

Sumaira Z. Aasi
David J. Leffell
Rossitza Z. Lazova

Atlas of Practical Mohs Histopathology



Springer

Atlas of Practical Mohs Histopathology

Sumaira Z. Aasi • David J. Leffell • Rossitza Z. Lazova

Atlas of Practical Mohs Histopathology

 Springer

Dr. Sumaira Z. Aasi
Stanford University School of Medicine
450 Broadway Street
Pavilion B, 4th Floor
Redwood City, CA 94063, USA

Dr. David J. Leffell
Yale School of Medicine
40 Temple Street
5th Floor, Suite 5A
New Haven, CT 06510, USA

Dr. Rossitza Z. Lazova
Yale School of Medicine
15 York Street, New haven,
CT 06519, USA

ISBN 978-1-4614-5160-0 ISBN 978-1-4614-5161-7 (eBook)
DOI 10.1007/978-1-4614-5161-7
Springer New York Heidelberg Dordrecht London

Library of Congress Control Number: 2012952729

© Springer Science+Business Media New York 2013

This work is subject to copyright. All rights are reserved by the Publisher, whether the whole or part of the material is concerned, specifically the rights of translation, reprinting, reuse of illustrations, recitation, broadcasting, reproduction on microfilms or in any other physical way, and transmission or information storage and retrieval, electronic adaptation, computer software, or by similar or dissimilar methodology now known or hereafter developed. Exempted from this legal reservation are brief excerpts in connection with reviews or scholarly analysis or material supplied specifically for the purpose of being entered and executed on a computer system, for exclusive use by the purchaser of the work. Duplication of this publication or parts thereof is permitted only under the provisions of the Copyright Law of the Publisher's location, in its current version, and permission for use must always be obtained from Springer. Permissions for use may be obtained through RightsLink at the Copyright Clearance Center. Violations are liable to prosecution under the respective Copyright Law.

The use of general descriptive names, registered names, trademarks, service marks, etc. in this publication does not imply, even in the absence of a specific statement, that such names are exempt from the relevant protective laws and regulations and therefore free for general use.

While the advice and information in this book are believed to be true and accurate at the date of publication, neither the authors nor the editors nor the publisher can accept any legal responsibility for any errors or omissions that may be made. The publisher makes no warranty, express or implied, with respect to the material contained herein.

Printed on acid-free paper

Springer is part of Springer Science+Business Media (www.springer.com)

To my beloved parents and siblings (Ghulam-Haider, Zubaida, Humaira, Irfan, Rummanah, and Salman) for their constant love, support, and faith even when I falter. To my mentors, particularly my two co-authors, who taught me Mohs surgery, dermatopathology, collegiality, and a determined will to achieve goals. And finally to my patients who teach me every day what it means to be a physician.

Sumaira Z. Aasi

To my fellows and students, whose curiosity is a great source of joy.

David J. Leffell

To my parents who raised me and taught me to be myself no matter what, to my son whom I love the most and have great expectations for, to my brother who is one of the kindest people I know and, most importantly, to the greatest husband in the Universe, Ken Robinson, with deep love and appreciation!

Rossitza Z. Lazova

Preface

This atlas is the product of combined clinical and laboratory experience of more than half a century. It represents a highly rewarding collaboration between cutaneous oncologists trained in Mohs microscopically controlled surgery and a dermatopathologist. In an age when technology such as whole exome sequencing of tumor DNA, optical coherence tomography of in vivo skin, and even spectrophotometric diagnosis of skin lesions is rapidly changing the way we understand skin malignancies and diagnose and treat them, it is remarkable that in a fundamental way we still rely on a method of microscopic diagnosis that is centuries old: the light microscope. The endurance of this “original technology” is less an indication of the absence of other cost-efficient diagnostic tools and more a reflection on the general reliability of conventional histopathology in making the majority of initial and often final diagnostic decisions about a cutaneous cancer.

Fundamental to the art and science of microscopic identification of cancer is the recognition of the wide range of variants for a particular entity and the need to view tissue in a flexible fashion. That is, one must master the fundamentals and understand what the images under the light microscope reflect biologically. Then, one must use that broader understanding of the images to make a clinically relevant and useful diagnosis. In essence, this atlas is intended not only to convey the fundamental features of each entity under discussion but also to highlight pathways to understand how those features may relate to others in a differential fashion so that a clinical decision can be made in real time. For this reason we have titled the book *Atlas of Practical Mohs Histopathology*. We hope you find this book a useful adjunct as you care for your patients with skin cancer.

Any errors or omissions in this text are ours alone. We would appreciate feedback and suggestions so that we may continue to improve both the quality and content of this first edition.

Sumaira Z. Aasi, M.D.
David J. Leffell, M.D.
Rossitza Z. Lazova, M.D.

Acknowledgments

This atlas, like any collaborative scholarly project, has required the input of many individuals. The information in this book is based on the academic work of those who came before us. Our goal was to distinguish this book with the highest quality images. In a day when internet-based teaching and digital imaging have revolutionized how we share information, in the world of Mohs microscopically controlled surgery the fundamental building block of quality in an atlas is the clinical material upon which the book is based. If the histologic slide is of poor quality, so too will be the photographic images upon which teaching is based. We have been fortunate over the past quarter century to have technicians who are supremely talented. Our staff has continually demonstrated dedication to patient care and achieving quality in the Mohs frozen sections which rivals that of permanent sections. Without their expertise and patience as we prepared the slides for this atlas, we would not have been able to craft a book that we hope will find a permanent place by your microscope. We would like to thank Ursula Carlson, Sylwia Kaczowka, Lezlie Roark, and the other technicians of the Yale Dermatologic Surgery Mohs lab. Ann Putio typed the manuscript in a professional and thorough fashion. It goes without saying that the fundamental *raison d'être* of this book is to enhance the care of patients. Over the past quarter of a century we have been fortunate to have remarkable staff and colleagues including nurses, clerical staff, and departmental administrators. Dr. Lazova would like to acknowledge Dr. A. Bernard Ackerman and Dr. Glynis Scott who taught her so much and inspired her. We would also like to acknowledge Richard L. Edelson, M.D., chairman of the Department of Dermatology at the Yale School of Medicine since 1985, who has fostered a culture of scholarship and patient-centered care in an environment that has allowed our cutaneous oncology and dermatopathology programs to thrive.

Contents

1	How to Use This Atlas	1
2	Normal Skin	3
	Folliculo-Sebaceous Unit	3
	Nerves	10
	Skeletal Muscle	13
	Smooth Muscle	15
	Vessels	17
	Eccrine Glands	19
	Salivary Glands	20
	Apocrine Glands	23
	Periosteum	24
	Scar Tissue	25
3	Basal Cell Carcinoma	27
4	Infiltrative Basal Cell Carcinoma	47
	Histologic Features	47
	Histopathologic Differential Diagnosis	48
	Syringoma	48
	Desmoplastic Trichoepithelioma	48
	Microcystic Adnexal Carcinoma	48
	Infiltrative Basal Cell Carcinoma with Perineural Invasion	49
5	Differentiating Basal Cell Carcinoma from Normal and Benign Histologic Findings	65
	Differentiating Basal Cell Carcinoma from Hair Follicles	66
	Differentiating Basal Cell Carcinoma with Follicular Differentiation from Hair Follicles	66
	Differentiating Basal Cell Carcinoma from Eccrine Glands	67
	Differentiating Basal Cell Carcinoma from Vessels	67
	Differentiating Basal Cell Carcinoma from Inflammation	68
6	Adnexal Tumors	111
	Syringoma	111
	Histologic Features	111
	Histopathologic Differential Diagnosis	111
	Desmoplastic Trichoepithelioma (DTE)	112
	Histopathologic Differential Diagnosis	112
	Sebaceous Carcinoma	113
	Histologic Features	113
	Muir-Torre Syndrome and Its Cutaneous Anifestations	113

7 Microcystic Adnexal Carcinoma	129
Histologic Features	129
Differentiating Features Between Microcystic Adnexal Carcinoma and Desmoplastic Trichoepithelioma	130
Differentiating Features Between Microcystic Adnexal Carcinoma and Infiltrative Basal Cell Carcinoma	130
8 Differentiating Infiltrative Basal Cell Carcinoma from Other Tumors	145
Infiltrative Basal Cell Carcinoma and Desmoplastic Trichoepithelioma	145
Infiltrative Basal Cell Carcinoma and Microcystic Adnexal Carcinoma	146
Infiltrative Basal Cell Carcinoma and Syringoma	146
9 Squamous Cell Carcinoma In Situ and Actinic Keratoses	153
Histologic Features	153
Histopathologic Differential Diagnosis	153
Actinic Keratosis	153
Intraepidermal Paget's Disease	153
Malignant Melanoma In Situ	154
10 Squamous Cell Carcinoma	179
Histologic Features	179
Subtypes of SCC	180
Infiltrative Squamous Cell Carcinoma	180
Spindle Cell Squamous Cell Carcinoma	180
Acantholytic Squamous Cell Carcinoma	180
Differential Diagnosis	180
Inflamed Seborrheic Keratosis	180
Verruca	180
Tangential Sectioning of the Epidermis	181
Pseudoepitheliomatous Hyperplasia (PEH)	181
11 Differentiating Squamous Cell Carcinoma from other entities	245
Hypertrophic Lupus Erythematosus	245
Squamous Cell Carcinoma and Atypical Fibroxanthoma	245
Squamous Cell Carcinoma and Pseudoepitheliomatous Hyperplasia	246
12 Dermatofibrosarcoma Protuberans	257
Histologic Features	257
Differentiating Dermatofibrosarcoma Protuberans and Scar Tissue	257
13 Other Non-melanocytic Skin Cancer	273
Atypical Fibroxanthoma	273
Histologic Features	273
Atypical Fibroxanthoma and Squamous Cell Carcinoma	273
Extramammary Paget's Disease	274
Histologic Features	274
A Note on Immunohistochemistry Stains	274
Immunohistochemical Staining Characteristics of Spindle Cell Neoplasms	274

14 Pitfalls and Incidental Findings	285
Incidental Findings	285
Nevus	285
Neurofibroma	285
Epidermal Inclusion Cyst	285
Seborrheic Keratosis	285
Solar Lentigo	285
15 Artifacts	309
Bibliography	317
Index	319

The incidence of skin cancer continues to rise and with it there is an increasing focus on the need to treat malignant skin tumors in an effective and cost-efficient fashion. Mohs surgery, more specifically referred to as Mohs microscopically controlled surgery, is a tissue sparing method for the stepwise removal of skin cancer. The approach, performed in the office setting under local anesthesia, permits maximal normal tissue preservation while optimizing the cure rate. It is the treatment of choice for a variety of skin cancers on the face, head and neck, trunk and extremities. Originally developed at the University of Wisconsin by Frederick Mohs, the method used a fixed tissue approach through the application of zinc chloride. In the early 1970s, this method gave rise to the frozen section Mohs technique. *This book focuses exclusively on the frozen section method. We do not discuss special stains and limit our discussion to hematoxylin and eosin-stained tissue.* While some Mohs surgeons may use other methods, in order to make this text applicable most broadly we have focused on the most commonly used method of tissue preparation. Ultimately, as the reader will see, Mohs histopathology is much more about pattern recognition and understanding cellular features than about the particular stain that is used.

A critical element of the Mohs technique is that the properly trained Mohs surgeon is also the individual who maps, oversees the processing of, and interprets the specimen. This reduces the chance for error in tumor mapping and is probably a key element in the high cure rate observed with the technique. To this end, of course, the ability to interpret specimens is paramount. It is not possible to perform Mohs surgery properly without adequate training in the interpretation of Mohs frozen section histopathology slides. This atlas is intended as an aid to slide interpretation. We have specifically focused on normal skin as a foundation and have highlighted common variations of abnormal in each of the disease categories normally treated by Mohs surgery. Use of this text presumes knowledge of dermatopathology. That is, the terminology assumes proper exposure to skin pathology whether through dermatology, pathology, or other specialty training.

This is not an introductory level text nor is it a how-to manual. Interpreting Mohs histopathology slides is both an art and a science. The distinction of cancerous tissue from non-cancerous tissue is not always clear-cut, nor always absolute, even among similarly trained colleagues within the subspecialty. There is nuance in interpretation of the cells as well as the various patterns of cellular alignment that are informative for the diagnosis of cutaneous malignancies. Rather, this text is intended to serve as an adjunct for people who have pursued formal training in Mohs surgery or dermatopathology. We hope this atlas will serve as an effective aid in addressing both routine Mohs surgery cases and clinical-pathologic conundrums that arise. To be certain, the range of complexities in a given case, such as a spindle cell carcinoma, can be vast. There are ancillary studies such as immunohistochemistry that can often help clarify obtuse cases. Such discussion is beyond the scope of this text. However, the common points of confusion, from the point of view of differential diagnosis, are specifically addressed in many of the chapters where the potentially confusing entities are compared feature by feature. While not to be used as a checklist, this structure will help organize your thinking as you approach challenging cases. More specifically what distinguishes this atlas and perhaps makes it most clinically relevant for the Mohs surgeon is that it discusses the false negatives and false positives that form the basis of the inevitable question that a Mohs surgeon faces at each moment, with each case and each stage: "Is this cancer or not, do I excise more or not?" By comparing and contrasting normal or benign histologic findings, studying challenging cases from low to high magnification in different sections and deeper cuts into the specimen, the atlas will uniquely allow the reader to appreciate the rationale when no absolute answers exist and develop the skills to make such decisions when faced with their own clinical conundrums.

We hope that the extensive effort invested in producing the highest quality rendition of actual Mohs histopathology specimens will provide you with the level of image detail you require to make the greatest use of this text.

The skin is generally considered to consist of three major layers: epidermis, underlying dermis, and subcutaneous fat. Depending on anatomic site, there are four to five layers of the epidermis. The layer closest to the basement membrane is the stratum basalis (or basal layer), which consists of a single layer of cuboidal cells that have a slightly basophilic cytoplasm and high nucleus to cytoplasm ratio. The stratum spinosum (or spinous layer) is above the stratum basalis and is so-called because of the prominent intercellular connections and pointed ends of the cells. The stratum granulosum (or granular layer) consists of flattened cells that contain coarse, basophilic granules. The stratum corneum (keratinous layer) is most superficial and consists of anucleate cells arranged in a basketweave pattern. On acral skin an additional layer called stratum lucidum is also present. The dermis consists of papillary dermis, consisting of a fine network of collagen and elastic fibers located immediately beneath the epidermis, and reticular dermis, which consists of thicker dense collagen bundles and extends to the subcutaneous fat. The thickness of the epidermis and dermis varies depending on the region of the body. Finally, the subcutis is composed of lobules of adipocytes separated by fibrous septae. Within the septae are blood vessels, lymphatics, and nerves.

The skin contains within it numerous adnexal structures such as hair follicles, sebaceous glands, eccrine and apocrine glands, as well as neurovascular elements. The number and appearance of adnexal structures vary at different body sites and can be a clue to a specific location on the body. For example, on facial skin there are numerous small

vellus hair follicles rooted superficially in the dermis. Large sebaceous lobules are associated with those hair follicles. Apocrine glands, for example, are mostly present on certain body sites such as the axilla and on the genitalia. In addition, the amount of actinic damage signified by the presence of elastotic (fragmentation of the elastic fibers that appears as irregular basophilic clumps) material can also provide clues to location of site.

Folliculo-Sebaceous Unit

The folliculo-sebaceous unit consists of a hair follicle and its associated sebaceous unit. In vertically oriented sections, the mature hair follicle in anagen phase consists of three parts: lower segment, which extends from the base of the follicle to the attachment of the muscle of hair erection or arrector pili muscle, middle segment (or isthmus), which extends from the attachment of arrector pili muscle to the entrance of the sebaceous duct, and upper segment (or infundibulum), which extends from the entrance of the sebaceous duct to the ostium of the hair follicle. The area where the arrector pili muscle attaches is also known as follicular “bulge.” Emanating from the sides of the hair follicle, at the junction of infundibulum and isthmus, are symmetrical cords of epithelial cells that extend laterally for a short distance, and then descend parallel with the follicle. This is referred to as the mantle of the follicle. It gives rise to the sebaceous glands and ducts. The lowest part of a follicle is named the bulb because it resembles

Fig. 2.1 Longitudinally transected hair follicles with associated sebaceous glands

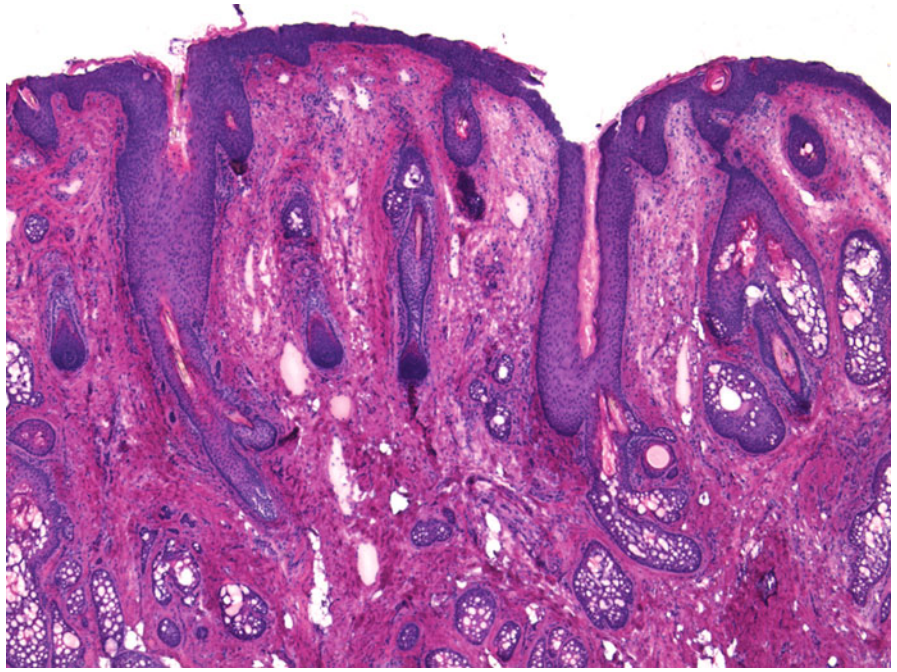
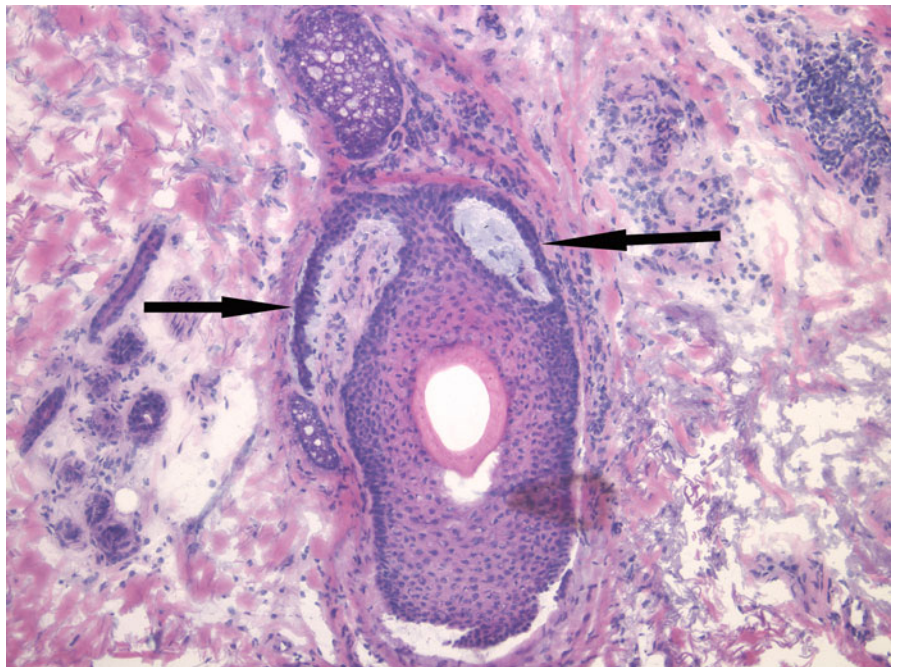


Fig. 2.2 Although seen as two cords of epithelial cells on longitudinal sections, the mantle (*arrows*) is actually an umbrella-like three-dimensional structure that encircles the hair follicles



the bulb of a tulip or an onion, and contains the matrix and germinative cells from which the hair shaft itself grows. The bulb also contains melanocytes, which are responsible for the color of the hair. The hair bulb surrounds a somewhat conical, highly vascularized area of connective tissue called

the papilla, which is responsible for blood supply to this area of high metabolic activity. The follicular papilla is separated from the epithelial cells by a basement membrane, which is continuous with the external glassy membrane surrounding the follicle.

Fig. 2.3 Follicular bulb (*B*) and papilla (*P*) of a hair follicle in anagen. The hair bulb hugs the follicular papilla, which is the fibrovascular core providing nourishment. The epithelium of the hair bulb consists of matrix cells admixed with melanocytes. Bright red trichohyalin granules are seen in the upper portion. A thin rim of fibrous tissue surrounds the follicle (*arrow*)

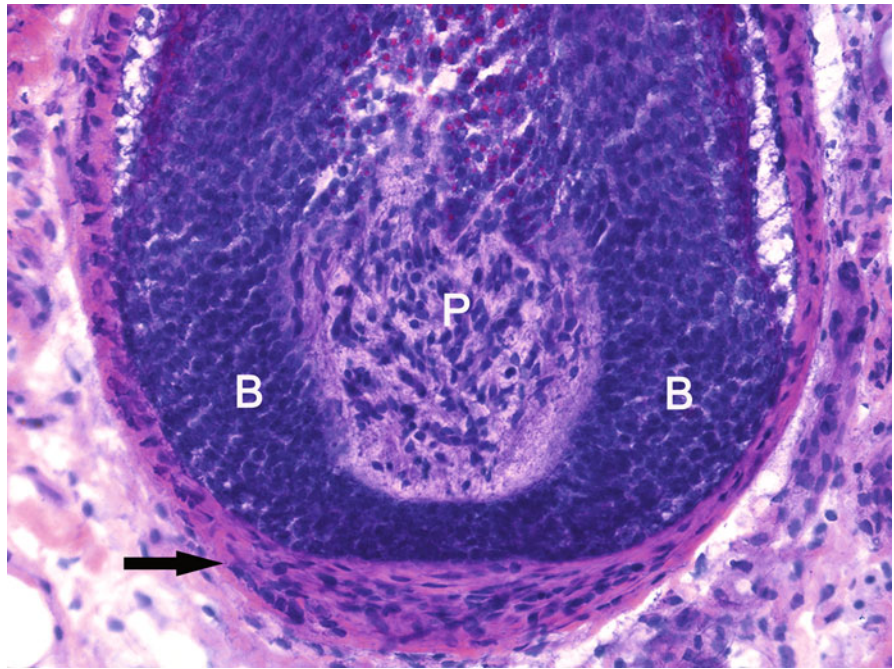
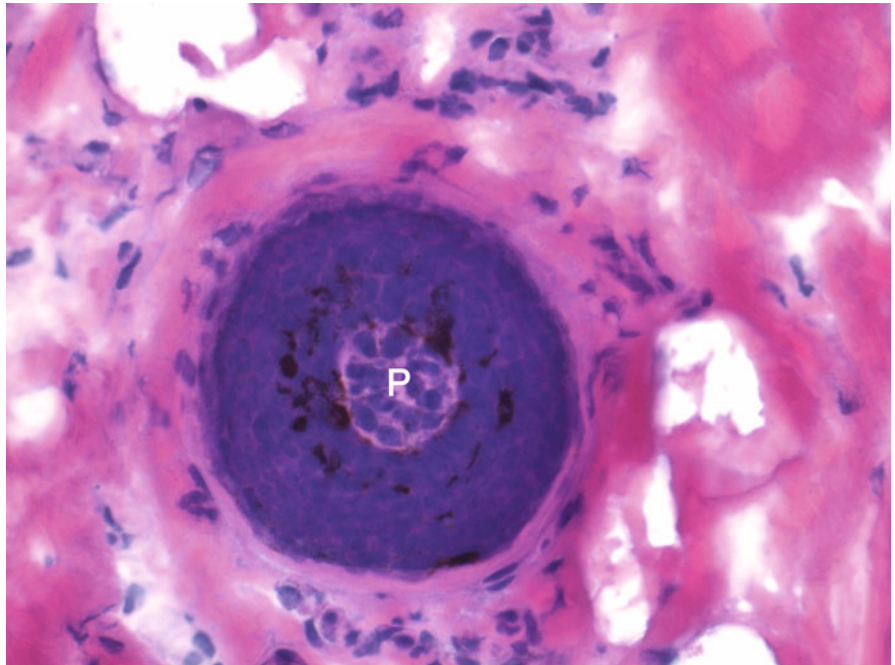


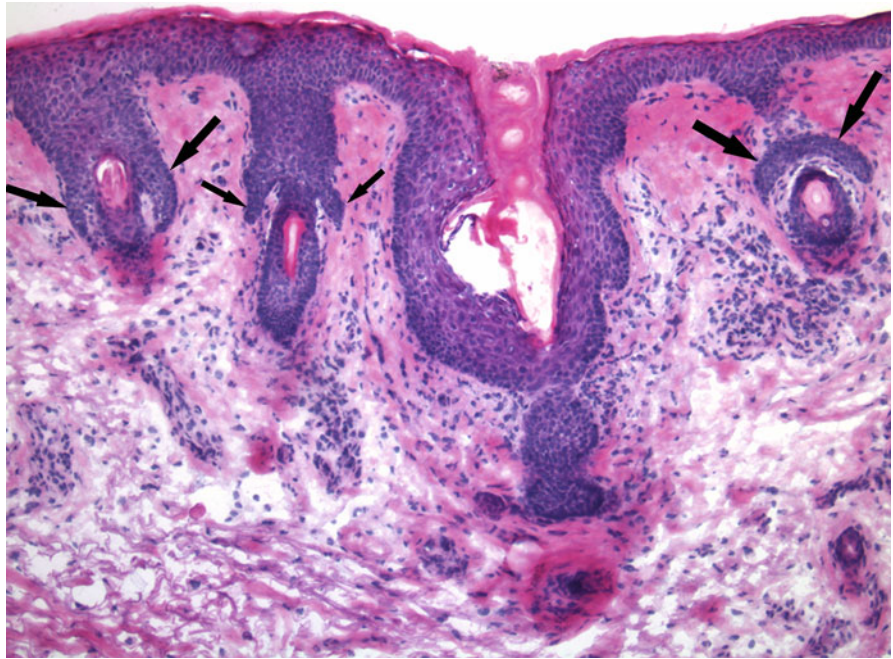
Fig. 2.4 A cross-section of a follicular bulb and a centrally placed papilla (*P*). Numerous melanocytes are admixed with matrix cells



Hair follicles undergo periods of growth and rest, which is reflected in changes in their microscopic appearance. Actively growing follicles penetrate deeply in the subcutaneous fat and demonstrate a prominent hair bulb. On the scalp and face, particularly in bearded areas of

men, terminal hair follicles are deeply rooted in the subcutaneous fat. In other areas of the face vellus hairs predominate, which are much smaller and superficially located. Their bulbs are present in either the superficial or mid reticular dermis.

Fig. 2.5 Vellus hair follicles on the face with prominent mantles (*arrows*)



The hair follicle consists of a series of concentric layers that form in the bulb and move progressively upward. These layers are often most obvious in the anagen growth phase. The outermost layer is a highly vascularized fibrous sheath. Immediately medial to that is a basement membrane followed by the outer root sheath. The cells of the outer root sheath are large, monomorphous, and with clear cytoplasm. Immediately medial to that area is the inner root sheath of the hair follicle consisting of a Henley's layer (which is the first of the lower follicle layers to keratinize), followed by the Huxley's layer (which also keratinizes and contains trichohyalin granules). The inner most layer is the hair shaft itself.

A sebaceous unit consists of a mature sebaceous gland comprised of several discrete sebaceous lobules and a sebaceous duct. The glands often appear clear or empty because they contain lipids that dissolve away during processing.

A sebaceous duct is a channel with thin, crenulated cornified epithelial lining that connects one or more sebaceous lobules to an infundibulum of the hair follicle. Each sebaceous lobule has a single row of immature sebocytes at the periphery and mature sebocytes in the center, which undergo complete disintegration and thus form the sebum in a process known as holocrine secretion. Sebocytes have scalloped nuclei and vacuolated, foamy cytoplasm.

Fig. 2.6 (a, b) Terminal hair follicles in anagen with follicular bulbs, papillae, and discernable follicular epithelial layers

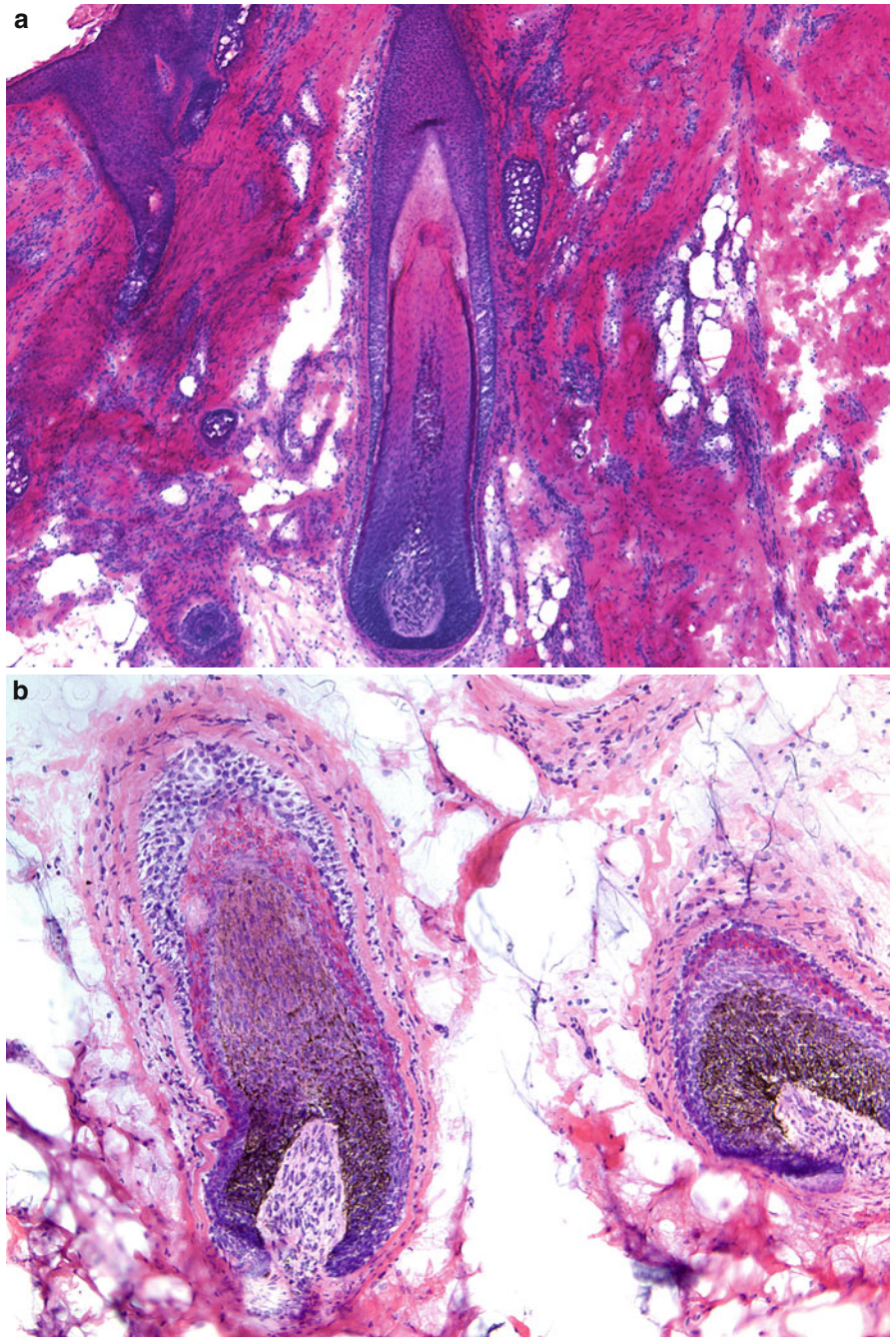


Fig. 2.7 Cross-section of hair follicles in anagen with hair shafts in the center and one miniaturized hair follicle (*arrow*)

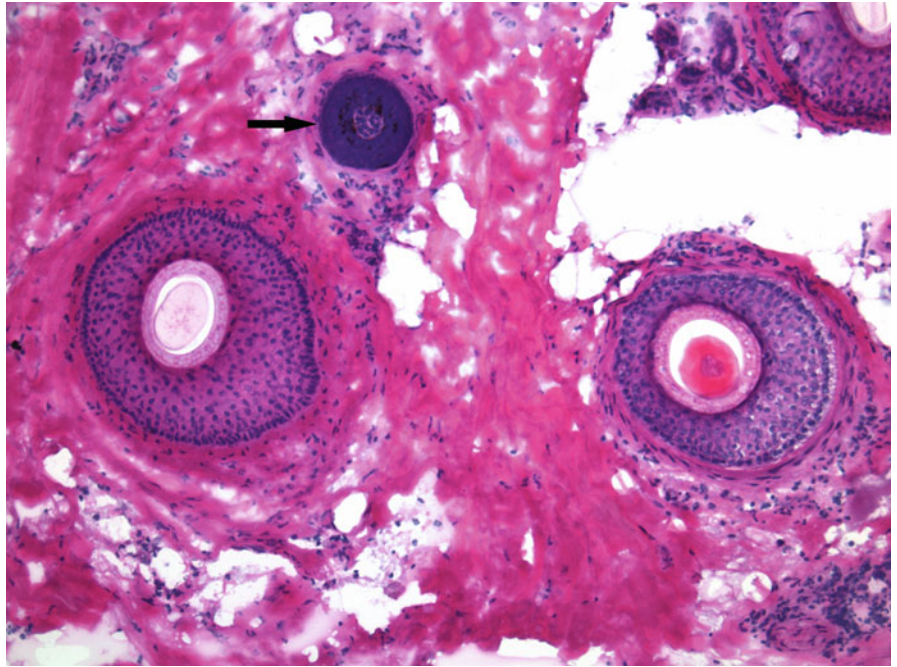


Fig. 2.8 Cross-section of hair follicles at the level of the sebaceous glands

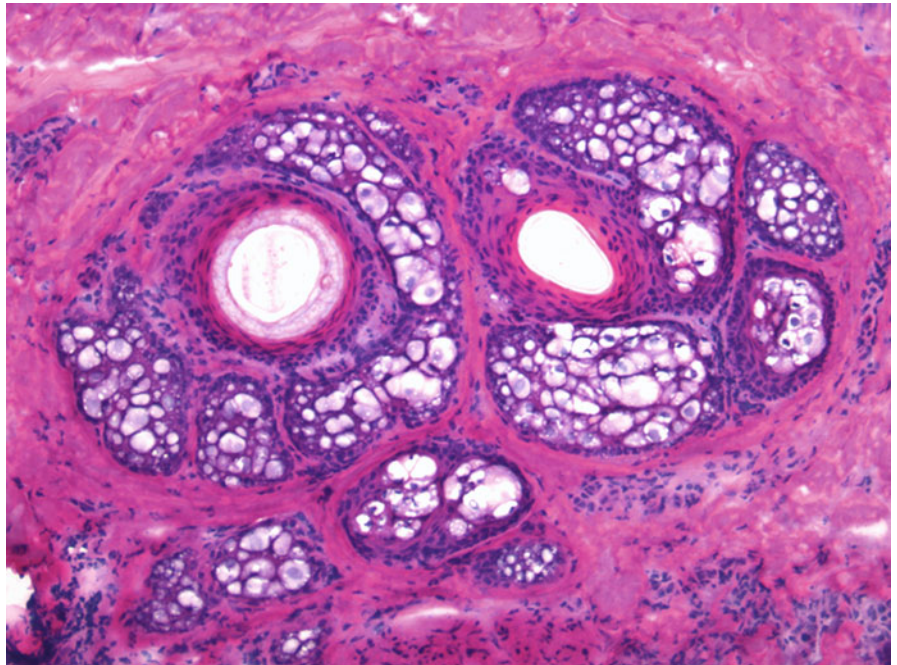
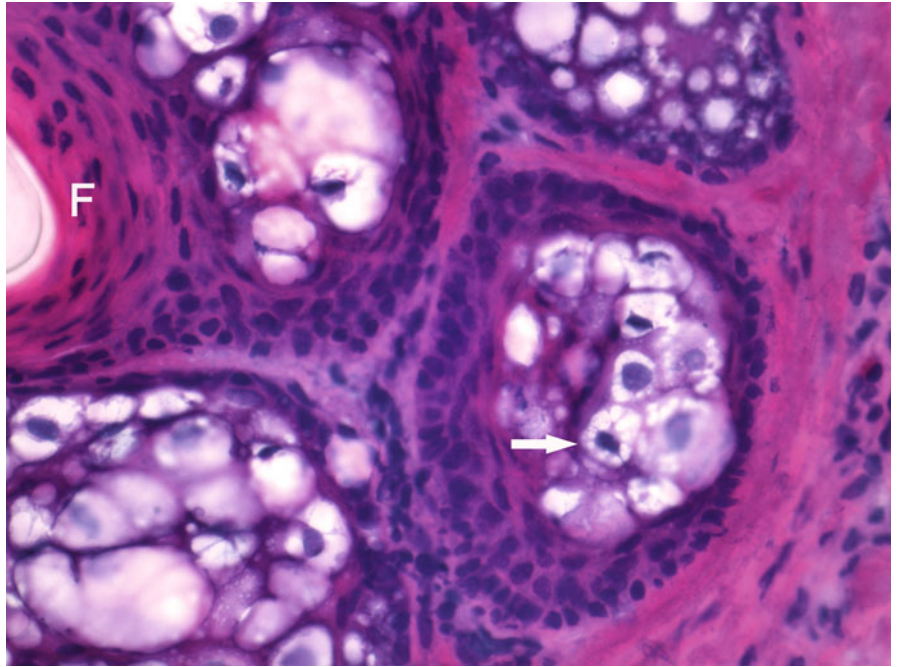


Fig. 2.9 Sebaceous glands surrounding a hair follicle (*F*), comprised of sebocytes, which have scalloped nuclei and vacuolated clear cytoplasm (*arrow*)



Nerves

Nerves are often seen in association with blood vessels as part of a neurovascular plexus. Nerves can be seen throughout the reticular dermis as well as in deeper tissues such as within subcutaneous fat and in between skeletal muscle fibers. The “basic unit” is a nerve fiber, which consists of an axon and the

surrounding Schwann cells. Multiple nerve fibers form nerve fascicles, which are surrounded by a sheath, called a perineurium. The space within the perineurium is called endoneurium. The endoneurium also contains fibroblasts, capillaries, and mast cells. Numerous nerve fascicles are grouped together into nerve bundles and are “held together” by a protective sheath referred to as epineurium. Often nerves are seen

Fig. 2.10 A medium sized longitudinally sectioned nerve (*N*) with surrounding collapsed blood vessels (*arrows*) and eccrine glands (*EG*) and ducts in the vicinity, all situated within the subcutaneous fat and adjacent to skeletal muscle (*SkM*)

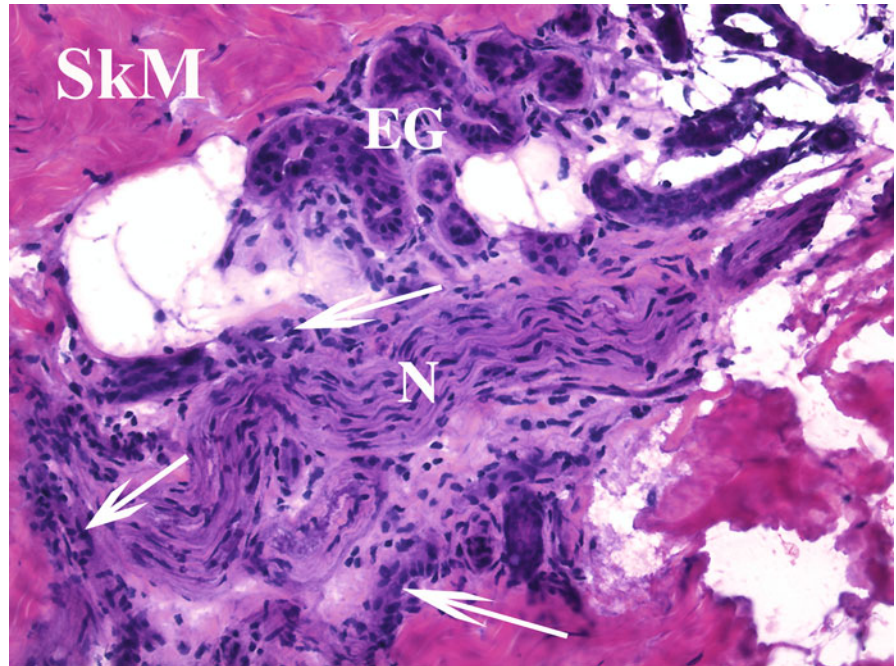


Fig. 2.11 Two longitudinally sectioned small nerves (*arrows*) surrounded by dense collagenous fibrous tissue called perineurium

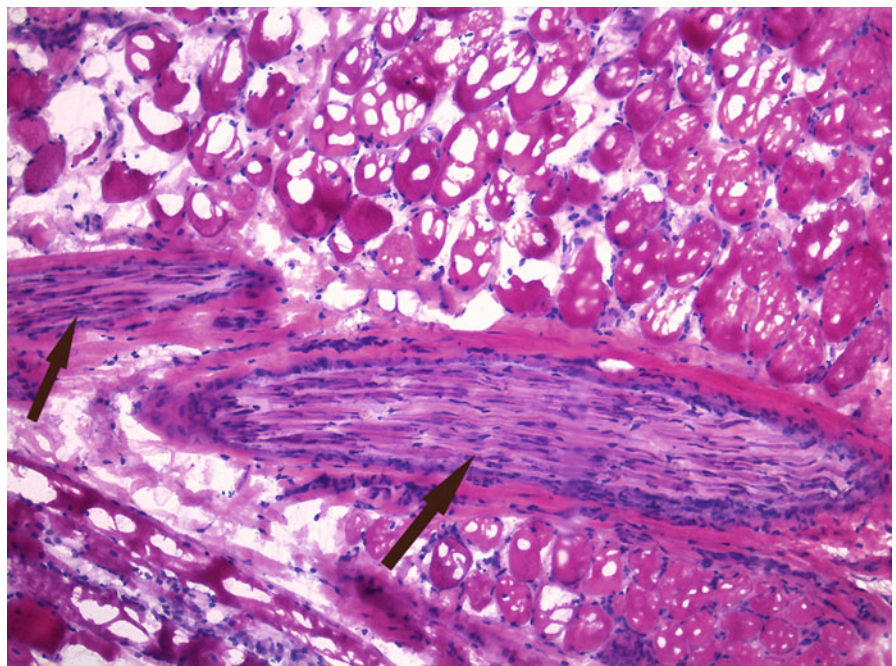


Fig. 2.12 Longitudinal zigzag alignment of nerve fibers with wavy, pointed nuclei

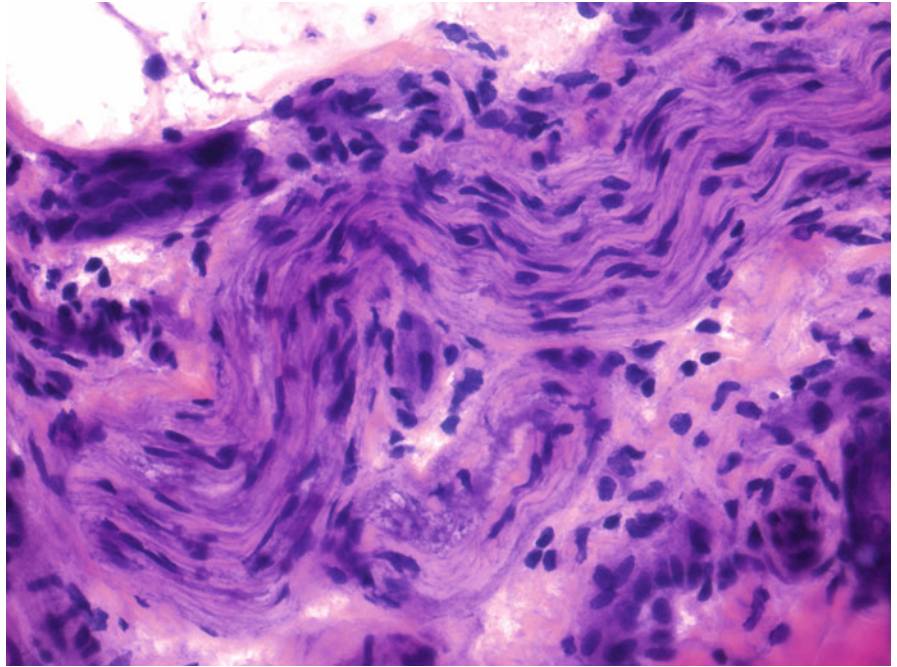
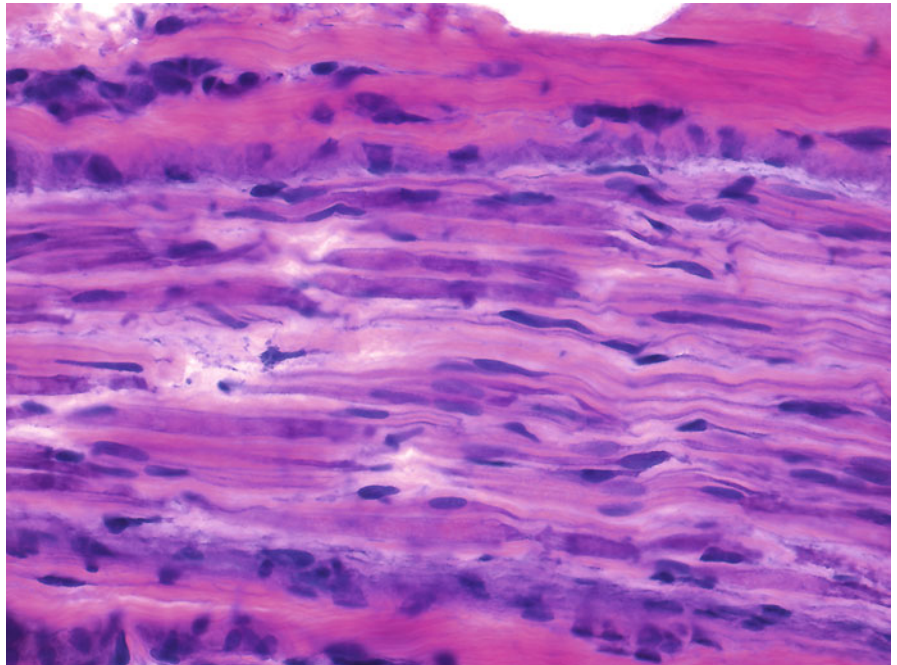


Fig. 2.13 Spindled pointed nuclei and long cytoplasmic processes oriented parallel to the long axis of the nerve fascicle



clumped together, some cut longitudinally and others cut transversely, but in close proximity to each other and each encased in a very thin fibrous sheath. When longitudinally sectioned, nerves show fascicles of spindled cells with

S-shaped nuclei and long thin cytoplasmic processes. Very often fine purple granules of different sizes are seen within the cytoplasm of the nerves. Small vacuoles are also noted in both longitudinal sections and cross sections.

Fig. 2.14 Three small nerves between skeletal muscles. The nerve on the right is longitudinally sectioned and the two nerves on the left are transversely cut

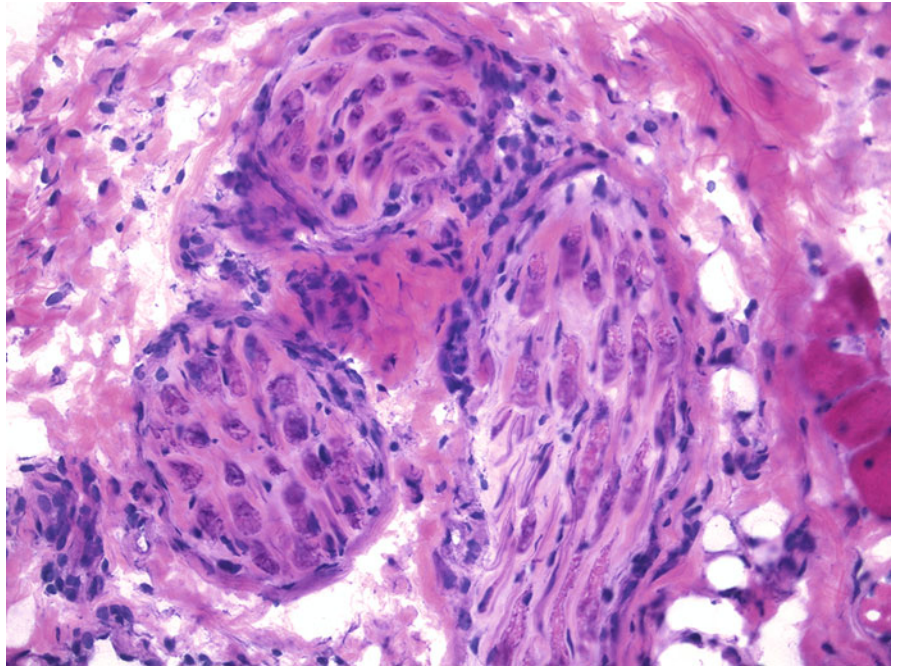
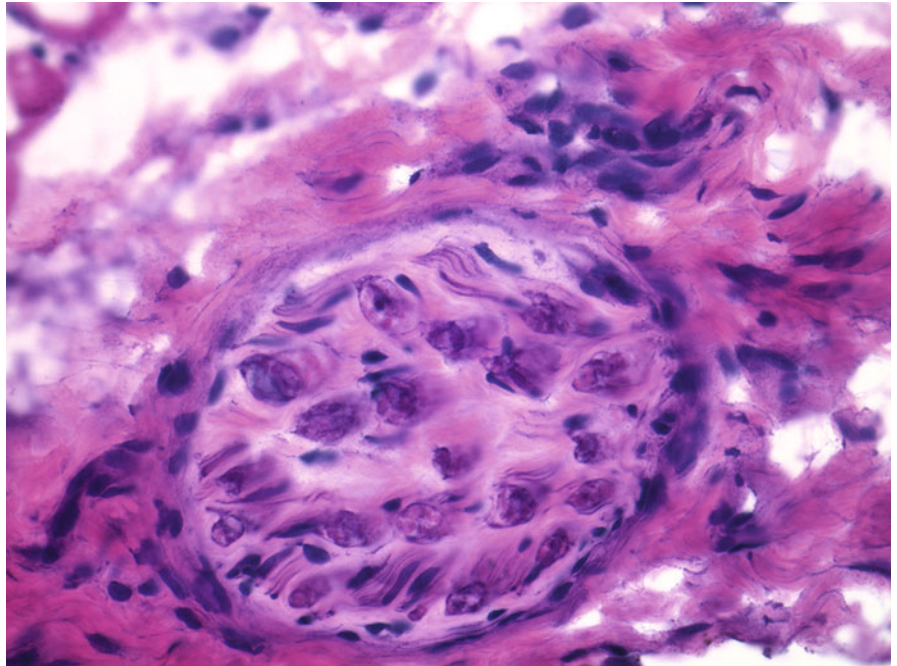


Fig. 2.15 Small nerve in a transverse section showing nerve axons in the center with a surrounding bubbly purple ring of myelin



Skeletal Muscle

Skeletal muscle fibers are typically located deep beneath the subcutaneous fat; however, depending on body site, they can be seen more superficially. The lip and eyelid are regions where skeletal muscle appears relatively superficially because of the lack of substantial subcutaneous adipose tissue in these areas. Skeletal muscle fibers are usually arranged in

large aggregates and fascicles. When longitudinally cut, the fascicles show a syncytium of cells with elongated blunt ended nuclei usually seen at the periphery, dense pink cytoplasm, and no distinct borders between the cells. In cross sections, skeletal muscle fibers are round, oval, or slightly angulated, containing round nuclei that are situated at the periphery. Dense pink non-vacuolated cytoplasm sometimes showing cross striations is seen in the center of the syncytium.

Fig. 2.16 Large fascicles of transversely cut skeletal muscle fibers, surrounded by a rim of fibrous tissue

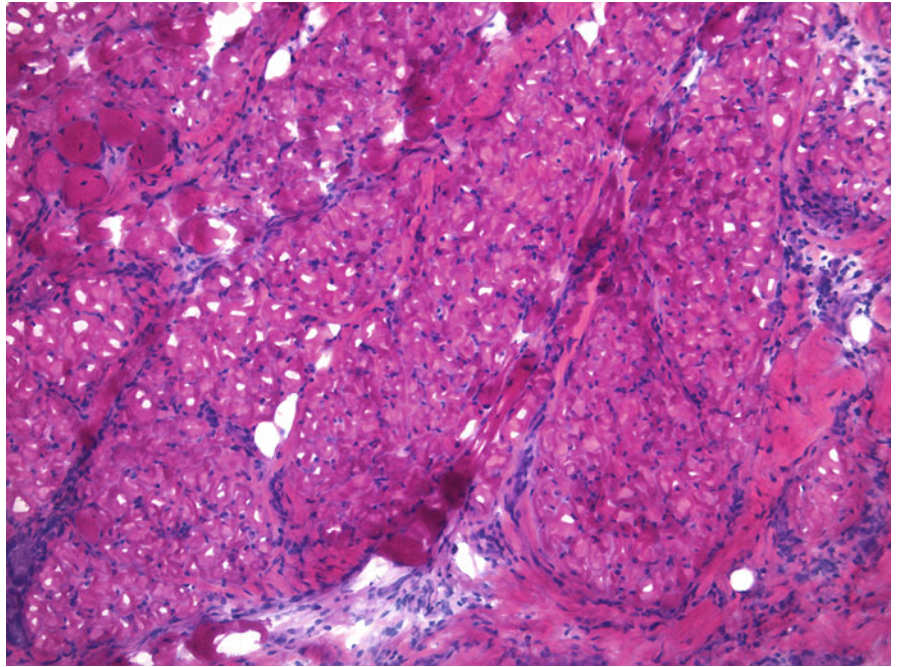


Fig. 2.17 Skeletal muscle fibers are a syncytium of cells without distinct borders

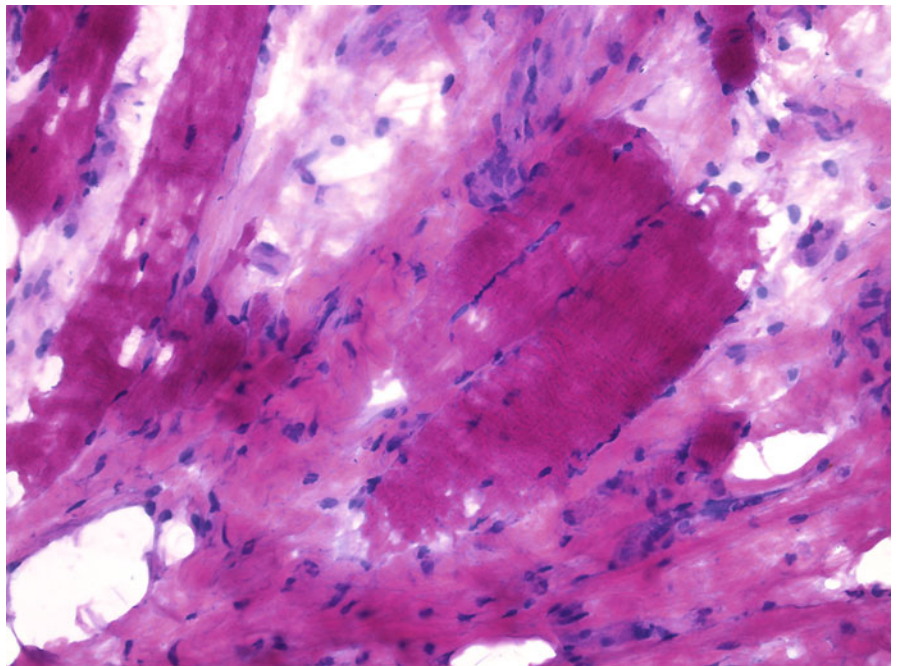


Fig. 2.18 The cells have elongated blunt ended nuclei and dense pink cytoplasm without vacuoles, distinguishing them from nerve fibers. Cross striations can be appreciated on high power (*arrows*)

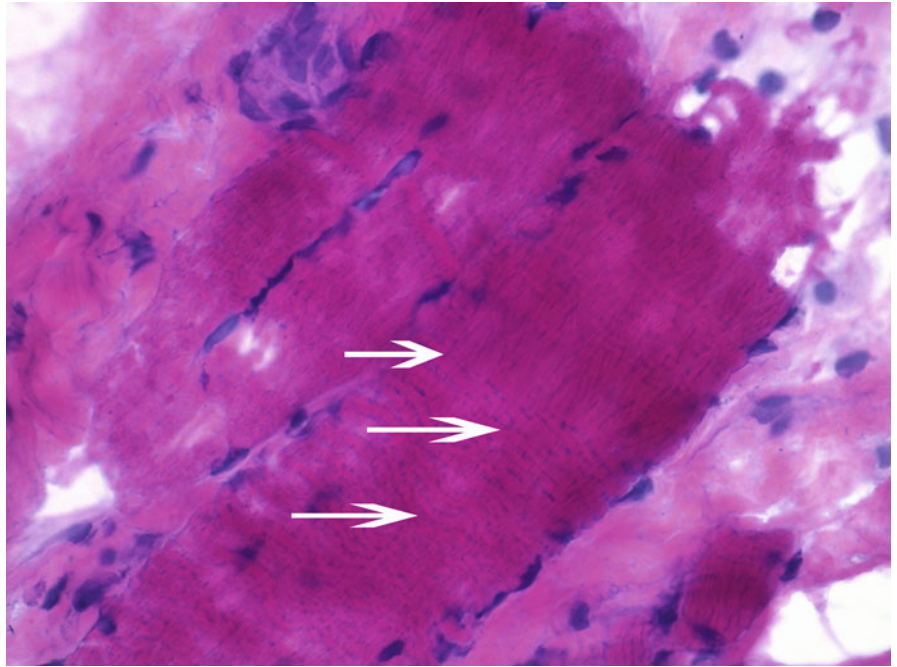
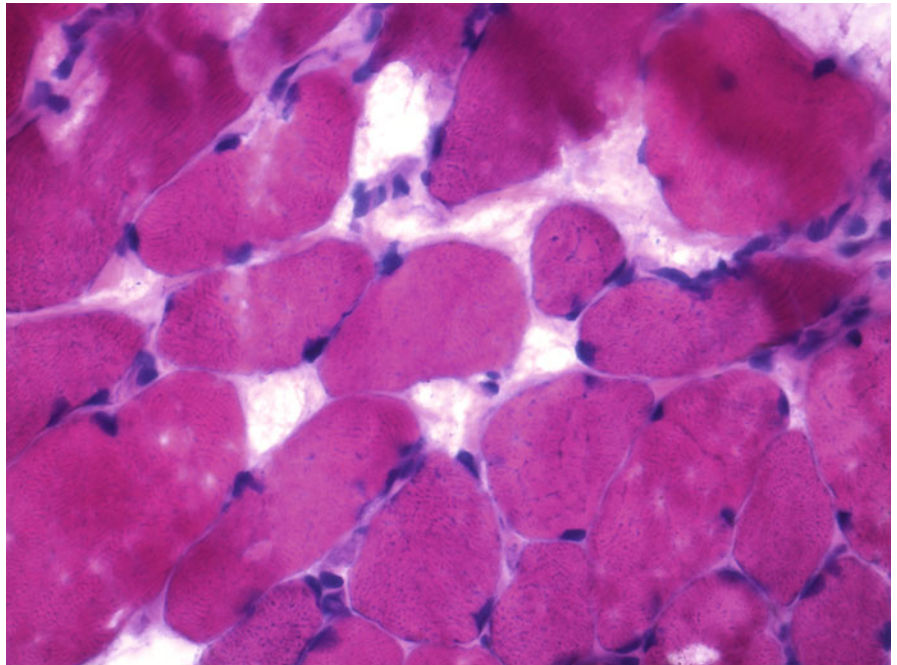


Fig. 2.19 Cross section of skeletal muscle fibers with round, oval, and slightly angulated contours



Smooth Muscle

Two types of smooth muscle are present in the skin: one is associated with hair follicles and the other is found in vessel walls. The muscle of hair erection (arrector pili or pilar muscle) is attached at a 45° angle in the mid-portion of the hair follicle, in the region of the mantle. Its upper portion attaches within the papillary dermis. When the pilar muscle contracts, it pulls the skin surface around the hair, which

elevates the hair shaft and produces what is known as “goose bumps.” Fascicles of pilar muscle can vary in shape and appear elongated, oval, or sometimes round. On longitudinal sections they reveal a syncitium of cells without distinct cellular borders, with elongated blunt ended nuclei, often oriented parallel to each other, and surrounded by eosinophilic cytoplasm. When cut transversely the nuclei appear round.

Fig. 2.20 Smooth muscle of hair erection (*arrows*) running at a 45° angle toward the mid portion of a hair follicle

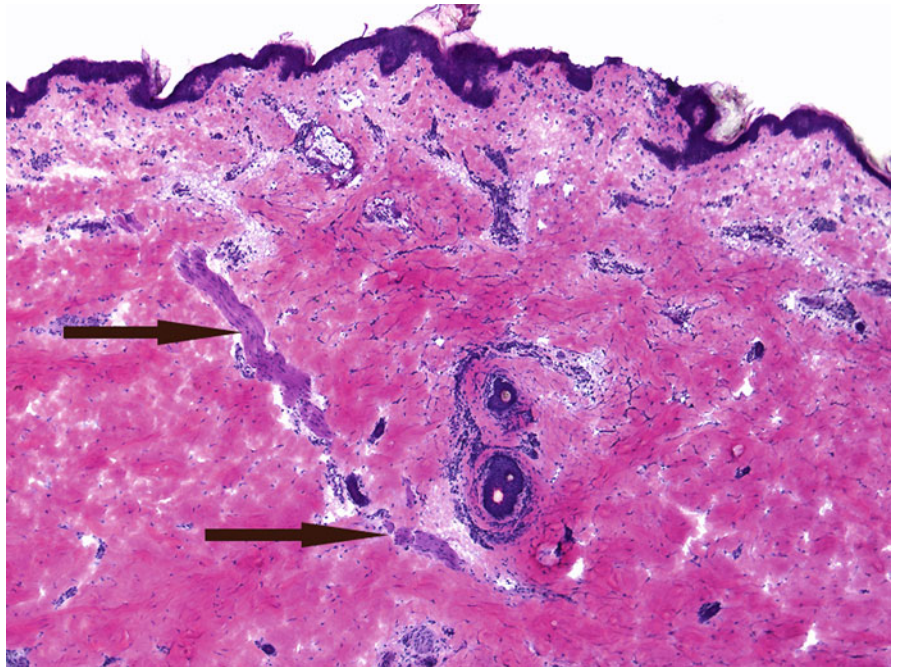
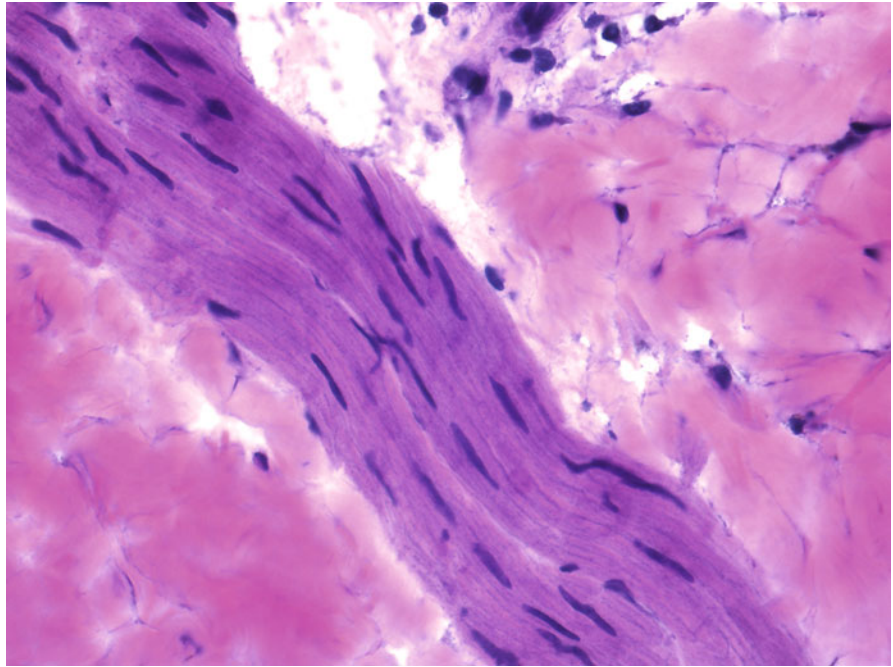


Fig. 2.21 Longitudinal section of smooth muscle with blunt ended elongated nuclei dispersed throughout the abundant eosinophilic cytoplasm that lacks cross striations



Nerves and smooth muscle can sometimes be difficult to differentiate for the novice. Aggregates of smooth muscle fibers are usually quite large as opposed to nerves especially in the superficial portion of the dermis. Large nerves are not seen there because they branch into smaller nerve fibers and present as nerve twigs in the most superficial portion of the dermis. Aggregates of pillar muscle have irregular shapes as opposed to nerves, which are either round, oval, or slightly elongated and encased in a thin fibrous sheath. Purple

granules seen within the cytoplasm of nerves are not observed within smooth muscle fibers. Smooth muscle fibers that are associated with a hair follicle and have as a main function erection of hair follicles are always seen in the upper, mid and, extremely rarely, in the lower reticular dermis. They are never present in the subcutaneous fat or in deeper soft tissues even when associated with terminal hair follicles deeply rooted in the subcutaneous fat as seen on the scalp and in bearded areas of the face in men.

Vessels

Dermal vasculature consists of superficial and deep vascular plexuses. The upper plexus is beneath the papillary dermis and the deep plexus is in the lower part of the reticular dermis. The arteries in the subcutaneous fat and larger arterioles

in the deep reticular dermis have three layers. The internal layer or “intima” contains endothelial cells and an internal elastic membrane. The second layer or “media” contains collagen, elastic fibers, and several concentric layers of smooth muscle cells. In muscular arteries, there is also an external elastic membrane. The outer layer is “adventitia”

Fig. 2.22 Nerves (*N*) and vessels (*V*) often run together

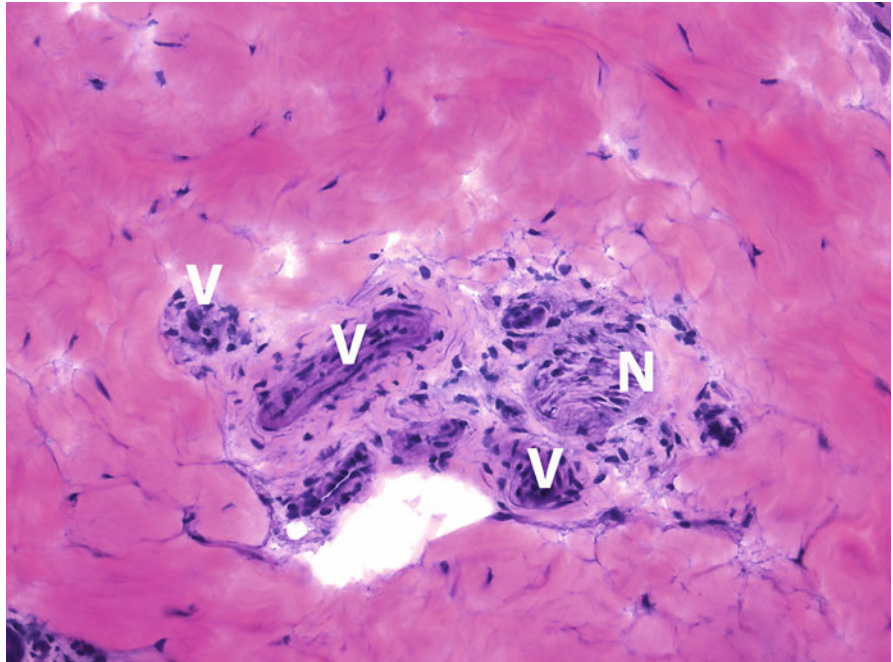
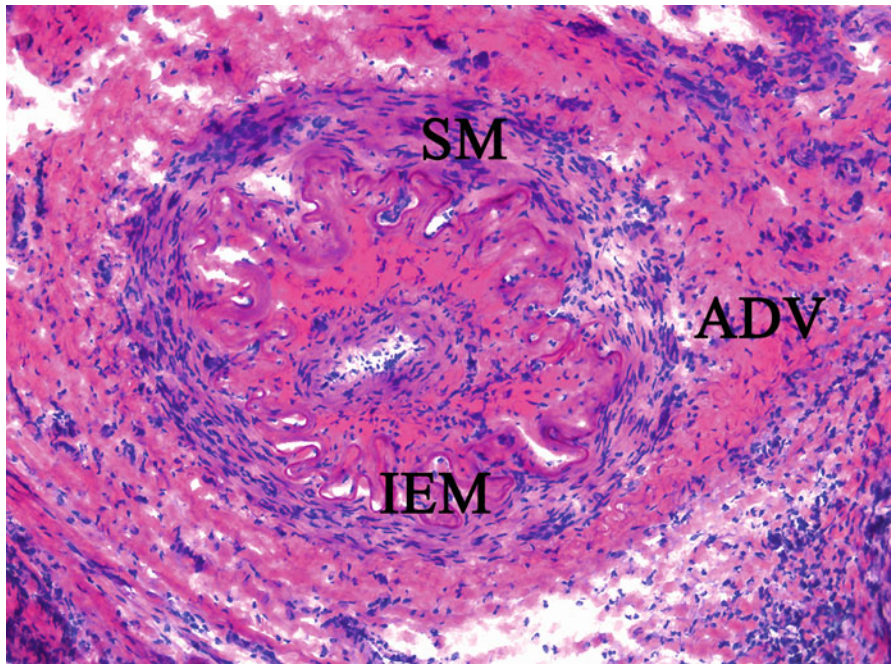


Fig. 2.23 A medium size artery with a small open lumen in the center, internal elastic membrane (*IEM*), smooth muscle layers (*SM*), and adventitia (*ADV*)



composed of fibrocytes, collagen, and elastic fibers. Small arterioles have only a single layer of smooth muscle cells. Capillaries are composed of a single layer of flattened

endothelial cells without a muscular or adventitial layer. Veins are distinguished by their thinner walls, wider lumina, and the presence of valves.

Fig. 2.24 A small artery (A) with a narrow lumen and a vein (Vn) with widely open lumen

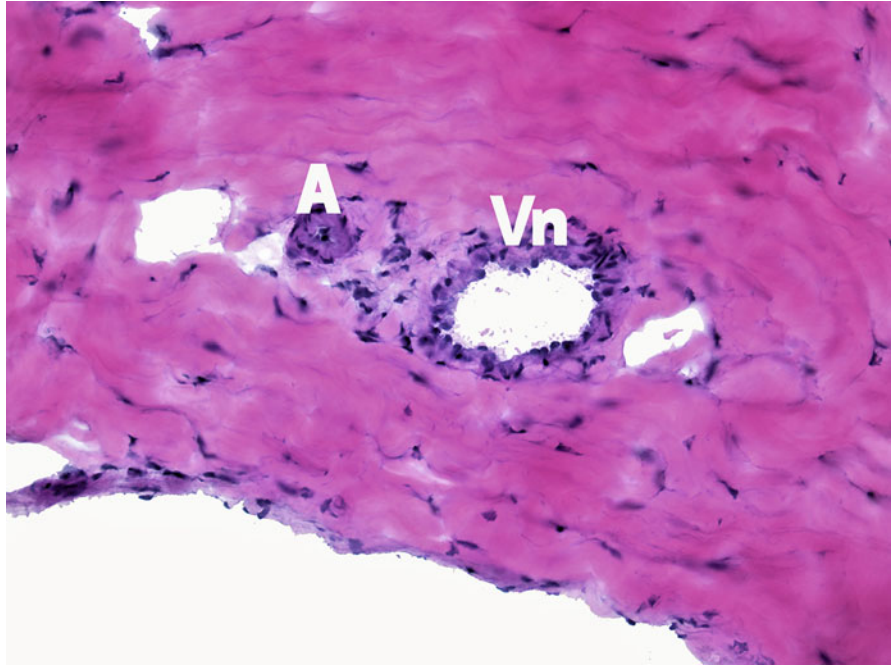
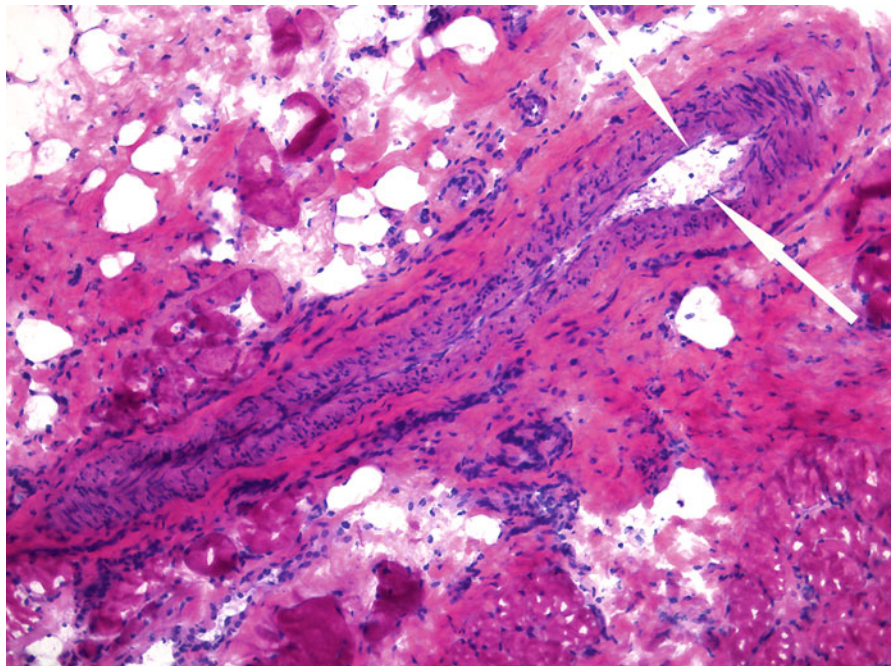


Fig. 2.25 A medium to large vein in longitudinal section with a patent partially collapsed lumen lined by flat endothelial cells (arrows)



Eccrine Glands

Sweat glands are unbranched, tubular structures that are composed of three segments: the intraepidermal duct (also known as the acrosyringium), the intradermal duct, and the secretory portion. The secretory portion of the gland forms a compact coil deep in the dermis and upper subcutaneous fat. In histologic sections, the glands appear as a mass of tubules cut in various planes. Eccrine glands are interspersed with

sections of the proximal part of the excretory duct. The eccrine glands consist of a single layer of large cuboidal or columnar cells surrounded by myoepithelial cells. The intradermal duct consists of a single layer of luminal cells and two or three rows of outer cells. The intraepidermal duct is composed of two layers of small, cuboidal basaloid cells. Unlike the secretory portion of the eccrine gland, the duct does not have a peripheral hyaline membrane zone but the lumen is lined with an eosinophilic cuticle.

Fig. 2.26 A longitudinally cut eccrine duct spiraling in its lower portion and leading to a group of eccrine glands located in the subcutaneous fat

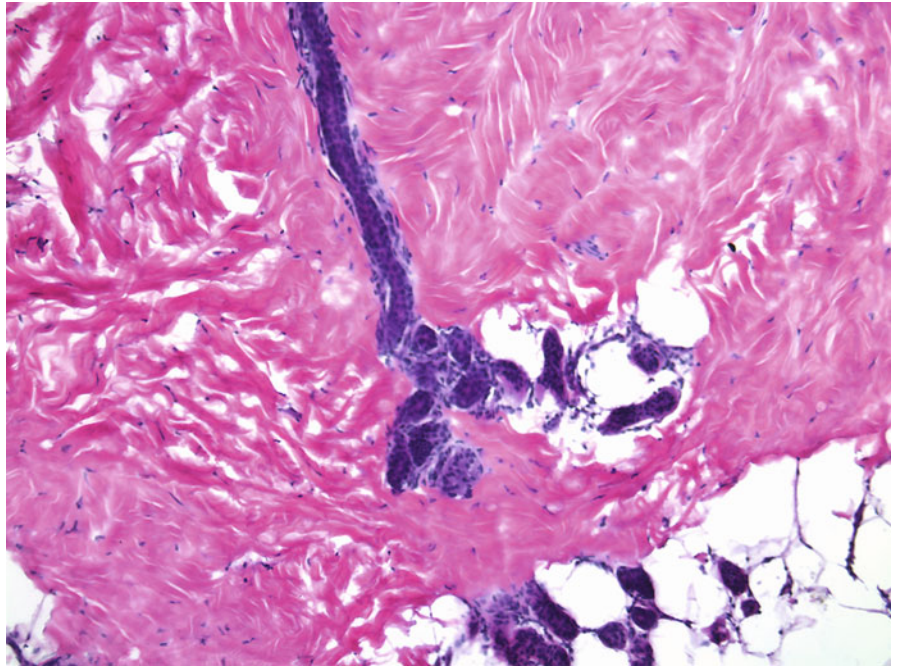
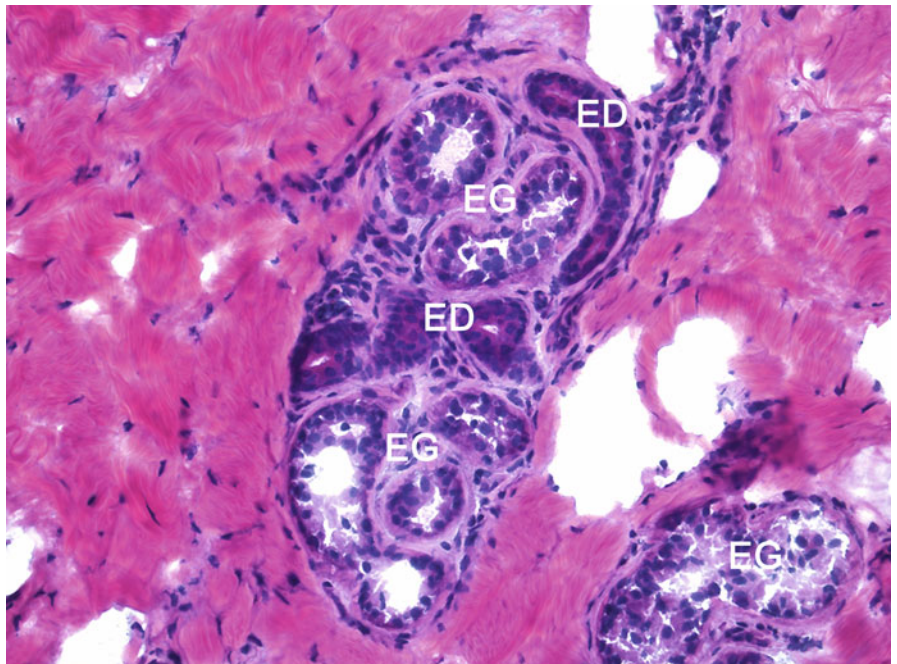


Fig. 2.27 A group of eccrine ducts (*ED*) with a lumen covered by a pink cuticle and eccrine glands (*EG*), which are lined by cuboidal cells and filled with pink secretion



Salivary Glands

Salivary glands are divided into numerous lobules each containing many secretory units. The glands consist basically

of ductal and acinar portions. Large excretory ducts have dilated lumina filled with secretions.

Fig. 2.28 A scanning magnification of a salivary gland comprised of lobules each containing secretory units and excretory ducts

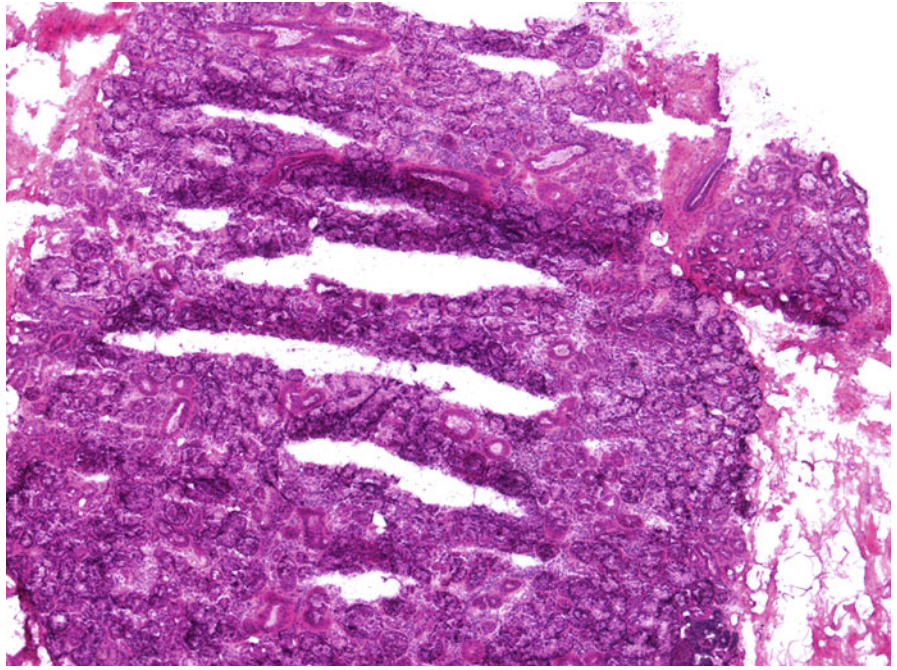


Fig. 2.29 The secretory units (*SU*) of the salivary glands are round and lined by cells that disintegrate to form holocrine secretions. The cell nuclei are positioned at the periphery of the glands. A thin rim of fibrous tissue (*arrow*) surrounds the entire glands. The salivary ducts (*SD*) are lined by two layers of cuboidal cells with eosinophilic cytoplasm. A thin layer of myoepithelial cells encircles the ducts. Pink amorphous secretions are seen in their patent lumina

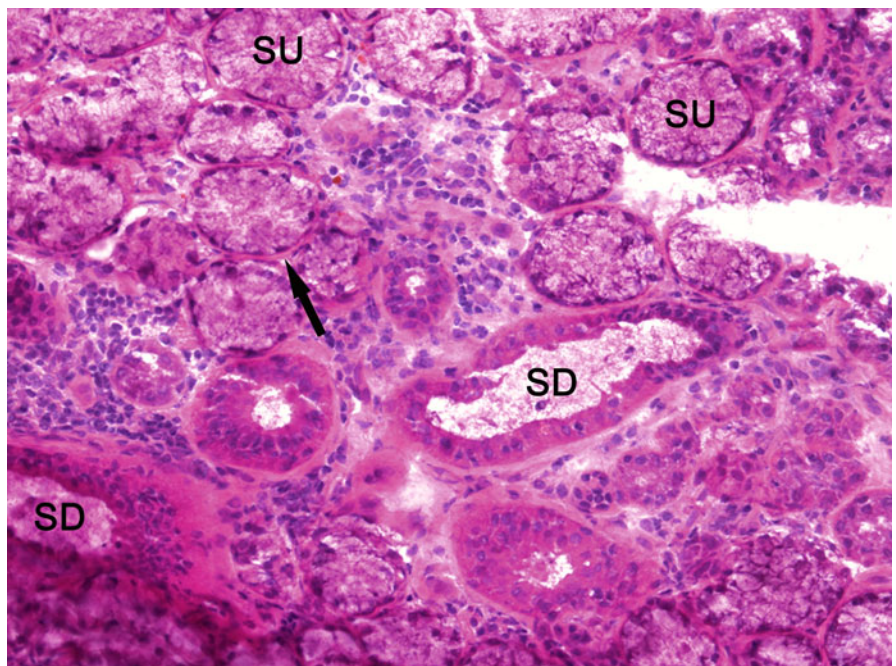


Fig. 2.30 Minor salivary gland: low power view of aggregates of a portion of minor salivary gland (*thin arrows*) deep in the subcutaneous tissue. Three large nerves in longitudinal sections are also seen (*thick arrows*)

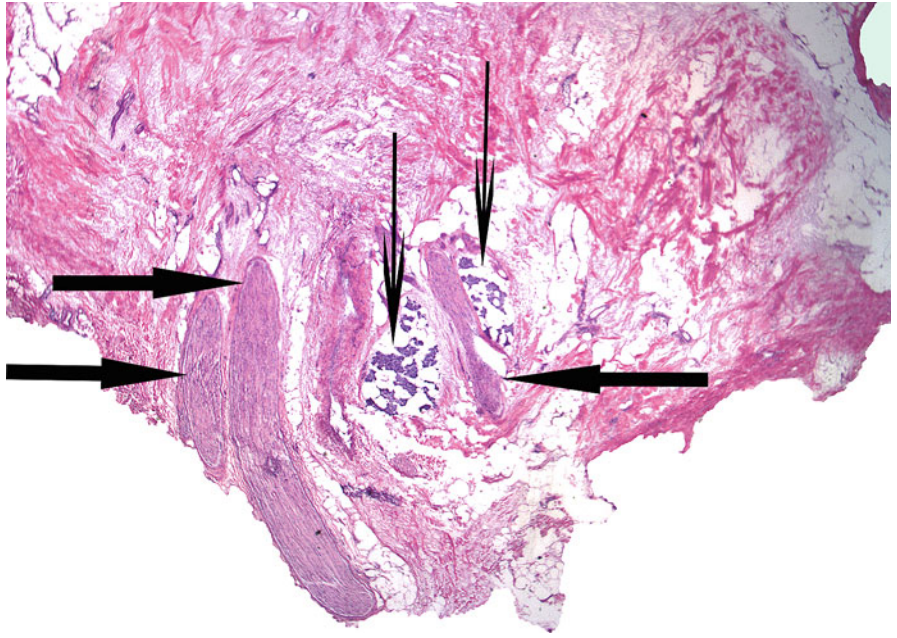


Fig. 2.31 Minor salivary gland: closer examination reveals that these are acini of a minor salivary gland with glandular structures organized in lobules with small lumina seen in the center of the acini

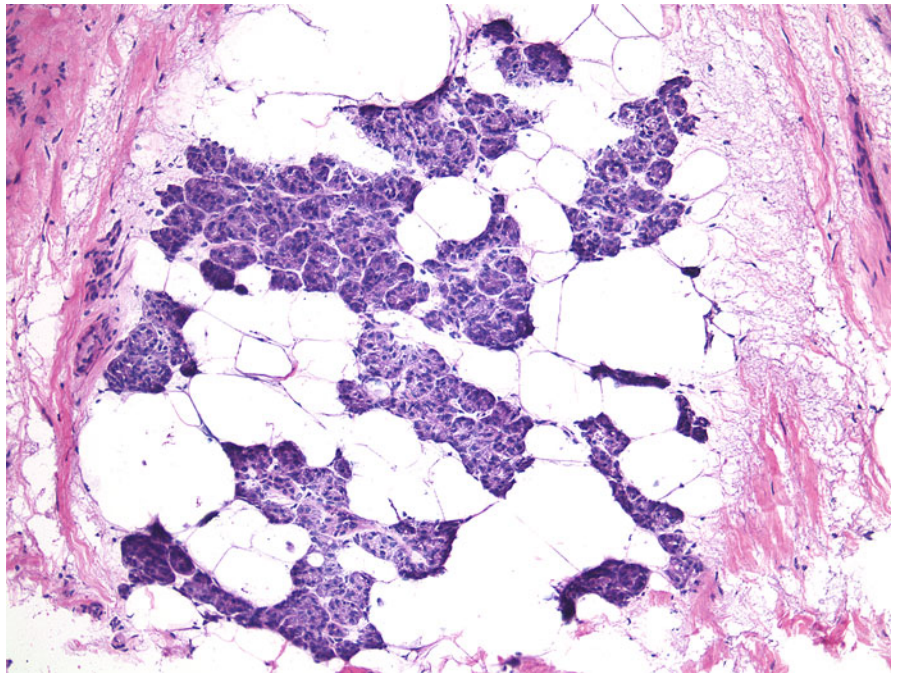


Fig. 2.32 Parotid gland: sheets of basophilic staining cells organized in clusters/groups

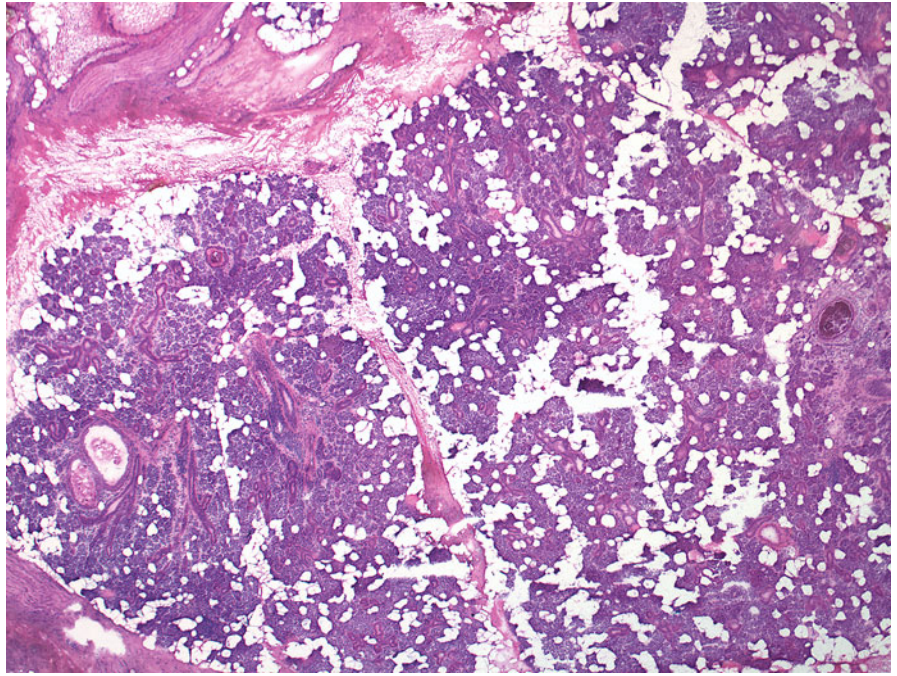
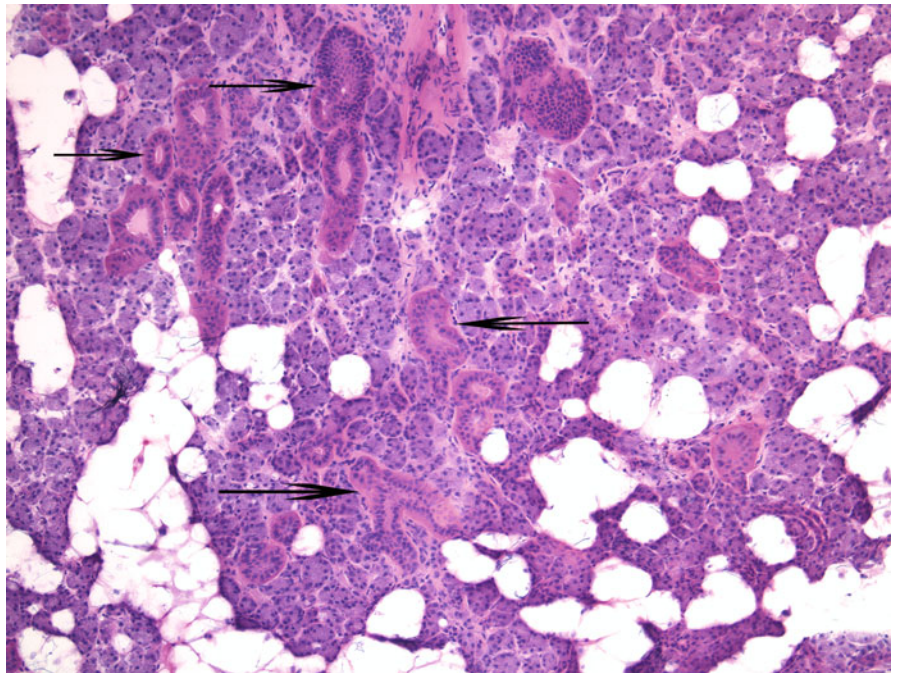


Fig. 2.33 Parotid gland: higher magnification reveals glands and ducts (arrows)



Apocrine Glands

Apocrine sweat glands are mainly confined to the axillae and the genital regions where they produce a viscid milky secretion. They can also be present on the forehead/scalp, areolae, as well as the periumbilical region. Apocrine glands are situated in the subcutaneous fat and their secretions are discharged into an adjacent hair follicle via a duct. Like eccrine glands, apocrine glands also consist of three segments: the intraepidermal duct, the intradermal duct, and the secretory portion. The secretory portion of

the gland is of the coiled, tubular type with widely dilated lumina. This portion of the apocrine glands consists of a single layer of cuboidal cells that have eosinophilic cytoplasm and are surrounded by a layer of myoepithelial cells. The snouting or budding of the apical portion of the cytoplasm is characteristic of the apocrine type of decapitation secretion. Like the eccrine duct, the apocrine duct is often lined by two layers of basophilic cuboidal cells with a periluminal eosinophilic cuticle, and an outer layer comprised of circumferentially arranged elongated myoepithelial cells.

Fig. 2.34 Apocrine glands: scanning magnification showing apocrine glands in the axilla

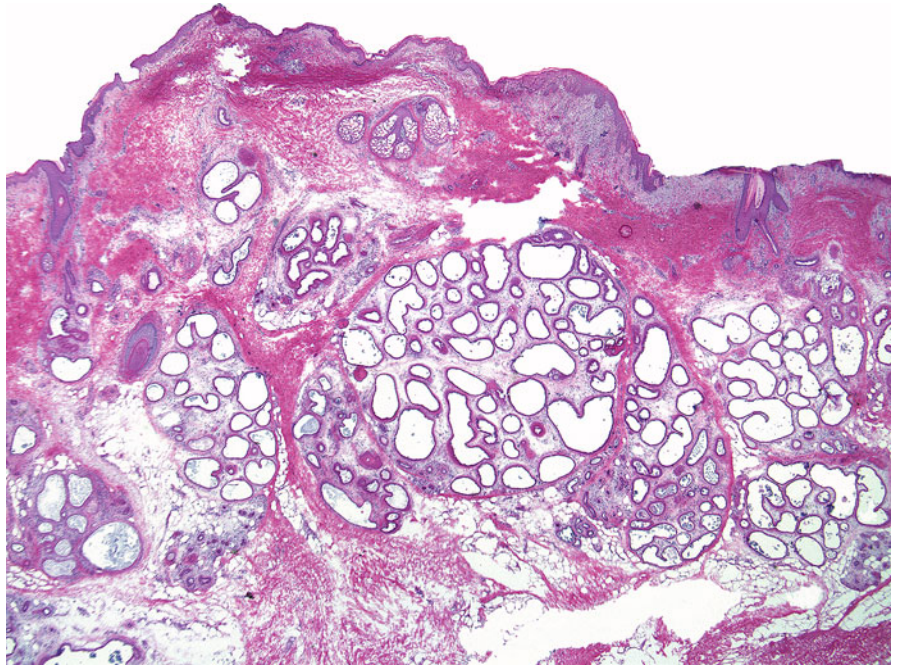
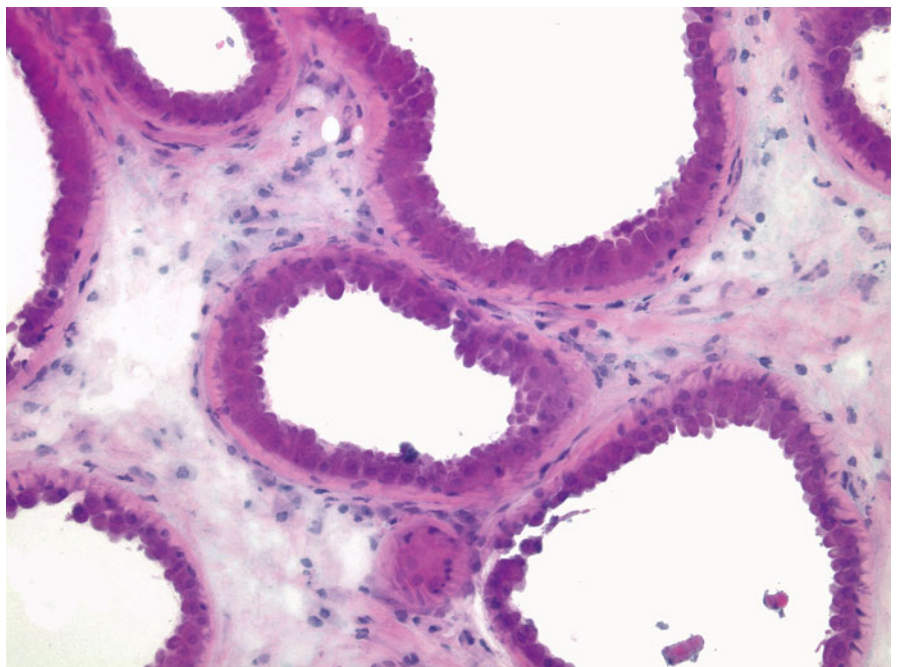


Fig. 2.35 Apocrine glands: widely dilated lumina of apocrine glands lined by two layers of cuboidal cells demonstrating decapitation secretions

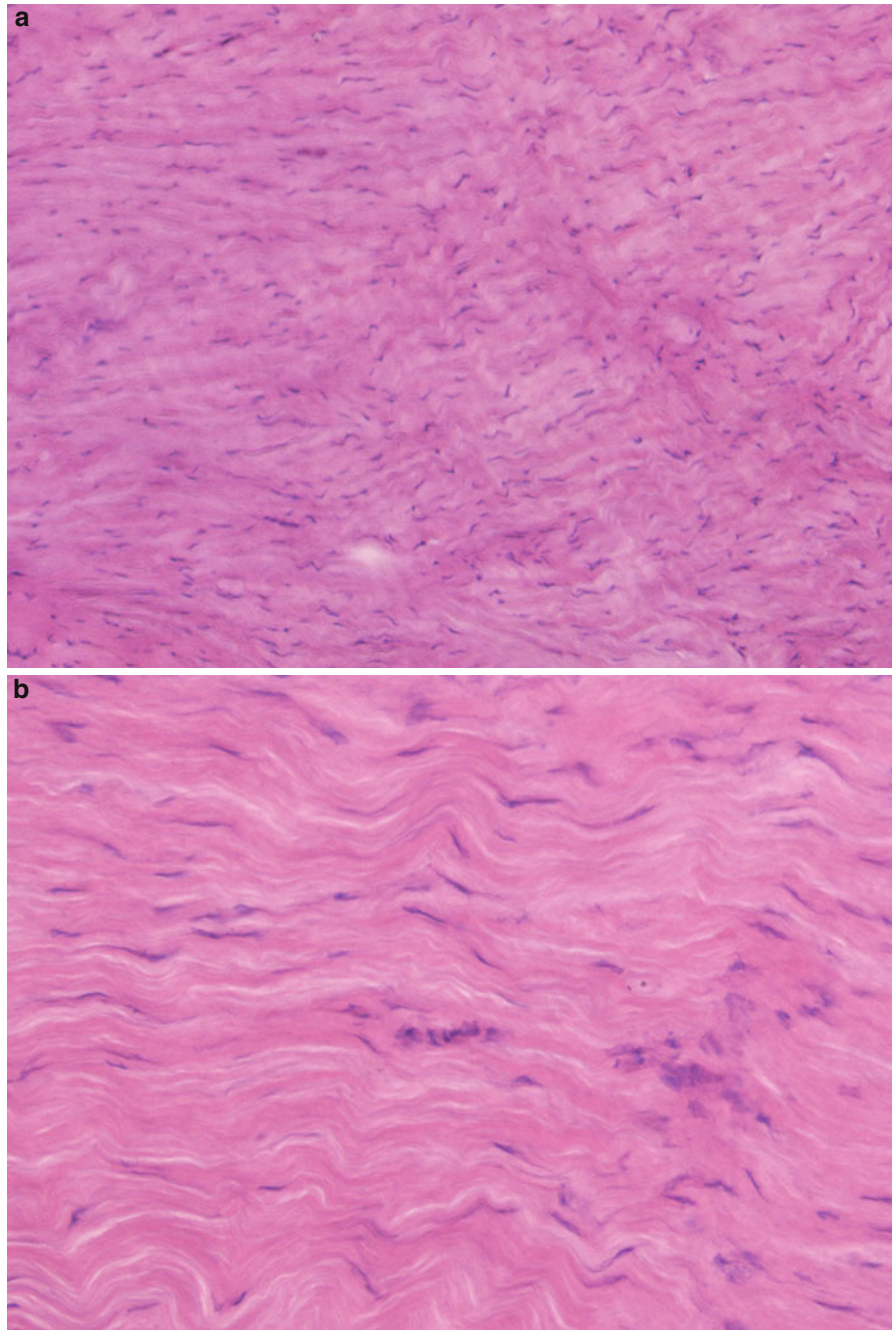


Periosteum

Periosteum is a layer of condensed fibrous tissue that covers the bone. It is comprised of cells arranged parallel to each

other that closely resemble fibroblasts with thin elongated nuclei embedded in dense eosinophilic fibrous stroma. The periosteum is richly supplied with blood vessels from adjacent connective tissue (Fig. 2.36).

Fig. 2.36 Periosteum: (a) Dense eosinophilic fibrous stroma with slender, wavy fibroblasts. (b) Higher magnification showing the compact nature of the eosinophilic stroma as well as the parallel arrangement of both the cells and the stroma



Scar Tissue

Immature (recent) scar tissue is composed of plump fibroblasts and slightly increased collagen bundles oriented parallel to the skin surface. There are vertically oriented,

newly formed blood vessels. As the scar matures, the fibroblasts become less discernable, slender, and fewer in number. The collagen fibers become more prevalent, thickened, and display horizontal orientation.

Fig. 2.37 Scar: a section taken from a recent biopsy, which shows significant scar tissue. There is epidermis on the left and a denuded area with immature scar underneath on the right

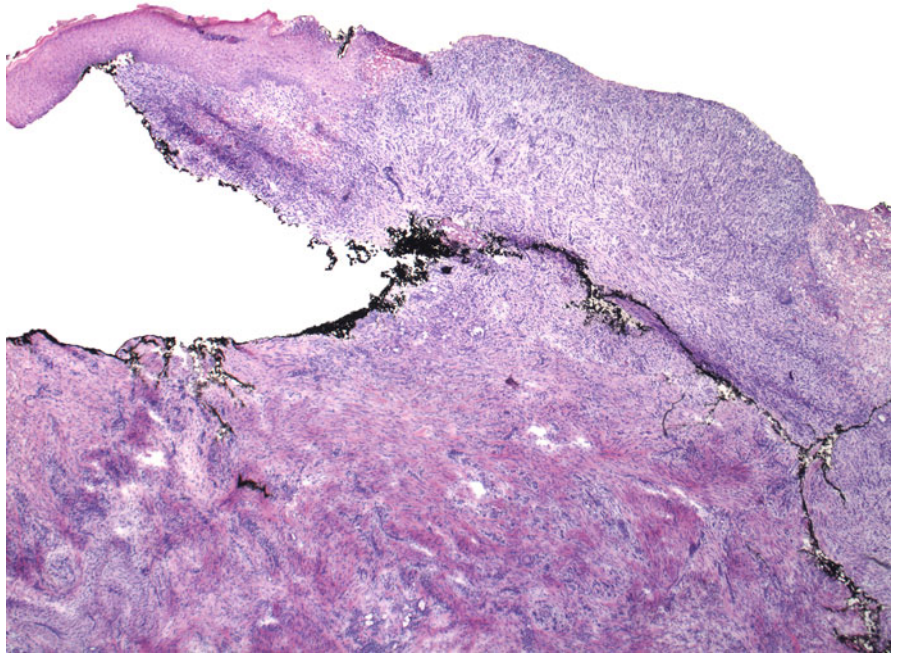


Fig. 2.38 Scar: a higher power view of immature scar tissue containing plump fibroblasts and numerous newly formed blood vessels lined by plump endothelial cells. Many vessels are aligned parallel to each other and perpendicular to the skin surface (*arrows*). Mild perivascular lymphocytic infiltrate is also seen. There is slight dermal edema

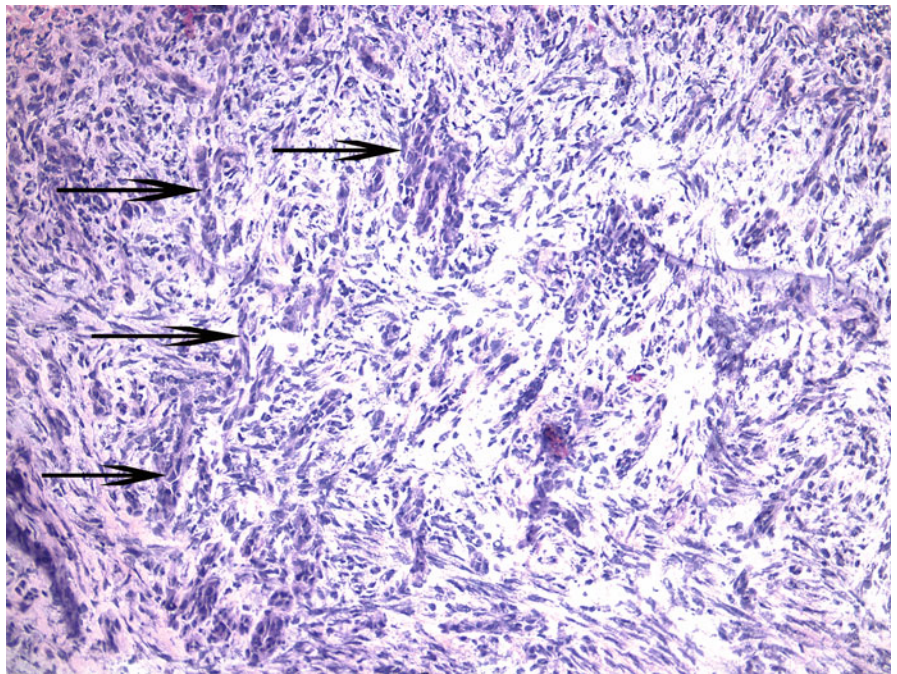
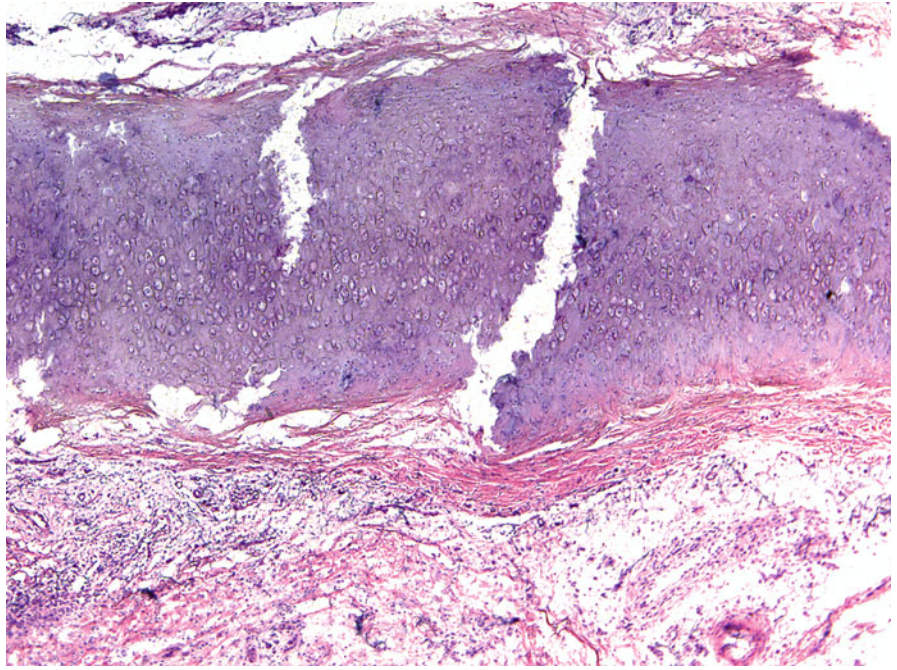


Fig. 2.39 Normal cartilage from the ear: cartilage is composed of chondrocytes positioned within lacunae



Basal cell carcinoma (BCC) shows the following histologic features:

- Neoplastic aggregates that vary in size and shape composed of basaloid cells
- Aggregates often arise from the undersurface of the epidermis or connect to adjacent hair follicles
- Peripheral palisading of nuclei within the tumor aggregates
- Retraction artifact between the aggregates and surrounding stroma
- Mucinous stroma surrounding the basaloid tumor aggregates
- Tumor cells have large, oval, or elongated nuclei and little cytoplasm
- Necrosis in the center of tumor aggregates and/or individual pyknotic/necrotic tumor cells
- Lack of striking cytologic atypia and mitoses
- Solar elastosis often in the surrounding dermis
- Tumor may have surrounding inflammatory infiltrate
- Calcifications may be present in long-standing lesions
- Within one BCC more than one histologic subtypes may be seen

Histologic types of basal cell carcinoma:

Superficial BCC

- Small buds of basaloid cells extending from the epidermis and hair follicle epithelium into the superficial dermis

Nodular BCC

- Basaloid aggregates of different shape and size in the dermis
 - (a) Macronodular subtype – large aggregates of basaloid cells
 - (b) Micronodular subtype – small aggregates of basaloid cells

Infiltrative BCC (also see Chap. 4)

- Angulated tumor aggregates and small strands and cords of basaloid cells infiltrating between normal structures in the dermis

Keratinizing BCC

- Basal cell carcinoma with areas of squamatization with large eosinophilic keratinocytes and keratin pearl formation

Infundibulocystic BCC

- Well circumscribed with numerous infundibular cysts filled with keratin and branching anastomosing basaloid aggregates

Pigmented BCC

- Basal cell carcinoma usually of nodular type with foci of prominent melanin pigment

Fibroepithelioma of Pinkus type of BCC

- Thin anastomosing strands of basaloid cells attached to the epidermis and embedded in loose stroma

BCC with sebaceous differentiation

- BCC with foci containing sebocytes and sebaceous duct-like structures

BCC arising from hair follicles

- Basaloid aggregates arising from different segments of the hair follicle
- Basaloid budding from the undersurface of the epidermis

Adenoid BCC

- Neoplastic cells are arranged in intertwining strands in a lace-like pattern suggesting tubular, gland-like structures.

Fig. 3.1 Superficial basal cell carcinoma: neoplastic aggregates emanating from the undersurface of the epidermis. Peripheral palisading and clefting is noted

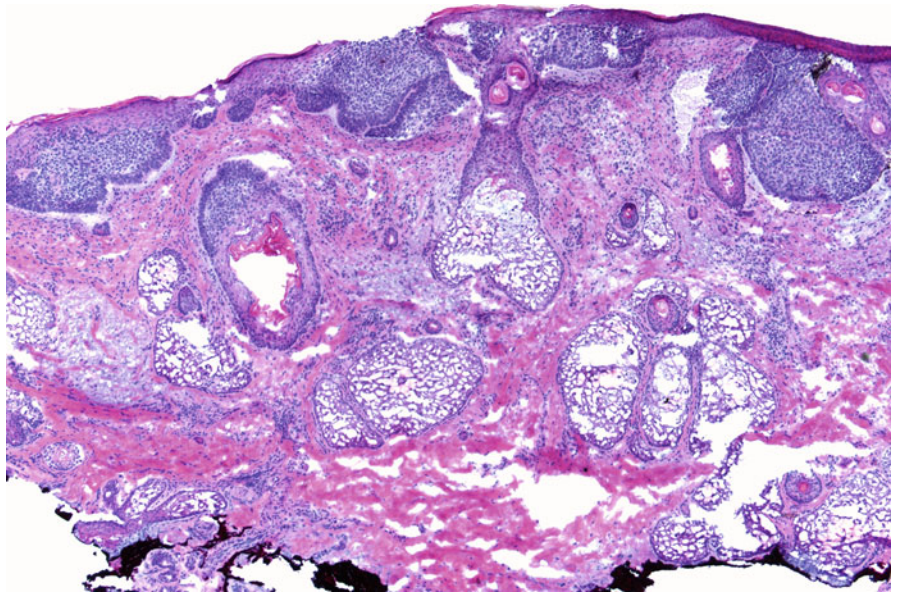


Fig. 3.2 Nodular and infiltrative basal cell carcinoma: irregular basaloid aggregates present throughout the dermis. These neoplastic aggregates are nodular and larger in the more superficial portion of the dermis and become more infiltrative as well as diminish in size with their descent into the dermis

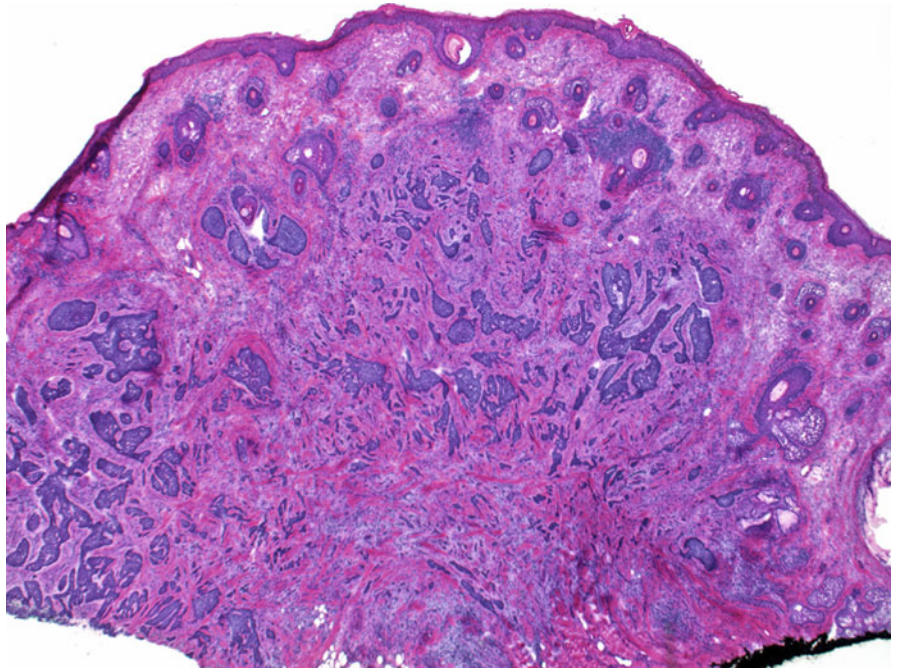


Fig. 3.3 Nodular and infiltrative basal cell carcinoma: infiltrative BCC with larger tumor aggregates near the epidermis that become smaller and angulated deeper in the dermis. Cords, strands, and individual neoplastic basaloid cells are seen at the bottom of the photograph

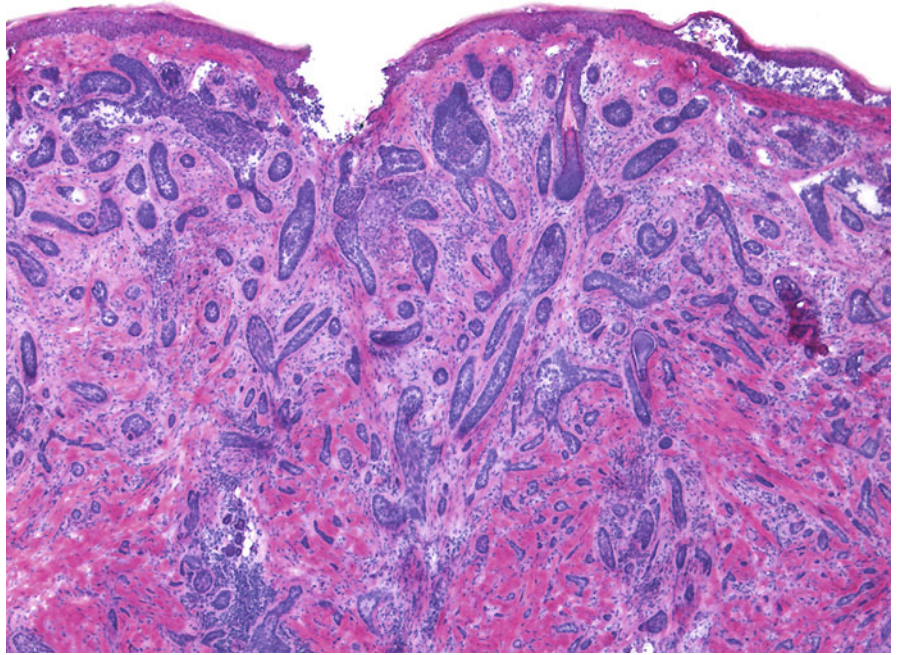


Fig. 3.4 Infundibulocystic basal cell carcinoma: cystically dilated follicular infundibula surrounded by branching basaloid aggregates. These aggregates also diminish as the tumor penetrates deeper in the dermis

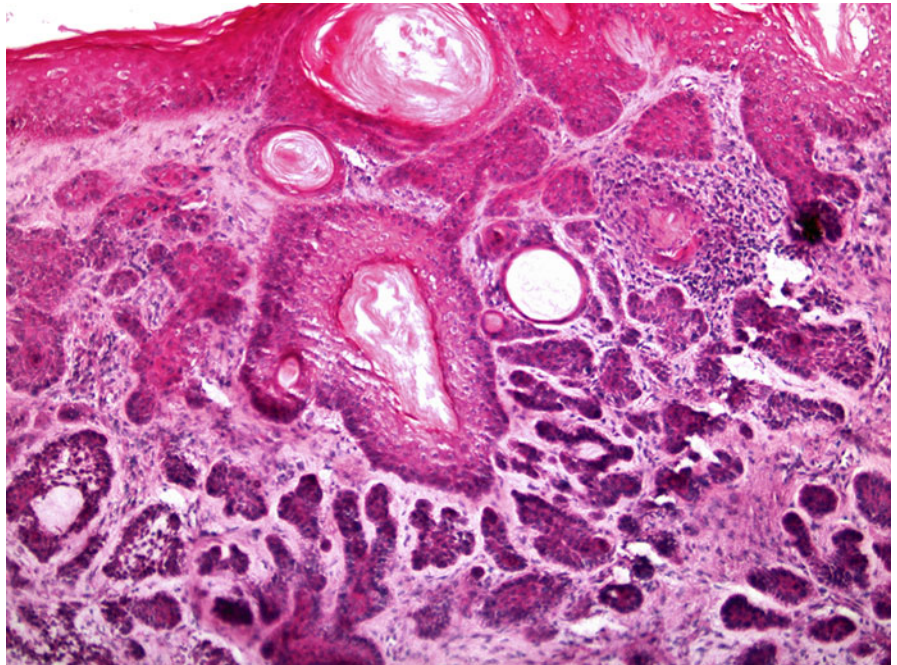


Fig. 3.5 Micronodular basal cell carcinoma: small, nodular, irregular aggregates of basaloid neoplastic cells surrounded by cellular myxoid stroma. Focal clefting is appreciated between the neoplastic aggregates and the stroma

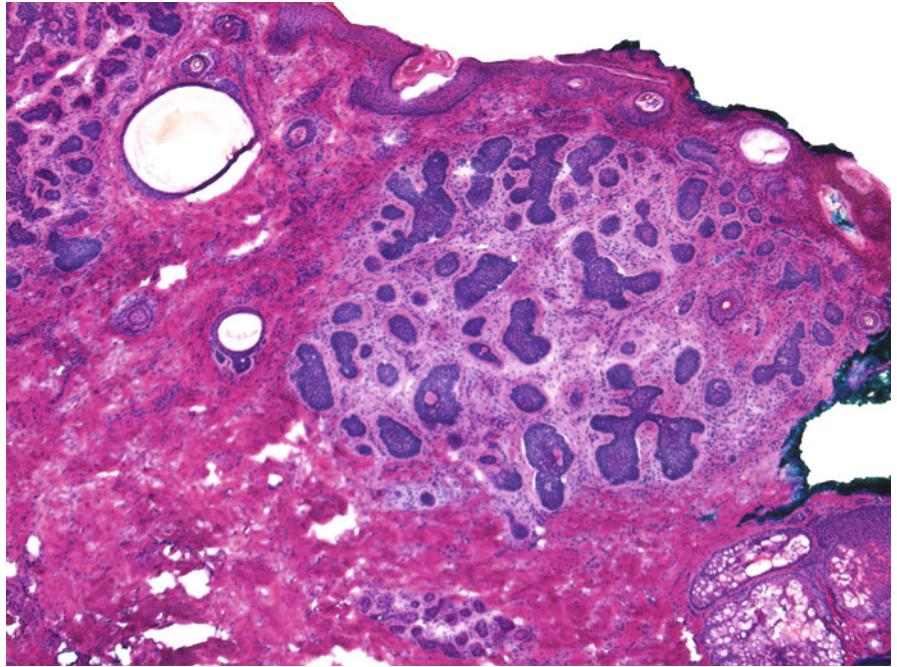


Fig. 3.6 Superficial basal cell carcinoma: superficial basal cell carcinoma originating from the surface epidermis as well as from the infundibular portion of the hair follicle

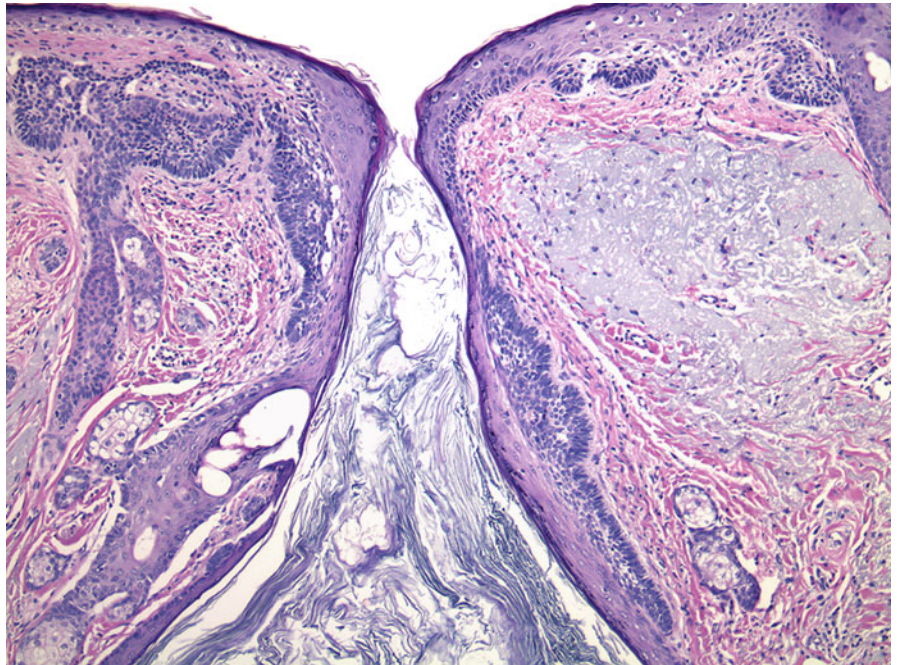


Fig. 3.7 Keratinizing basal cell carcinoma:
(a) At this magnification there are a few irregular basaloid aggregates in the superficial dermis, some showing angulated shapes. Within the center of a large aggregate is a keratin pearl (*arrow*).
(b) Higher magnification of the keratinizing BCC. At this power the neoplastic aggregates (*arrows*) are more obvious displaying peripheral palisading within the surrounding mucinous stroma

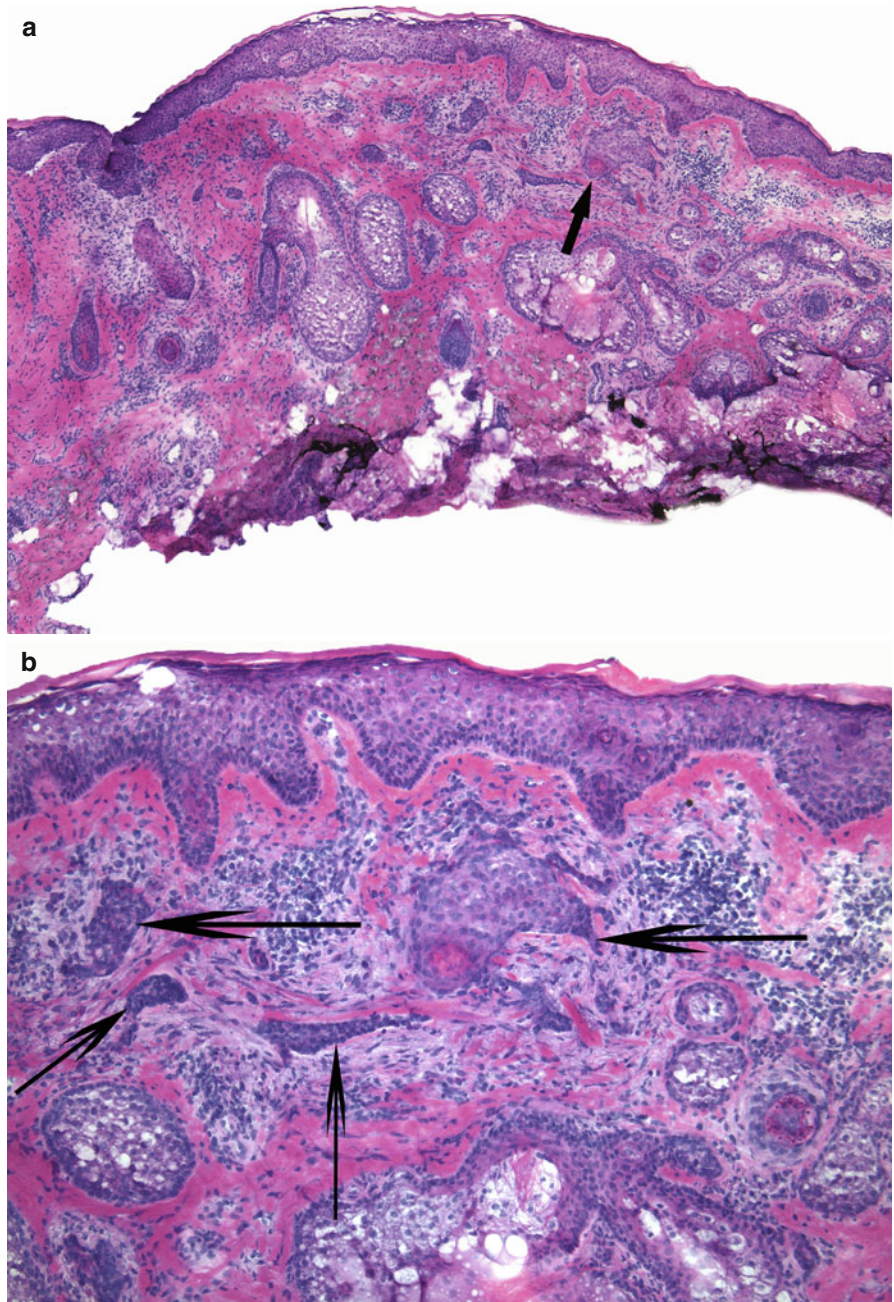


Fig. 3.8 Keratinizing basal cell carcinoma: (a) Aggregates of basal cell carcinoma demonstrating focal areas of keratinization in the center. (b) Some of the neoplastic cells in the center of these basaloid aggregates show squamoid features – i.e., they are larger, ovoid in shape, and with more abundant eosinophilic cytoplasm (*arrow*)

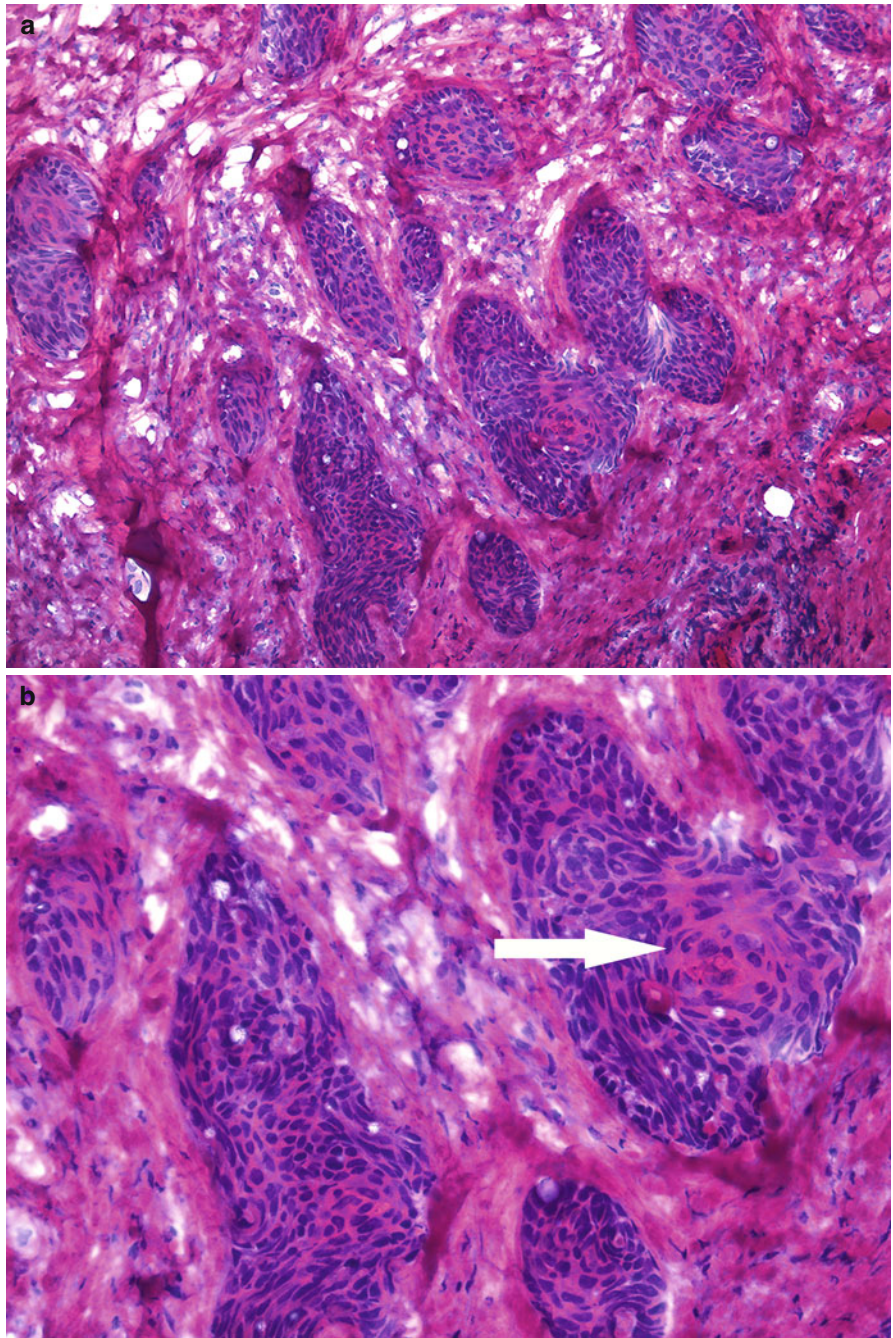


Fig. 3.9 Basal cell carcinoma: (a) Basal cell carcinoma with large areas of necrosis in the center of the aggregates (*arrows*). (b) Basal cell carcinoma with neoplastic cells that demonstrate a reticulated pattern

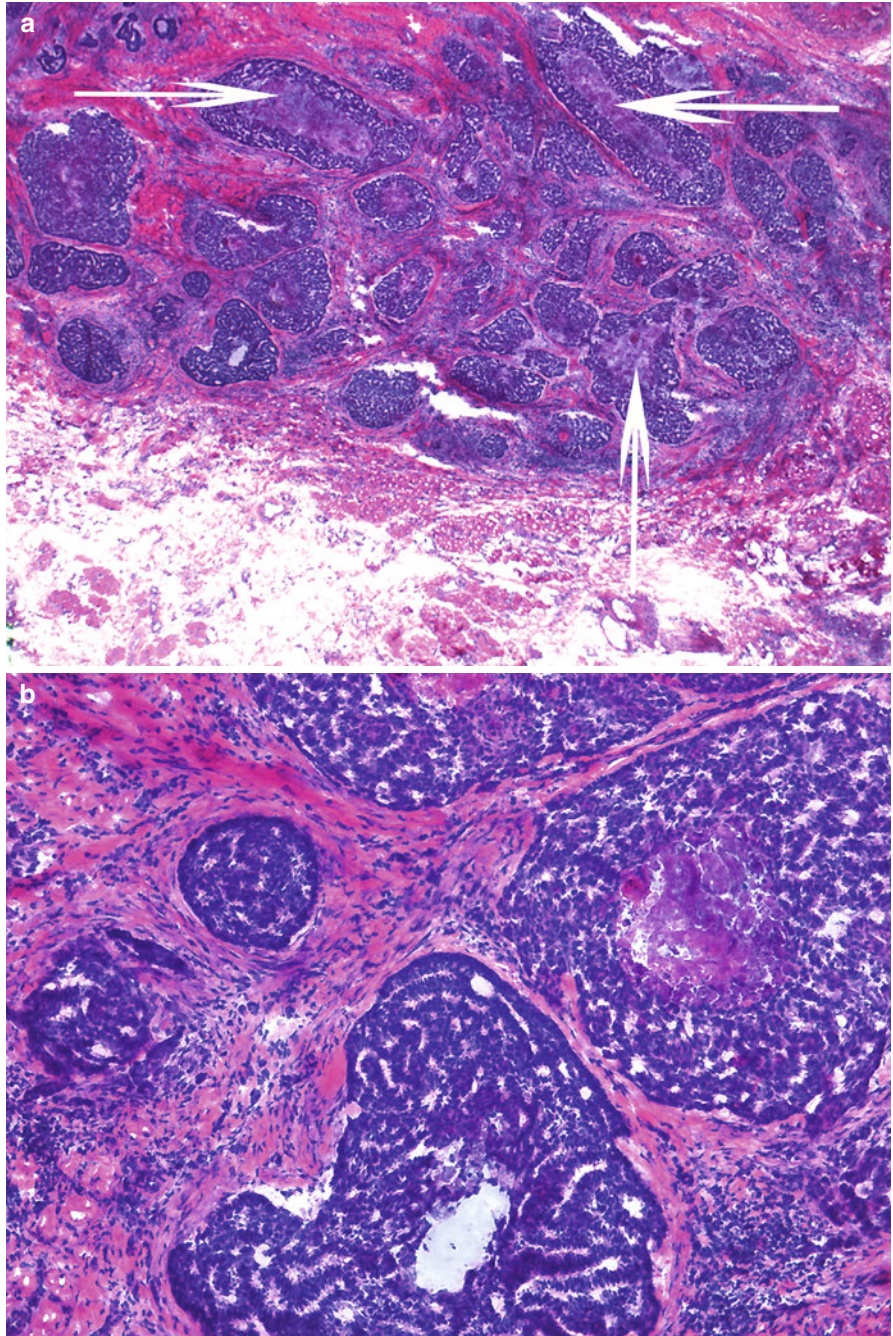


Fig. 3.10 Basal cell carcinoma: (a–c)
This example illustrates that the diagnosis of BCC is most easily made by evaluating the overall growth pattern and architecture of the tumor. Higher magnifications sometimes might be misleading and, as in this case, might lead the surgeon into making an erroneous diagnosis of Merkel cell carcinoma based on cytologic features alone

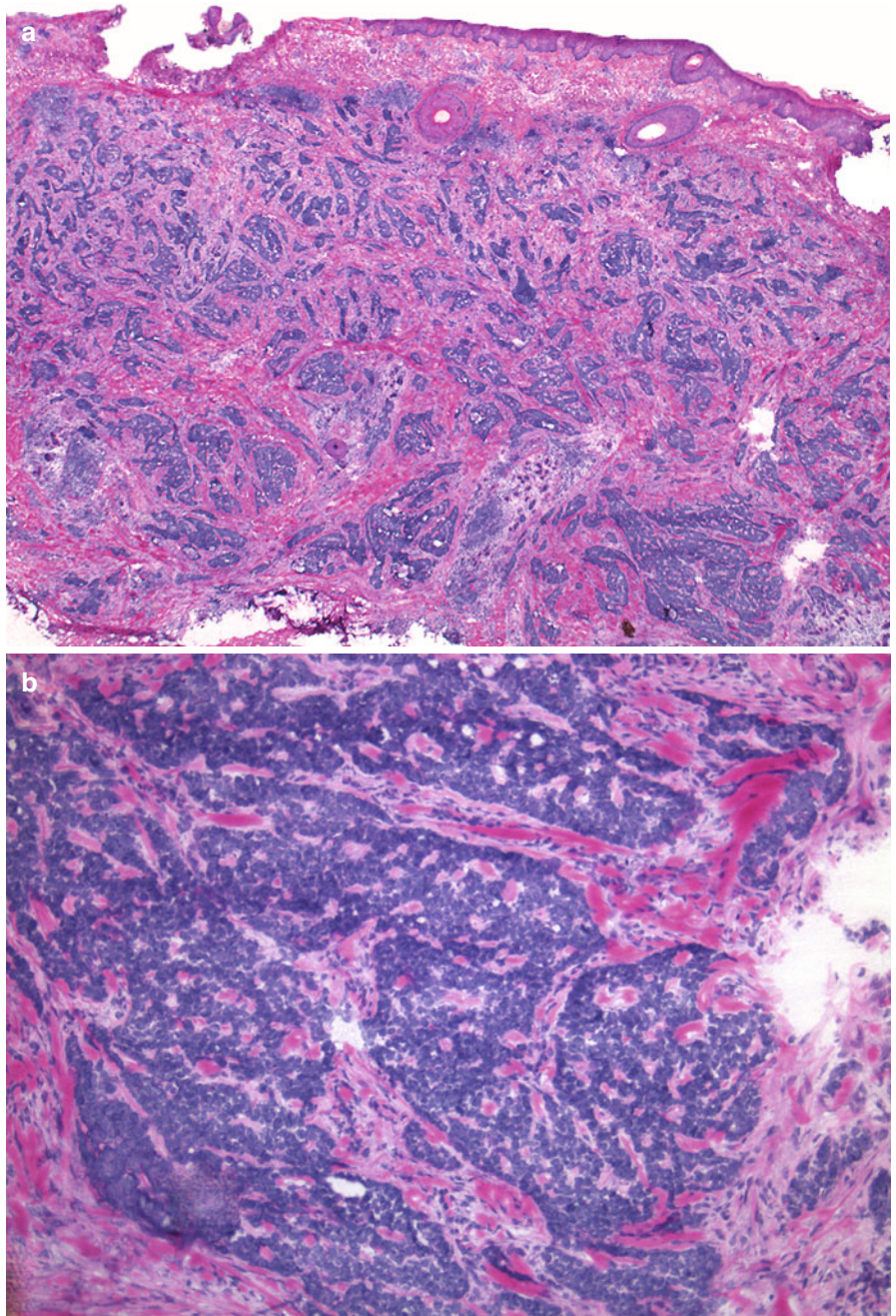


Fig. 3.10 (*continued*)

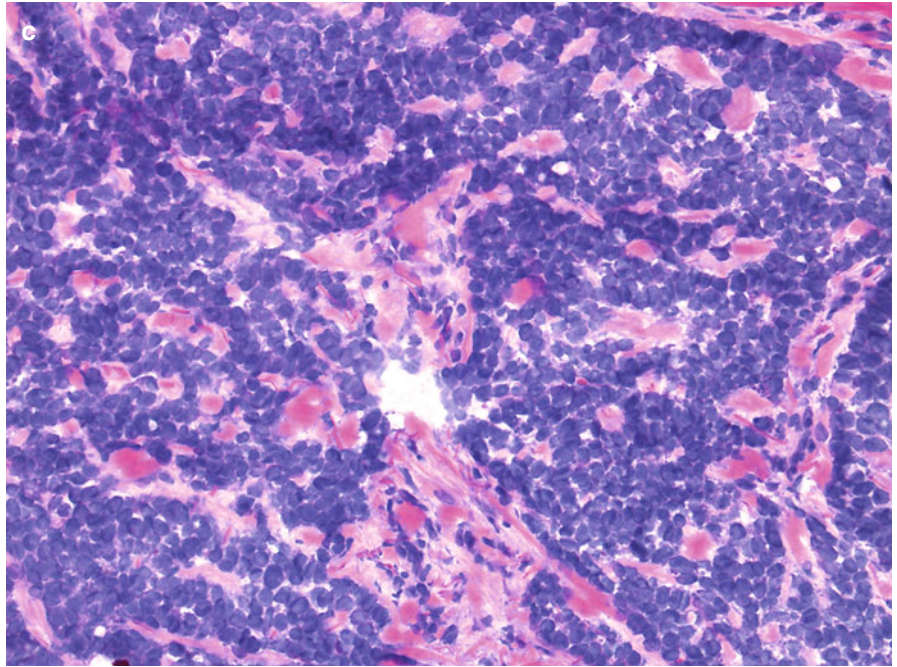


Fig. 3.11 Basal cell carcinoma: (a) This subtle basal cell carcinoma (*arrow*) is hidden among sebaceous glands and hair follicles. It can be easily overlooked because of its resemblance to a distorted hair follicle. A hair follicle at this level in the dermis would display organized and complex morphology as present in the surrounding folliculosebaceous units. (b) On higher magnification the presence of pyknotic nuclei, clefting, and pale surrounding stroma of these aggregates all support the diagnosis of basal cell carcinoma

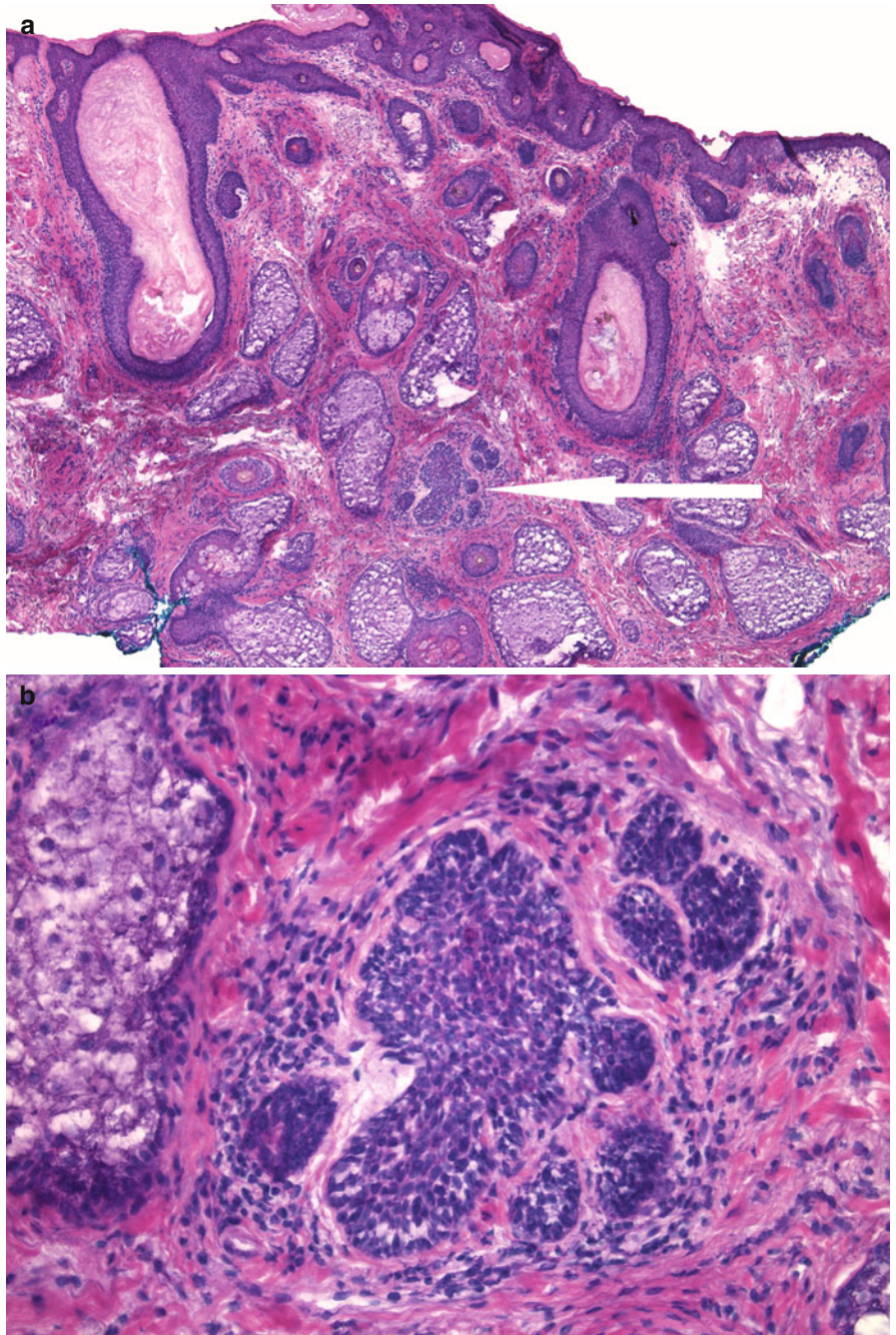


Fig. 3.12 Nodular basal cell carcinoma:

(a) Section of an eyelid showing both the cutaneous surface on top and the conjunctiva in the lower inked portion. Nodular basal cell carcinoma is present throughout the specimen. (b) At this magnification both the mucosa as well as the skin surface are appreciated. The skin is present superiorly in this photomicrograph transitioning into the lower portion where it becomes the conjunctiva. The mucosa lacks the stratum corneum and there is a lichenoid inflammatory infiltrate, which is commonly seen on conjunctival surfaces. (c) Transitional zone between skin on the left and conjunctival mucosa, containing Goblet cells (*arrows*) on the right. Conjunctival epithelium often has a disordered appearance

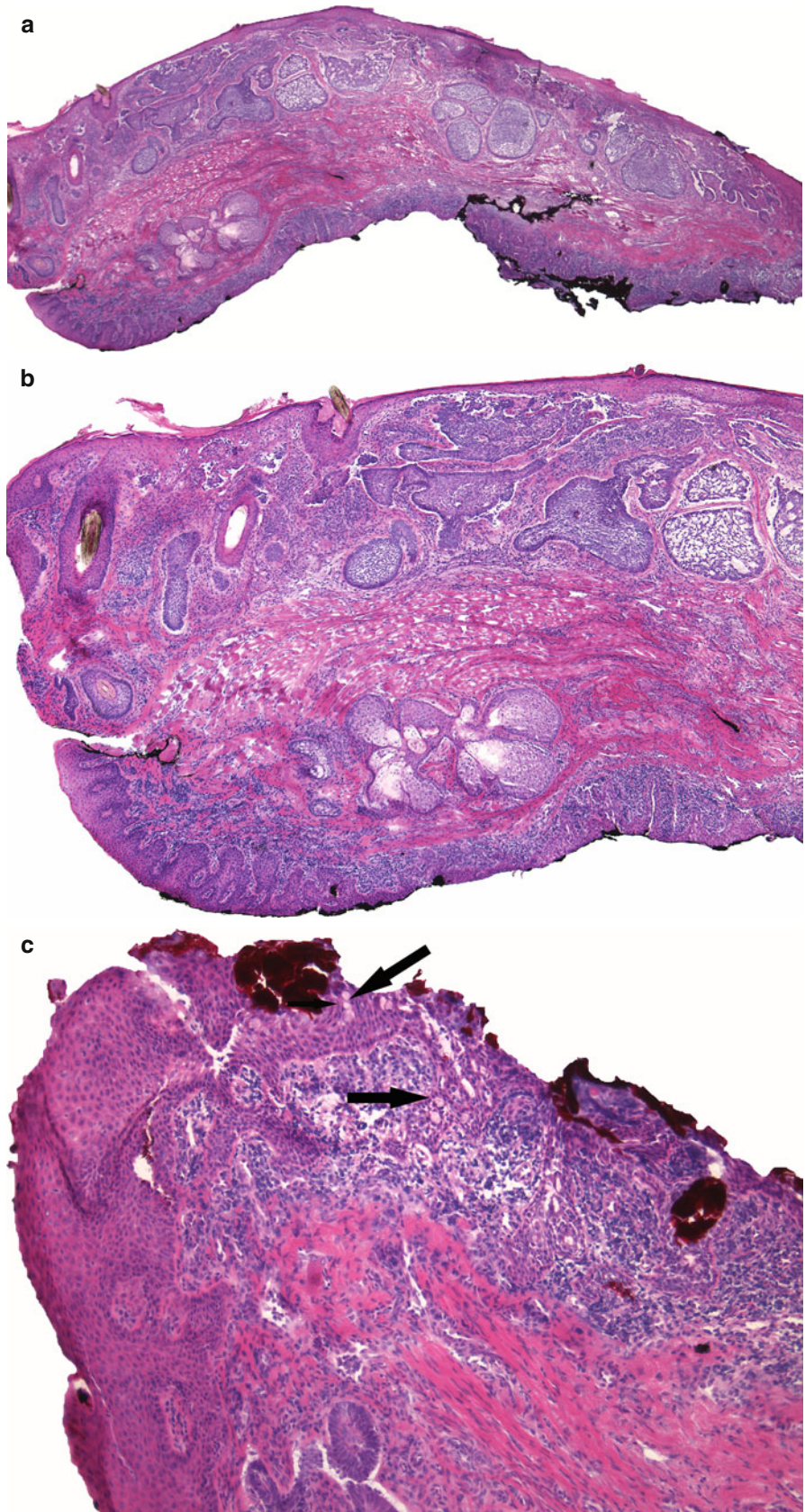


Fig. 3.13 Basal cell carcinoma: (a) Rare small islands of basal cell carcinoma are seen on the left of this photomicrograph. A few other neoplastic aggregates are present within areas of dense inflammation (arrows). The tumor is rather subtle. (b) At this high power the cohesiveness of the neoplastic cells forming small aggregates (arrows) is easily contrasted with the random, scattered appearance of the inflammatory cells

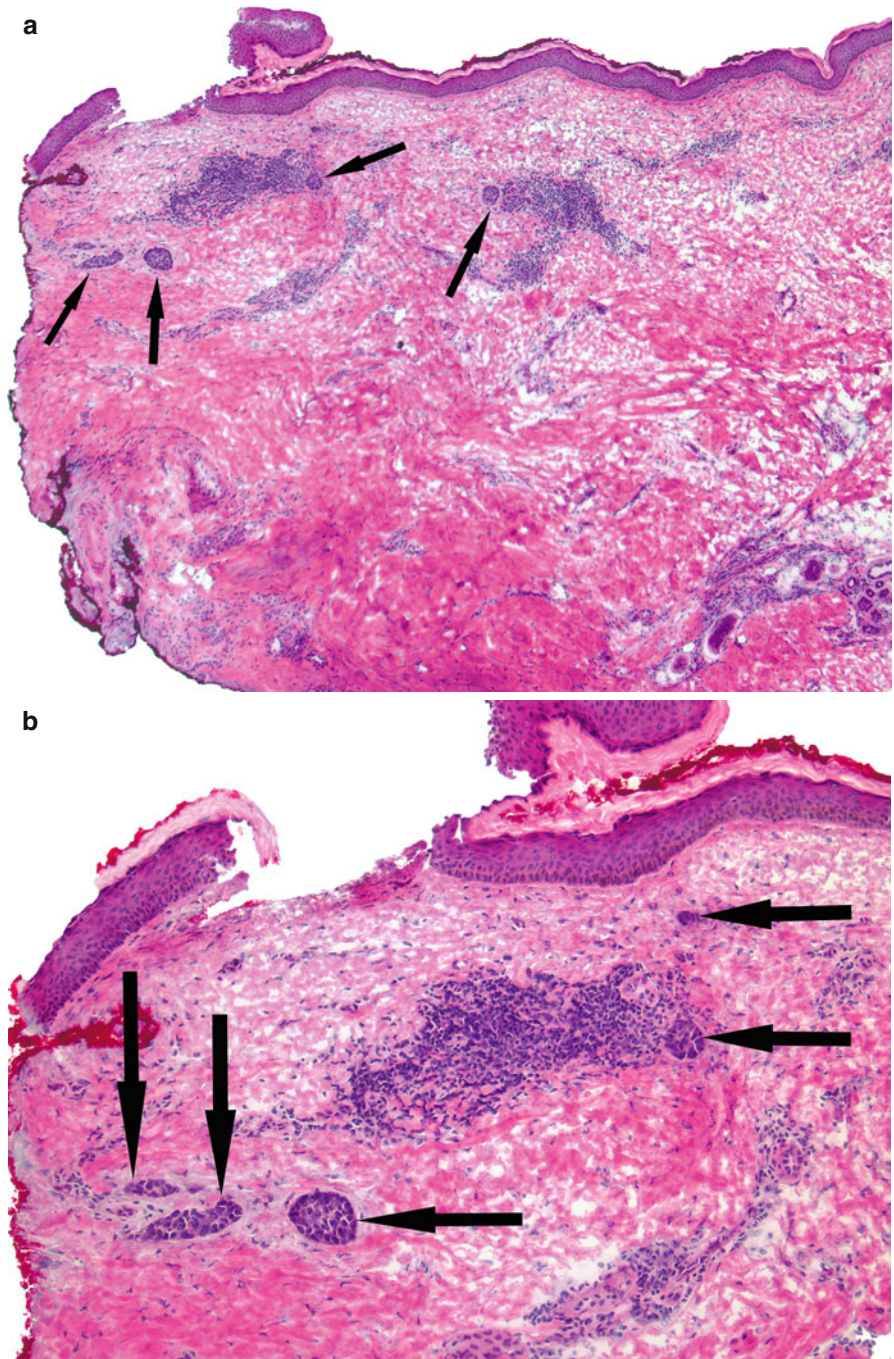


Fig. 3.14 Basal cell carcinoma:
(a) Scanning magnification shows a lobulated aggregate (*arrow*) mimicking an epithelial structure. It is difficult to make a diagnosis of basal cell carcinoma on this section at this power. (b) Upon closer examination, notable features such as focal palisading, nuclear pleomorphism, and focally hyperchromatic cells favor the diagnosis of basal cell carcinoma. There is also a narrow area of clefting between the aggregate and the surrounding stroma on the right. (c) Formalin-fixed permanent section of the original biopsy shows typical superficial basal cell carcinoma. An epithelioid appearing nodule that was similar to the one seen in the Mohs frozen section is seen to the left of the photomicrograph. This case illustrates the utility of reviewing the original biopsies of tumors prior to Mohs surgery

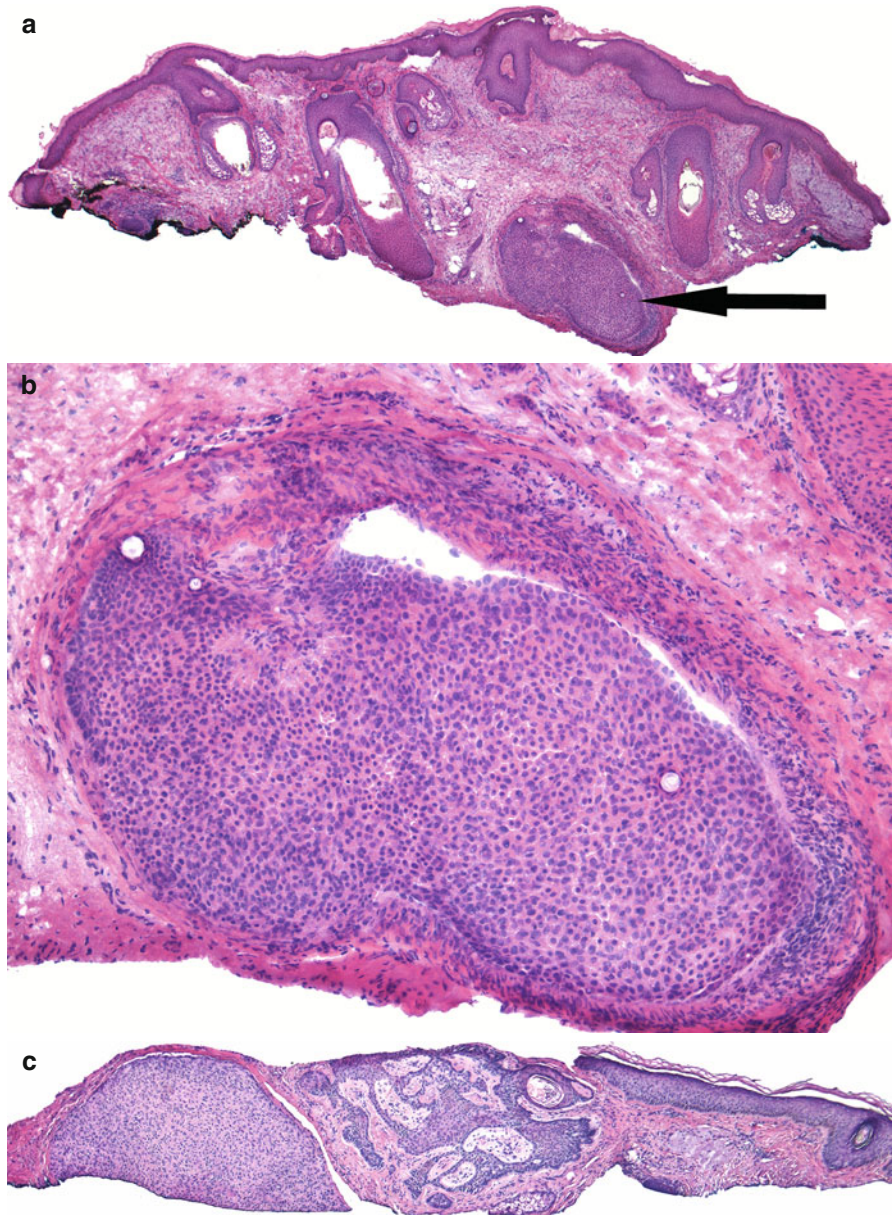


Fig. 3.15 Basal cell carcinoma:
(a) Scanning magnification shows focal areas of dense inflammation in the superficial and mid dermis on the left side of this photomicrograph. *Arrows* point to two small neoplastic aggregates that can be easily missed via a cursory examination of the specimen. (b) Neoplastic aggregates are more obvious on higher magnification (*arrows*)

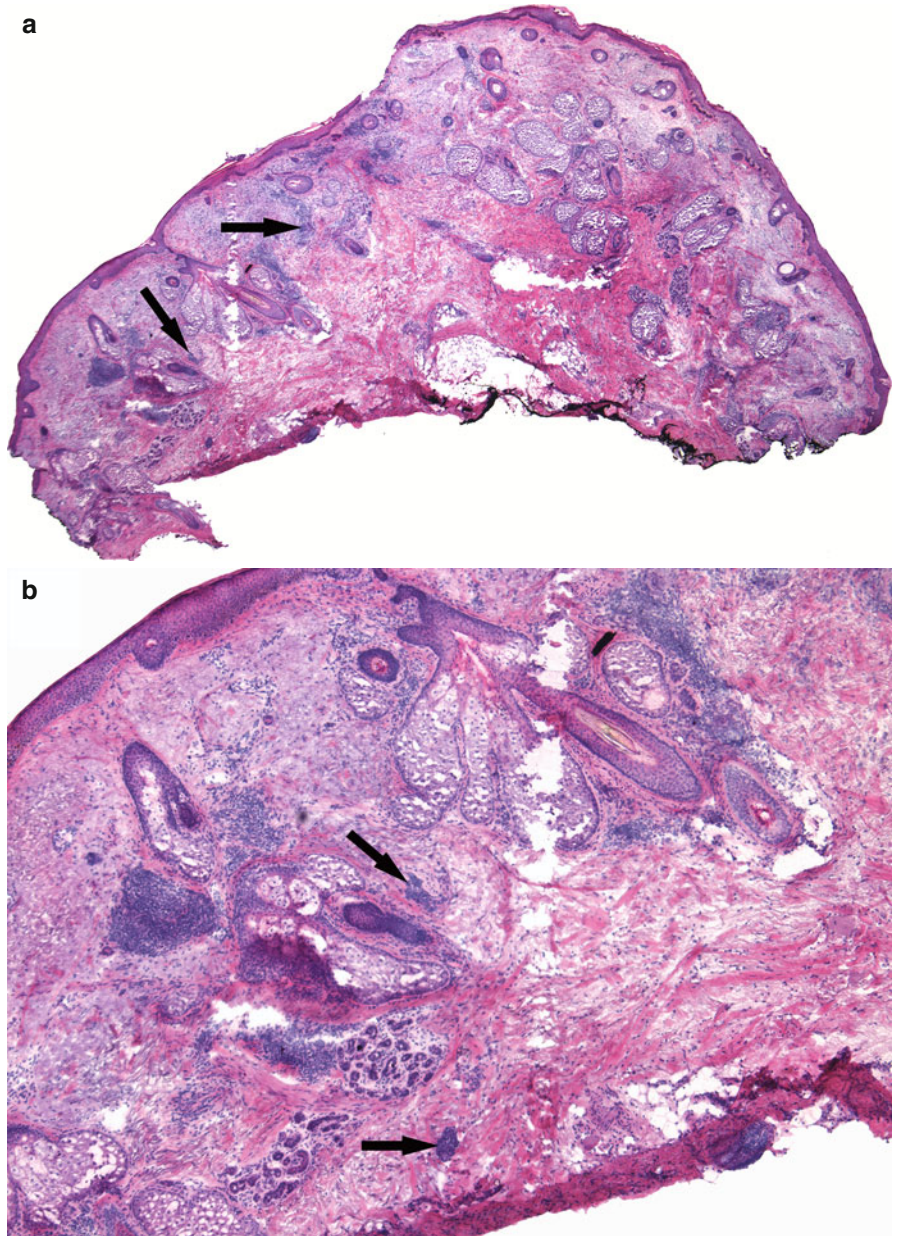


Fig. 3.15 (continued) (c) Further sectioning into this specimen shows additional basaloid aggregates consistent with basal cell carcinoma present in the areas of dense inflammation (arrow). This demonstrates that inflammation can also be a clue to the presence of nearby tumor. (d) Higher magnification revealing several aggregates of tumor (arrows) surrounded by inflammation

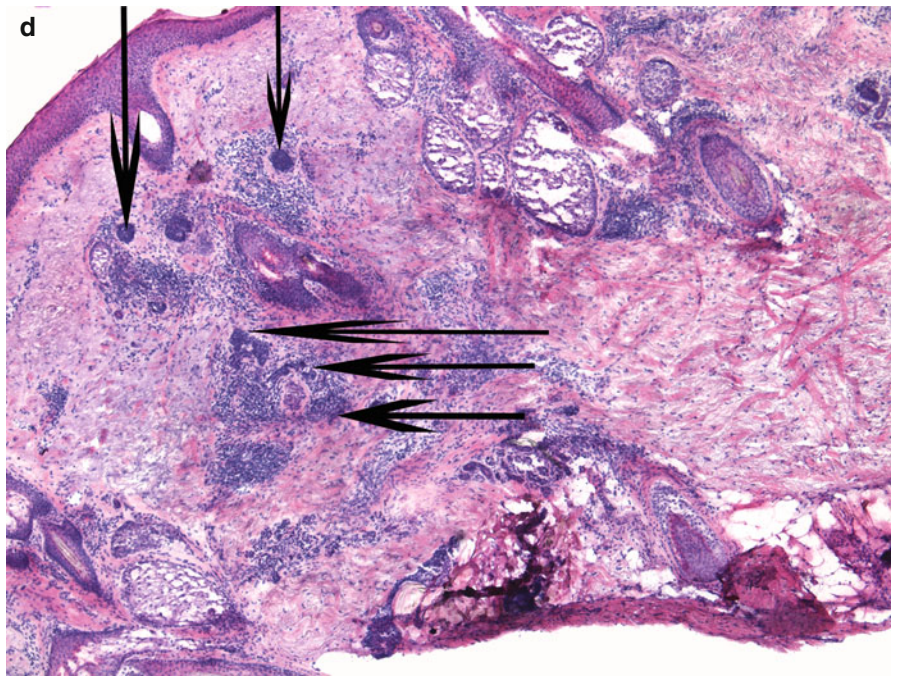
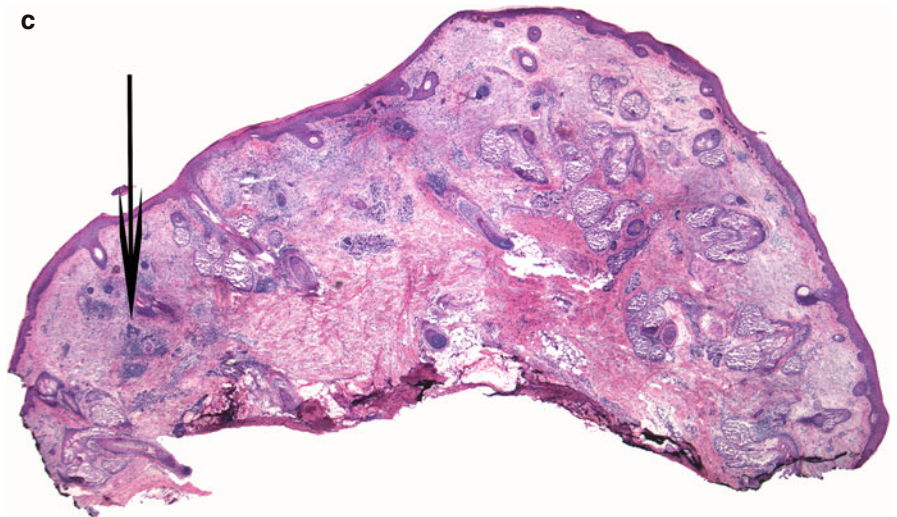


Fig. 3.16 Micronodular basal cell carcinoma: characteristically BCC of this subtype demonstrates a diminution in size of the tumor aggregates as they descend deeper into the tissue

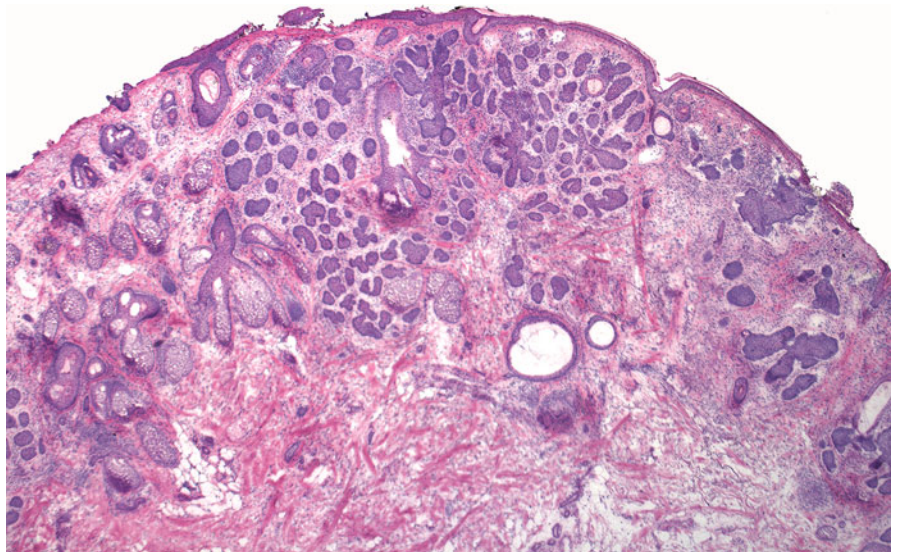


Fig. 3.17 Adenoid basal cell carcinoma: (a) Neoplastic cells are arranged in intertwining strands in a lace-like pattern suggesting tubular, gland-like structures (arrows). (b) Higher magnification

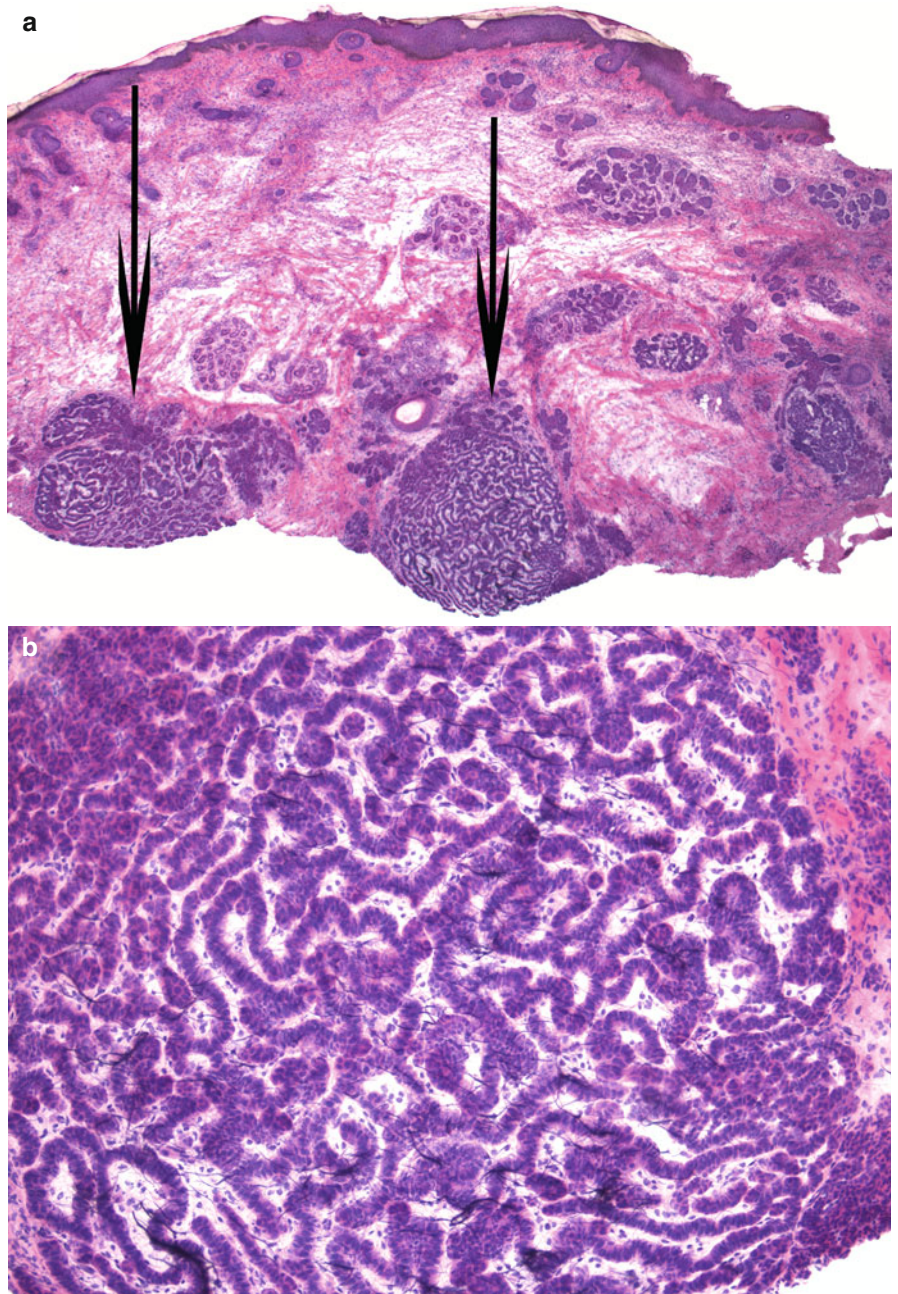


Fig. 3.18 Adenoid basal cell carcinoma: (a) At scanning magnification, the neoplastic aggregates look very similar to eccrine structures (*arrows*). (b) Compare the neoplastic aggregates (*thin arrows*) to the eccrine glands (*thick arrows*)

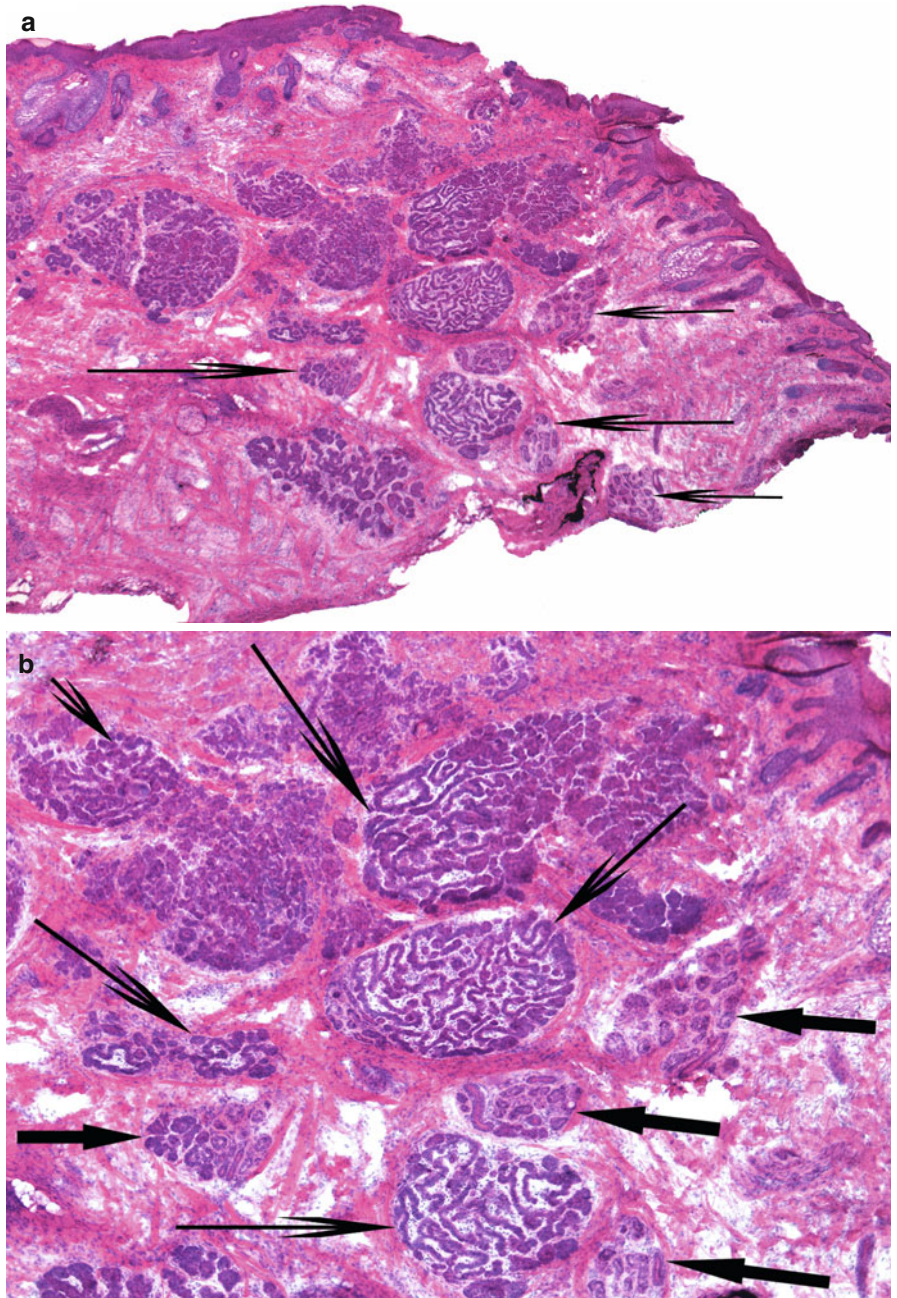


Fig. 3.18 (*continued*) (c) In the central portion of this photomicrograph is an area showing eccrine glands and ducts on the right (*rectangle*) and aggregates of basal cell carcinoma on the left (*ellipse*) and superiorly. Tumor aggregates have irregular and varying shapes and consist of hyperchromatic crowded cells

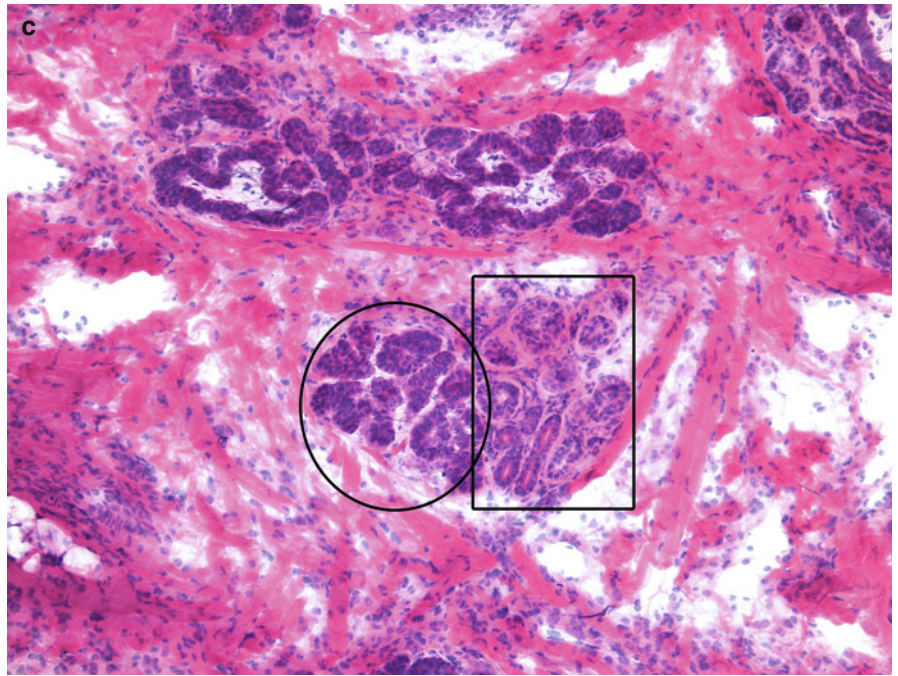


Fig. 3.19 Superficial basal cell carcinoma: (a, b) Low and medium power. Classic features such as basaloid aggregates emanating from the epidermis, peripheral palisading and clefting are present

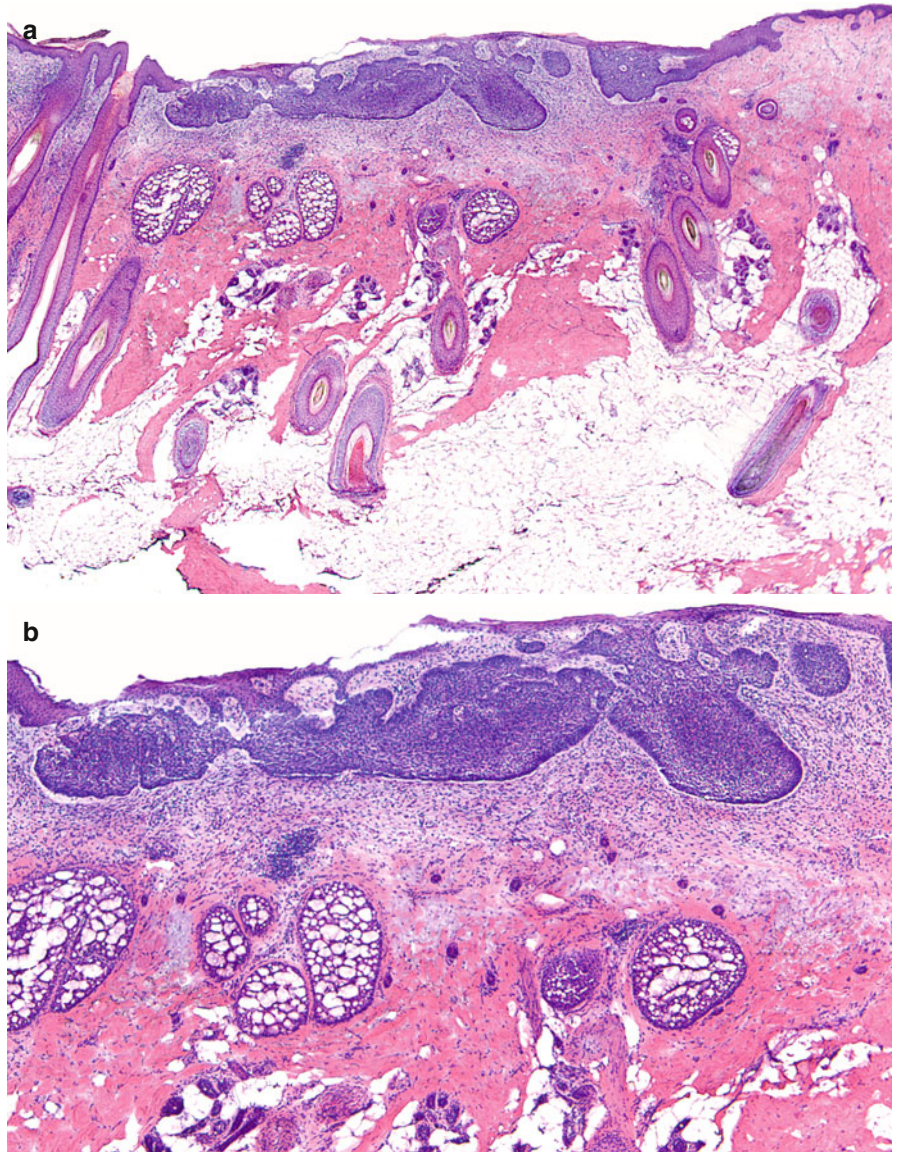
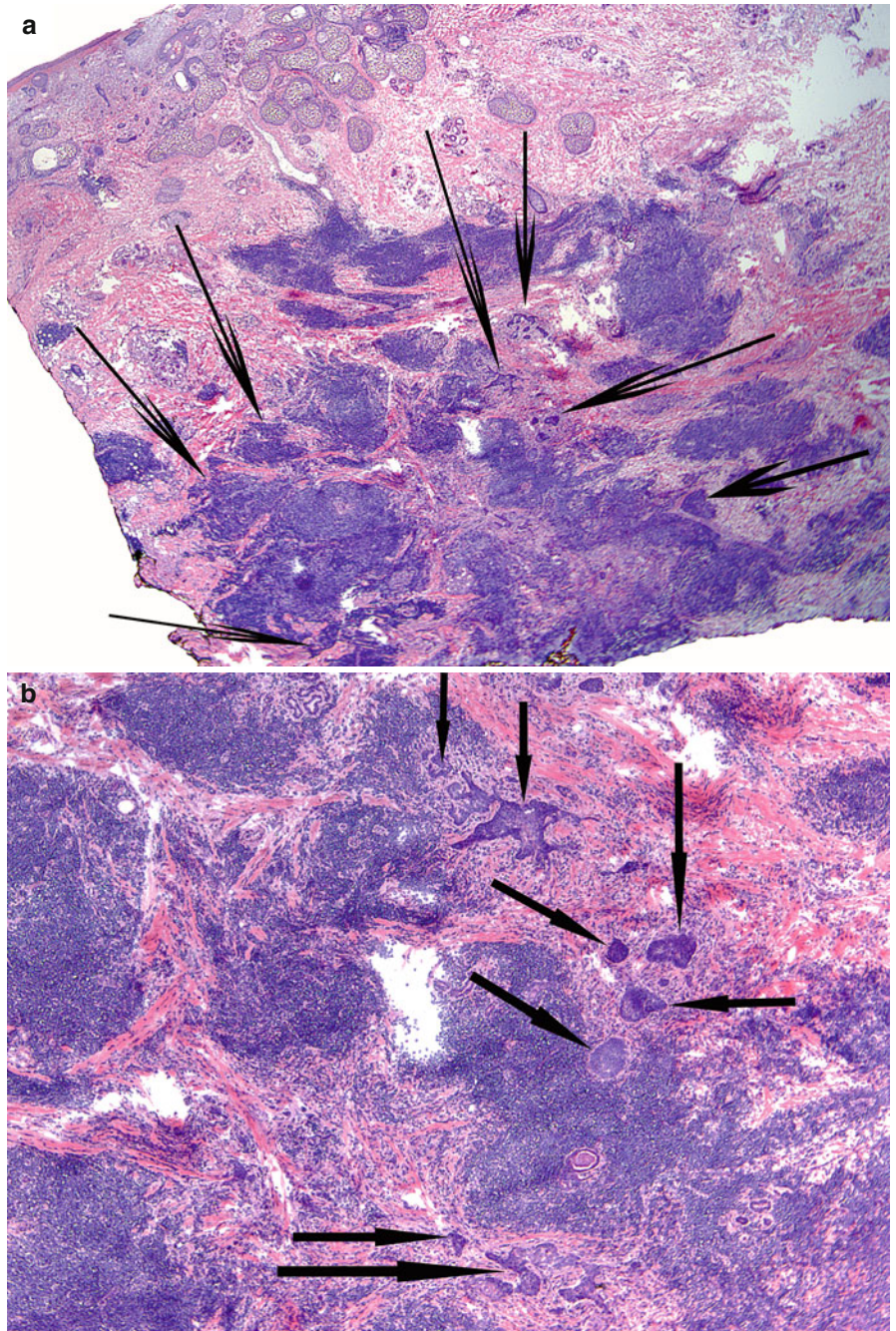


Fig. 3.20 (a) Basal cell carcinoma (*arrows*) in a patient with underlying chronic lymphocytic leukemia: this case demonstrates the dense lymphocytic and possibly leukemic infiltrate that is encountered in the skin of patients with CLL, which can make the evaluation of tumor very difficult. (b) Higher magnification reveals basaloid neoplastic aggregates (*arrows*) in between dense lymphocytic dermal infiltrate



Histologic Features

1. Tumor is often deeply infiltrative and poorly circumscribed.
2. Epidermal connection may be minimal to absent.
3. Aggregates of basaloid cells with different sizes and irregular shapes present usually in the more superficial portion of the dermis.
4. Size of the neoplastic aggregates usually diminishes in the deeper portion of the reticular dermis and toward the subcutaneous fat.
5. The aggregates show irregular angulated shapes and often contain only a few cell layers in width.
6. There is little to no peripheral palisading.
7. Clefts between the aggregates and the surrounding stroma may be present in the superficially located tumor masses. However, as the tumor strands invade deeper, there is little demarcation between tumor and stroma.
8. Little to no mucinous changes in the stroma surrounding the tumor aggregates. Stroma may even appear dense and fibrotic.
9. There is a variable irregularly scattered lymphocytic inflammatory infiltrate associated with the neoplastic stroma in a perivascular and perineural distribution.
10. Perineural invasion is sometimes present.

Histopathologic Differential Diagnosis

Syringoma

1. Well-demarcated tumor limited to the upper dermis.
2. Small epithelial aggregates with rounded, coma-like, or tadpole shapes, as well as elongated strands of epithelial cells.
3. Duct-like structures with homogeneous pink secretions in their lumina.
4. Dense sclerotic pink collagenized stroma surrounding the tumor aggregates.
5. No clefts between the tumor aggregates and the surrounding stroma.

Desmoplastic Trichoepithelioma

1. Well-circumscribed, symmetric plate-like growth pattern confined to the upper or mid dermis.
2. Epithelial aggregates that show evidence of follicular differentiation, i.e., infundibular cysts, trichohyaline granules, etc.
3. Presence of calcifications.
4. Absence of clefts around epithelial tumor aggregates and the surrounding stroma.
5. Dense collagenous stroma around tumor aggregates.

Microcystic Adnexal Carcinoma

1. Larger, asymmetric, poorly circumscribed, and deeply infiltrative neoplasm that often involves the subcutaneous fat and skeletal muscle.
2. Marked variation in size and shape of tumor aggregates.
3. Prominent perineural invasion.

Infiltrative Basal Cell Carcinoma with Perineural Invasion

1. When nerves are longitudinally sectioned, there are fascicles of spindled cells with S-shaped nuclei and long thin cytoplasmic processes. Very often fine purple granules of different sizes are seen within the cytoplasm of the nerves. Small vacuoles are also noted in both longitudinal and cross sections.
2. Perineural invasion refers to the presence of tumor cells in the perineural spaces of normal cutaneous nerves. Often there is inflammation in the vicinity of nerves showing perineural invasion.
3. Because of the increased possibility of perineural invasion associated with infiltrative BCC, the surgeon should examine areas of tumor involvement carefully.
4. Nerves within the area of the carcinoma and particularly at its periphery should be scrutinized to identify this subtle phenomenon.
5. It is a common practice to examine multiple sections when there is dense perineural inflammation to exclude the possibility of perineural invasion.

Fig. 4.1 (a, b) Infiltrative basal cell carcinoma: poorly circumscribed and deeply infiltrative tumor aggregates diminishing in size from superficial to deep dermis

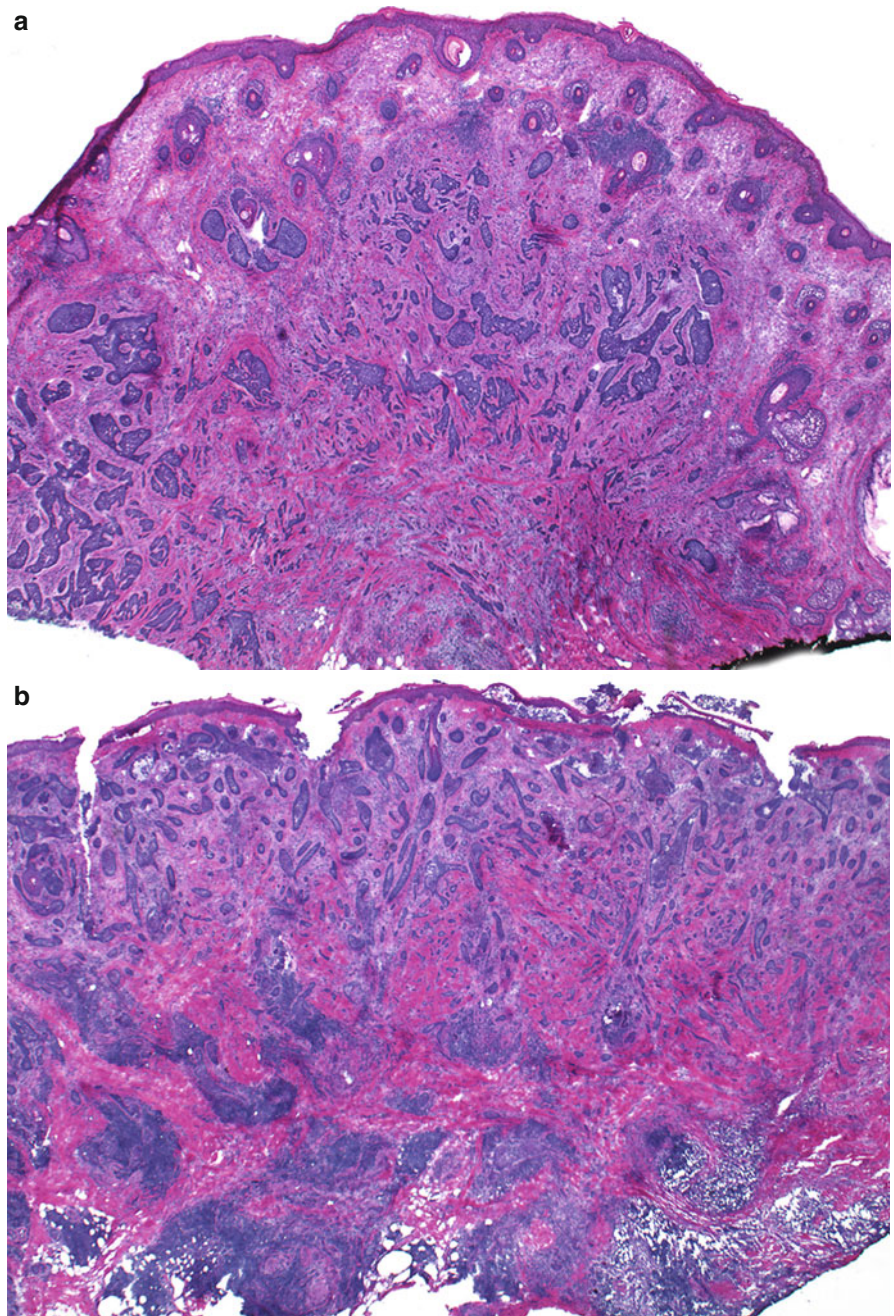


Fig. 4.2 (a, b) Infiltrative basal cell carcinoma: deeply infiltrative strands and cords, some consisting of a single layer of basaloid cells, and surrounded by thick collagen. Tumor aggregates are not always associated with an inflammatory response

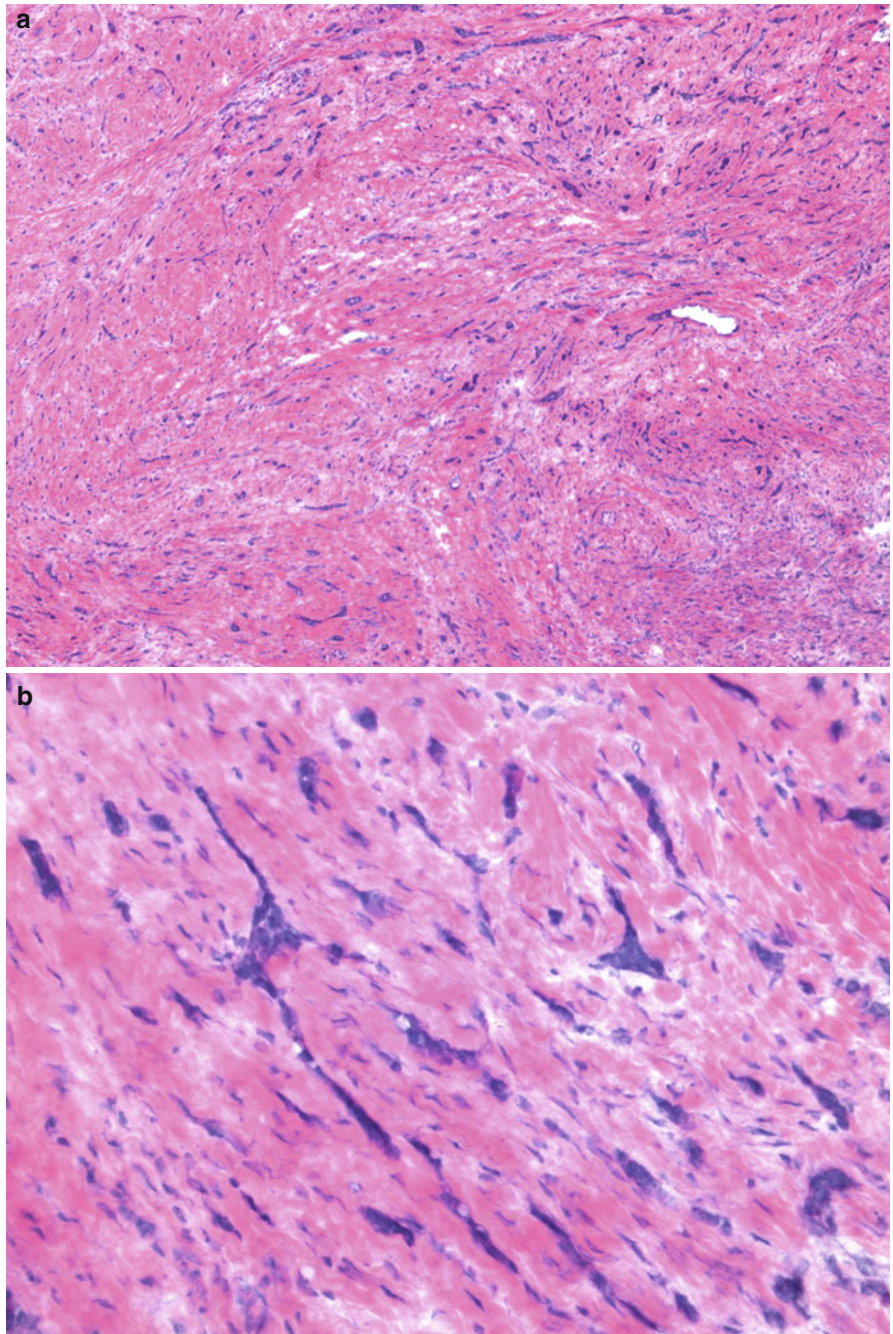


Fig. 4.3 (a, b) Infiltrative basal cell carcinoma: irregularly shaped strands, cords, and angulated aggregates of tumor cells among fibrotic stroma

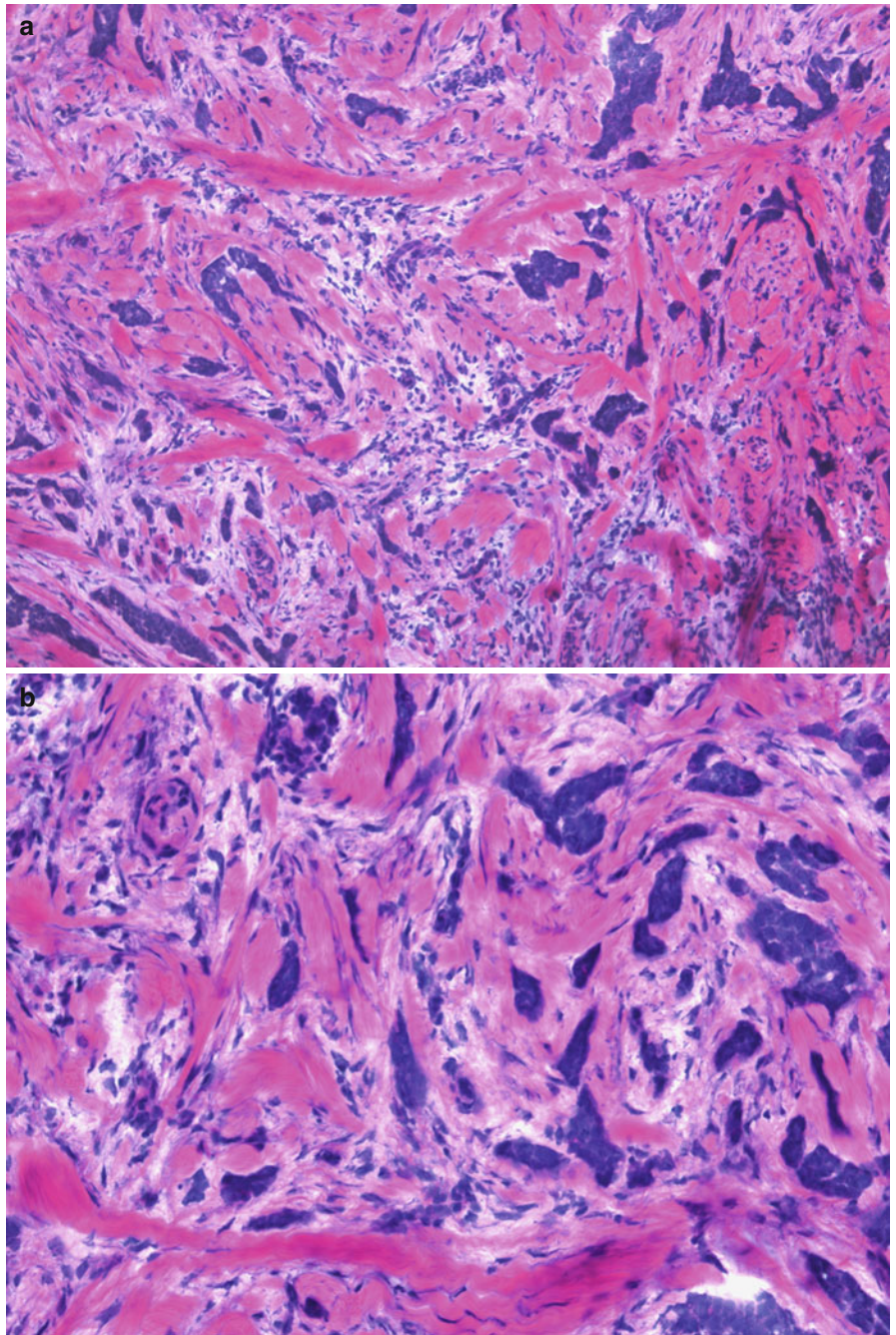
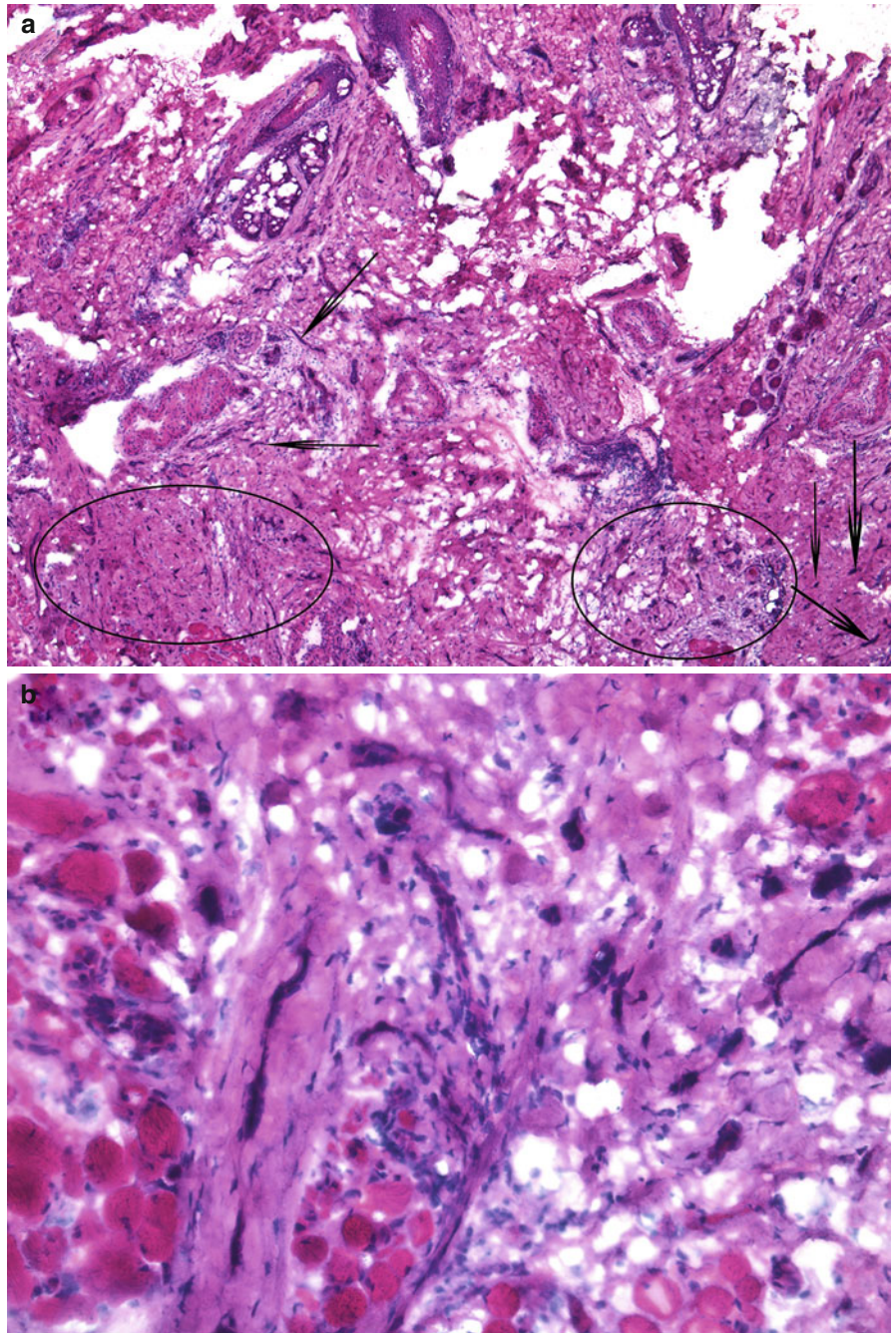


Fig. 4.4 Infiltrative basal cell carcinoma: (a) Tumor aggregates and strands (*arrows and ellipses*) infiltrating in between skeletal muscle. (b) Higher power view of slender tumor aggregates infiltrating in between skeletal muscles



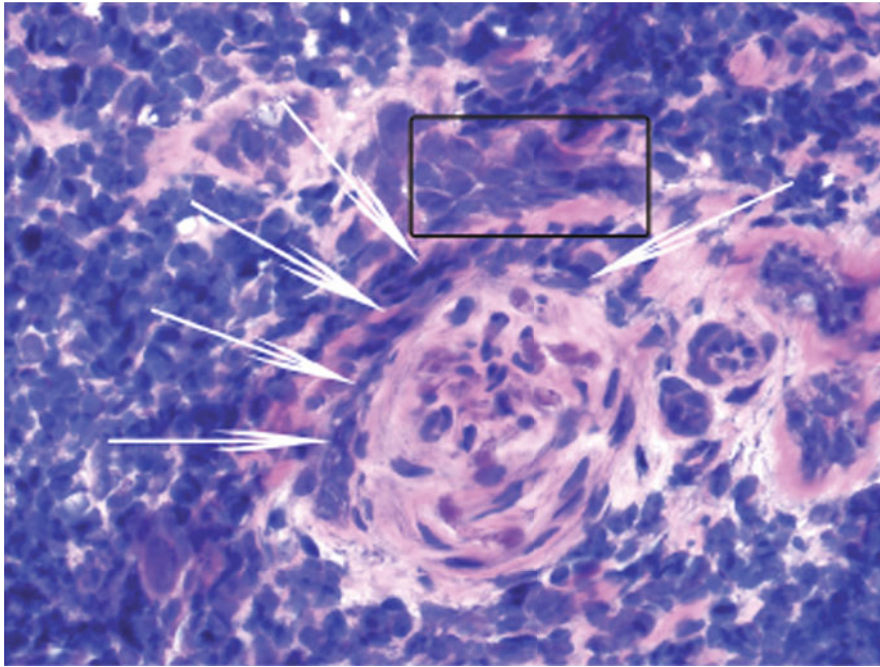
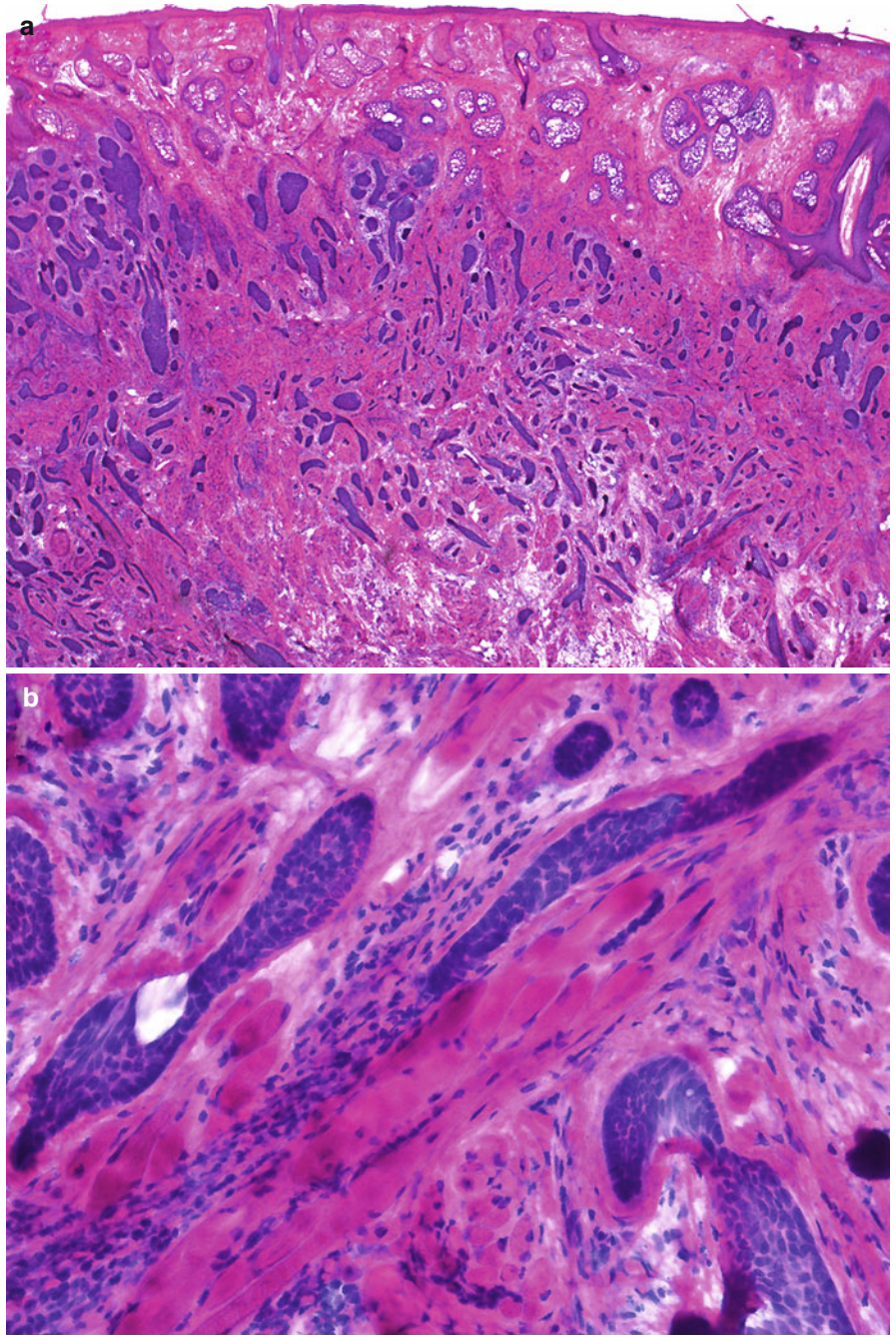


Fig. 4.5 Infiltrative basal cell carcinoma: a cross-sectioned nerve in the center of photograph encircled in a semilunar fashion (from 8 to 2 o'clock) by a tumor aggregate (*arrows*). Seen immediately above the perineural invasion of this nerve is an angulated neoplastic tumor aggregate (*rectangle*). Dense diffuse lymphocytic inflammation is present. Differentiating features between the inflammatory cells and the neoplastic cells are the following: (1) Pleomorphic and somewhat larger nuclei of the neoplastic cells compared to the more monomorphic and

relatively smaller nuclei of inflammatory cells. (2) The tumor cells, which form irregular and often angulated neoplastic aggregates, display a somewhat cohesive nature and group together in comparison to the almost random, disorderly, scattered and overlapping inflammatory cells. (3) Although both neoplastic and inflammatory cells have a high nuclear to cytoplasmic ratio, there is still some cytoplasm visible in the neoplastic cells that give these cells an overall pink to purplish hue compared to the more uniform blue nature of the inflammatory cells

Fig. 4.6 Infiltrative basal cell carcinoma:
(a) A scanning magnification of infiltrative basal cell carcinoma showing basaloid aggregates of various sizes and shapes, many with angulated appearance, that decrease in size from superficial to the deep portion of the neoplasm.
(b) High-power view of infiltrative basal cell carcinoma showing angulated basaloid aggregates infiltrating in between skeletal muscle fibers



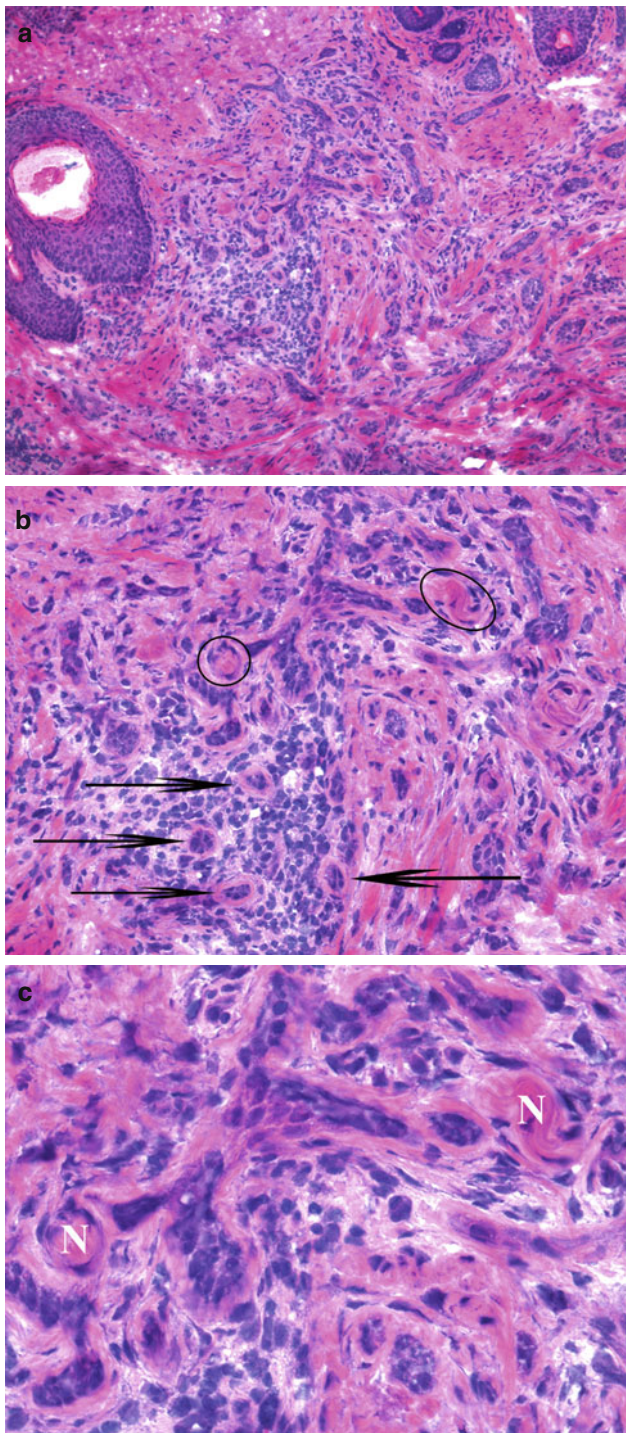


Fig. 4.7 Infiltrative basal cell carcinoma: (a) Aggregates of infiltrative basal cell carcinoma in the superficial and mid dermis. (b) Neoplastic aggregates are seen in close proximity to a small nerve, focally sectioned transversely (*circle*), and, in other areas, longitudinally (*ellipse*). There are oval basaloid neoplastic aggregates that mimic eccrine ducts. The eccrine ducts (*arrows*), unlike aggregates of BCC, are surrounded by eosinophilic fibrous sheath. (c) At this high magnification the proximity of the neoplastic aggregates to the nerve fibers (marked with 'N') can be appreciated

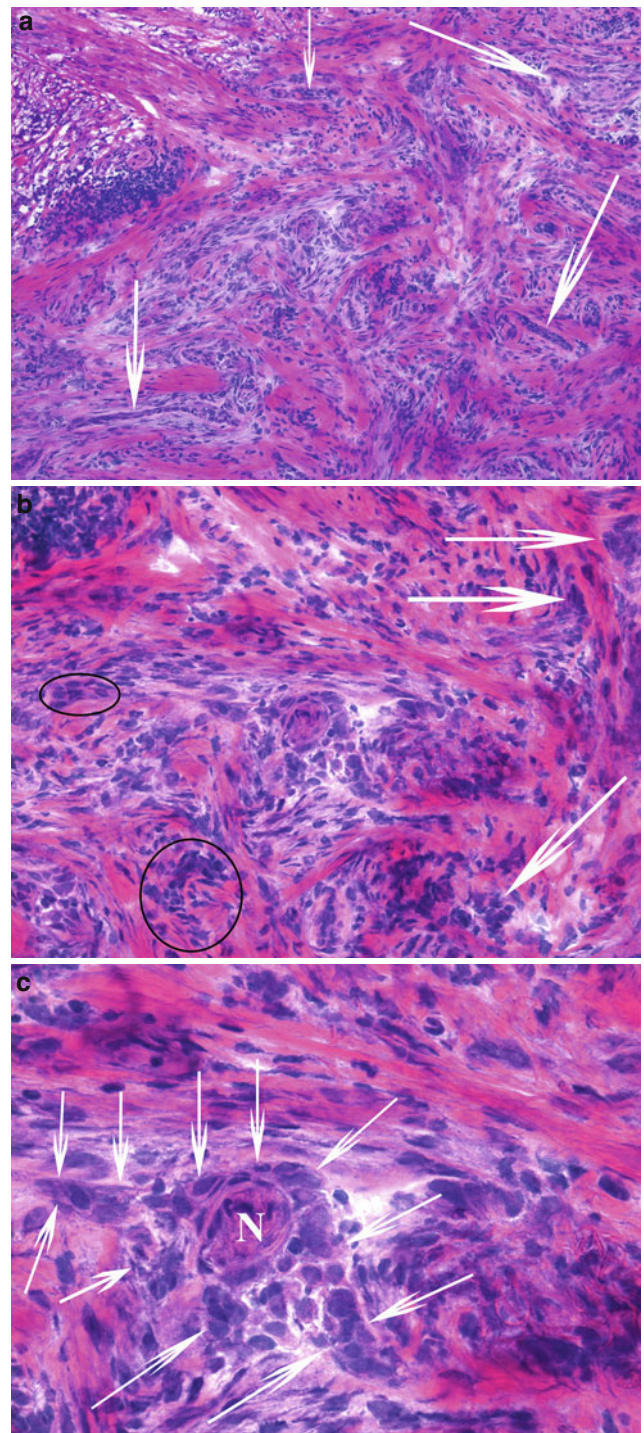


Fig. 4.8 Infiltrative basal cell carcinoma: (a) Irregular basophilic neoplastic aggregates (some of which are designated by *arrows*) infiltrating within the dermis. (b) A triangular neoplastic aggregate wrapped around a small nerve in the center of the photomicrograph. In addition to this neoplastic aggregate, there are other tumor aggregates (*arrows and ellipses*) in the photomicrograph that are ill defined and could be misinterpreted as inflammatory cells. However, the cohesiveness and irregular shapes of the aggregates (as opposed to the disorderly, randomly organized inflammatory cells) confirms their neoplastic nature. (c) Higher magnification of the above photomicrograph. A transversely sectioned small nerve (N) is completely encircled by an irregular tumor aggregate (outlined by *arrows*). Note the pleomorphic nuclei of the neoplastic cells

Fig. 4.9 Infiltrative basal cell carcinoma: (a) A low-power magnification showing numerous irregular neoplastic aggregates throughout the superficial and mid dermis. (b) Medium power magnification showing a muscle of hair erection (SM) with an elongated tumor aggregate at its periphery (arrow). Below the smooth muscle bundle is an elongated nerve (N), which contains slender, wavy, s-shaped nuclei and cytoplasm with deep purple color

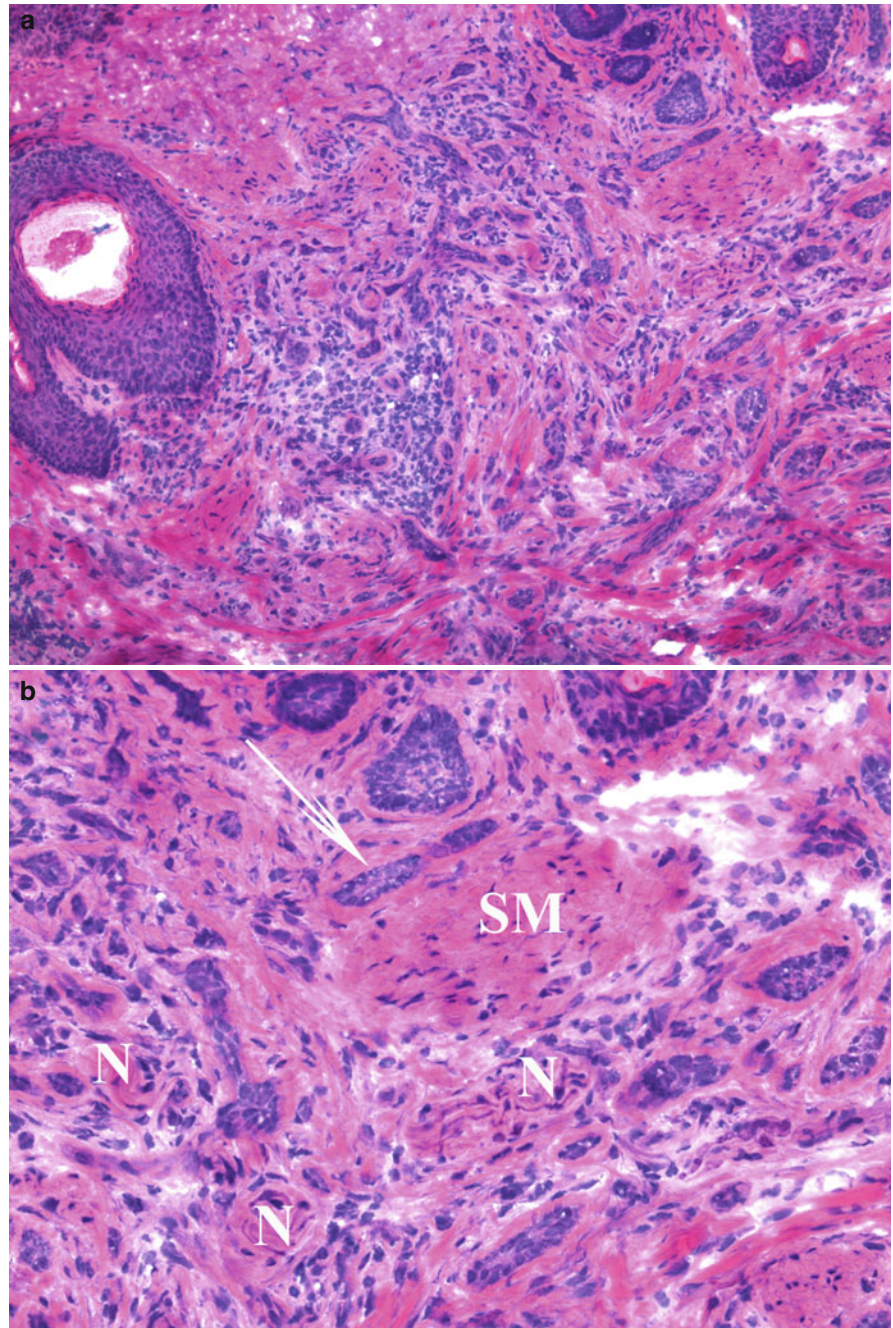


Fig. 4.9 (*continued*) (c) In this high-power photomicrograph, the characteristic features of the erector pilar muscle (SM), with an oval shape and composed of syncytium of cells with oval elongated nuclei and abundant eosinophilic cytoplasm, are easily identified. In contrast, the nerve (N) below shows an oval shape and consists of elongated cells with wavy nuclei and purple cytoplasm. Wrapping around the right upper pole of the nerve are a few neoplastic cells (*arrow*) with high nuclear to cytoplasmic ratio and darkly staining nuclei, which represents a perineural invasion. A few small neoplastic aggregates (*circle*) are seen in the adjacent dermis

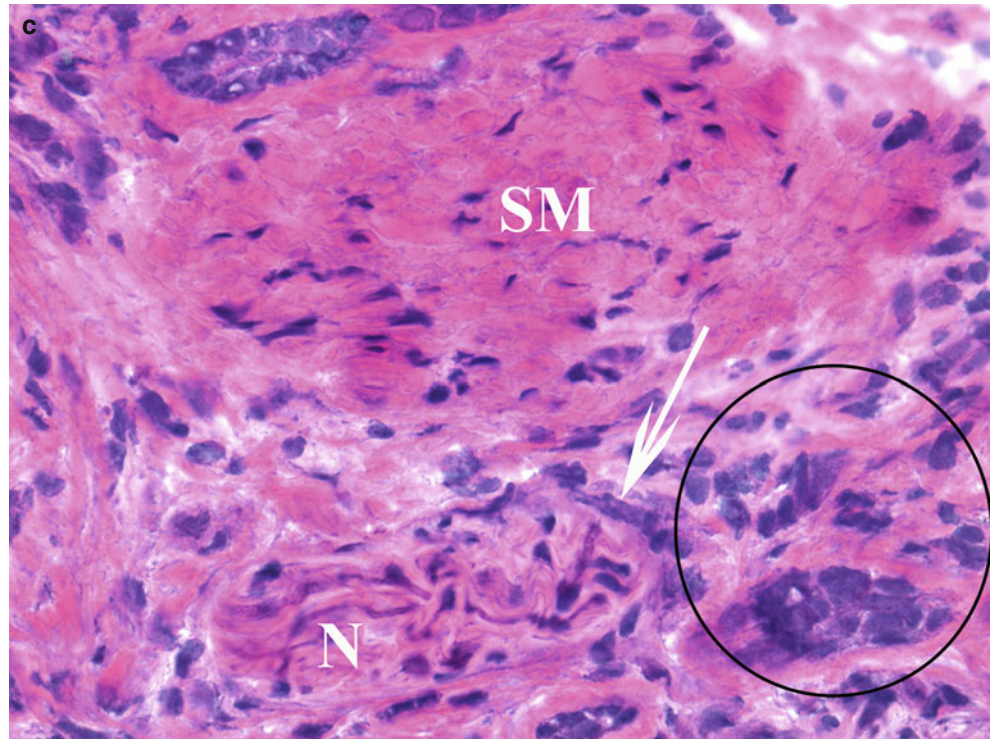
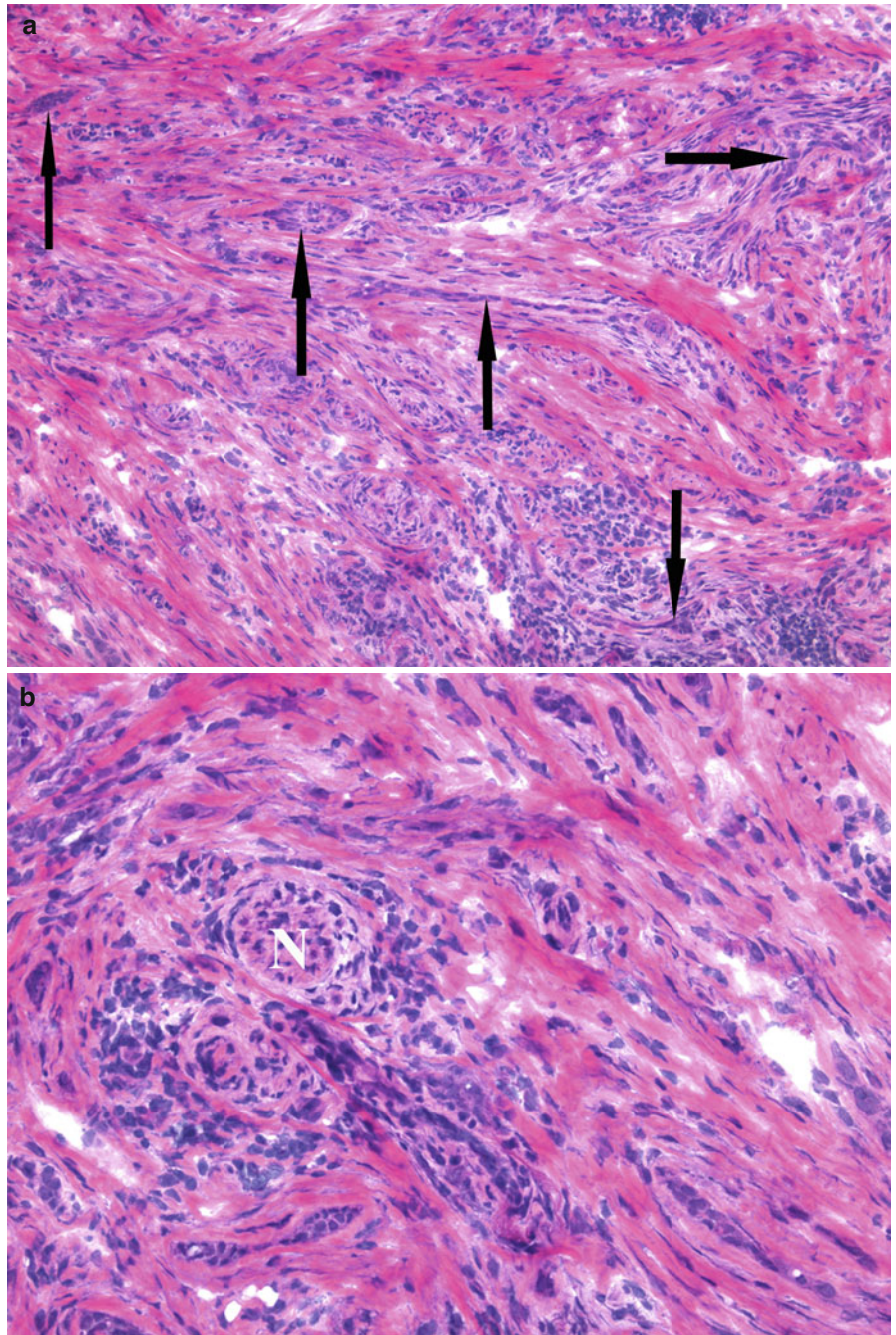


Fig. 4.10 Infiltrative basal cell carcinoma: (a) At this medium power it is not easy to identify tumor aggregates (some of which are designated by *arrows*) hidden among collagen bundles and admixed with inflammatory cells. The difficulty in identifying the tumor aggregates is due to the fact that in many areas they are composed of one to two layers of neoplastic cells arranged as strands and cords. A few of the tumor aggregates are angulated. (b) Subtle example of perineural invasion (nerve marked by "N"). It is challenging to discern the irregular tumor strands and cords from the surrounding inflammatory cells even at high magnification



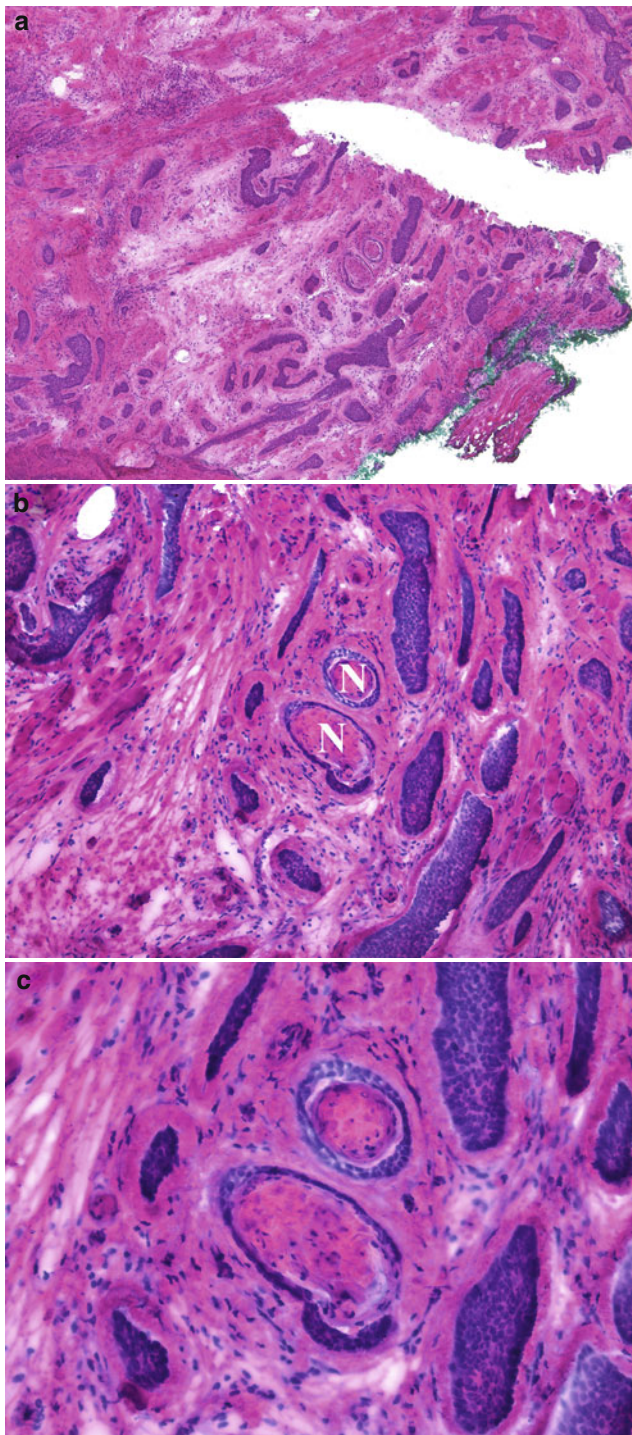


Fig. 4.11 (a) Infiltrative BCC with perineural invasion: scanning magnification showing irregular tumor aggregates in the dermis and in between skeletal muscle, as well as areas of perineural involvement. (b) Medium power photomicrograph showing numerous tumor aggregates in between skeletal muscle fibers. In the center there are two nerves (N) encircled by neoplastic cells. (c) Tumor aggregates circumferentially surrounding two transversely cut small nerves

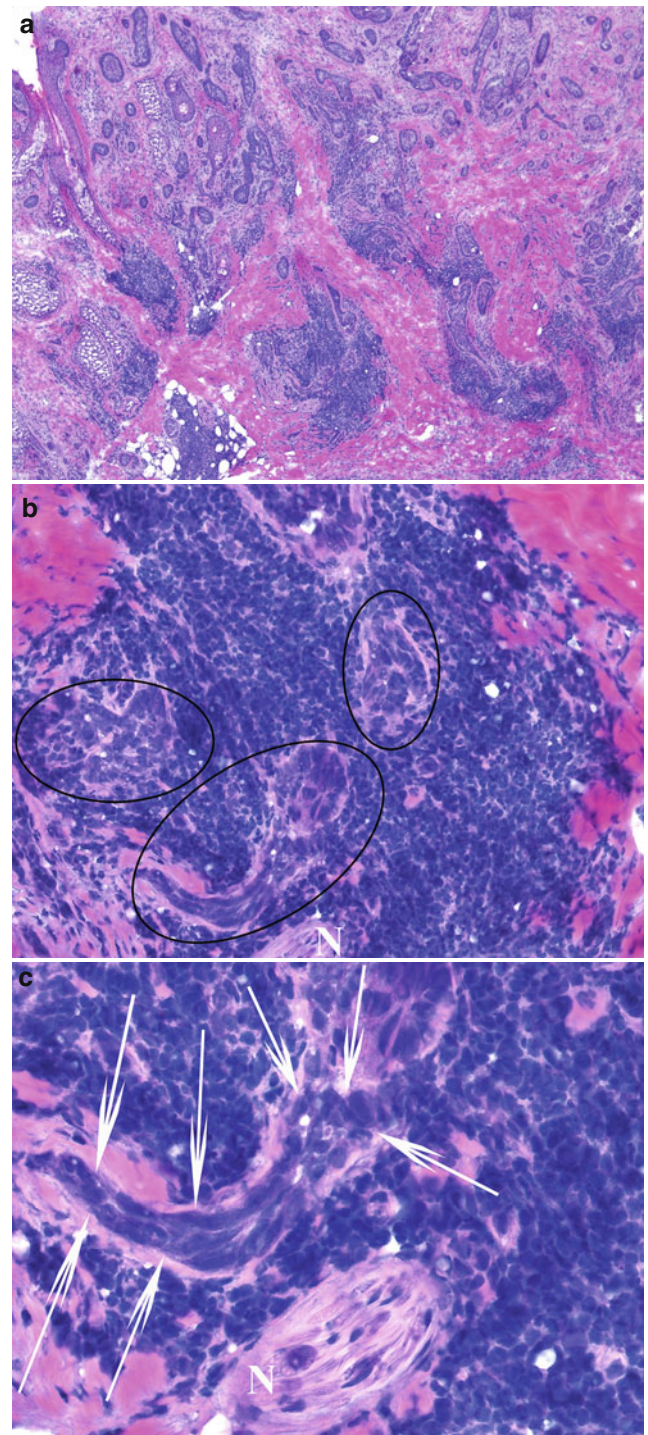


Fig. 4.12 (a) Nodular and infiltrative basal cell carcinoma: basoid neoplastic aggregates in various shapes and sizes throughout the dermis. (b) A few irregular angulated tumor aggregates (*ellipses*) are hidden among dense inflammation. A portion of a small nerve (N) is seen in the central lower pole of the photomicrograph. Note the following differences between neoplastic cells and inflammatory cells: inflammatory cells have a more uniform blue hue, compared to the *purplish/blue* color of the tumor cells; inflammatory cells have a high nuclear to cytoplasmic ratio as do neoplastic cells but in contrast, the neoplastic epithelial cells have the presence of a small amount of pink cytoplasm; and neoplastic cells maintain cohesiveness and cluster together in aggregates versus the random, irregular and somewhat disorderly nature of the inflammatory cells. (c) High magnification showing a tadpole-shaped neoplastic aggregate delineated by *arrows*, immediately above a nerve (N) and surrounded by a dense inflammatory infiltrate

Fig. 4.13 Perineural inflammation: a small transversely cut nerve (*arrow*) is seen in the center of the photograph surrounded by scattered large lymphocytes. No obvious tumor aggregates are appreciated

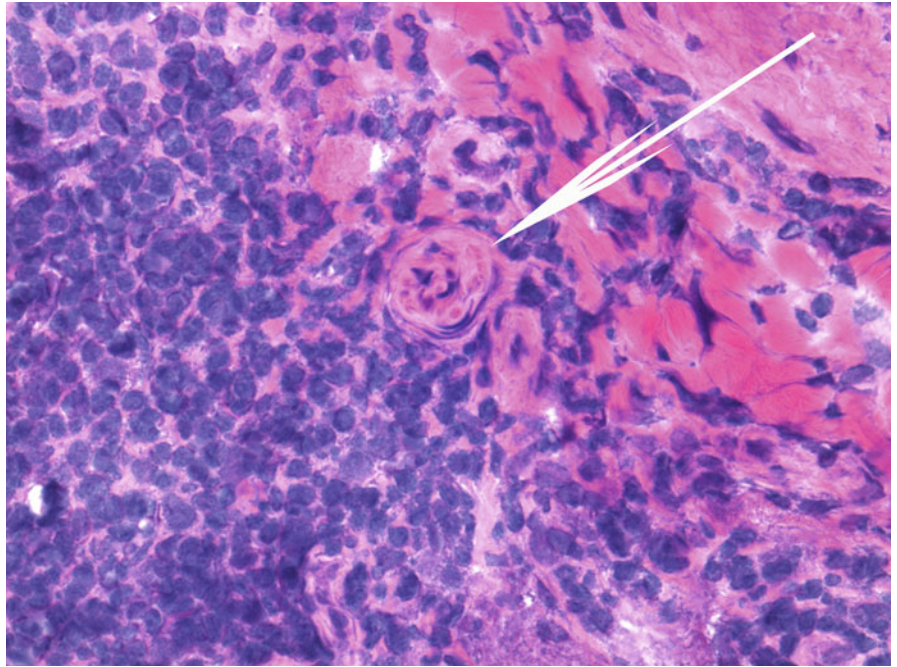


Fig. 4.14 Infiltrative basal cell carcinoma: (a) The subtle presence of tumor aggregates (*circle*) can be missed upon a cursory examination of the specimen. Higher magnification is necessary to determine whether these are inflammatory cells or represent infiltration by cancer. (b) Higher magnification of BCC in the previous figure. The slender and short cords and strands of neoplastic basaloid cells (*arrows*) are more obvious

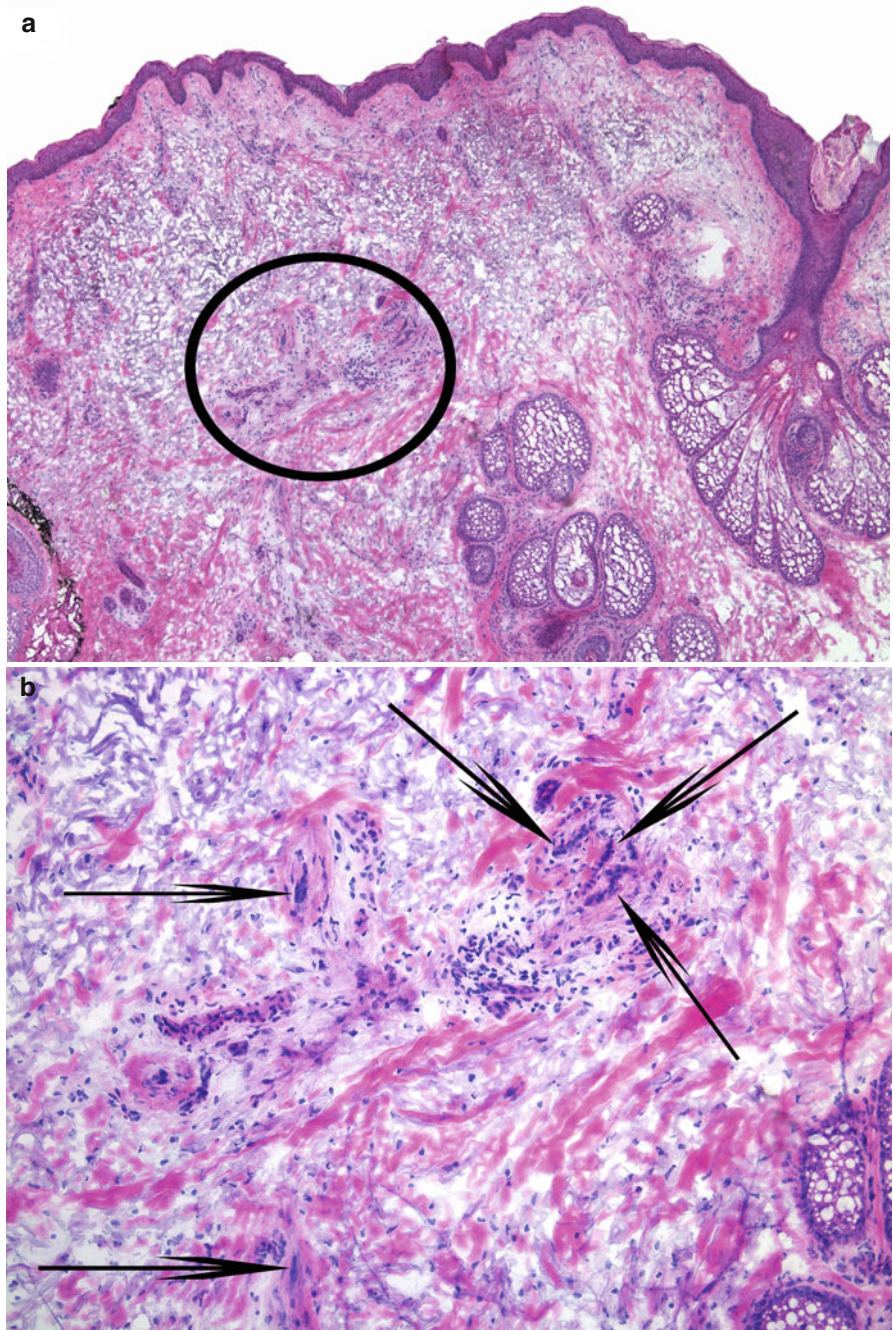


Fig. 4.14 (continued) (c) Deeper cuts into the specimen demonstrate the presence of more obvious infiltrative basal cell carcinoma (ellipse). (d) Tumor cords, strands, and slender angulated aggregates are even better appreciated at higher magnification

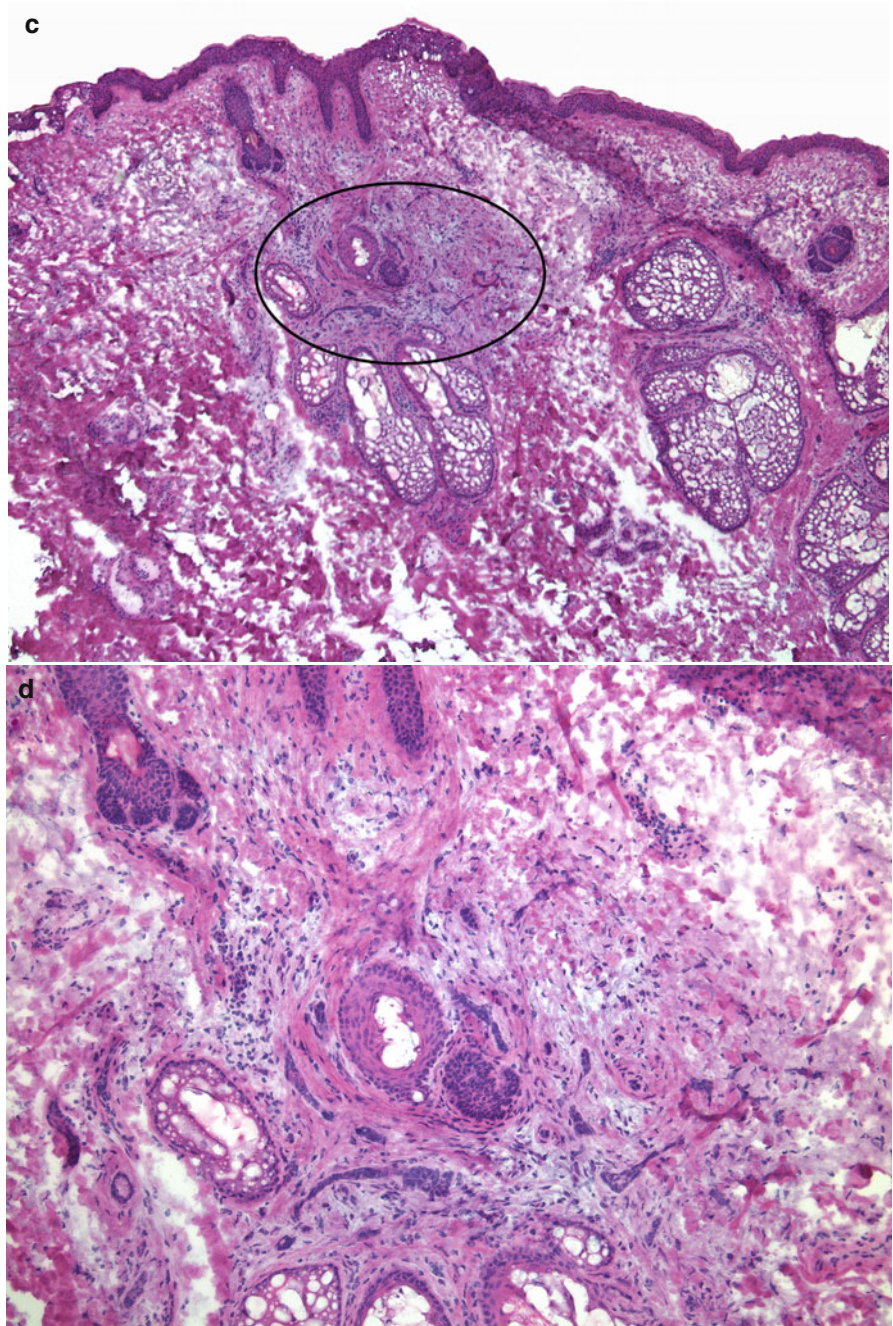


Fig. 4.15 Infiltrative basal cell carcinoma: (a) Below the subcutaneous fat there are subtle small basaloid strands, focally embedded within mucinous stroma (*ellipse*), which can be easily mistaken for inflammation. (b) The strands of basaloid tumor aggregates are more obvious at this magnification (*ellipse*)

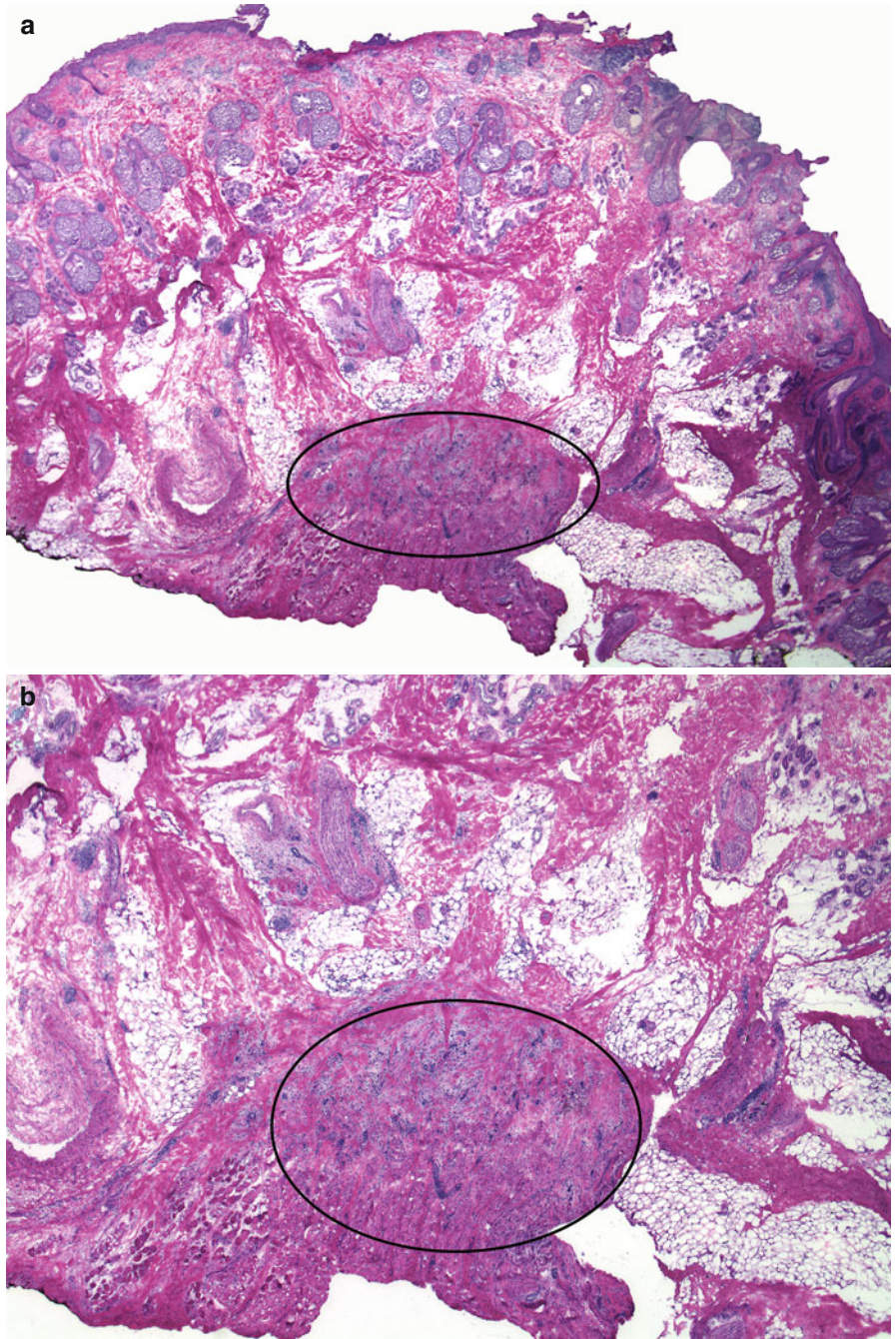
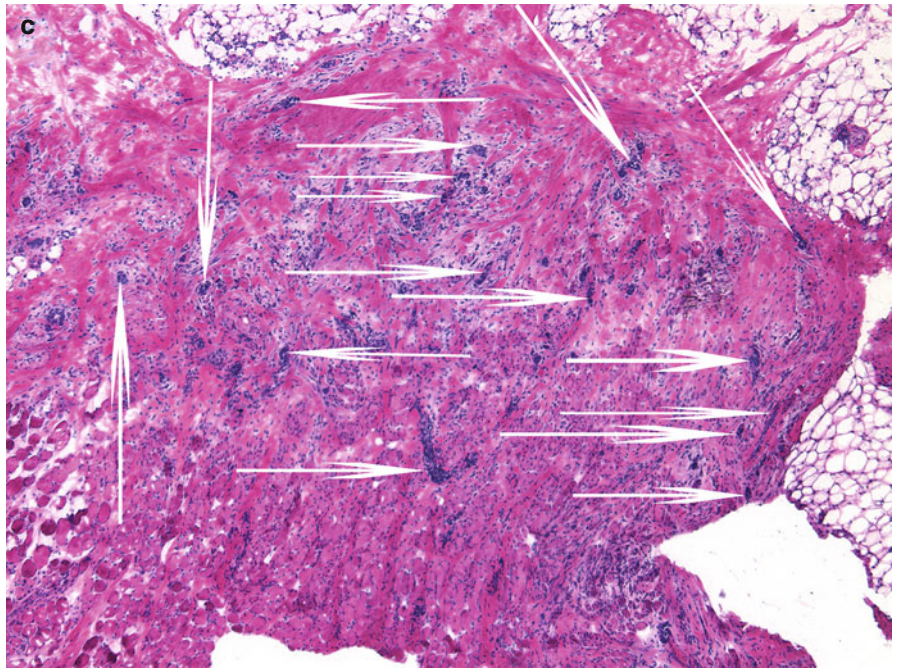


Fig. 4.15 (continued) (c) *Arrows* indicate some of the tumor aggregates of this basal cell carcinoma. Multiple *arrows* are being used to demonstrate the small and subtle nature of the tumor aggregates percolating in between skeletal muscle fibers



Differentiating Basal Cell Carcinoma from Normal and Benign Histologic Findings

5

The fundamental challenge for the Mohs surgeon is the histologic differentiation of benign entities from malignant as the goal of Mohs surgery is not only to extirpate the cancer but also to conserve healthy tissue. Often dense inflammation, scar tissue, transected follicles, and other normal or benign structures can be very difficult to differentiate from tumor aggregates. This chapter provides some guidance on features that help differentiate benign from malignant.

One of the most common challenges for cases of basal cell carcinoma in particular is the differentiation of tumor from “funny-looking” follicular structures. Many Mohs surgeons and pathologists feel that basal cell carcinoma, like other cutaneous tumors, causes follicular induction, somewhat akin to a proliferative epiphenomenon. Because basal cell carcinomas often arise adjacent to hair follicles, it can sometimes be virtually impossible to distinguish cancer from oddly shaped follicular structures. Two entities that share similarities with basal cell carcinoma are basaloid follicular hamartoma (BFH) and folliculocentric basaloid proliferation (FBP). Basaloid follicular hamartoma is an epithelial proliferation of basaloid cells that are arranged in a radial and anastomosing pattern representing malformed and distorted follicles. Keratin cysts may also be present. The features that may help distinguish this entity from basal cell carcinoma include the presence of bland epithelial cells without nuclear pleomorphism, absent or rare mitotic activity, and lack of necrosis. Peripheral palisading, stromal changes, and clefting can be variably present (although less predominant than in BCC), thus highlighting the difficulty in differentiating between these benign structures and basal cell carcinoma. Folliculocentric basaloid proliferation is thought to be a reactive phenomenon originating from mantle epithelium of follicles. FBP has an overall vertical orientation and is folliculocentric where the basaloid cords of cells create a pinwheel formation. Again, in this benign entity, nuclear pleomorphism, mitoses, cellular necrosis, and stromal changes are absent. Another finding that can help differentiate FBP from BCC is the presence of a thick hyaline basement membrane around many of the aggregates in FBP. It is also thought that keratin cysts are not present in FBP as they are in BFH but this is not absolute. As one can imagine, at times, BCC with follicular differentiation, FBP and BFH can be virtually indistinguishable from one another and perhaps until genetic molecular techniques can help differentiate between these, it is really the clinical judgment that will guide the Mohs surgeon in providing the best care of patients.

Differentiating Basal Cell Carcinoma from Hair Follicles

Features of basal cell carcinoma	Features of hair follicles
1. Irregularly shaped angulated aggregates of basaloid cells with high nuclear to cytoplasmic ratio	1. Hair follicles depending on their profile are usually round or oval and do not appear irregularly shaped or angulated
2. Peripheral palisading in neoplastic aggregates	2. Often a centrally placed hair shaft surrounded by layers of follicular epithelium and a perifollicular fibrous sheath
3. Clefts between the neoplastic aggregates and the surrounding stroma	3. Lack of clefts between follicular structures and adjacent dermis
4. Atypical pleomorphic cells may be present	4. Usually monomorphic cells
5. Neoplastic cells comprised of mostly nuclei with very little cytoplasm	5. Cells with small or moderate amount of eosinophilic cytoplasm
6. Individually pyknotic/necrotic keratinocytes	6. Rare individual pyknotic/necrotic keratinocytes within follicular epithelium
7. No trichohyalin granules present	7. Sometimes trichohyalin granules seen
8. Loose mucinous stroma surrounding tumor aggregates	8. Fibrous sheath surrounding hair follicles
9. Neoplastic aggregates are usually surrounded by inflammation	9. Focal inflammation particularly in cases of rosacea and other inflammatory conditions
10. No sebaceous glands in the vicinity of neoplastic aggregates	10. Sebaceous glands associated with follicular structures in the upper portion of the reticular dermis

Differentiating Basal Cell Carcinoma with Follicular Differentiation from Hair Follicles

Features of basal cell carcinoma with follicular differentiation	Features of normal follicular structures
1. Aggregates of basaloid cells with irregular angulated shapes arising mostly from the infundibular portion of the hair follicle.	1. Hair follicles when cut longitudinally or transversely show round or oval shapes and basaloid cells at the periphery. However, cells with more abundant pink cytoplasm are present in the center of the follicles, exhibiting trichohyalin keratinization
2. Peripheral palisading within the aggregates	2. Sometimes peripheral palisading within mainly transversely cut hair follicles
3. No hair shafts in the center of neoplastic aggregates and no Demodex	3. Hair shafts sometimes in the center of follicular structures. Demodex occasionally seen in the follicular infundibulum
4. Focally clefts are present between the basaloid aggregates and the surrounding stroma	4. Lack of clefts between the follicular epithelium and the fibrous sheaths
5. Often individually necrotic/pyknotic cells within the neoplastic aggregates	5. Occasional individual necrotic/pyknotic cells within follicular epithelium
6. Spindle cell stroma rich in mucin surrounding the neoplastic aggregates	6. Often a thin rim of fibrous tissue without mucin tightly encircling follicular structures
7. No structures resembling follicular bulbs and papillae	7. Follicular bulbs and papillae usually in the lower reticular dermis or subcutaneous fat
8. Often central areas of necrosis within the neoplastic aggregates	8. No areas of necrosis
9. Slightly pleomorphic cells with no discernable cytoplasm	9. Monomorphic cells with small or moderate amount of eosinophilic cytoplasm
10. Usually no sebaceous glands associated with tumor aggregates	10. Sebaceous glands in the vicinity of follicular structures in the upper portion of the reticular dermis
11. No mantle zone	11. Presence of mantles, i.e., symmetrical cords of epithelial cells that emanate from the sides of a follicle, extend laterally for a short distance, and then descend parallel with the follicle

Differentiating Basal Cell Carcinoma from Eccrine Glands

Features of basal cell carcinoma	Features of eccrine glands and ducts
1. Irregularly shaped angulated aggregates of basaloid cells with high nuclear to cytoplasmic ratio	1. Rounded eccrine glands and ducts grouped together
2. Aggregates lack lumina	2. Eccrine glands lined by a layer of large cuboidal cells with a centrally placed lumen containing pink secretion
3. Lack of structures resembling ducts	3. Eccrine ducts lined by two layers of small cuboidal cells and a peripheral layer of myoepithelial cells. Narrow lumen lined by pink cuticle
4. Mild perivascular and peritumoral lymphocytic inflammation	4. Usually no inflammation
5. Central necrosis in large tumor islands or individual necrotic cells	5. No necrotic or pyknotic cells

Differentiating Basal Cell Carcinoma from Vessels

Features of basal cell carcinoma	Features of vessels
1. Aggregates lack lumina	1. A round or compressed lumen lined by flat endothelial cells
2. No smooth muscle associated with tumor aggregates	2. Smooth muscle wall of various thickness depending on caliber of vessel
	3. Erythrocytes and serum within vessel lumina
	4. Thin rim of surrounding fibrous tissue
	5. Usually no surrounding inflammation

Differentiating Basal Cell Carcinoma from Inflammation

Features of basal cell carcinoma	Features of inflammatory cell aggregates
1. Irregularly shaped cohesive aggregates of basaloid cells with high nuclear to cytoplasmic ratio	1. Ill-defined collections of cells resembling swarms of bees or interstitially scattered individual cells
2. Neoplastic cells showing at least some pleomorphism	2. Relatively monomorphic cells
3. Mitoses present and often atypical	3. Mitoses seen rarely and not atypical
4. Necrotic/pyknotic cells present	4. No necrotic/pyknotic cells
Neoplastic cells	Inflammatory and other cells
	<i>Lymphocytes</i>
1. Large cells with variation in nuclear to cytoplasmic ratio	1. Small cells (7–8 μm) with high nuclear to cytoplasmic ratio and almost no discernible cytoplasm
2. Pleomorphic cells with variation in size, shape, and staining characteristics	2. Cells relatively monomorphic with no prominent pleomorphism
3. Hyperchromatic nuclei with irregular nuclear contours	3. Round uniform nuclei with smooth dense chromatin pattern
4. Sometimes prominent nucleoli	4. No prominent nucleoli
5. High nuclear to cytoplasmic ratio usually	5. High nuclear to cytoplasmic ratio in small lymphocytes
6. Mitotic figures, some of which atypical	6. Mitotic figures rare
7. Individually necrotic/pyknotic cells among neoplastic cells	7. Rare necrotic/pyknotic cells
8. Aggregates of neoplastic cells with peculiar irregular shapes; sometimes clefts around tumor aggregates and surrounding stroma	8. Lymphocytes usually clumped together without particular shape of aggregations; no clefts between aggregations and surrounding dermis
	<i>Histiocytes</i>
	1. Large cells with large vesicular nuclei, small nucleoli, and abundant irregularly shaped cytoplasm
	2. Nuclei are either round or oval but not angulated
	3. Vesicular nuclei with fine nuclear chromatin
	4. Always low nuclear to cytoplasmic ratio; i.e., abundant cytoplasm
	5. Sometimes grouped together in aggregations without discernible shape, forming small granulomas
	6. No clefts between the aggregations and the surrounding dermis
	7. No associated mucin
	8. Mitoses seen rarely and not atypical
	9. No necrotic/pyknotic cells

Fig. 5.1 Superficial BCC with follicular differentiation: Prominent basaloid budding at the bottom of elongated rete ridges and connection of the superficial basal cell carcinoma to the infundibulum of the hair follicle. The normal lining of the follicular infundibulum resembles the surface epidermis with a basal cell layer, a spinous layer, a thin granular cell layer, and basket-woven keratin. In addition, a hair shaft can be seen in the infundibulum. No budding of basaloid epithelium should be normally seen in the infundibular portion of the hair follicle. Basaloid budding refers to proliferations of basaloid cells coming off from the undersurface of the epidermis and showing signs of follicular germs only with no follicular papillae. Lack of follicular papillae as well as the basaloid budding off of the infundibulum favors a superficial basal cell carcinoma and not follicular induction

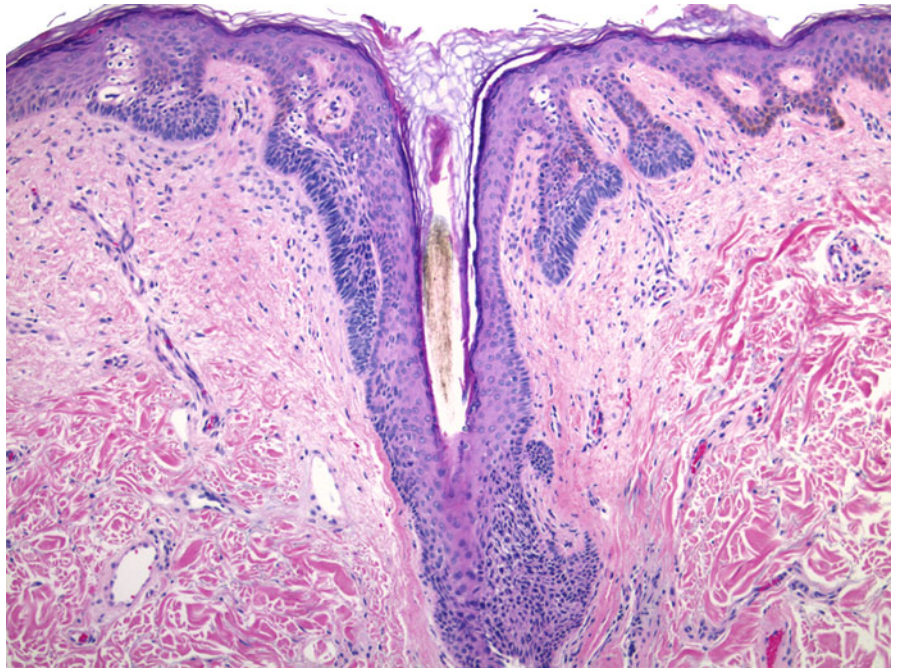


Fig. 5.2 (a) There are multiple hair follicles in this section. The central vellus hair follicle has an angulated basaloid proliferation (*thick arrow*), which resembles the mantle of the hair follicle. However, the high nuclear to cytoplasmic ratio and different staining pattern compared to the surrounding follicular structures favors basal cell carcinoma. To the right of this is another hair follicle where the infundibulum is seen. It can be debated whether there is basal cell carcinoma as the outer portion displays a basaloid layer which appears to be palisading (*thin arrow*). In these cases further sectioning of the specimen may occasionally help resolve the quandary. (b) Higher magnification of the irregular angulated basaloid proliferation coming off from the vellus hair follicle on the left (*ellipse*)

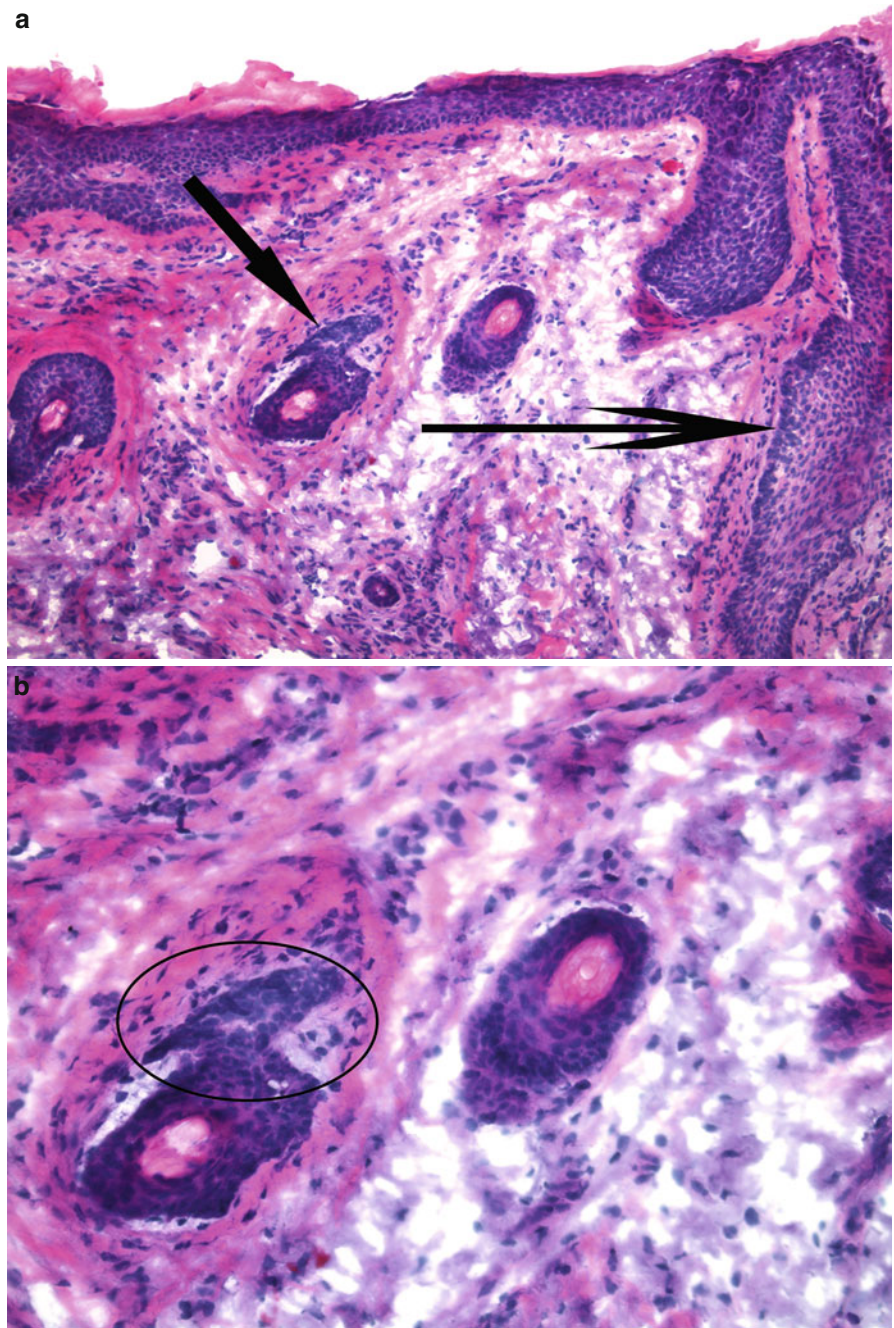


Fig. 5.3 BCC with follicular differentiation: **(a)** Hair follicles in this photomicrograph are cross-sectioned at different levels. Several of these follicles have adjacent basal cell carcinoma. **(b)** Cystically dilated follicular infundibulum containing a keratin plug with a large crescent-shaped aggregate of basal cell carcinoma with adjacent mucinous fibrous stroma. In the left lower corner of the photograph is a normal hair follicle adjacent to a neoplastic aggregate

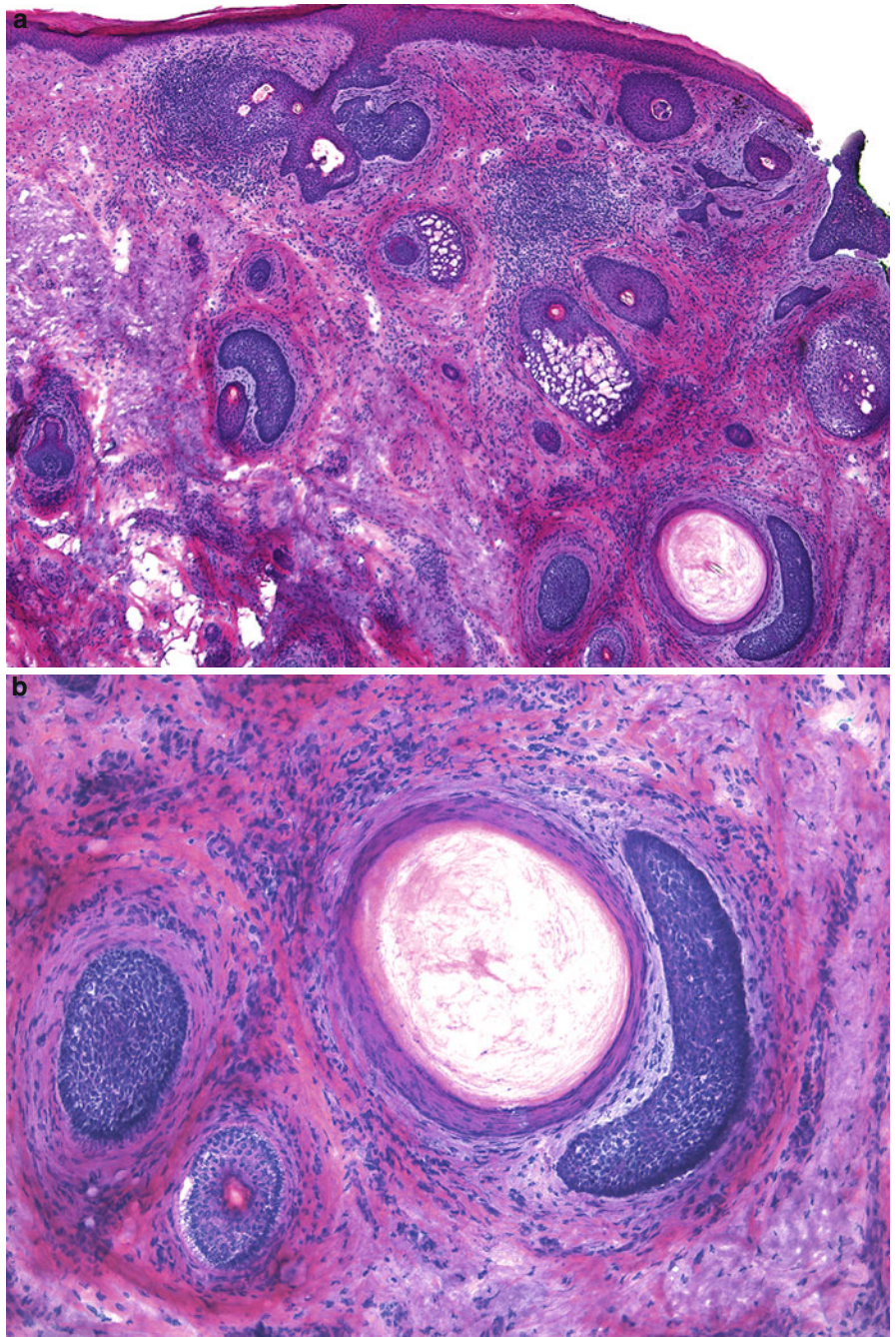


Fig. 5.3 (continued) (c) In the lower center of the photomicrograph is a normal hair follicle, in which all follicular layers are seen including a basaloid layer at the periphery, epithelial layers with cells with eosinophilic cytoplasm and a brightly eosinophilic cuticle-like area in the center. Adjacent to this hair follicle on the left is an oval aggregate of neoplastic basaloid cells with peripheral palisading. No particular follicular layers can be discerned in this aggregate, there is no evidence of keratinization, and no central channel for a hair shaft is present. Lack of clefting and stromal changes; however, can be a confounding feature highlighting the challenge in differentiating follicular structures from BCC

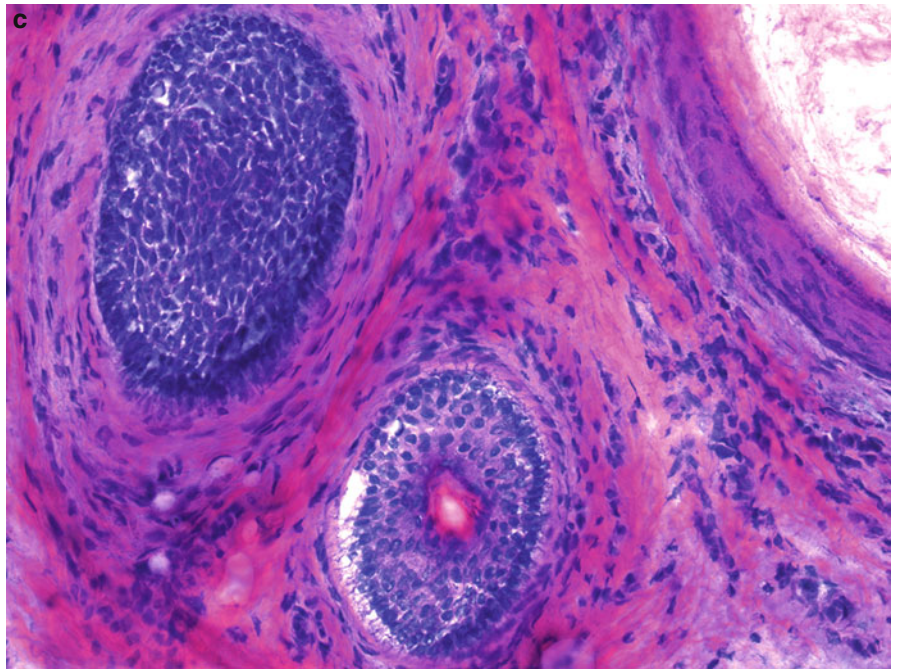


Fig. 5.4 Superficial basal cell carcinoma in the central portion of the photograph. The basaloid aggregates are coming off from the infundibular portion of the follicular epithelium. In the right lower corner there is a darkly stained hair follicle with slightly discernible crescent papilla in the lower pole and bulbar area above it (*thin arrow*). Immediately above this area is a hair follicle with an aggregate of basal cell carcinoma attached to it (*thick arrow*). Mucinous stroma surrounds the aggregate

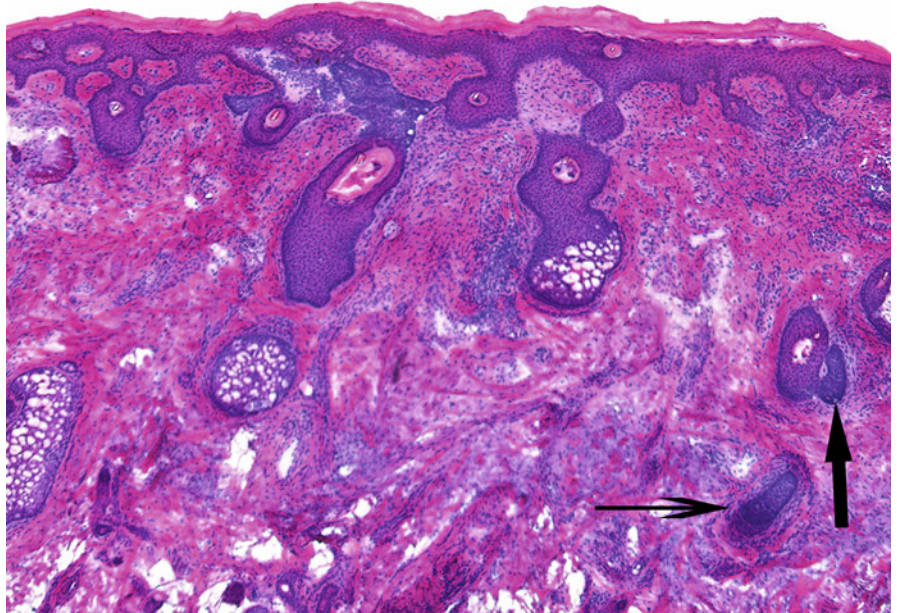


Fig. 5.5 Comparison of hair follicle and BCC: (a) Vellous hair follicle and BCC: A normal hair follicle in cross section in the right upper corner of the photograph. In the left portion of the photograph is an irregular aggregate of pleomorphic basaloid cells surrounded by cellular mucinous stroma. There is no particular organization of the neoplastic cells in layers as we see in the hair follicle. No clefting is observed. (b) Follicular bulb and papilla mimicking BCC: At the edge, on the left side of this photomicrograph, is a structure suspicious for basal cell carcinoma (*circle*)

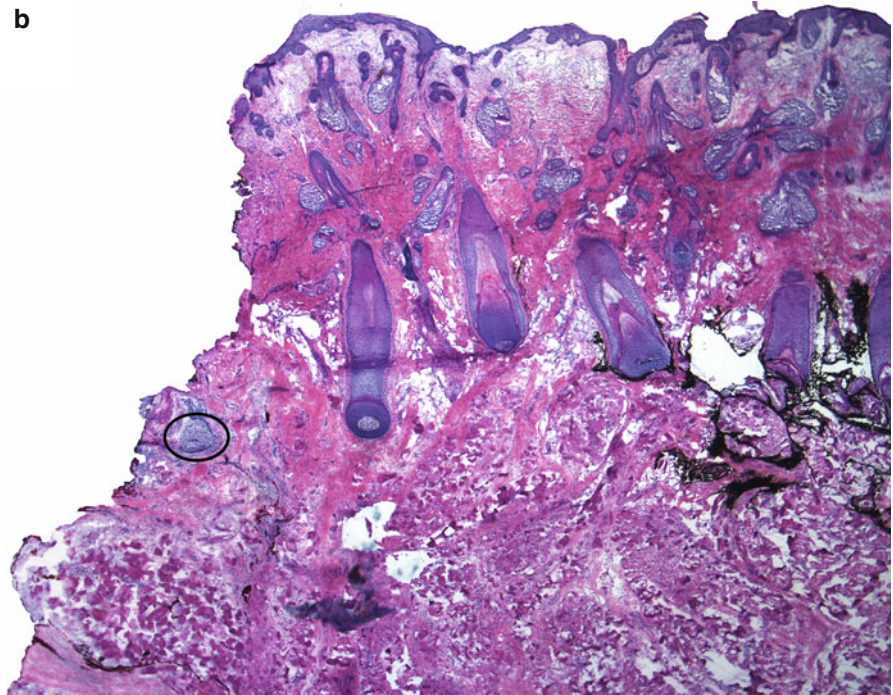
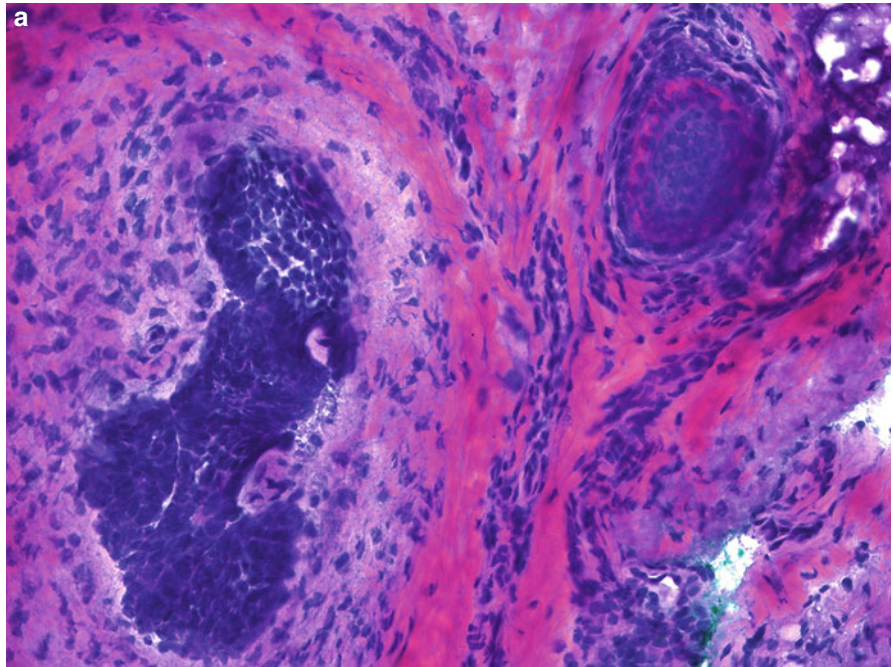


Fig. 5.5 (continued) (c) At higher magnification, there are great similarities between the central round area on the left, suspicious for basal cell carcinoma, and the area of adjacent follicular papilla on the right (*arrow*). This distorted and crushed follicular epithelium superior to the area of follicular papilla (*circle*) could be easily mistaken for basal cell carcinoma. (d) Cross-sectioned follicular papilla (*circle*) with bulbar epithelium in the upper pole

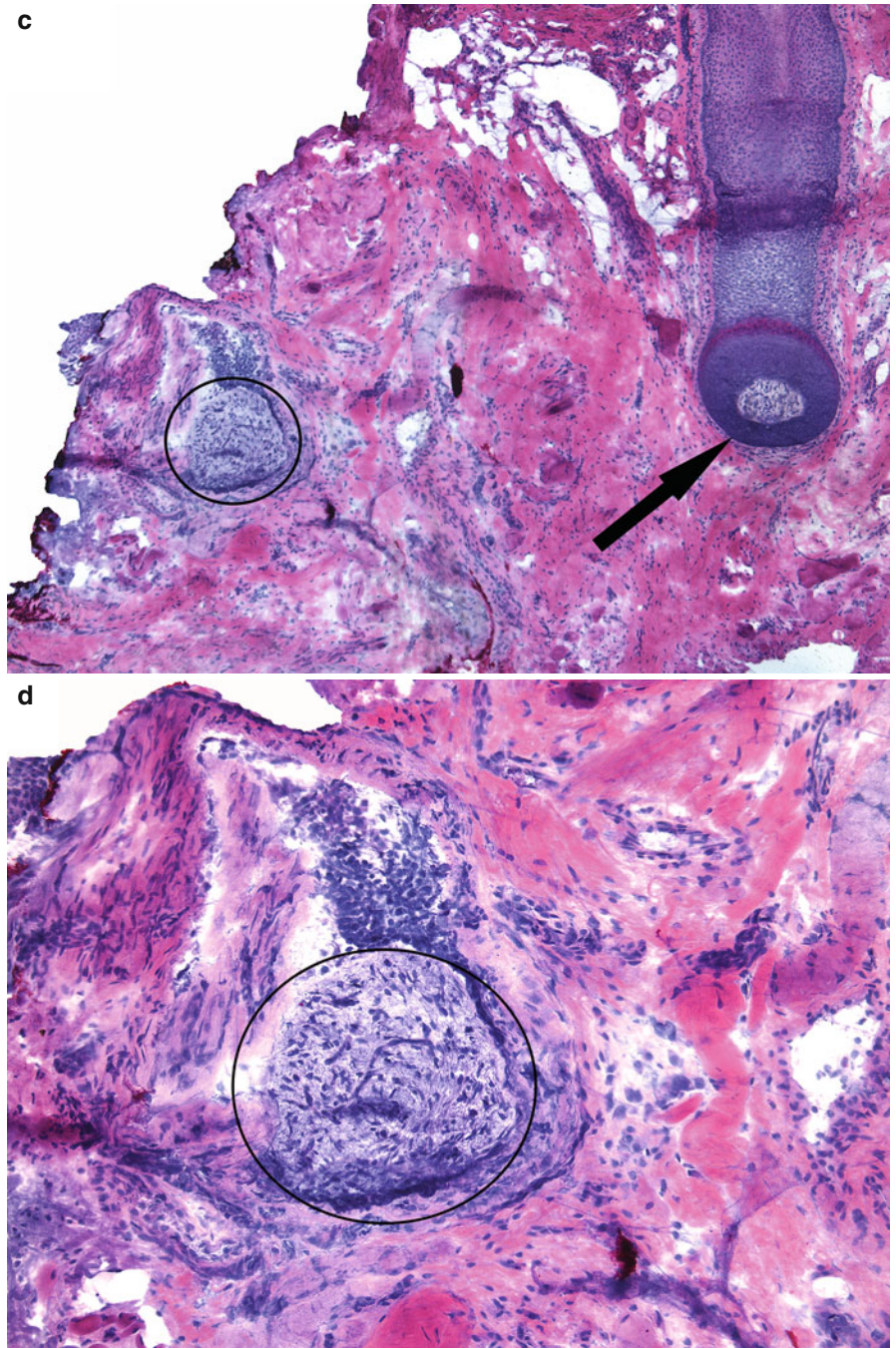


Fig. 5.5 (continued) (e) A consecutive deeper section demonstrates the papilla and its associated circumferential epithelium (arrow). (f) Higher magnification showing similarities between the follicular papillae in both hair follicles

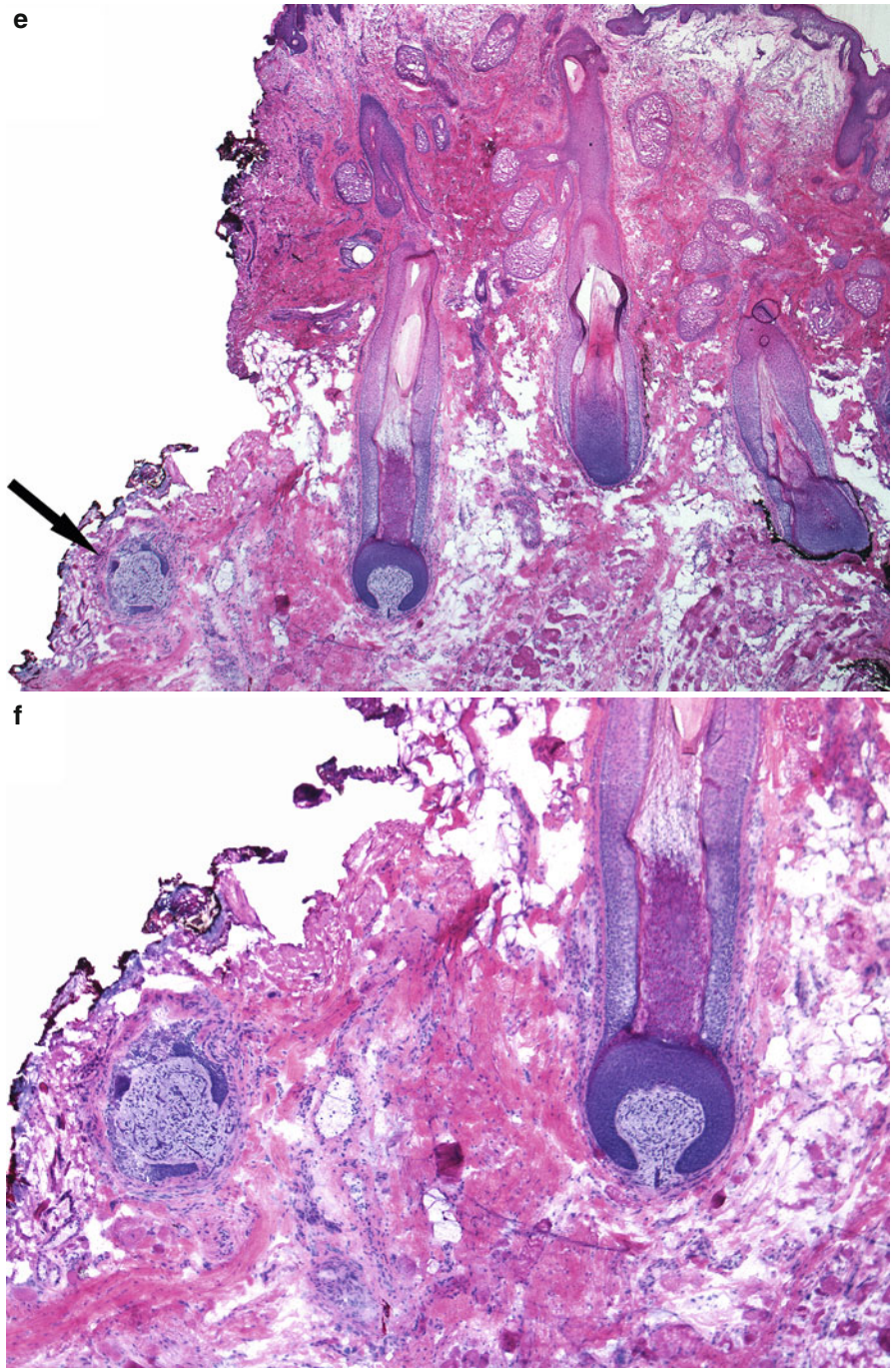


Fig. 5.5 (continued) (g) At this magnification the blood vessels within the follicular papilla can be appreciated (arrows). (h) Crushed and distorted lower portion of a hair follicle may be confused for BCC due to their basaloid staining when seen in this format (i.e., sectioned in this manner without the rest of the follicle being visible). However, the most helpful feature in identifying the follicle is the eosinophilic, corrugated perifollicular fibrous sheath (arrow)

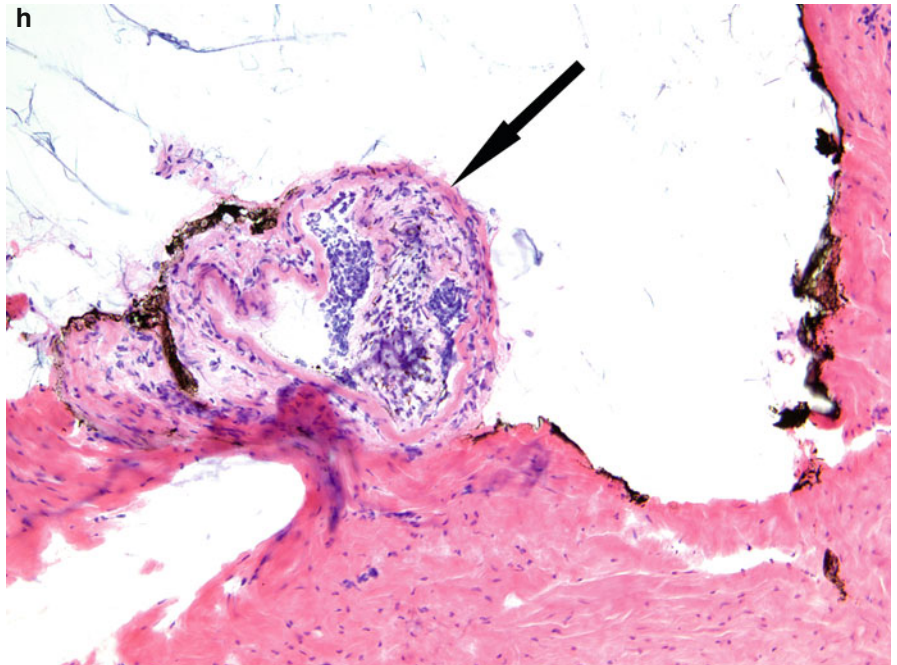
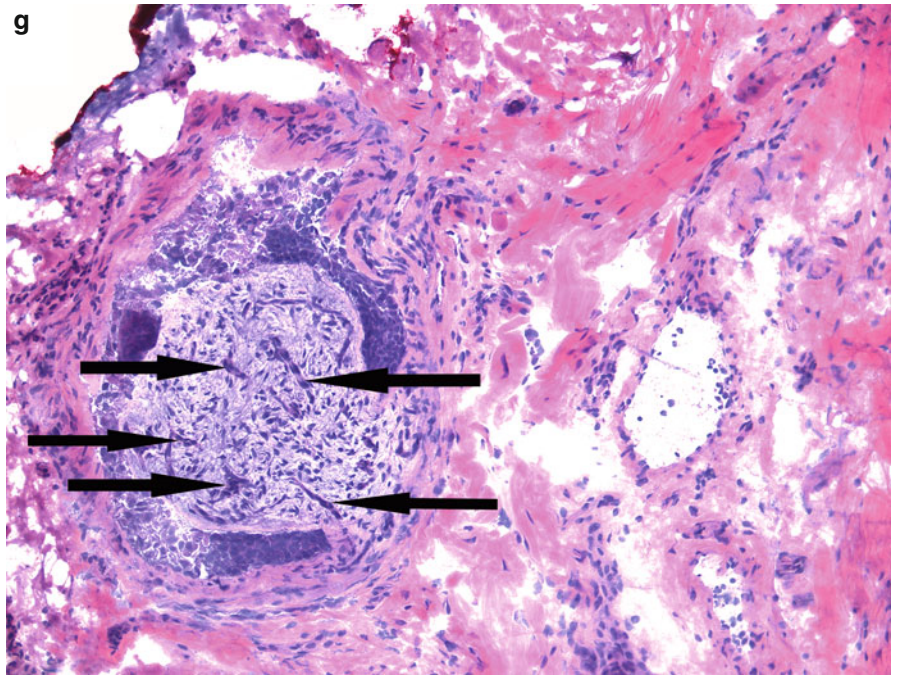


Fig. 5.6 Infiltrative basal cell carcinoma: (a) Scanning magnification reveals a suspicious small, angulated, slender basaloid aggregate around a hair follicle (*arrow*). At this magnification, this can easily be overlooked or misinterpreted as a component of a follicular structure (i.e., mantle). Perhaps the only helpful clue is the slightly more basophilic staining of the aggregate in comparison to the nearby follicles. (b) Higher magnification reveals that this basaloid aggregate is composed of hyperchromatic and pleomorphic cells (*arrow*). However, it is still challenging to discern whether this is carcinoma due to the lack of features such as stromal changes, clefting, peripheral palisading, and even any surrounding inflammation. (c) Further sectioning into the tissue block reveals angulated and irregularly shaped aggregates, now making the diagnosis obvious for basal cell carcinoma

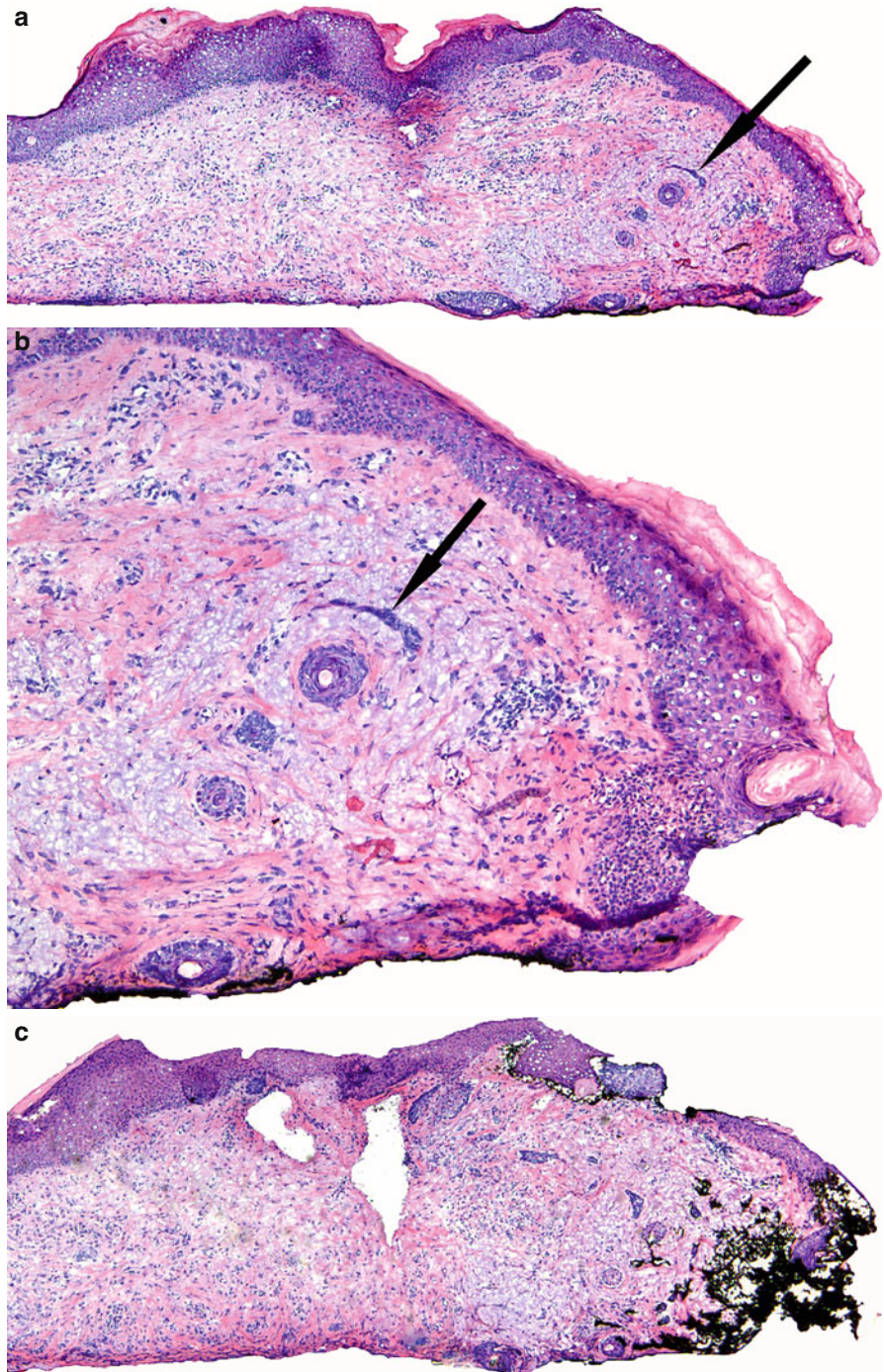


Fig. 5.6 (continued) (d) Higher magnification of the neoplastic aggregates composed of basaloid cells with large, pleomorphic and hyperchromatic nuclei

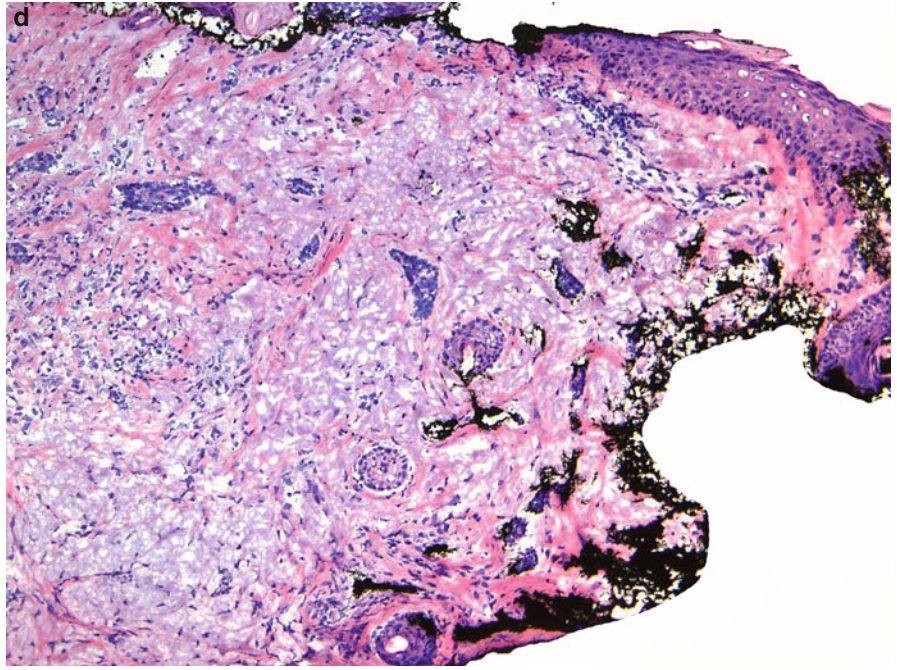


Fig. 5.7 BCC and hair follicle: (a) A normal hair follicle in cross section in the left lower portion of the photomicrograph surrounded by a thin fibrous sheet (*arrow*). Three irregular aggregates of basal cell carcinoma embedded in thick fibrous stroma. The aggregates are comprised of neoplastic cells with high nuclear to cytoplasmic ratio. The cells appear more eosinophilic toward the center but there is no discrete organization as one would appreciate in a normal hair follicle. (b) Higher magnification showing a small lumen surrounded by irregular crenulated eosinophilic material representing a sebaceous duct completely surrounded by neoplastic basaloid cells of basal cell carcinoma. Although this could be confused with a distorted hair follicle, the lack of organized layers and lack of trichohyalin keratinization is consistent with a basal cell carcinoma. The follicular differentiation of the BCC is demonstrated by the presence of a sebaceous duct within the neoplastic aggregate

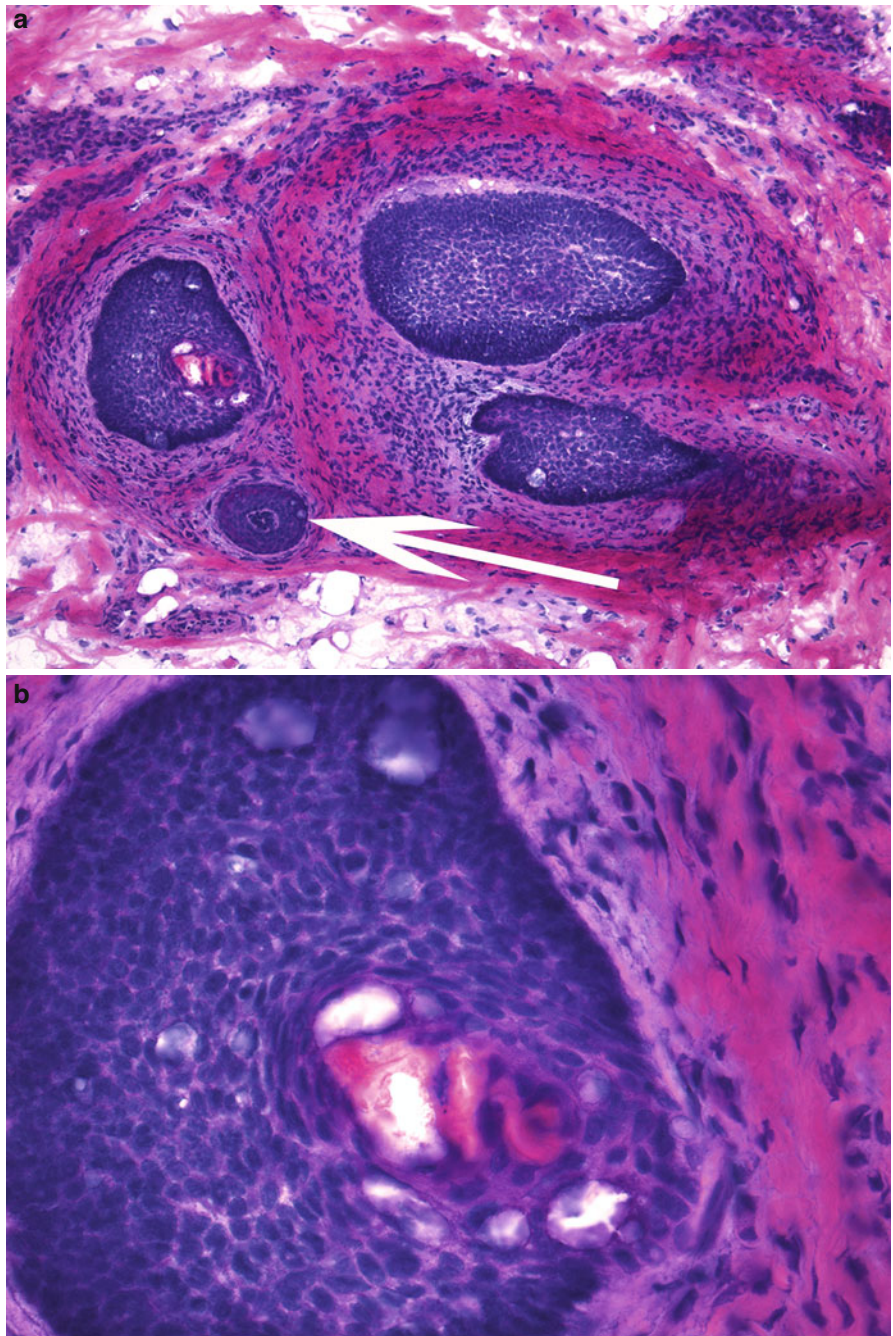


Fig. 5.8 Comparison of hair follicles and BCC. Hair follicles show small aggregates of sebocytes (*ellipse*) and occasional sebaceous ducts (*rectangle*). There is a layering in the appearance of the follicular epithelium with a basaloid layer peripherally and more eosinophilic layers centrally. The nuclei of the follicular epithelium are uniform and monomorphic. In contrast, the neoplastic aggregates (*arrow*) are more irregularly shaped and contain larger cells with hyperchromatic nuclei, and focal peripheral palisading

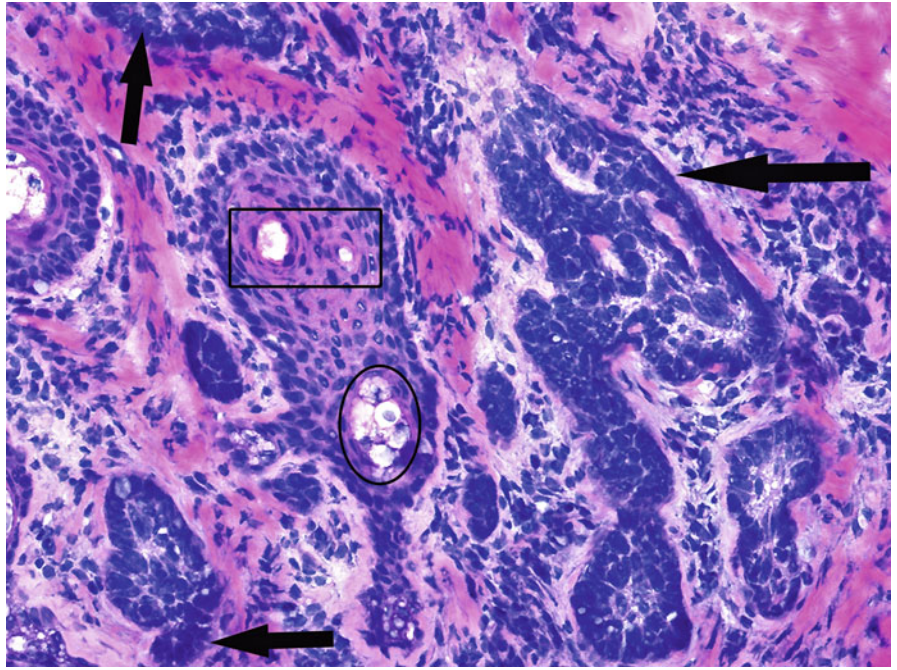


Fig. 5.9 (a) Basal cell carcinoma (*ellipse*) arising from the lower portion of a hair follicle. (b) Higher magnification demonstrating angulated shape, peripheral palisading, hyperchromasia, pleomorphism, and stromal changes

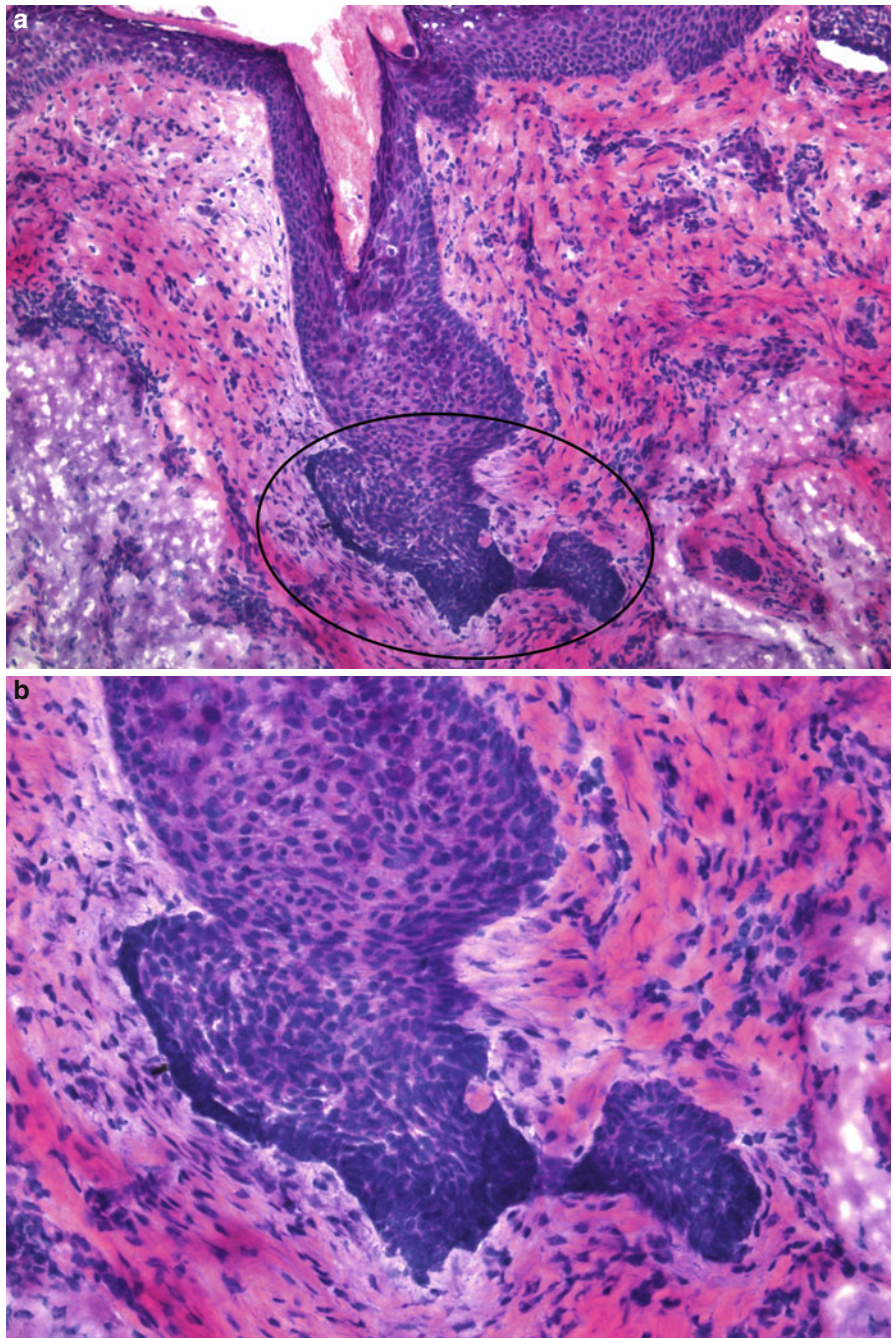


Fig. 5.10 BCC with FBP: (a) Obvious nodular basal cell carcinoma is appreciated in this section. (b) Irregular angulated and round basal cell aggregates are appreciated in the lower dermis. Surrounding stromal changes can also be seen. Centrally, there is a hair follicle from which angulated basaloid aggregates emanate. It appears that these are connected to the underlying basal cell carcinoma. *Arrows* point to two hair follicles from which the basal cell aggregates arise. One can appreciate the difference in the deep basophilic color of the aggregates in contrast to the more eosinophilic follicular epithelium

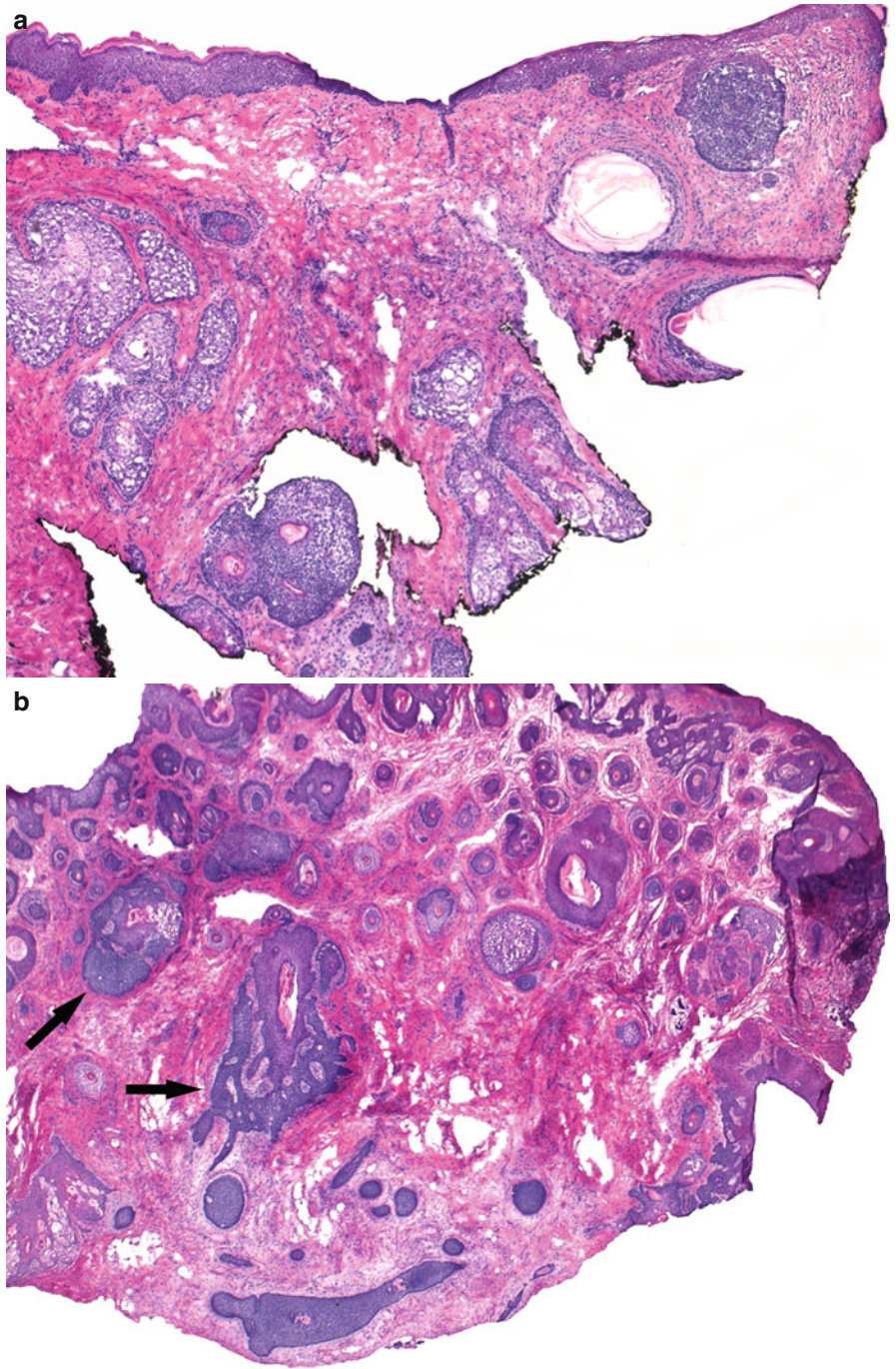


Fig. 5.10 (continued) **(c)** In a subsequent section of this case, there are many hair follicles with elaborate shapes. Sebaceous ducts can be appreciated within the hair follicles. The hair follicles are vertically oriented. There is no stromal change around them. Some peripheral palisading, however, can be appreciated. Nevertheless, we believe that these are banal follicular structures and are not consistent with basal cell carcinoma and may demonstrate a proliferative epiphenomenon. **(d)** A subsequent stage and section showing indisputable BCC on the right and probable folliculocentric basaloid proliferation (FBP) on the left. In certain cases it might be impossible to distinguish between the two entities

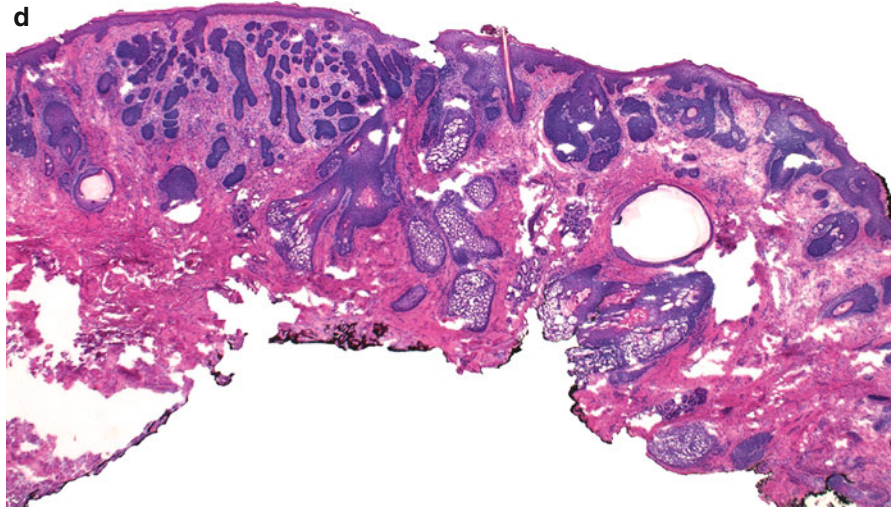
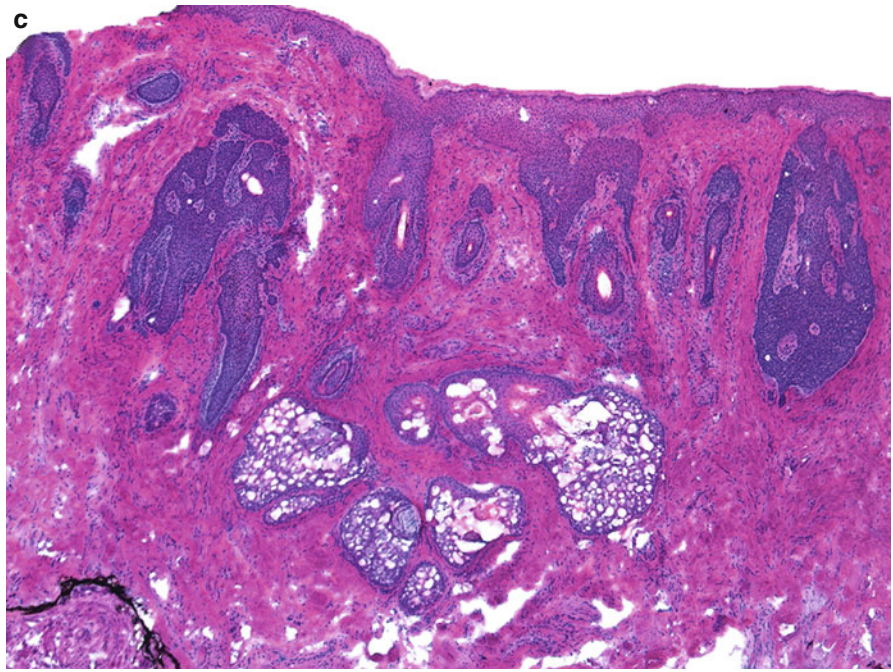
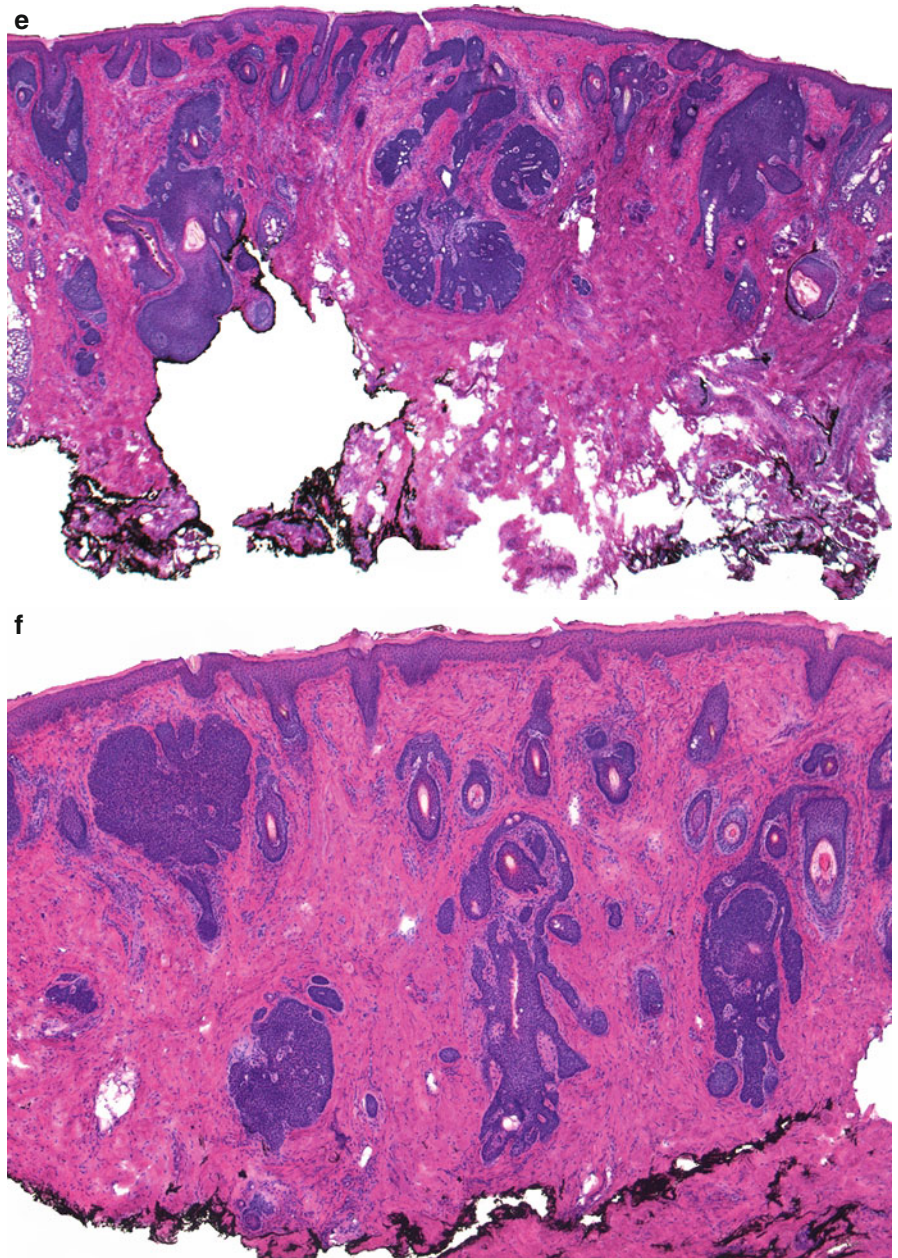


Fig. 5.10 (continued) (e) Sections like these are frustrating for Mohs surgeons. There are structures within the central portion of these sections that have the overall configuration of a hair follicle. However, the stromal changes as well as the presence of basaloid aggregates emanating from these follicles make the diagnosis of BCC versus FBP very challenging. (f) The overall vertical architectural pattern favors a benign FBP



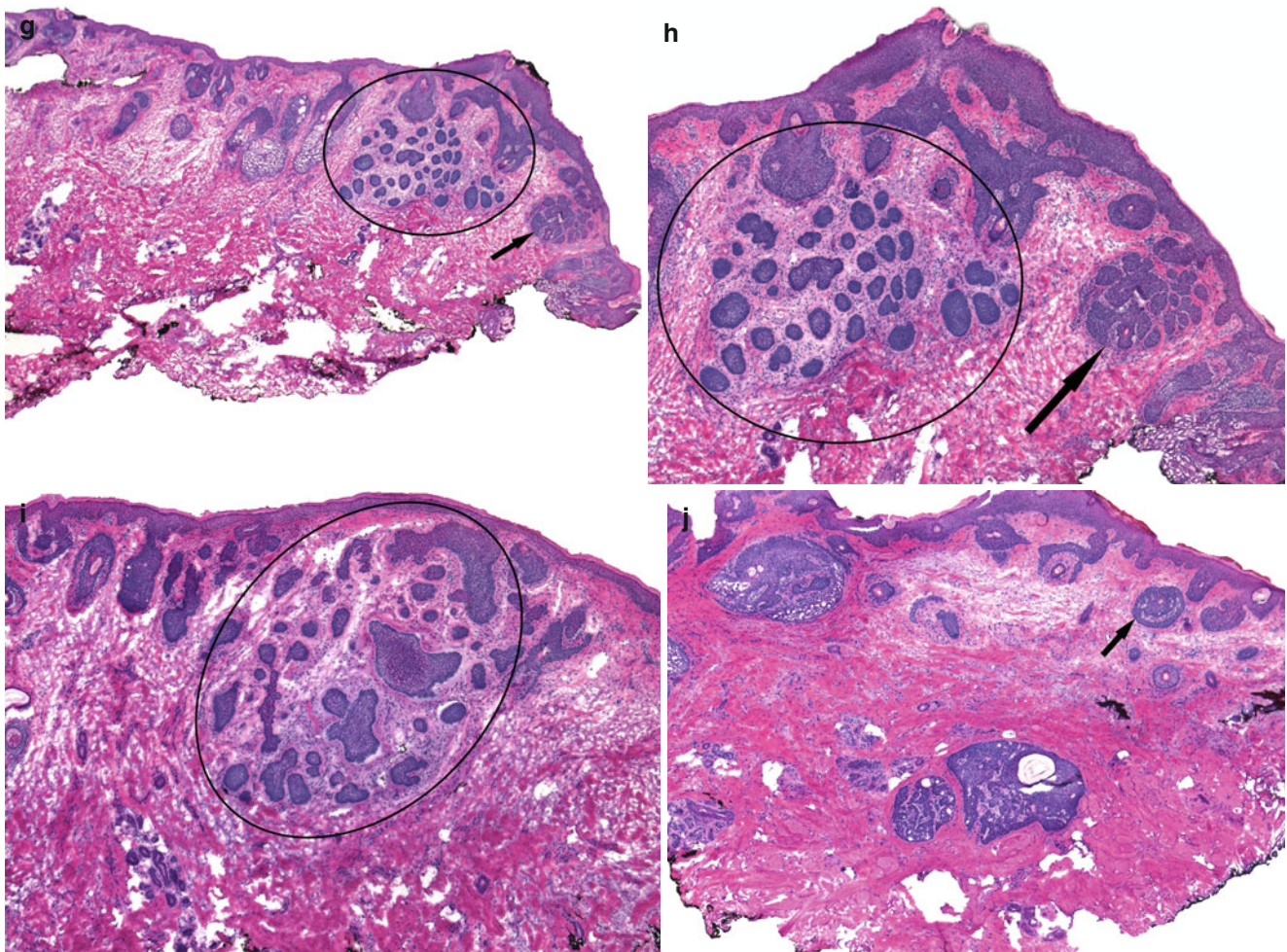


Fig. 5.10 (continued) (g–j) This case of BCC included sections, which had follicular structures that were not classic for FBP (arrows) as well as areas concerning for and others consistent with BCC (ellipses). This proliferative phenomenon is not uncommonly encountered with BCC on the nose and presents a significant challenge for Mohs surgeons.

(h) The stromal changes and peripheral palisading of the neoplastic aggregates from the basal cell carcinoma can be better appreciated here in the central portion of this section (ellipse). In addition, the more eosinophilic epithelial aggregates emanating from the hair follicle on the right show different appearance (arrow)

Fig. 5.10 (continued) (k) Higher magnification showing irregular follicular structures with a hair shaft in one of them (arrow)

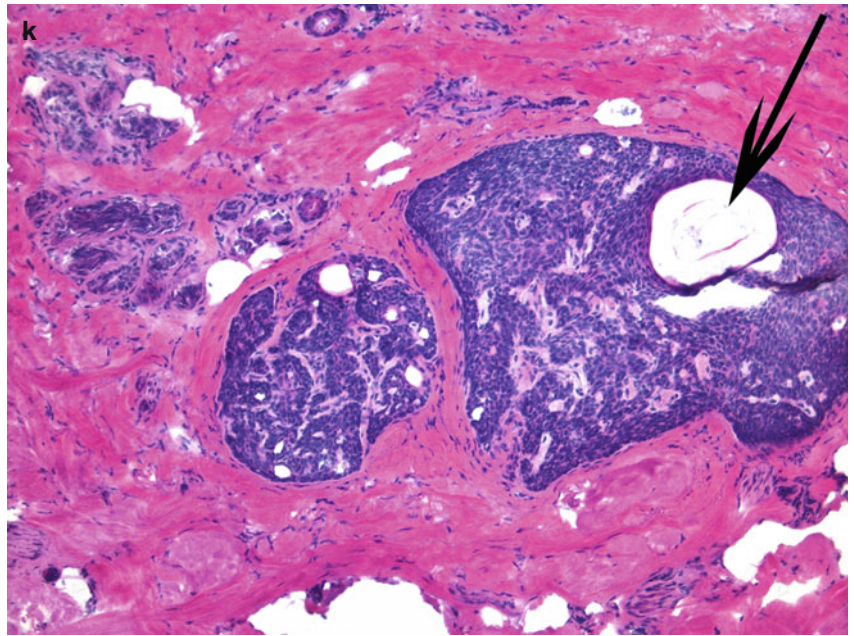


Fig. 5.11 (a, b) A central distorted follicle with anastomosing epithelial proliferation of basaloid cells, which represents a basaloid follicular hamartoma (BFH) (ellipse)

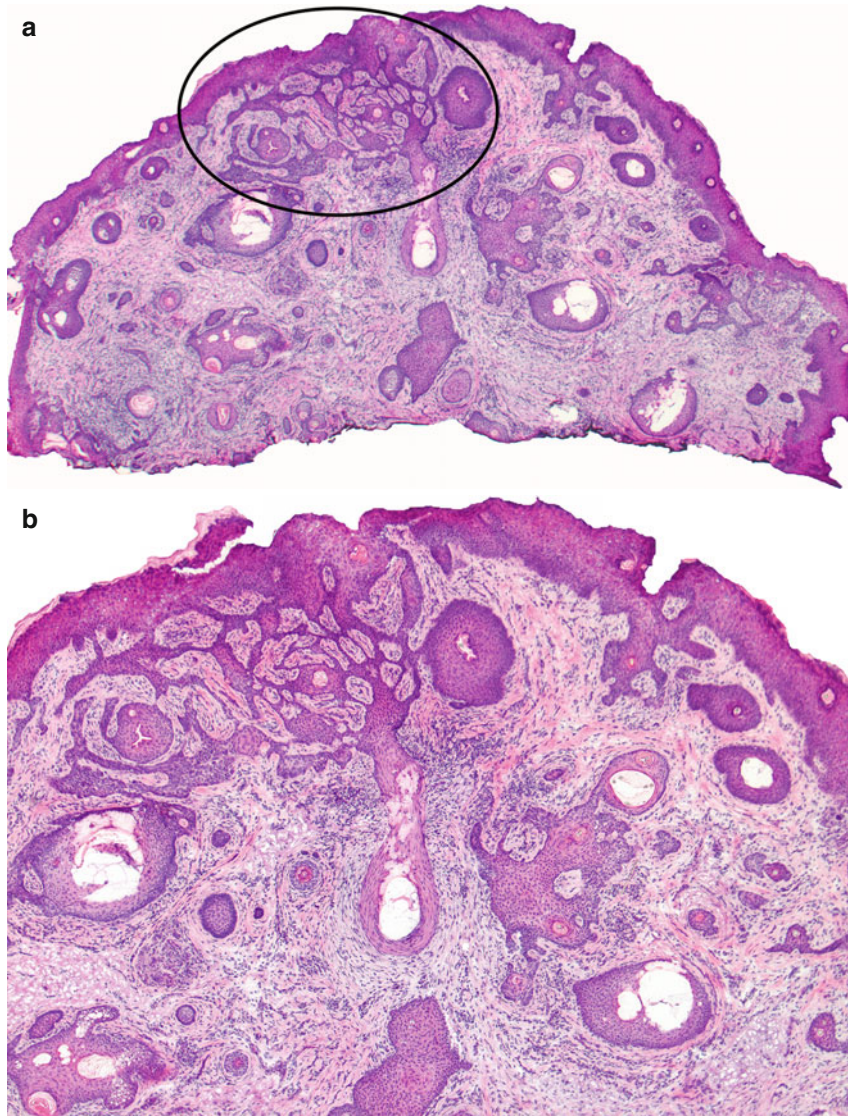


Fig. 5.12 BCC and BFH: (a) This photomicrograph shows a section with superficial basal cell carcinoma on the left and basaloid follicular hamartomas on the right (*circle* and *rectangle*). (b) Higher magnification demonstrates a complex follicular basaloid structure with aggregates that connect with each other. Clear-cut features of basal cell carcinoma such as peripheral palisading, clefting, and mucinous stroma are not present

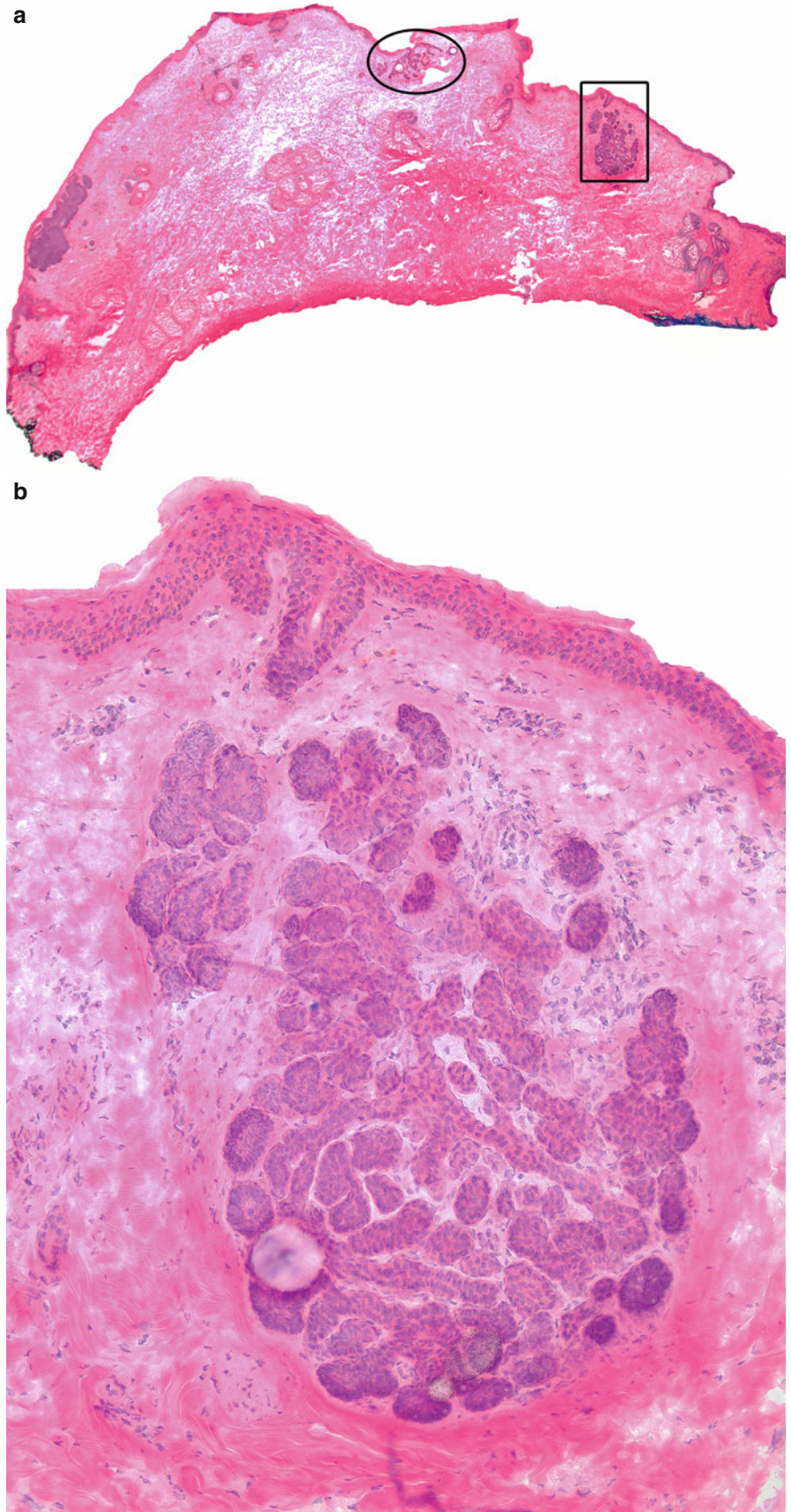


Fig. 5.12 (continued) (c) In another section of the same case, there is basal cell carcinoma (*ellipse*) adjacent to BFH around a dilated follicular infundibulum

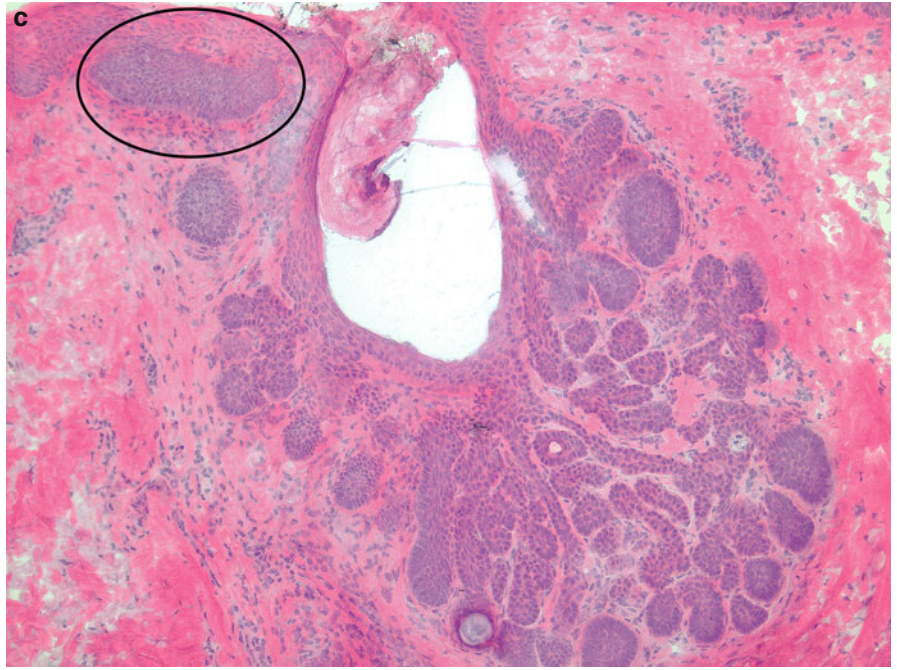


Fig. 5.13 BFH: Complex epithelial structures that resemble hair follicles are seen together with cystically dilated sebaceous ducts lined by pink cuticle. The epithelial aggregates arise from and connect to the epidermis

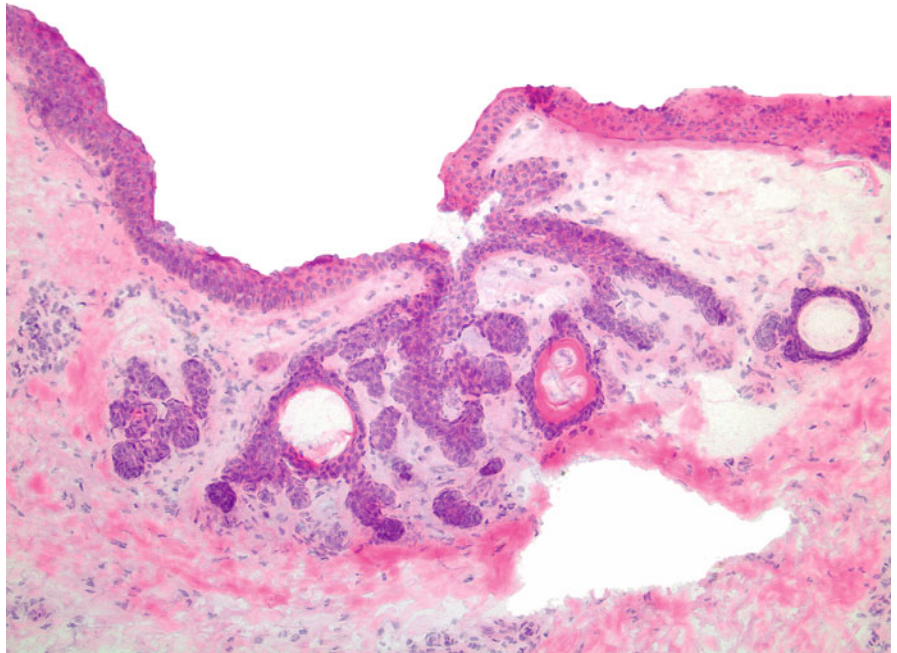


Fig. 5.14 (a) Two complex follicular structures that may present a challenge for the Mohs surgeon. On the right there are multiple anastomosing basaloid epithelial aggregates concerning for BCC. On the left there is a BFH. (b) Higher magnification of the BFH

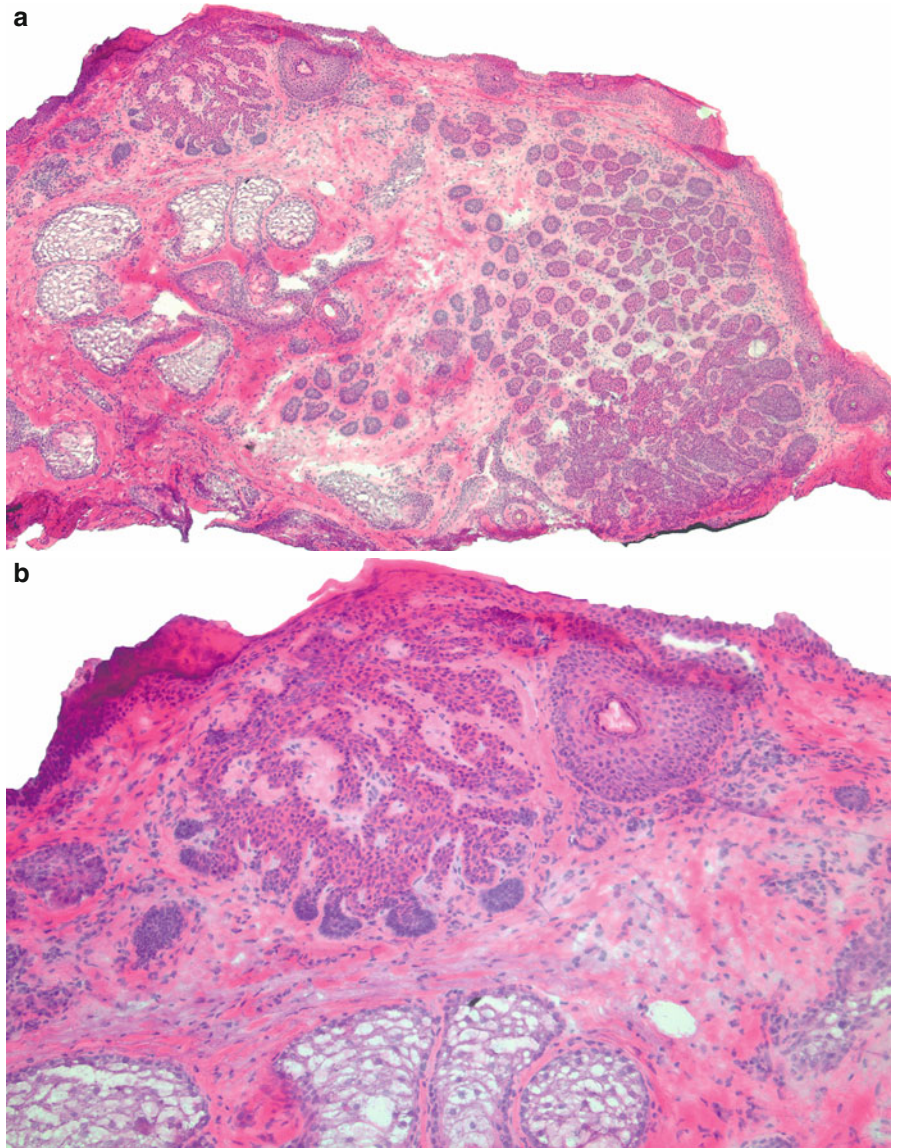


Fig. 5.15 BFH: Well-differentiated elaborate follicular epithelial proliferation connected to the overlying epidermis

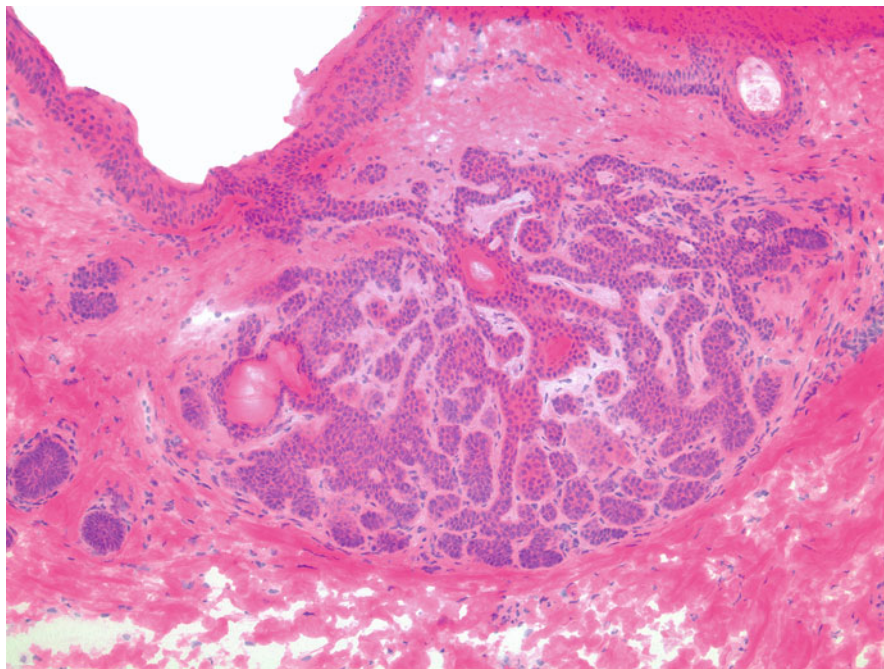


Fig. 5.16 (a) Infiltrative BCC (*arrows*) and immature follicular structures (*circles*). (b) Irregular follicular proliferation: Basaloid aggregates mimicking BCC in the mid reticular dermis. Note the lack of peripheral palisading, stromal reaction, and clefting characteristic of BCC. Lack of these features support the diagnosis of a benign follicular proliferation

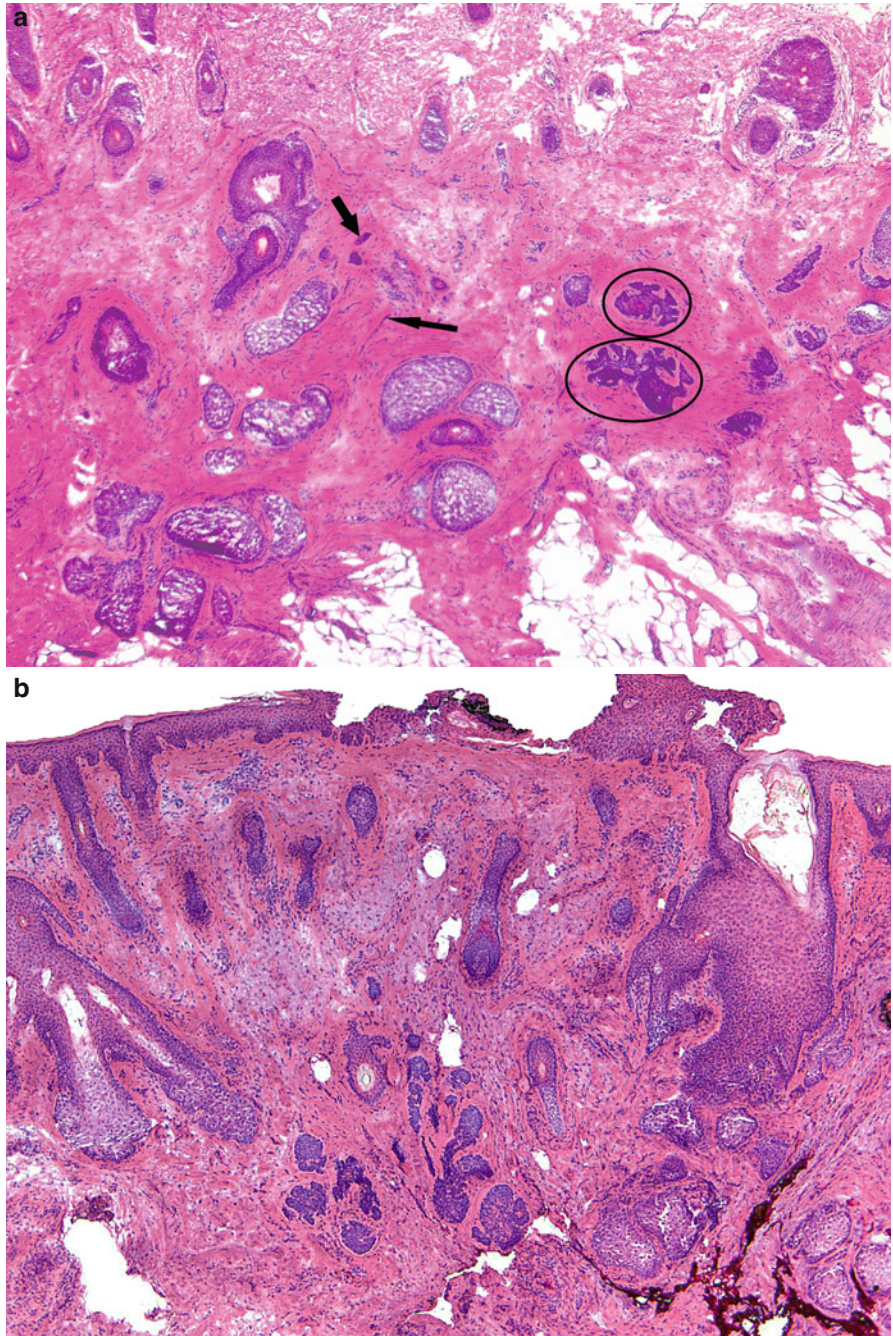


Fig. 5.17 BCC versus hair follicle: (a) A “funny looking” hair follicle showing a bulb and papilla (*ellipse*). Note the dense fibrous perifollicular sheath. (b) In contrast, this aggregate of basal cell carcinoma shows an irregular contour and surrounding inflammation (*circle*)

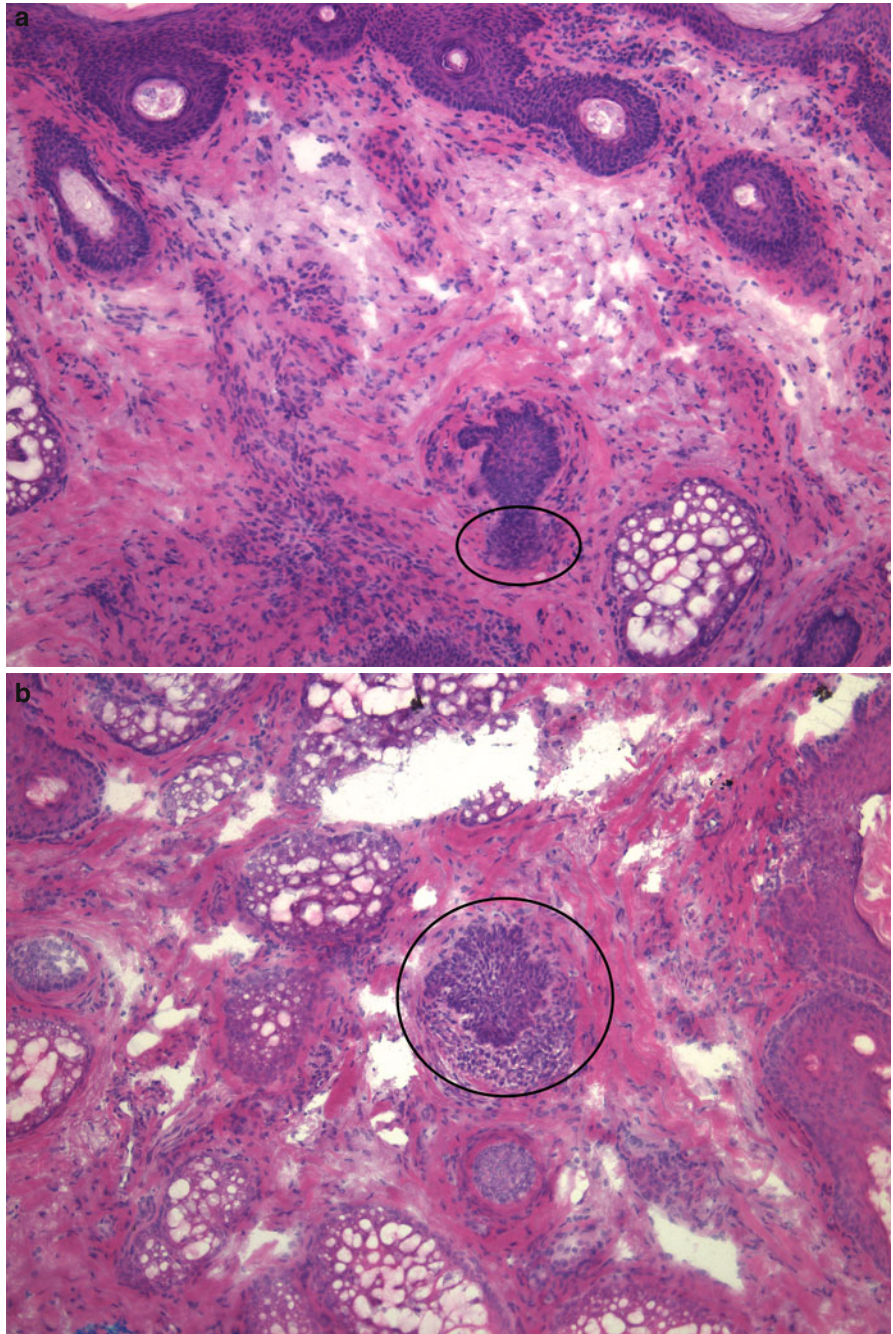


Fig. 5.17 (continued) (c) At higher magnification pyknotic cells (*arrows*) and pleomorphic hyperchromatic nuclei are noted within this tumor aggregate. Focal palisading is present. No fibrous sheath is identified and there is prominent surrounding inflammation

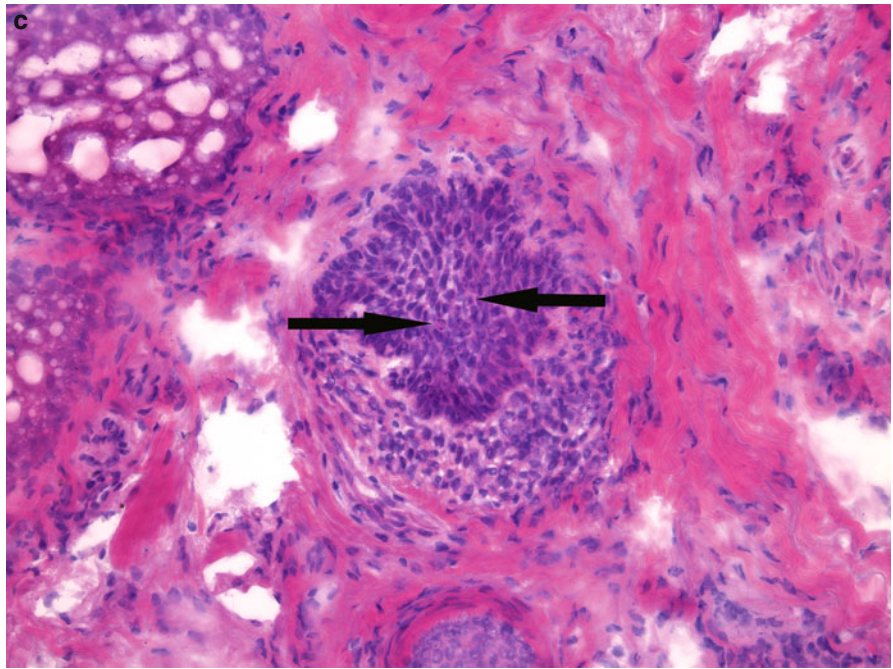


Fig. 5.18 (a) Irregular follicular proliferation adjacent to basal cell carcinoma: the neoplastic aggregates in this section demonstrate the classic features of BCC: peripheral palisading, stromal reaction, and clefting. (b) Surrounded by BCC is a central area of benign-appearing follicular structures (*ellipse*)

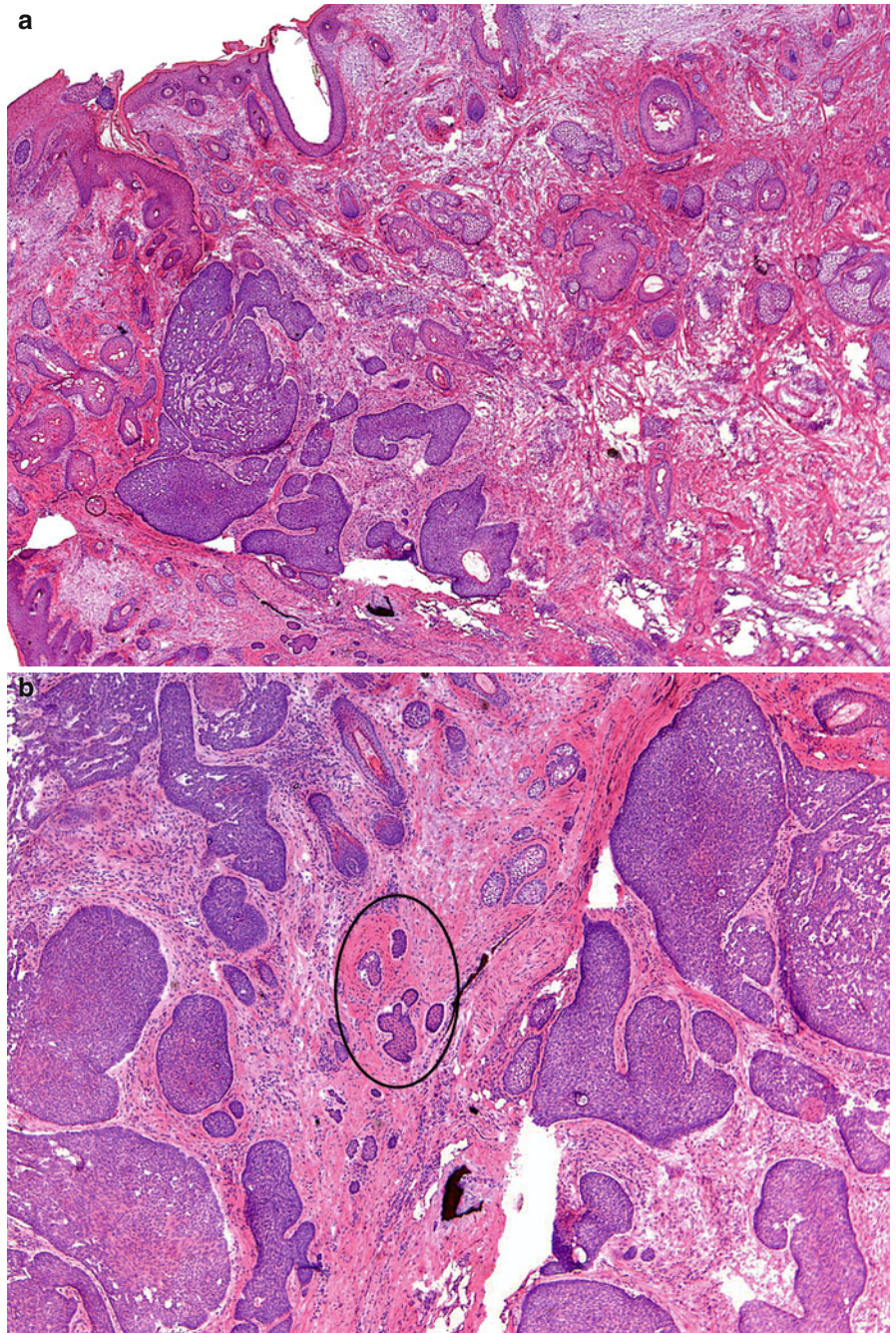


Fig. 5.18 (continued) (c) At higher magnification the follicular structures reveal a basaloid outer layer and more eosinophilic follicular epithelium with small, monomorphic cells centrally. Some of the follicular structures are surrounded by prominent eosinophilic perifollicular fibrosis (*arrow*). In contrast, the BCC on the far right displays prominent peripheral palisading and contains basaloid cells with large pleomorphic nuclei in disordered pattern

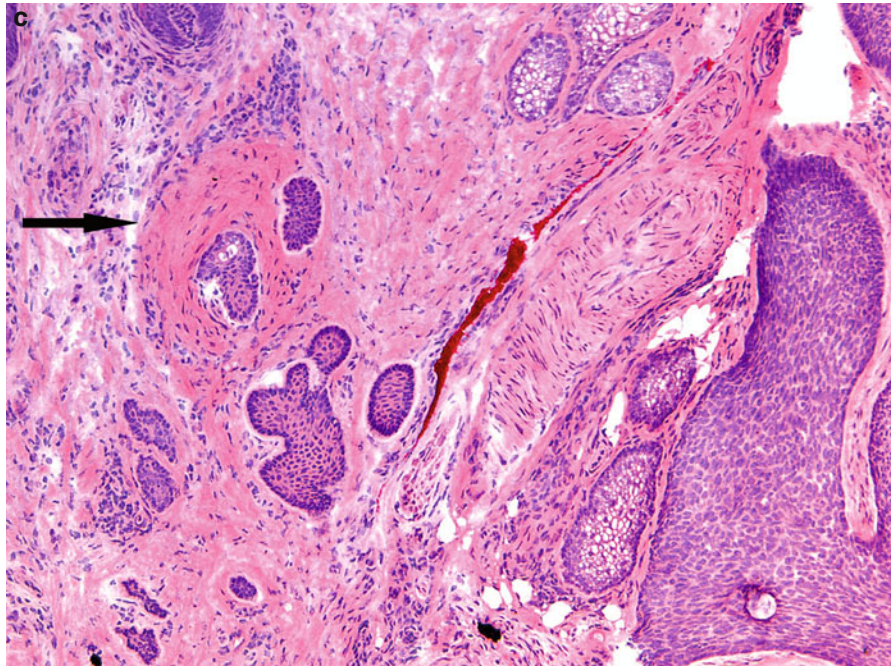


Fig. 5.19 Follicle versus BCC: **(a)** A basaloid follicular structure concerning for possible BCC is present in the center of this tissue section. **(b)** The overall architecture and the presence of sebaceous areas containing sebocytes with vacuolated cytoplasm support the diagnosis of a follicle

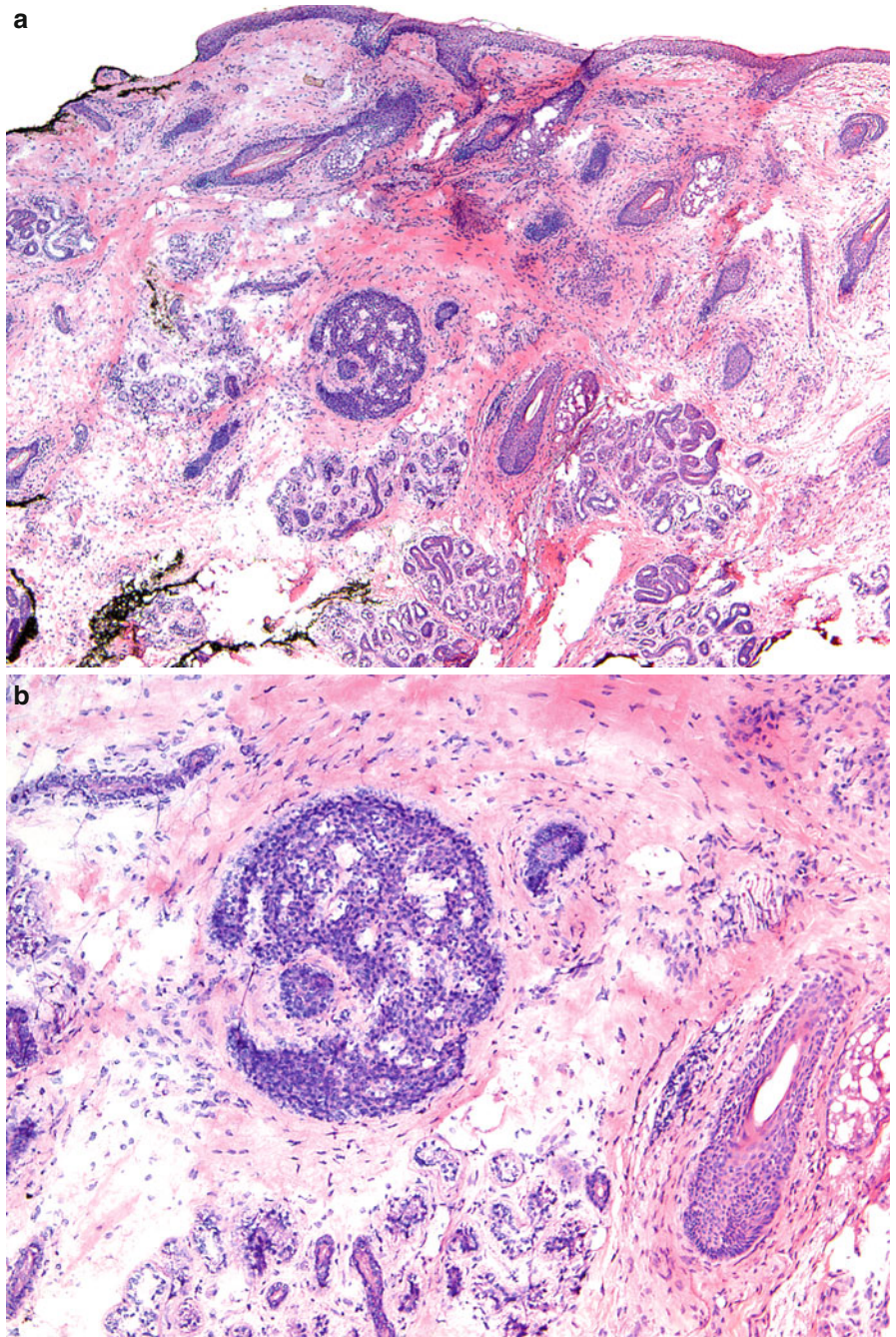


Fig. 5.20 BCC vs. follicle: (a, b) Basal cell carcinoma embedded within a scar and resembling follicular structures. The tumor aggregates are very basophylic, lacking any eosinophilic centers that are often seen within hair follicles

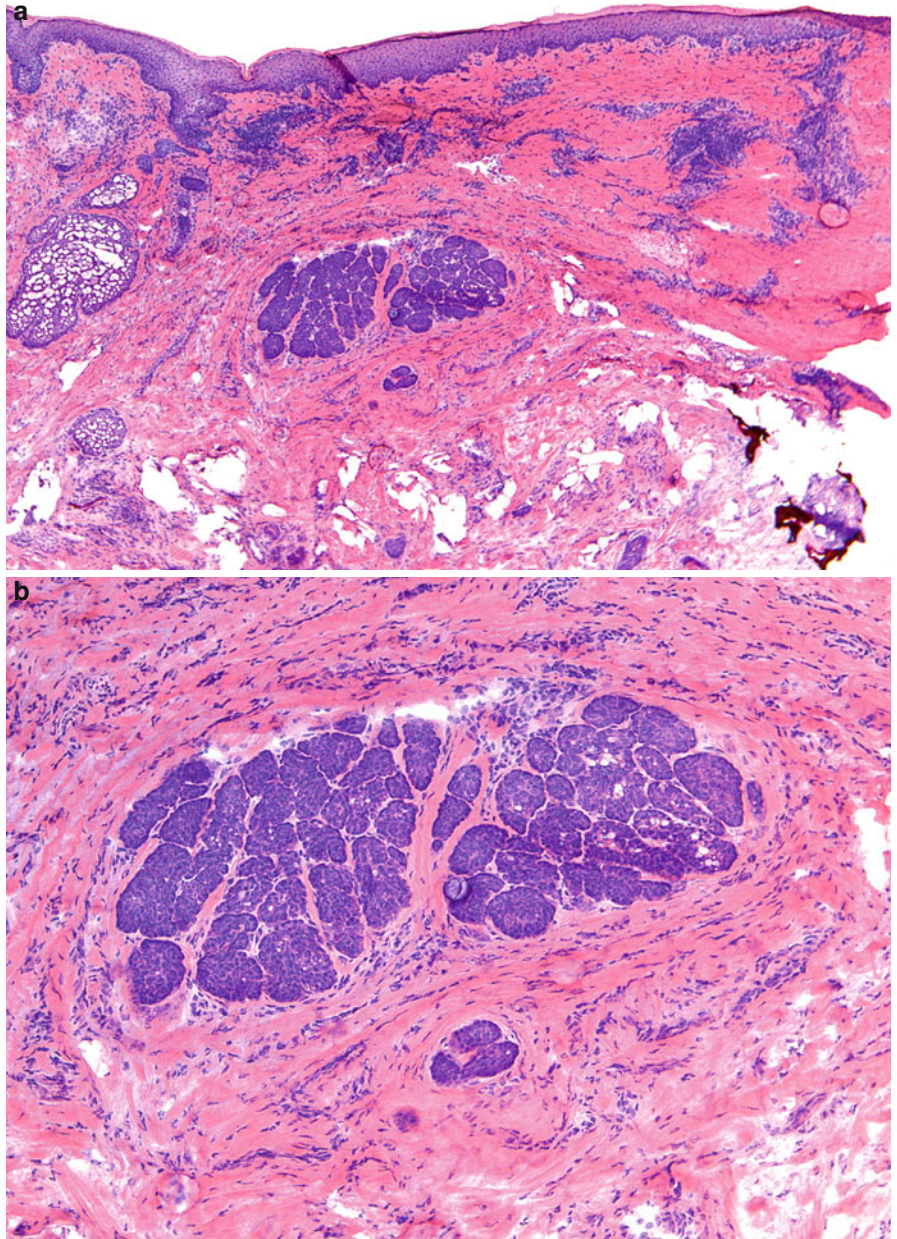


Fig. 5.20 (continued) (c) In a subsequent section there are angulated basaloid tumor aggregates in the deep tissue on the right side (arrows) confirming the diagnosis of BCC

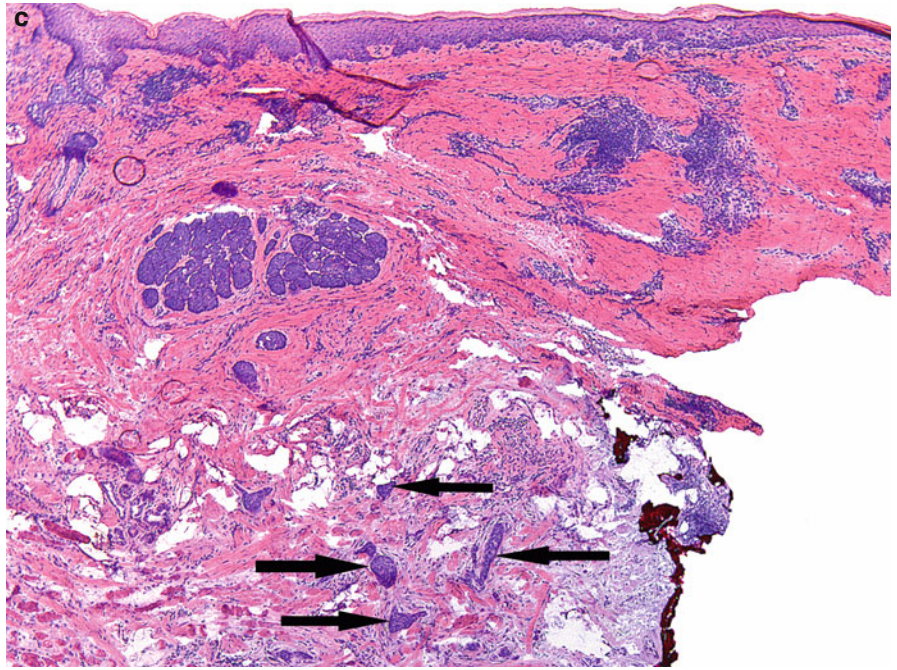


Fig. 5.21 BCC vs. follicle: (a) An irregular follicular structure is present at the bottom of this tissue section (*ellipse*). Compare the similar overall architecture of this to the more obvious follicular-sebaceous unit on the left (*rectangle*). (b) Several features help support the diagnosis of benign follicular structure over carcinoma: the central more eosinophilic staining epithelial cells, the presence of sebocytes with vacuolated cytoplasm and scalloped nuclei (*thin arrow*), a surrounding pink fibrous sheath as well as adjacent erector pili muscles (*thick arrow*)

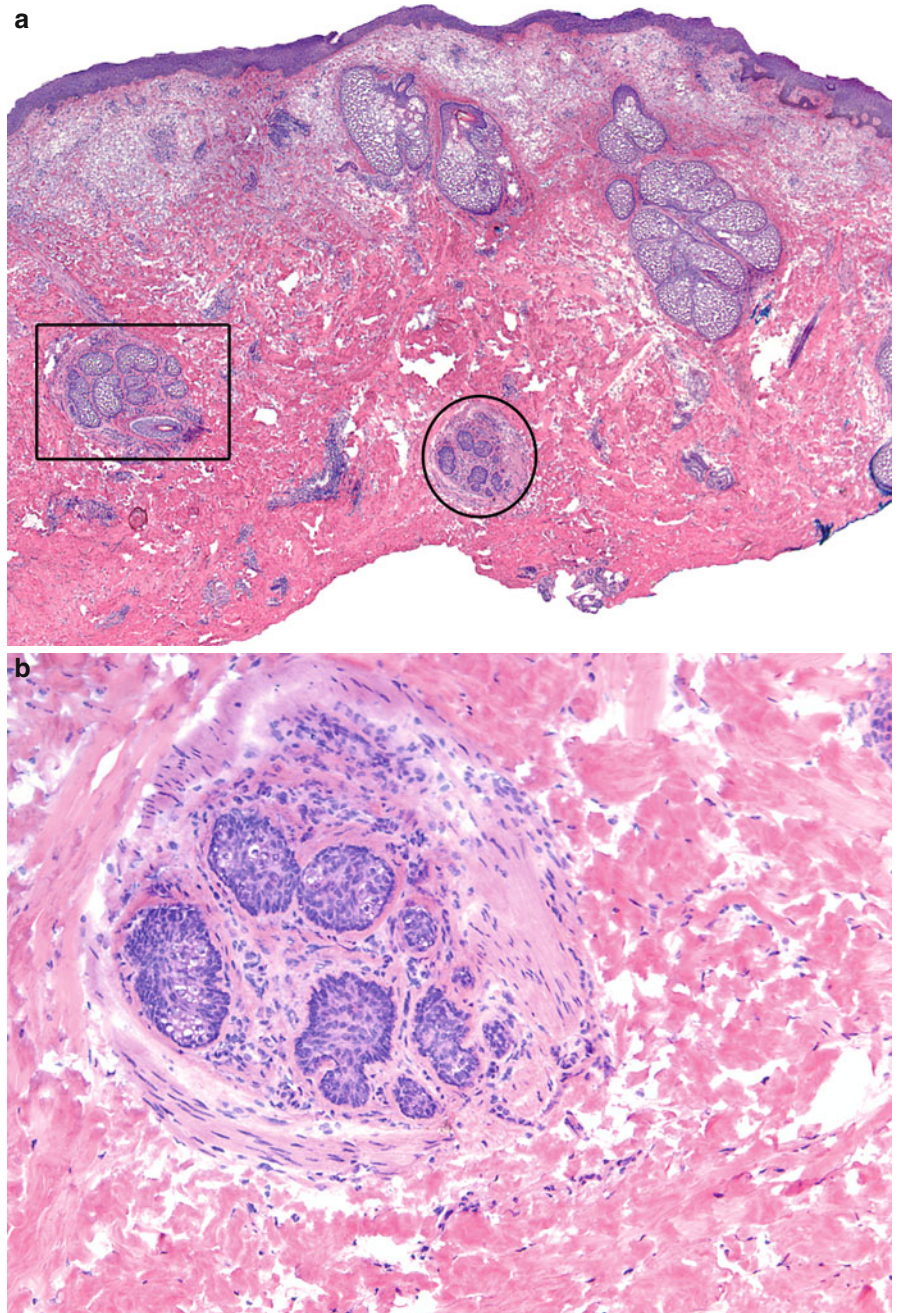


Fig. 5.21 (continued) (c) Further sectioning into the tissue block can help clarify the diagnosis. In this case a deeper section reveals an indisputable hair follicle. (d) Higher magnification demonstrates monomorphic, more glassy and eosinophilic staining epithelial cells in the center of the aggregates as well as the presence of vacuolated sebocytes. These findings confirm the diagnosis of a folliculo-sebaceous unit. Note the lack of pertinent findings for carcinoma such as clefting, peripheral palisading, and pleomorphic or apoptotic cells

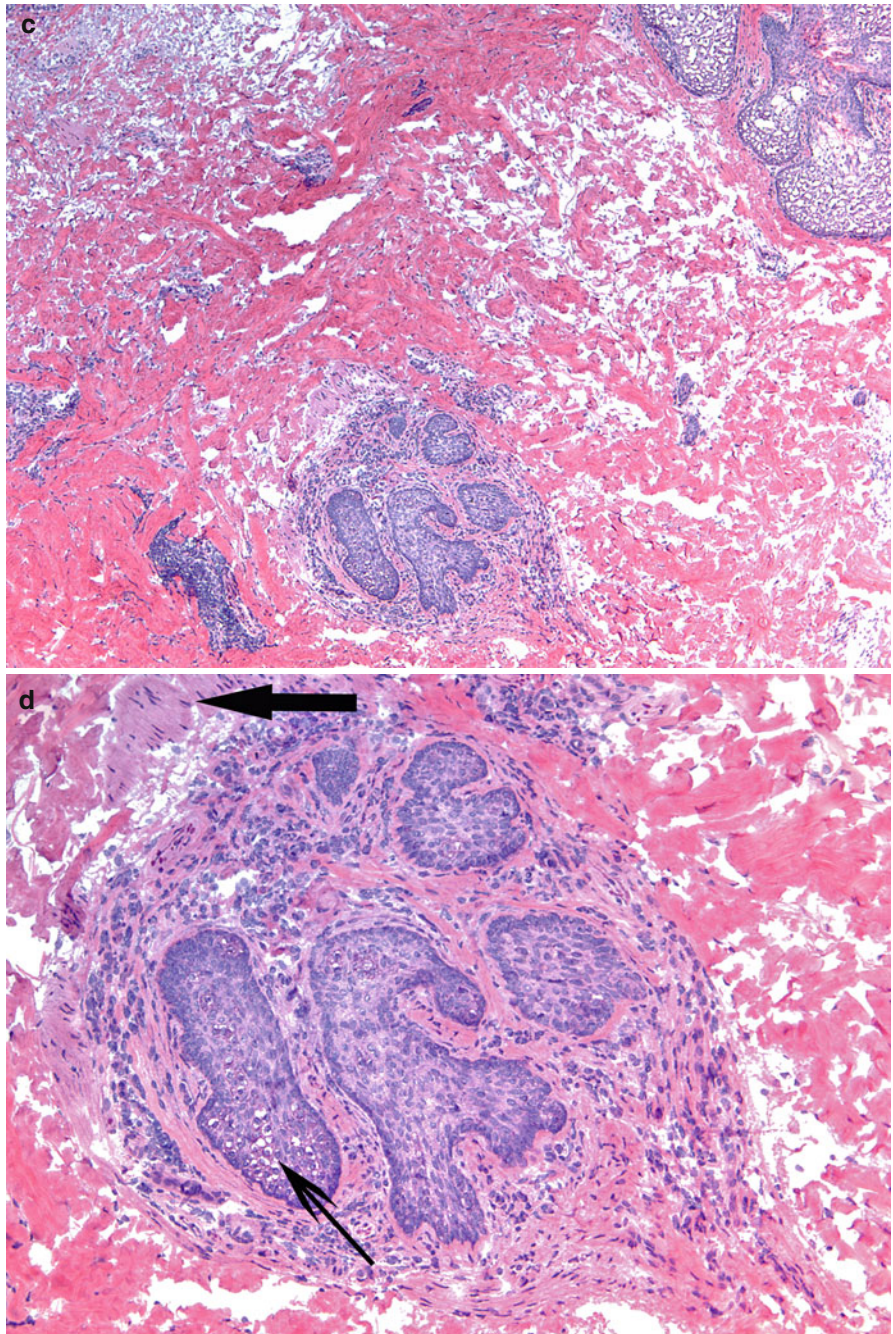


Fig. 5.22 BCC vs. follicle: (a) A group of large basaloid aggregates are seen in the reticular dermis. (b) On higher magnification this appears to be a tangentially sectioned hair follicle and not basal cell carcinoma. Although peripheral palisading is present, there is lack of artifactual clefting or stromal changes

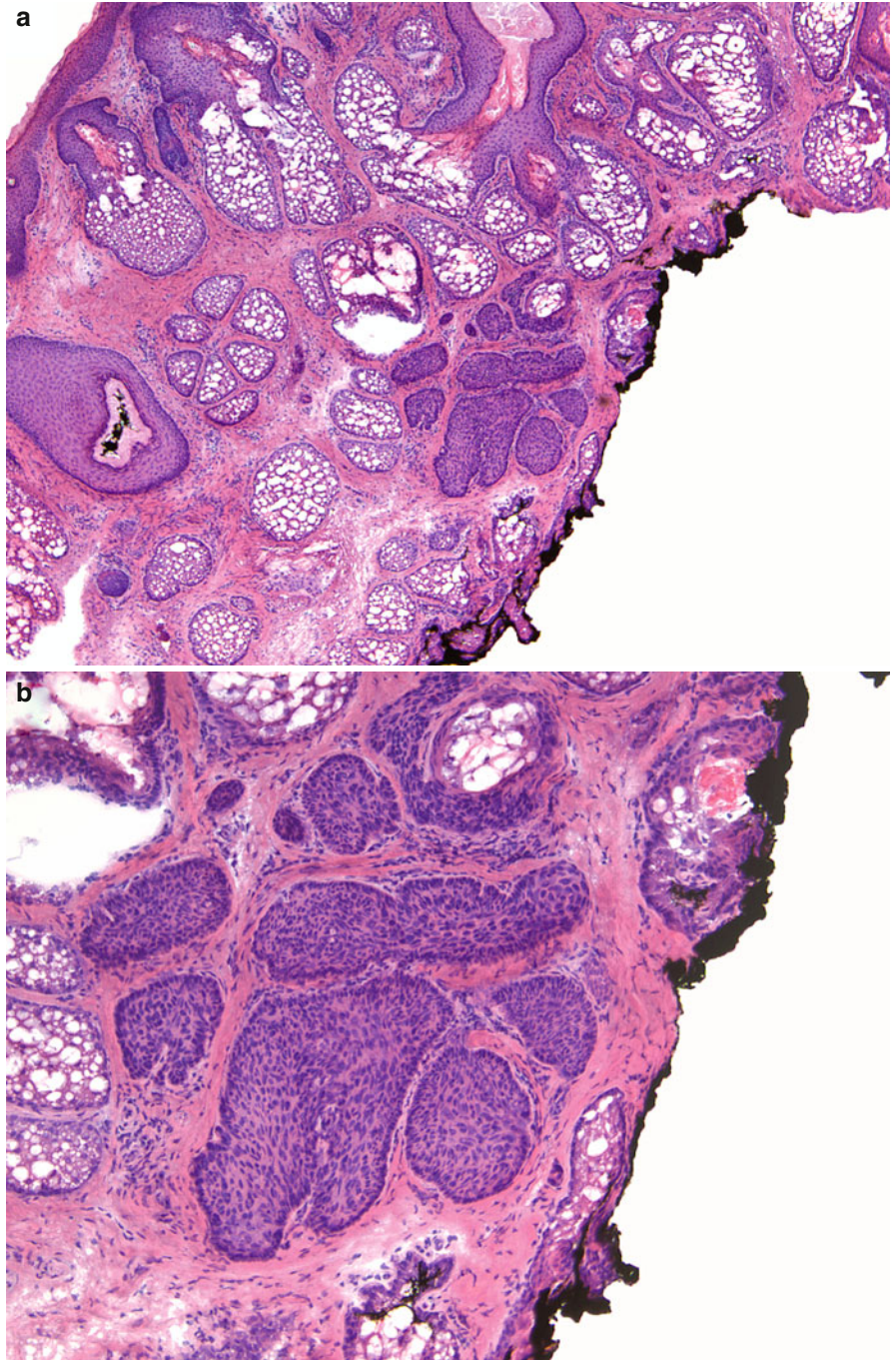


Fig. 5.22 (continued) (c) Deeper cuts into this tissue block support the finding that this is a follicular structure rather than carcinoma. (d) Note the dilated sebaceous duct of the hair follicle

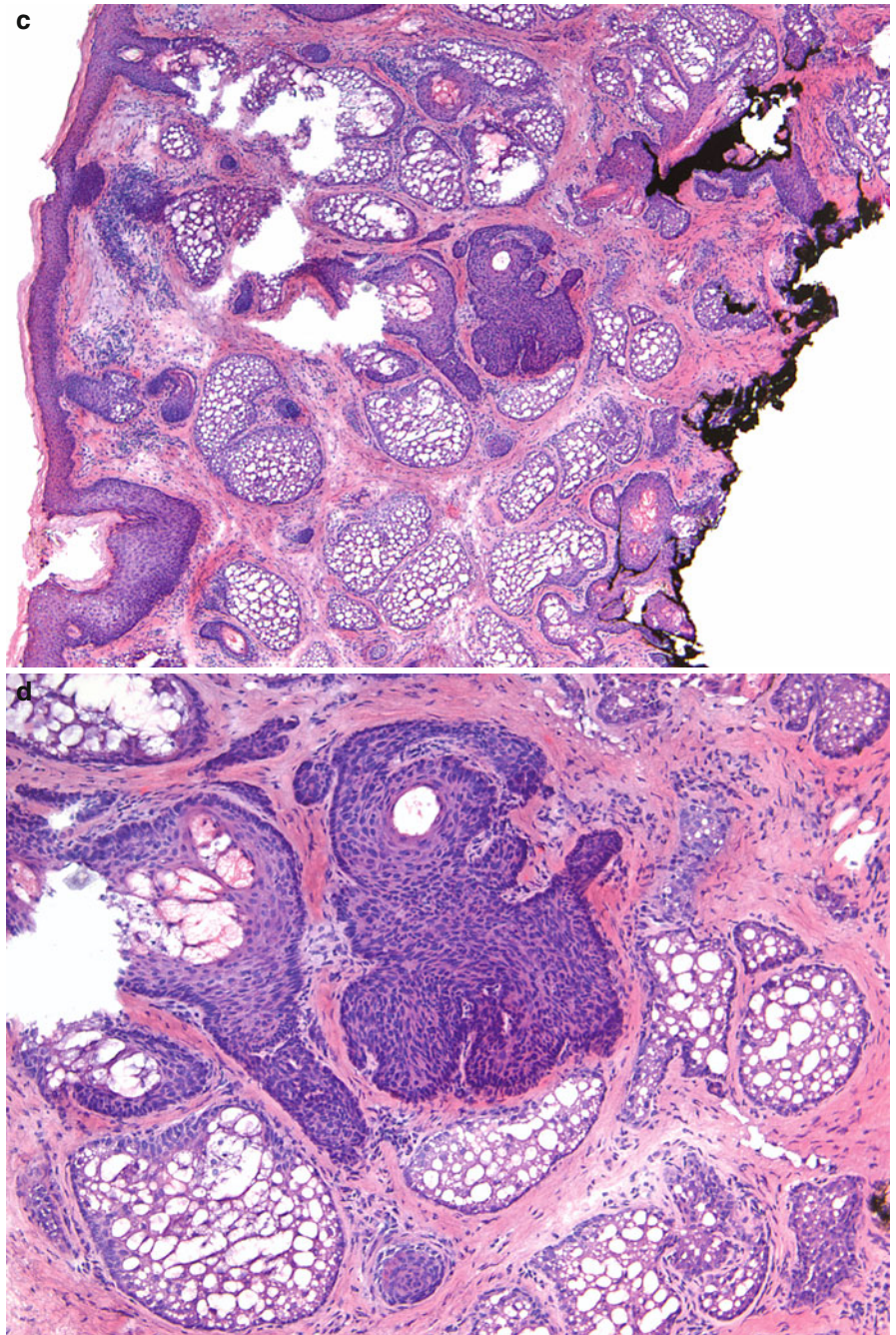


Fig. 5.23 Malformed follicular structure: note the overall architecture and appearance of a hair follicle and lack of features for a BCC (clefting, peripheral palisading, and mucinous stromal changes)

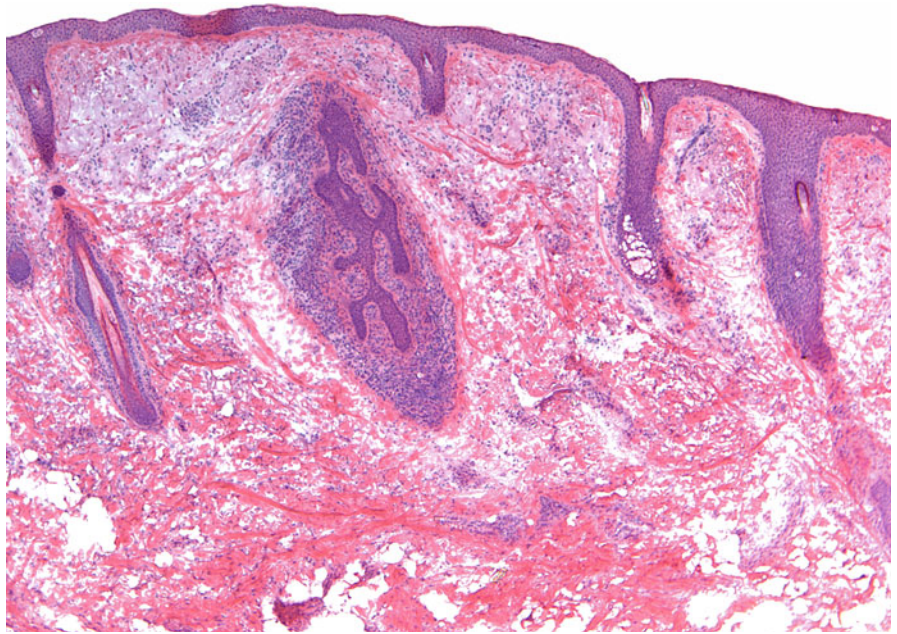


Fig. 5.24 BFH: (a) Basaloid aggregates arising from a hair follicle. (b) At closer examination, a follicular bulb and papilla at the bottom of this hair follicle are apparent. In addition, there is a dilated infundibulum and surrounding basaloid aggregates, which represent portions of follicular epithelium and sebaceous lobules

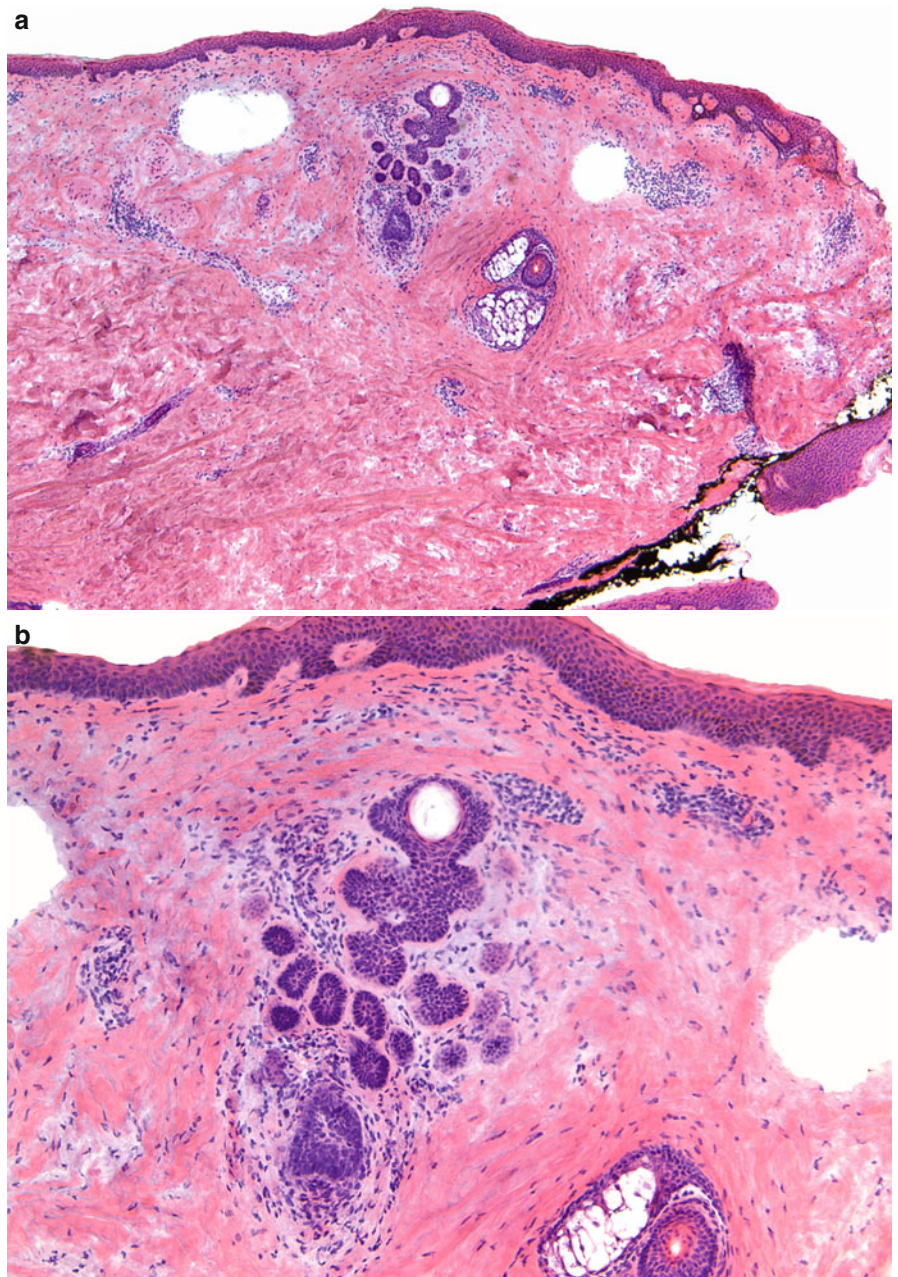


Fig. 5.25 FBP: (a) Vertically oriented, folliculocentric proliferations, with an axial distribution, lacking an epidermal attachment. The basaloid aggregates have a floret-like configuration. (b) Note the lack of stromal changes, clefting, and peripheral palisading typical for BCC. There is a dilated follicular infundibulum and the overall architecture resembles that of a hair follicle

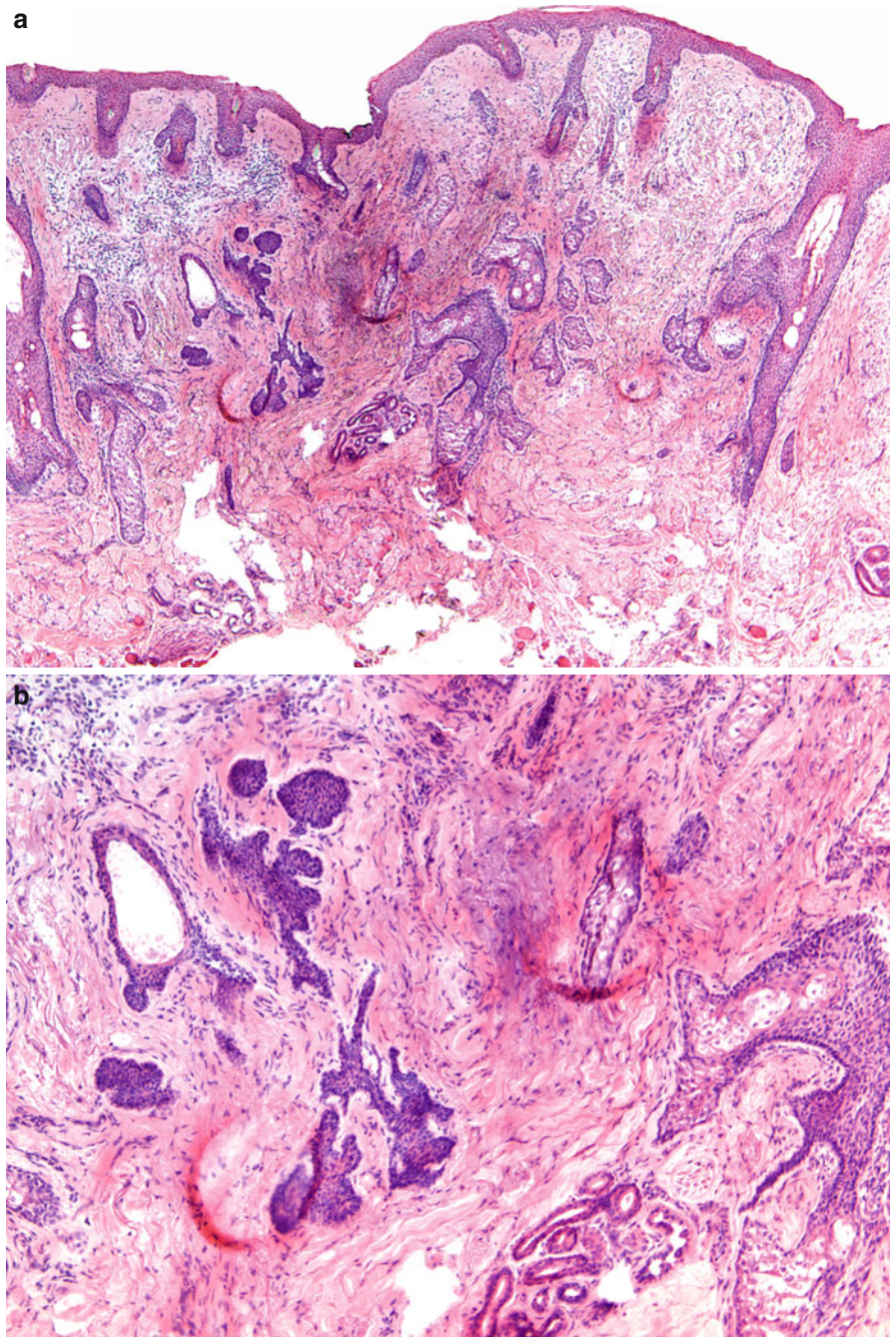


Fig. 5.26 BCC and eccrine structures: A cluster of eccrine ducts in the center of the specimen surrounded by inflammatory cells (*ellipse*). The ducts are lined by a double layer of cells with dark nuclei and are surrounded by a brightly pink sheath. Another cluster of eccrine ducts is seen in the right lower corner (*smaller ellipse*). Scattered throughout the photograph in between skeletal muscle are irregular basaloid aggregates of neoplastic cells (*arrows*). Unlike the rounded and oval-shaped eccrine ducts the neoplastic aggregates are irregular, often angulated, and do not have lumina or eosinophilic sheets around them

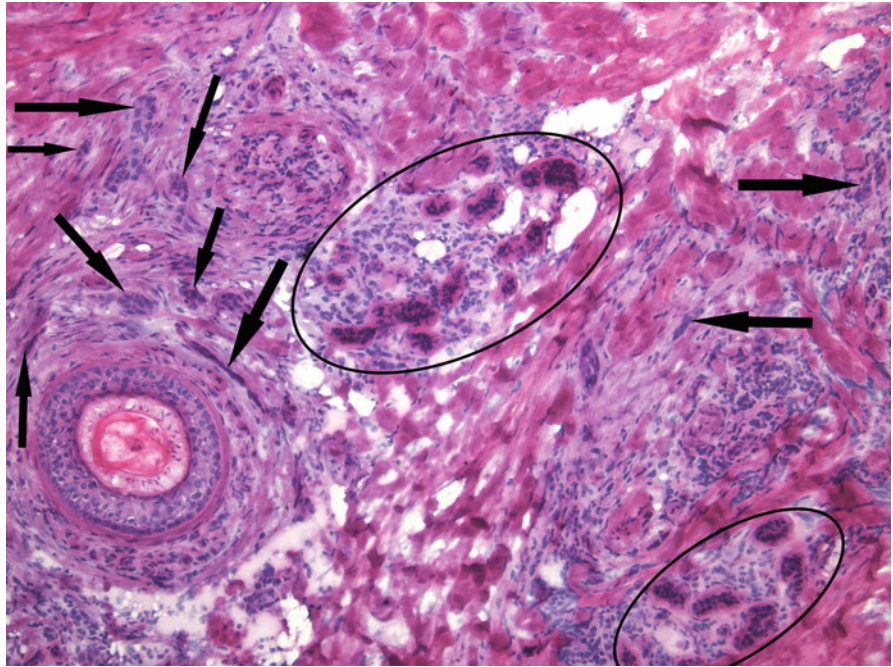
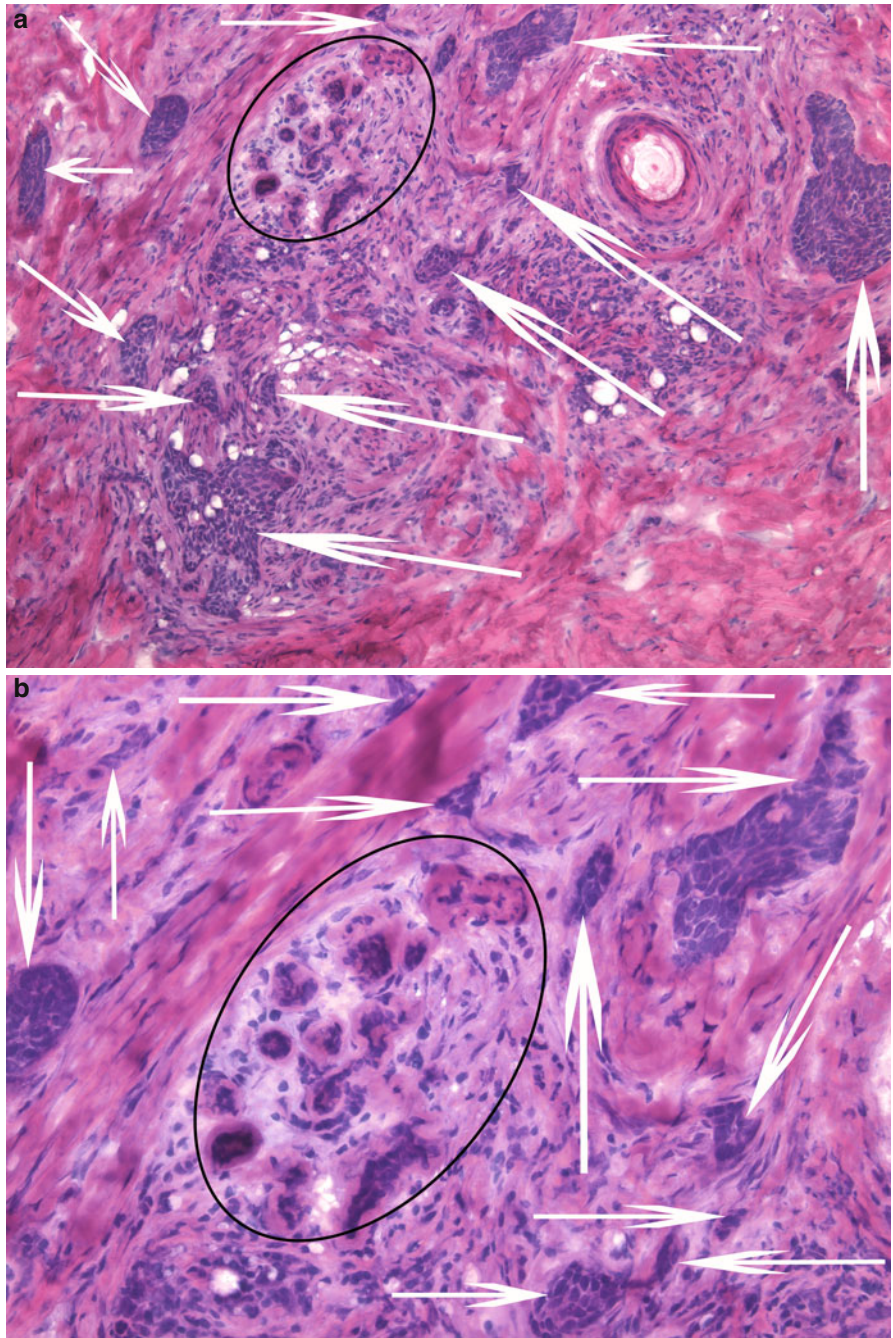


Fig. 5.27 BCC and eccrine structures: (a) In general, it is more helpful to appreciate the contrast between the eccrine ducts (*ellipse*) and neoplastic aggregates (*arrows*) on lower power looking at the overall architectural pattern and organization of the ducts. (b) Higher magnification with a collection of eccrine ducts centrally in the photomicrograph (*ellipse*). The cells of the eccrine ducts are not pleomorphic, smaller in size, and appear to lie on top of each other. In contrast the neoplastic aggregates (many of which are designated by *arrows*) show large pleomorphic cells, without the encircling bright eosinophilic sheath



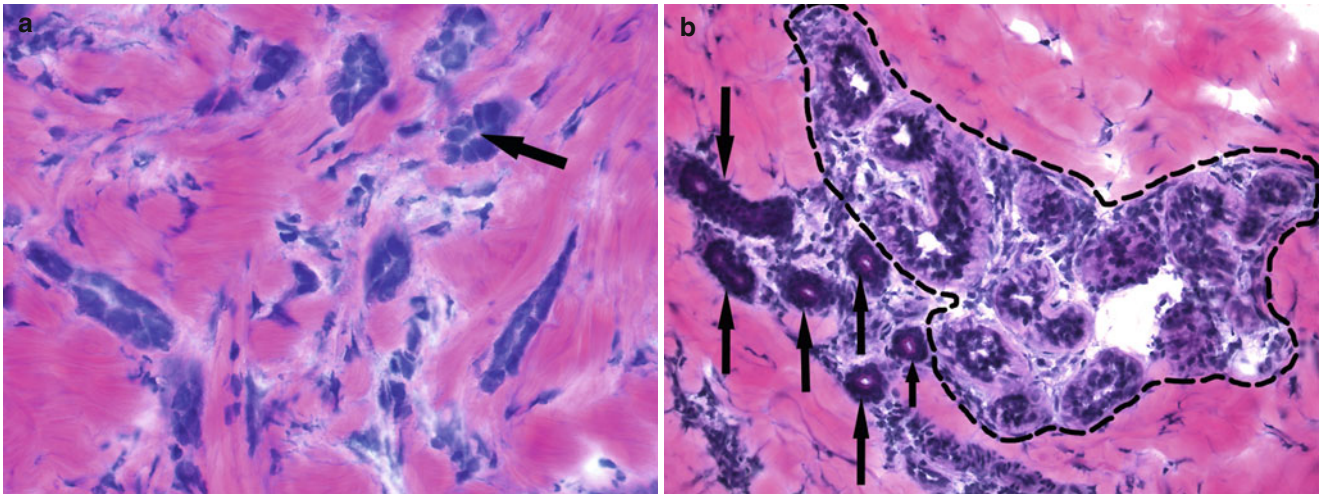


Fig. 5.28 Comparing BCC to eccrine structures: (**a**, **b**) The photomicrograph on the left shows neoplastic aggregates with both oval as well as round shapes. Some of these neoplastic aggregates appear to have pseudolumina (*arrow*). In addition, there are smaller aggregates consisting of two to three cells with hyperchromatic nuclei. Bright eosinophilic collagen surrounds the aggregates. In contrast, the photomicrograph on the right shows a collection of both eccrine ducts (*arrows*) and glands outlined. The overall architectural pattern and organization is helpful in discerning the two entities. For example, the eccrine glands and ducts are positioned in close proximity to each other within a confined area whereas there is variable distance between the neoplastic aggregates.

The eccrine glands are larger than the eccrine ducts and have irregular elongated or oval shapes. The cells lining the glands are large and have a moderate amount of eosinophilic cytoplasm. There are rounded or elongated lumina in the center of the glands, sometimes containing secretions. Often a thin layer of myoepithelial cells is seen surrounding the glands. In contrast, eccrine ducts are comprised of two closely opposed layers of cuboidal cells with dark nuclei and very little cytoplasm. When cut transversely they show round shapes with a round lumen lined by pink cuticle. In longitudinally sectioned parts of the duct, the lumen is elongated and covered by a thin eosinophilic layer

Fig. 5.29 BCC and an eccrine duct: There are numerous neoplastic aggregates in a loose mucinous stroma and surrounded by bright pink eosinophilic collagen bundles. In the right upper corner there is an eccrine duct (*arrow*) lined by two cell layers, which has more eosinophilic appearance due to the small amount of cell cytoplasm as well as the pink cuticle. The cells that comprise the eccrine duct are much smaller and less pleomorphic than the cells comprising the neoplastic aggregates

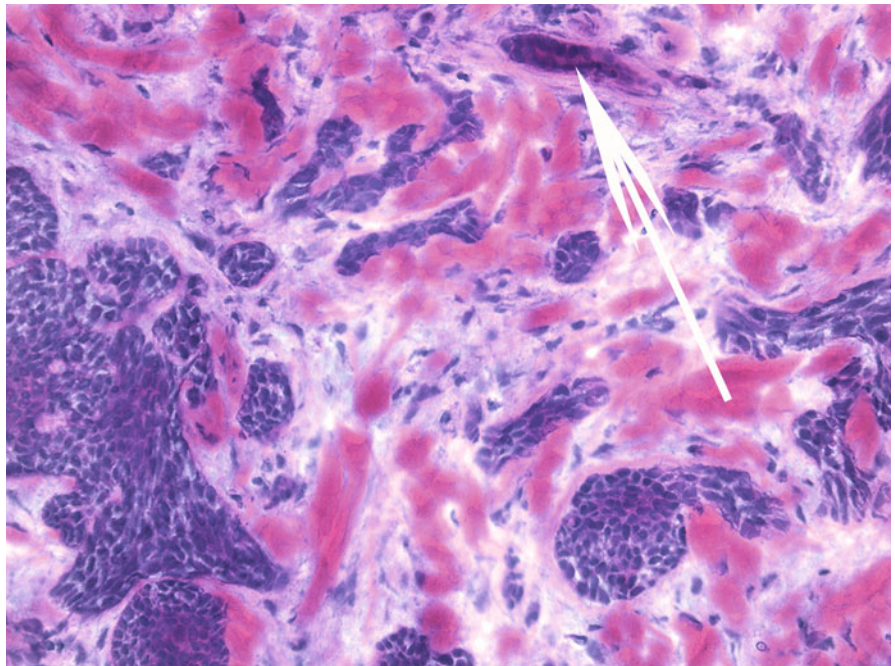
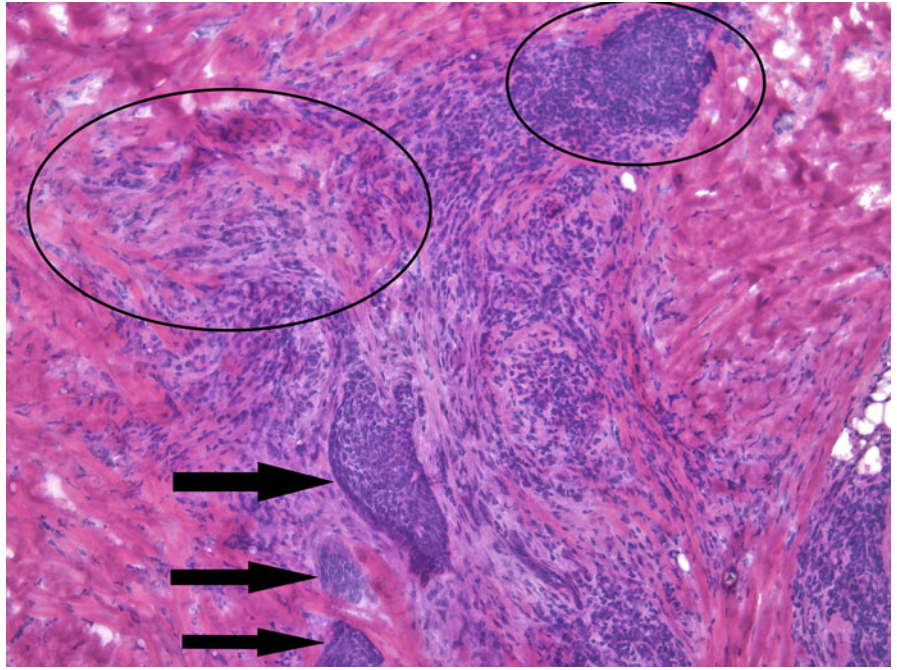


Fig. 5.30 BCC and inflammation: Several neoplastic aggregates that vary in size and shape can be seen (*arrows*). They appear cohesive forming either oval or angulated structures. In contrast, the inflammatory infiltrate shows dense collections along with individual scattering of cells interstitially in between collagen bundles in a patternless distribution (*ellipses*). The neoplastic cells are slightly pleomorphic unlike the inflammatory cells, which are monomorphic and have higher nucleus to cytoplasmic ratio, particularly the lymphocytes. In addition, peripheral palisading can be appreciated within the larger neoplastic aggregates, whereas the dense collections of inflammatory cells show no evidence of peripheral palisading or any other organization



Although the benign adnexal tumors discussed in this chapter are not an indication for treatment with Mohs micrographic surgery, it is critical for the Mohs surgeon to be familiar with their histopathology for a number of reasons. Sometimes a superficial biopsy may lead to an erroneous diagnosis and the patient is inadvertently referred to Mohs surgery. The Mohs layers then can help reveal the correct diagnosis. In addition, it is not uncommon to find these benign adnexal tumors on the face, adjacent to basal cell carcinomas and the ability of the Mohs surgeon to delineate these benign growths from cancerous lesions will minimize surgery and morbidity for the patient.

Syringoma

Histologic Features

1. Benign dermal tumor of eccrine duct origin
2. No epidermal connection
3. Well demarcated, non-encapsulated tumor in the superficial to mid reticular dermis
4. Tumor comprised of small epithelial aggregates with round, coma-like, or tadpole shapes, as well as elongated strands of epithelial cells
5. Tumor aggregates push surrounding adnexal structures but do not infiltrate them
6. Duct-like structures with homogeneous pink secretions in their lumina admixed with the tumor aggregates
7. The tumor cells are monomorphous, lacking atypia, and mitotic figures
8. No individually pyknotic or necrotic cells within epithelial tumor aggregates
9. Dense sclerotic pink collagenized stroma surrounding the tumor aggregates
10. No clefts between the tumor aggregates and the surrounding stroma
11. No solar elastosis or mucin within the stroma of the tumor
12. Minimal inflammatory infiltrate associated with the tumor
13. Neoplastic cells can be arranged in strands and cords as in infiltrative basal cell carcinoma; however, numerous round epithelial aggregates and tubular structures predominate in this tumor
14. In the clear cell variant of syringoma, large epithelial cells with clear cytoplasm comprise the tumor aggregates

Histopathologic Differential Diagnosis

Infiltrative Basal Cell Carcinoma

1. Asymmetric, poorly circumscribed, and often involves deeper tissues
2. Comprised of strands and cords and lack ductal structures
3. Necrotic tumor cells and mitotic figures are present

Desmoplastic Trichoepithelioma

1. Larger and deeper neoplasm composed of epithelial elements that show evidence of follicular differentiation, i.e., infundibular cysts, trichohyaline granules, etc.

Microcystic Adnexal Carcinoma

1. Larger, asymmetric, poorly circumscribed, and deeply infiltrative neoplasm that often involves the subcutaneous fat and skeletal muscle
2. Marked variation in size and shape of tumor aggregates
3. Prominent perineural invasion

Desmoplastic Trichoepithelioma (DTE)

1. Benign follicular tumor confined to the upper to mid dermis.
2. Tumor has a symmetric plate-like growth pattern that is well circumscribed but not encapsulated.
3. Central epidermal dell-like depression is often present.
4. Tumor comprised of small cords and aggregates of basaloid cells with scant cytoplasm.
5. No clefts around epithelial tumor aggregates and the surrounding stroma.
6. Horn cysts, particularly in the upper portion of the lesion.
7. Often presence of a granulomatous response with histiocytes and multinucleated giant cells to free keratin from ruptured cysts.
8. Calcifications often present.
9. Dense collagenous stroma with increased number of fibroblasts around tumor aggregates.
10. Tumor cells are relatively monomorphous and with high nuclear to cytoplasmic ratio.
11. Rare pyknotic or necrotic keratinocytes.
12. Lymphocytic inflammatory infiltrate may or may not be present at the periphery of the lesion or surrounding epithelial aggregates.

Histopathologic Differential Diagnosis**Infiltrative Basal Cell Carcinoma**

1. Asymmetric, poorly circumscribed, and often involving deeper tissues
2. Comprised of basaloid aggregates, sometimes with bizarre angulated shapes, as well as strands and cords that vary markedly in size and shape
3. Horn cysts are rarely seen in BCC
4. Clefts are often seen between aggregates of basal cell carcinoma and the surrounding stroma. In DTE, clefts may be seen within the stroma but not between aggregates and the stroma
5. Necrotic tumor cells and mitotic figures are often present in BCC

Syringoma

1. Smaller and more superficially located
2. Horn cysts, foreign body granulomas, or calcifications rarely present
3. Lack of narrow strands of tumor cells

Microcystic Adnexal Carcinoma

1. Larger, asymmetric, poorly circumscribed, and deeply infiltrative neoplasm that often involves the subcutaneous fat and skeletal muscle
2. Marked variation in size and shape of tumor aggregates
3. Prominent perineural invasion

Sebaceous Carcinoma

Two types:

- Ocular
- Extraocular

Histologic Features

1. Located superficially or deep
2. Asymmetric, poorly circumscribed, with infiltrative borders
3. Aggregations of neoplastic sebocytes that vary in size and shape and bear poor resemblance to normal sebaceous lobules
4. Mixture of immature (non-vacuolated) and mature (vacuolated) neoplastic sebocytes
5. Markedly pleomorphic neoplastic cells with hyperchromatic irregular nuclei
6. Numerous mitoses, many of which may be abnormal
7. Necrosis of neoplastic sebocytes as solitary units and en masse
8. Intra-epidermal involvement by neoplastic cells more often seen in the ocular form
9. Can often be discontinuous and multicentric

Muir-Torre Syndrome and Its Cutaneous Manifestations

- Syndrome characterized by the development of:
 - Sebaceous tumors, often multiple
 - Visceral neoplasms
- Autosomal dominant inheritance
- Sebaceous tumors vary from just one to more than one hundred lesions
- Cutaneous tumors may precede or follow the manifestation of the visceral cancer
- Visceral tumors usually of the gastrointestinal tract:
 - Polyps of the large bowel
 - Adenocarcinomas
- Cutaneous sebaceous neoplasms sometimes difficult to classify
- Cystic sebaceous tumors described as marker lesions for the Muir-Torre syndrome
- Sebaceous tumors associated with the syndrome:
 - Sebaceous adenoma
 - Sebaceoma
 - Sebaceous carcinoma
 - Basal cell carcinoma with sebaceous differentiation

Fig. 6.1 Syringoma: (a) Well-delineated small tumor comprised of epithelial aggregates embedded in fibrotic stroma. (b) Round, oval, and tadpole-shaped cords and strands of basaloid tumor cells. There are brightly eosinophilic collagen bundles and increased number of fibroblasts in the surrounding stroma

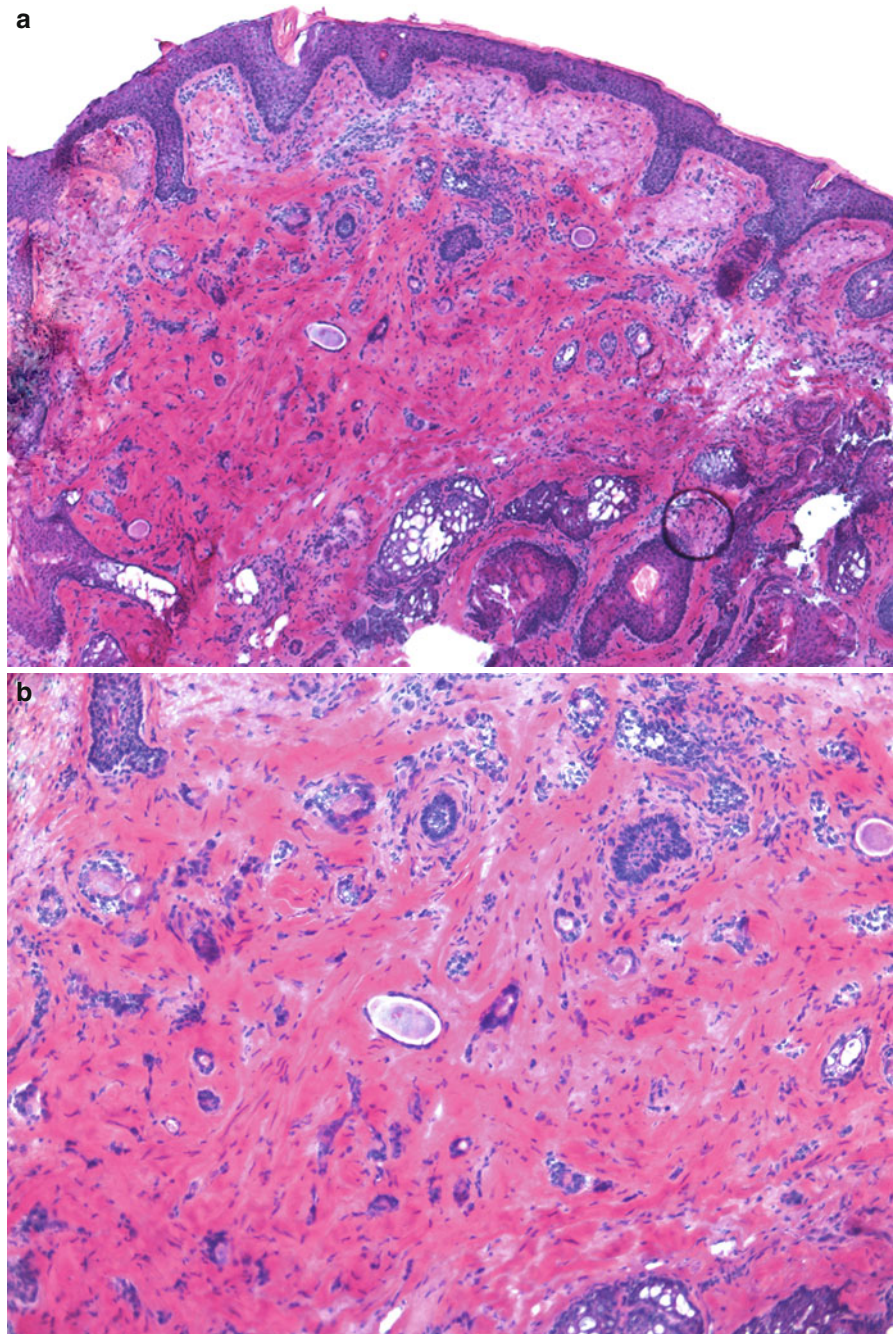


Fig. 6.2 Syringomas: (a) Multiple syringomas (*arrows*) with the typical tadpole-shaped aggregates embedded in fibroblastic stroma. It appears that there are multiple syringomas with areas of normal skin in between. (b) Higher power magnification of this benign tumor

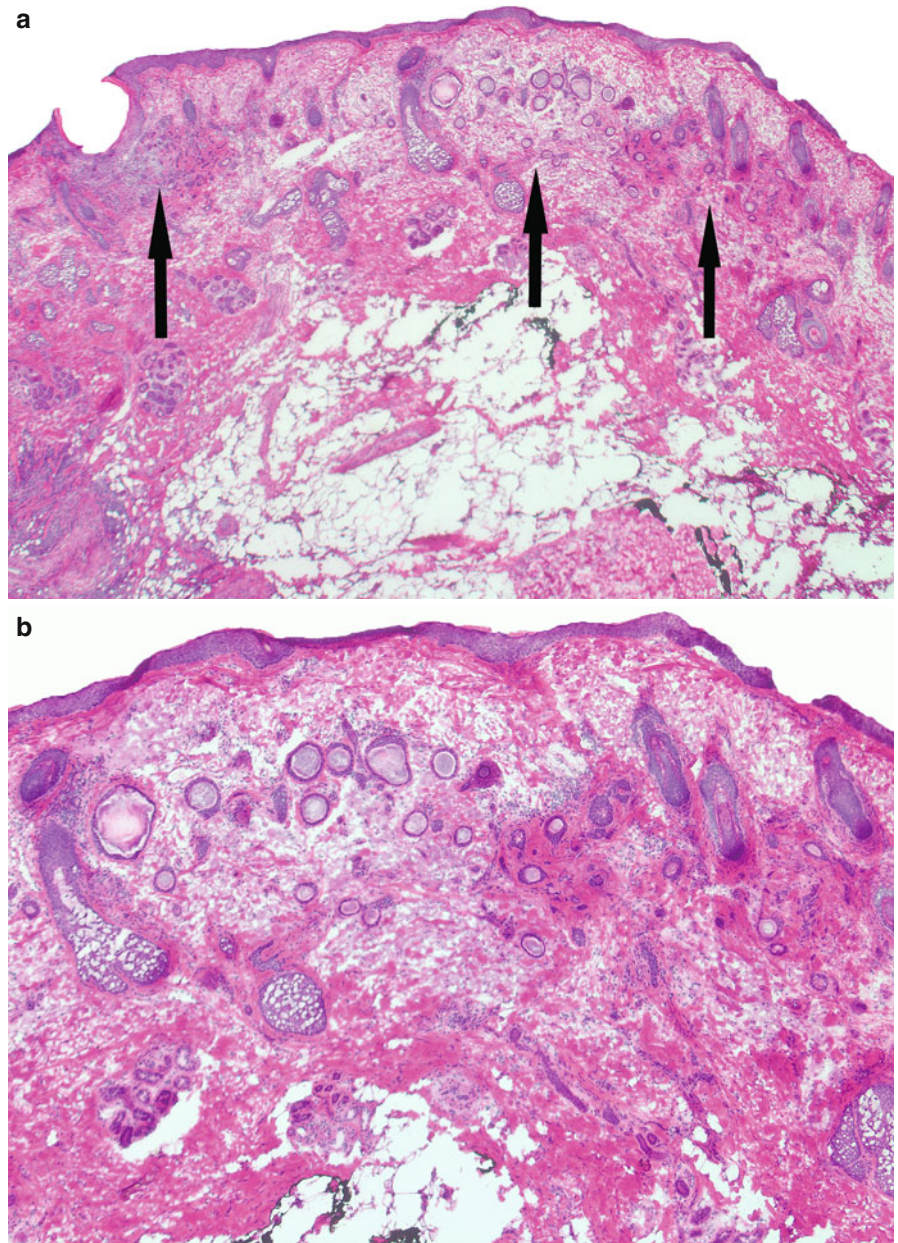


Fig. 6.3 Syringoma – clear cell variant: (a) Numerous ductal structures lined by two layers of cells and containing pink dense secretion in their lumina. (b) Large epithelial cells with abundant clear cytoplasm form tumor aggregates and line ductal structures

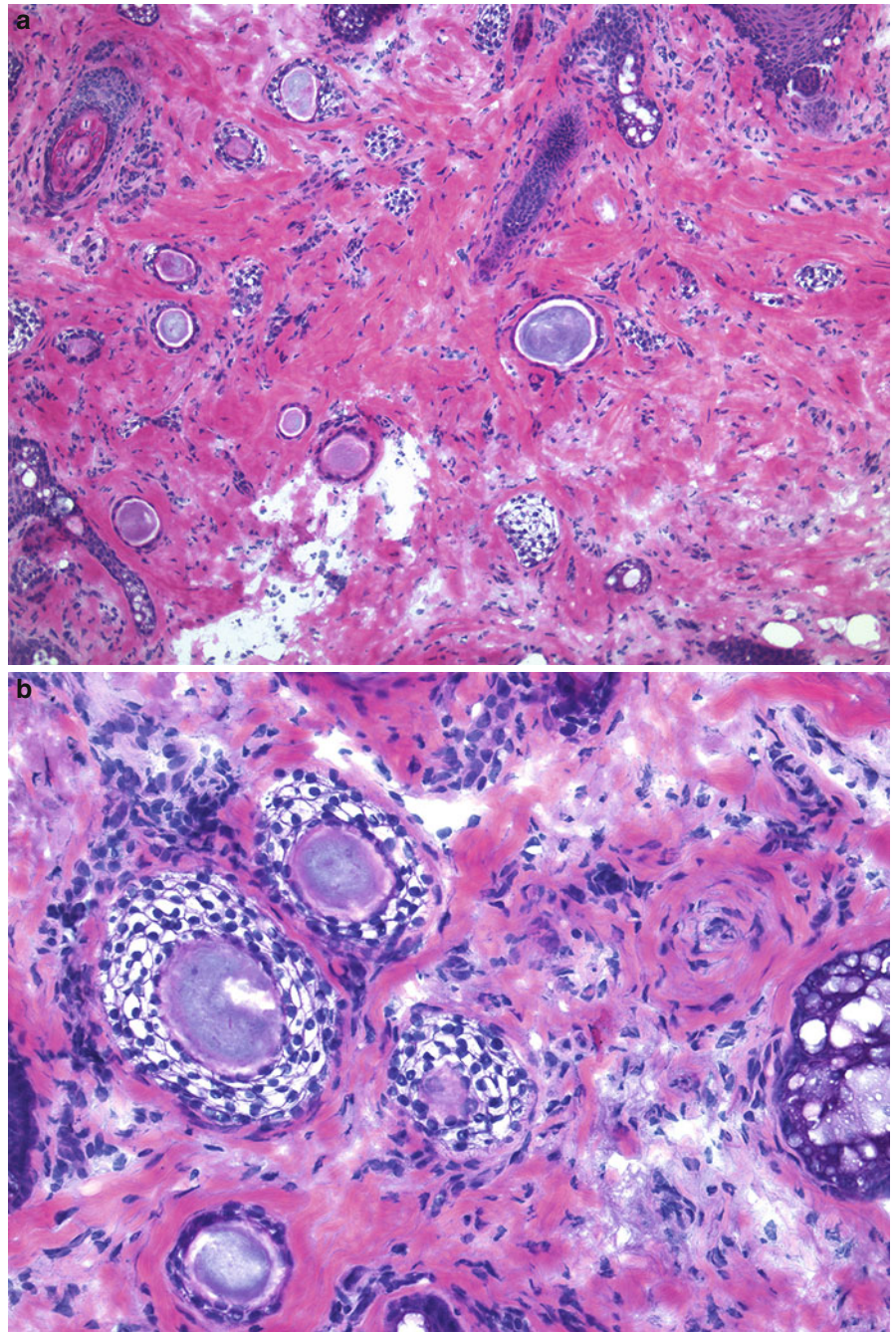


Fig. 6.4 Desmoplastic trichoepithelioma (DTE): (a) Plate-like distribution of tumor aggregates in a formalin-fixed section. The tumor is confined to the upper three-quarters of the reticular dermis. (b) Focal foreign body-type granulomatous reaction to free keratin in the dermis is often present as a sequela of ruptured horn cysts. There is an area of calcification centrally (*arrow*). Clefting is present within the stroma

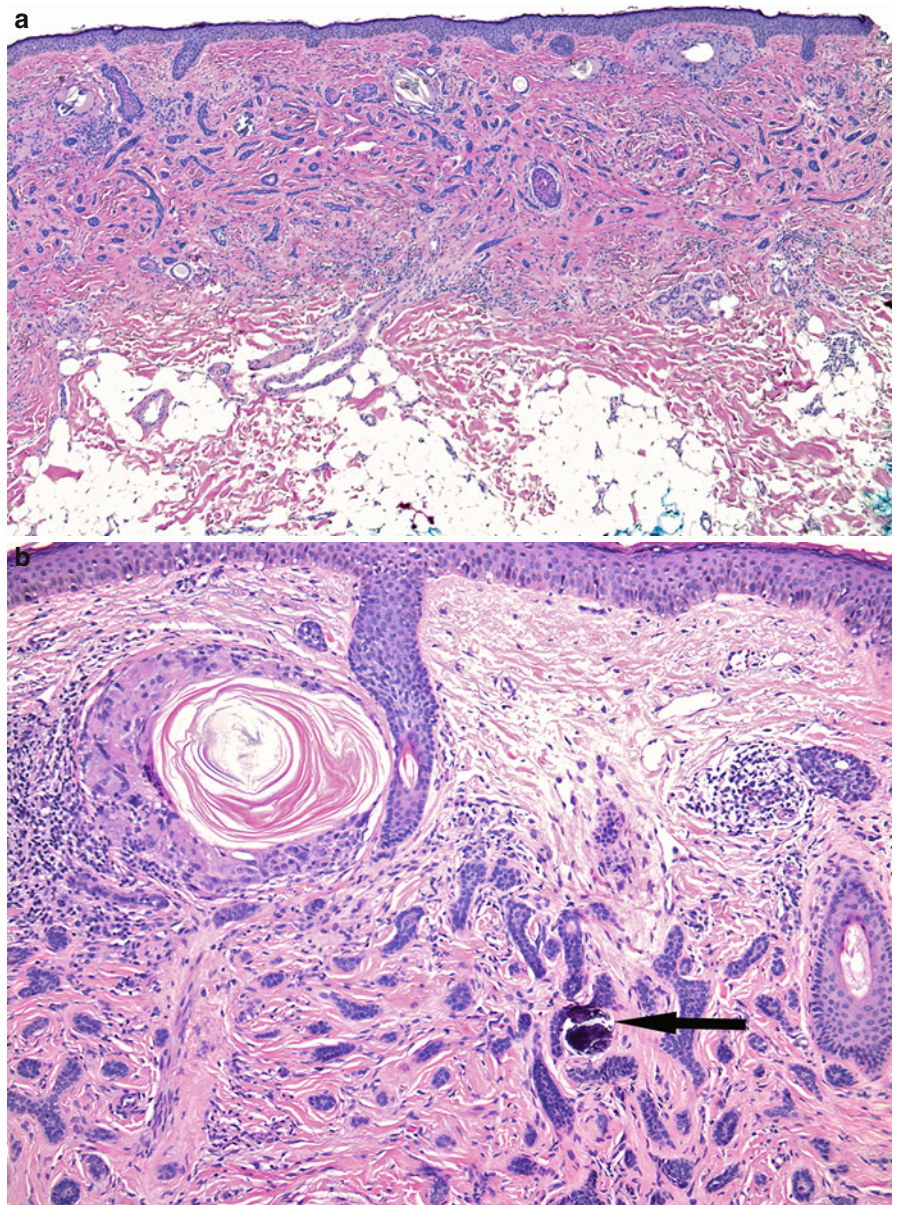


Fig. 6.5 Desmoplastic trichoepithelioma (DTE): (a) Relatively symmetrical tumor in mid-reticular dermis comprised of basaloid aggregates with variation in size and shape. Lymphocytic inflammatory infiltrate is seen at the periphery of the tumor and focally surrounding tumor aggregates. (b) Small horn cysts, strands, and cords of basaloid tumor cells embedded in fibrotic stroma containing brightly eosinophilic collagen. No clefts around tumor aggregates and surrounding stroma. Focal lymphocytic inflammation is present

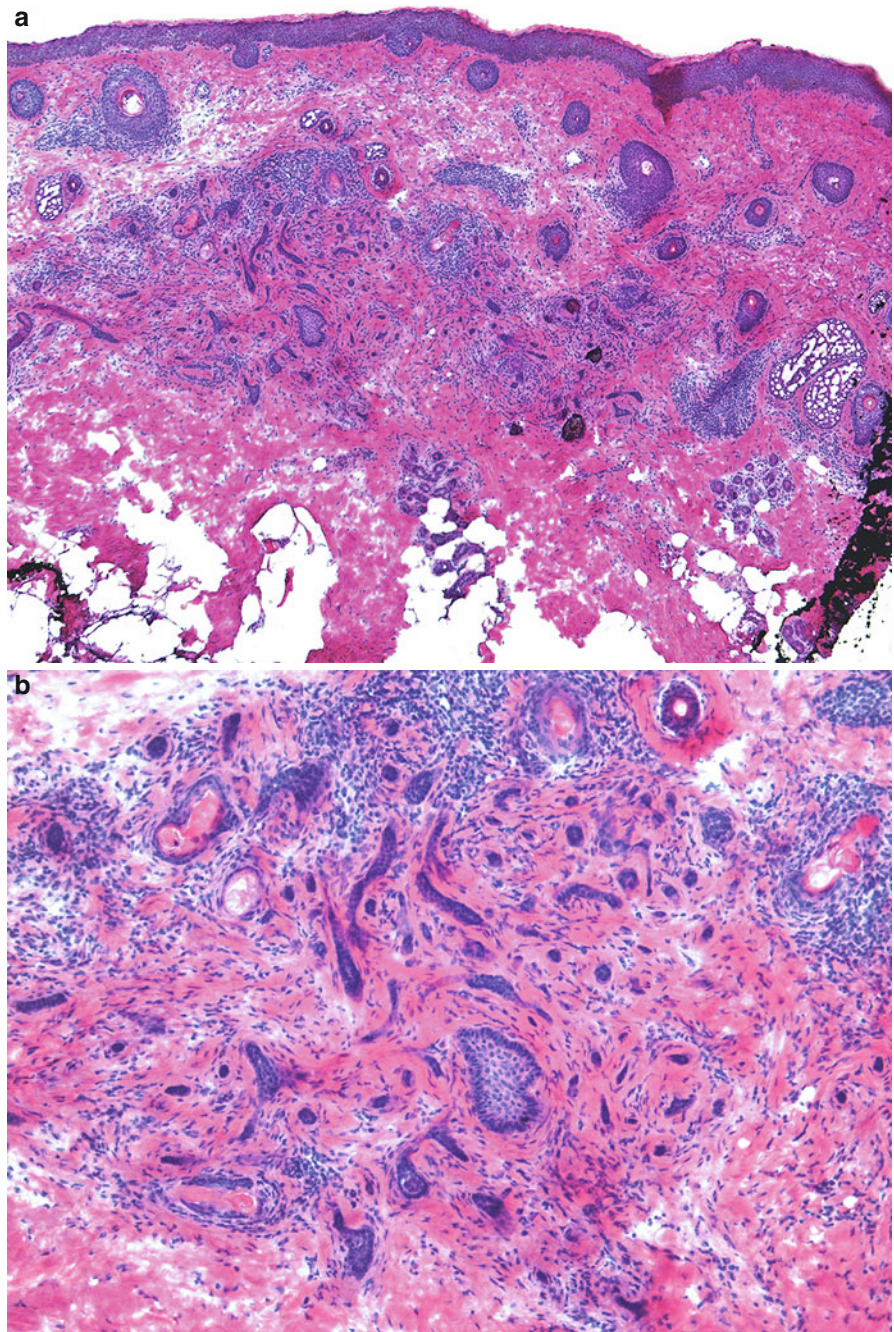


Fig. 6.5 (*continued*) (c) Cords and strands of tumor cells that are monomorphous, lack pleomorphism, and pyknotic or necrotic cells. Mitotic figures are absent. Note lack of clefting between tumor aggregates and stroma

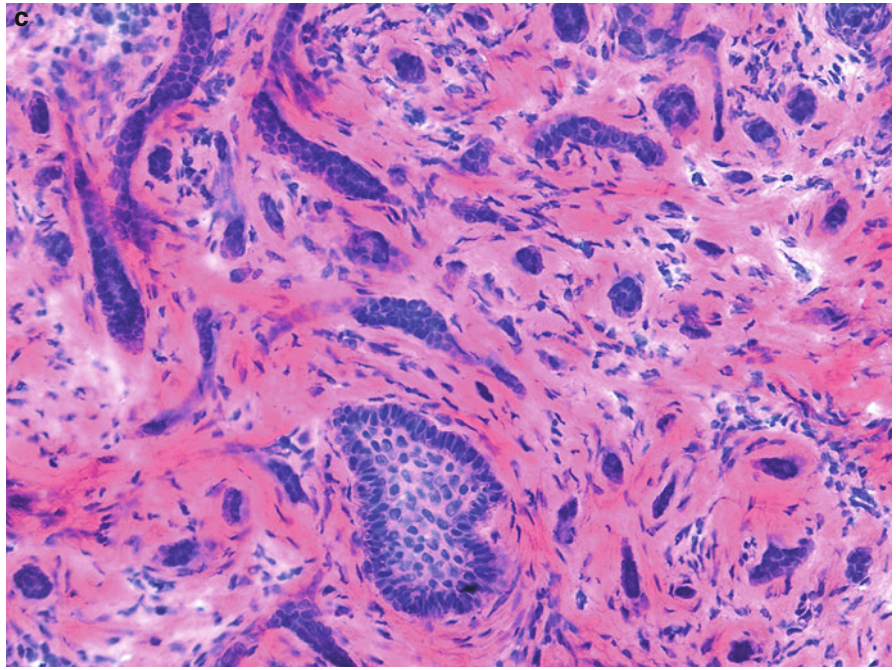


Fig. 6.6 Sebaceous carcinoma:

(a) Scanning magnification of formalin fixed tissue depicting irregularly shaped asymmetric neoplasm comprised of aggregates of neoplastic cells connected to the epidermis. (b) A medium power view of areas showing mature sebocytes forming small lobules toward the left of the photograph and sheets of immature sebocytes with dark blue nuclei and very scant cytoplasm. A few sebaceous ducts lined by pink cuticle are seen throughout the immature component of the neoplasm. (c) Numerous neoplastic sebaceous lobules connecting directly to the epidermal surface and not associated with hair follicles. Within the lobules there is a mixture of dark immature sebocytes and mature sebocytes with scalloped nuclei and vacuolated cytoplasm. Cystically dilated spaces filled with sebum presumably represent sebaceous ducts and duct-like structures

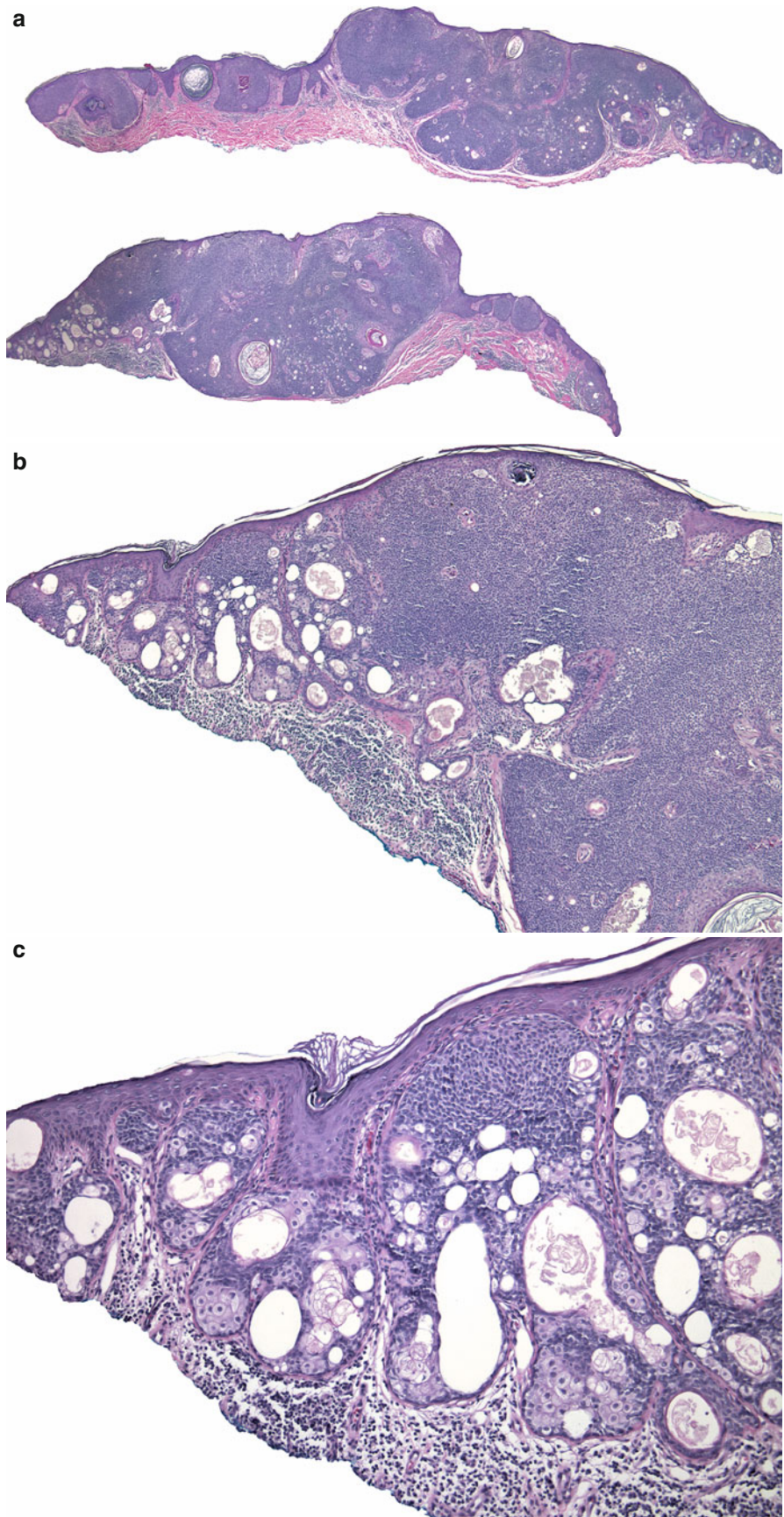


Fig. 6.7 Sebaceous carcinoma: sometimes areas of sebaceous carcinomas can be entirely composed of immature basaloid sebocytes with high nuclear to cytoplasmic ratio. Only focally rare mature sebocytes can be seen (*arrow*). On the left side of the photomicrograph there are aggregates of immature sebocytes within the epidermis itself, which represents intraepidermal involvement by the neoplasm

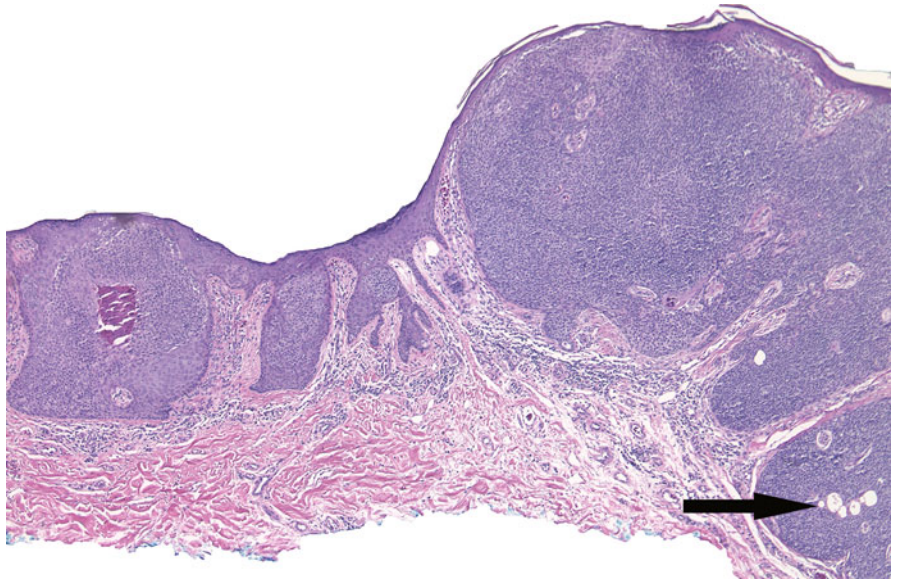


Fig. 6.8 Sebaceous carcinoma: (a) Low-power view of an epithelioid basaloid aggregate still connected to the epidermis and surrounded by scar tissue in the dermis. On the left side of the photomicrograph are more mature appearing sebocytes within the epidermis. (b) Collection of mature and immature sebocytes scattered within the epidermis

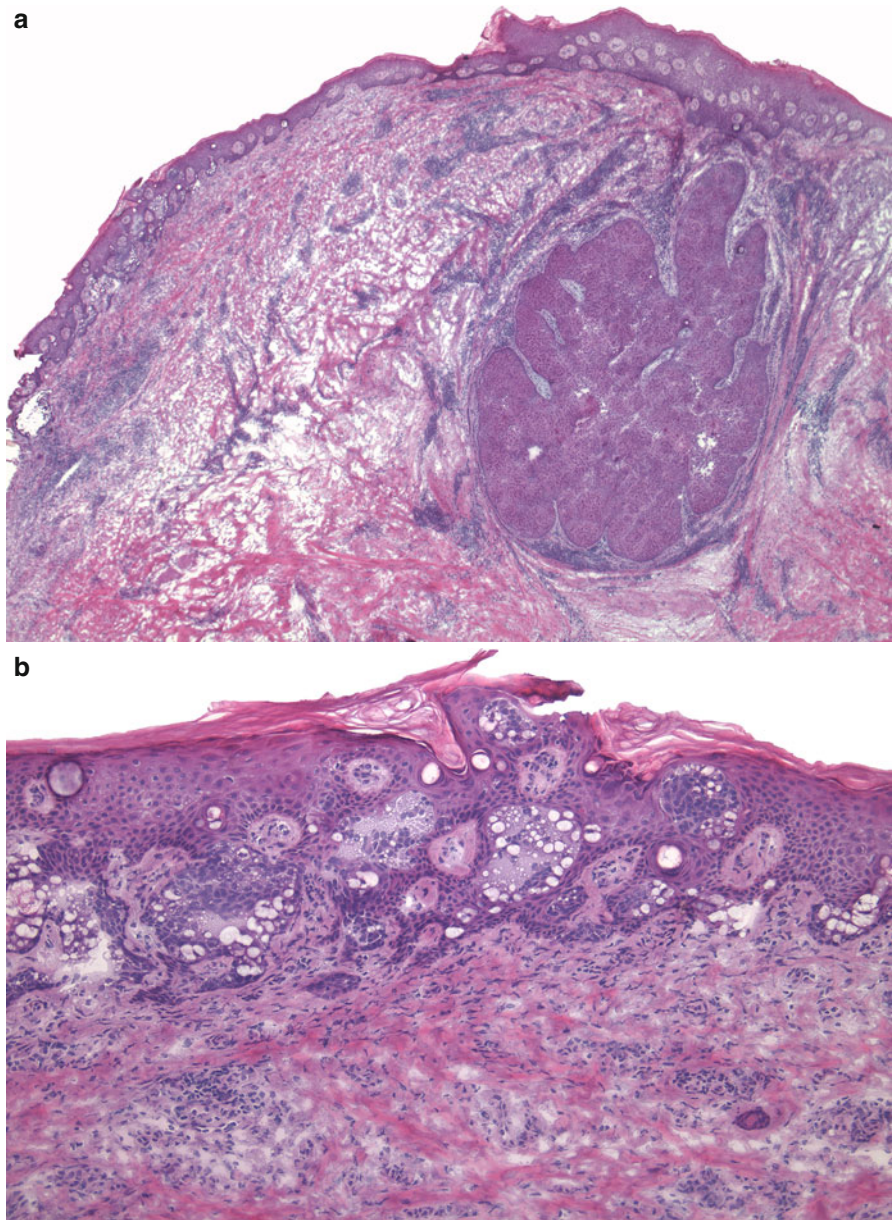


Fig. 6.9 Sebaceous carcinoma: **(a)** A formalin fixed tissue section (non-frozen section). Irregular neoplastic aggregates connecting to the epidermal surface showing variation in size and shape. The overlying epidermis is ulcerated and covered by a crust. **(b)** Round, oval, polygonal, and angulated neoplastic aggregates comprised of cells that vary from immature sebocytes with dark nuclei and scant cytoplasm to mature sebocytes with abundant vacuolated cytoplasm. Many aggregates have a central duct-like opening containing eosinophilic secretions

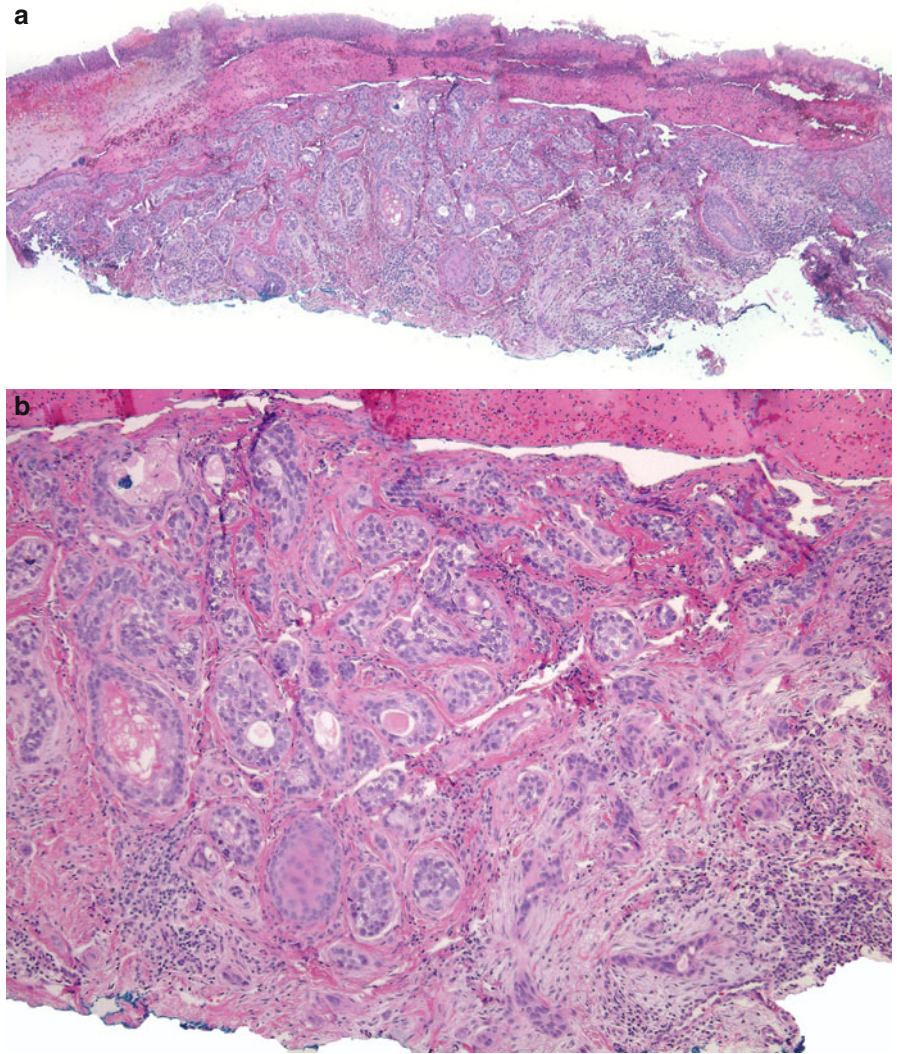


Fig. 6.9 (continued) (c) Round and angulated aggregates of immature and mature sebocytes. Mature sebocytes have scalloped nuclei and vacuolated cytoplasm (*thick arrow*). A mitotic figure is seen in the adjacent area (*thin arrow*). (d) Ocular sebaceous carcinoma often involves the overlying epidermis and extends down pre-existing normal follicular structures as seen in this photomicrograph (*arrow*). Numerous mitotic figures are seen throughout the neoplastic aggregates

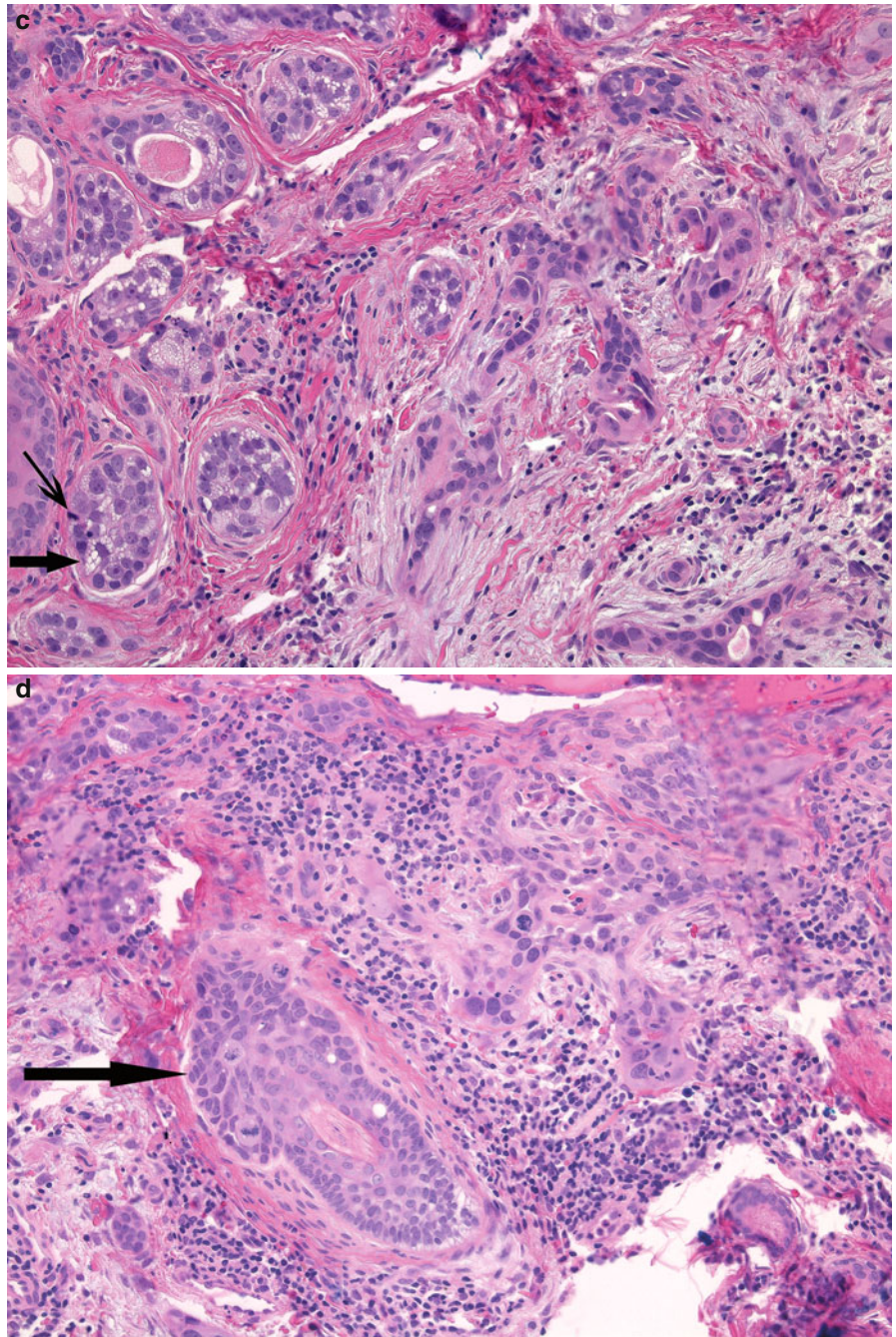


Fig. 6.9 (continued) (e) Low-power magnification of a Mohs frozen section of the neoplasm depicted above. Involving the epidermis and extending down into the superficial dermis are irregular aggregates of neoplastic cells with hyperchromatic nuclei and scant cytoplasm. In this example of sebaceous cell carcinoma, there is a broad connection of the tumor with the overlying epidermis. (f) The overlying epidermis is almost completely replaced by neoplastic sebocytes. The majority of the sebocytes are immature with hyperchromatic nuclei and scant cytoplasm. Focally mature sebocytes with vacuolated cytoplasm are noted (*thick arrow*). In the right lower corner there are sebaceous ducts lined by pink cuticle (*thin arrows*)

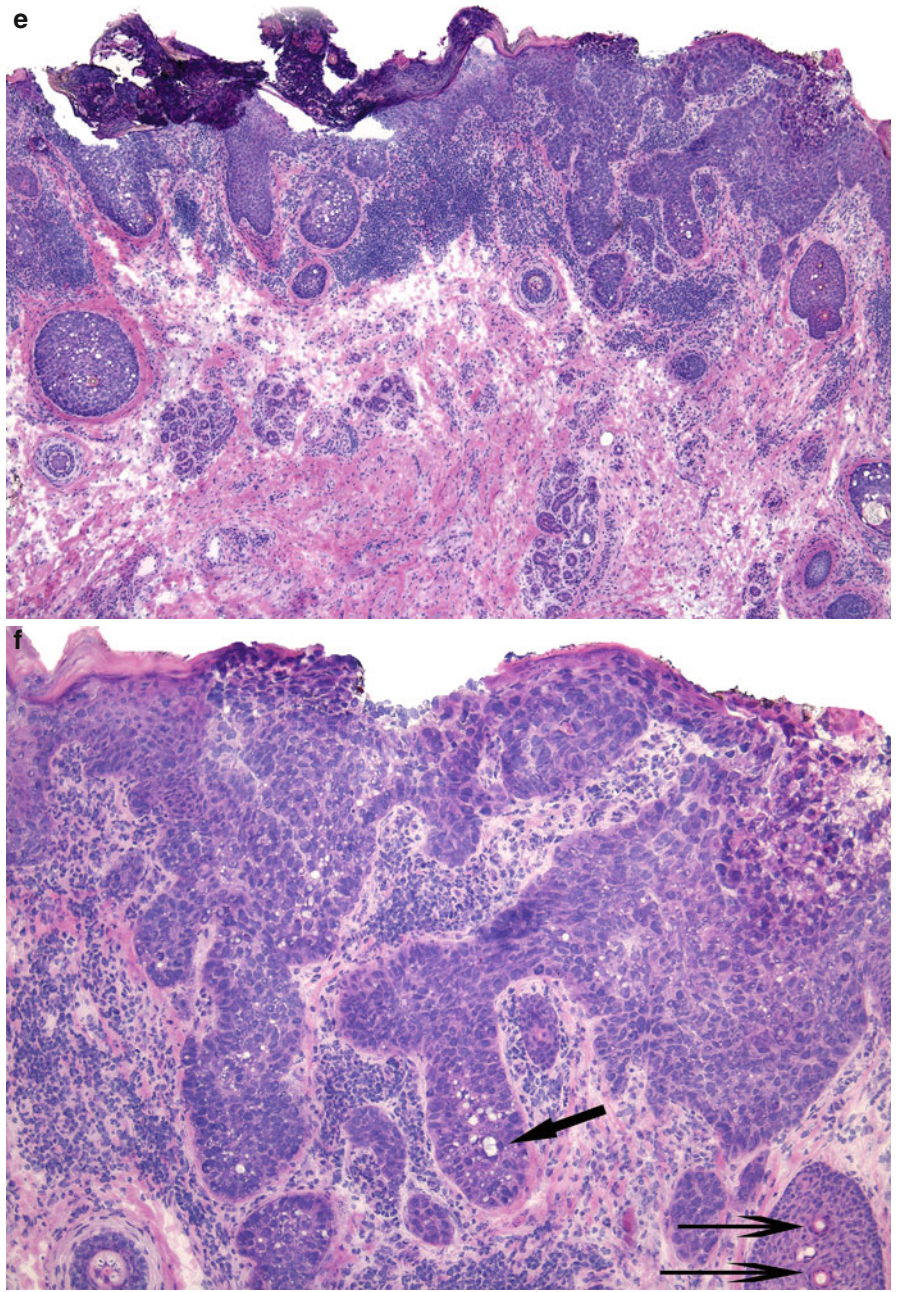


Fig. 6.10 Sebaceous carcinoma: (a) There are large neoplastic lobules with central necrosis en mass in the dermis. Normal overlying epidermis is focally seen. (b) The neoplastic lobules are organized in a trabecular pattern. The majority of the neoplastic cells are immature basaloid-staining sebocytes at the periphery with more mature vacuolated sebocytes in the center. There is significant edema of the surrounding stroma

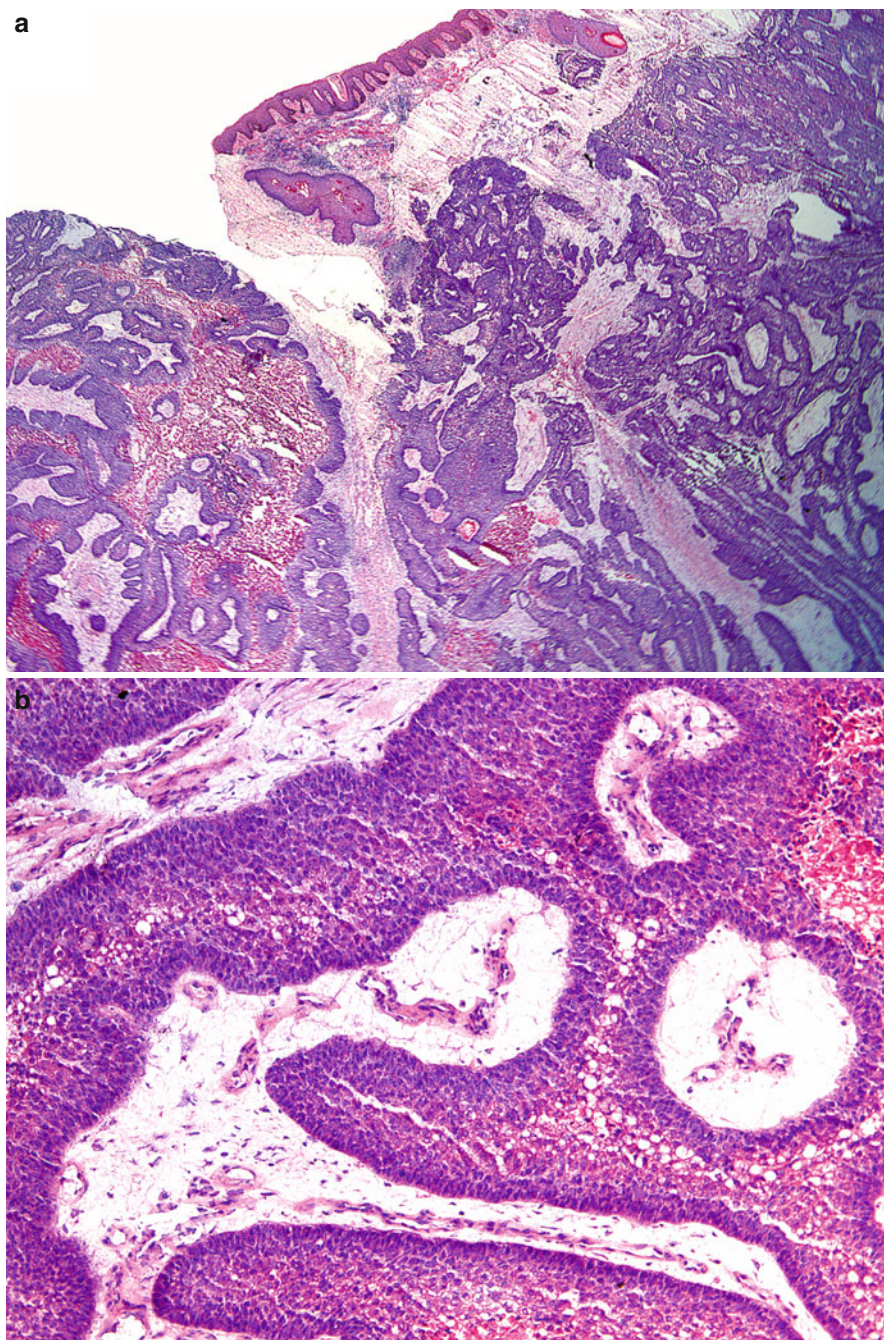
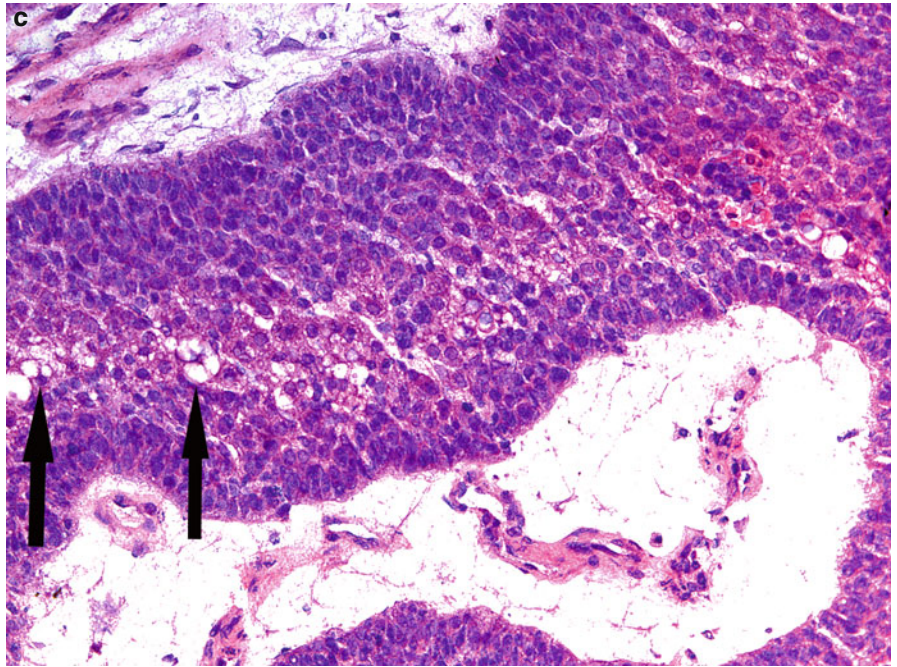


Fig. 6.10 (*continued*) (c) The sebocytes in the center of the neoplastic aggregates are mature and show scalloped nuclei and vacuolated cytoplasm (*arrows*). They are surrounded by immature, basaloid sebocytes, which predominate



Histologic Features

1. Malignant neoplasm with eccrine differentiation.
2. Plate-like growth pattern within the reticular dermis and extending deep into the subcutaneous fat and/or skeletal muscle in an infiltrative fashion.
3. Neoplastic aggregates are larger superficially and diminish in size in deeper tissue.
4. Small epithelial aggregates with irregular often angulated shapes, and cords and strands traversing in between collagen bundles.
5. The cords and strands may be very thin and are sometimes comprised of just one cell layer.
6. Pseudohorn cysts containing laminated keratin may be present in the superficial portion of the neoplasm.
7. Rarely granulomatous inflammation around ruptured cysts is present.
8. Some neoplastic aggregates are ductal in nature and have luminal centers often lined by a pink cuticle.
9. Adnexal structures are diminished or destroyed where tumor is present.
10. Perineural invasion is a prominent feature.
11. Dense hyalinized stroma comprised of thickened collagen bundles surrounds the neoplastic aggregates.
12. Lack of clefting between the epithelial aggregates and the surrounding stroma.
13. Neoplastic cells are usually basaloid, bland, uniform, with monomorphous nuclei with vesicular chromatin, high nuclear to cytoplasmic ratio, and scant cytoplasm.
14. In some cases, pleomorphism and mitotic figures may be prominent.

Differentiating Features Between Microcystic Adnexal Carcinoma and Desmoplastic Trichoepithelioma

Microcystic adnexal carcinoma	Desmoplastic trichoepithelioma
1. Large neoplasm	1. Small neoplasm
2. Asymmetric	2. Symmetric plate-like growth pattern
3. Poorly circumscribed	3. Well circumscribed
4. Deeply infiltrative, often extending to the subcutaneous fat and skeletal muscle	4. Confined to upper or mid dermis
5. No epidermal changes	5. Central epidermal dell-like depression
6. Marked variation in size and shape of tumor aggregates	6. Slight variation in size and shape of tumor aggregates
7. Neoplastic aggregates are larger superficially and diminish in size in deeper tissue	7. Minimal change in the size of aggregates in deeper dermis
8. Horn cysts may be present superficially	8. Horn cysts more common, particularly in the upper portion of the lesion
9. Ductal structures present	9. Lack of ductal structures
10. Prominent perineural invasion	10. No perineural invasion
11. Neoplastic cells may be pleomorphic and atypical	11. Neoplastic cells relatively monomorphous
12. Mitotic figures may be present	12. Mitotic figures are absent

Differentiating Features Between Microcystic Adnexal Carcinoma and Infiltrative Basal Cell Carcinoma

See also Chap. 8.

Microcystic adnexal carcinoma	Infiltrative basal cell carcinoma
1. Variation in size and shape of tumor aggregates	1. Greater variation in size and shape of tumor aggregates
2. Horn cysts may be present superficially	2. Lack of horn cysts
3. Often granulomatous inflammation around ruptured cysts	3. Lack of granulomatous inflammation
4. No foci of typical nodular basal cell carcinoma	4. Foci of typical nodular basal cell carcinoma present sometimes
5. No clefts between aggregates and stroma	5. Clefts between neoplastic aggregates and surrounding stroma
6. Inflammation usually absent	6. Inflammation usually present
7. No connection of the neoplastic aggregates to the overlying epidermis	7. Often connection of the neoplastic aggregates to the overlying epidermis
8. Ductal structures present	8. No ductal structures

Fig. 7.1 Microcystic adnexal carcinoma:
(a) A low-power view of a non-circumscribed and very infiltrative tumor throughout the entire reticular dermis with extension into the subcutaneous fat.
(b) Numerous small irregular basaloid aggregates surrounded by sclerotic stroma and inflammation. There is no connection between the tumor and the overlying epidermis

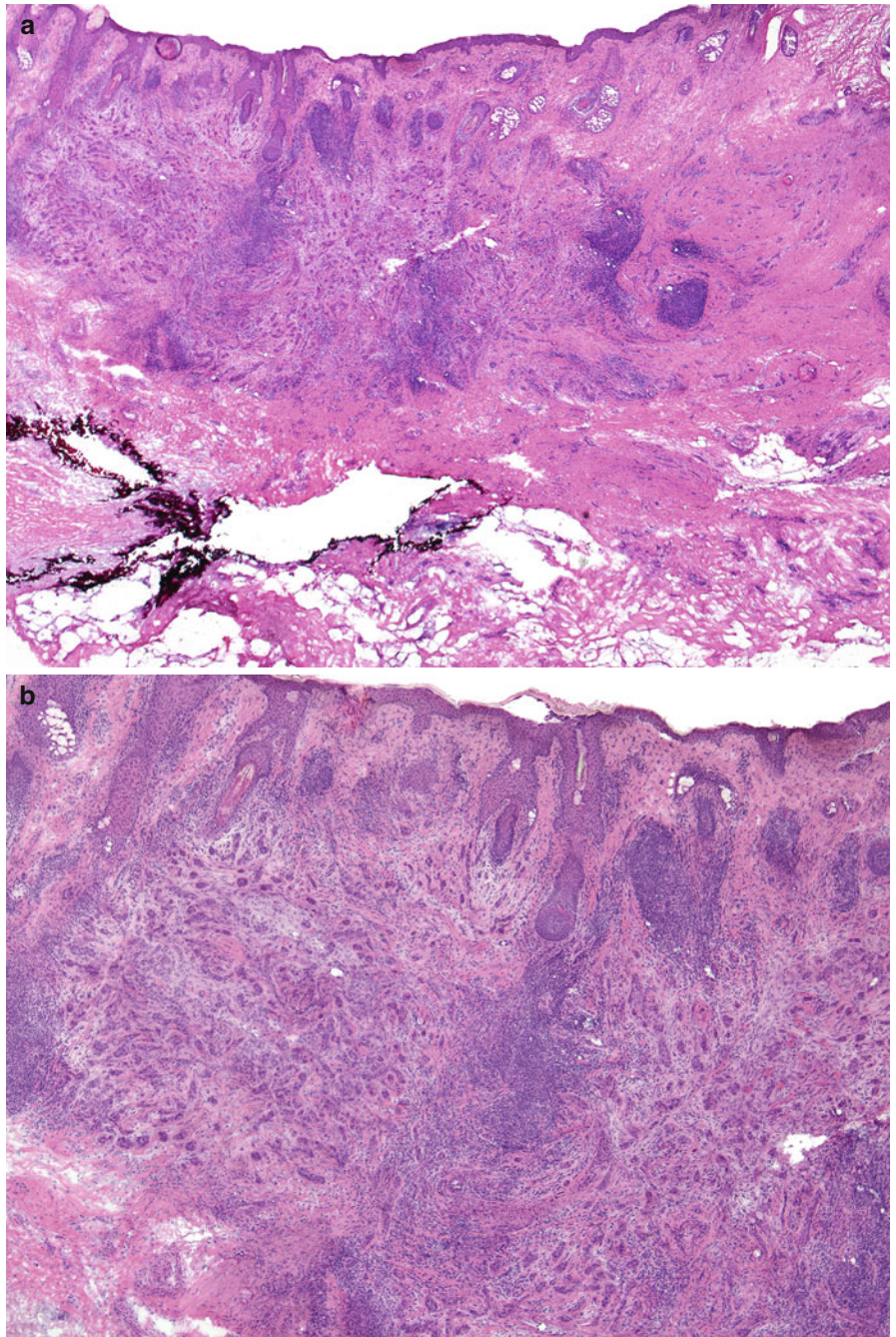


Fig. 7.1 (*continued*) (c) The tumor aggregates are composed of one to two cell layers. The neoplastic cells are relatively bland showing some hyperchromasia and pleomorphism. (d) On the right of this medium power photomicrograph the tumor transitions into an infiltrative pattern. The neoplastic aggregates are mainly cords and strands, surrounded by dense eosinophilic stroma

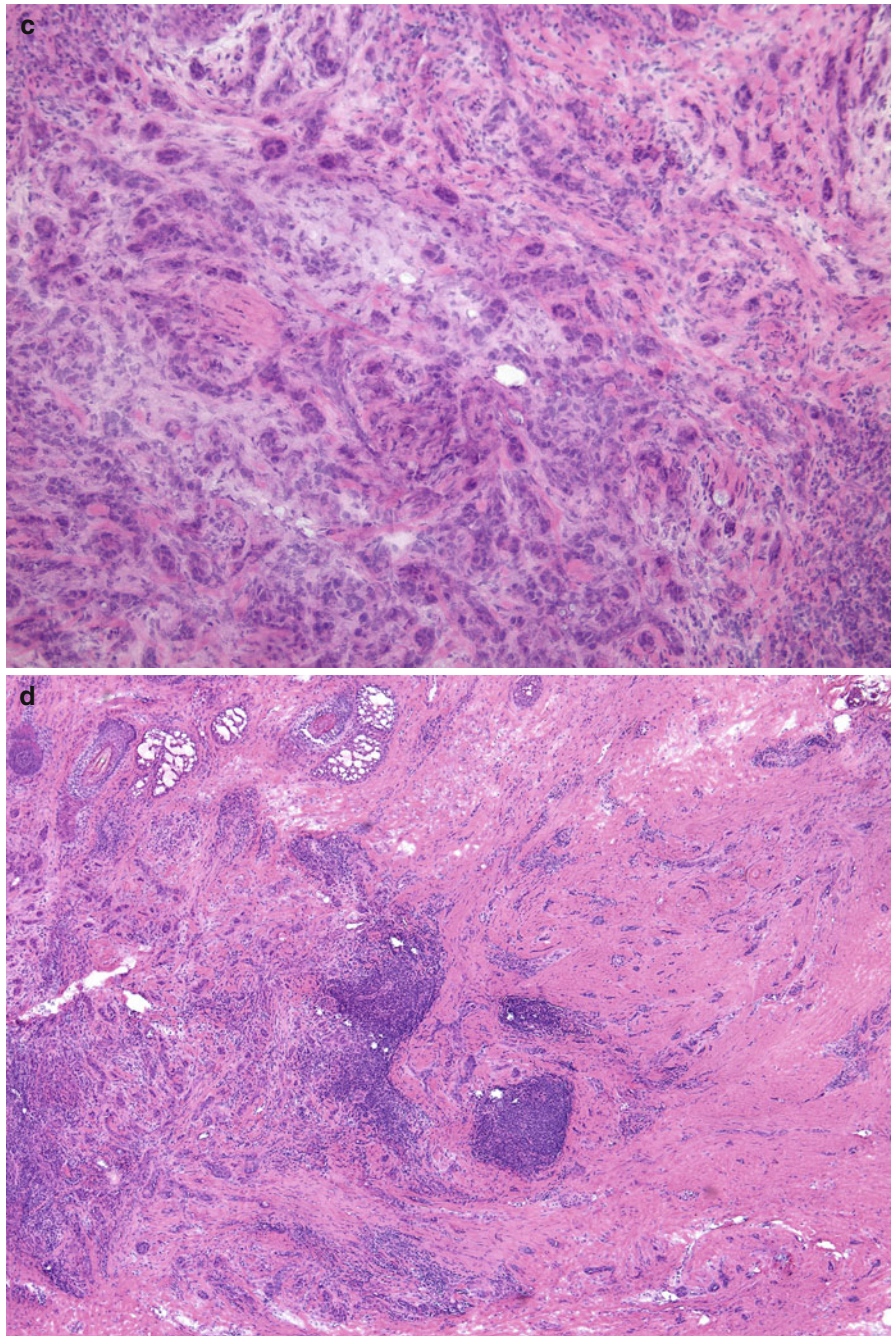


Fig. 7.1 (continued) (e) A high-power view of the sclerotic region depicting small tumor aggregates and focal surrounding inflammation

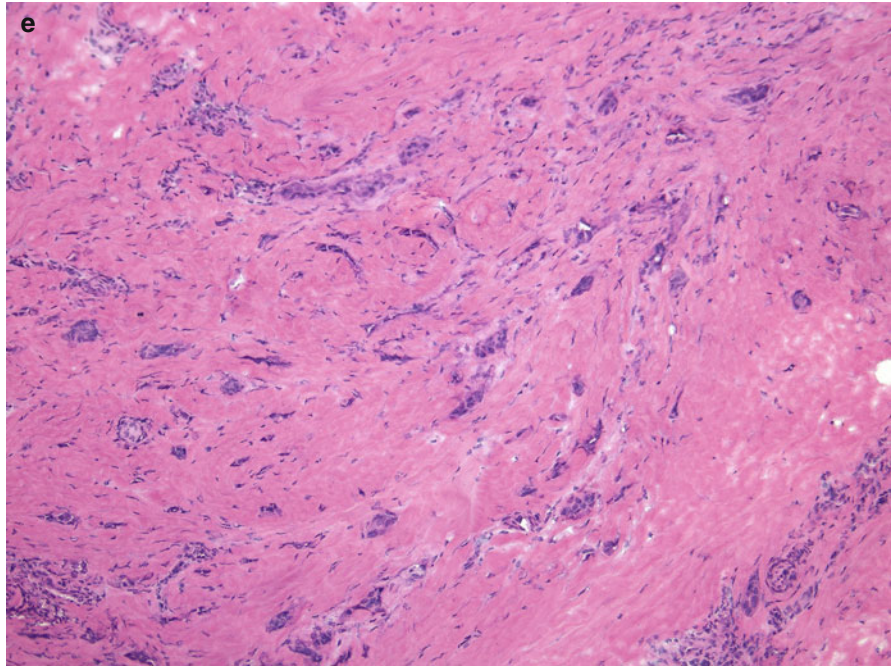


Fig. 7.2 Microcystic adnexal carcinoma: (a) Scanning magnification demonstrating the subtle nature of this rather infiltrative tumor. Only a few tumor aggregates are seen in the low reticular dermis with minimal surrounding inflammation (*ellipses*). Below the subcutaneous fat and within skeletal muscle are a few large nerves with focal dense inflammation. (b) Within the skeletal muscle are multiple nerves wrapped around and infiltrated by aggregates of tumor cells. There is focal patchy inflammation

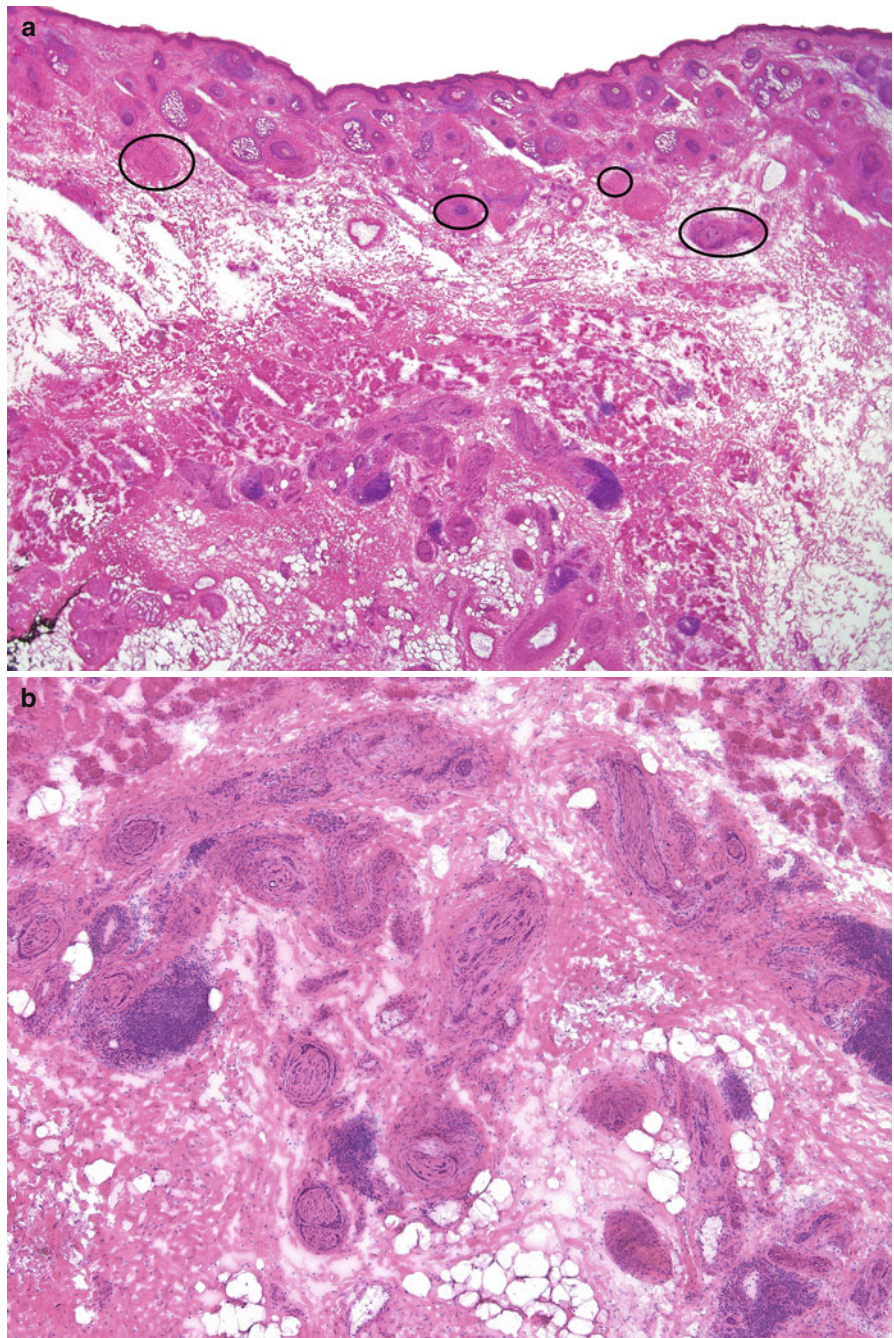


Fig. 7.2 (*continued*) (c) The neurotropic nature of this tumor can be appreciated by the presence of hyperchromatic aggregates of tumor cells infiltrating and surrounding nerve fibers. (d) Within the subcutaneous fat and skeletal muscle is an area showing dense inflammation, concentrated around nerves. The hyperchromatic cells of the carcinoma are hardly discernible

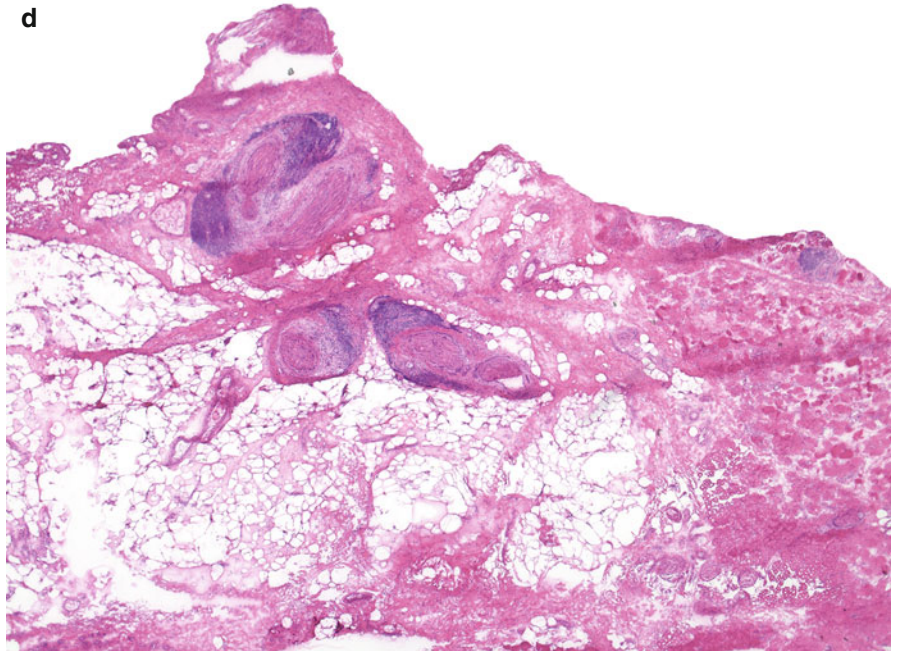
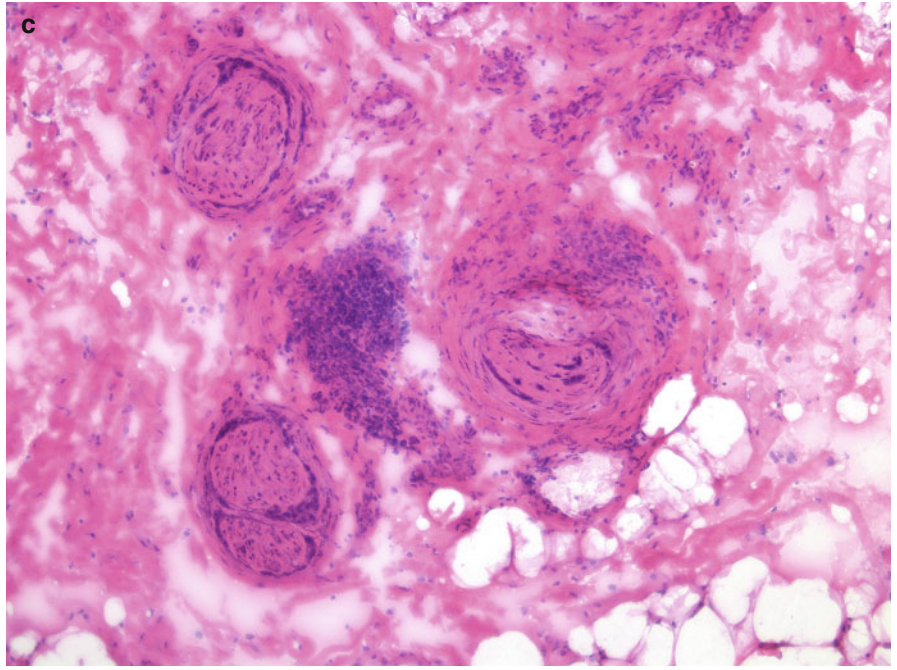


Fig. 7.2 (*continued*) (e) At a higher magnification one can appreciate strands and cords of tumor cells wrapping around and seen within the nerve fibers. This emphasizes the importance of close examination of areas which show dense inflammation. No tumor aggregates are seen anywhere else in this view except in association with nerve fibers and inflammation

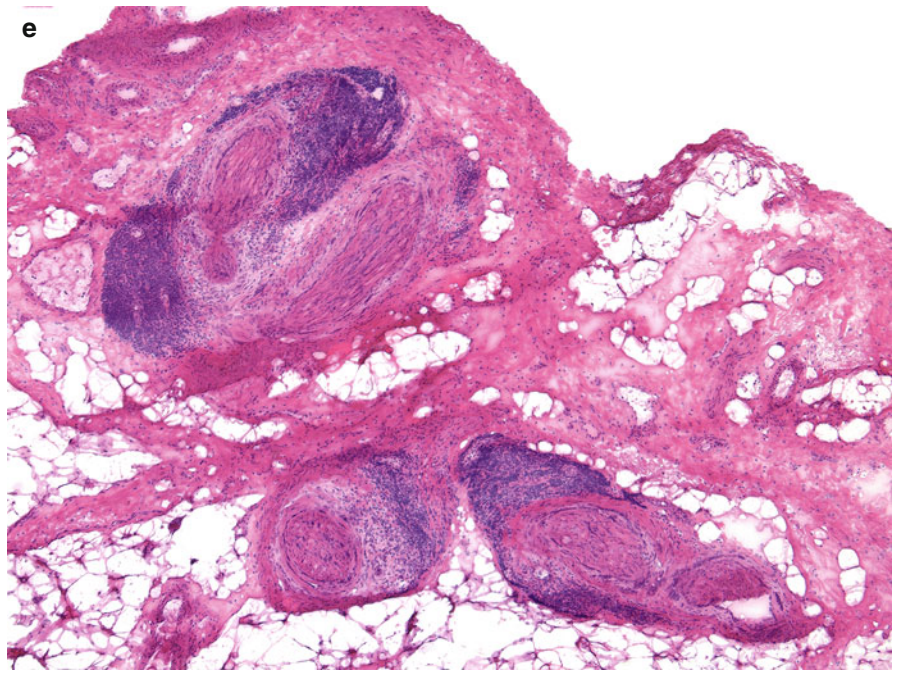


Fig. 7.3 Microcystic adnexal carcinoma:
(a) The lower reticular dermis contains very small hyperchromatic tumor aggregates.
(b) Small round and elongated tumor aggregates within fibrotic stroma stand out solely because of their hyperchromasia. They may easily be misinterpreted as normal constituents of the dermis such as eccrine ducts

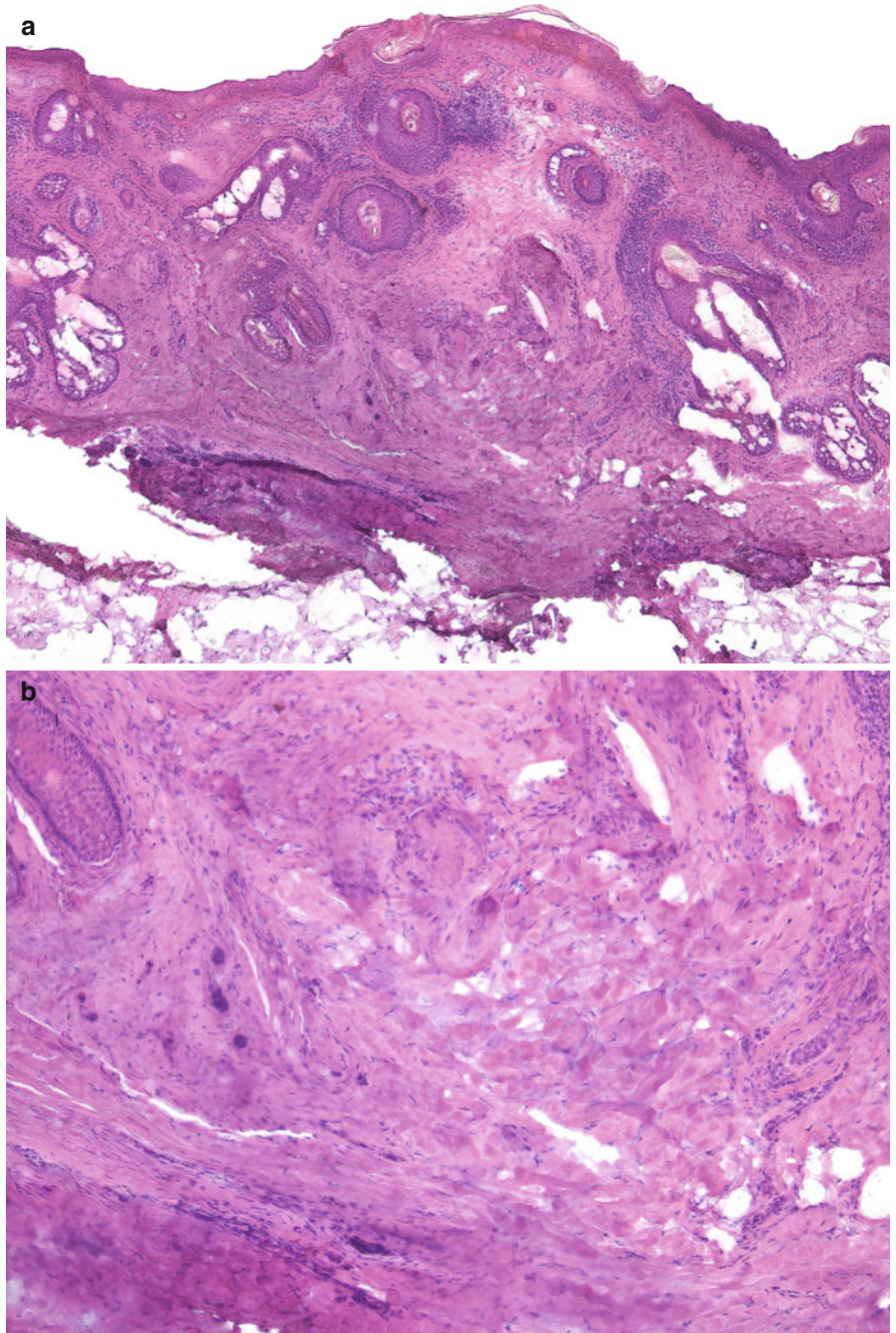


Fig. 7.4 Microcystic adnexal carcinoma: there are subtle small tumor aggregates throughout the dermis. Even at this magnification a few foci of perineural involvement are apparent

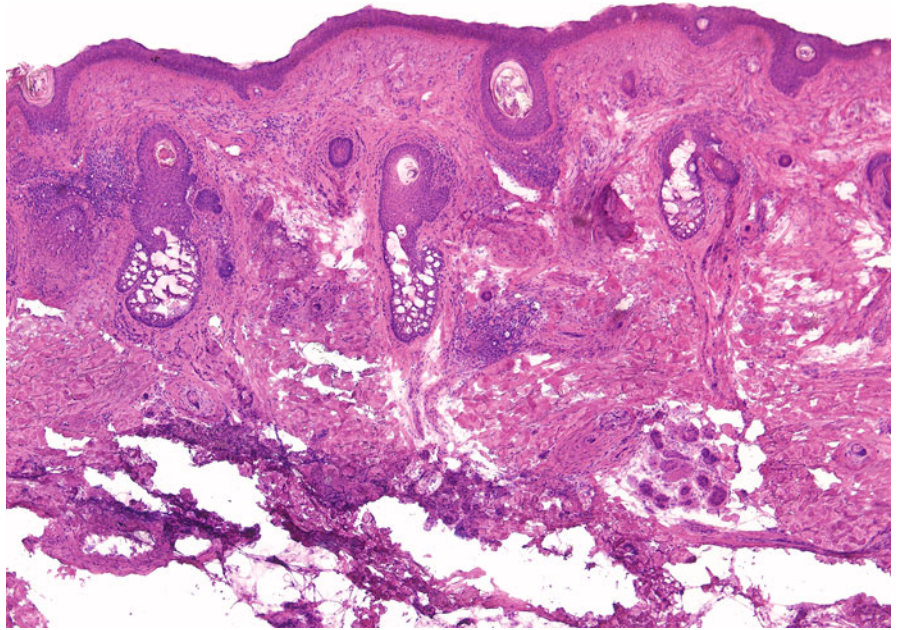


Fig. 7.5 Microcystic adnexal carcinoma: hyperchromatic tumor cells surrounding two small nerves (arrows). The importance of closely examining the entire tissue sections cannot be emphasized enough

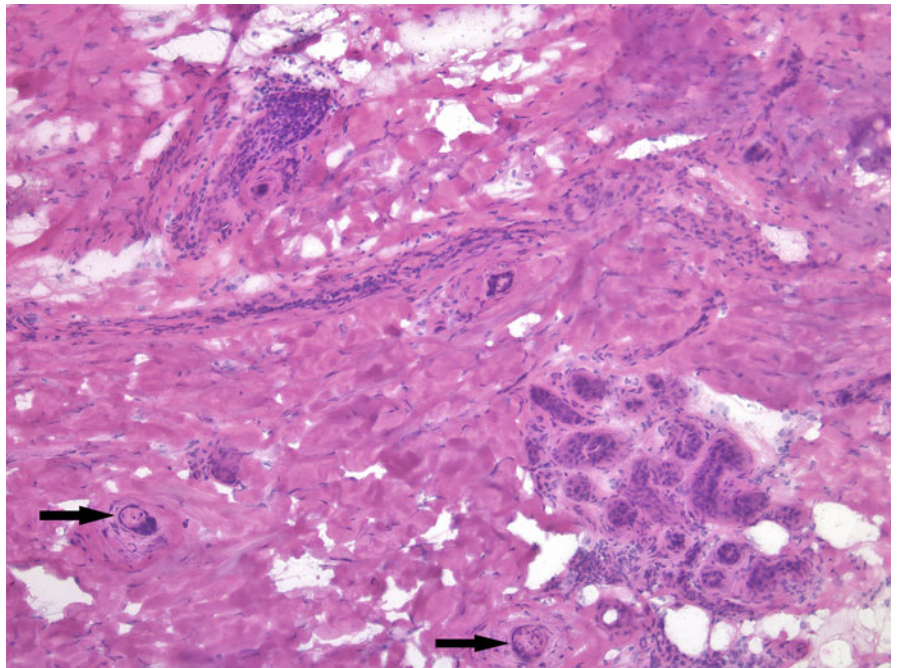


Fig. 7.6 Microcystic adnexal carcinoma:
(a) Below skeletal muscle and subcutaneous fat are infiltrative small tumor aggregates that invade the periosteum.
(b) Cords and strands of hyperchromatic neoplastic cells are seen below the skeletal muscle in the upper portion of the photomicrograph and extend into the periosteum

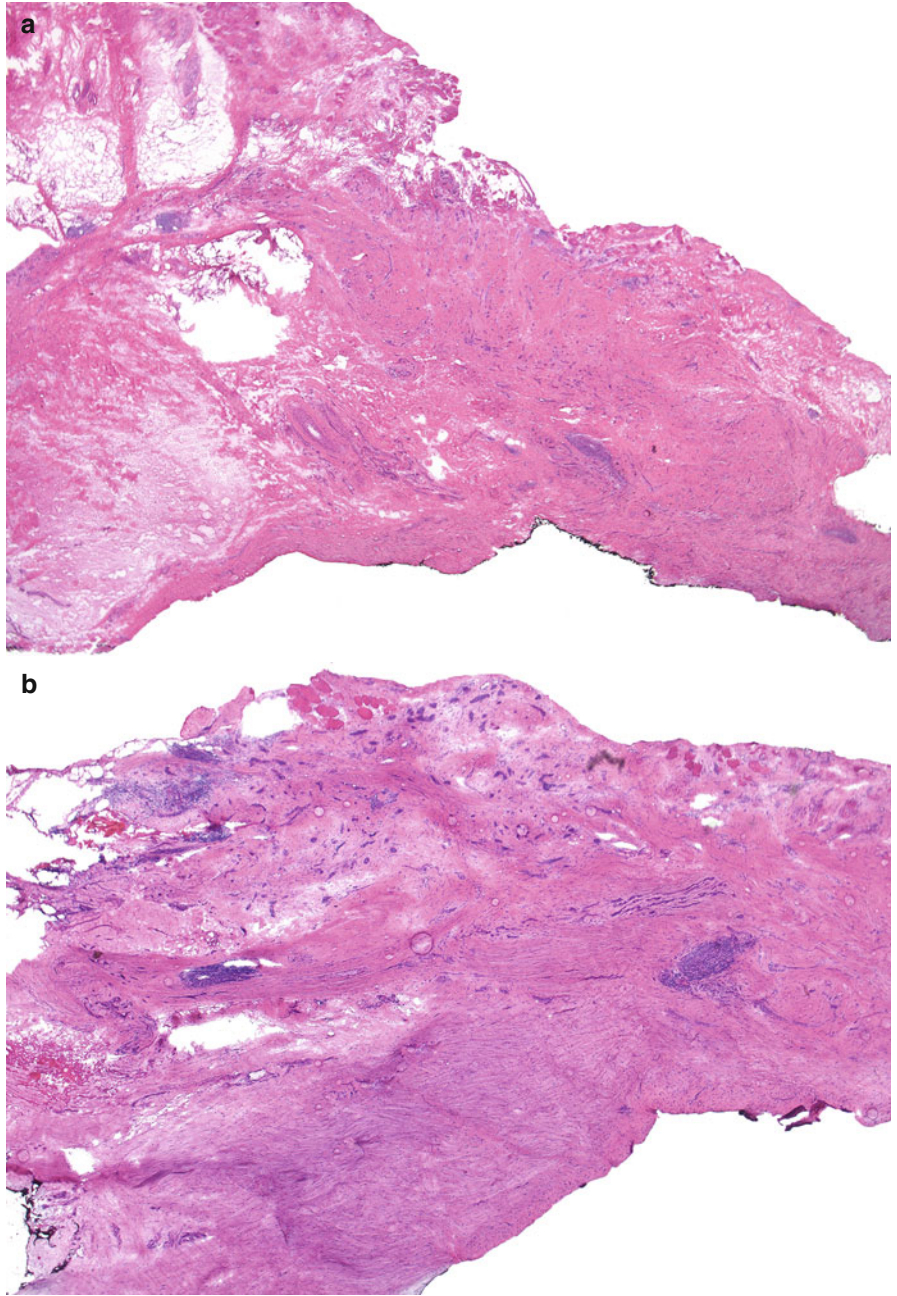


Fig. 7.6 (continued) (c) Higher magnification showing numerous small angulated or strand-like hyperchromatic tumor aggregates infiltrating the fibrotic periosteum (P). (d) Within the wavy eosinophilic periosteum are strands and cords of hyperchromatic tumor aggregates

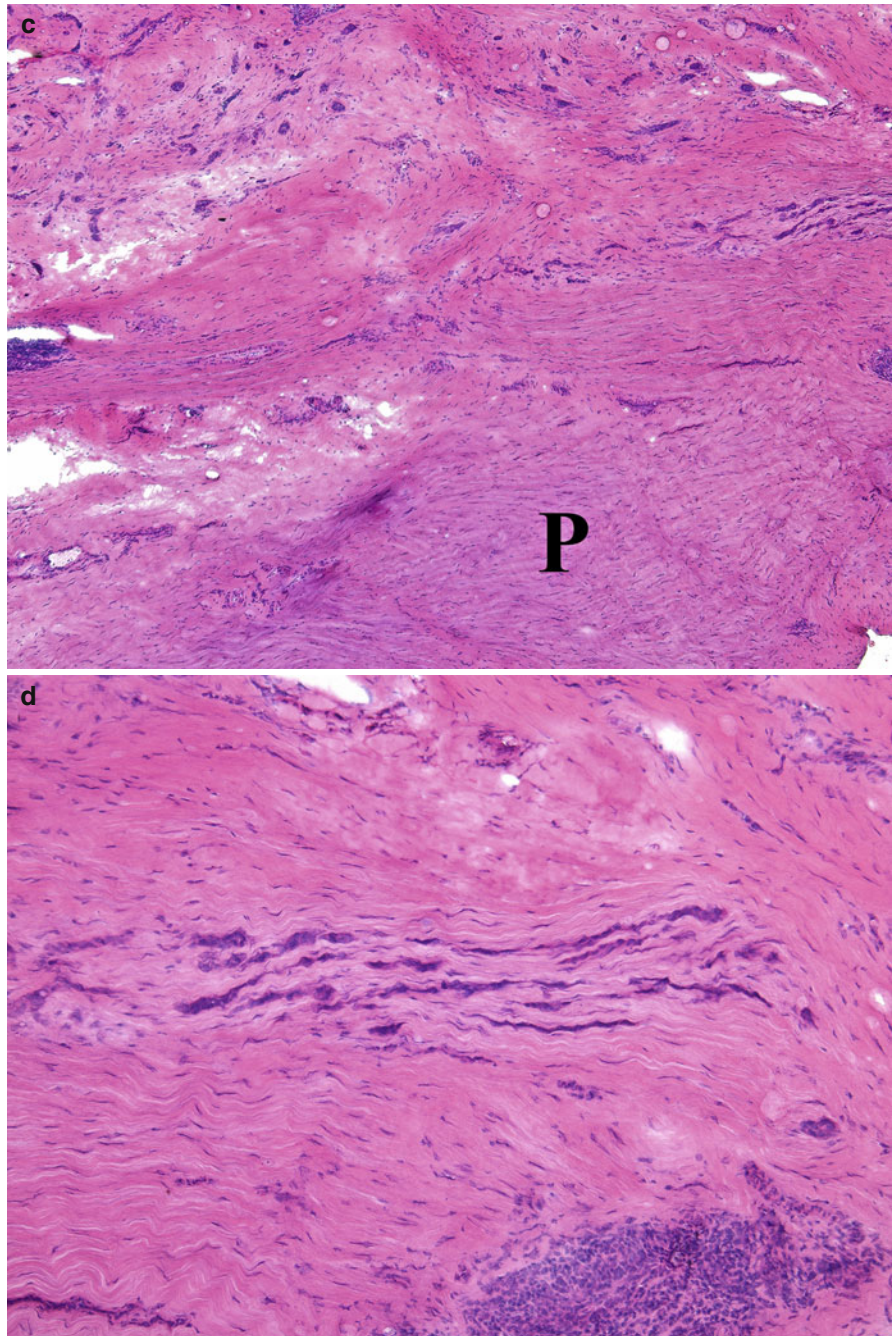


Fig. 7.7 Microcystic adnexal carcinoma: (a) Small round and angulated tumor aggregates are seen in the lower dermis extending and infiltrating into the subcutis and fascia. (b) Numerous bland round, oval, and elongated neoplastic islands infiltrating dermis and subcutis

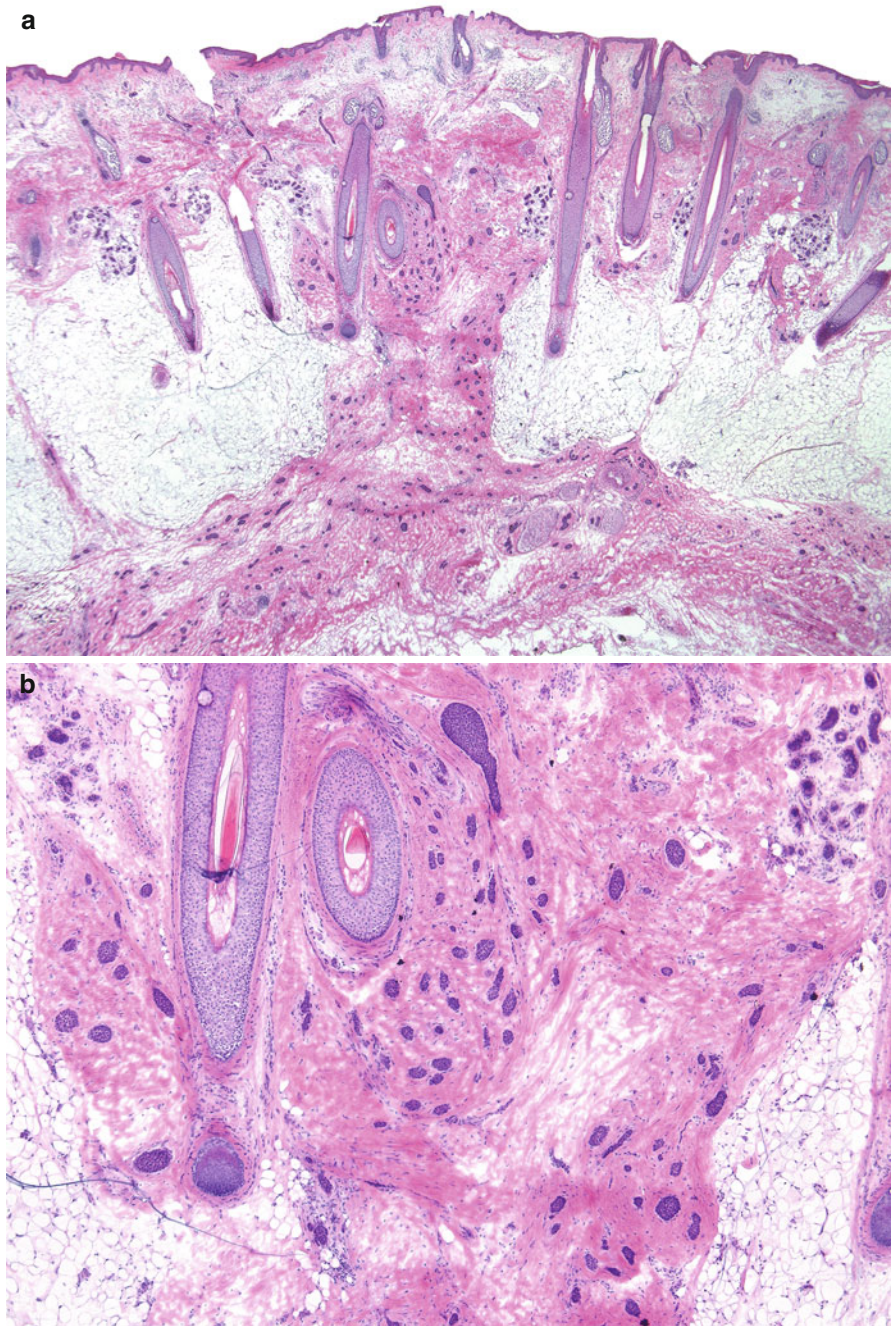


Fig. 7.7 (continued) (c) The neoplastic aggregates vary slightly in size and shape and display tubular and elongated appearance. Small lumina are seen within the center of some of them. (d) This low-power photomicrograph includes epidermis, dermis, subcutaneous fat, and underlying fascia. In this subsequent stage tumor is only seen deep within fascia

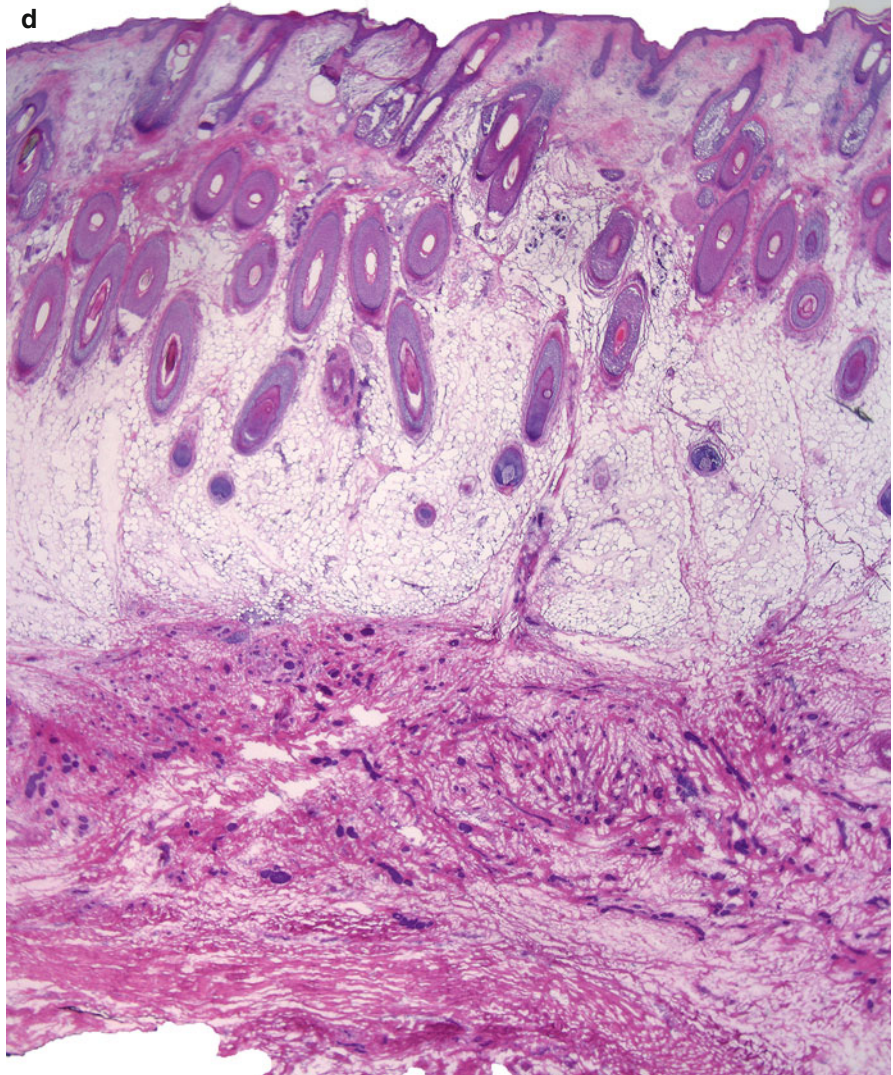
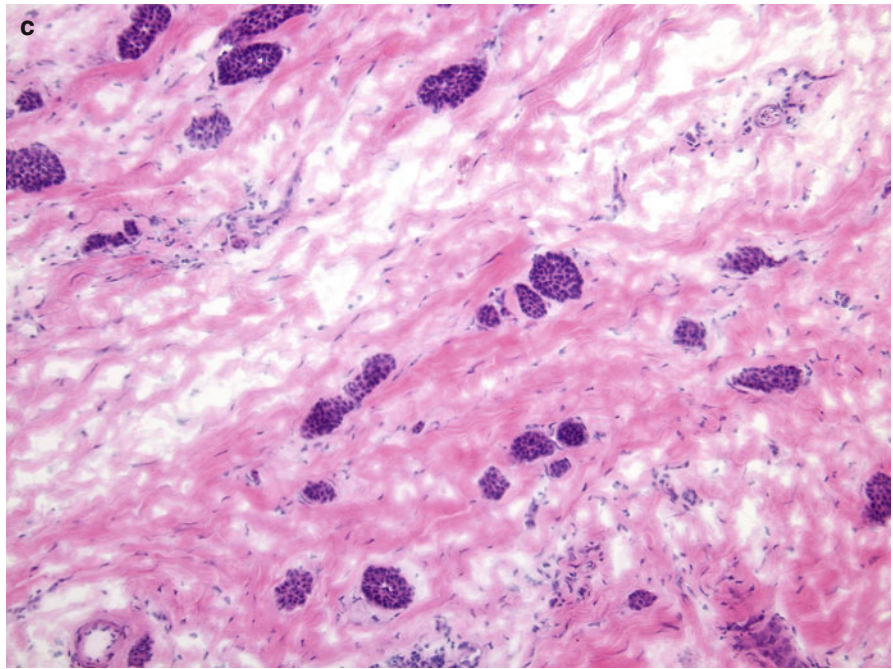


Fig. 7.7 (continued) (e) Higher magnification of the neoplastic aggregates surrounded by collagenous fibrotic stroma within fascia. (f) Many of the neoplastic aggregates show ductal lumina in their center

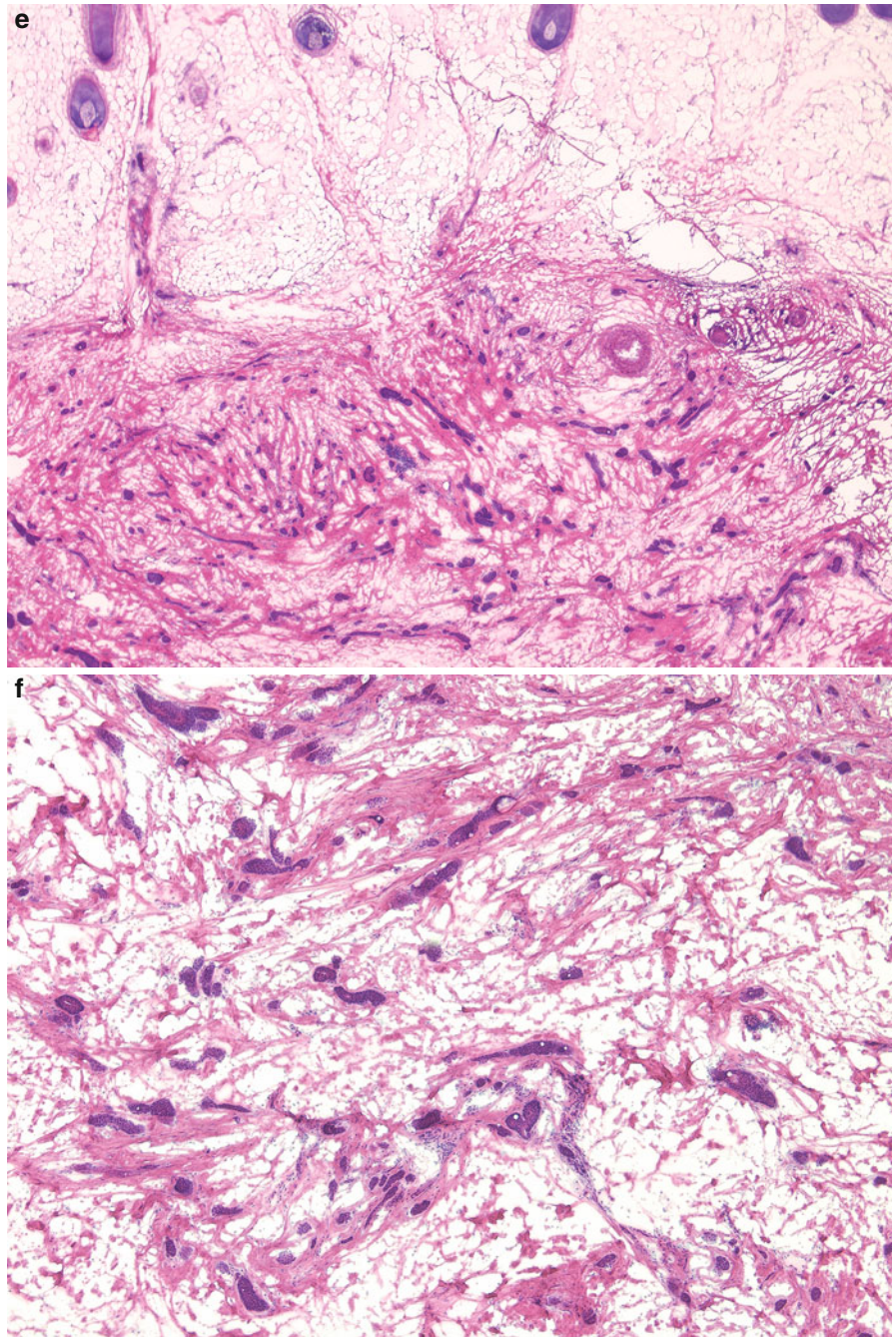
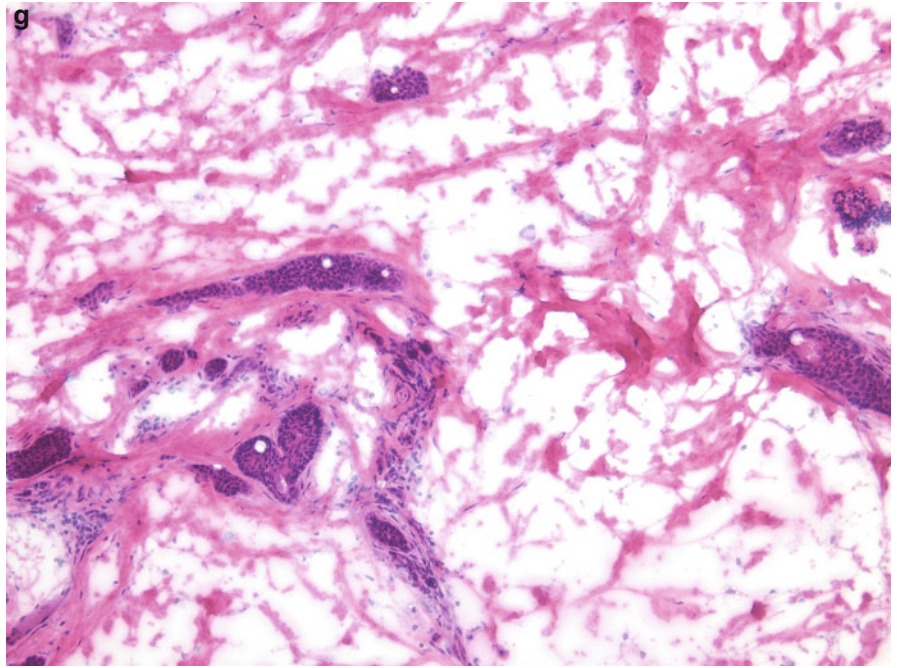


Fig. 7.7 (*continued*) (g) The neoplastic cells are fairly uniform. They are bland and do not display pleomorphism. Within some of these aggregates ductal lumina can be appreciated



Infiltrative Basal Cell Carcinoma and Desmoplastic Trichoepithelioma

Infiltrative basal cell carcinoma	Desmoplastic trichoepithelioma
1. Large neoplasm	1. Small neoplasm
2. Often deeply infiltrative, involving the entire dermis and extending to the subcutaneous fat and skeletal muscle	2. Plate-like growth pattern confined to the upper or mid dermis
3. Asymmetric growth pattern	3. Symmetric growth pattern
4. Poorly circumscribed	4. Well circumscribed
5. Neoplastic aggregates focally connecting with the undersurface of the epidermis	5. Central epidermal dell-like depression
6. Marked variation in size and shape of tumor aggregates	6. Slight variation in size and shape of tumor aggregates
7. Neoplastic aggregates larger superficially but diminishing in size in deeper tissue	7. Minimal change in the size of aggregates in deeper dermis
8. Basaloid aggregates may display bizarre angulated shapes or may be organized as strands and cords	8. Bizarre angulated shaped aggregates rarely present
9. Rare horn cysts may be present superficially	9. Horn cysts more common, particularly in the upper portion of the lesion
10. Clefts may be seen between tumor aggregates and surrounding stroma	10. Clefts may be seen within the stroma but not in between aggregates and stroma
11. Granulomatous inflammation rarely present	11. Granulomatous response with histiocytes and multinucleated giant cells to free keratin from ruptured cysts often present
12. Calcifications occasionally encountered	12. Calcifications often present
13. Perineural invasion may be present	13. No perineural invasion
14. Neoplastic cells may be pleomorphic and atypical	14. Neoplastic cells relatively monomorphous
15. Pleomorphism, mitotic figures, and pyknotic tumor cells may be seen	15. Slight pleomorphism may be present; mitotic figures absent

Infiltrative Basal Cell Carcinoma and Microcystic Adnexal Carcinoma

Infiltrative basal cell carcinoma	Microcystic adnexal carcinoma
1. Greater variation in size and shape of tumor aggregates	1. Variation in size and shape of tumor aggregates
2. Lack of horn cysts	2. Horn cysts may be present superficially
3. Lack of granulomatous inflammation	3. Granulomatous inflammation around ruptured cysts may be present
4. Foci of typical nodular basal cell carcinoma often present	4. No foci of typical nodular basal cell carcinoma
5. Clefts between neoplastic aggregates and surrounding stroma	5. No clefts between aggregates and stroma
6. Inflammation usually present	6. Inflammation usually absent
7. Often connection of the neoplastic aggregates to the overlying epidermis	7. No connection of the neoplastic aggregates to the overlying epidermis
8. No ductal structures	8. Ductal structures present

Infiltrative Basal Cell Carcinoma and Syringoma

Infiltrative basal cell carcinoma	Syringoma
1. Large neoplasm	1. Small neoplasm
2. Often deeply infiltrative involving the entire dermis and extending to the subcutaneous fat and skeletal muscle	2. Rounded, non-encapsulated tumor in the superficial to mid reticular dermis
3. Asymmetric growth pattern	3. Symmetric growth pattern
4. Poorly circumscribed	4. Well demarcated
5. Neoplastic aggregates focally connecting with the undersurface of the epidermis	5. No connection with the overlying epidermis
6. Marked variation in size and shape of tumor aggregates	6. Slight variation in size and shape of aggregates
7. Neoplastic aggregates larger superficially but diminishing in size in deeper tissue	7. Minimal change in the size of aggregates. In general tumor aggregates do not extend beyond mid reticular dermis.
8. Basaloid aggregates may display bizarre angulated shapes or may be organized as strands and cords	8. Small epithelial aggregates with round, coma-like, or tadpole shapes, as well as elongated strands of epithelial cells
9. Neoplastic cells mostly arranged in strands and cords	9. Numerous round epithelial aggregates and tubular structures predominate over cords and strands
10. Presence of stroma variable	10. Dense pink sclerotic collagenized stroma surrounding tumor aggregates; lack of solar elastosis or mucin within the stroma
11. Clefts may be seen between tumor aggregates and surrounding stroma	11. Clefts between aggregates and stroma not present
12. No ductal structures present	12. Duct-like structures with homogeneous pink secretions in their lumina admixed with the tumor aggregates
13. Perineural invasion may be present	13. No perineural invasion
14. Neoplastic cells may be pleomorphic and atypical	14. Neoplastic cells relatively monomorphous
15. Tumor aggregates highly infiltrative in between normal structures	15. Tumor aggregates push surrounding adnexal structures but do not infiltrate them
16. Pleomorphism, mitotic figures, and pyknotic tumor cells may be seen	16. Monomorphous tumor cells, lacking atypia and mitotic figures; no individual pyknotic cells
17. Inflammation common	17. Minimal inflammatory infiltrate associated with the tumor

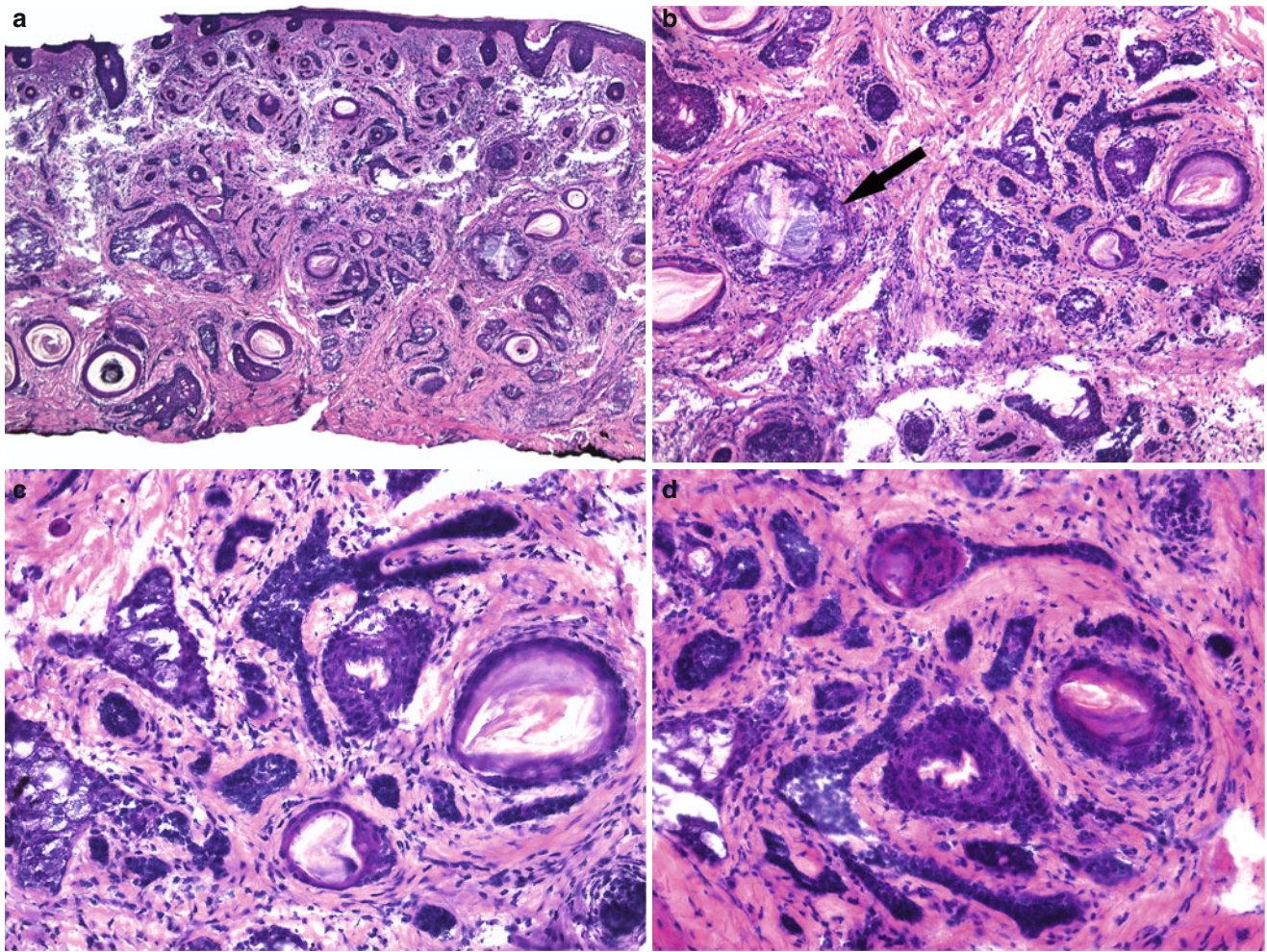


Fig. 8.1 Basal cell carcinoma: (a) This basal cell carcinoma at first glance resembles desmoplastic trichoepithelioma. The infiltrative borders and the large angulated aggregates are features of BCC. (b) There is variation of size and shape of the neoplastic aggregates. Keratinizing cysts and surrounding foreign body type granulomatous reaction

(arrow) are not uncommon in BCC as in this case. (c) Although there are two small cysts filled with keratin, which often favor DTE, the presence of irregular basaloid aggregates confirms the diagnosis of BCC. (d) Rarely ductal tadpole-like structures, similar to those present in syringoma, can be seen in BCC

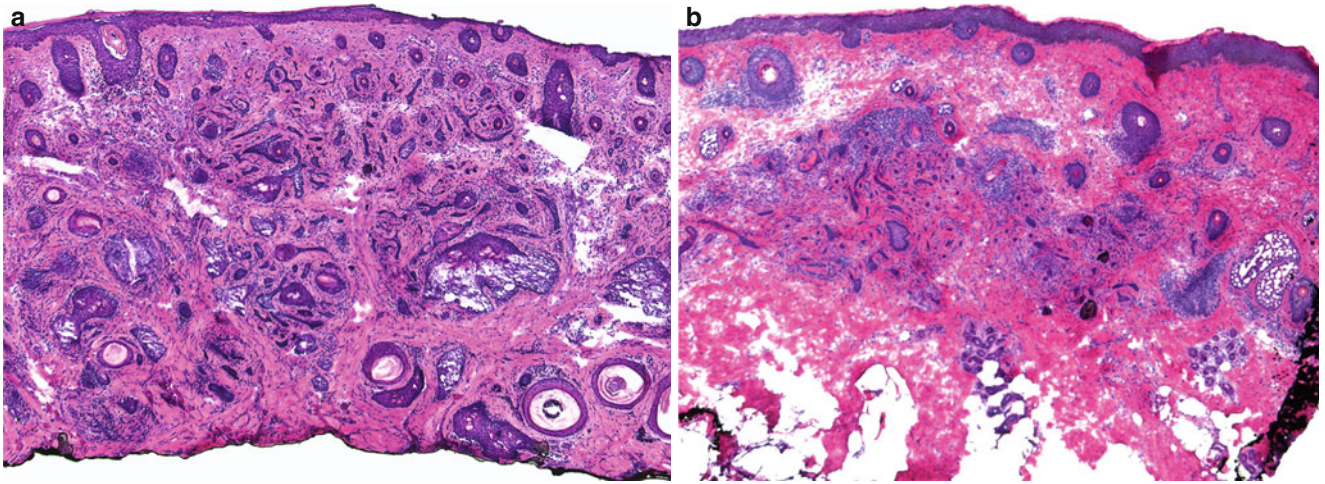


Fig. 8.2 BCC versus DTE: (a) Basal cell carcinoma: tumor is poorly circumscribed and deeply infiltrating. There is a connection with the epidermis. Tumor aggregates vary considerably in size and shape

(b) Desmoplastic trichoepithelioma (DTE): well-demarcated and non-encapsulated plate-like neoplasm. A few follicular cysts surrounded by inflammation can be appreciated even at scanning magnification. Dense fibrotic stroma is seen around the epithelial aggregates

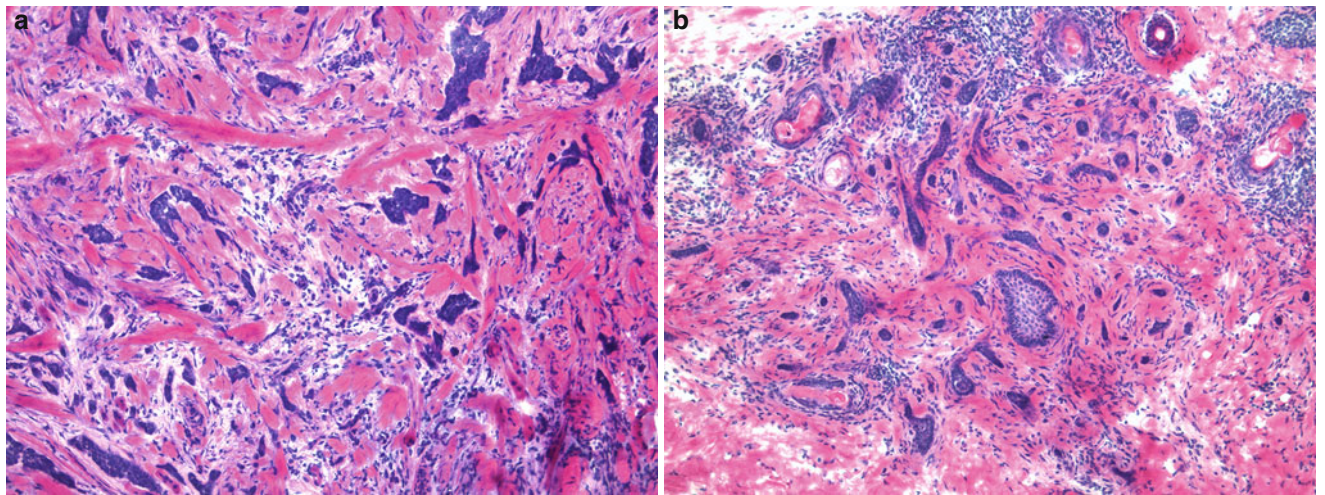


Fig. 8.3 BCC versus DTE: (a) Basal cell carcinoma: angulated and hyperchromatic tumor aggregates with focal clefting between tumor aggregates and surrounding stroma. Aggregates vary considerably in size and shape

(b) Desmoplastic trichoepithelioma (DTE): epithelial aggregates showing less variation in size and shape. All aggregates are relatively small and are embedded in fibrotic stroma

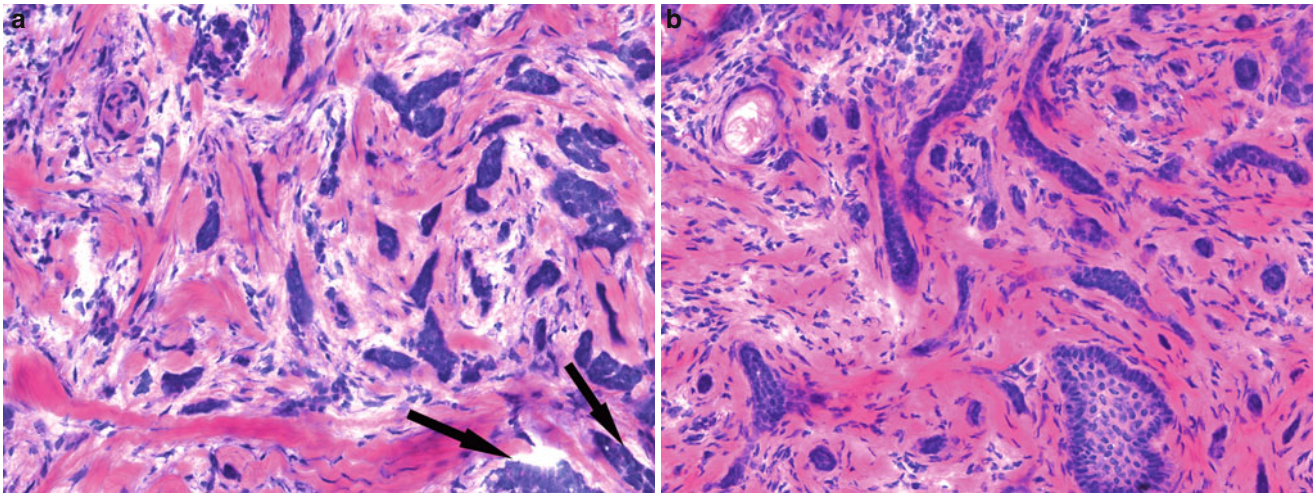


Fig. 8.4 BCC versus DTE: (a) Basal cell carcinoma: hyperchromatic neoplastic cells forming irregular, angulated tumor aggregates embedded in sclerotic and slightly mucinous stroma. Note focal clefting between the tumor aggregates and the stroma (*arrows*)

(b) Desmoplastic trichoepithelioma (DTE): free keratin surrounded by inflammation and foreign body type granulomatous reaction in the left upper corner of the photomicrograph. There is lack of clefting between the tumor aggregates and the surrounding stroma. Although these aggregates are slightly variable in size and angulated (similar to BCC) the cells that form these aggregates are smaller and rather monomorphic

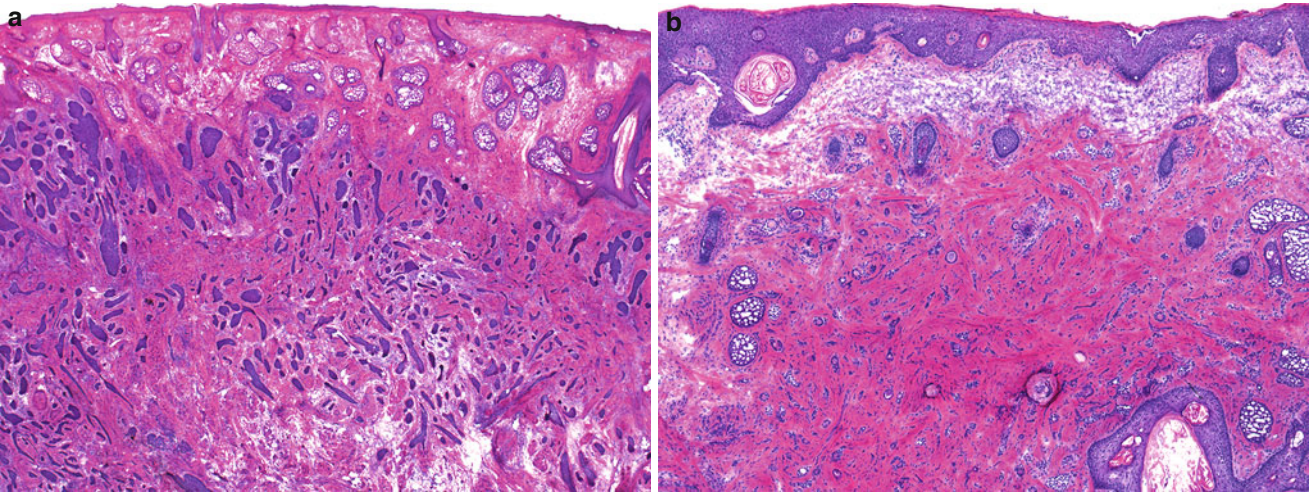


Fig. 8.5 BCC versus Syringoma: (a) Basal cell carcinoma: basaloid tumor aggregates throughout the reticular dermis showing considerable variation in size and shape. Note how the neoplastic aggregates diminish in size with their descent into the deeper tissue

(b) Syringoma: well-delineated tumor composed of epithelial aggregates and ductal structures. The tumor is limited to the dermis and has no epidermal connection. The tumor aggregates are similar in size and shape throughout the entire lesion and are surrounded by pink, fibrotic stroma

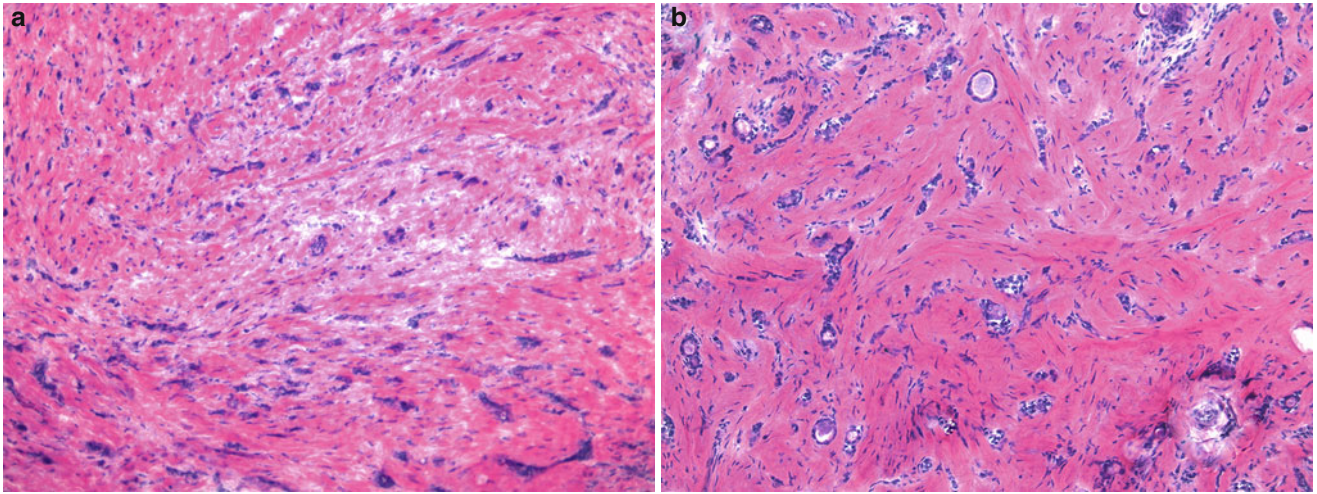


Fig. 8.6 BCC versus Syringoma: (a) Basal cell carcinoma: strands, cords, and elongated tumor aggregates with significant variation in size, embedded in a dense collagenous stroma

(b) Syringoma: round, elongated, or tadpole-shaped epithelial aggregates embedded in pink collagenous stroma. Small ducts, lined by two layers of epithelial cells, containing pink secretions in their lumina are intermingled with the other epithelial structures

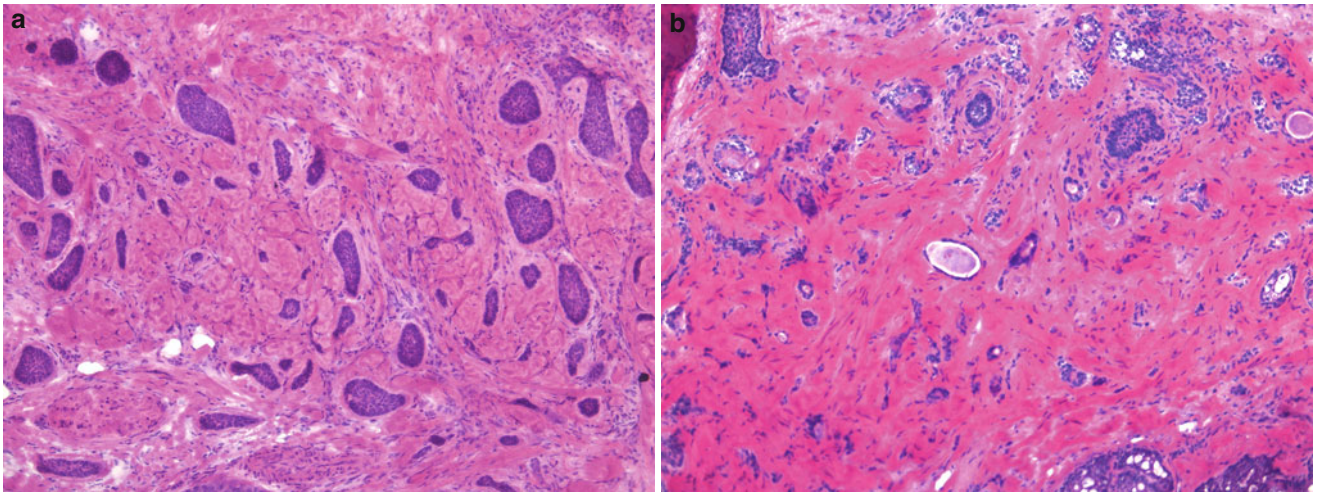


Fig. 8.7 BCC versus Syringoma: (a) Basal cell carcinoma: irregular solid basaloid aggregates with prominent variation in their size and shape infiltrating in between skeletal muscle. Incidentally, some of the tumor aggregates have tadpole shapes; however, ductal lumina are not present

(b) Syringoma: round-, oval-, and tadpole-shaped epithelial aggregates, many with central lumina containing eosinophilic secretions. They are embedded in pink collagenous stroma

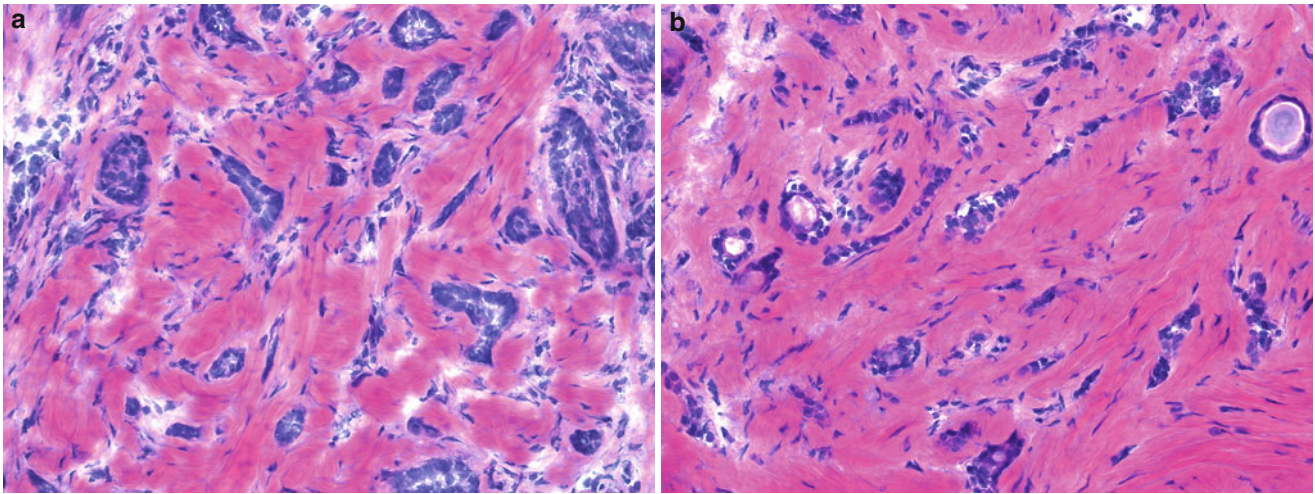
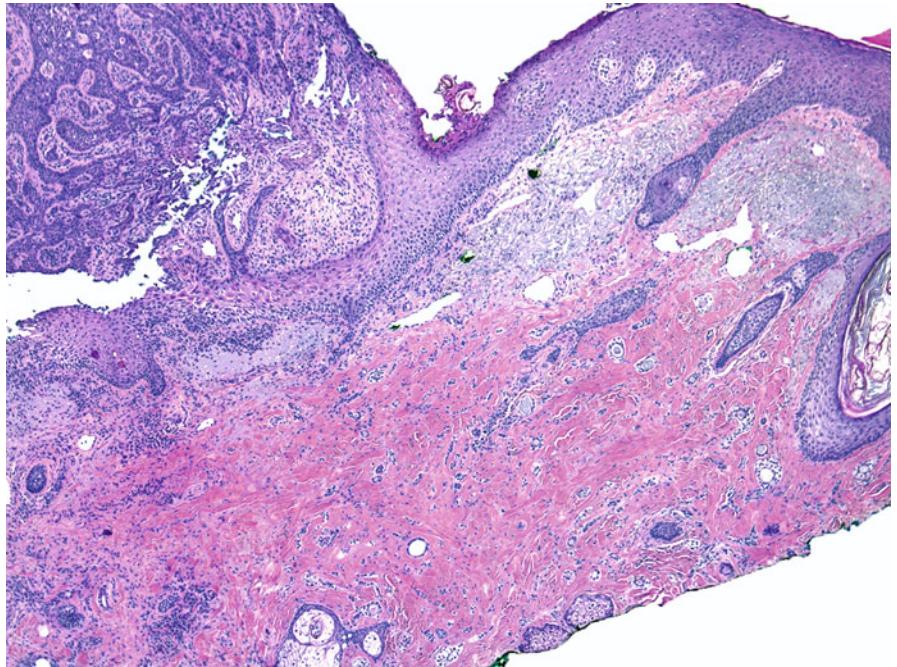


Fig. 8.8 BCC versus Syringoma: (a) Basal cell carcinoma: variation in size and shape of tumor aggregates. Some aggregates are angulated and others resemble strands and cords

(b) Syringoma: Mostly oval-, round-, or tadpole-shaped epithelial aggregates surrounded by eosinophilic dense stroma. The presence of ductal structures with lumina and pink secretions helps differentiate this syringoma from basal cell carcinoma. The cells are small and monomorphous unlike the neoplastic cells of BCC

Fig. 8.9 Basal cell carcinoma and syringoma: this is a formalin fixed section with BCC in left upper corner and an incidental syringoma in the adjacent dermis on the right



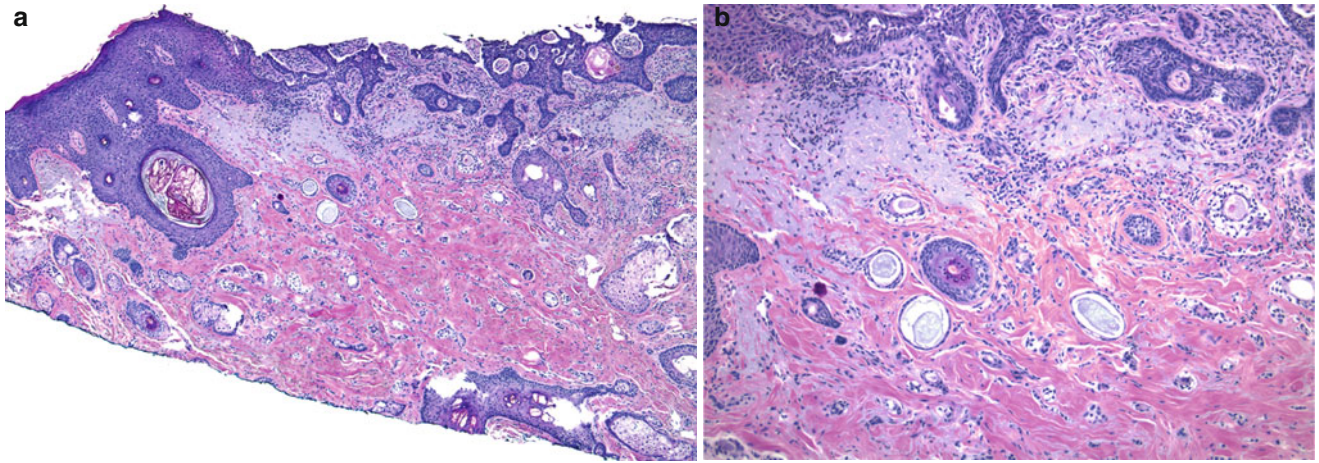


Fig. 8.10 Basal cell carcinoma and syringoma: **(a)** Basal cell carcinoma is evident on the right and a well-demarcated incidental syringoma is present in the adjacent dermis below and on the left

(b) The dense pink stroma of the syringoma contrasts with the solar elastosis seen immediately under the basaloid neoplastic aggregates of the BCC

Histologic Features

1. Keratinocytic atypia involving the entire thickness of the epidermis.
2. Crowding of the keratinocytes in the basal layer of the epidermis with disorganization and a “wind blown appearance.”
3. Focal alignment of the keratinocytes at the basal cell layer forming a row of darkly stained keratinocytes with high nuclear to cytoplasmic ratio, the so-called “eyeliner sign.”
4. Lack of maturation of the keratinocytes with their ascent to the upper layers.
5. Lack of normal keratinization, i.e., overlying parakeratosis as opposed to normal basket-woven keratin layer.
6. Large pleomorphic keratinocytes with hyperchromatic, irregular nuclei, and abundant eosinophilic cytoplasm. Atypia may range from subtle to severe.
7. Multinucleated keratinocytes may be present.
8. Keratinocytes often appear vacuolated.
9. Individual dyskeratotic/necrotic cells. Discernible intercellular bridges.
10. Premature keratinization in some of the neoplastic keratinocytes with dense pink keratin in their cytoplasm.
11. Increased number of mitotic figures, many of which are atypical.
12. Often a lichenoid lymphocytic infiltrate in the papillary dermis.
13. Intact basement membrane.
14. Atypical keratinocytes can involve the follicular epithelium.

Histopathologic Differential Diagnosis

Actinic Keratosis

1. Alternating ortho and parakeratosis.
2. Lack of full thickness atypia of the epidermis. The atypia is appreciated only in the lower levels of the epidermis.
3. Keratinocytic atypia does not involve follicular structures.
4. No eyeliner sign.
5. Rarely mitotic figures.

Intraepidermal Paget’s Disease

1. Large epithelioid cells in small groups or as individual cells scattered at all levels of the epidermis but with some cells present at the dermal epidermal junction.
2. The cells have vesicular nuclei, often basophilic nucleoli and abundant pale cytoplasm.
3. Low nuclear to cytoplasmic ratio, i.e., abundant cytoplasm and no intercellular bridges.
4. Rarely the neoplastic cells contain pigment in their cytoplasm the so-called pigmented Paget’s disease variant.

Malignant Melanoma In Situ

1. Neoplastic cells in nests that vary in size and shape positioned at the dermal epidermal junction and above it.
2. The main histopathologic activity is at the dermal epidermal junction where the majority of single melanocytes and nests of melanocytes are present.
3. No intercellular bridges.
4. Often melanin pigment within the cytoplasm of the cells.
5. Usually low to moderate nuclear to cytoplasmic ratio, i.e., the cells have a small to moderate amount of cytoplasm.
6. No eyeliner sign.
7. Usually no overlying parakeratosis.

Fig. 9.1 Squamous cell carcinoma in situ (SCCIS): (a) Acanthotic epithelium with large atypical keratinocytes throughout the full thickness of the epidermis. There is also overlying parakeratosis. (b) Higher magnification demonstrating the atypical, pleomorphic nuclei as well as the overall disorganized wind-blown appearance of the keratinocytes

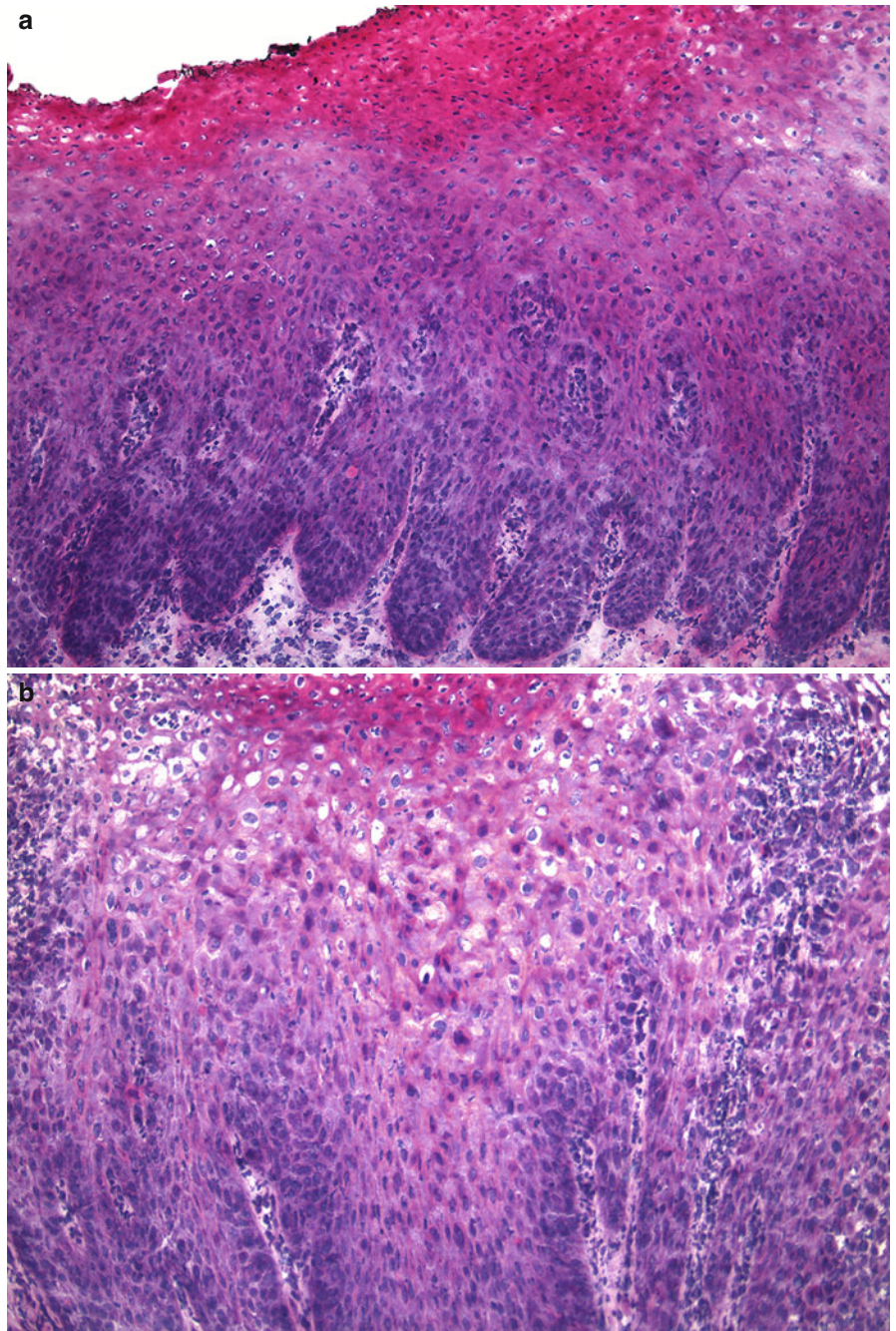


Fig. 9.1 (continued) (c) Crowding of hyperchromatic pleomorphic keratinocytic nuclei in the lower levels of the epidermis. (d) Individual dyskeratotic/necrotic keratinocytes with pyknotic nuclei and brightly eosinophilic cytoplasm (*arrows*)

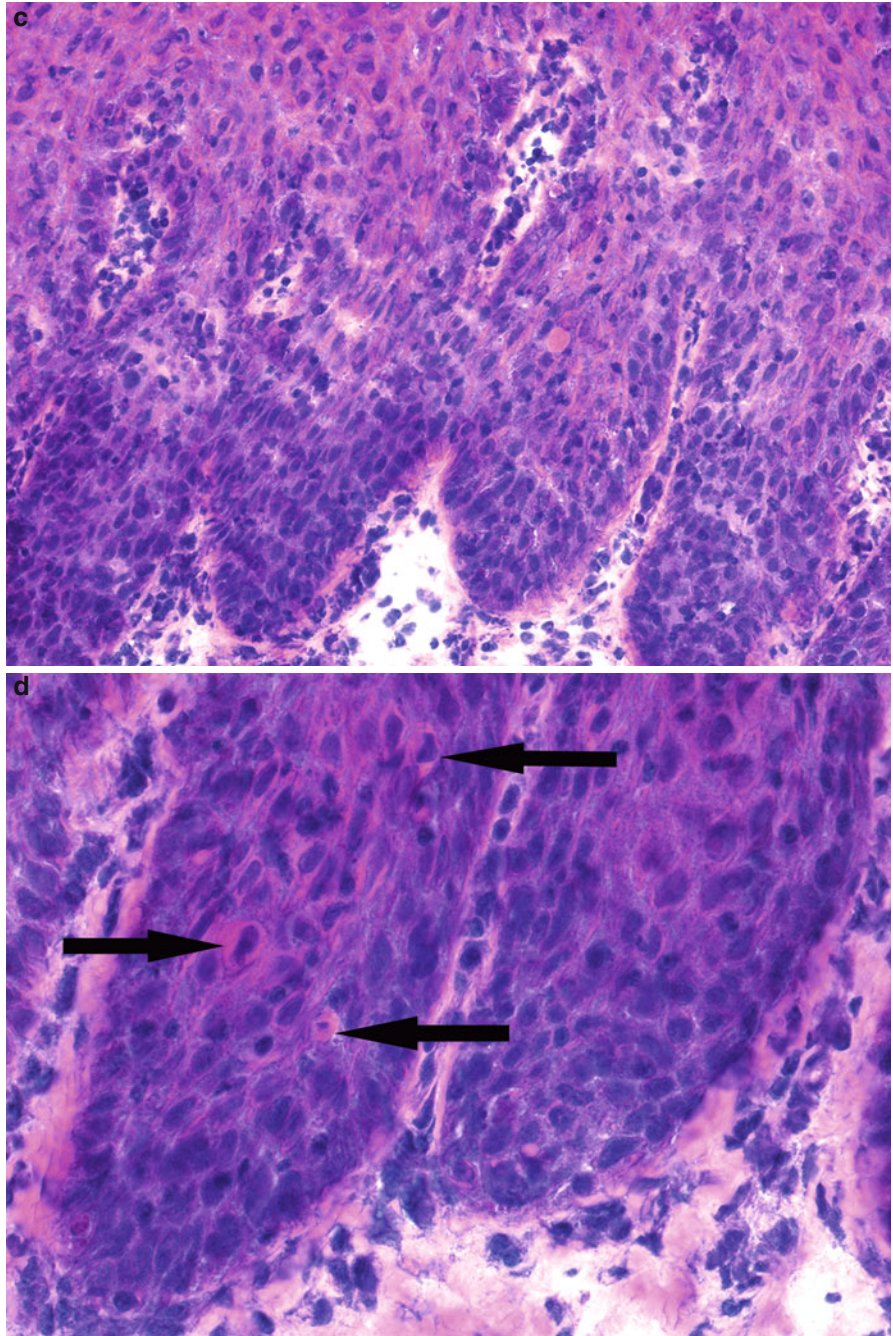


Fig. 9.1 (continued) (e) Pleomorphic, hyperchromatic, and crowded keratinocytic nuclei with scattered mitotic figures (arrow)

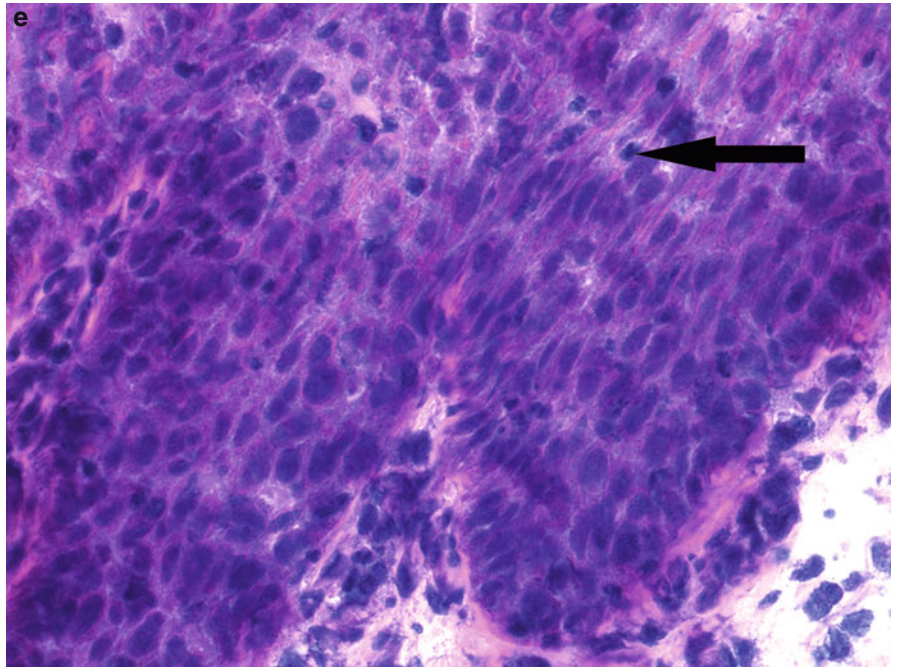


Fig. 9.2 SCCIS: prominent “eyeliner sign” with a row of hyperchromatic keratinocytes aligned at the basal layer of the epidermis. Overlying parakeratosis forming a parakeratotic pearl in the left upper corner of the photograph. Absence of granular cell layer is indicative of the lack of maturation. There is also a dense lichenoid lymphocytic infiltrate in the superficial dermis

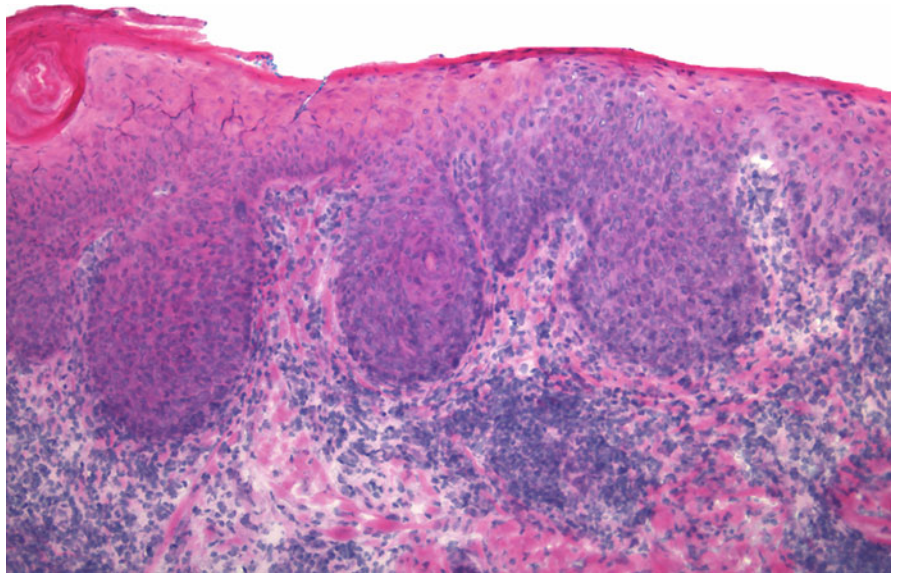


Fig. 9.3 Actinic keratosis: (a) Crowded keratinocytes within the lower part of the epidermis and overlying parakeratosis. Inflammatory cell infiltrate is noted in the underlying dermis. (b) Higher magnification showing slightly pleomorphic keratinocytes with hyperchromatic nuclei crowded together in the lower third of the epidermis. In actinic keratosis there is maturation of the keratinocytes toward the surface of the epidermis in contrast to squamous cell carcinoma in situ, where the entire epidermis is replaced by large neoplastic keratinocytes. The granular cell layer is usually lost and there is overlying parakeratosis as in this case

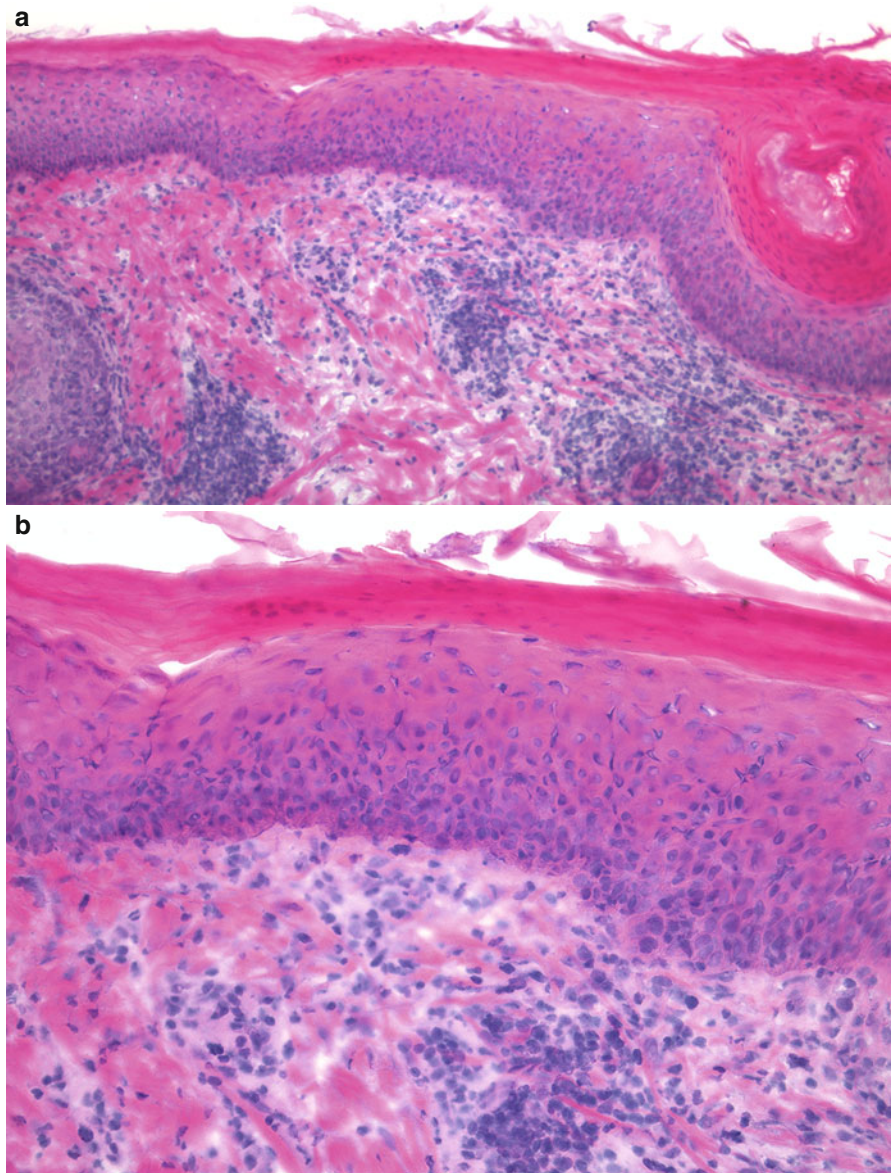


Fig. 9.4 SCCIS: (a) At low power the most notable feature alerting to the presence of SCC in situ is the epidermal acanthosis and overlying parakeratosis. Note how the epidermis on the right is markedly thicker than the normal epidermis on the left (*arrow*). (b) Acanthosis, enlarged, atypical keratinocytes in a disorderly arrangement, and abnormal maturation with an overlying parakeratotic layer. The presence of basal keratinocytes aligned in a row with the contrasting disarray of the overlying cells creates the appearance of an “eye-liner” sign (*arrow*). (c) The epidermis in this photomicrograph represents a transition between the SCCIS and normal epidermis. There is mild disarray of the keratinocytes and hyperkeratosis

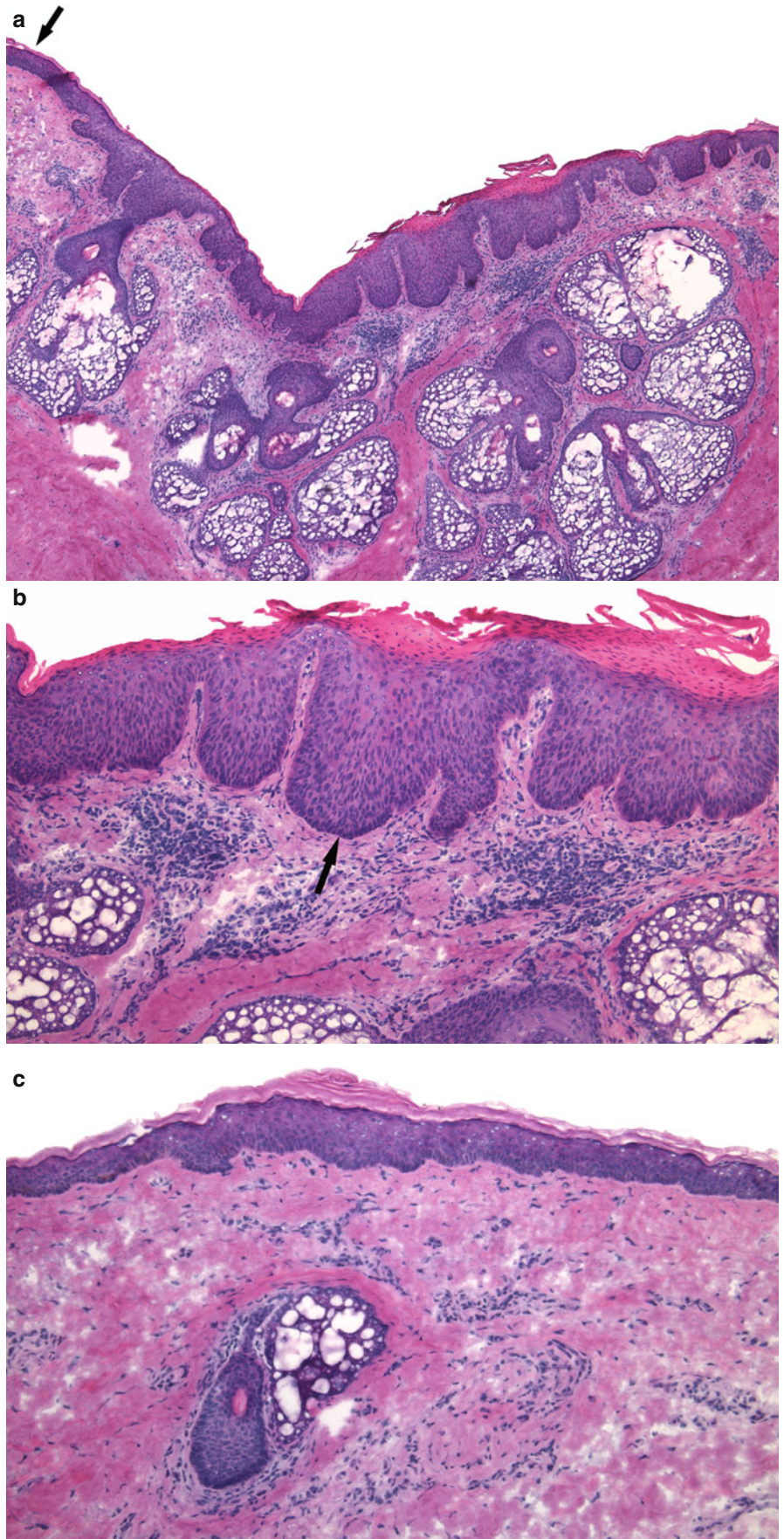


Fig. 9.5 (a) Tangential sectioning of an area adjacent to SCC in situ creates pseudo-acanthosis and can make the diagnosis challenging. Although there is minimal keratinocytic disarray, there are not sufficient criteria to make the diagnosis of SCC in situ. (b) High power view of this tangentially sectioned area shows mild keratinocytic atypia, occasional keratinocytes with pyknotic nuclei, yet presence of maturation

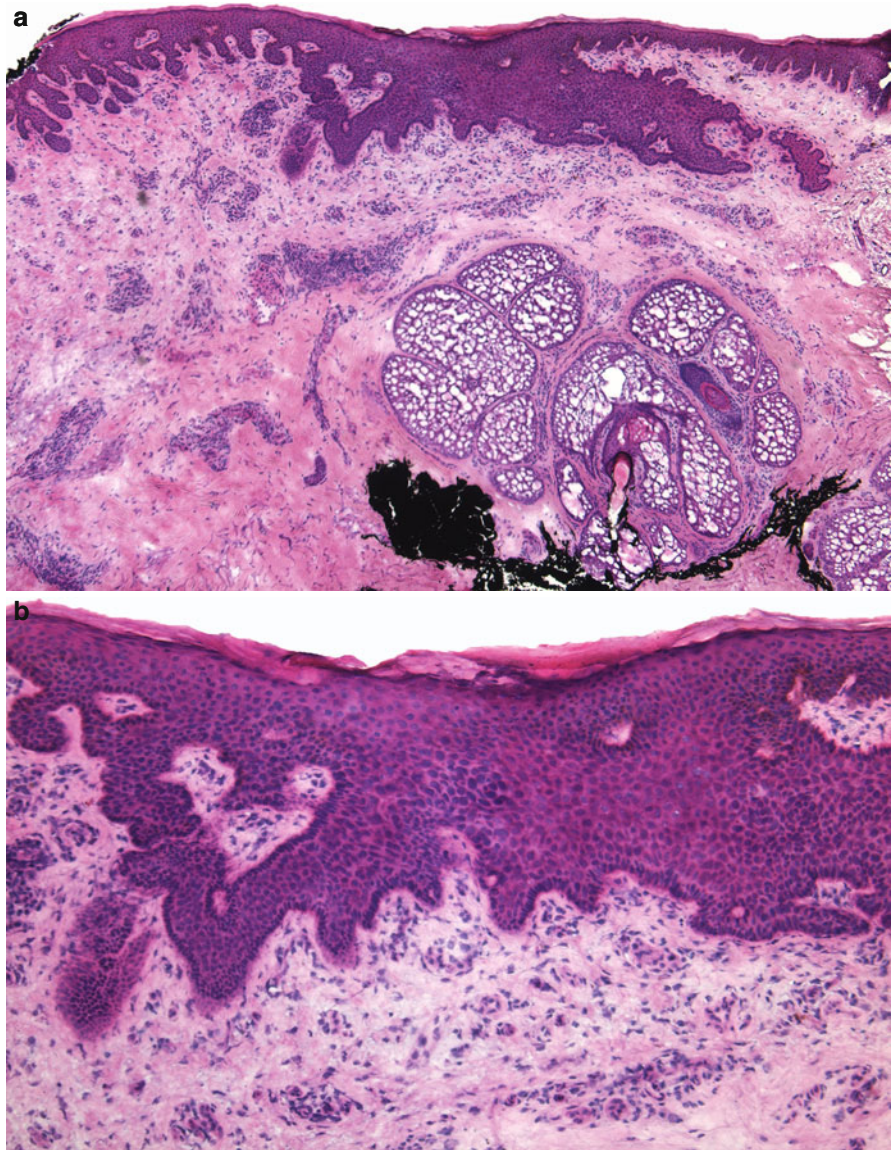


Fig. 9.6 SCCIS: (a) Acanthotic epidermis with keratinocytic disarray. (b) Large pleomorphic epithelial cells throughout the entire thickness of the epidermis

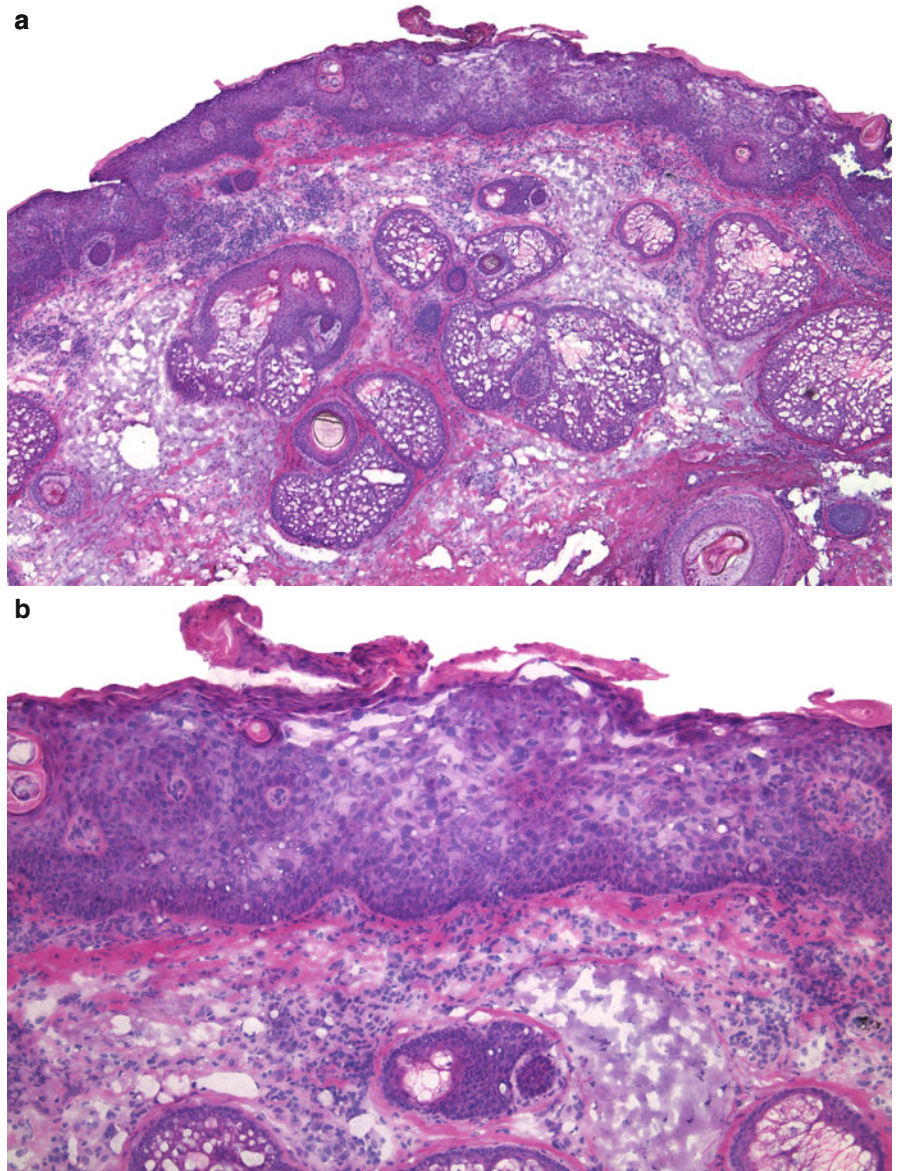


Fig. 9.7 (a) Hypertrophic squamous cell carcinoma in situ. (b) Thickened epidermis with downward projections and darkly stained neoplastic cells with high nuclear to cytoplasmic ratio contrasts with the epithelium of the follicular infundibula, which is more eosinophilic. (c) Tangentially cut thickened neoplastic epithelium with overlying parakeratosis

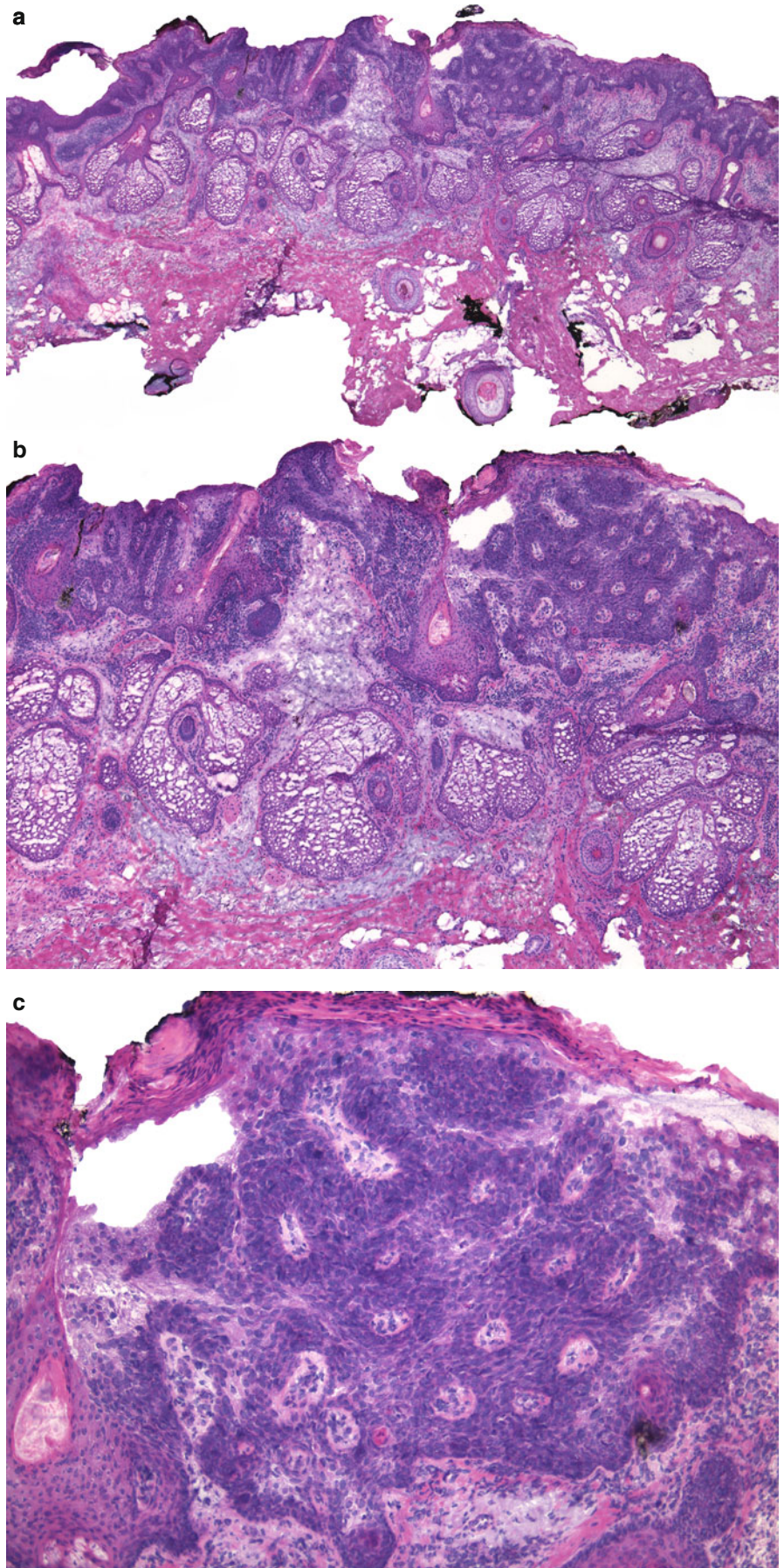


Fig. 9.8 SCCIS: in the epidermis on the right, there is full thickness keratinocytic atypia, lack of maturation, and loss of the stratum granulosum

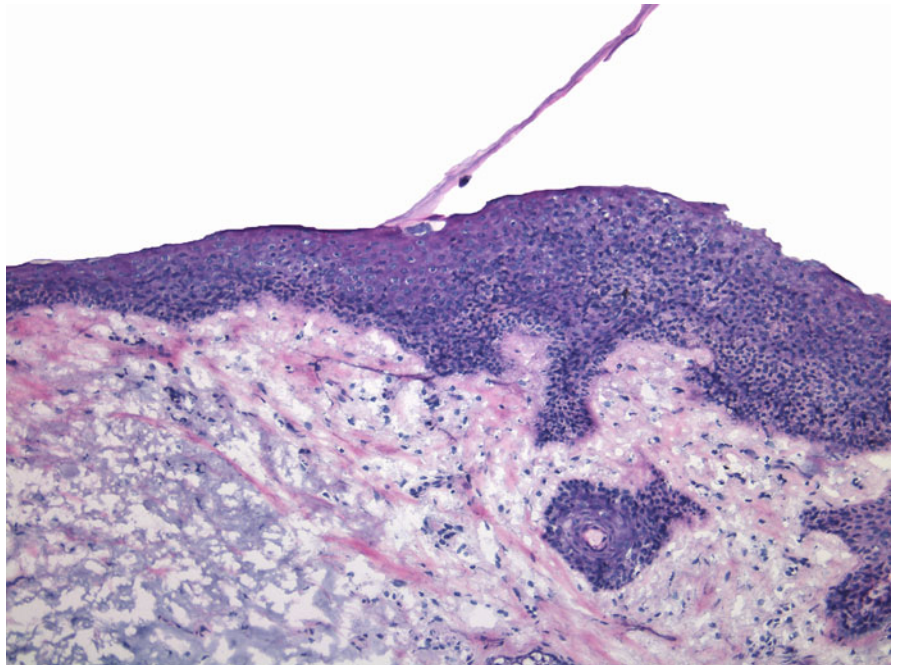


Fig. 9.9 SCCIS: (a) Normal epidermis on the left and adjacent SCCIS on the right. Increased hyperchromasia of the atypical keratinocytes can be appreciated at this magnification. (b) Complete disorder of the cells in the epidermis. The pleomorphic neoplastic cells extend into the follicle. (c) Transitional zone between SCCIS and normal epidermis. Note the sheer disarray, crowdedness, and pleomorphism of the keratinocytes on the right compared to the normal epidermis on the left

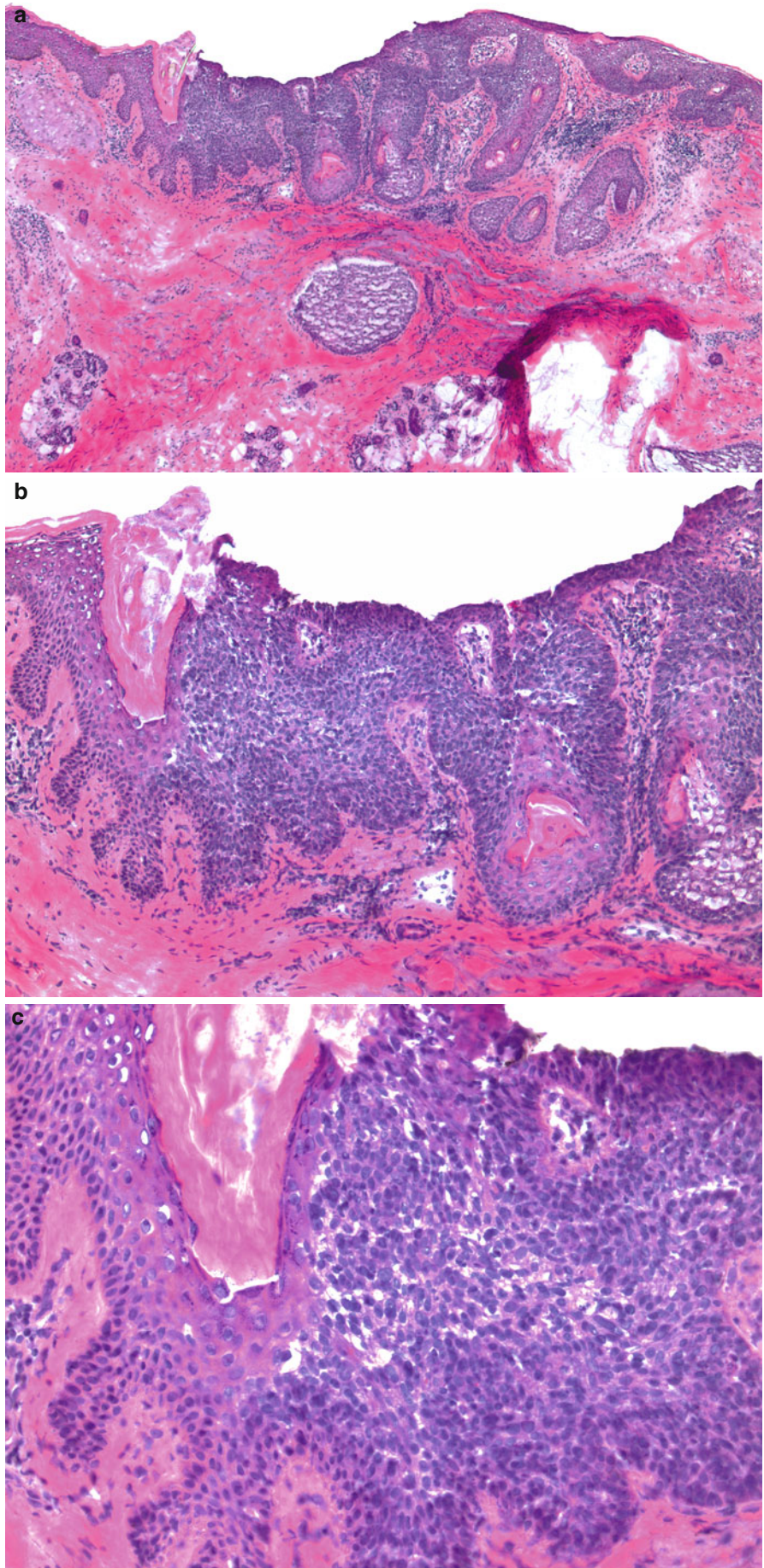


Fig. 9.10 (a) SCCIS sparing follicular epithelium. (b) SCCIS on either side of this hair follicle

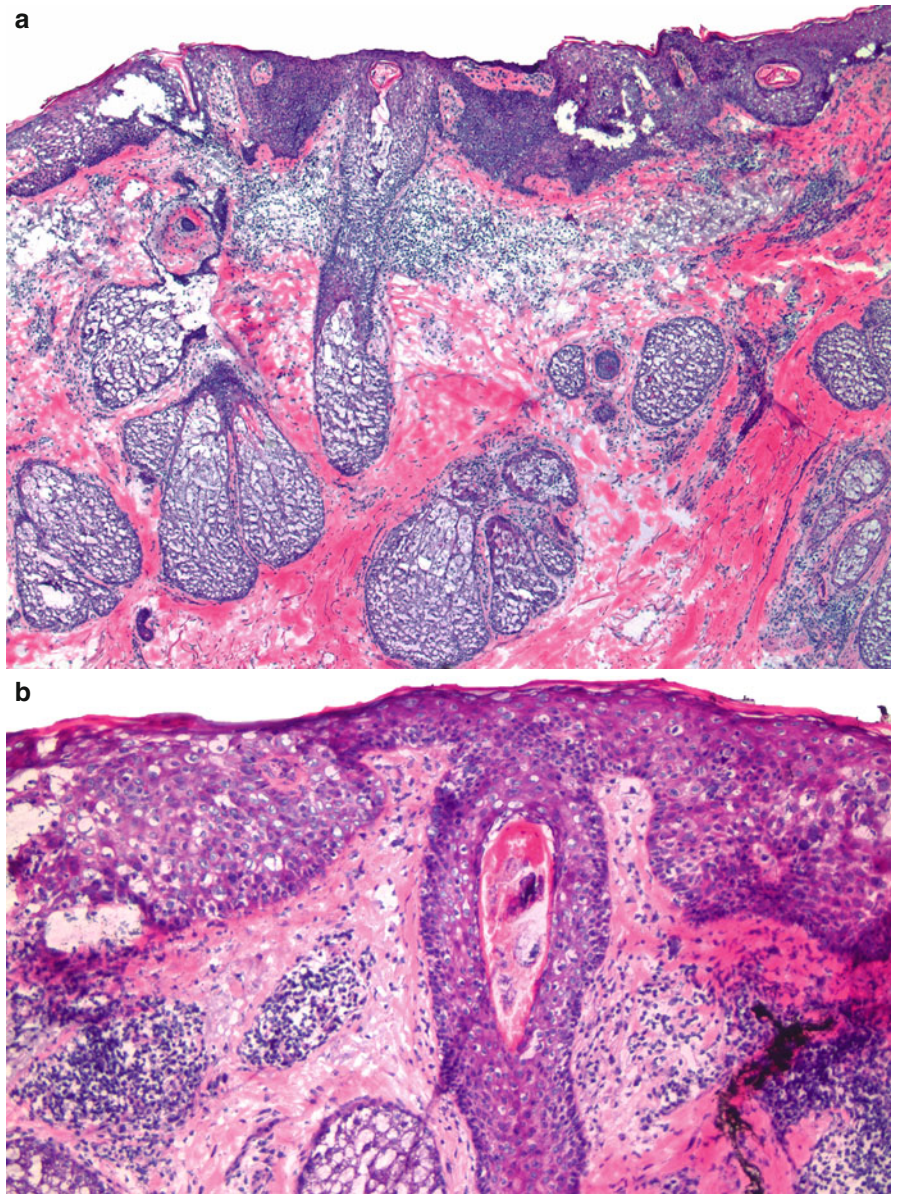


Fig. 9.10 (continued) (c) This photomicrograph shows the transition from actinic keratosis to SCCIS. The actinic keratosis can be seen on the right where there is keratinocytic disarray and atypia in the lower levels of the epidermis. The maturation is still preserved unlike the SCCIS in the center and the left portion of the photomicrograph. (d) Higher magnification of the transition from AK to SCCIS

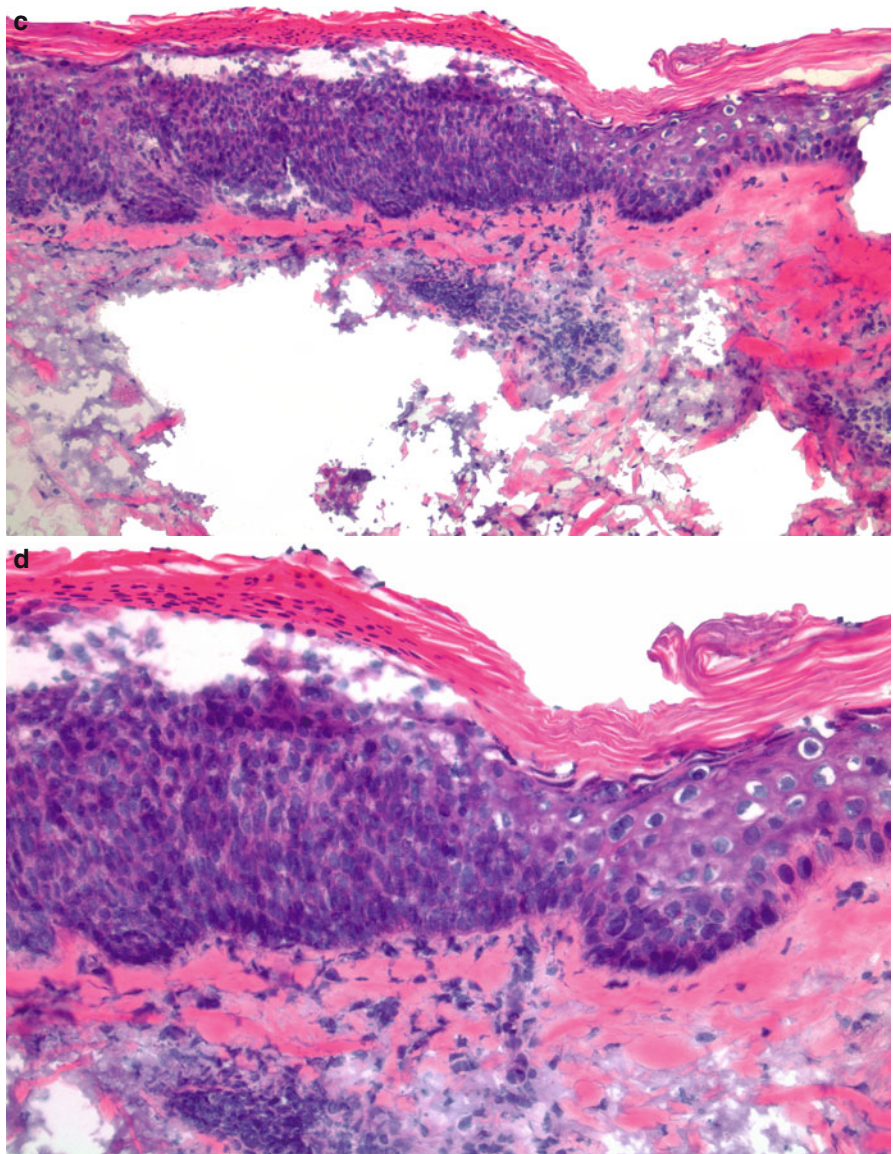


Fig. 9.11 SCCIS extending down hair follicle: **(a)** Scanning magnification shows acanthosis of the epidermis with full-thickness keratinocytic atypia extending into a follicle. **(b)** Higher magnification demonstrates large pleomorphic and hyperchromatic keratinocytes throughout the epidermis and involving follicular epithelium

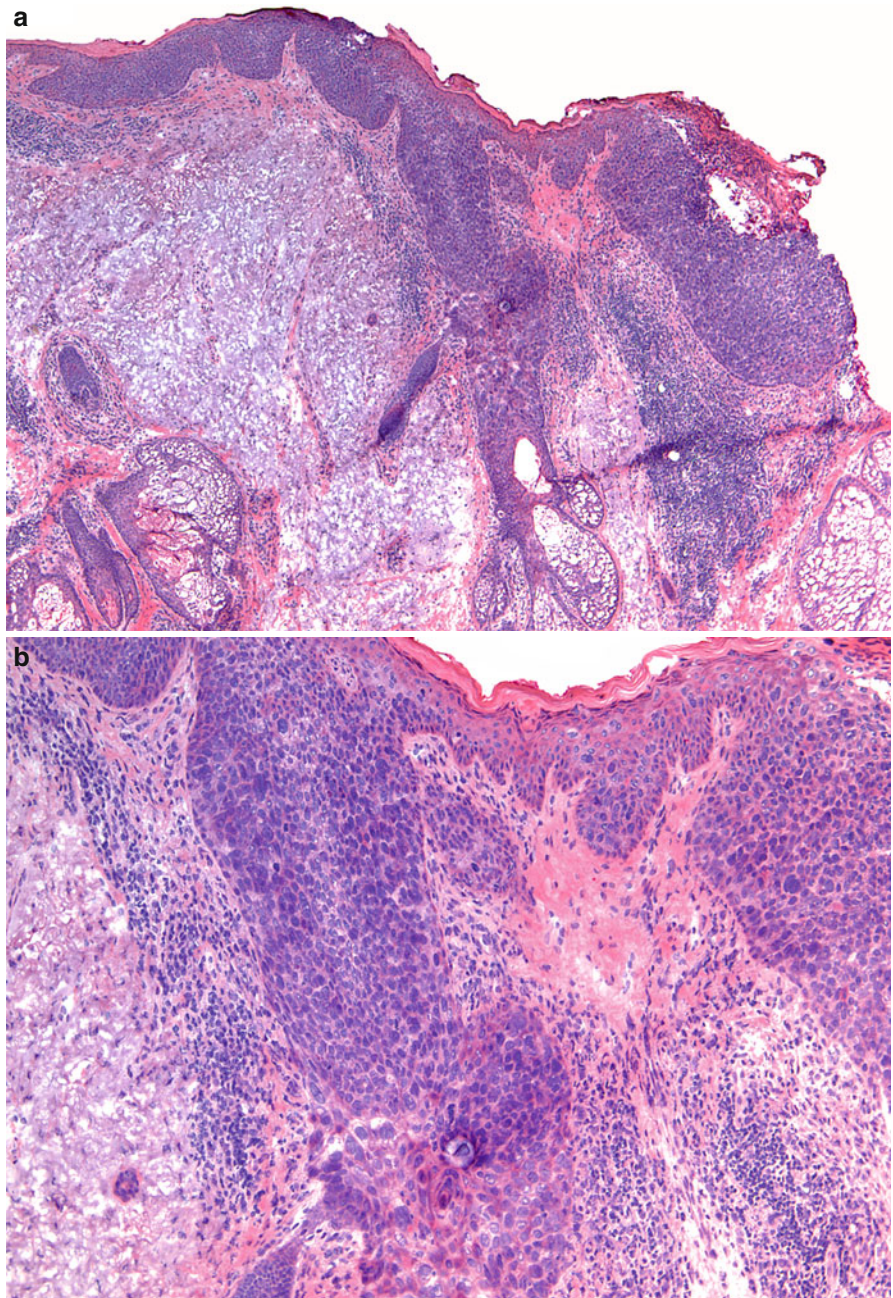


Fig. 9.11 (continued) (c) Large, hyperchromatic and atypical keratinocytes have replaced the follicular epithelium

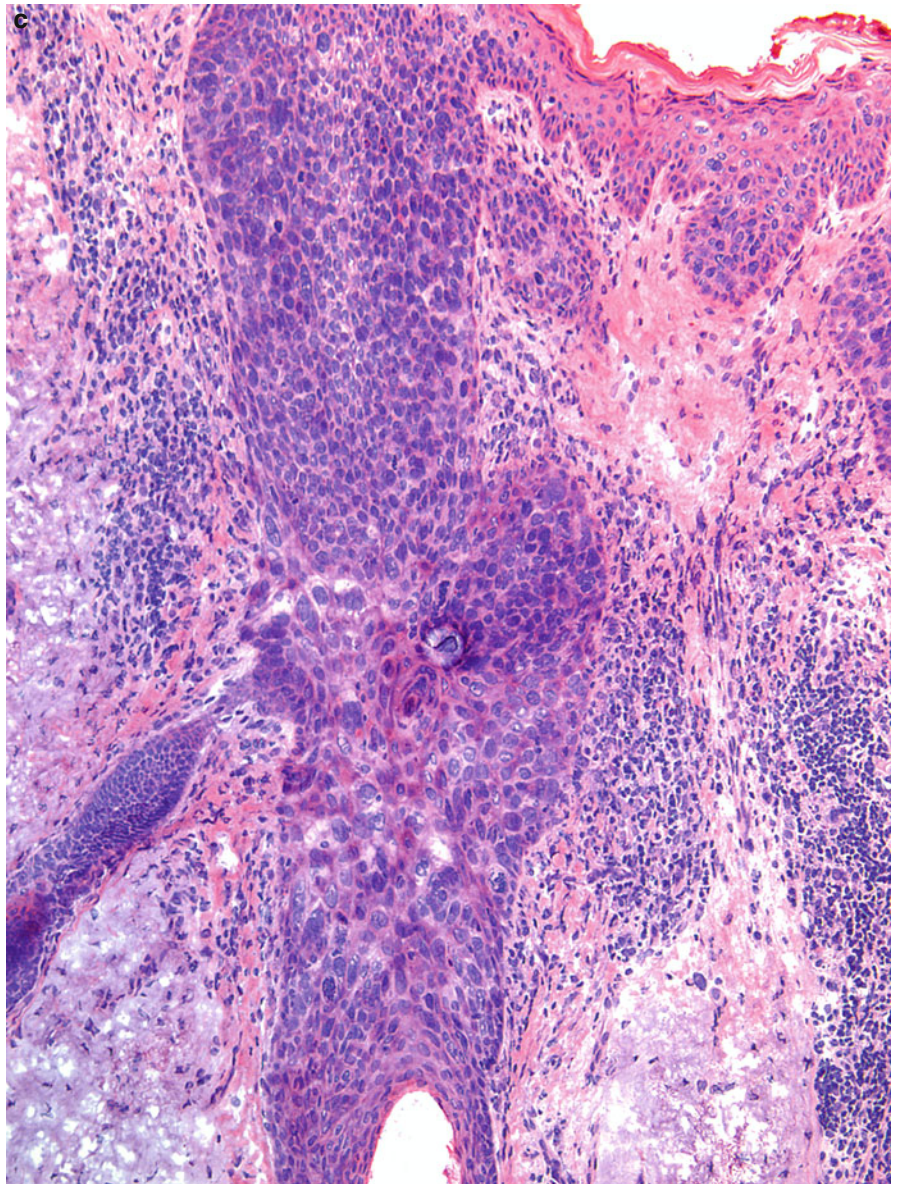


Fig. 9.12 SCCIS: (a) There are multiple broad epidermal projections, some of which, due to tangential sectioning, appear as if they are disconnected from the epidermis. (b) Although there is overall maturation and differentiation of epidermis (note the presence of a granular cell layer in various parts of the section), there is still cellular disarray and atypia, occasional large and hyperchromatic cells, as well as a focus of squamatization (*arrow*)

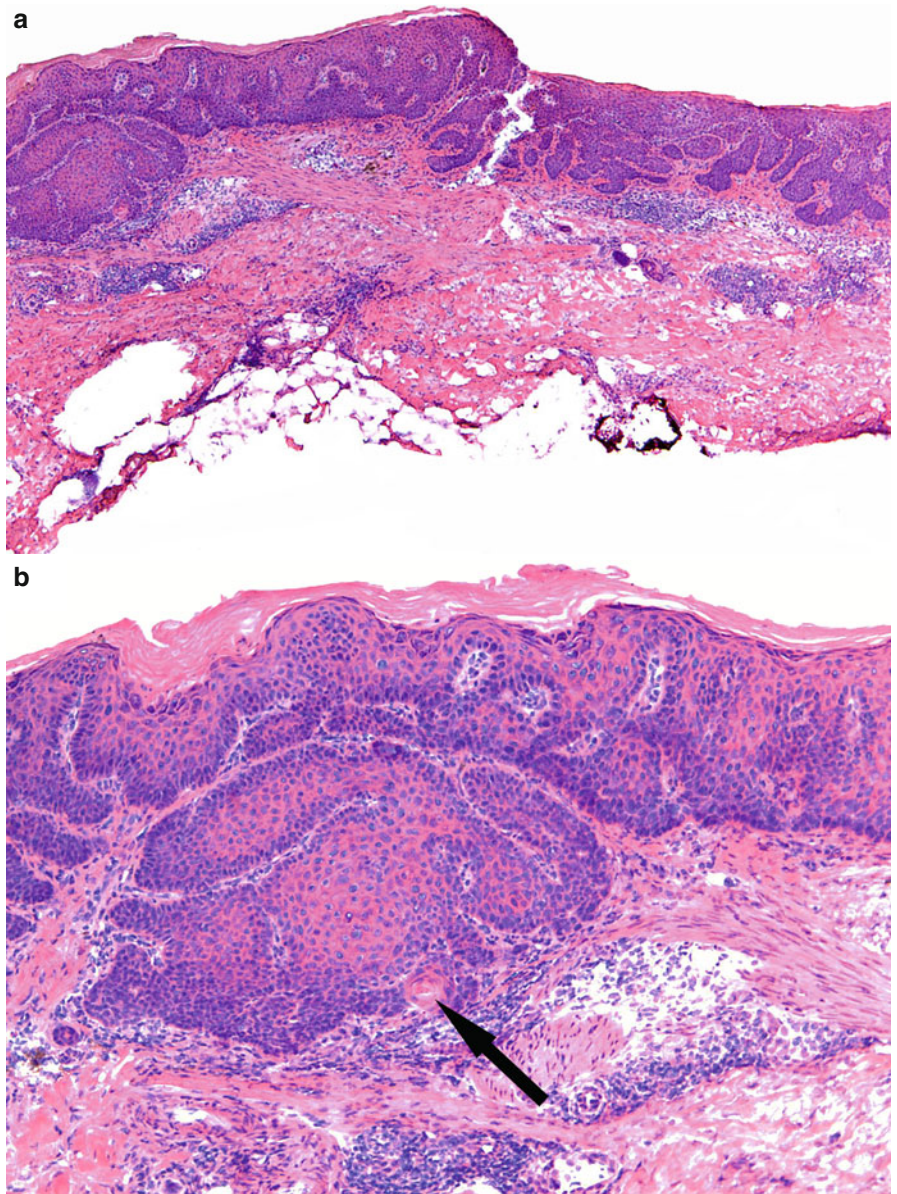


Fig. 9.12 (continued) (c) Another tissue section reveals full-blown atypia with formation of multiple squamous eddies and, possibly, early invasive squamous cell carcinoma. Sometimes, it is difficult to determine if the tumor aggregates are attached to the overlying (tangentially cut) epidermis or are infiltrating the superficial dermis. (d) Higher magnification of SCCIS with questionable superficial invasion

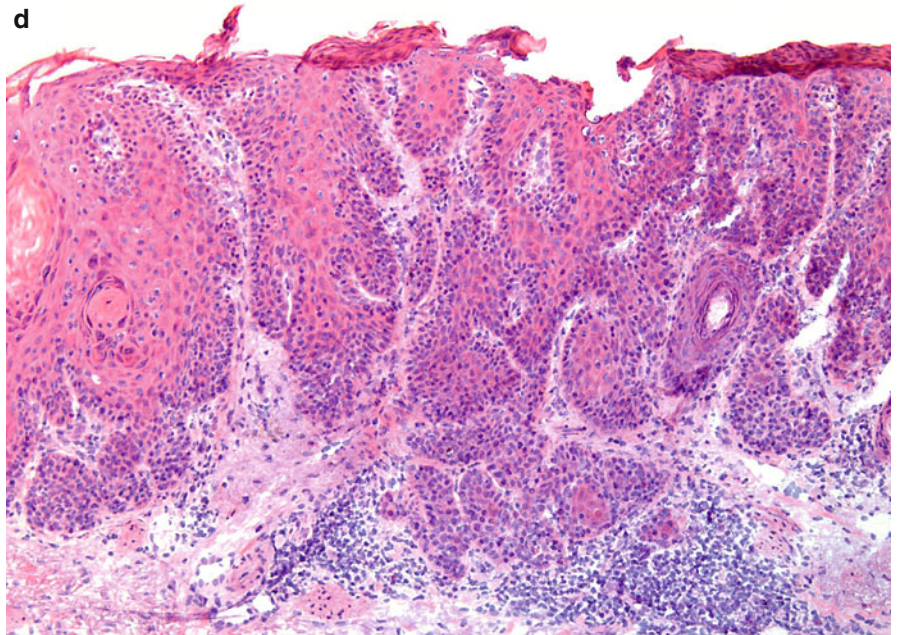
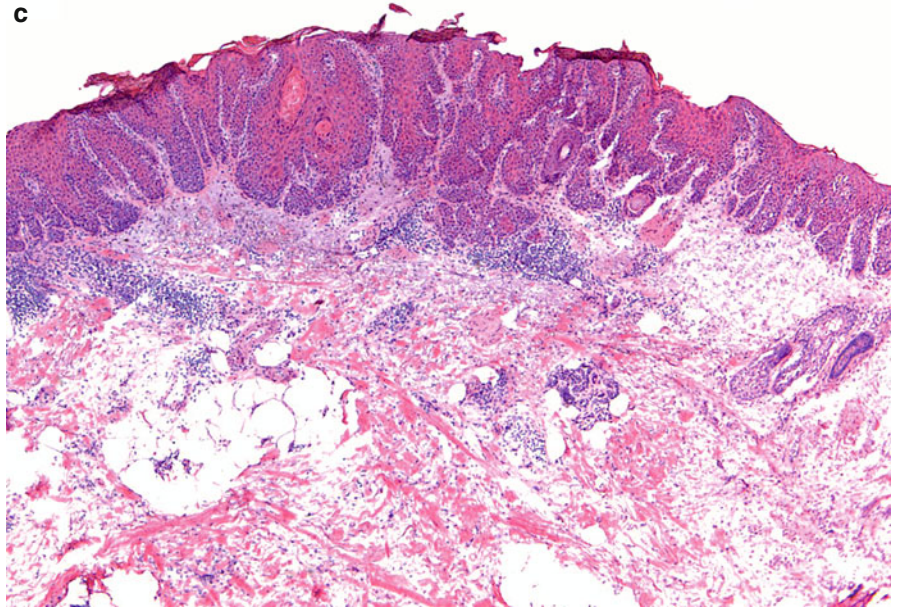


Fig. 9.13 (a) SCCIS with focal invasive SCC: there is a basophilic cellular nodule in the deep dermis. (b) Higher magnification of the surface epidermis. There is full thickness epidermal atypia and underlying inflammatory infiltrate

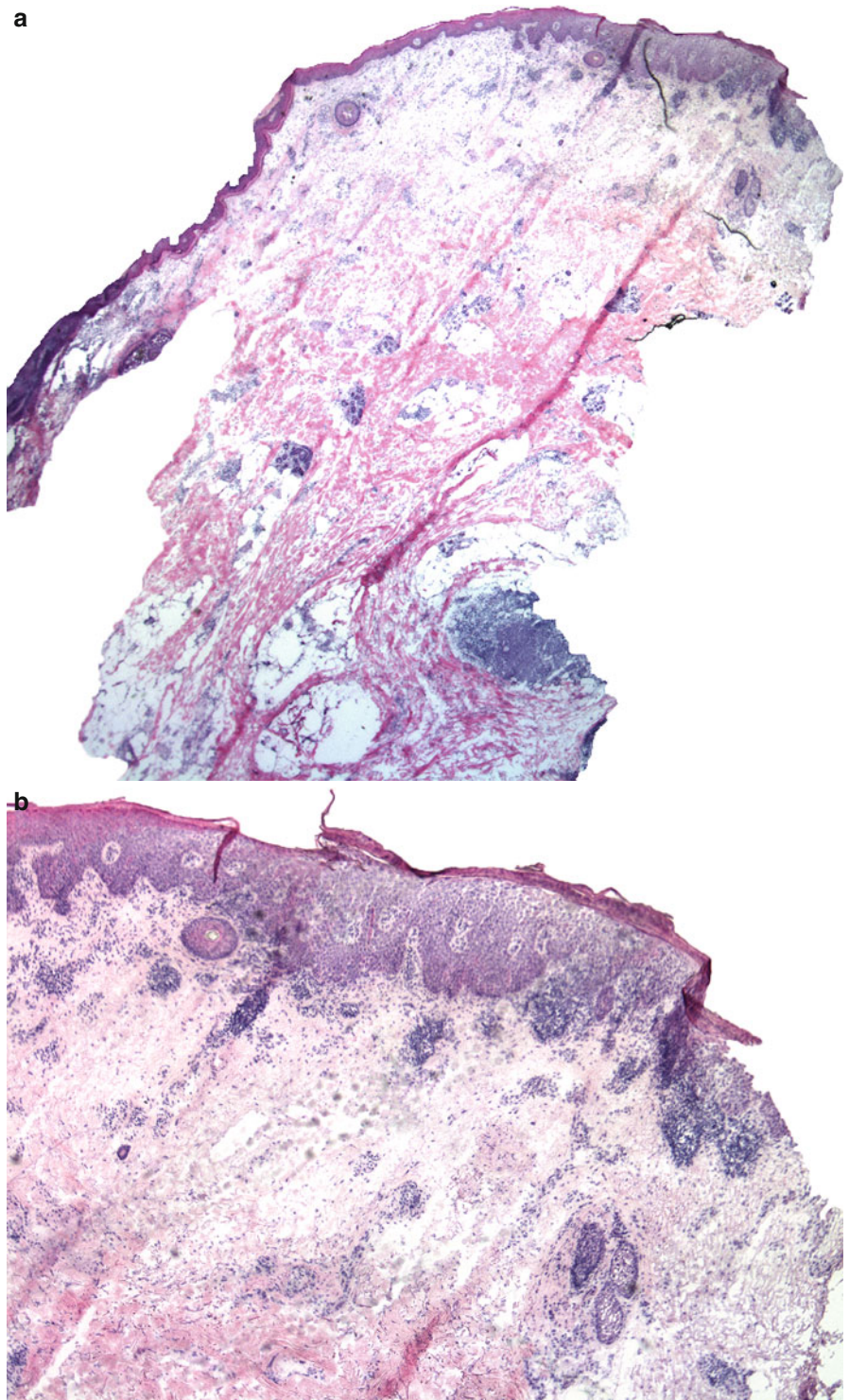


Fig. 9.13 (continued) (c) Higher magnification of the basophilic cellular nodule in the deep dermis. Large neoplastic cells of SCC (*ellipse*) surrounded by dense inflammation. (d) In another section, the slightly different staining pattern helps distinguish the neoplastic cells from the dense inflammatory infiltrate

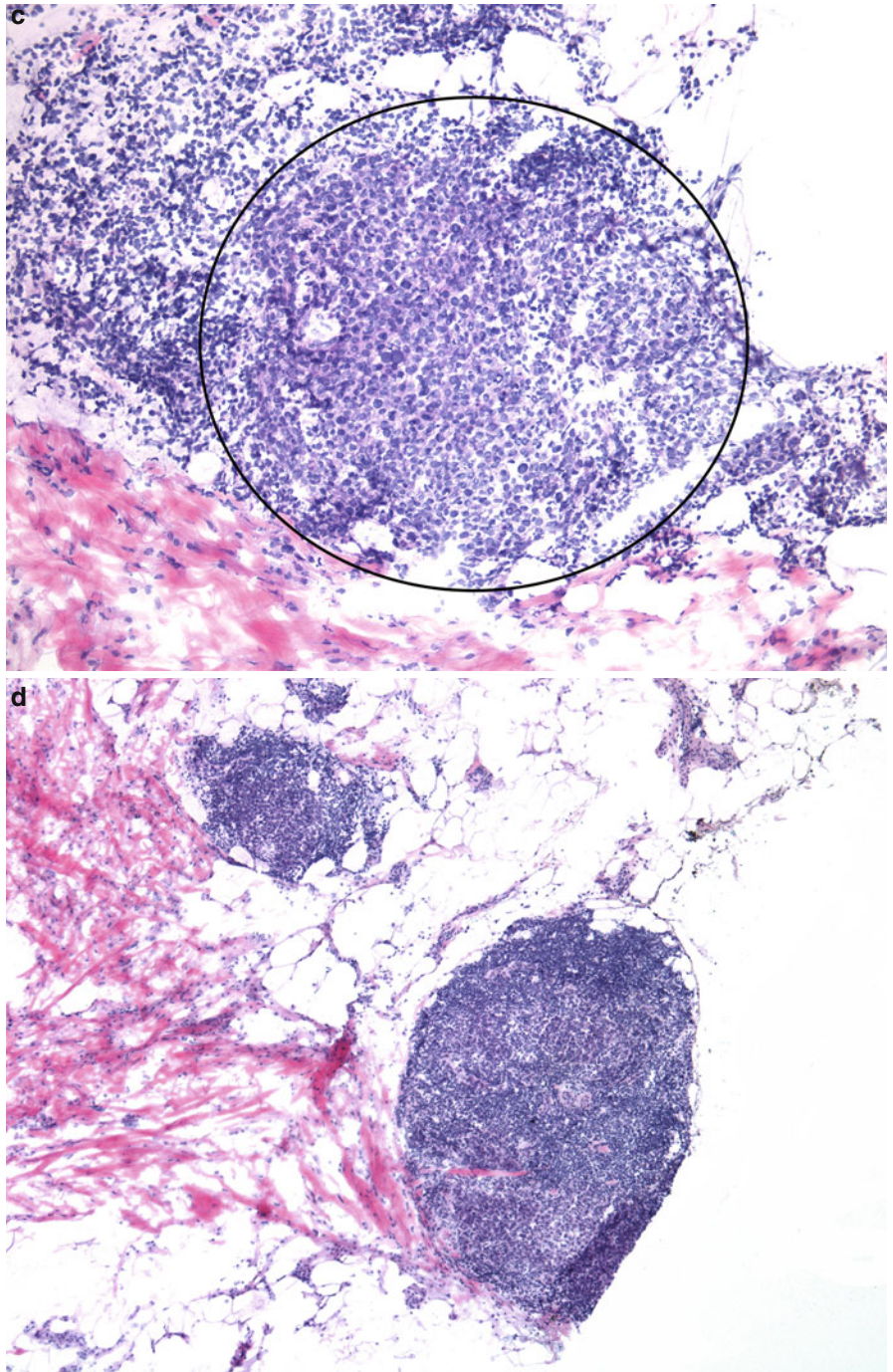


Fig. 9.13 (continued) (e) Arrows point out aggregates of SCC

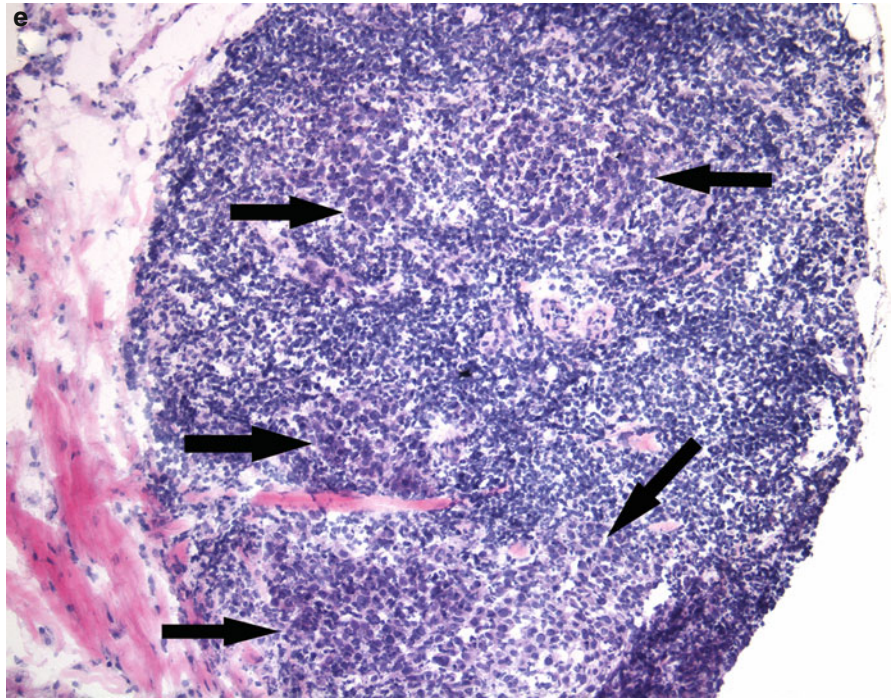


Fig. 9.14 (a) SCCIS and seborrheic keratosis: a seborrheic keratosis on the right adjacent to SCCIS on the left. (b) SCCIS and seborrheic keratosis: the seborrheic keratosis on the right shows acanthosis, hyperkeratosis, and cystically dilated follicular structures. In contrast, the SCCIS shows disarray of the keratinocytes in the epidermis and lack of maturation

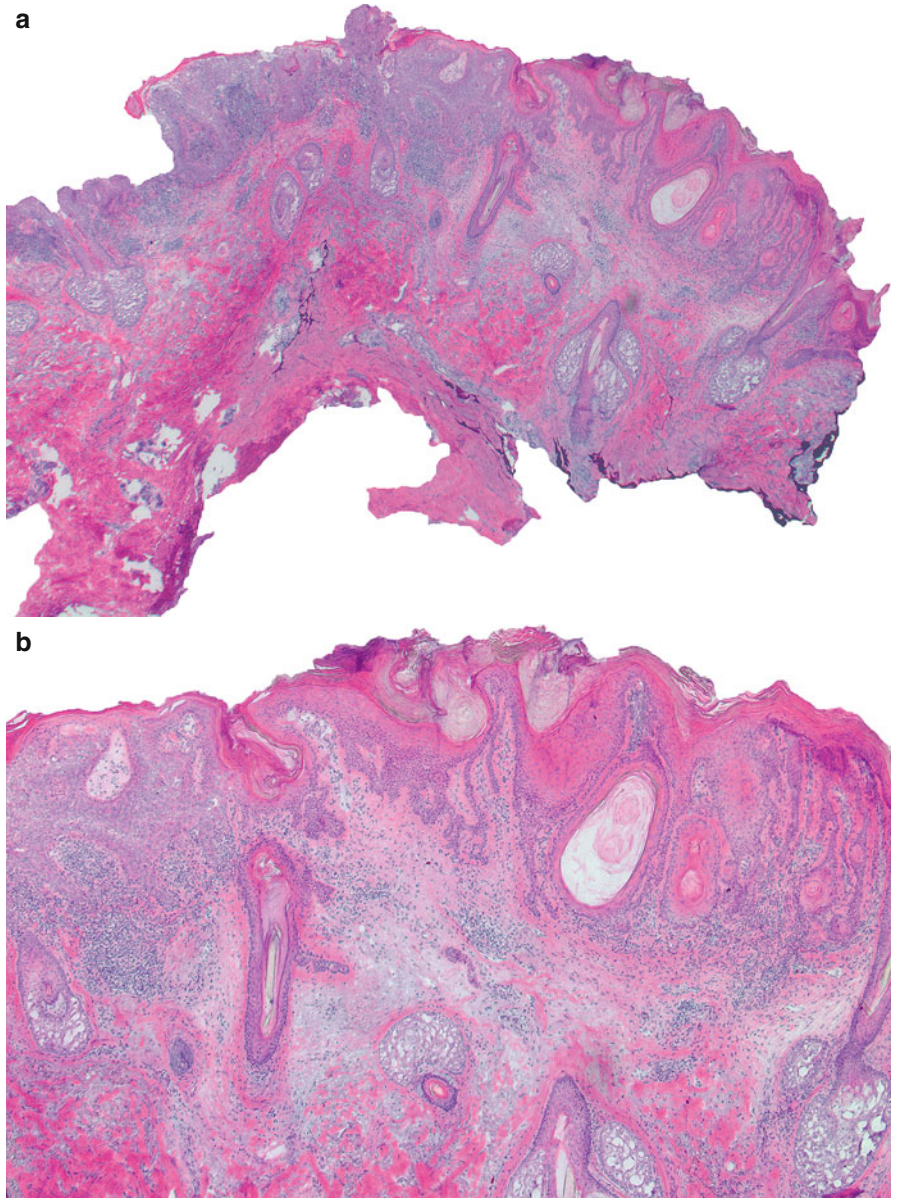


Fig. 9.14 (continued) (c) Higher magnification showing florid SCCIS with underlying inflammation. There is lack of maturation, absence of granular cell layer, and overlying parakeratosis. The neoplastic cells are jumbled on top of each other and show variable pleomorphism

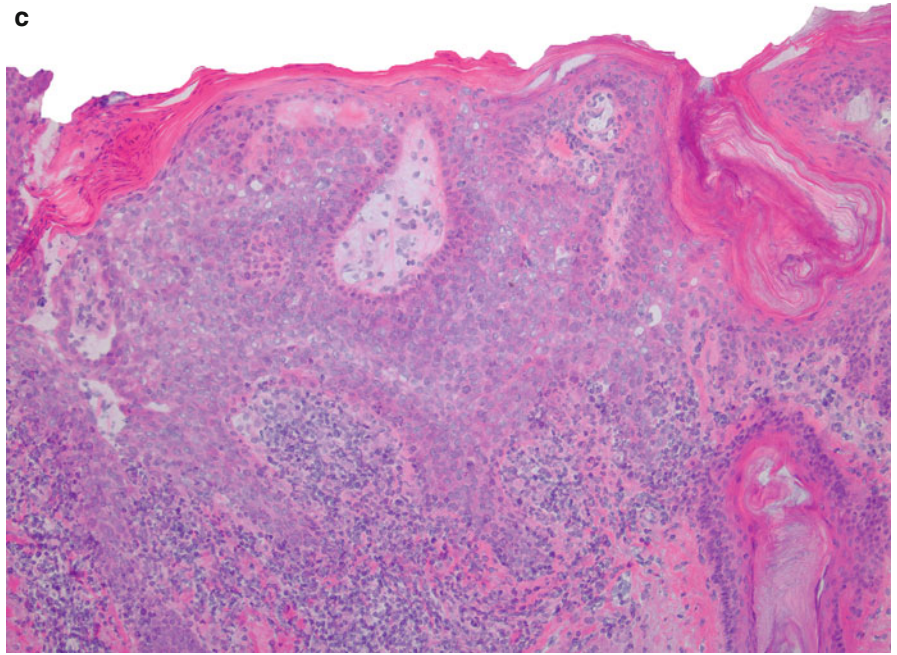


Fig. 9.15 Acantholytic actinic keratosis: Large and atypical keratinocytes in the lower portion of the epidermis with foci of acantholysis (loss of cellular cohesion)

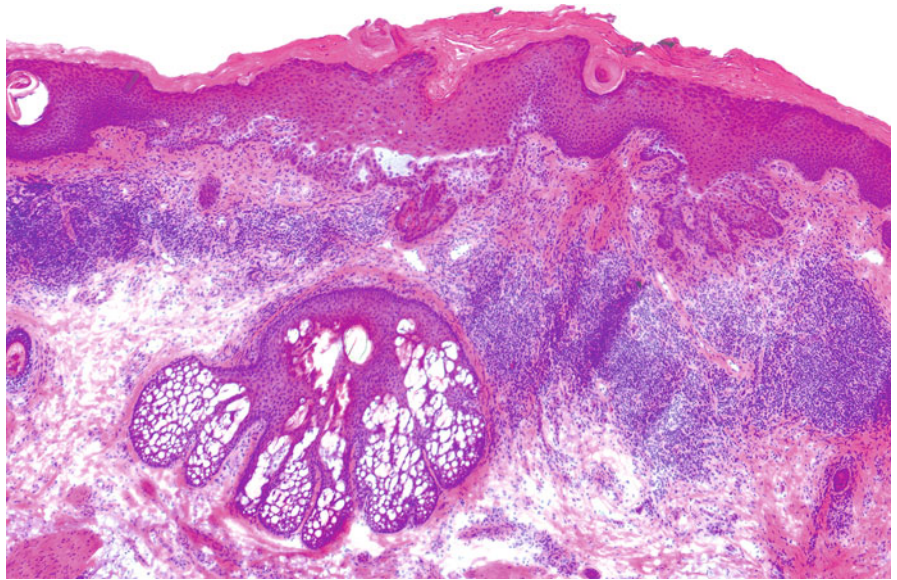


Fig. 9.16 (a) Actinic keratosis: scanning magnification. (b) Thickened epidermis and cellular disarray in the lower portion of the epidermis on the left

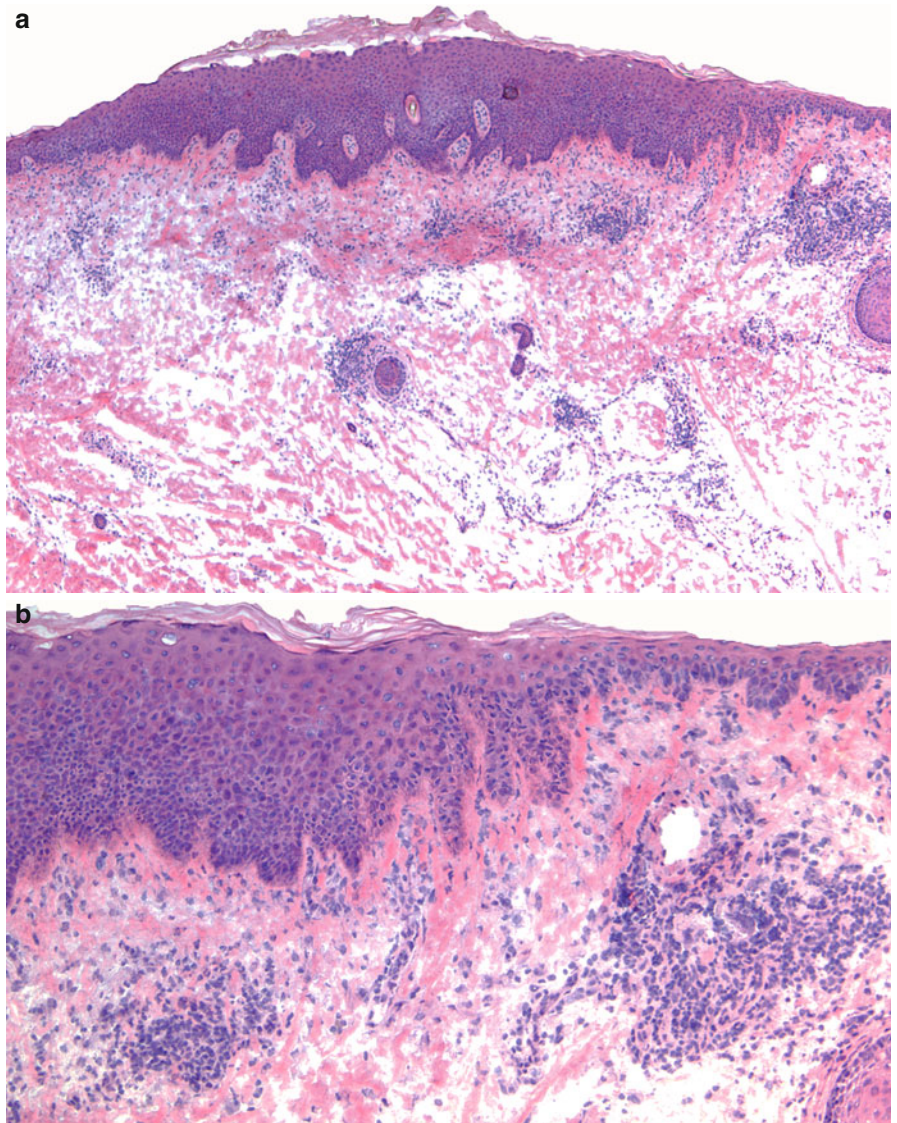


Fig. 9.17 SCCIS in association with seborrheic keratosis: tangentially cut section with seborrheic keratosis on the left and epidermal atypia with darkly stained keratinocytes on the right

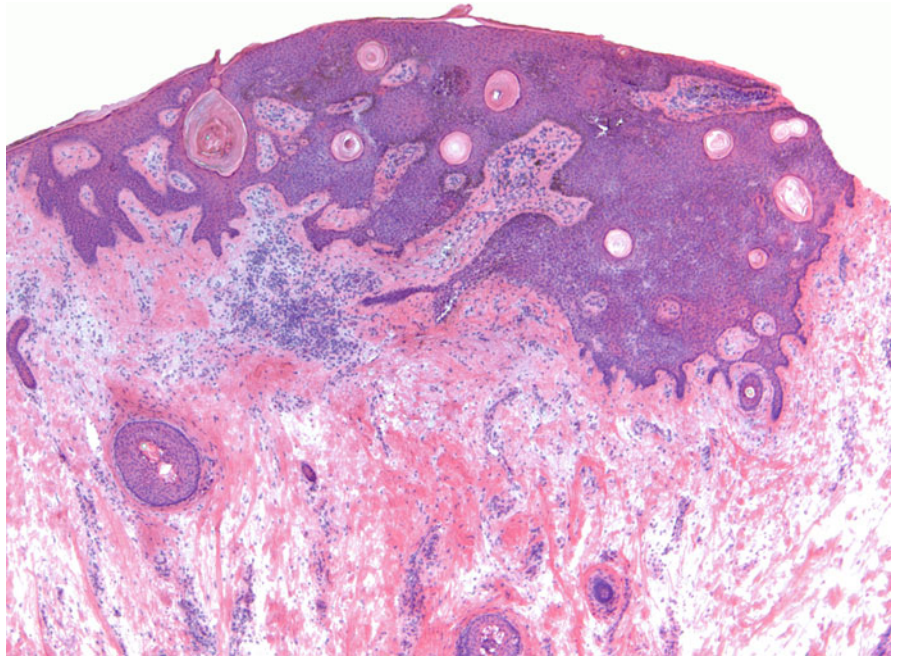


Fig. 9.18 (a) Actinic keratosis in association with seborrheic keratosis: tangentially cut epidermis with AK on the left and SK containing pseudohorn cysts on the right. (b) Higher magnification of actinic keratosis adjacent to seborrheic keratosis

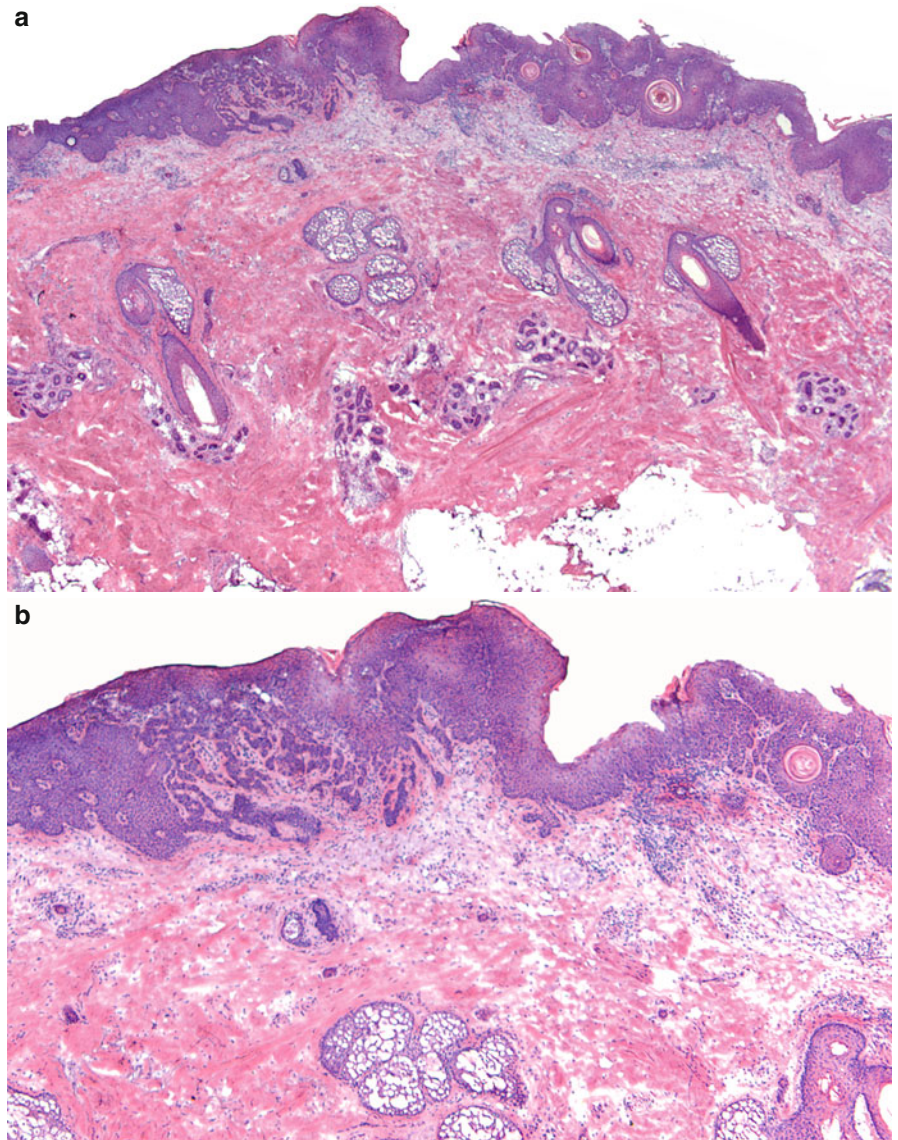
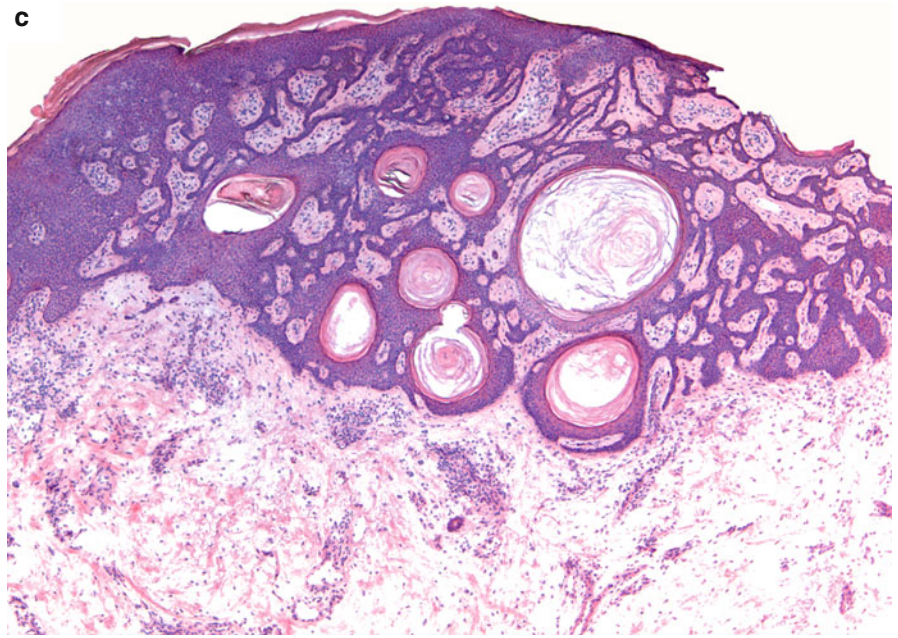


Fig. 9.18 (continued) (c) Further sectioning into the tissue block shows tangentially cut seborrheic keratosis with multiple pseudohorn cysts on the right and actinic keratosis on the left



Histologic Features

1. Irregular aggregates of neoplastic keratinocytes arising from the epidermis and invading the dermis.
2. Poorly circumscribed epithelial aggregates that vary markedly in size and shape.
3. Concentric whorls of parakeratotic cells as well as keratin pearls within the aggregates in well- and moderately differentiated tumors.
4. Neoplastic epithelial cells have vesicular nuclei, purple nucleoli, and abundant eosinophilic cytoplasm.
5. Nuclear pleomorphism with atypical hyperchromatic nuclei and large nucleoli.
6. Evidence of keratinization, i.e., dense eosinophilic material, within the cytoplasm of neoplastic cells.
7. Dyskeratotic cells showing pyknotic nuclei and homogenous bright, eosinophilic cytoplasm.
8. Increased number of mitotic figures, some of which are atypical, within neoplastic aggregates.
9. Areas of focal necrosis.
10. Prominent solar elastosis in the superficial dermis with or without actinic keratosis in the overlying or adjacent epidermis.
11. Inflammatory infiltrate around aggregates of neoplastic cells.
12. Intercellular bridges between the epithelial neoplastic cells can be appreciated on high power, although they may not be present in poorly differentiated tumors.
13. Invasion of perineurium or endoneurium by neoplastic aggregates or individual tumor cells from SCC.
14. Perineural invasion should be suspected in lesions demonstrating inflammation around nerves.

Subtypes of SCC

Infiltrative Squamous Cell Carcinoma

Histologic Features

1. Neoplastic cells arranged as strands, cords, or single-cell rows.
2. Single neoplastic cells infiltrate between collagen bundles.
3. Evidence of keratinization may be sparse.
4. Connection to the epidermis may be subtle.
5. Inflammatory infiltrate around aggregates of neoplastic cells.
6. The neoplastic cells may be elongated as opposed to polygonal or oval.

Spindle Cell Squamous Cell Carcinoma

Histologic Features

1. Spindle-shaped neoplastic epithelial cells.
2. Sheets or fascicles of neoplastic cells in a storiform pattern. Sometimes individual neoplastic cells are infiltrating in between collagen bundles.
3. The neoplastic cells are elongated with spindle-shaped nuclei.
4. Bizarre, pleomorphic giant cells may be present.
5. Evidence of keratinization may be sparse.
6. Connection to the epidermis may be a helpful clue to the diagnosis.
7. Tumor often infiltrates into the deep dermis.

Acantholytic Squamous Cell Carcinoma

Histologic Features

1. Acantholysis of neoplastic cells creates pseudoglandular islands.
2. The polygonal neoplastic cells are aligned around a space resembling a lumen that might contain free-floating (acantholytic) neoplastic keratinocytes.
3. The acantholytic, dyskeratotic cells and tumor islands may be seen in only a portion of or present throughout the lesion.
4. Focal keratinization can be helpful for diagnosis.
5. Acantholytic actinic keratosis may be seen adjacent to the tumor.

Differential Diagnosis

Inflamed Seborrheic Keratosis

- Reactive atypia, keratin pearls, and overlying parakeratosis
- Inflammatory infiltrate in the papillary dermis
- Pseudohorn cysts, melanin pigmentation, and a sharp, linear, well-demarcated flat base
- No invasion into the dermis
- Occasional mitoses

Verruca

- Digitated and acanthotic epidermis with hypergranulosis
- Koilocytes in the upper epidermal layers

- Dilated capillaries in the dermal papillae
- No true keratinocytic atypia

Tangential Sectioning of the Epidermis

- The presence of dermal papillae surrounded by epidermis with normal maturation of keratinocytes and without cytologic atypia distinguishes this artifact from SCC.

Pseudoepitheliomatous Hyperplasia (PEH)

- Proliferation of epithelium resembling SCC.
- Originates from the adnexal epithelium.
- The epithelial aggregates are angulated and composed of large uniform keratinocytes with abundant eosinophilic cytoplasm. Reactive cytologic atypia, mitoses, and keratin pearls may be present.
- Deeper sectioning into the block may be helpful.
- Epithelioid aggregates are jagged, uneven, and sharply pointed.
- Keratinocytes are well differentiated. Nuclear atypia, hyperchromasia, and pleomorphism are absent.
- Neutrophilic intraepidermal abscesses may be seen.

Fig. 10.1 Squamous cell carcinoma: (a) Irregular aggregates of glassy, eosinophilic epithelial cells immediately beneath a hyperplastic tangentially cut epidermis. (b) The neoplastic epithelial aggregates vary markedly in size and shape and some are angulated. They consist of polygonal cells with pleomorphic and hyperchromatic nuclei. In the center of the aggregates the neoplastic epithelial cells show abundant brightly eosinophilic cytoplasm with evidence of keratinization. Scattered lymphocytes are seen in the vicinity

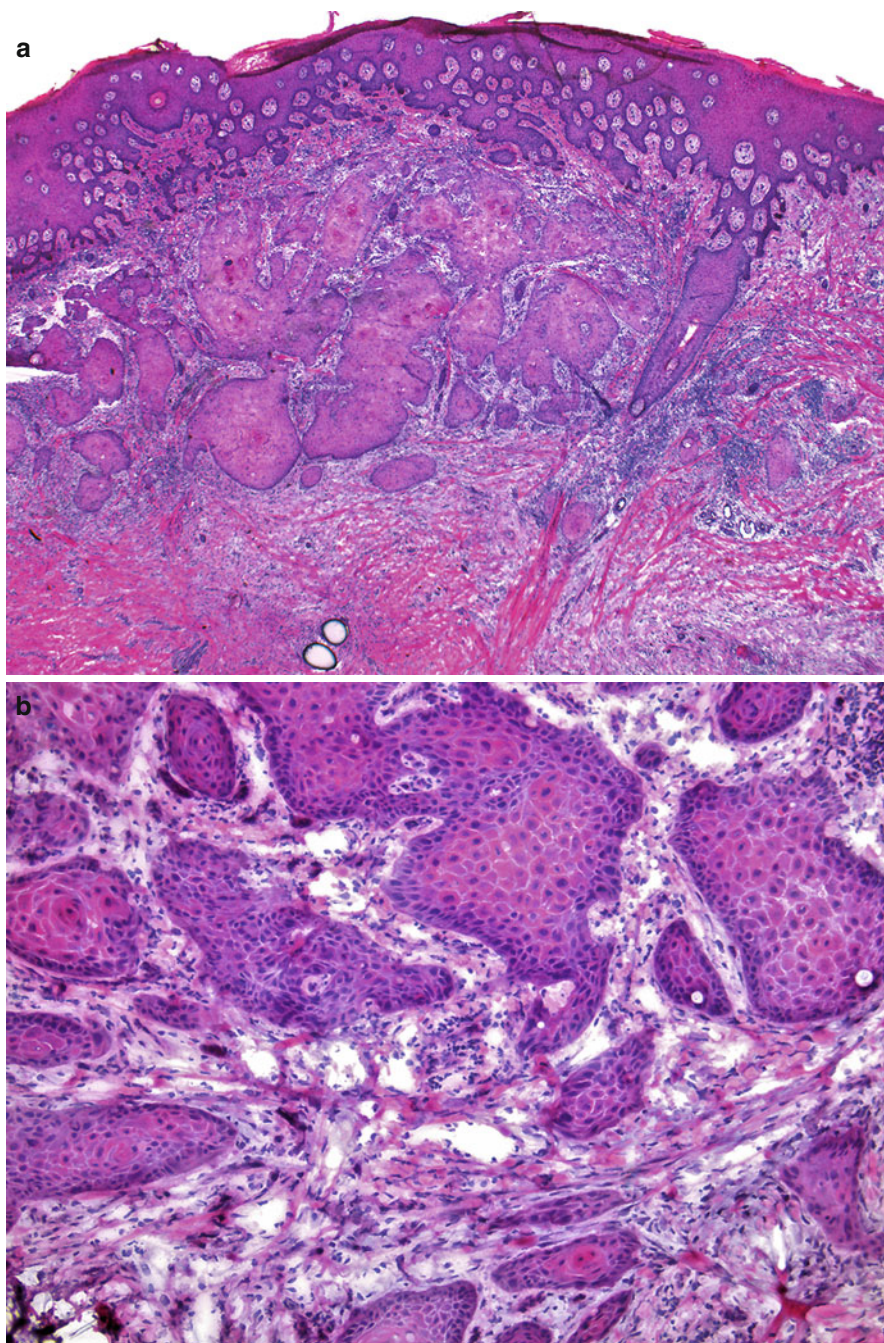


Fig. 10.2 Squamous cell carcinoma: prominent whorls of parakeratotic cells in the center of neoplastic aggregates. There is focal acantholysis in other areas

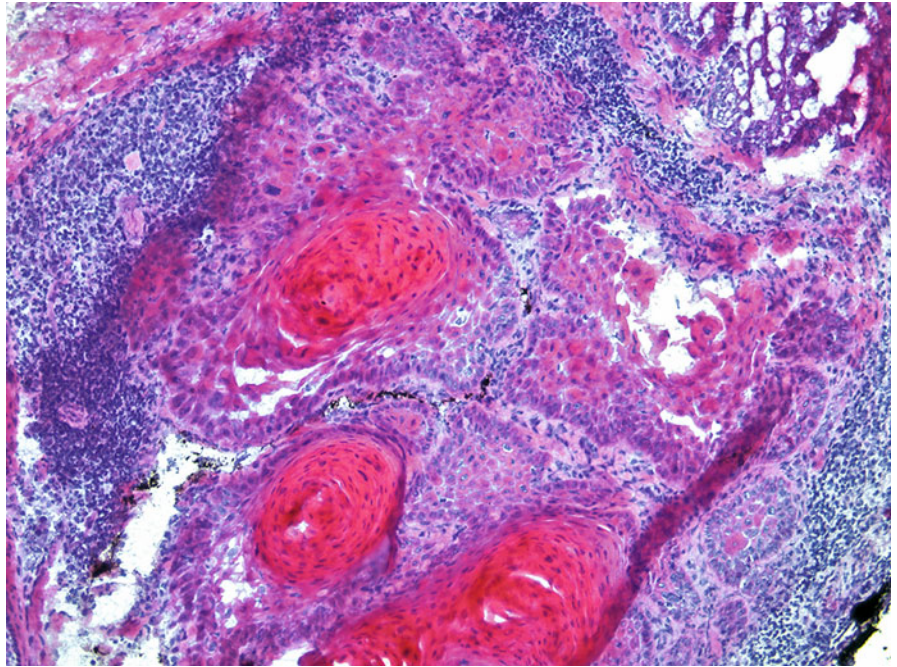


Fig. 10.3 Squamous cell carcinoma: keratin pearls containing brightly eosinophilic whorled keratin surrounded by dense lymphocytic inflammation

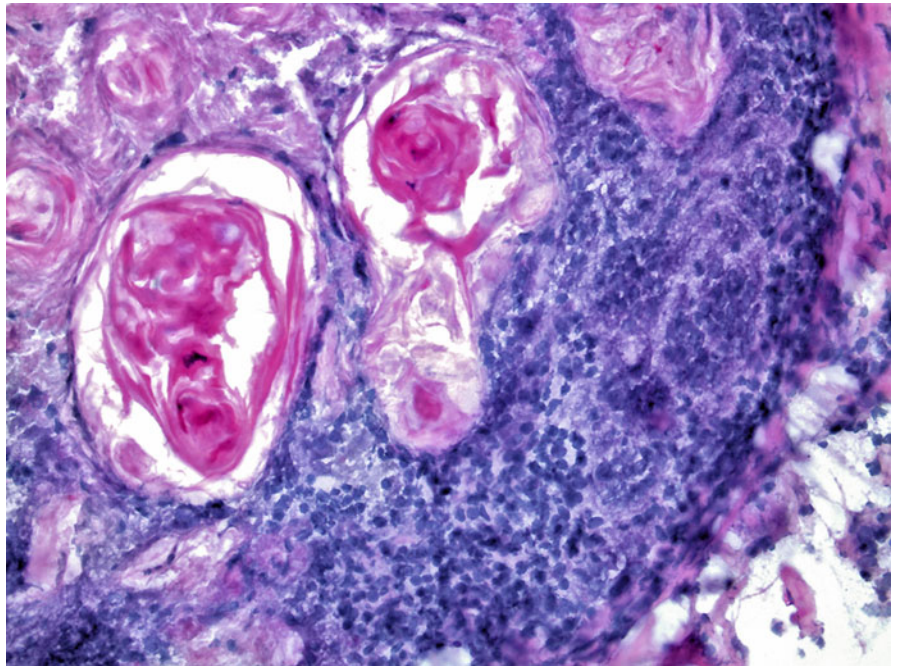


Fig. 10.4 Squamous cell carcinoma: dyskeratotic neoplastic keratinocytes with hyperchromatic nuclei and bright eosinophilic dense cytoplasm. Marked pleomorphism of the neoplastic cells with variation in nuclear size, staining pattern, and shape

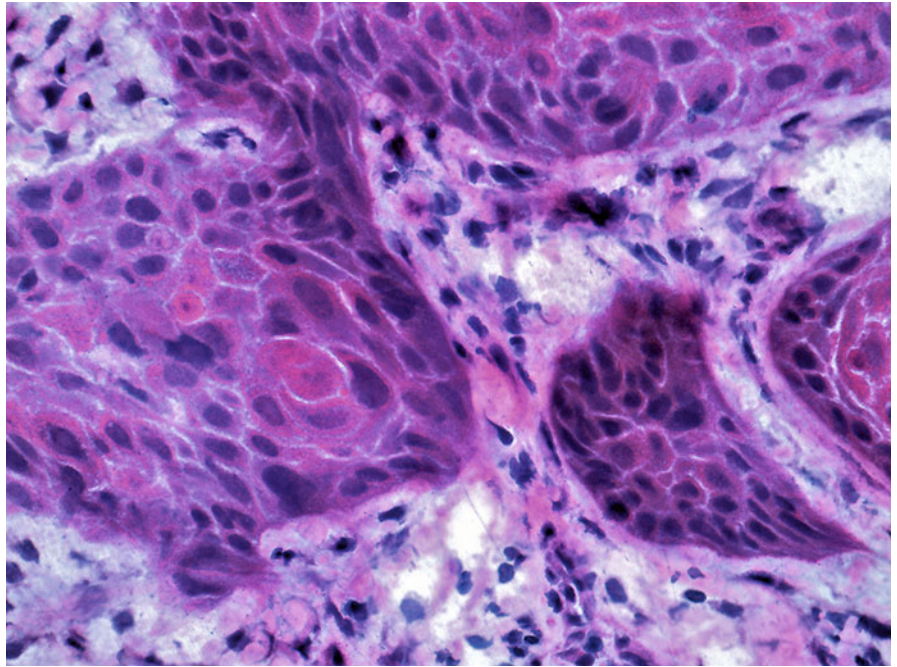


Fig. 10.5 Squamous cell carcinoma: an atypical mitotic figure (*arrow*). Intercellular bridges between the epithelial cells can be seen

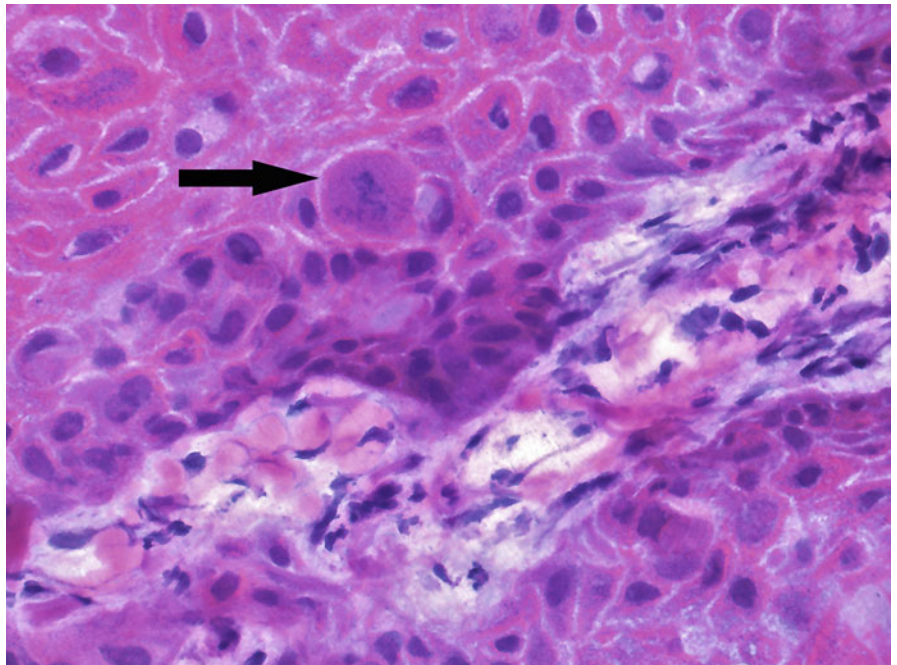


Fig. 10.6 Squamous cell carcinoma:

(a) A low-power magnification shows patchy lymphocytic inflammation in the reticular dermis with a few areas containing pink globular material. Focal actinic keratosis is present in the overlying epidermis in the left upper corner.

(b) Within the dense lymphocytic inflammation are clumps of cells with larger nuclei and more cytoplasm compared to the surrounding lymphocytes. In the right lower corner, there is pink eosinophilic keratinous material surrounded by irregular clumps of neoplastic cells and a lymphocytic infiltrate at the periphery. The tumor cells adhere together and form either clumps or nests whereas the inflammatory cells are erratic, dispersed, and often solitary.

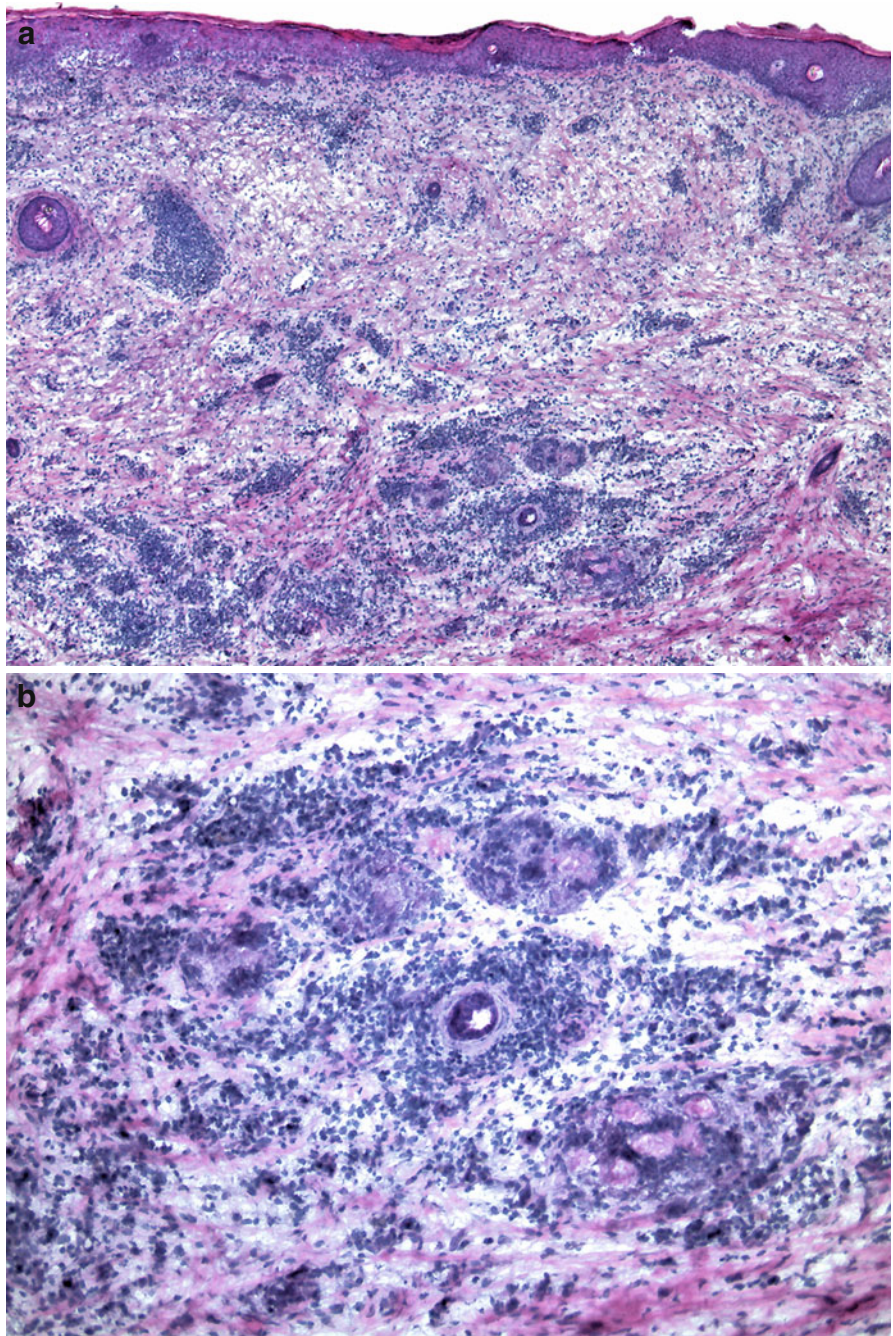


Fig. 10.6 (continued) (c) Higher magnification of the pink keratinous material surrounded by neoplastic keratinocytes and inflammatory cells. (d) Neoplastic keratinocytes admixed and obscured by the dense lymphocytic infiltrate. Helpful features to discern tumor from inflammation include the following: (1) Neoplastic nuclei are clumped together. (2) The neoplastic keratinocytes have a high nuclear to cytoplasmic ratio. (3) The neoplastic keratinocytes stain with eosinophilic hue unlike the dark blue staining of the lymphocytes. (4) The neoplastic nuclei are larger than the nuclei of lymphocytes

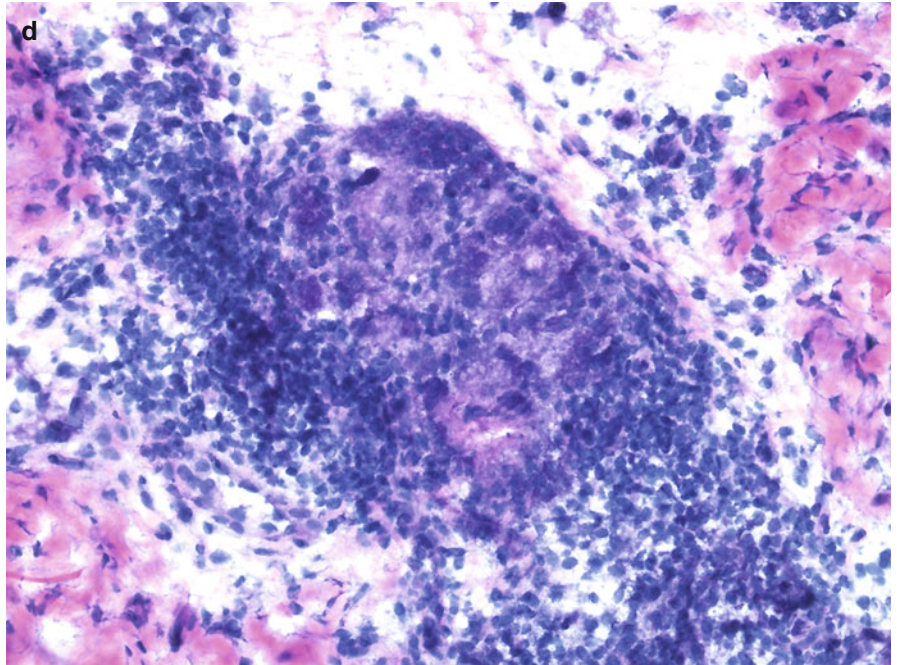
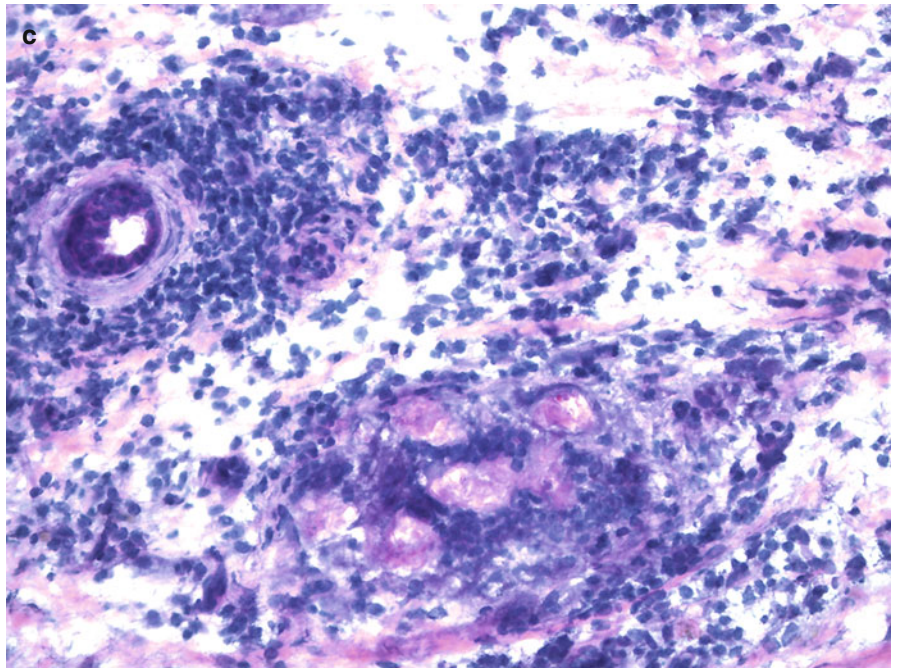


Fig. 10.7 Squamous cell carcinoma:
(a) Carcinoma on the right and scar tissue on the left at the base of the section.
(b) Closer examination of the area above the scar shows neoplastic aggregates with surrounding inflammation (*arrows*)

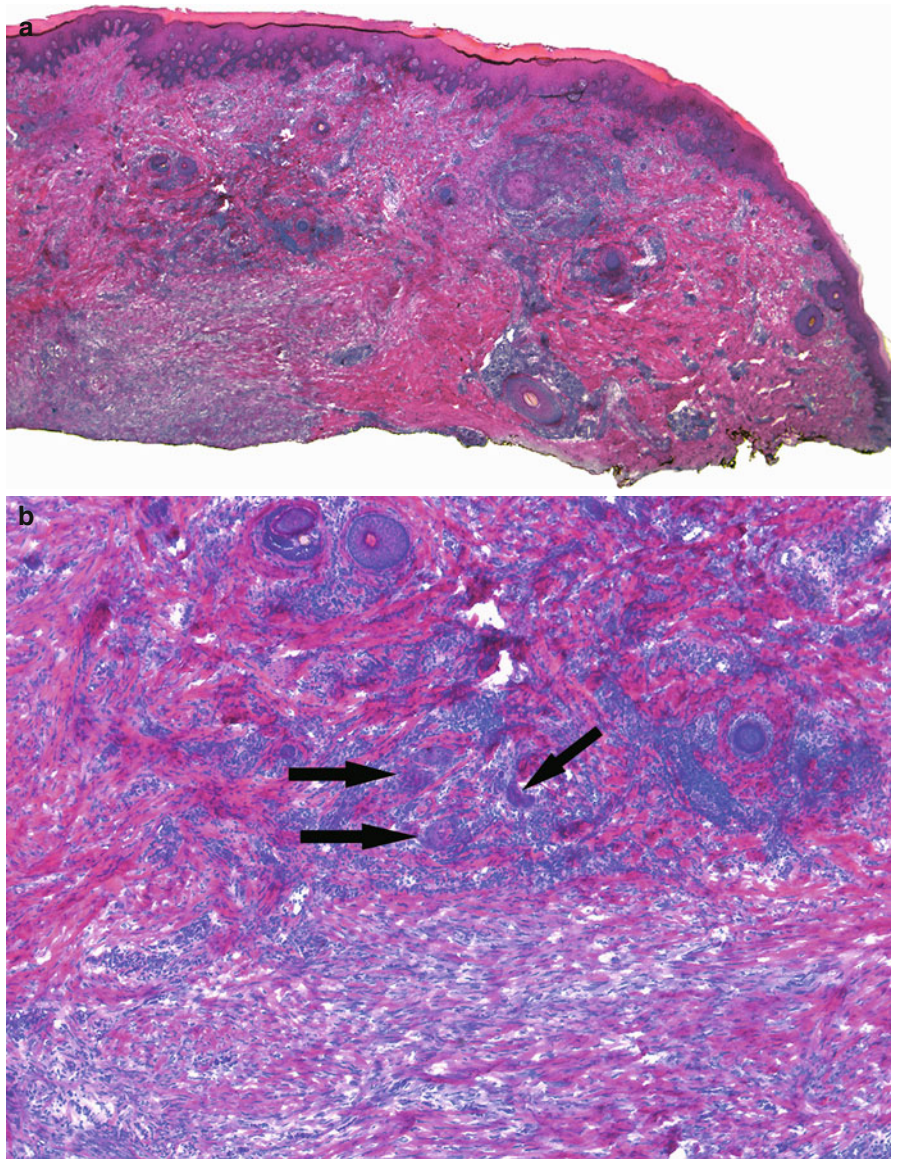


Fig. 10.7 (continued) (c) At this magnification, irregularly shaped angulated neoplastic aggregates with pleomorphic cells and focal keratinization are more obvious. (d) One neoplastic aggregate with bright eosinophilic keratin clump is present in the top center of the section. In the lower portion of this photomicrograph is a scar. There are bright eosinophilic thickened collagen bundles and plump fibroblasts, oriented horizontally

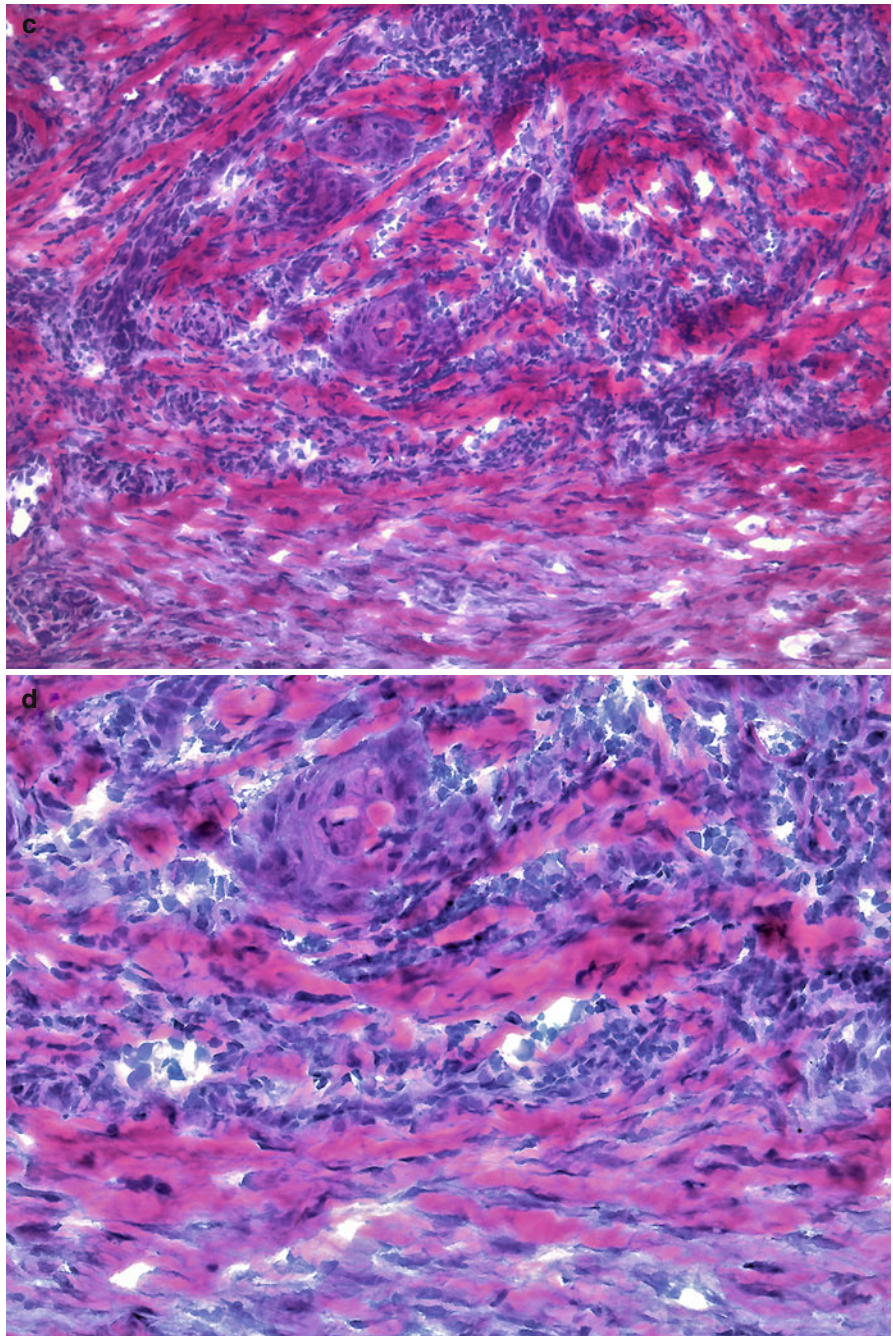


Fig. 10.8 Well-differentiated squamous cell carcinoma: (a) Note a small oval bright eosinophilic neoplastic aggregate in the right lower corner (circle). (b) This cancer may easily be missed if areas of scars are not carefully examined

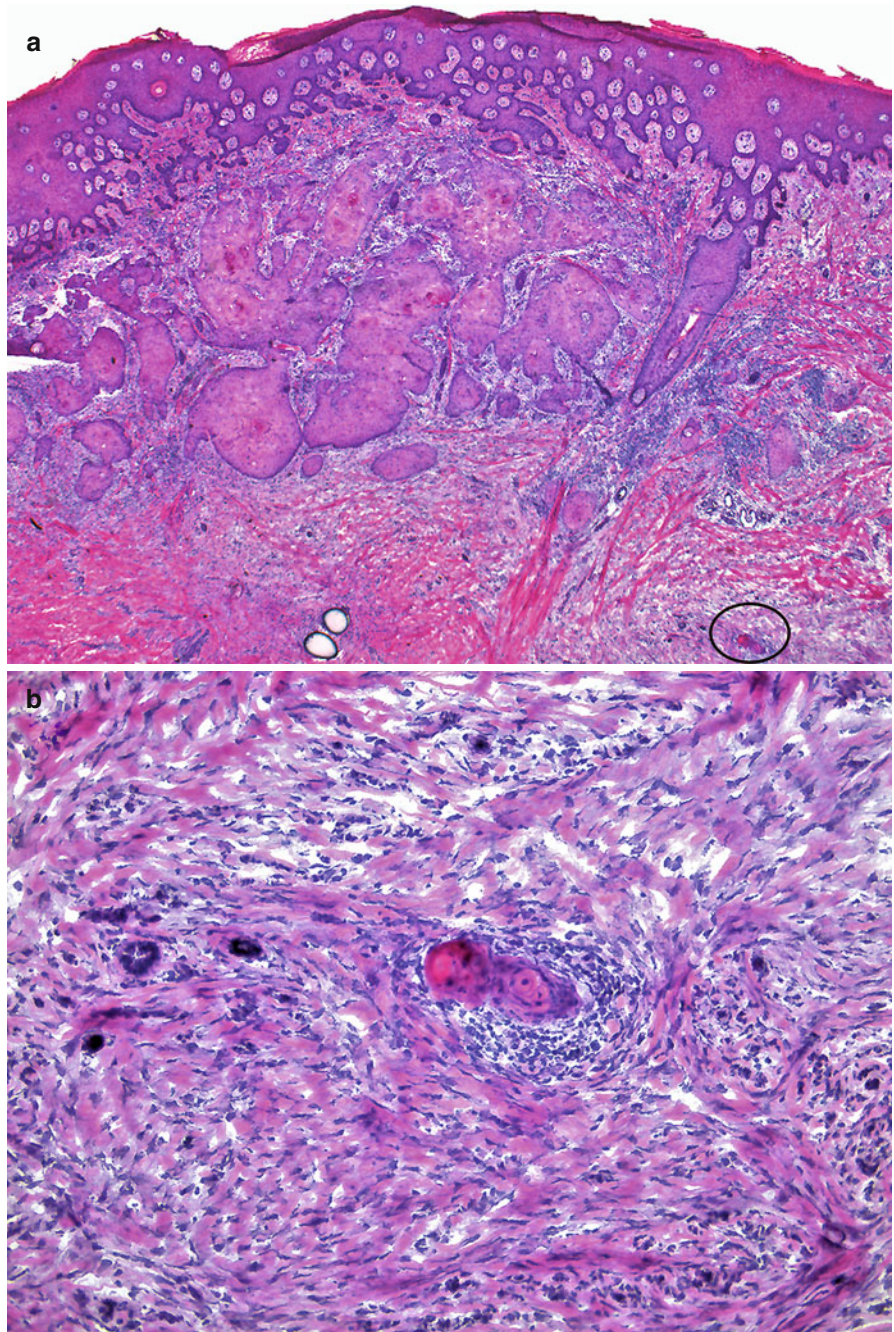


Fig. 10.9 Squamous cell carcinoma:
(a) Irregularly shaped keratinizing neoplastic epithelial aggregates. Basophilic neoplastic aggregates transitioning into keratinizing eosinophilic tumor islands.
(b) Neoplastic aggregates with variable keratinization. Small lymphocytes are dispersed among the neoplastic aggregates

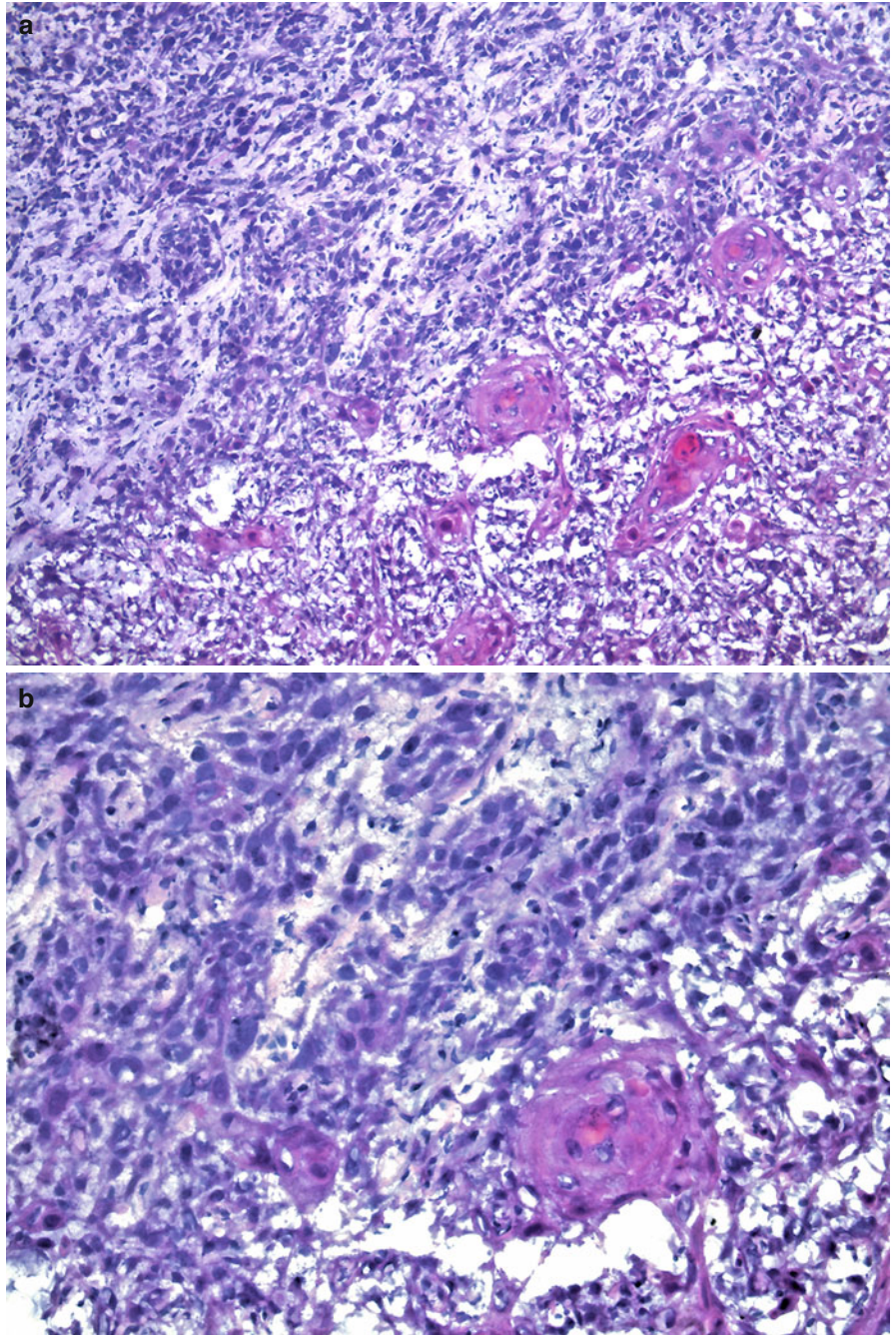


Fig. 10.10 Squamous cell carcinoma:
(a) Unremarkable dermis with a large basophilic nodule within the subcutaneous fat. (b) The nodule is composed of arborizing aggregates of neoplastic epithelial cells with eosinophilic cytoplasm and focal keratinization (*arrow*)

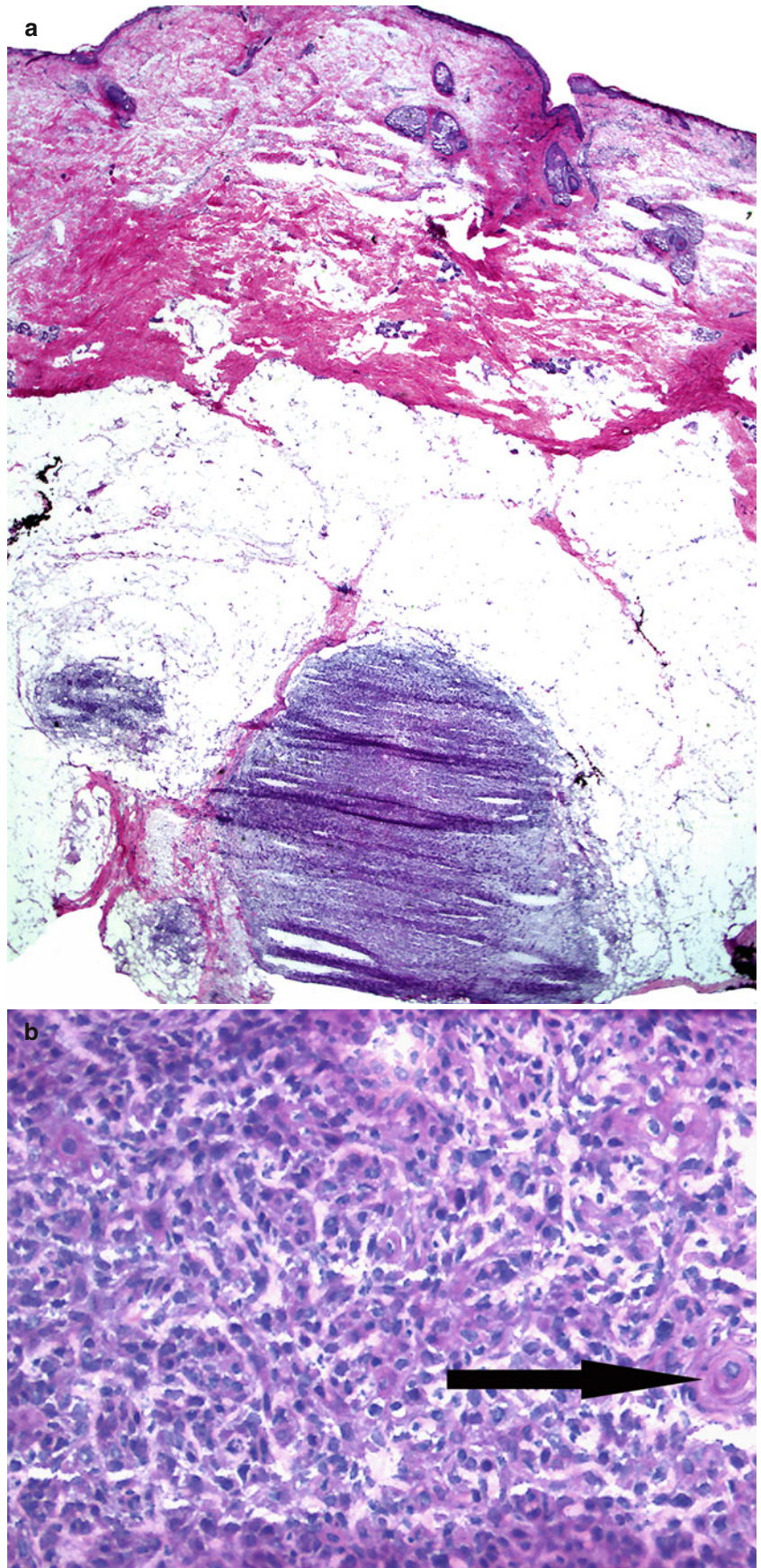


Fig. 10.11 Squamous cell carcinoma: (a) Although at this magnification tumor is not obvious, the presence of inflammation, mucinous stroma, and increased cellularity in the deep dermis and subcutis should alert the surgeon to examine the section more closely. (b) Solitary atypical keratinocytes and very small neoplastic aggregates (arrows) are noted infiltrating between collagen bundles

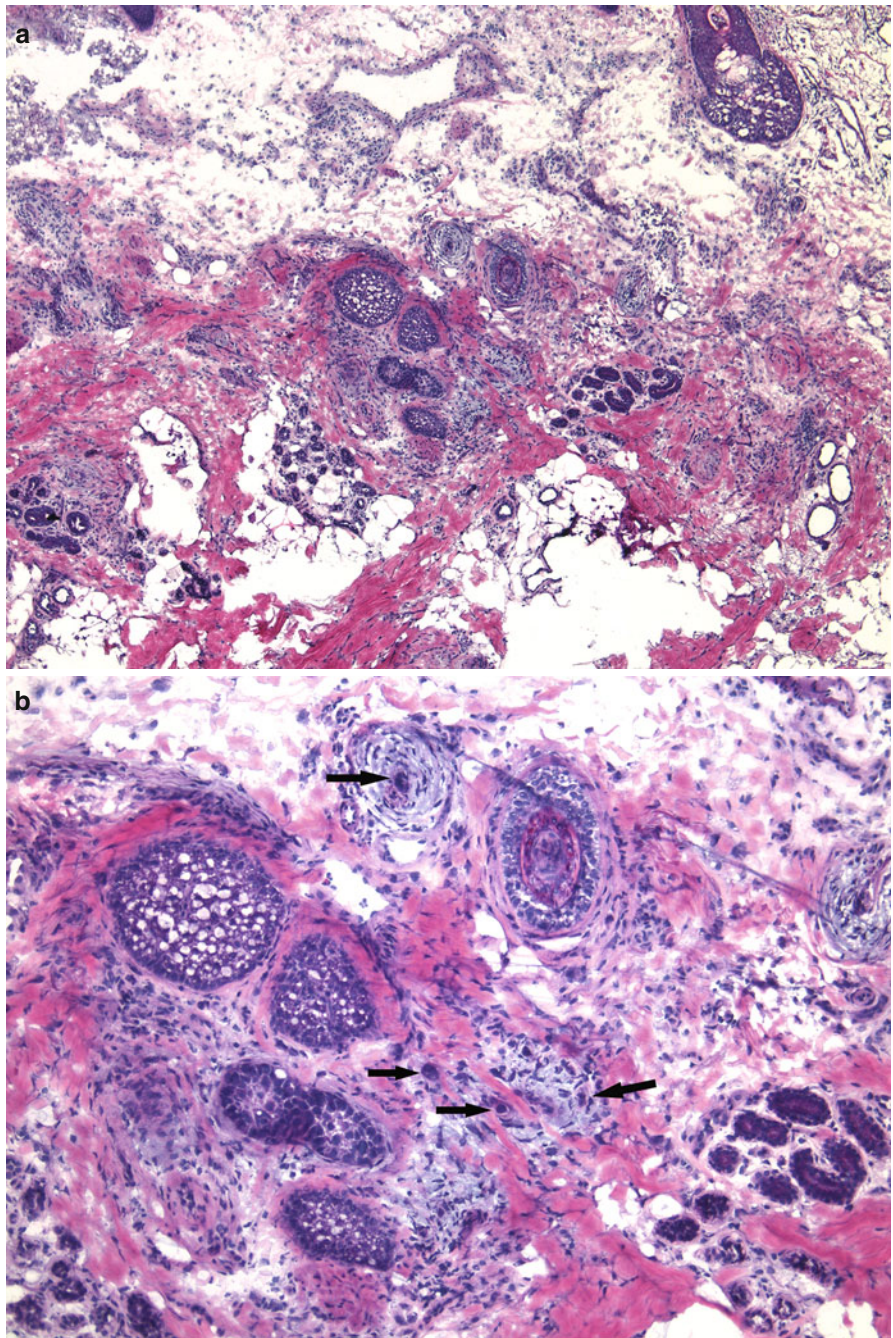


Fig. 10.11 (continued) (c) Squamous cell carcinoma with perineural invasion: a neoplastic aggregate (*thick arrow*) adjacent to a nerve (*thin arrow*) demonstrating perineural invasion

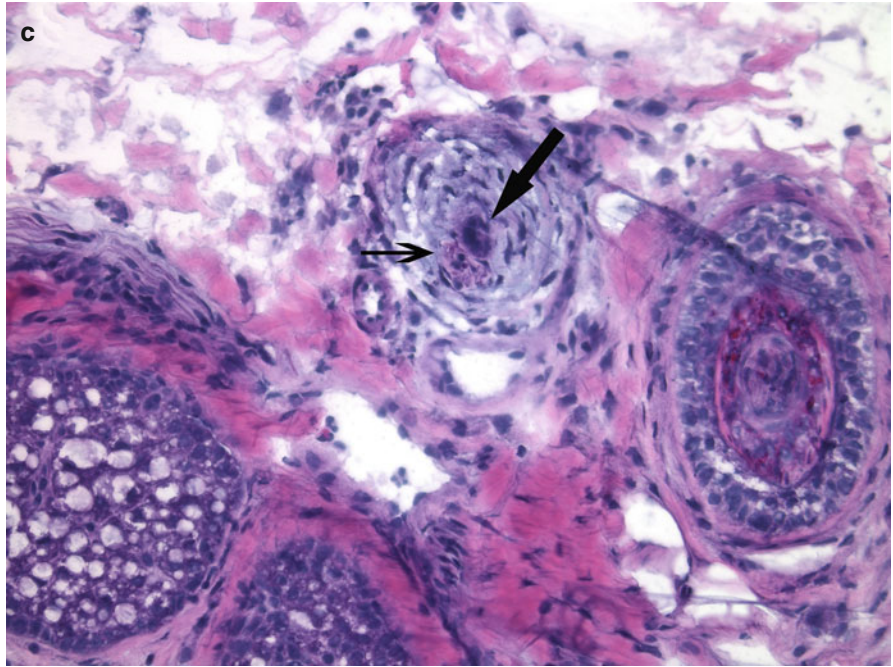


Fig. 10.12 Squamous cell carcinoma: (a) Potentially easily overlooked scattered tumor aggregates (*arrow*). (b) Tumor aggregates surrounded by mucinous stroma are more obvious at this magnification

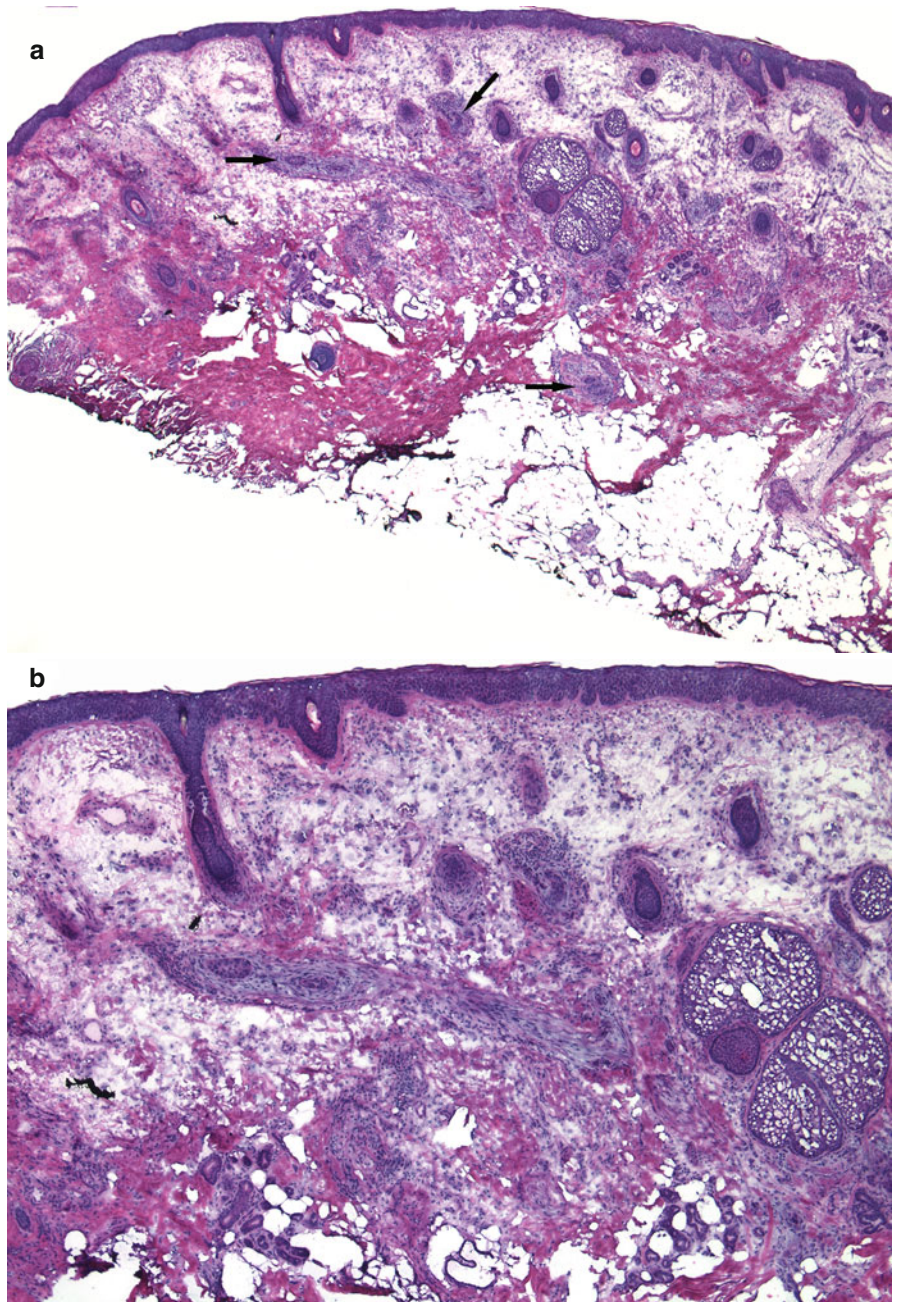


Fig. 10.12 (continued) (c, d) Arrows point to variably sized and inconspicuous tumor aggregates

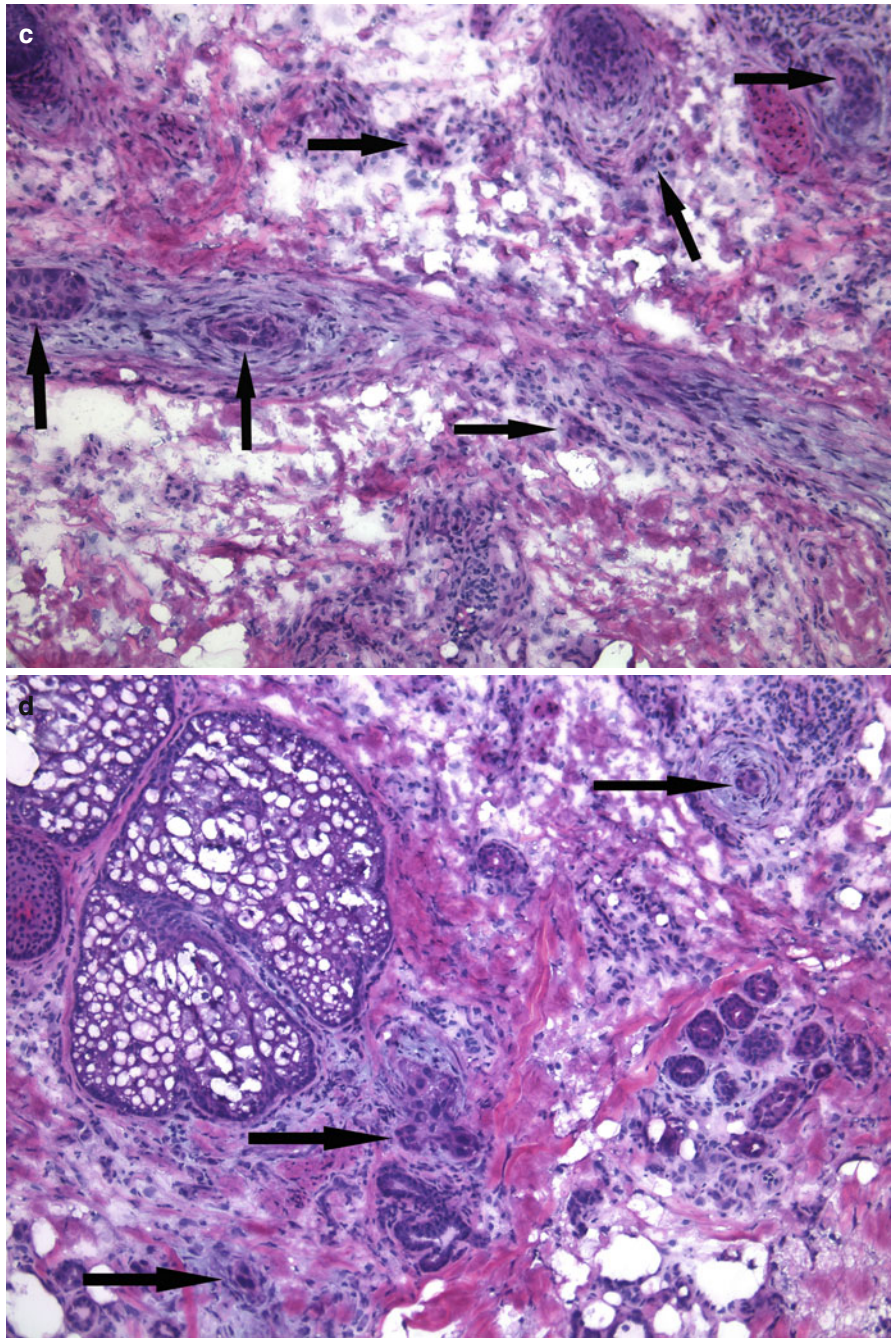


Fig. 10.12 (*continued*) (e) Squamous cell carcinoma with perineural invasion: a nerve cut in cross section infiltrated with neoplastic keratinocytes

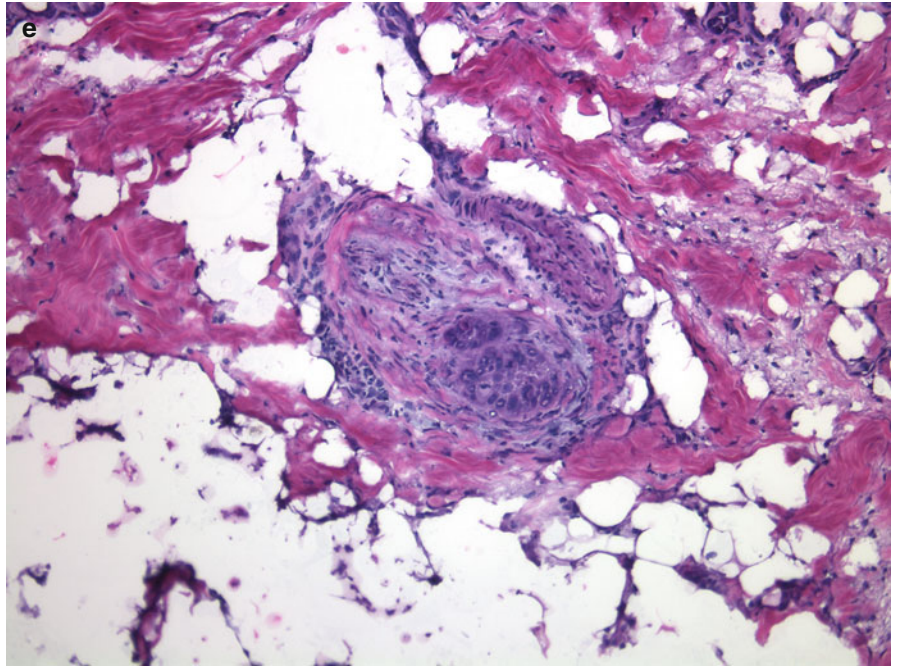


Fig. 10.13 Squamous cell carcinoma:
(a) Epithelioid islands of tumor cells within
the subcutaneous fat. (b) The neoplastic
aggregates are easily discernible at this
magnification

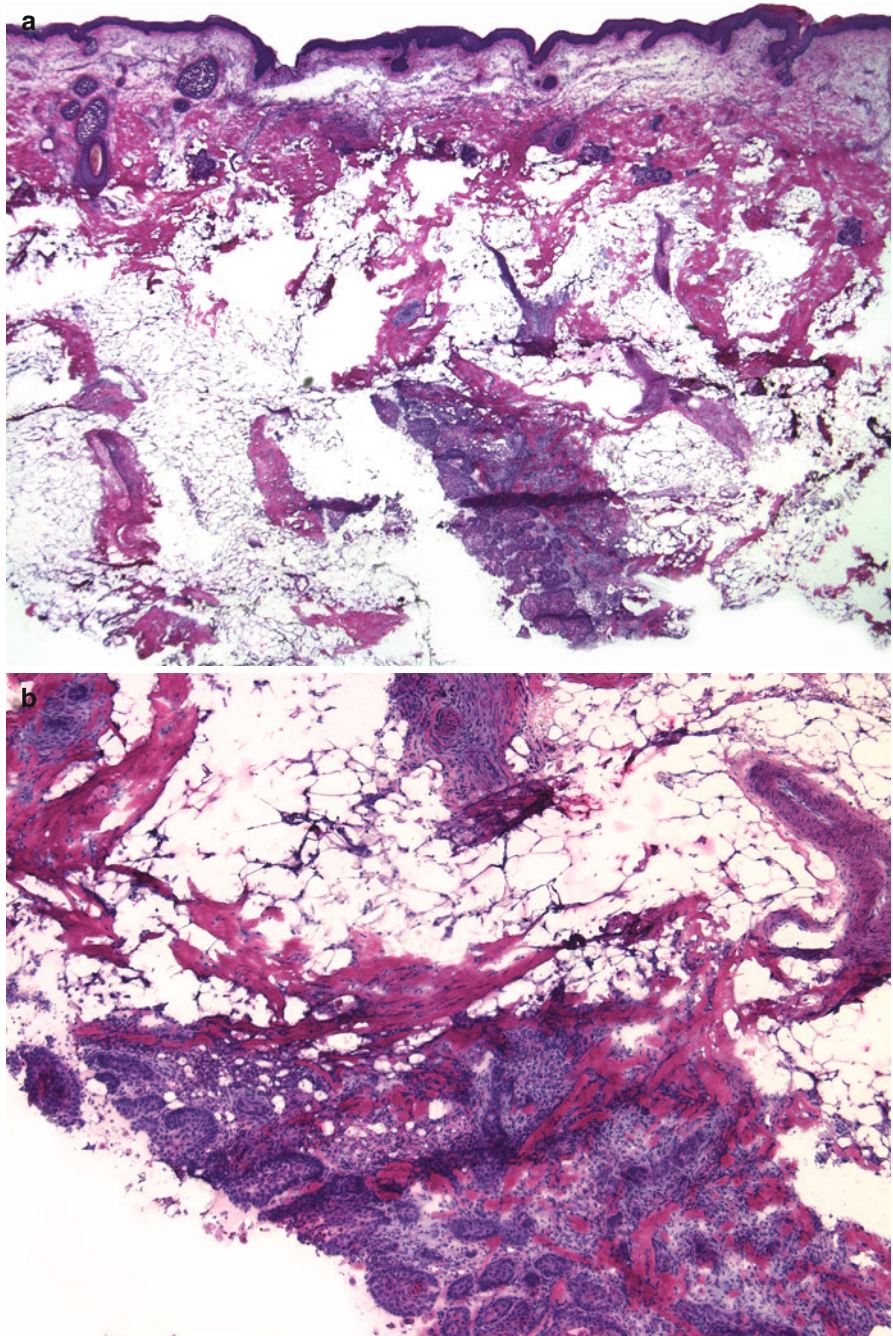


Fig. 10.13 (continued) (c) Although this tumor is deeply infiltrative it retains its keratinizing feature. (d) Two small neoplastic aggregates within a fibrous septum of the subcutis

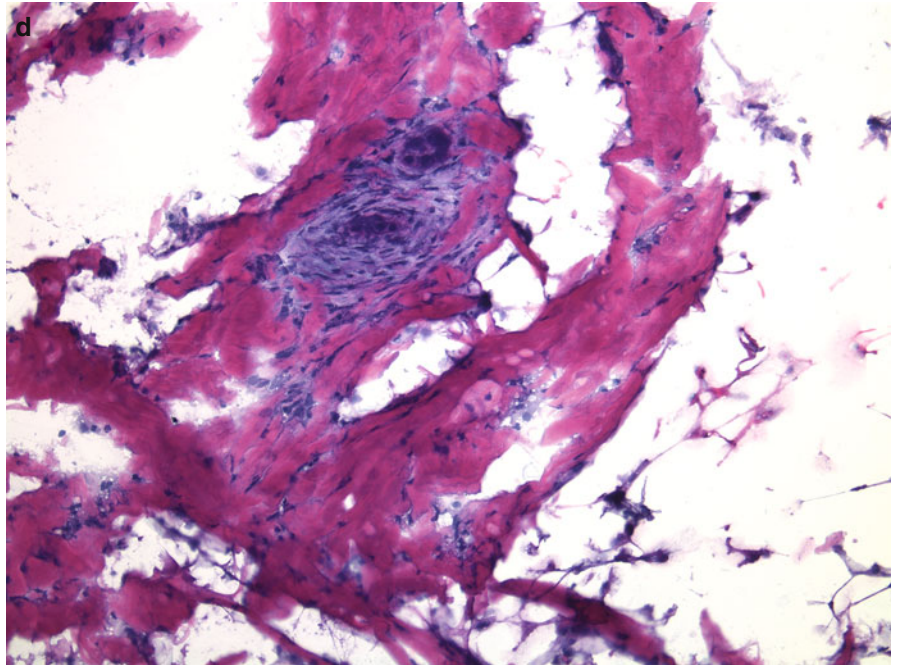
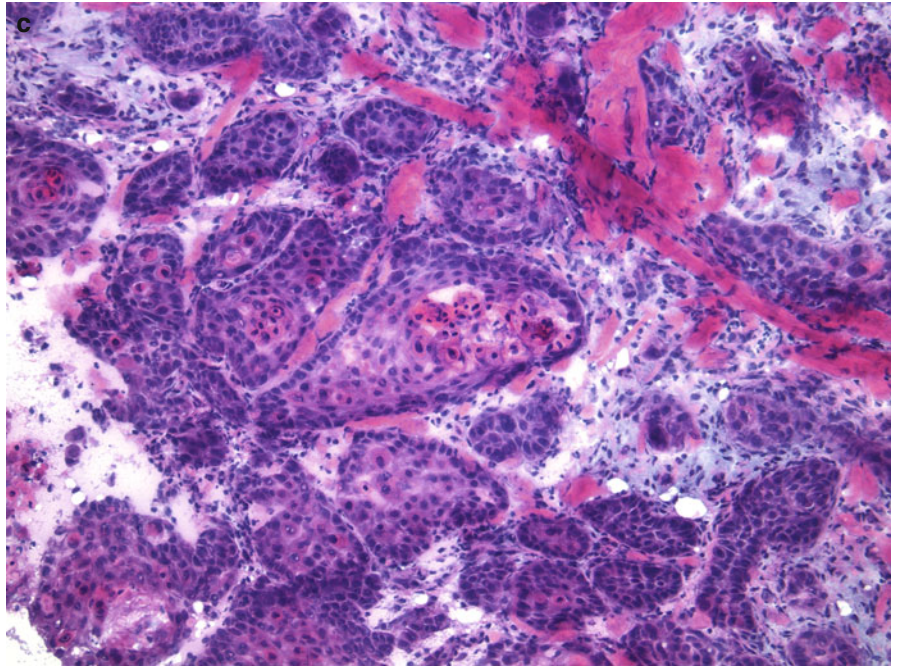


Fig. 10.14 Perineural squamous cell carcinoma: **(a)** A medium-size nerve surrounded by dense lymphocytic inflammation. Nests of neoplastic keratinocytes (designated by arrows) are obscured by dense inflammatory infiltrate. Features that help differentiate tumor from inflammation include the cohesiveness of the neoplastic cells, the larger nuclear and cell size, and the scant but still discernible eosinophilic cytoplasm. **(b)** In contrast to the large pleomorphic neoplastic cells the lymphocytes are smaller, with darker nuclei, and no visible cytoplasm

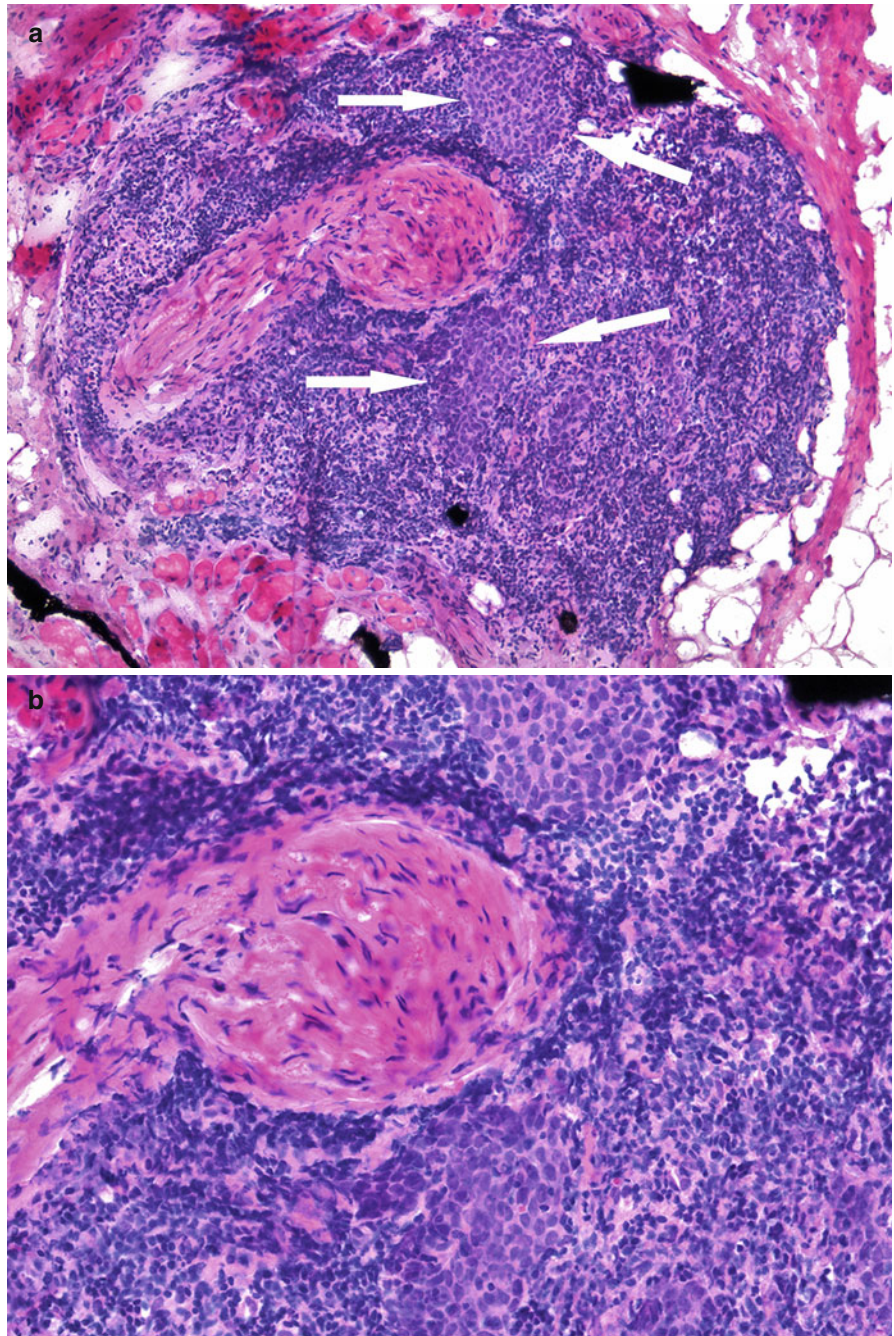


Fig. 10.15 Acantholytic squamous cell carcinoma: **(a)** There is acantholysis in the lower portion of the epidermis and pseudoglandular pattern of the tumor in the superficial dermis. **(b)** Round neoplastic aggregates showing pseudolumina in their centers

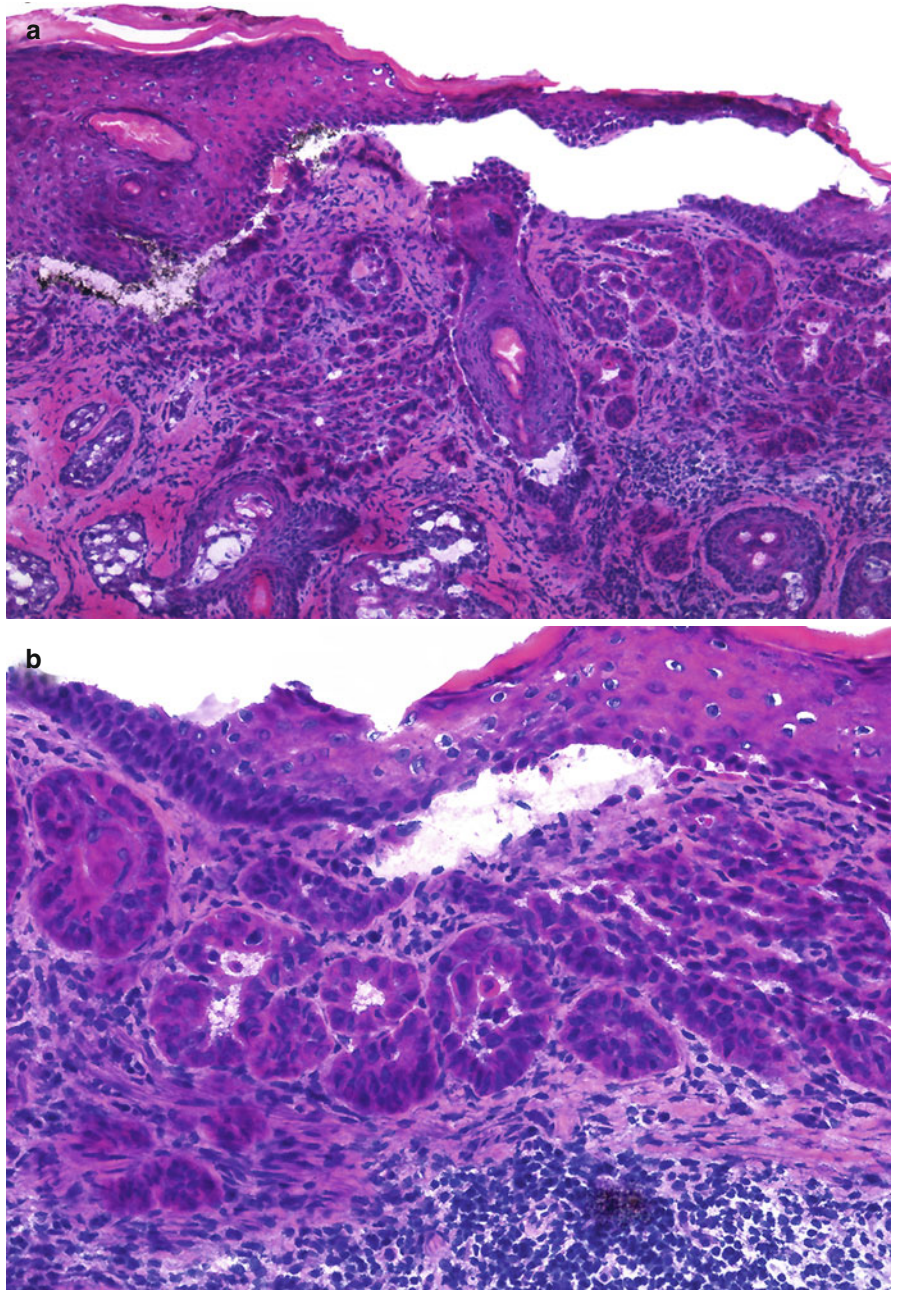


Fig. 10.15 (*continued*) (c) Higher magnification of the gland-like tumor aggregates as well areas showing focal keratinization

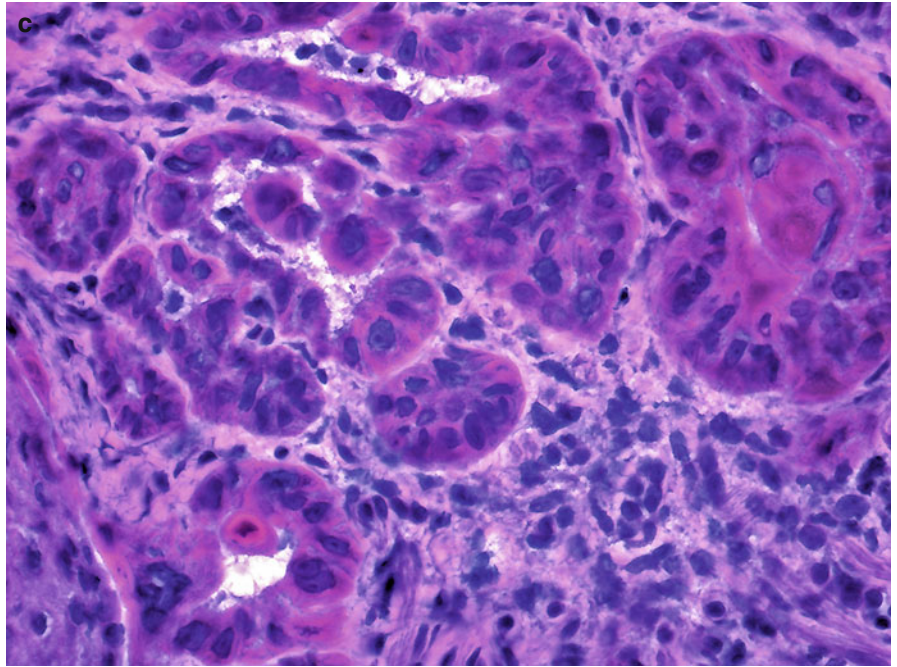


Fig. 10.16 Squamous cell carcinoma:
(a) Collection of darkly stained cells and inflammation in the dermis in the center of the specimen warrants a closer examination.
(b) At this magnification, a basophilic cellular area is noted

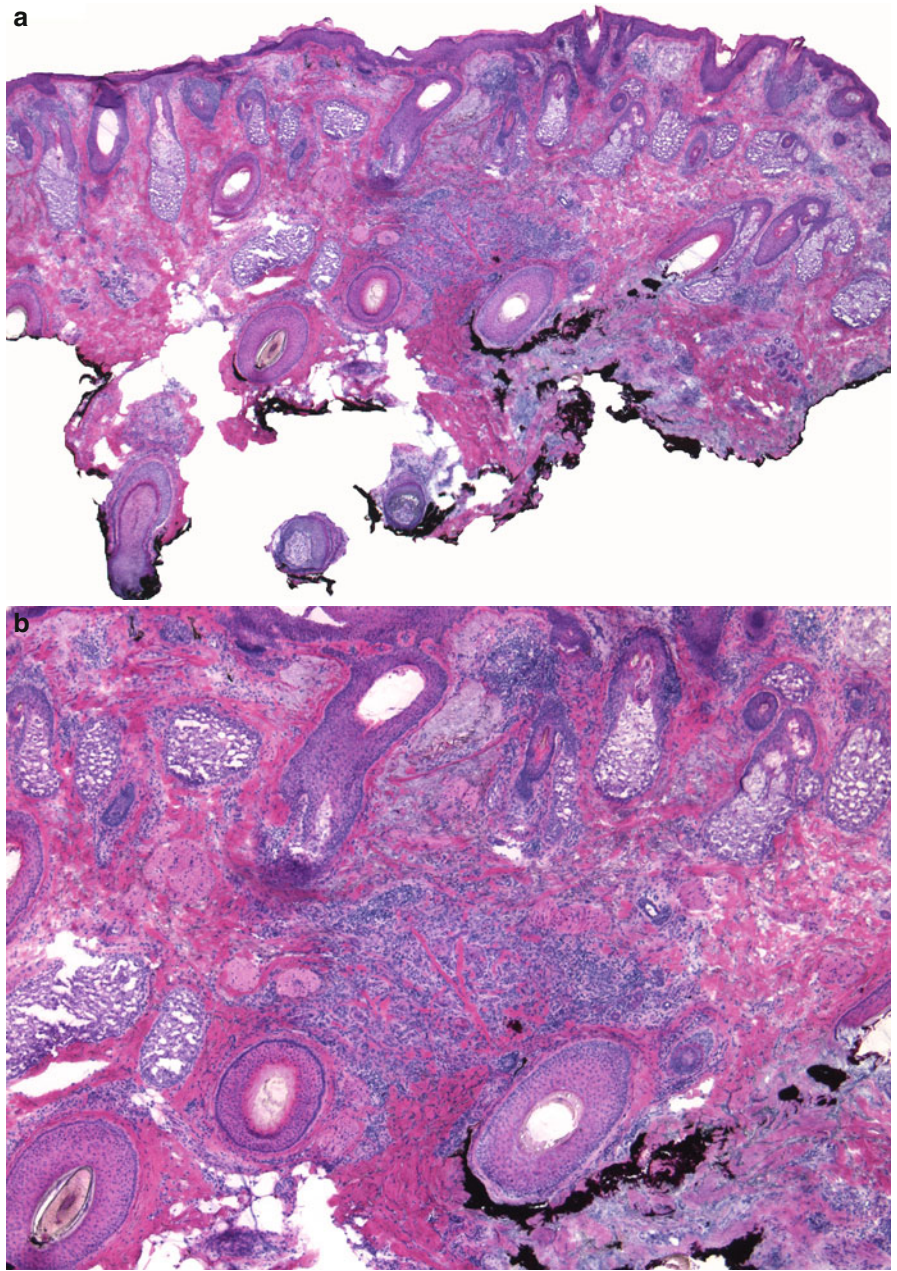


Fig. 10.16 (*continued*) (c) The neoplastic aggregates are angulated and irregular and many contain central foci of keratinization

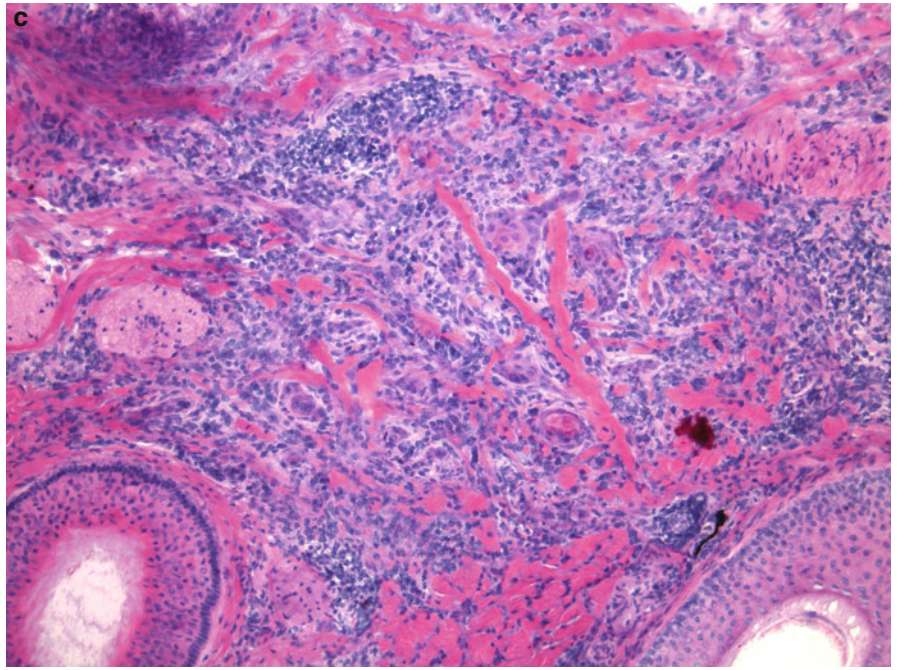


Fig. 10.17 Squamous cell carcinoma: (a) Under a scar in the superficial dermis are neoplastic aggregates that resemble hair follicles. (b) On the left and in the right lower corner are tumor aggregates with a central pearl of parakeratin (*arrows*). Focal granulomatous reaction with multinucleated giant cells surrounding free keratin in the dermis is also seen. To the right is a scar with bright eosinophilic newly formed collagen bundles and plump fibroblasts

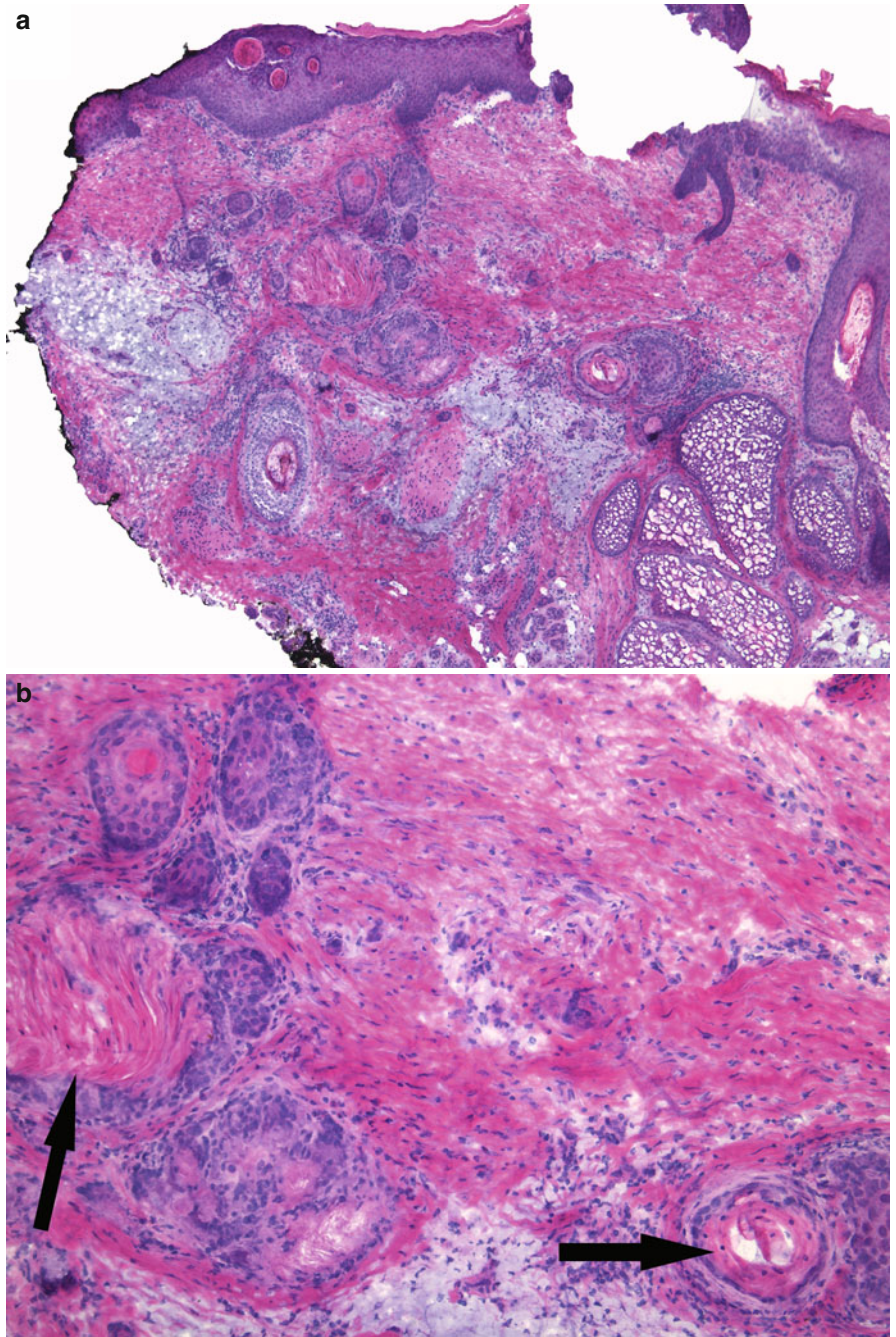


Fig. 10.18 Squamous cell carcinoma: (a) At scanning magnification this squamous cell carcinoma, hidden in between sebaceous lobules in the dermis, can be easily overlooked. (b) A few suspicious foci for tumor are seen mainly in the area between sebaceous lobules

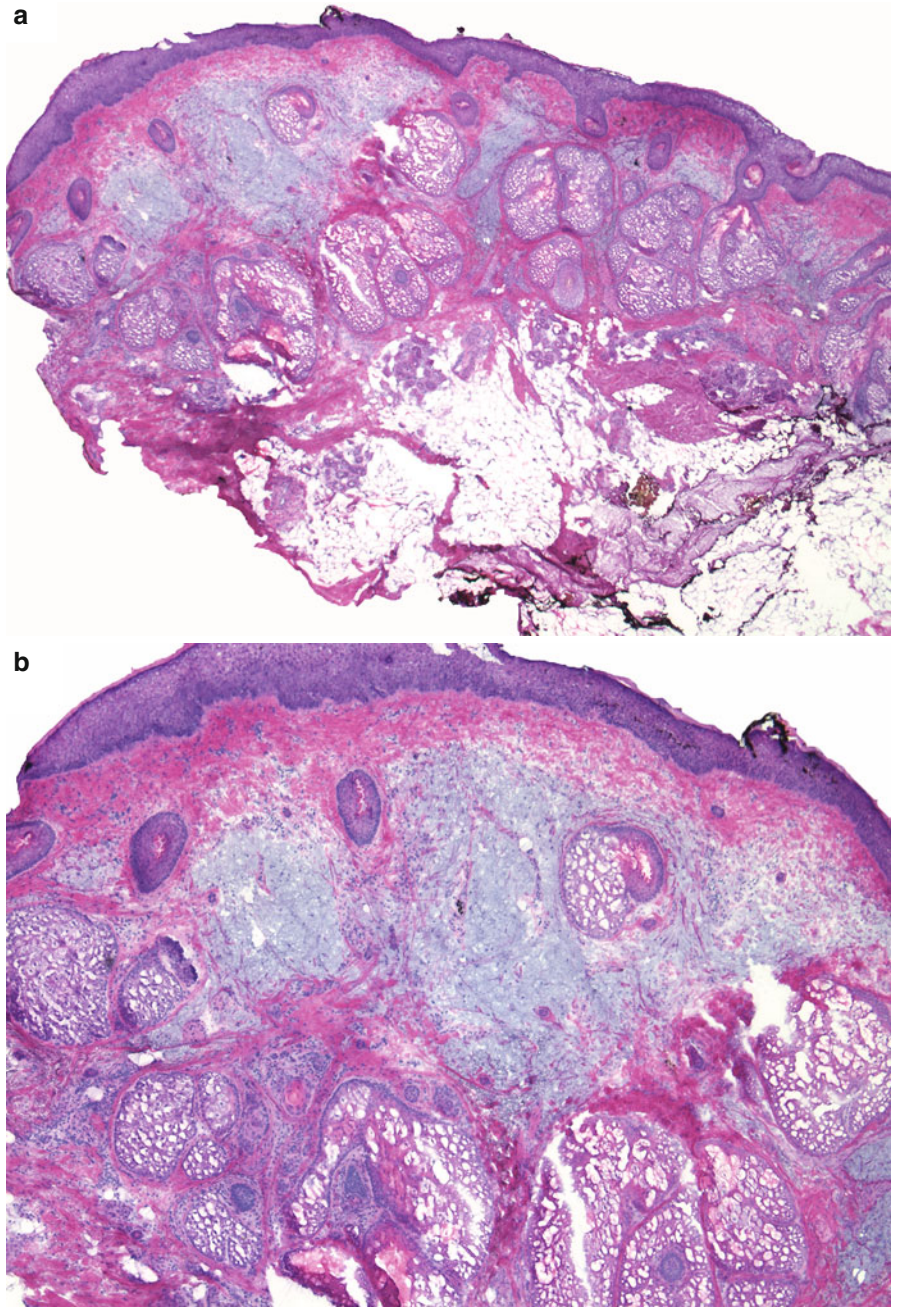


Fig. 10.18 (continued) (c) Aggregates of squamous cell carcinoma (*thick arrows*) versus follicular bulbs and papillae (*thin arrows*). In contrast to follicular epithelium, the neoplastic aggregates have irregular shapes, more eosinophilic staining, and faulty keratinization. (d) The lack of surrounding inflammation makes the tumor aggregates (*arrows*) quite inconspicuous

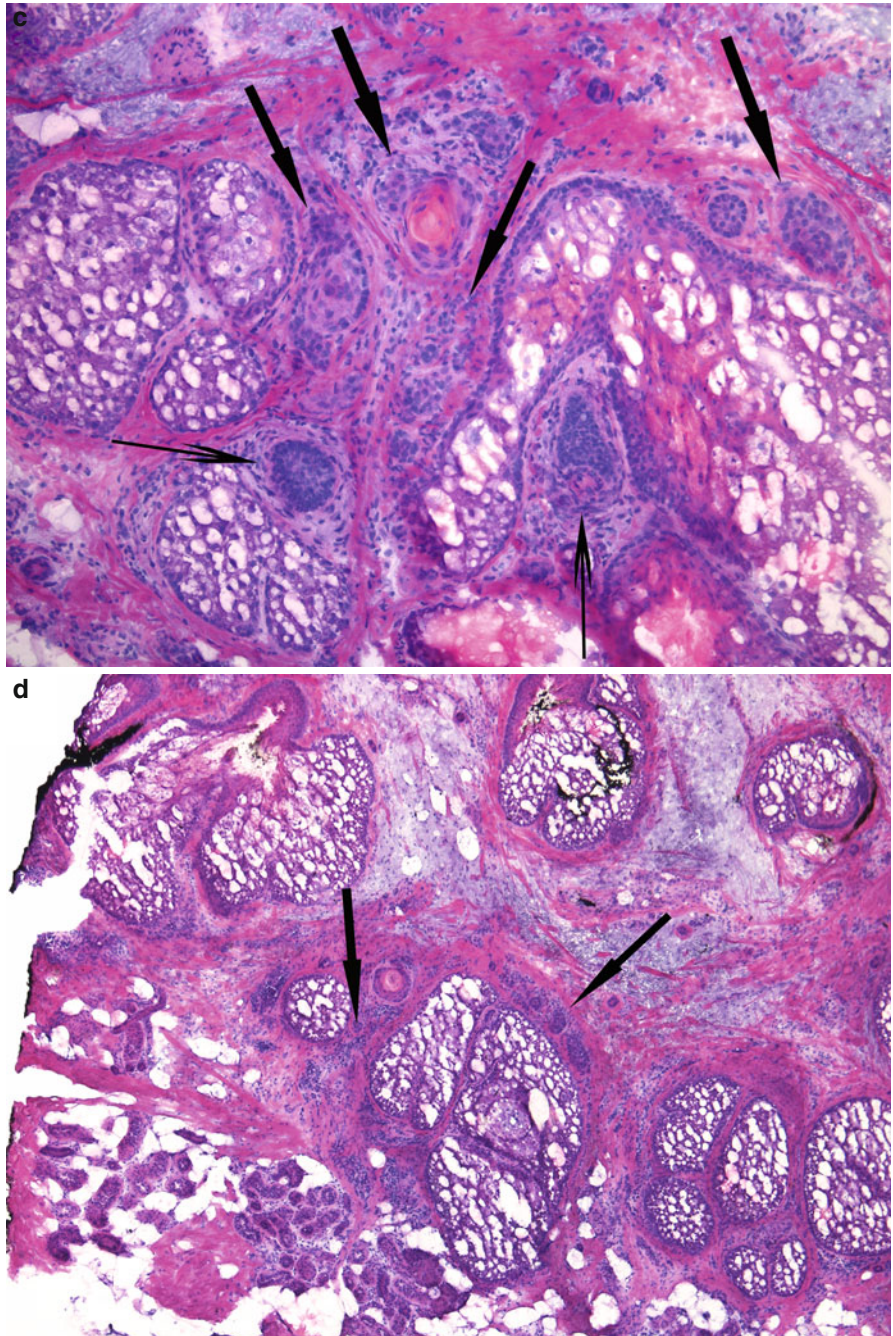


Fig. 10.18 (*continued*) (e) The only clue to the neoplastic nature of these tumor aggregates (*arrows*) is their hyperchromasia and minimal accompanying inflammation

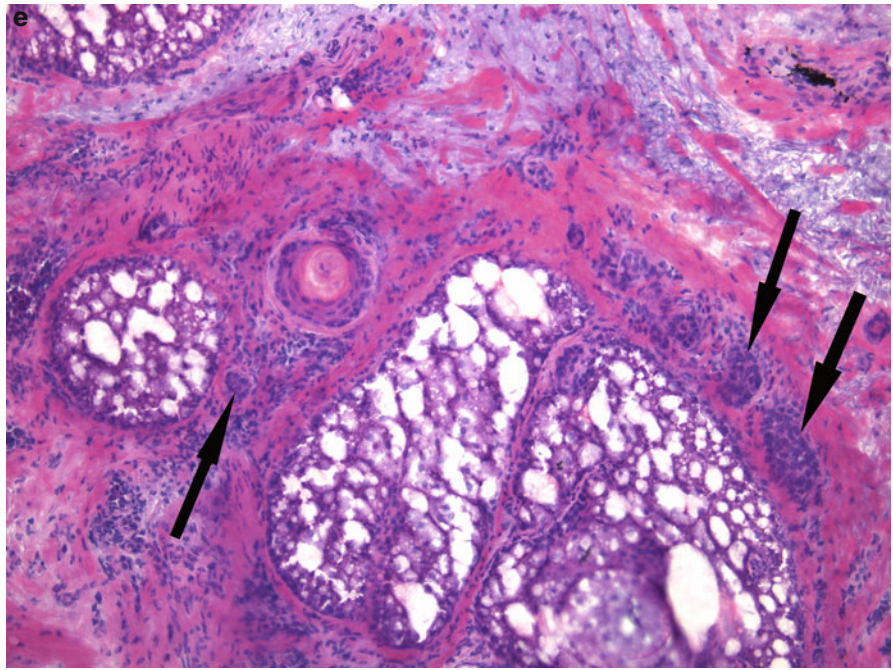


Fig. 10.19 Small hyperchromatic tumor aggregates in sea of solar elastosis: (a) *Arrows* point to the small and widely scattered neoplastic aggregates. (b) The neoplastic aggregates are surrounded by the folliculosebaceous unit in the center of the photomicrograph. *Arrows* point to other small nests of neoplastic cells, which can possibly be mistaken for eccrine ducts

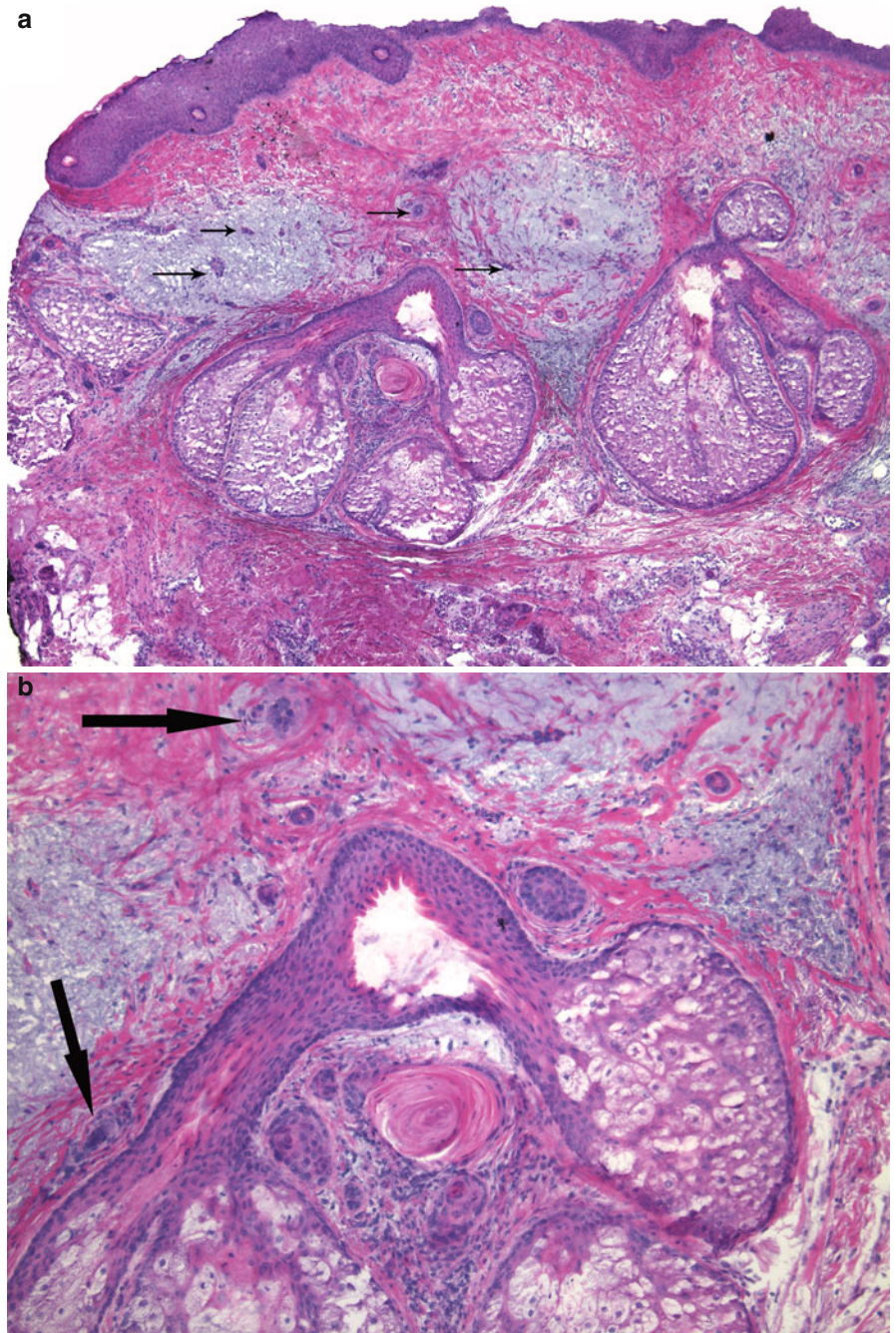


Fig. 10.19 (*continued*) (c) Unlike the two eccrine ducts designated by *thin arrows*, which have a central lumen lined by pink cuticle, the small round neoplastic aggregate (*thick arrow*) is composed of large hyperchromatic cells and lacks a lumen

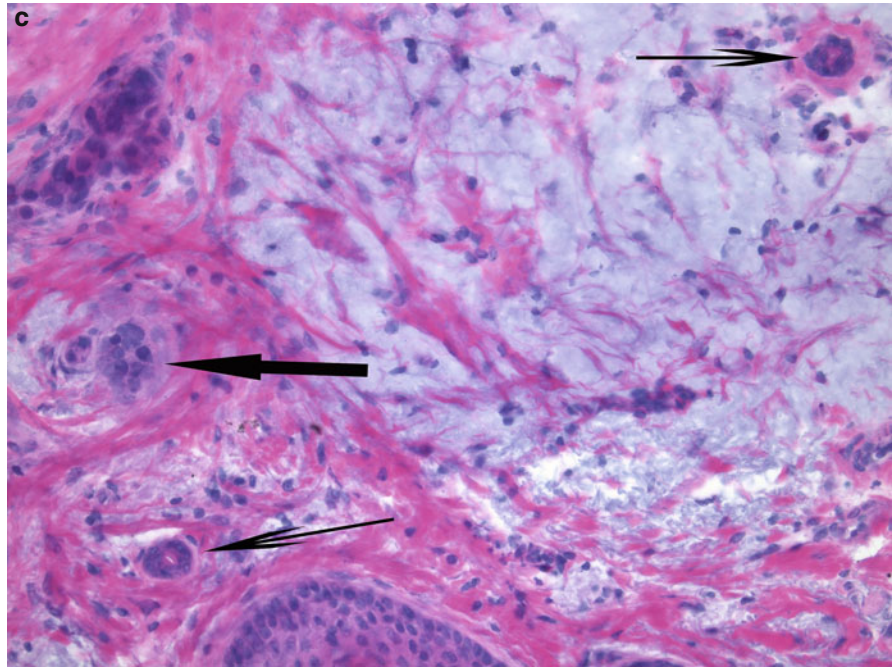


Fig. 10.20 Infiltrative squamous cell carcinoma: **(a)** Neoplastic cells infiltrate most of the section. **(b)** The tumor consists of small epithelial aggregates, cords, and strands

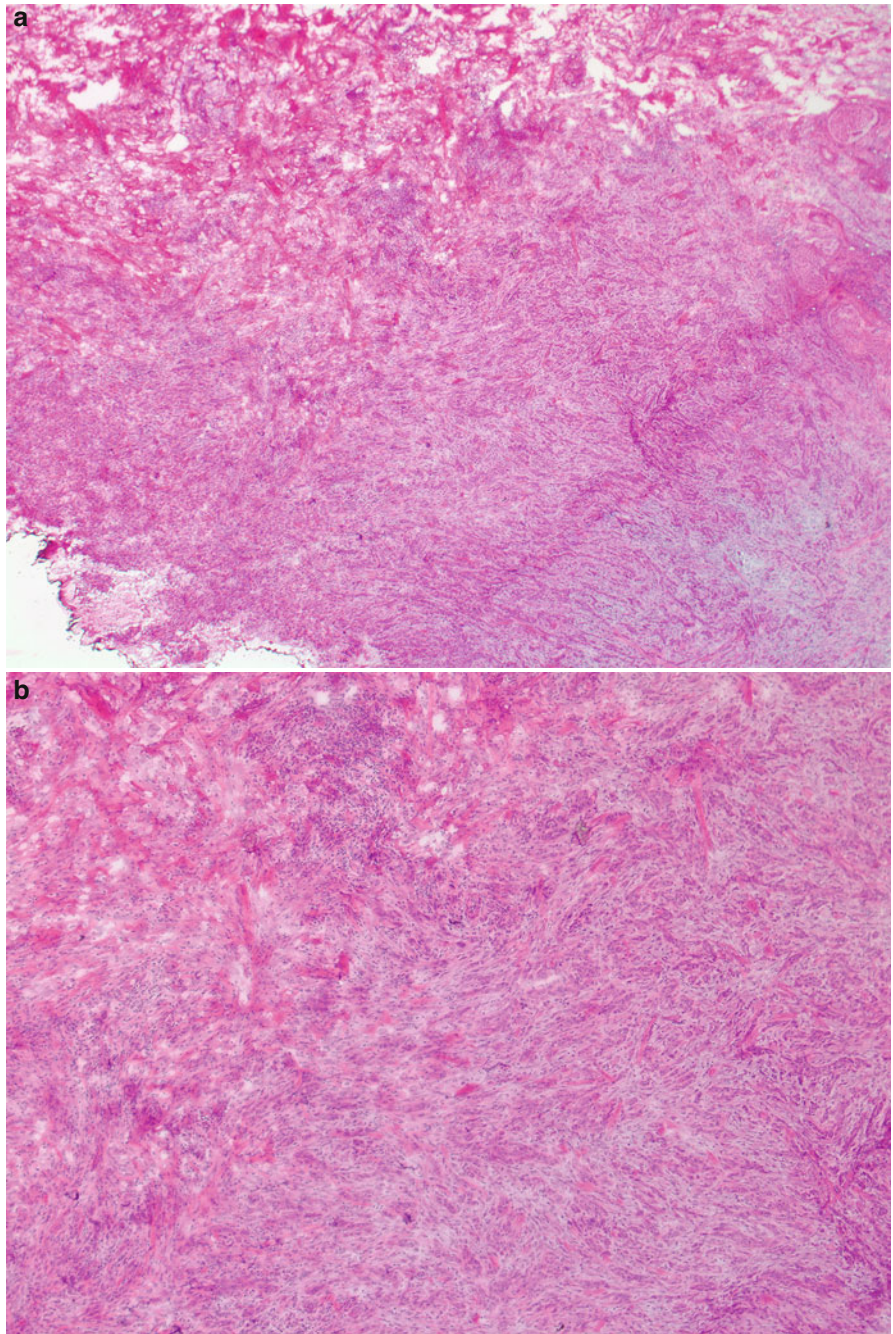


Fig. 10.20 (*continued*) (c) The neoplastic cells have a polygonal or round shape, basophilic nuclei, and scant, glassy eosinophilic cytoplasm

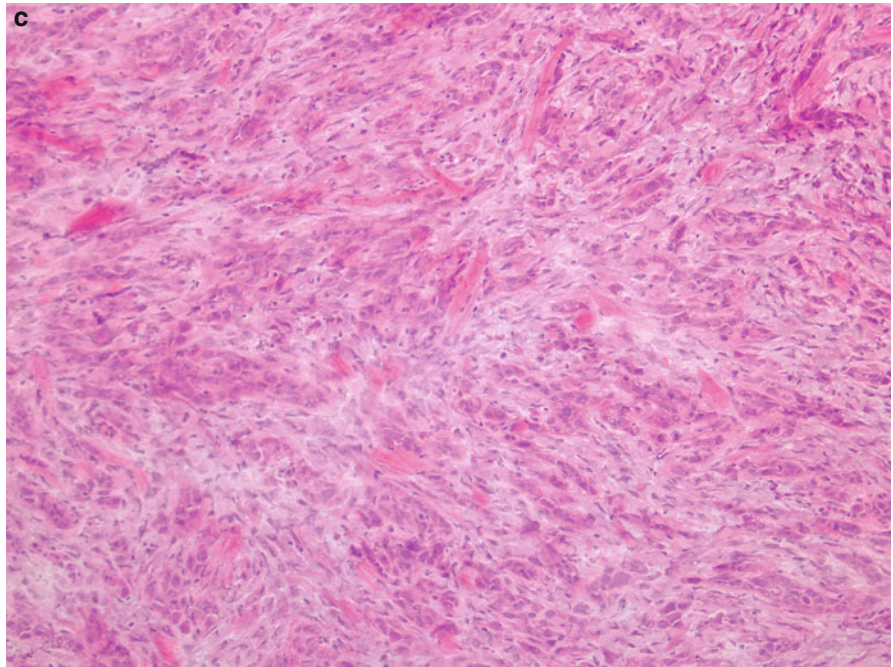


Fig. 10.21 Infiltrative squamous cell carcinoma: **(a)** The neoplastic aggregates of infiltrative SCC may be small and obscured by dense inflammation, therefore careful examination of the tissue section is imperative. **(b)** In this tumor there are areas containing solitary neoplastic cells as well as small collections of a few neoplastic cells with glassy eosinophilic cytoplasm

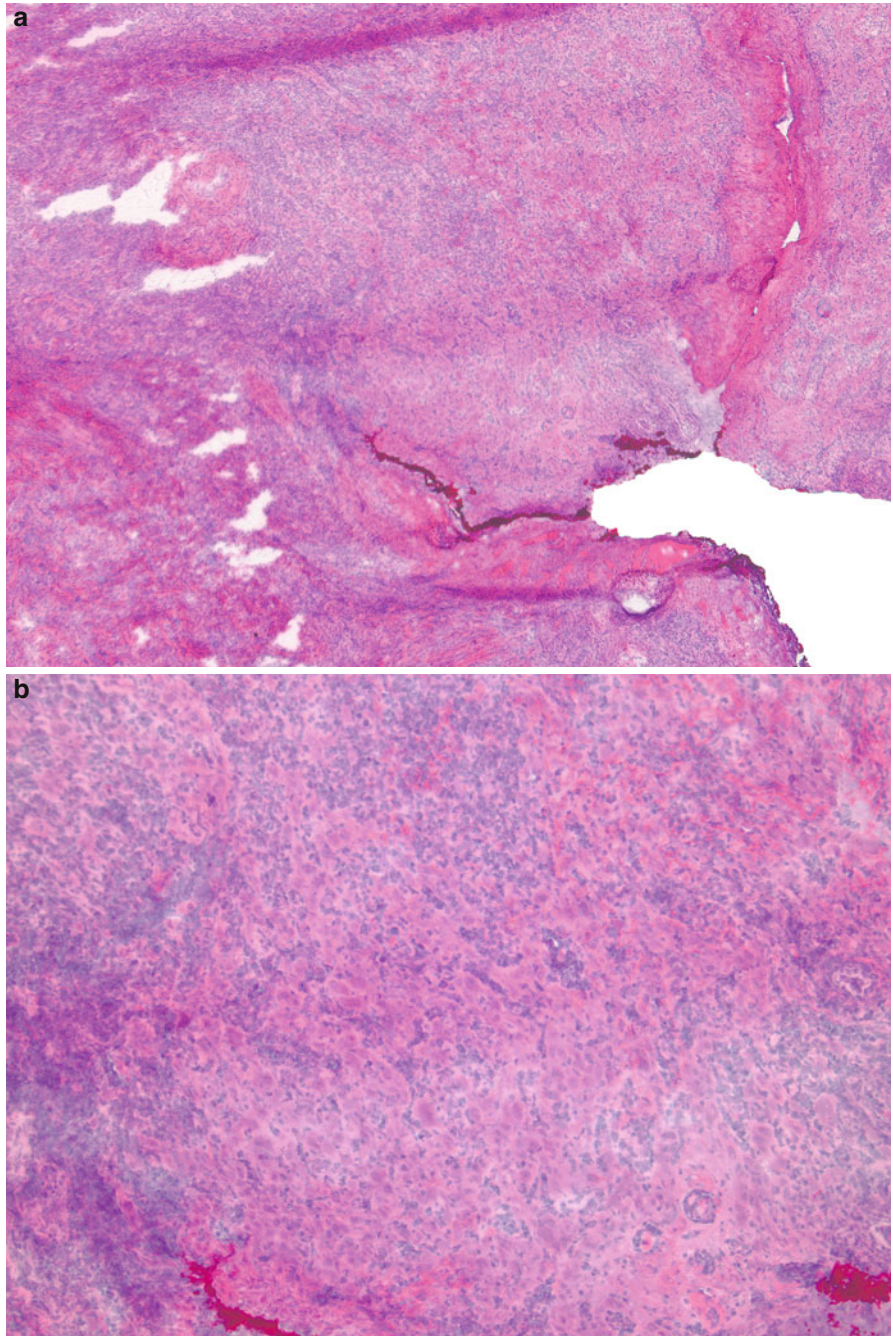


Fig. 10.22 Squamous cell carcinoma:
(a) Well-differentiated carcinoma is present in the lower dermis in the center of the specimen. (b) Higher magnification reveals cellular atypia and formation of squamous eddies in these two neoplastic aggregates

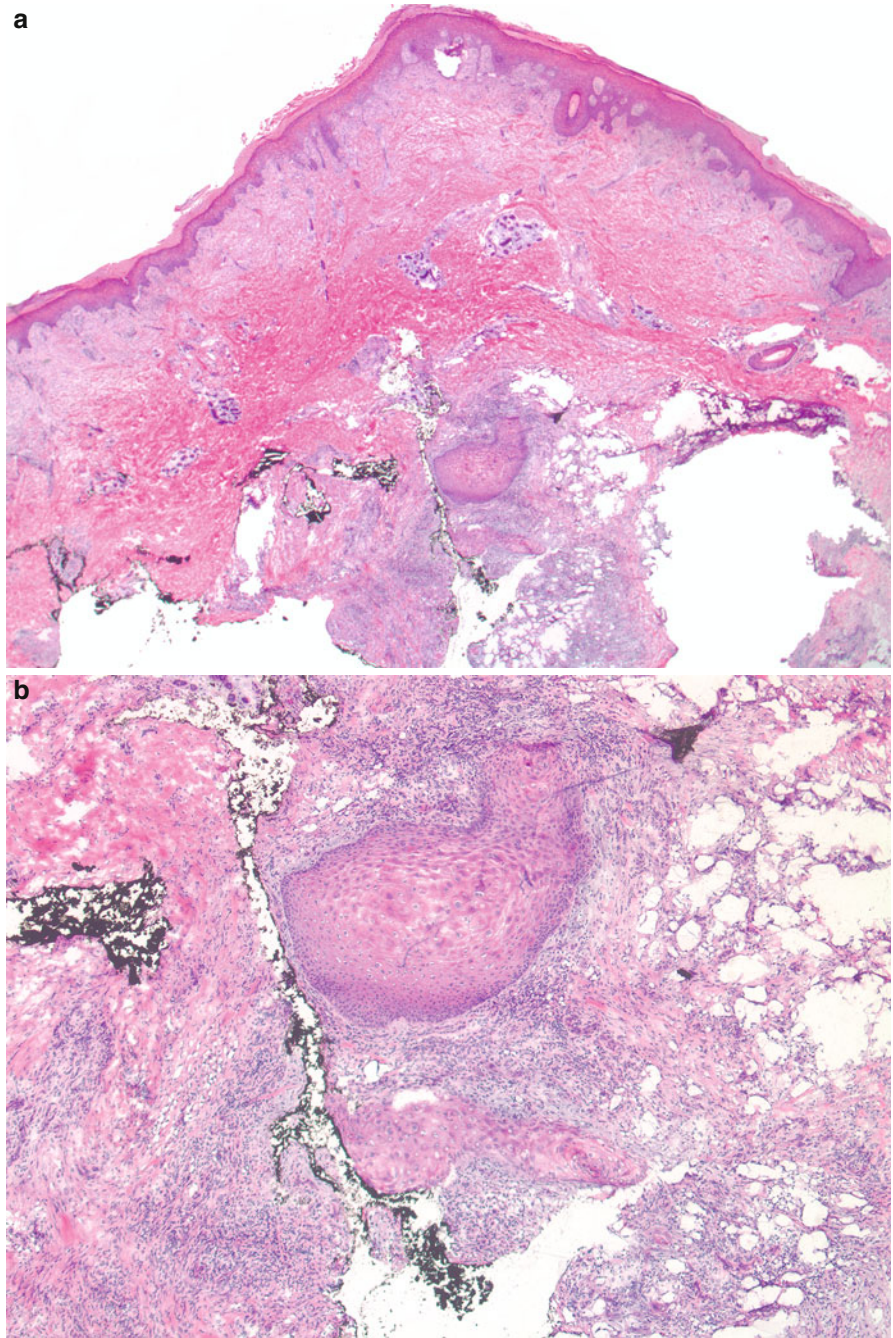


Fig. 10.23 Squamous cell carcinoma: (a) Areas of dense inflammation are seen at scanning magnification. (b) Upon closer examination, glassy, eosinophilic, epithelioid tumor cells are seen within the center of the dense inflammation. The neoplastic cells are large, with basophilic nuclei, and moderately abundant eosinophilic cytoplasm, in contrast to the lymphocytic inflammatory cells

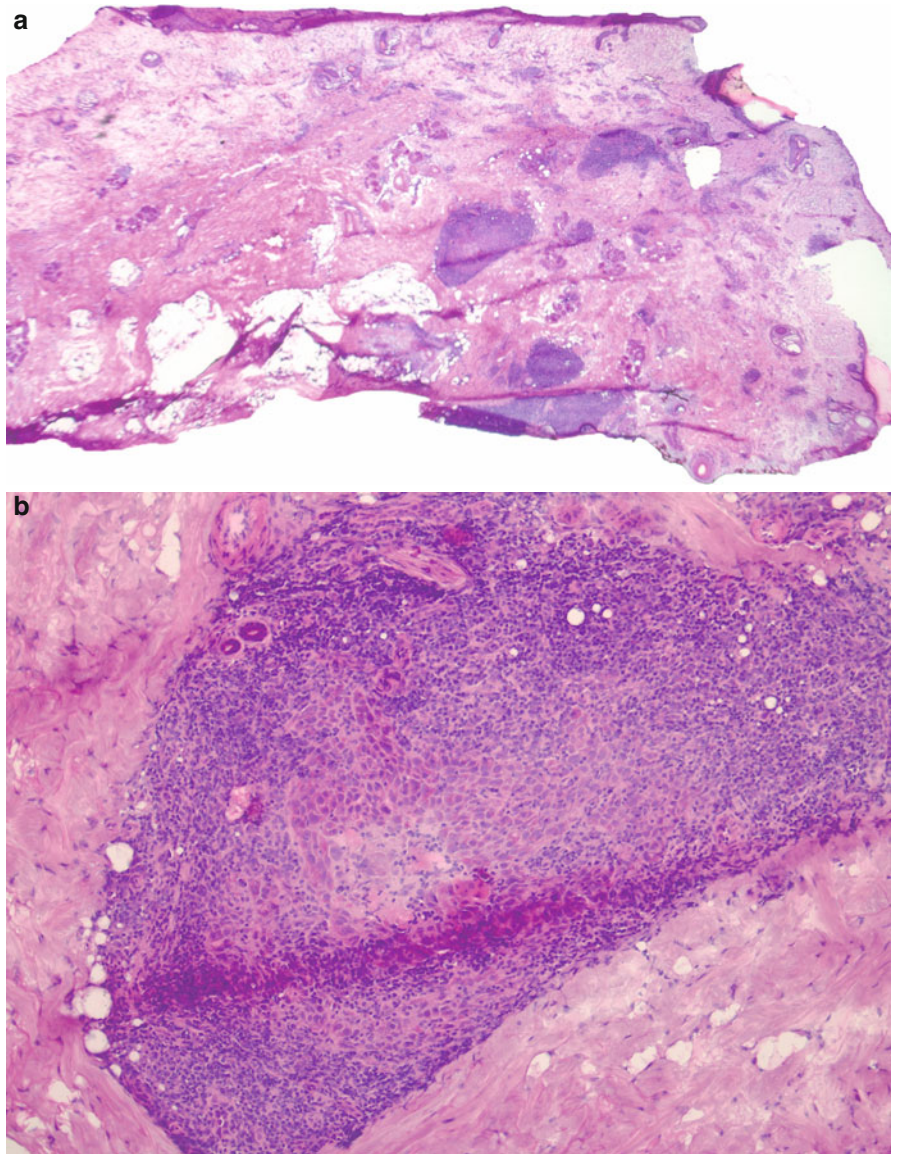


Fig. 10.23 (*continued*) (c) Dense lymphocytic inflammation surrounds nerves. Small neoplastic nests and single cells are present within the inflammation (*arrows*). The neoplastic cells have large pleomorphic nuclei and scant eosinophilic cytoplasm. They do not form large tumor aggregates and, therefore, are not readily perceived

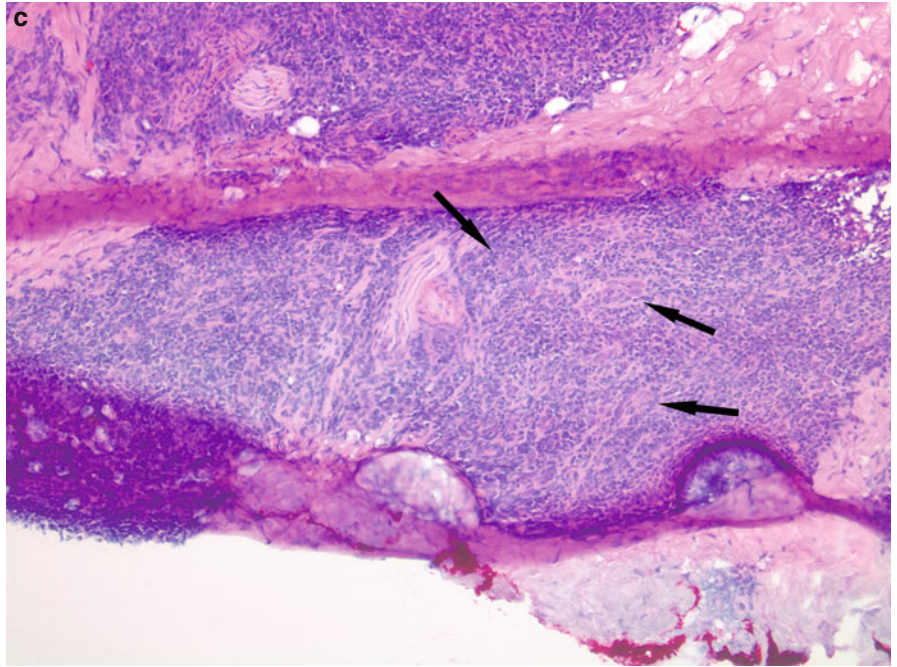


Fig. 10.24 Infiltrative squamous cell carcinoma: **(a)** An area of increased cellularity is seen within the deep dermis at low-power. **(b)** Higher magnification reveals angulated cords and linear strands, many with Indian-filing of single cells in a mucinous stroma admixed with inflammatory cells

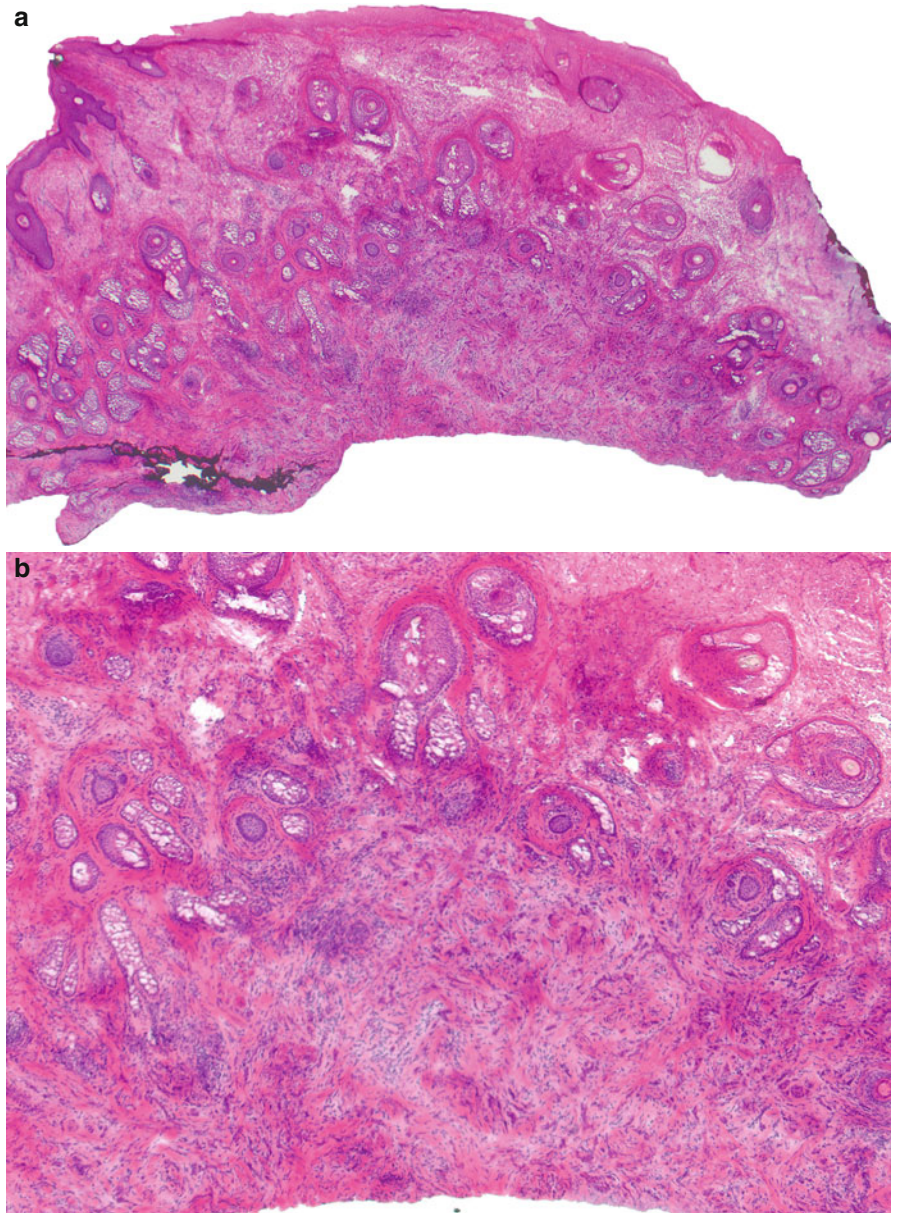


Fig. 10.24 (continued) (c) Hyperchromatic neoplastic cells forming small nests, strands and cords. (d) Scanning magnification of another section of this subtle infiltrative squamous cell carcinoma

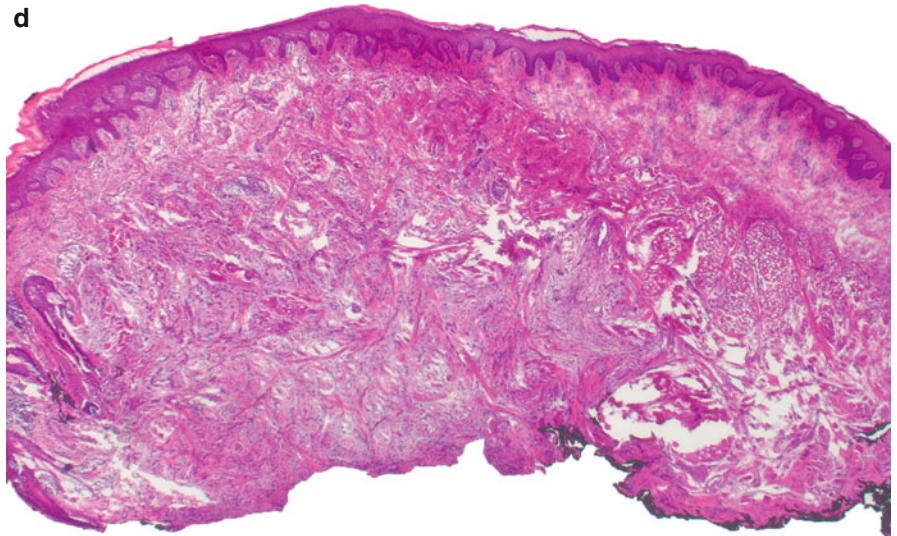
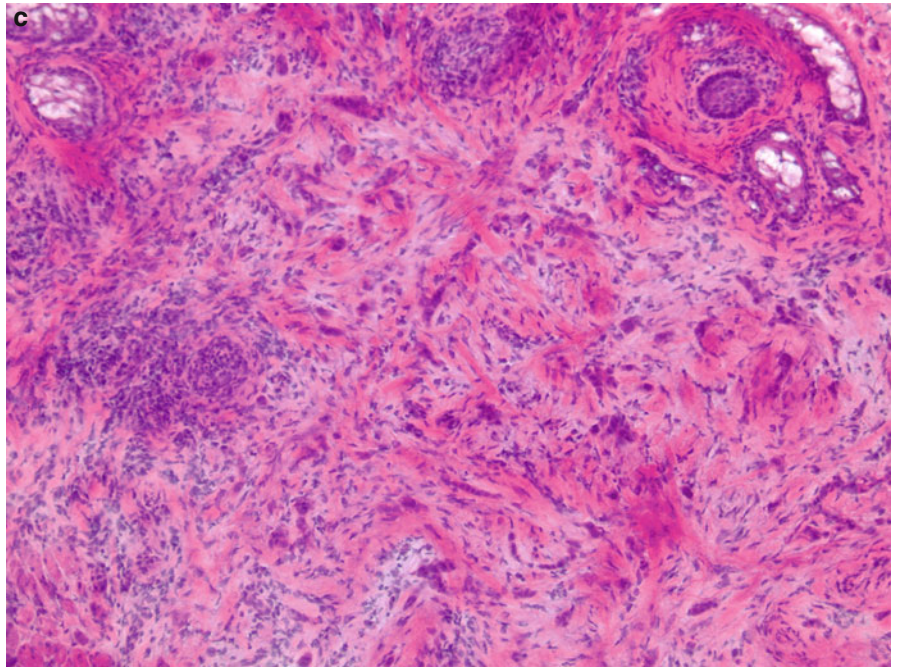


Fig. 10.24 (*continued*) (e) Infiltrating strands and cords of basophilic neoplastic cells are seen in between collagen bundles. (f) Rows of single neoplastic cells with Indian-filing are seen surrounded by thickened eosinophilic collagen. The hyperchromasia and pleomorphism of the malignant cells can be better appreciated at this magnification

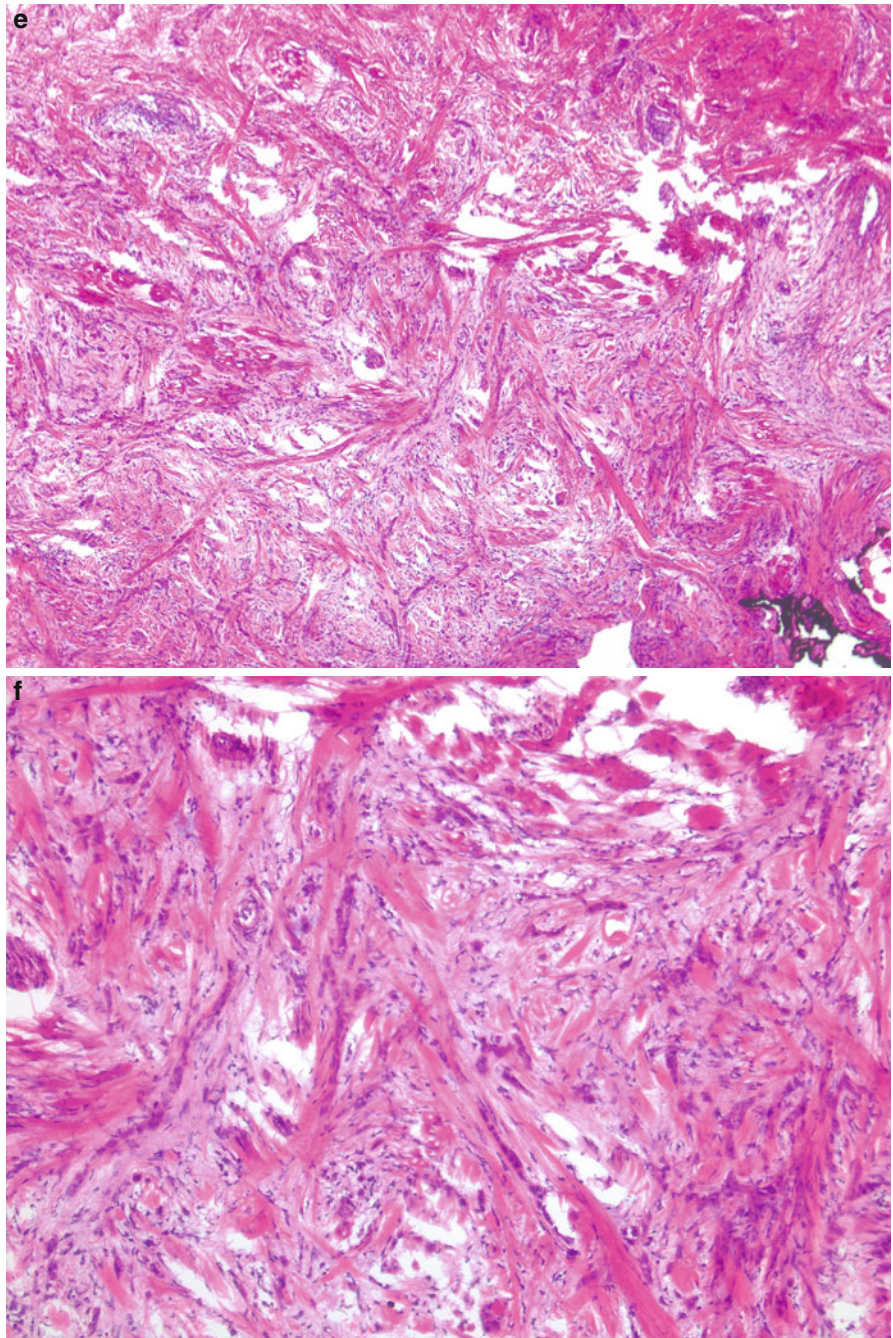


Fig. 10.24 (*continued*) (g) Hyperchromatic neoplastic cells in cords and strands. Evidence of keratinization is not seen

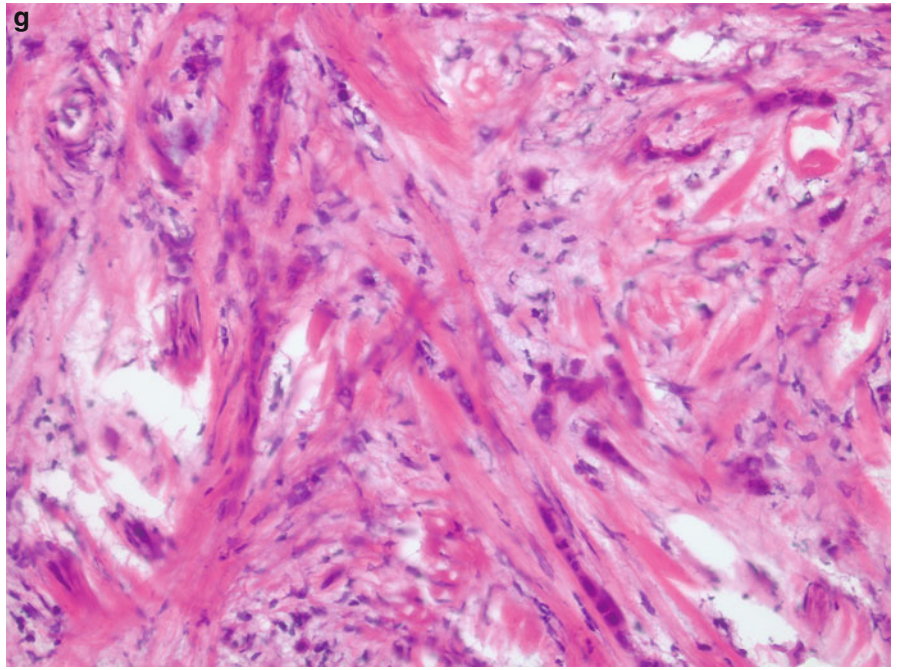


Fig. 10.25 Infiltrative squamous cell carcinoma: **(a)** Scanning magnification reveals tumor infiltrating the entire dermis with associated inflammation. Angulated neoplastic aggregates are seen arising from the undersurface of the epidermis. **(b)** Some neoplastic aggregates are well-differentiated showing evidence of squamatization and keratin pearl formation. Other aggregates are poorly differentiated forming angulated slender cords and strands

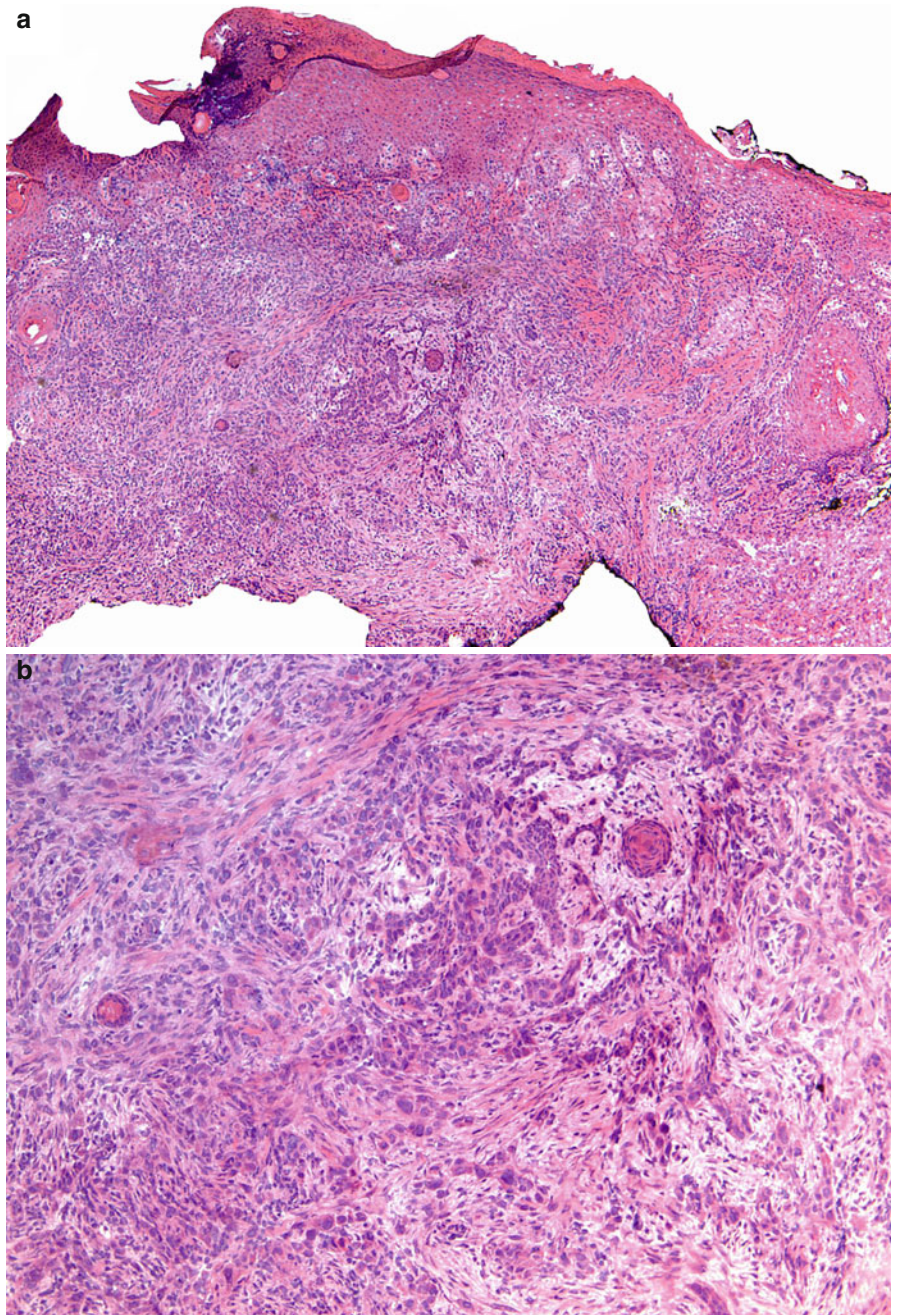


Fig. 10.25 (*continued*) (c) Densely cellular dermis filled with neoplastic cells. (d) Neoplastic cords and strands break into smaller islands and even single cells towards the base, demonstrating the aggressive nature of this carcinoma

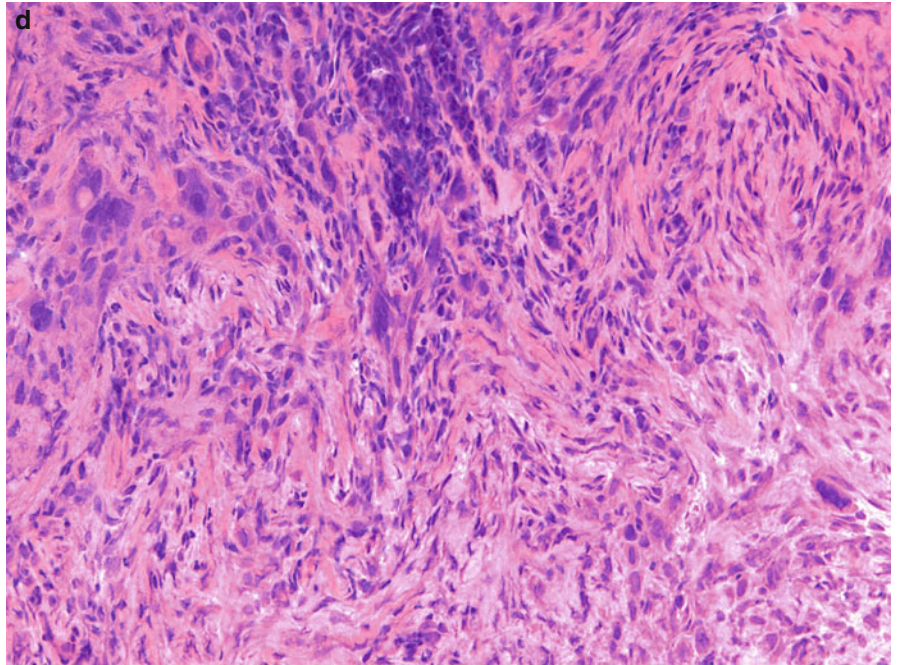
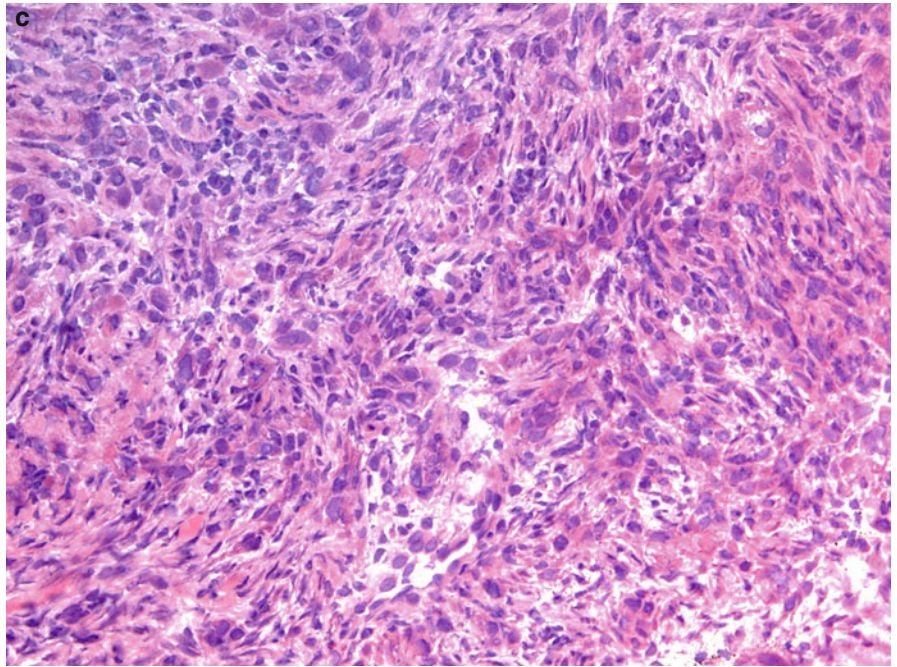


Fig. 10.26 Recurrent infiltrative squamous cell carcinoma: (a) Scanning magnification reveals tumor and associated inflammation within a scar from a prior excision. (b, c) Slender and not easily discernible tumor aggregates in the dermis surrounded by fibrosis

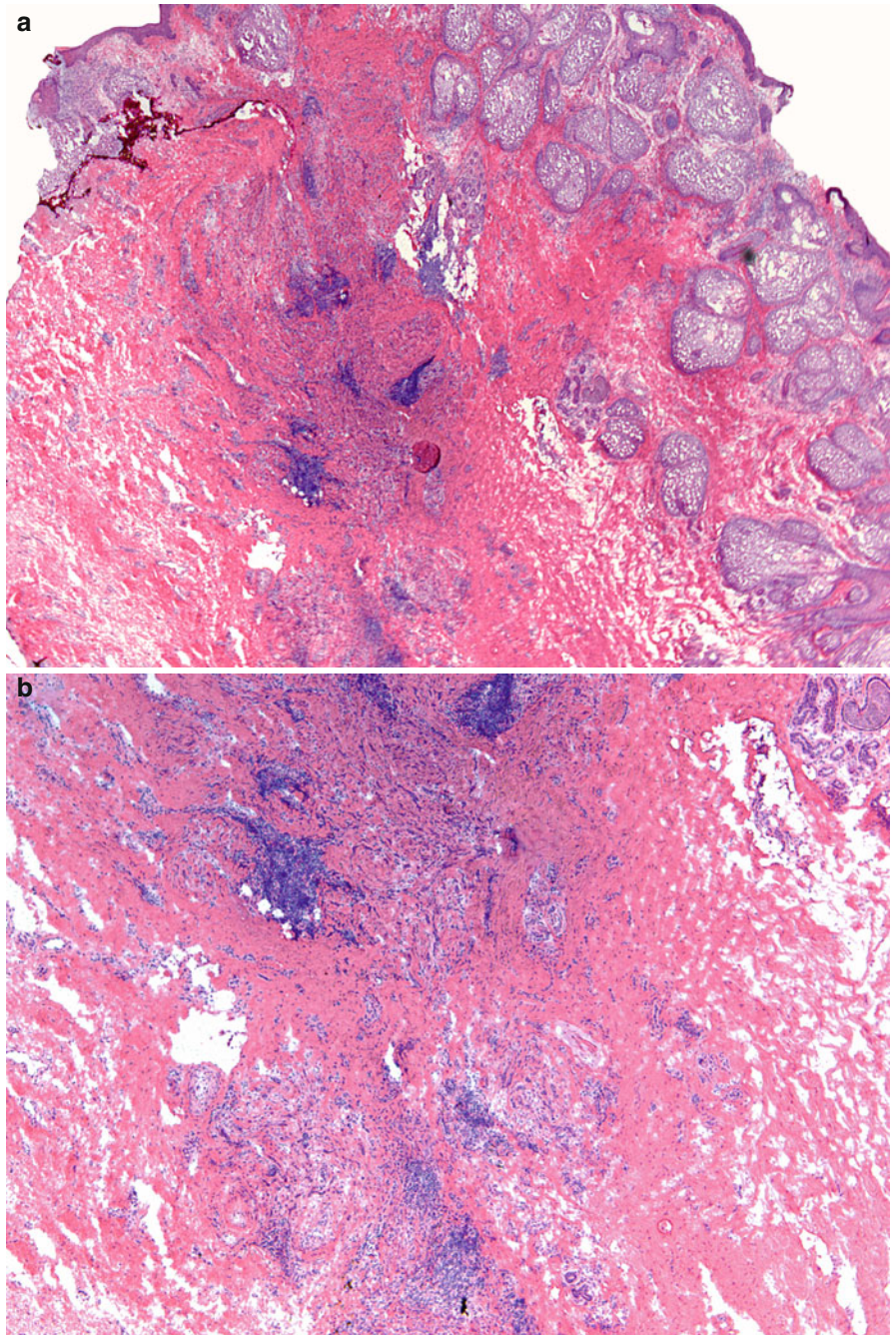


Fig. 10.26 (continued) (d) The tumor strands in between sclerotic collagen may be easily missed. However, their angulated shapes and hyperchromatic nuclei confirm the presence of carcinoma

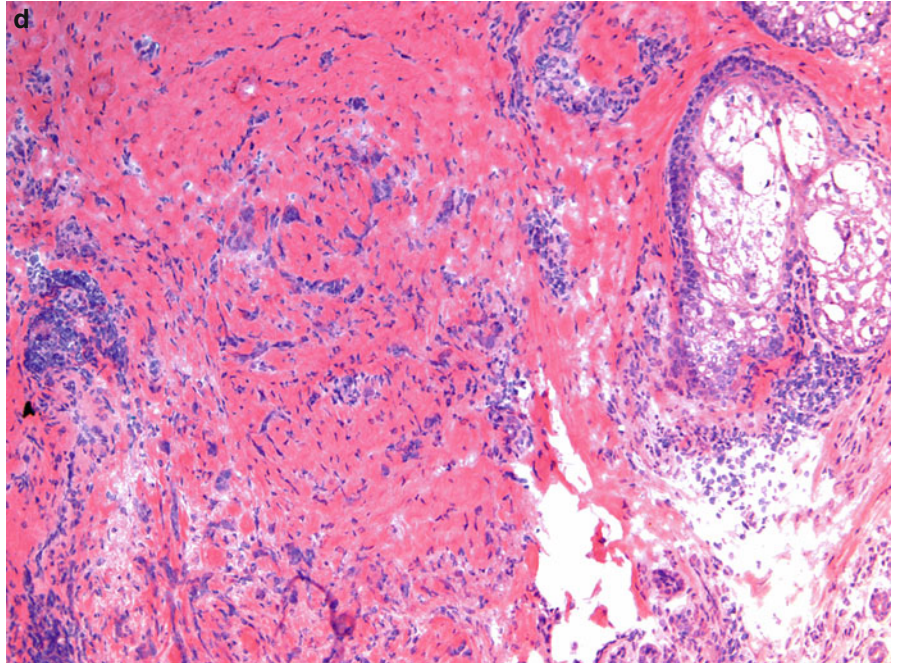
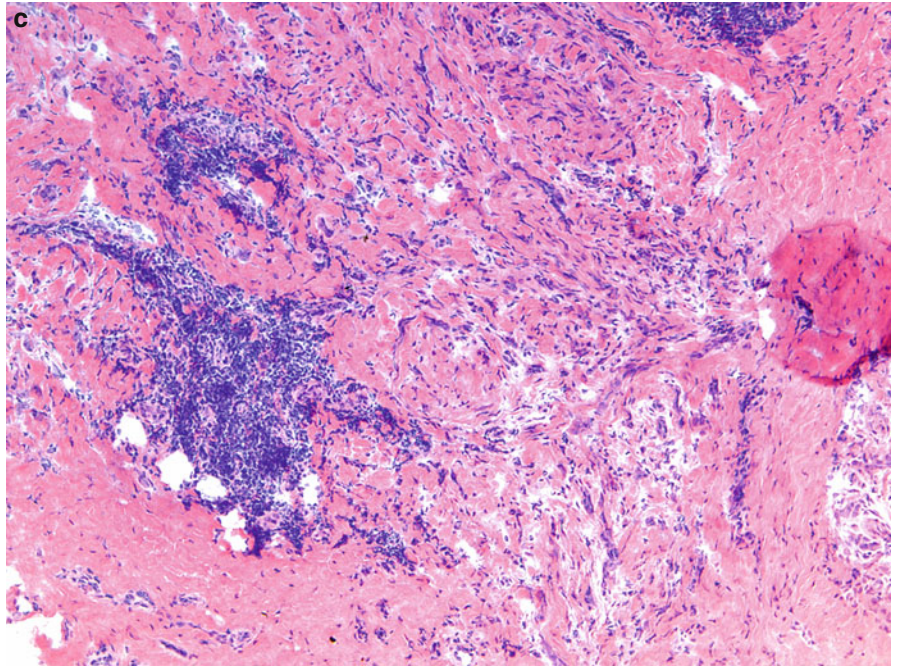


Fig. 10.26 (*continued*) (e) In addition to the slightly larger neoplastic aggregates superficially, there are slender cords and strands of tumor cells infiltrating the dermis. (f) Numerous neoplastic cells arranged as single cells infiltrating in between collagen bundles. There are also small, angulated tumor aggregates, as well as cords and strands containing hyperchromatic cells

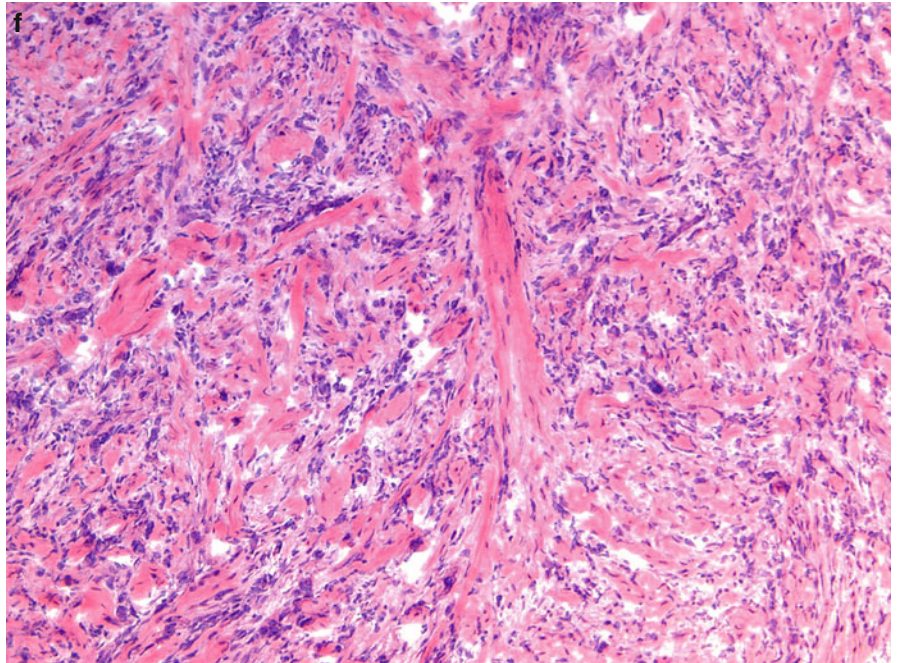
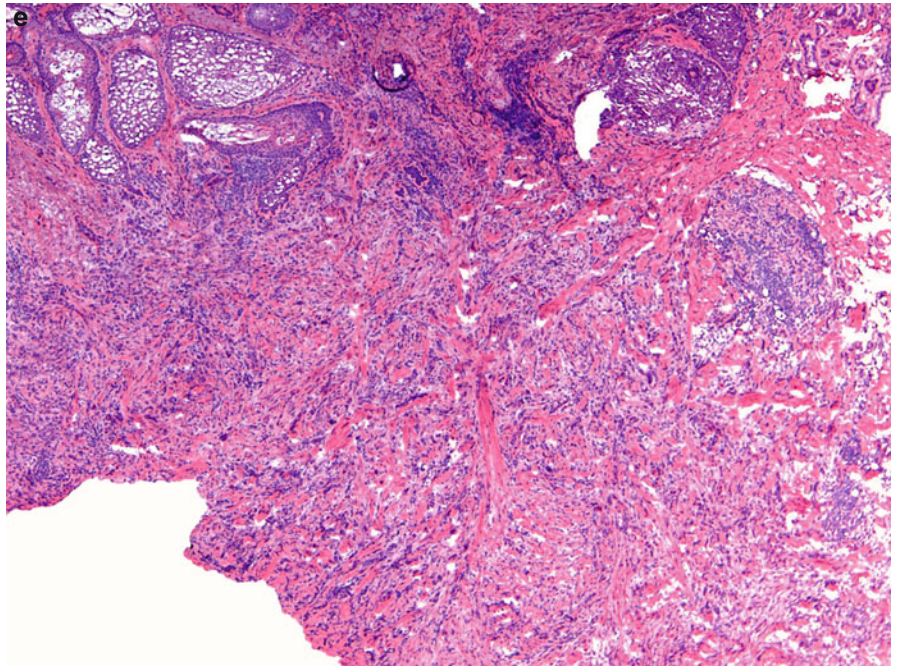


Fig. 10.27 Infiltrative squamous cell carcinoma: **(a)** Variably sized hyperchromatic epithelial neoplastic aggregates, some of which show keratinization. **(b)** The tumor cells are distinguished from the surrounding inflammatory cells by their large size, darkly stained and irregular nuclei, and rim of eosinophilic cytoplasm

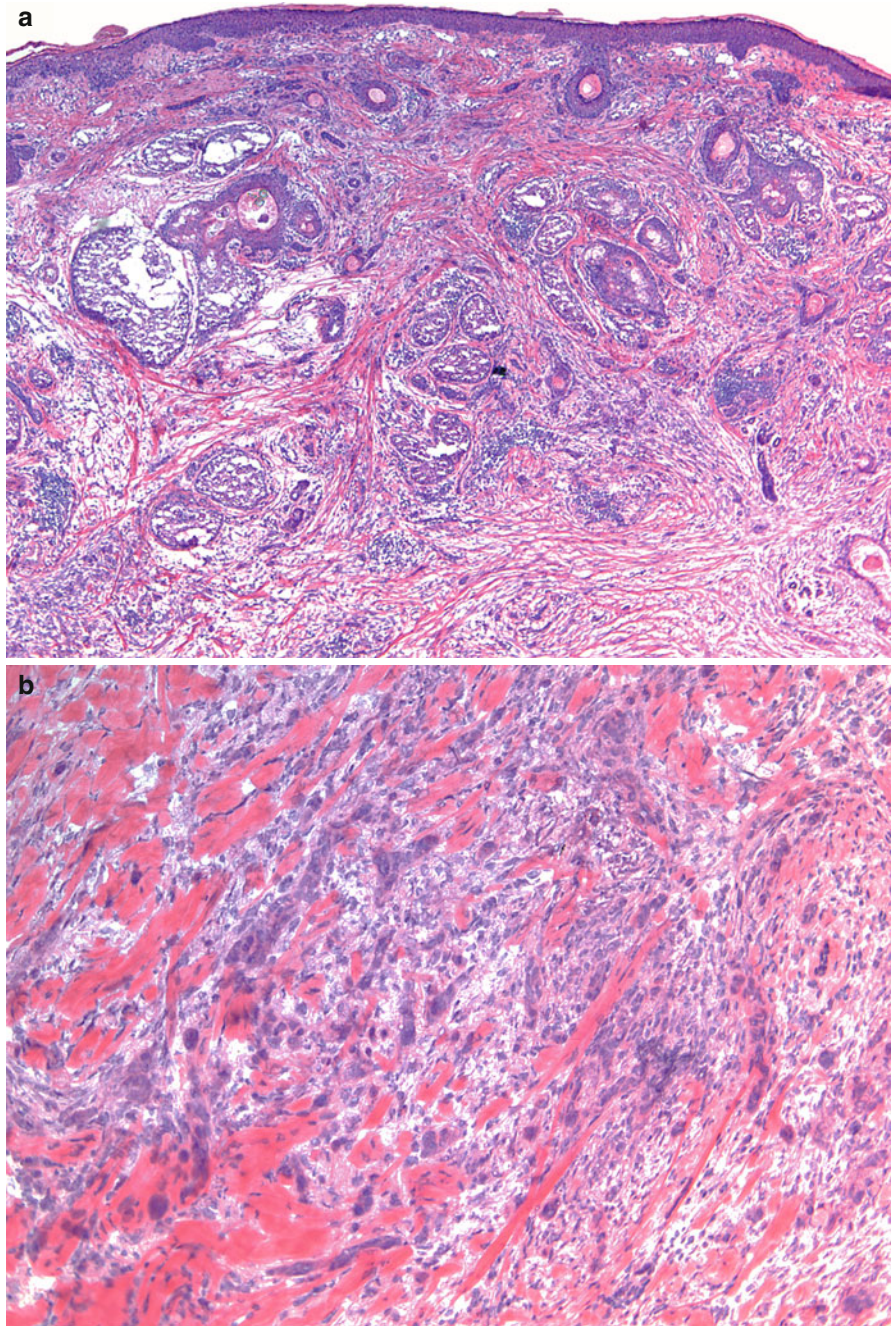


Fig. 10.28 Squamous cell carcinoma:
(a) A few tumor aggregates in the superficial dermis. (b) The neoplastic aggregates are well-differentiated and may be mistaken for normal adnexal structures (arrows)

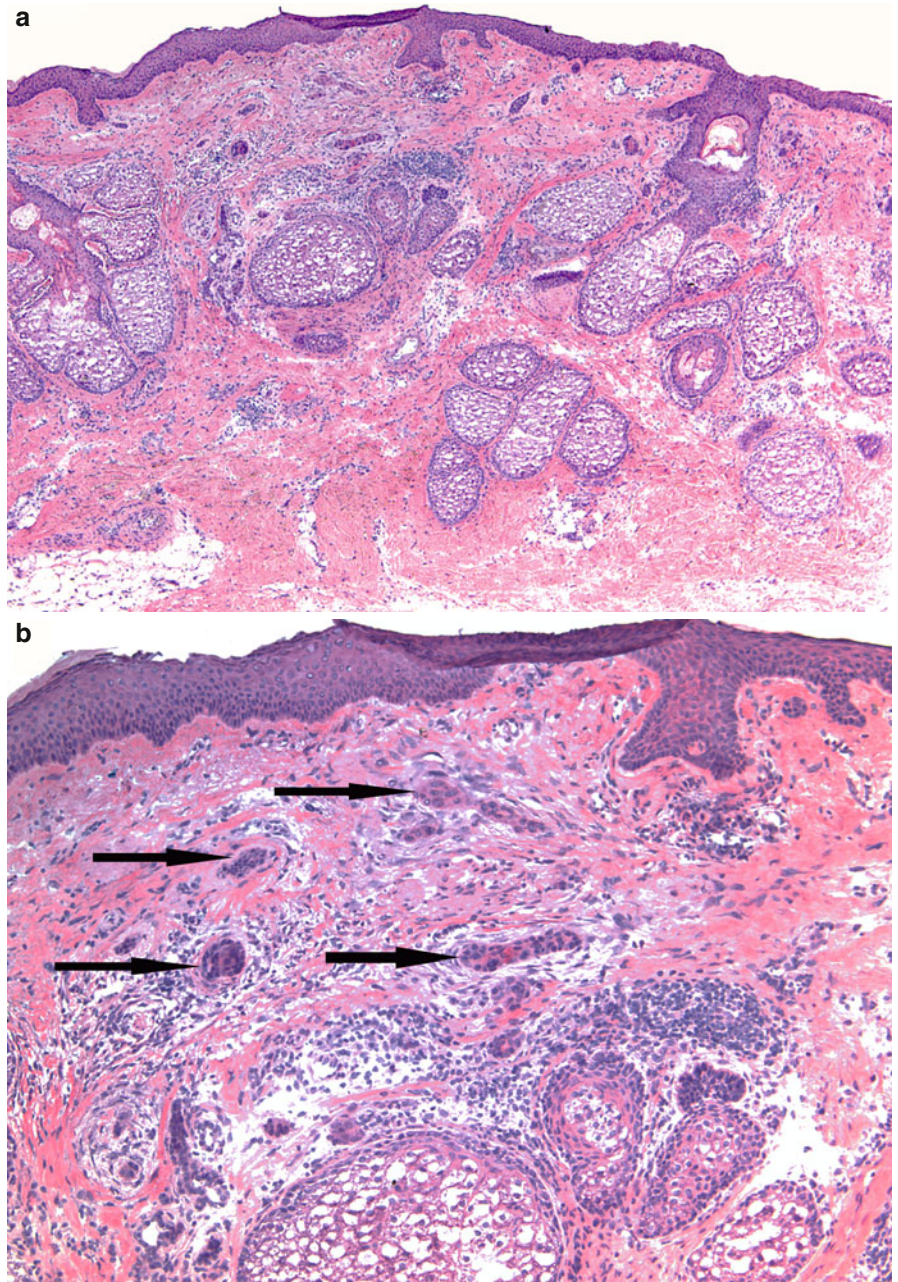


Fig. 10.28 (continued) (c) Here the tumor demonstrates its highly infiltrative nature (arrows point to some of the neoplastic cells)

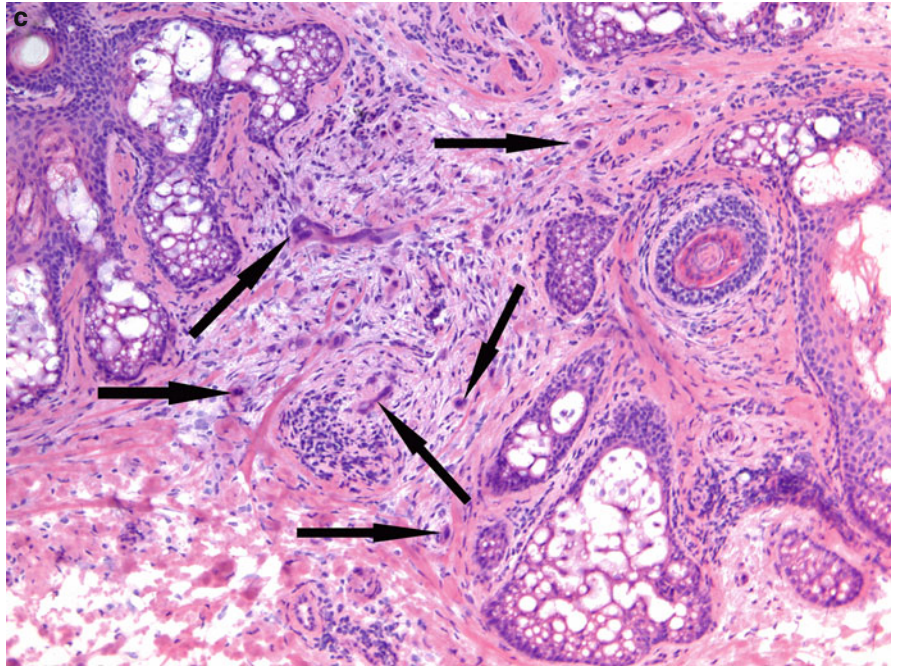


Fig. 10.29 Infiltrative squamous cell carcinoma: (**a, b**) The cancer is well differentiated superficially where squamous eddies are noted (*ellipses*) and becomes less differentiated and breaks into smaller, one to two-cell aggregates, as it infiltrates deeper on subsequent sections

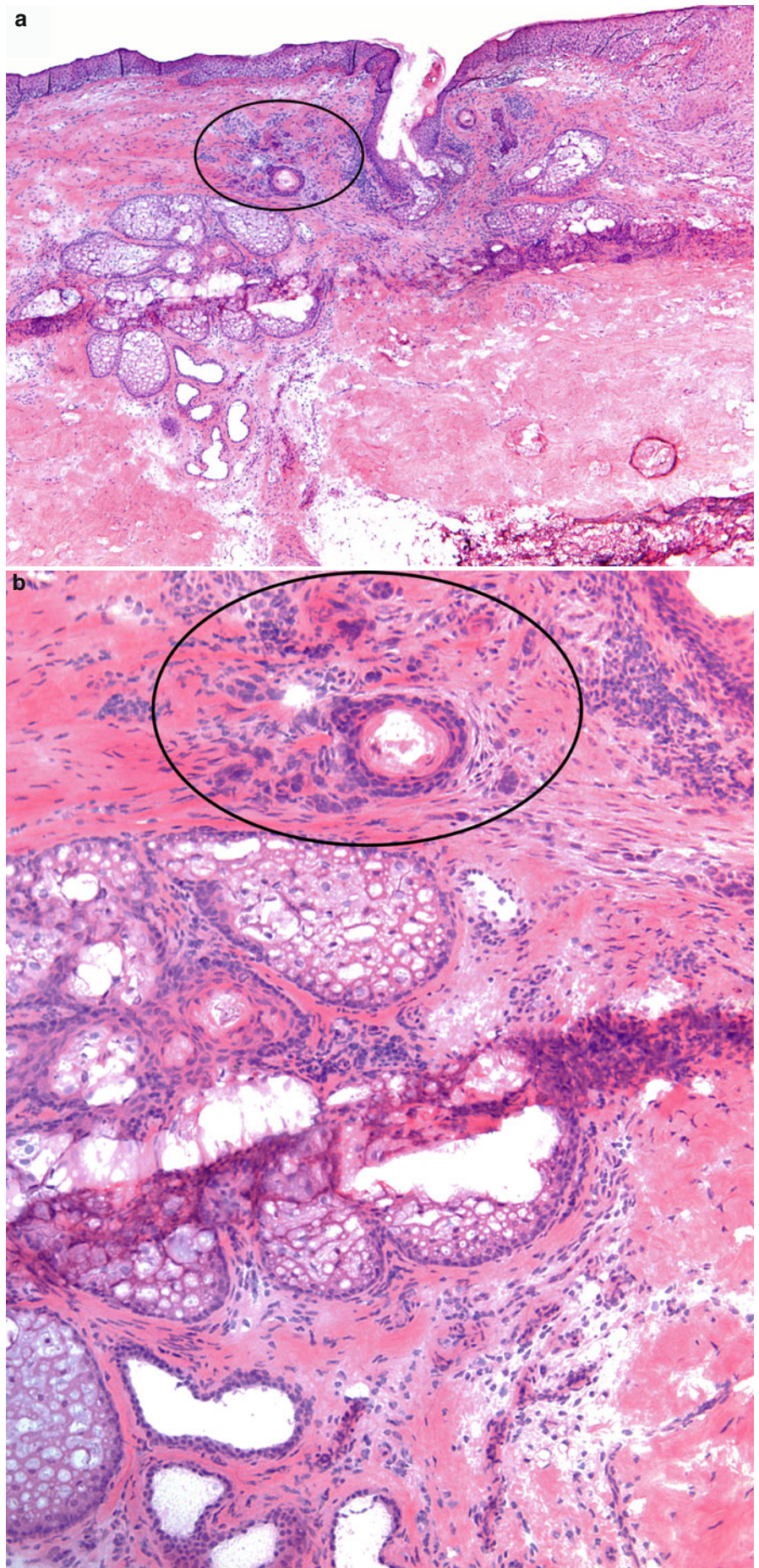


Fig. 10.29 (*continued*) (c, d) Another section shows a focus of tumor and inflammation in the deep reticular dermis and subcutaneous tissue at low and medium power

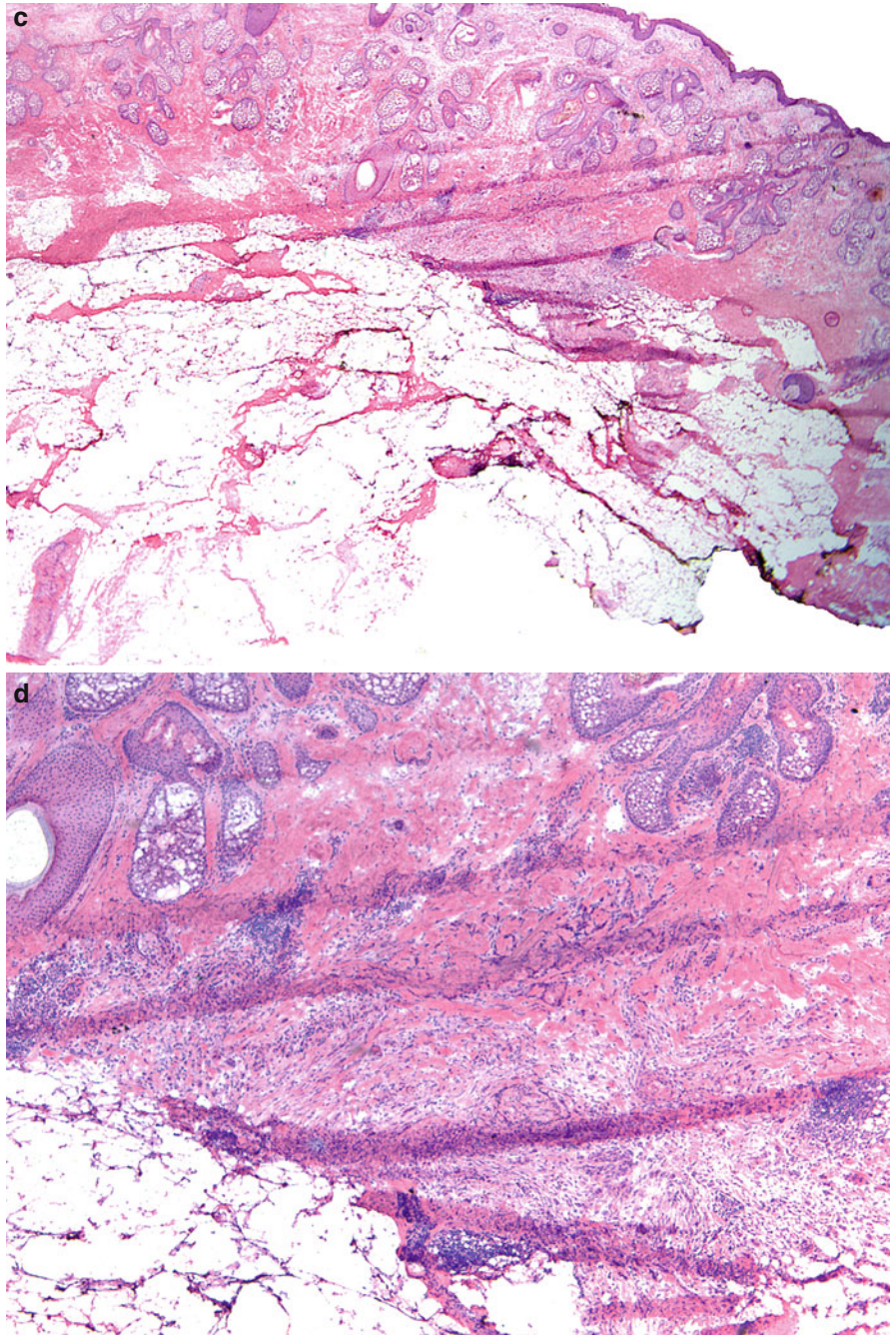


Fig. 10.29 (continued) (e) At this higher magnification the hyperchromatic and pleomorphic neoplastic cells can be better appreciated. (f, g) Relatively large nerve (N) in the subcutaneous fat with neoplastic aggregates surrounding and infiltrating it (arrows)

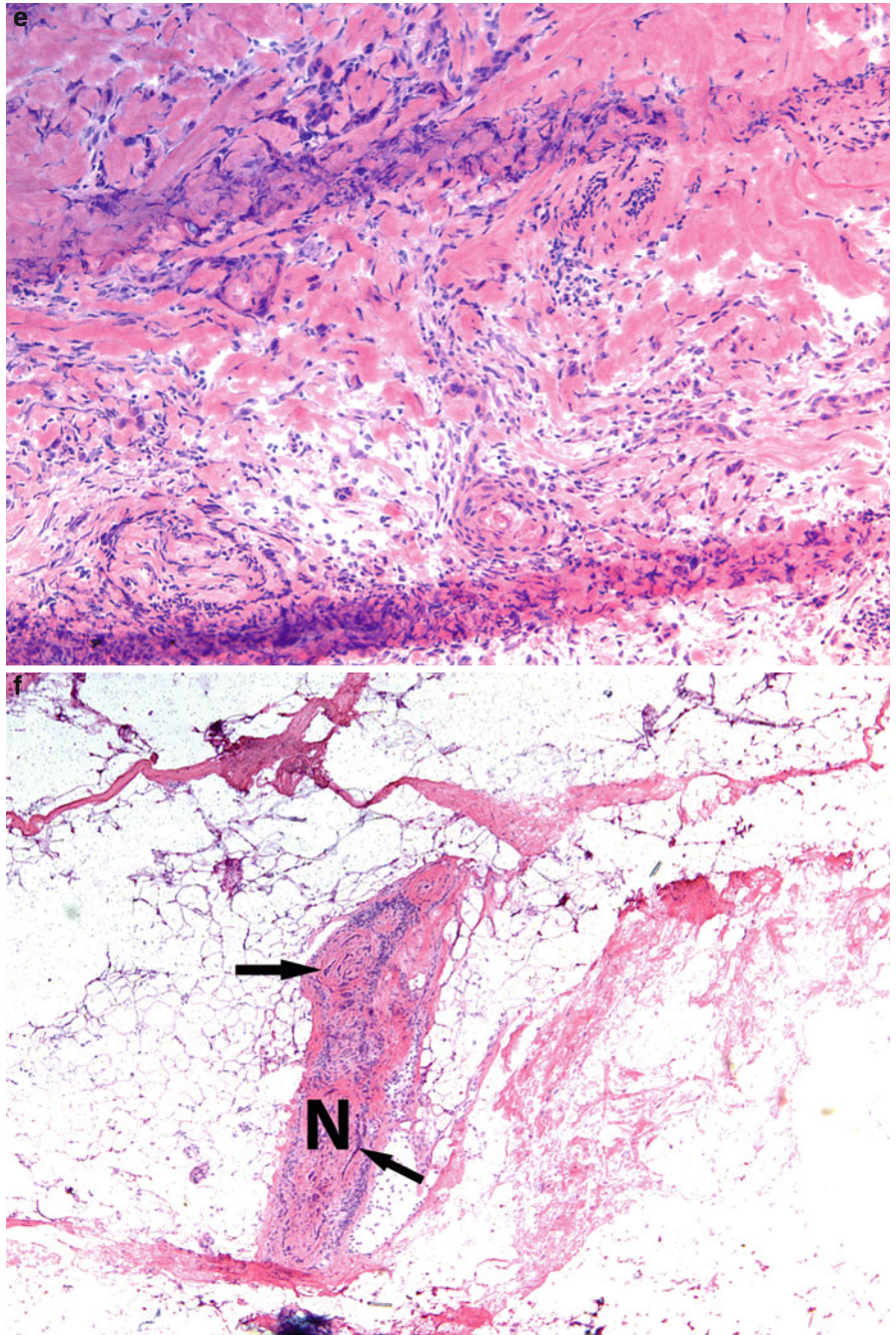


Fig. 10.29 (continued)

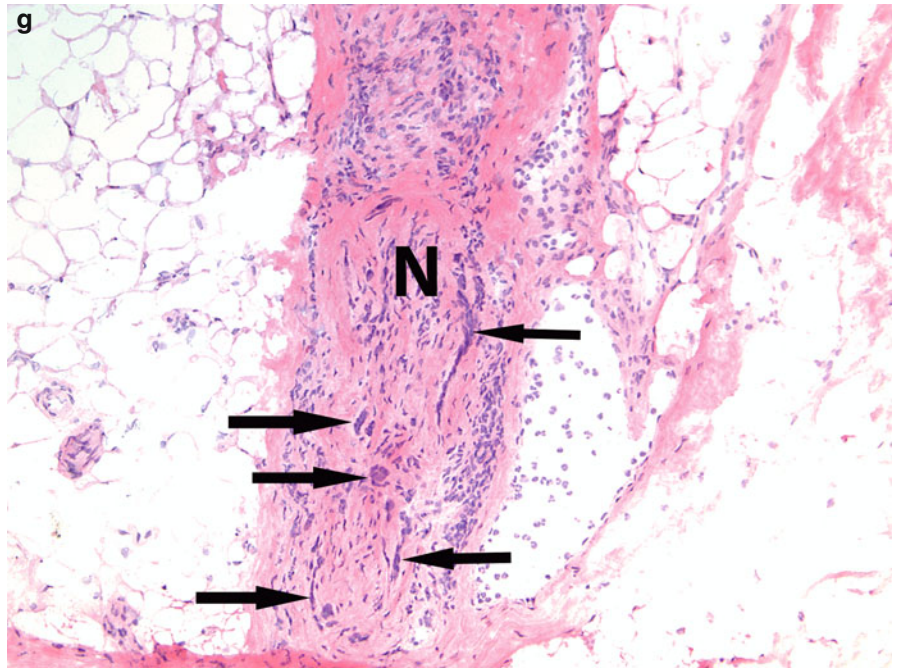


Fig. 10.30 Squamous cell carcinoma with perineural invasion: **(a)** Neoplastic aggregates with minimal surrounding inflammation are present in skeletal muscle below the subcutis. **(b)** Angulated neoplastic aggregate wrapping around a small nerve within skeletal muscle

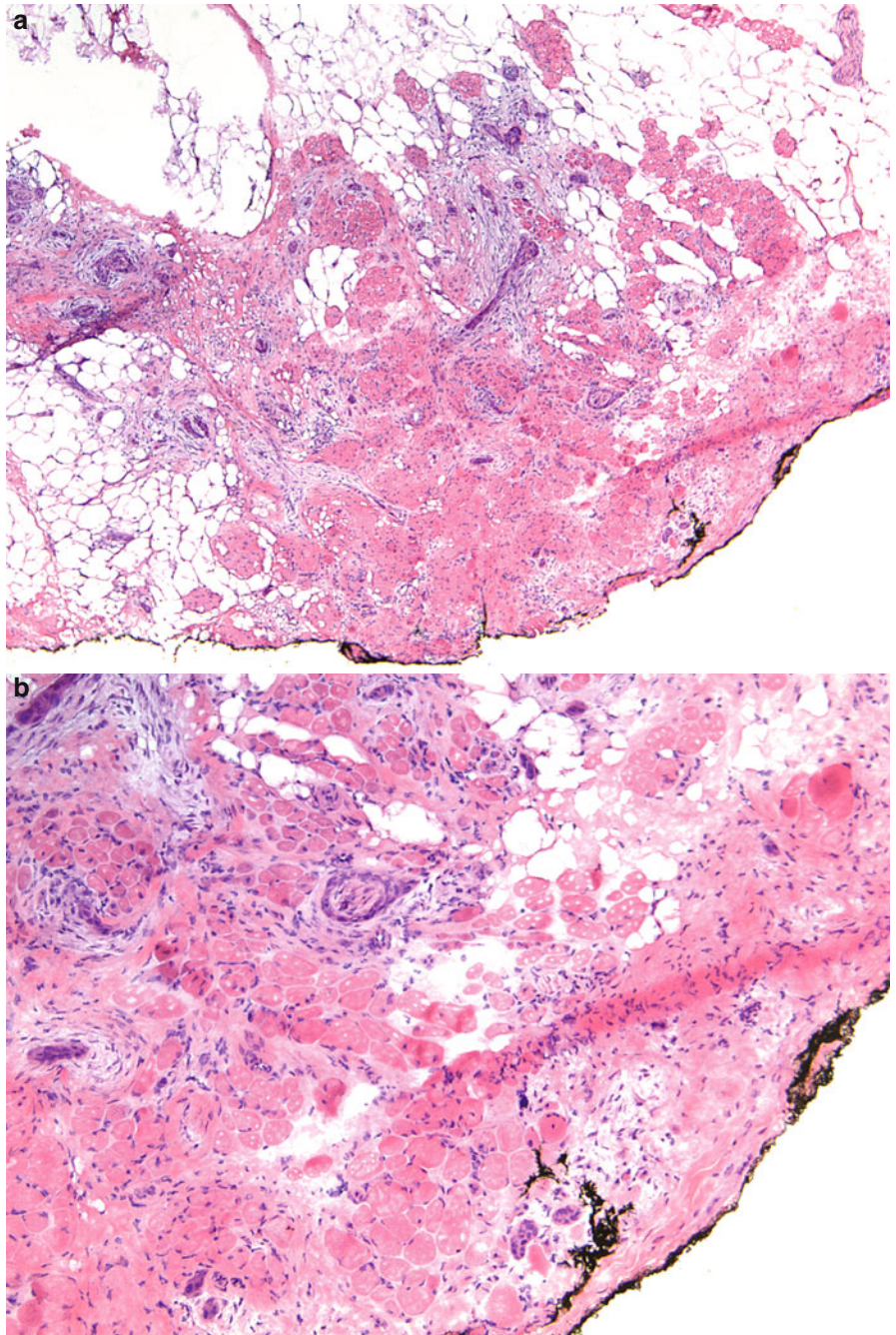


Fig. 10.31 Squamous cell carcinoma in situ and invasive well-differentiated squamous cell carcinoma: (a) Scanning magnification reveals squamous cell carcinoma in situ, focally present in the epidermis, and a cluster of irregular basaloid aggregates in the lower dermis. (b, c) The irregular shapes and focal central necrosis attest to the neoplastic nature of these aggregates. The tumor cells are hyperchromatic peripherally and become eosinophilic towards the center. Some dyskeratotic cells are also present

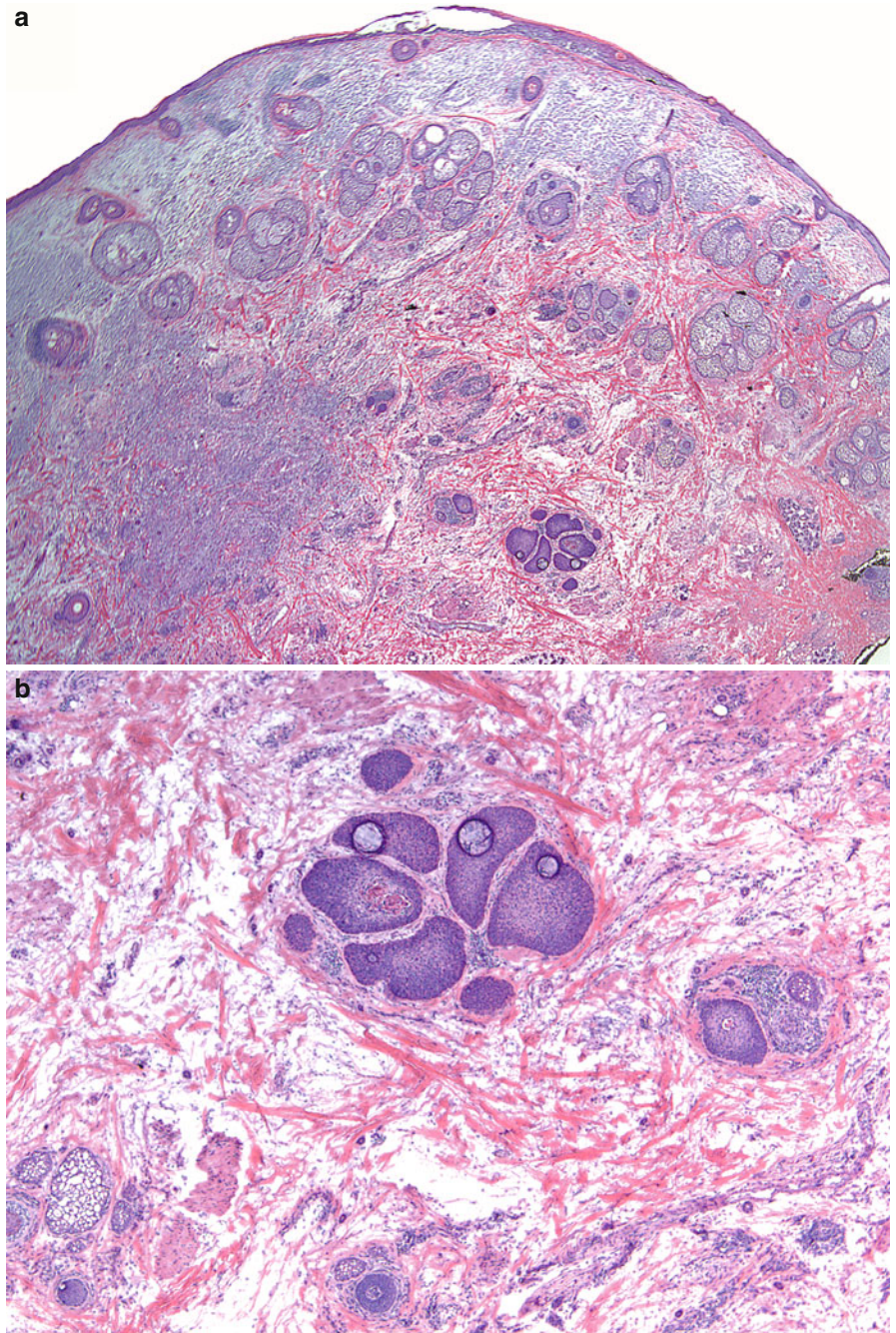


Fig. 10.31 (continued) (d) SCCIS with an invasive well-differentiated squamous cell carcinoma: Sometimes an initial superficial biopsy shows only SCCIS. However, Mohs sections may reveal invasive SCC as was the case here

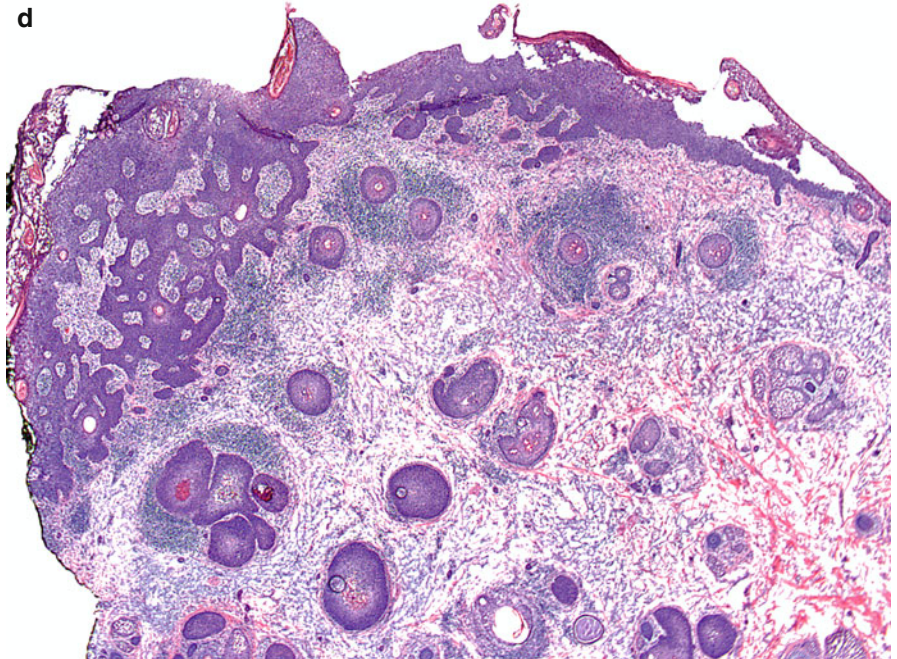


Fig. 10.31 (continued) (e, f) The neoplastic aggregates demonstrate necrosis, calcification, and squamatization

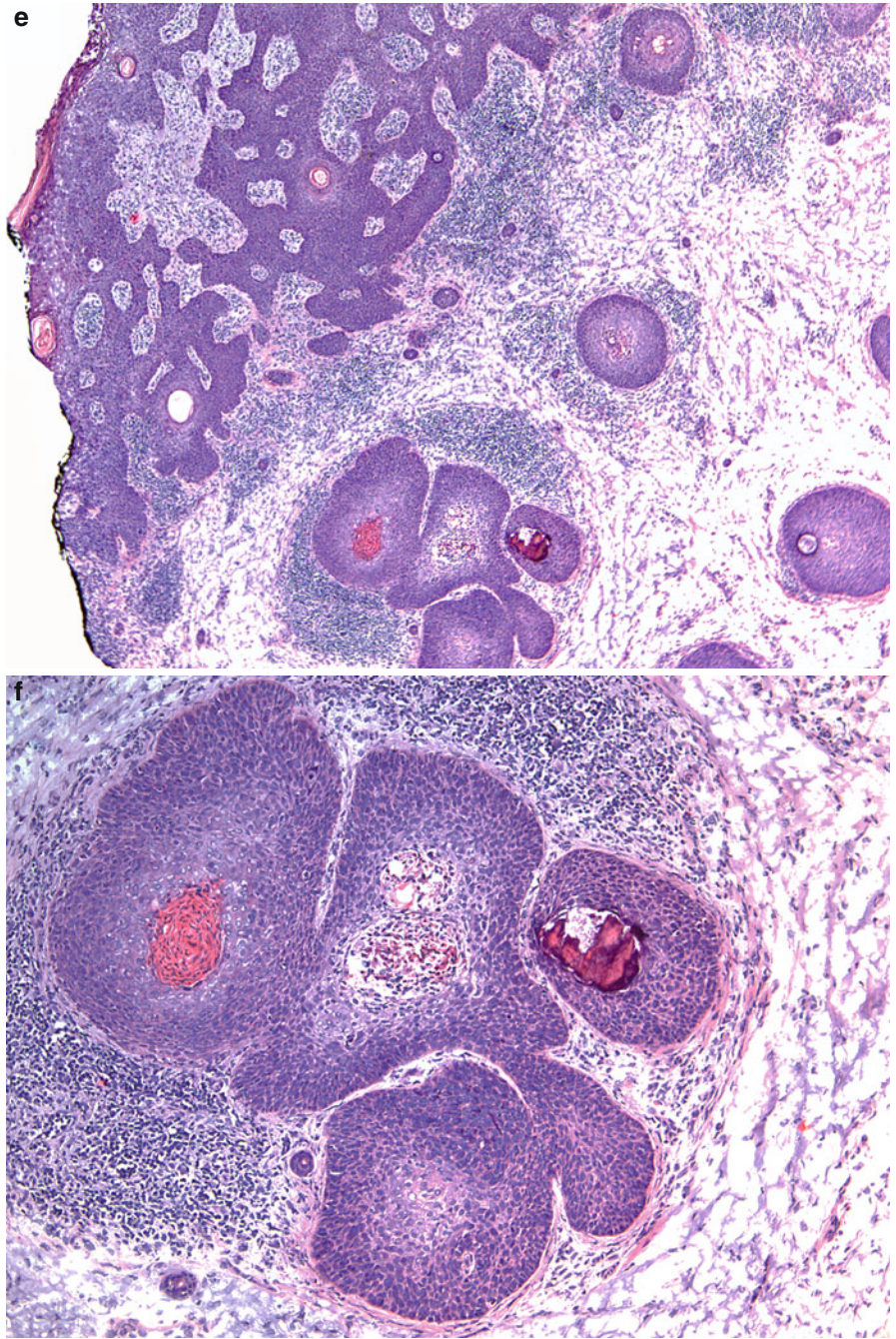


Fig. 10.32 Well-differentiated squamous cell carcinoma: (a) Multiple keratinous cysts within eosinophilic neoplastic aggregates are seen. (b) Well-differentiated squamous cell carcinoma: higher magnification

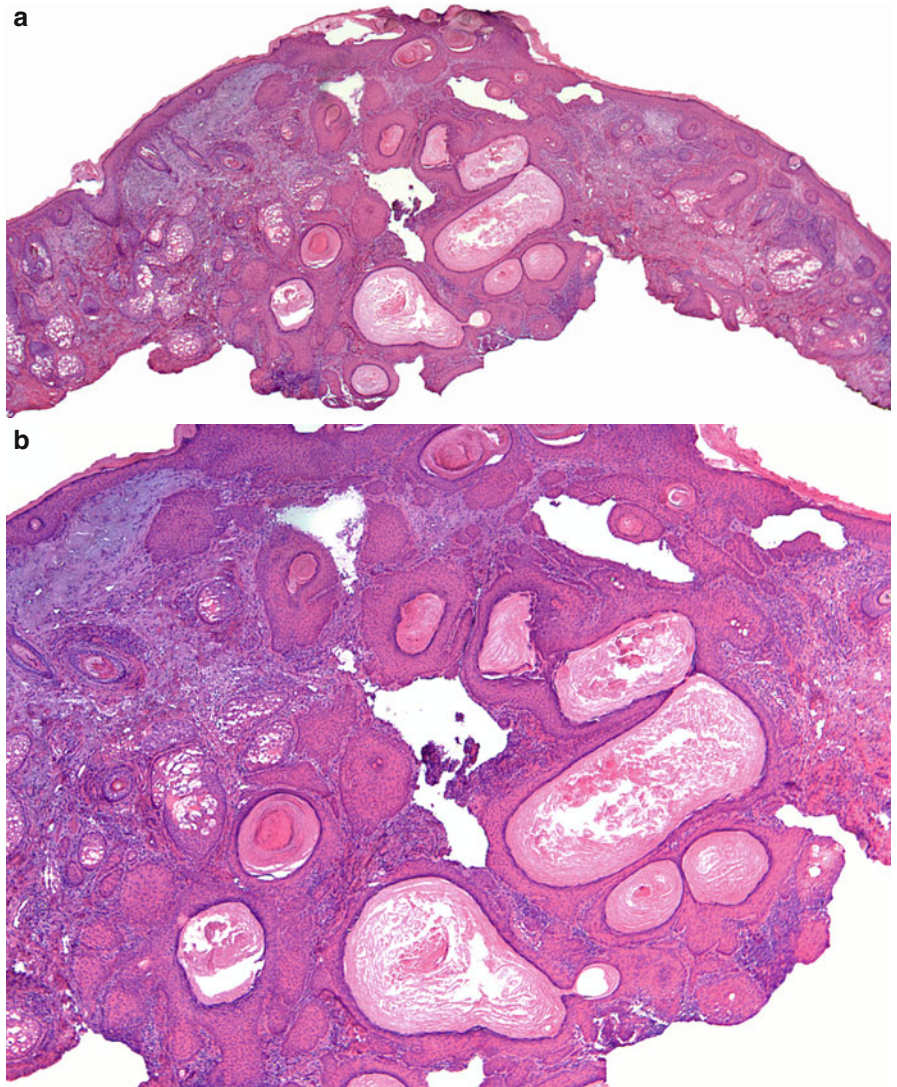


Fig. 10.33 Squamous cell carcinoma:
(a) Focus of inflammation in the deep reticular dermis. (b) A few small neoplastic aggregates surrounded by inflammatory cells

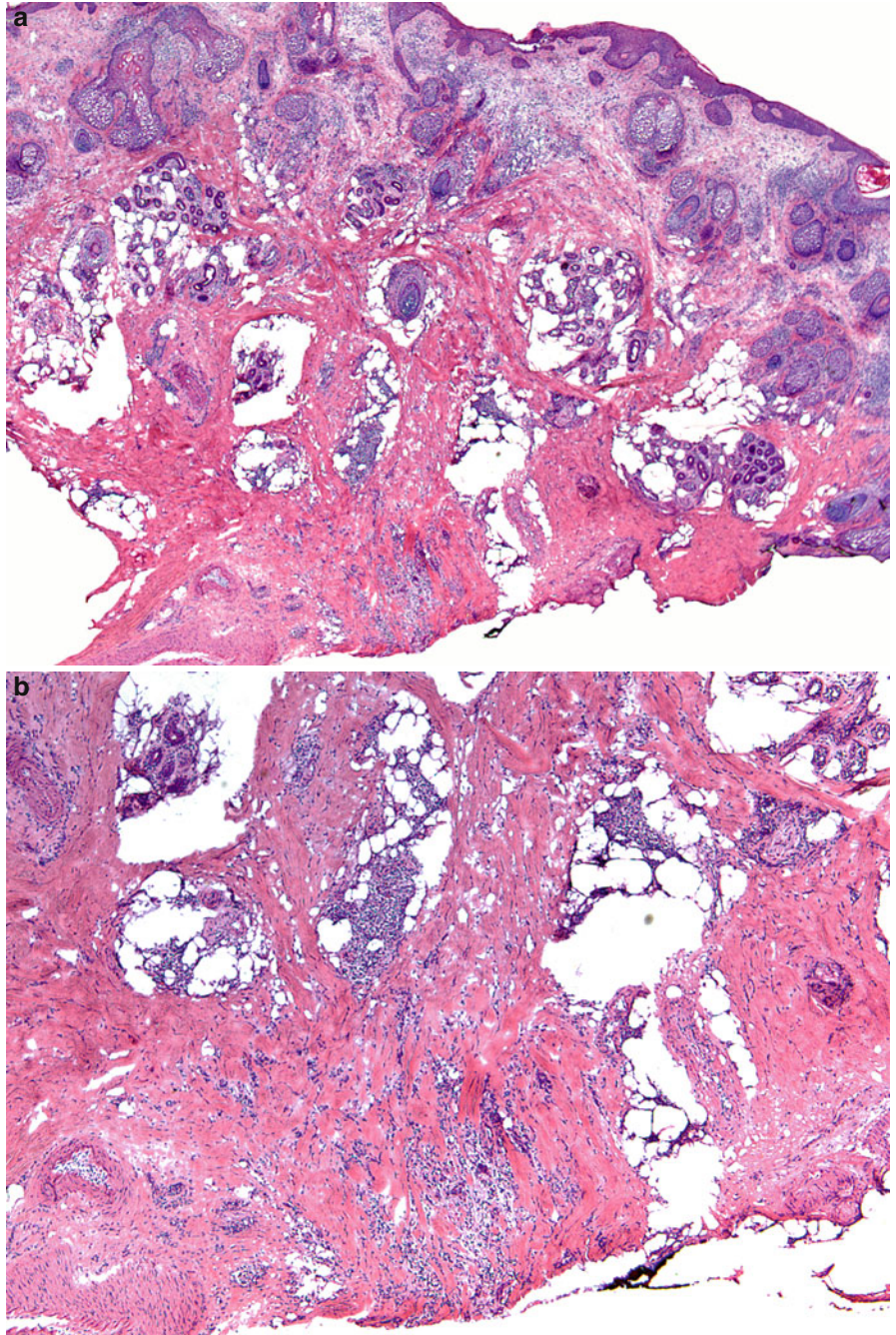


Fig. 10.33 (continued) (c) Small neoplastic aggregates as well as single neoplastic cells with glassy, eosinophilic cytoplasm and hyperchromatic, pleomorphic nuclei are present (*arrows*). (d–f) CK116 immunohistochemical stain performed on permanent sections highlighting the neoplastic cells

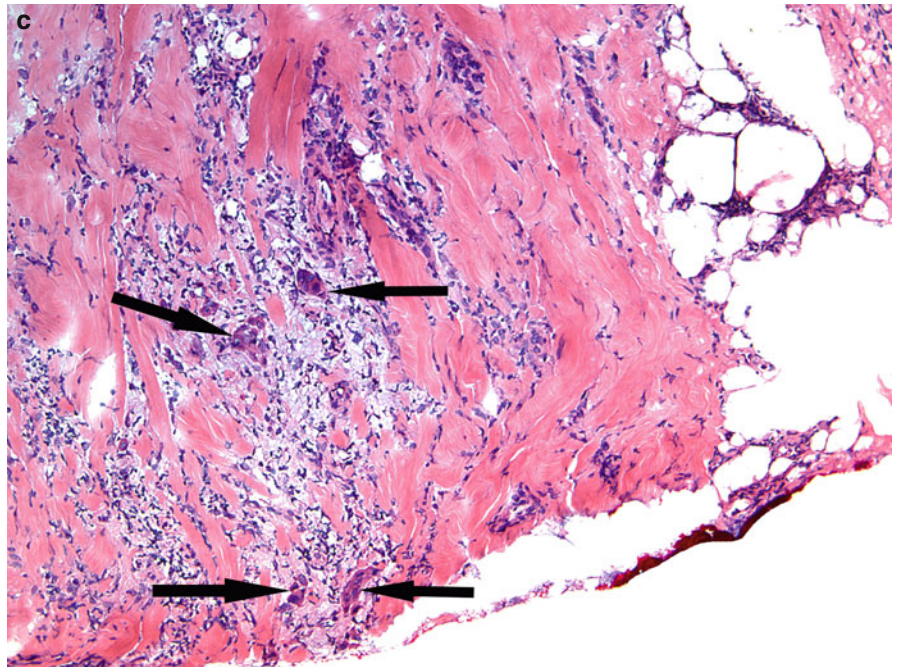


Fig. 10.33 (continued)

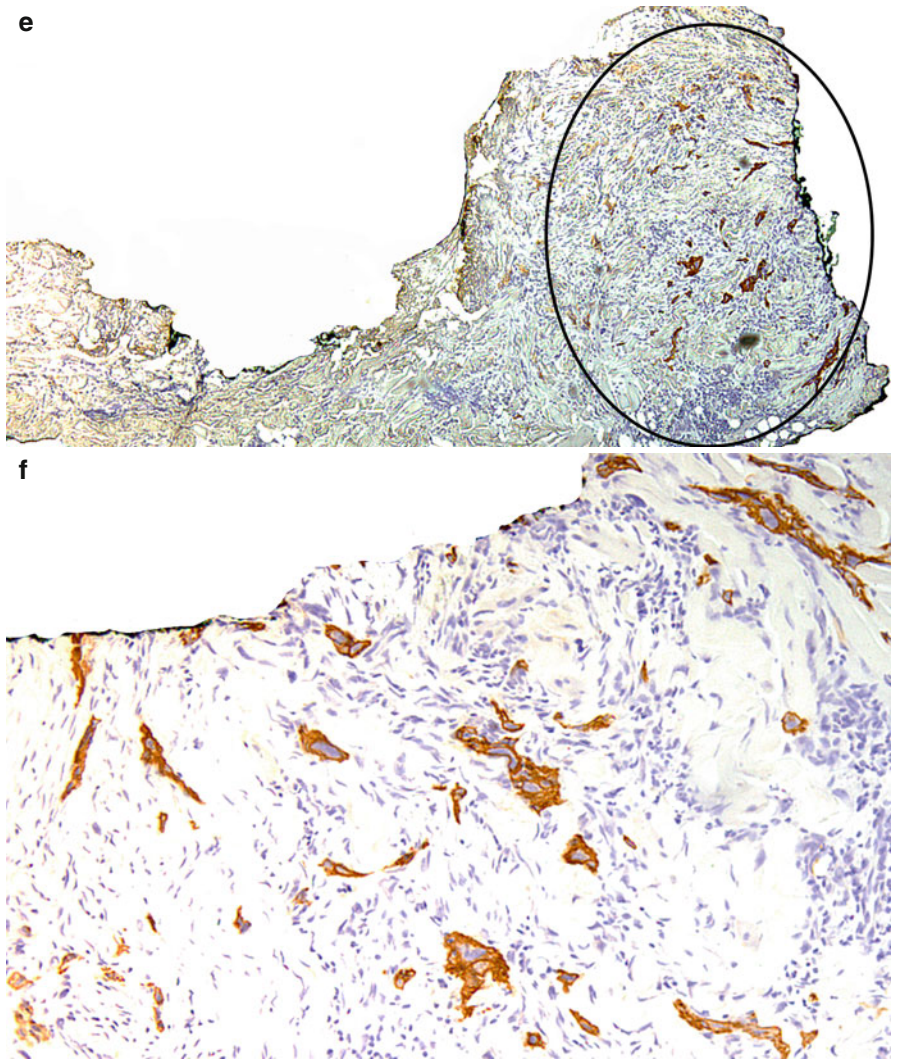


Fig. 10.34 Squamous cell carcinoma:
(a) A few small foci containing eosinophilic neoplastic aggregates are seen surrounded by dense inflammation. (b) The neoplastic aggregates show foci of squamatization

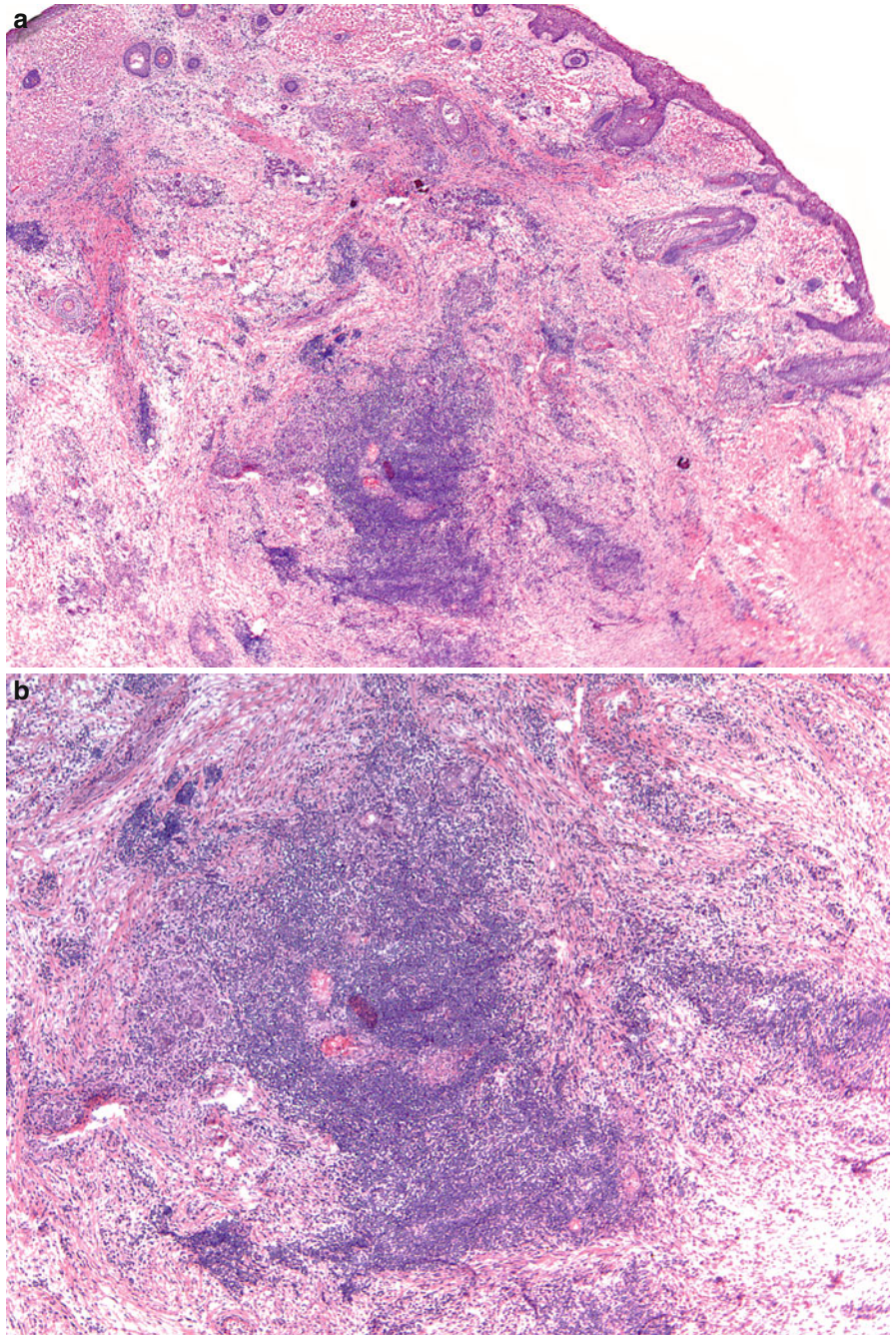


Fig. 10.34 (*continued*) (c) Note the larger size and pleomorphic nuclei of the neoplastic cells in contrast to the surrounding lymphocytes

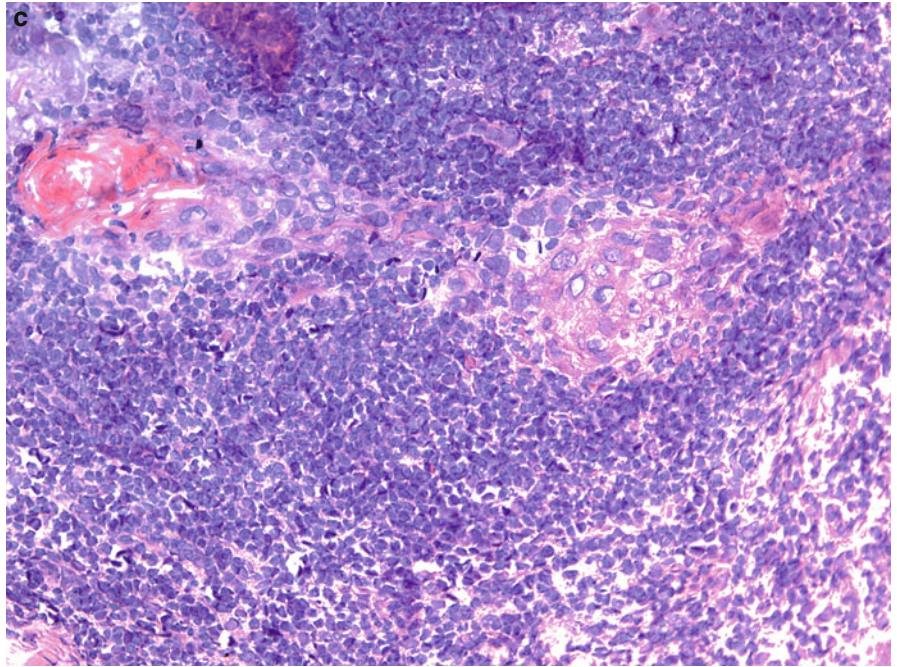


Fig. 10.35 Squamous cell carcinoma:
(a) A focus of infiltrative squamous cell carcinoma in the dermis on the left. Scar is seen on the right. (b) Strands and cords of neoplastic aggregates surrounded by inflammation

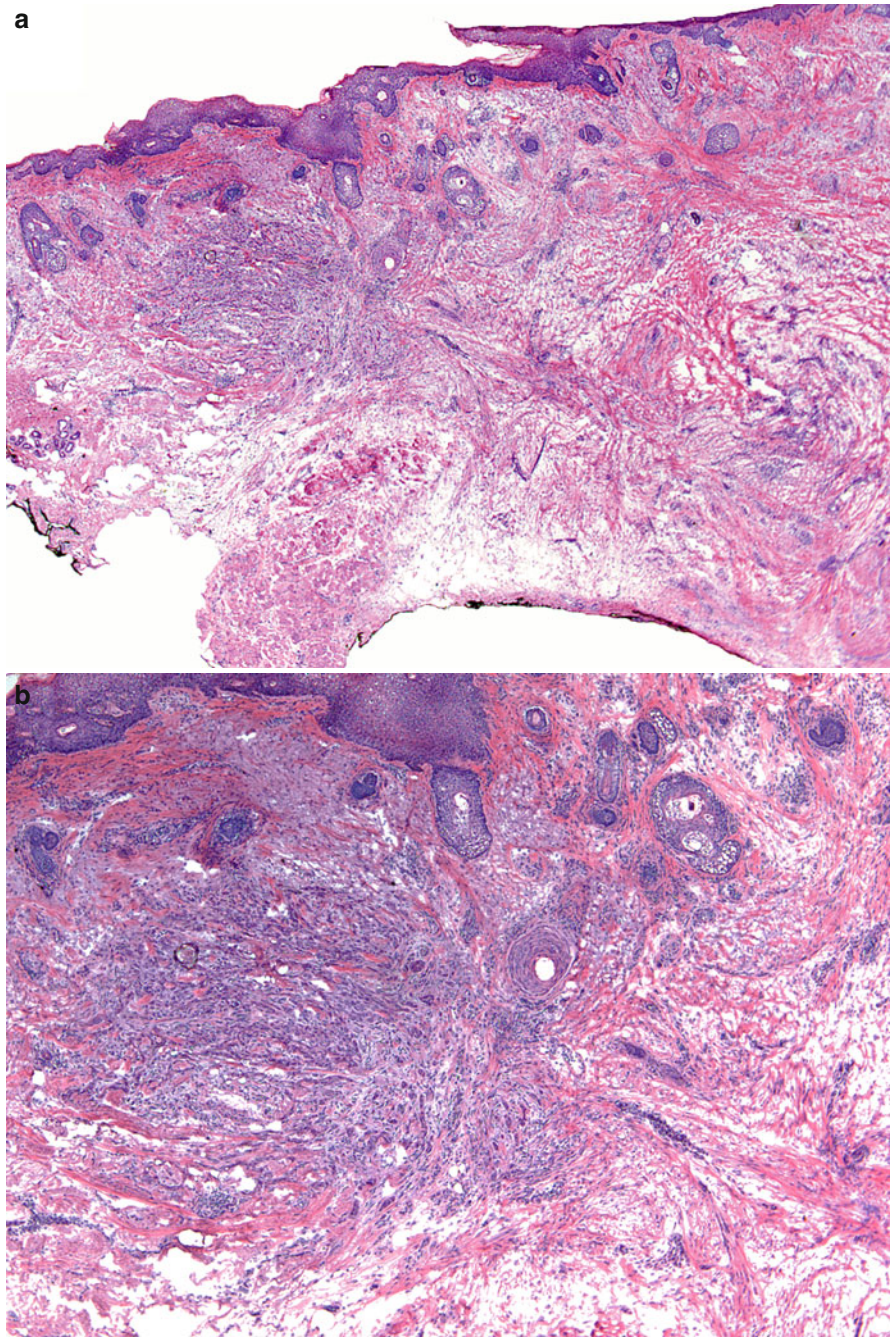


Fig. 10.35 (*continued*) (c) Many of the neoplastic aggregates consist of only a few cells. (d) This is another section from the bisected tissue block. In the center of the specimen there are thickened collagen bundles and mild perivascular inflammatory infiltrate. Adnexal structures are effaced and solar elastosis is absent in the area of the scar

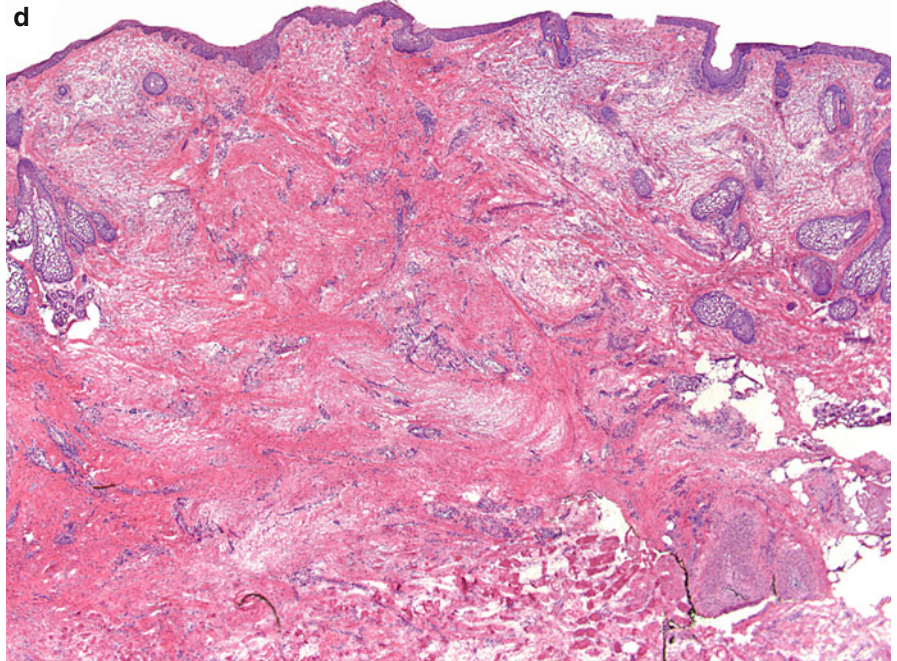
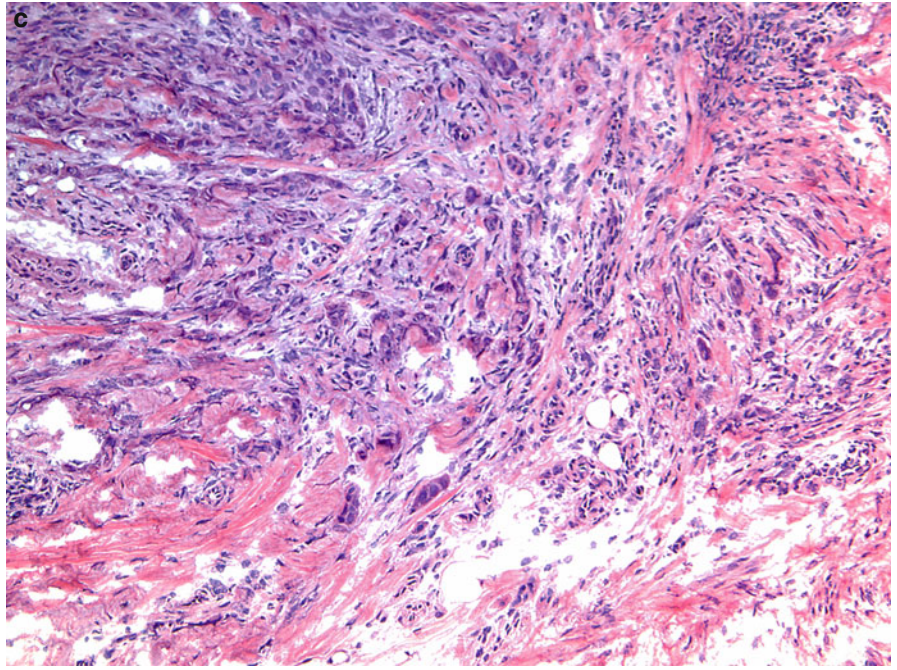
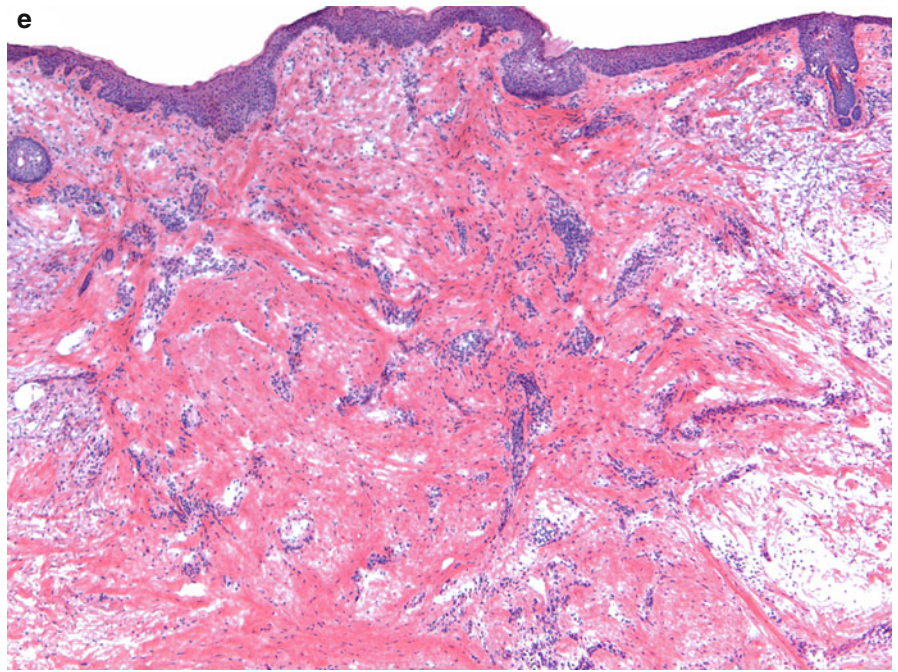


Fig. 10.35 (*continued*) (e) There are a few vertically oriented blood vessels with mild perivascular lymphocytic inflammation



Hypertrophic Lupus Erythematosus

Hypertrophic lupus erythematosus may mimic squamous cell carcinoma when there is prominent keratinocytic atypia, particularly if a superficial biopsy is performed.

Features that are helpful in making the diagnosis of lupus are:

1. Irregularly hyperplastic epidermis with keratinocytic atypia
2. Follicular plugging
3. Dense lichenoid lymphocytic infiltrate obscuring the dermal epidermal junction
4. Focal vacuolar changes of the basal epidermal layer and occasional necrotic keratinocytes
5. Focal thickening of the basement membrane
6. Prominent melanophages in the papillary dermis signifying a preceding destruction of keratinocytes
7. Superficial and deep perivascular and periadnexal lymphocytic infiltrate

Squamous Cell Carcinoma and Atypical Fibroxanthoma

Squamous cell carcinoma	Atypical fibroxanthoma
1. Large pleomorphic keratinocytes with hyperchromatic irregular nuclei and abundant eosinophilic cytoplasm with evidence of premature keratinization within the cytoplasm	1. Large pleomorphic cells with bizarre, atypical, and hyperchromatic nuclei with prominent nucleoli and moderately abundant pink cytoplasm
2. Intercellular bridges in between the neoplastic cells	2. No intercellular bridges between neoplastic cells
3. Aggregates of neoplastic cells varying in size and shape	3. Sheet-like growth pattern of the neoplastic cells in the dermis
4. Extension of atypical squamous cells from the overlying epidermis into the dermis. Adjacent actinic keratosis may be present	4. No connection between the neoplastic cells in the dermis with the overlying epidermis, which is often ulcerated
5. Multinucleated neoplastic cells are rare	5. Bizarre atypical multinucleated giant neoplastic cells are often present
6. Mitotic figures present and may be atypical	6. Numerous mitotic figures, many of which are atypical
7. Keratinization often present	7. No evidence of keratinization

Squamous Cell Carcinoma and Pseudoepitheliomatous Hyperplasia

Pseudoepitheliomatous hyperplasia (PEH) is a benign condition, characterized by hyperplasia of the epidermis and adnexal epithelium, closely simulating squamous cell carcinoma. PEH may be present in a number of conditions characterized by prolonged inflammation and/or chronic infection, as well as in association with many cutaneous neoplasms. PEH, also known as pseudocarcinomatous hyperplasia, is difficult to distinguish from SCC.

Squamous cell carcinoma	Pseudoepitheliomatous hyperplasia
1. Neoplastic keratinocytes are derived from epidermis	1. The hyperplastic epithelium originates from adnexal epithelium
2. Horizontally oriented	2. Vertically oriented
3. Asymmetric	3. Symmetric
4. Whorls of parakeratotic cells (“horn pearls”) common	4. No whorls of parakeratotic cells; cornification tends to be orthokeratotic
5. Dyskeratotic cells numerous	5. Few, if any, dyskeratotic cells
6. Suprabasal (“pseudoglandular”) spaces containing acantholytic dyskeratotic cells common	6. No formation of suprabasal (“pseudoglandular”) spaces or of acantholytic cells
7. Epithelial cells often in cords between collagen bundles	7. Epithelial cells not in cords between collagen bundles
8. Nuclei crowded and often markedly atypical	8. Nuclei not crowded or strikingly atypical
9. Nuclei sometimes spindle-shaped	9. Nuclei not spindle-shaped
10. Multinucleate epithelial cells often	10. No multinucleate epithelial cells
11. Mitotic figures range from few to many	11. Mitotic figures range from none to few
12. Mitotic figures may be atypical	12. No atypical mitotic figures
13. Contiguous actinic keratosis or Bowen’s disease often present	13. No contiguous superficial squamous-cell carcinoma in the form of Bowen’s disease or adjacent actinic keratosis
14. No identifiable underlying process, except for changes such as solar elastosis or radiation sclerosis	14. Underlying process, e.g., granular-cell tumor, deep fungal infection, etc., usually identifiable

Fig. 11.1 Lupus erythematosus mimicking superficial squamous cell carcinoma: (a) Irregular downward projections of the epidermis showing keratinocytic atypia in the background of prominent solar elastosis. An erroneous diagnosis of superficial squamous cell carcinoma was made in this case. However, features of lupus erythematosus include the presence of interface changes with a lichenoid lymphocytic infiltrate, occasional necrotic keratinocytes, and follicular plugging. (b) The first stage of Mohs surgery in this case showed a dense superficial and deep perivascular and periadnexal inflammatory infiltrate. (c) Numerous hair follicles transversely sectioned and surrounded by a dense lymphocytic inflammatory infiltrate

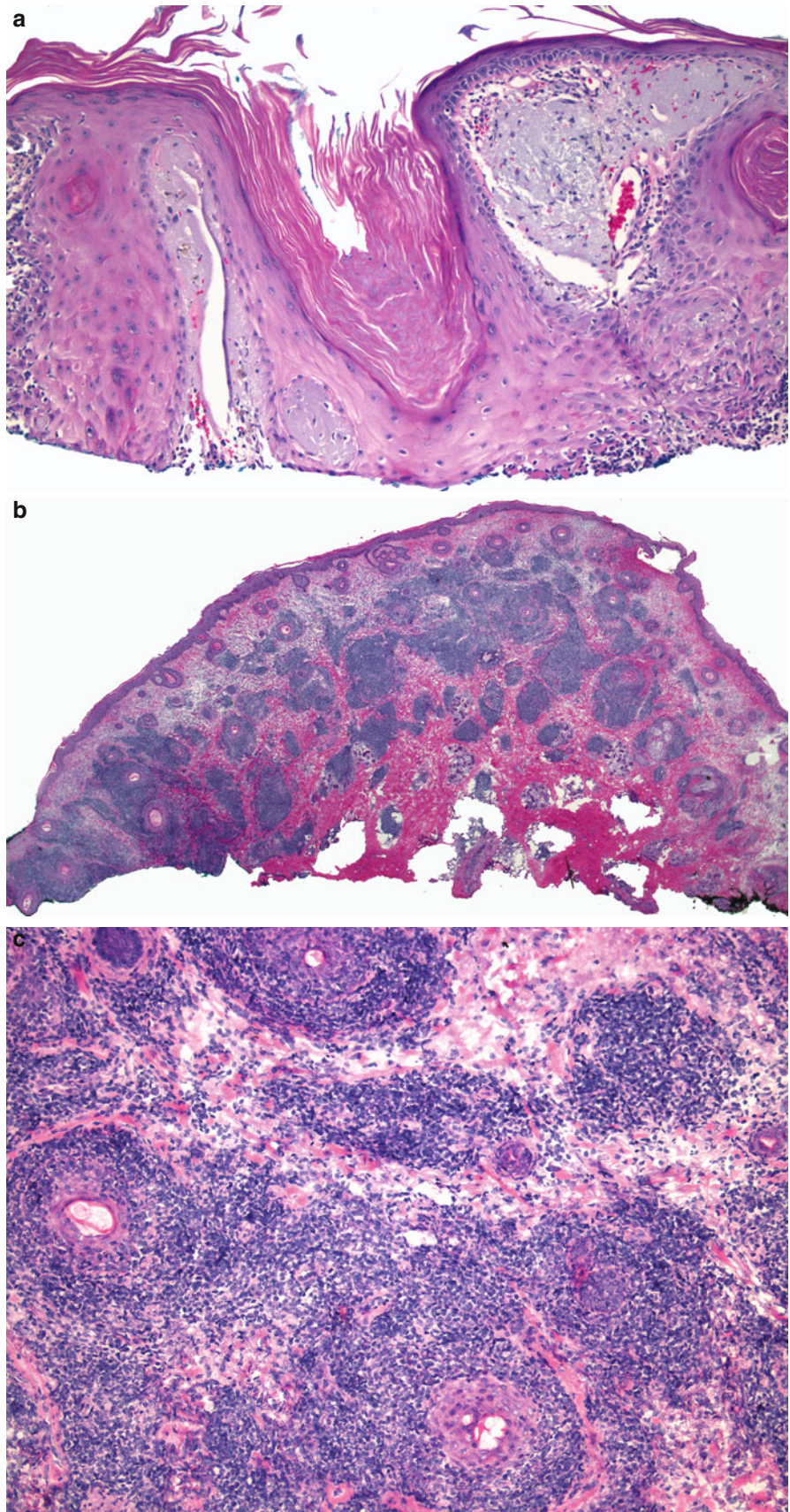


Fig. 11.2 Hypertrophic lupus erythematosus: (a, b) Mimicking SCC. Irregularly hyperplastic epithelium with follicular plugging and dense lichenoid lymphocytic infiltrate

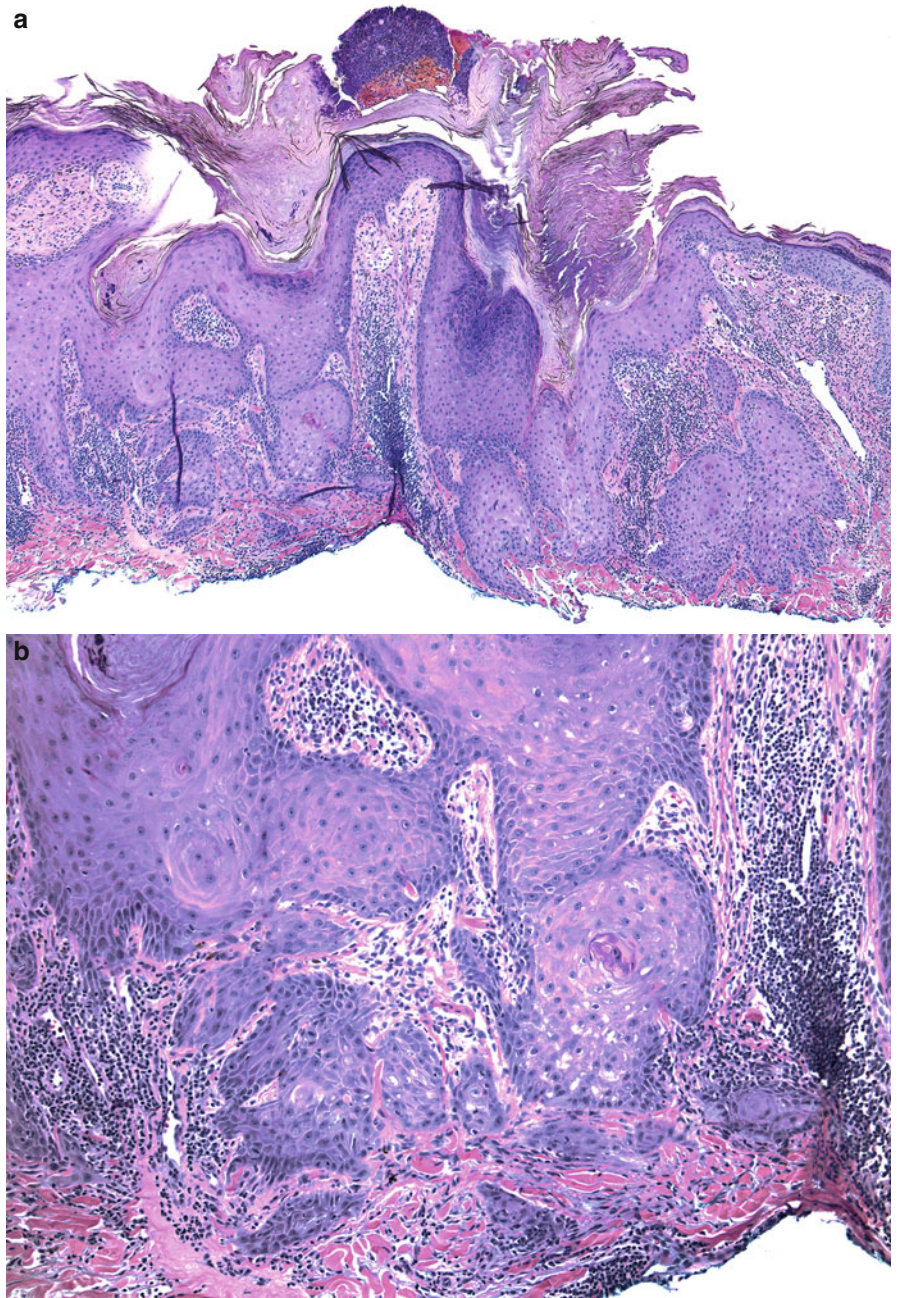


Fig. 11.3 Pseudoepitheliomatous hyperplasia: (a) Superficial scar with re-epithelialization on the left. Elongated acanthotic downward projections of the epidermis with variable depth and jagged borders adjacent to the scar on the right. Many of the aggregates have angulated outlines. (b) The epithelial downward projections mimic tumor aggregates of squamous cell carcinoma. However, the squamous epithelium of PEH is well differentiated and lacks keratinocytic atypia

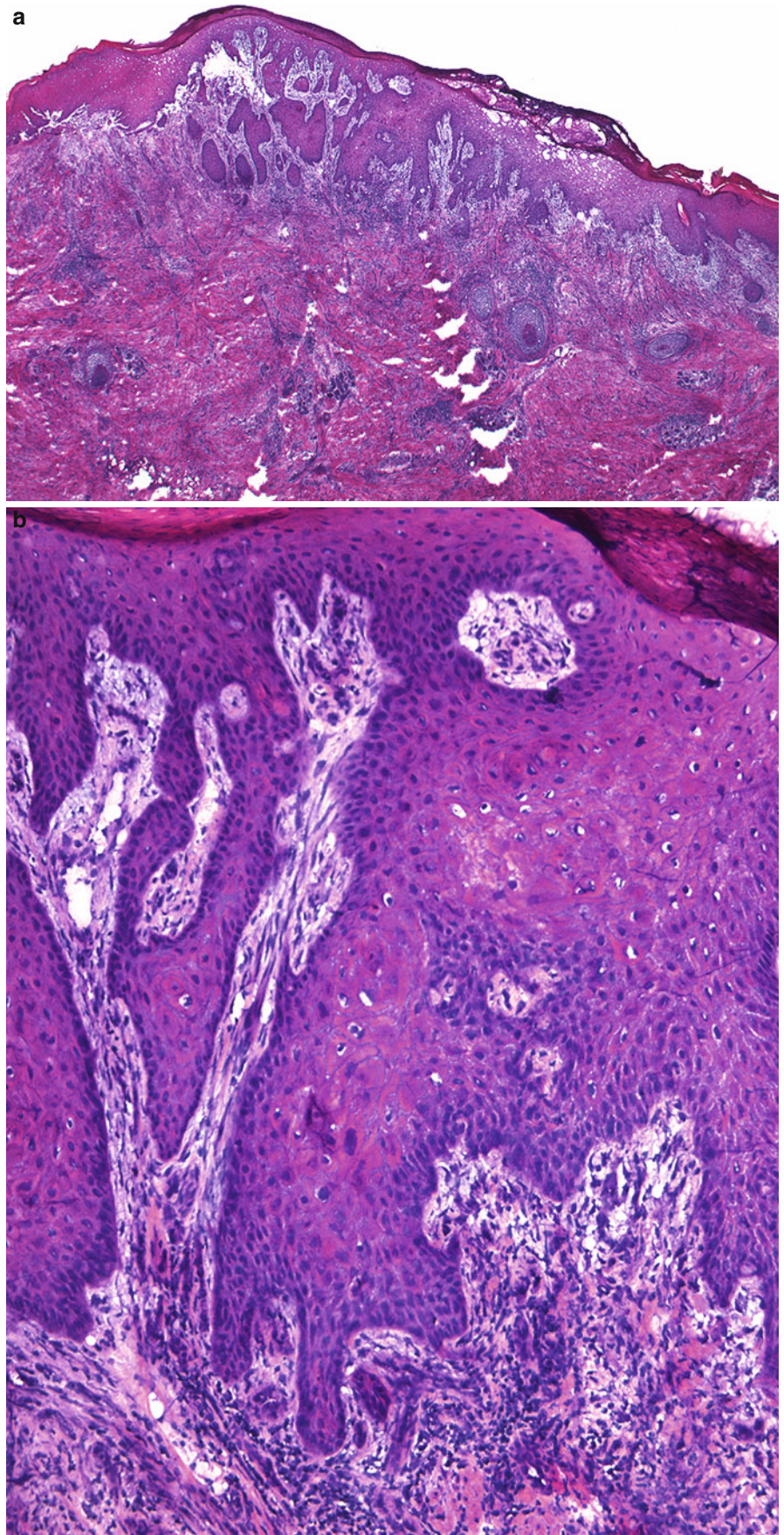


Fig. 11.3 (continued) (c) The keratinocytes are monomorphous and show normal maturation. Keratin pearls and mitotic figures are rare

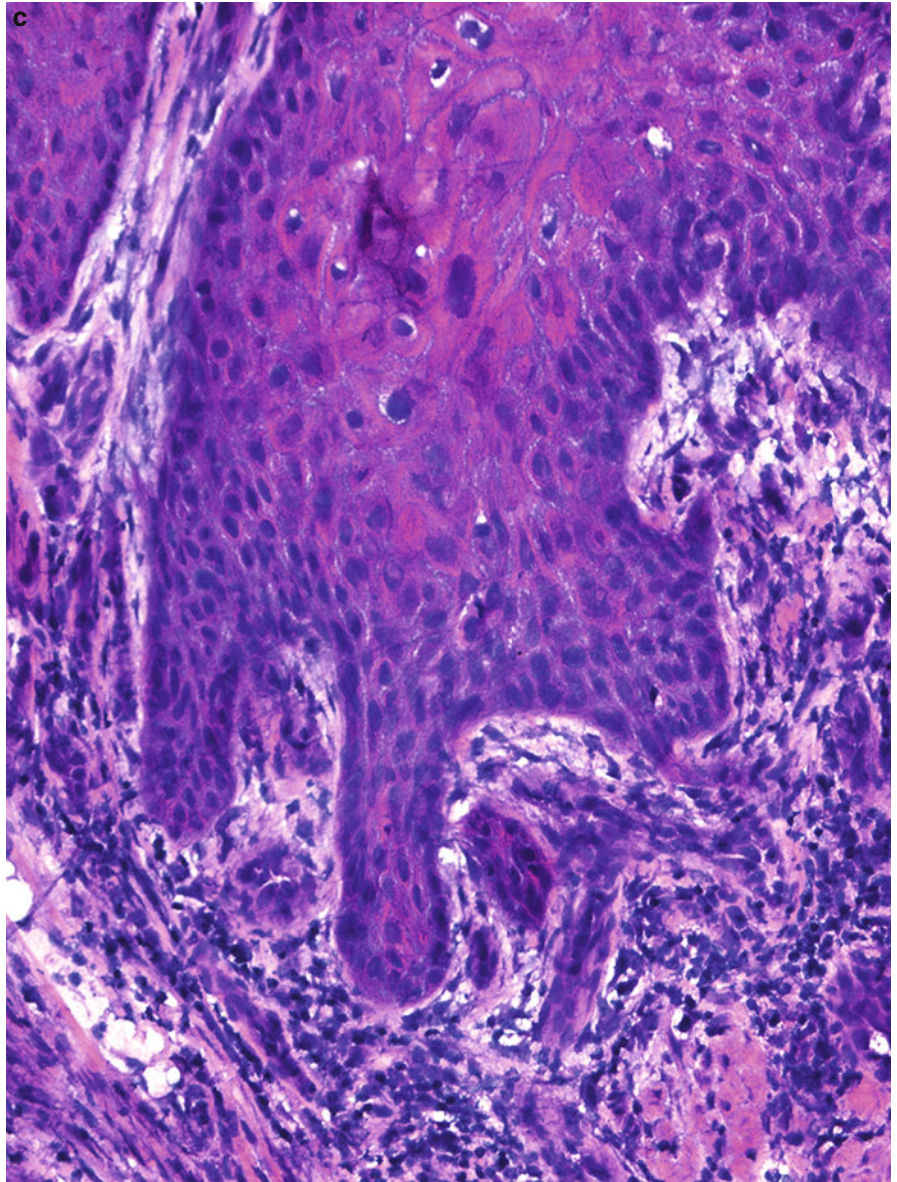


Fig. 11.4 Pseudoepitheliomatous hyperplasia: prominent pseudo-epitheliomatous hyperplasia in association with stasis. Note the angulated downward projections of the acanthotic epidermis

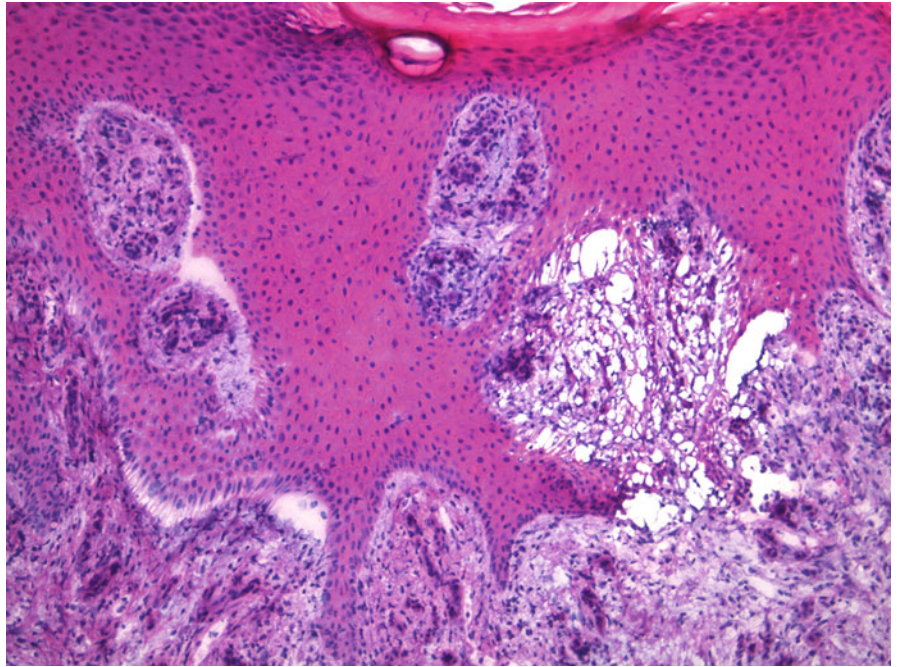


Fig. 11.5 Pseudoepitheliomatous hyperplasia: (a) Another example of PEH. (b) Seemingly disconnected epithelial aggregates may be mistaken for well-differentiated SCC

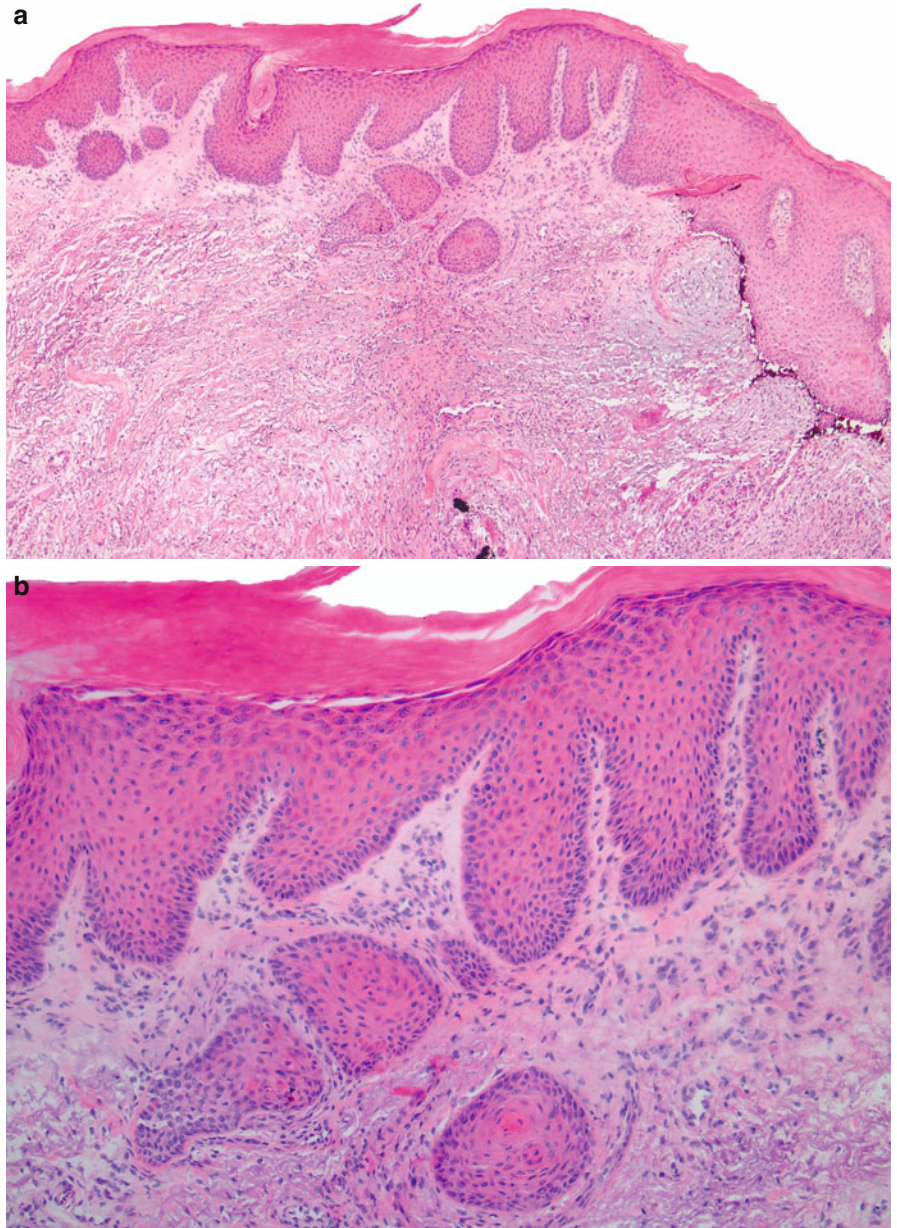


Fig. 11.5 (*continued*) (c) Squamous cell carcinoma: this is the biopsy of the Mohs specimen illustrated above which shows well-differentiated squamous cell carcinoma with squamous eddies that is markedly different from the PEH

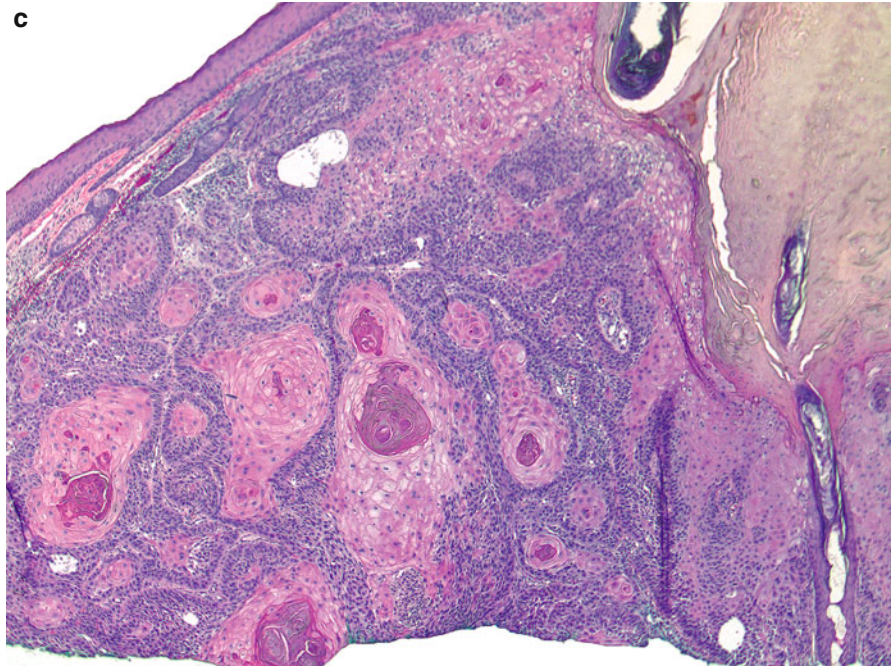


Fig. 11.6 Pseudoepitheliomatous hyperplasia: (a) PEH and dense lichenoid inflammation in the dermis. (b) The features of PEH are better appreciated at this magnification: elongated and jagged downward projections of the epidermis, many with a sharply pointed base. The epidermis is thickened. The keratinocytes are large and eosinophilic but not atypical

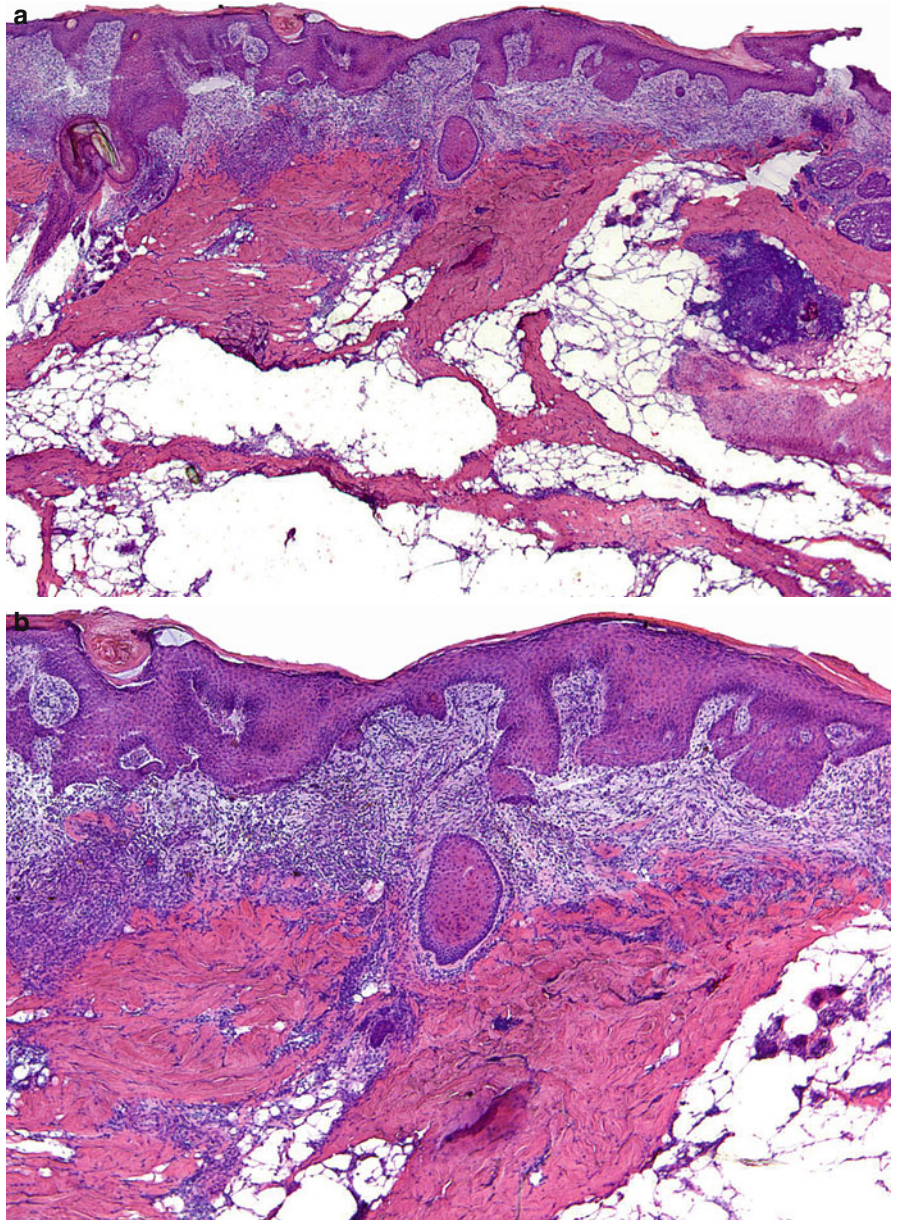


Fig. 11.7 Squamous cell carcinoma with overlying pseudoepitheliomatous hyperplasia: there is thickened epidermis representing PEH. Eosinophilic aggregates of squamous cell carcinoma are seen in the dermis surrounded by dense inflammation

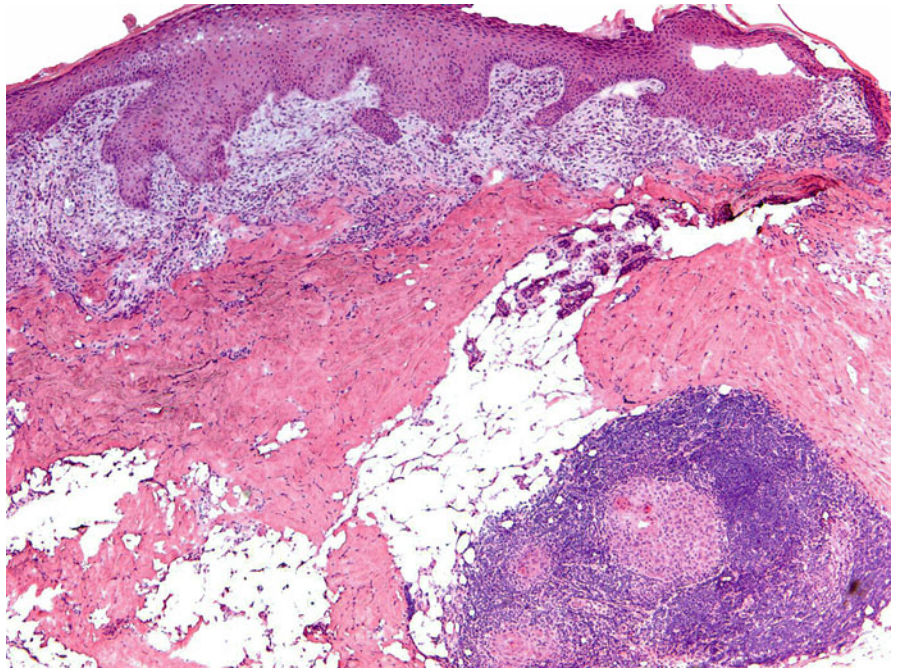
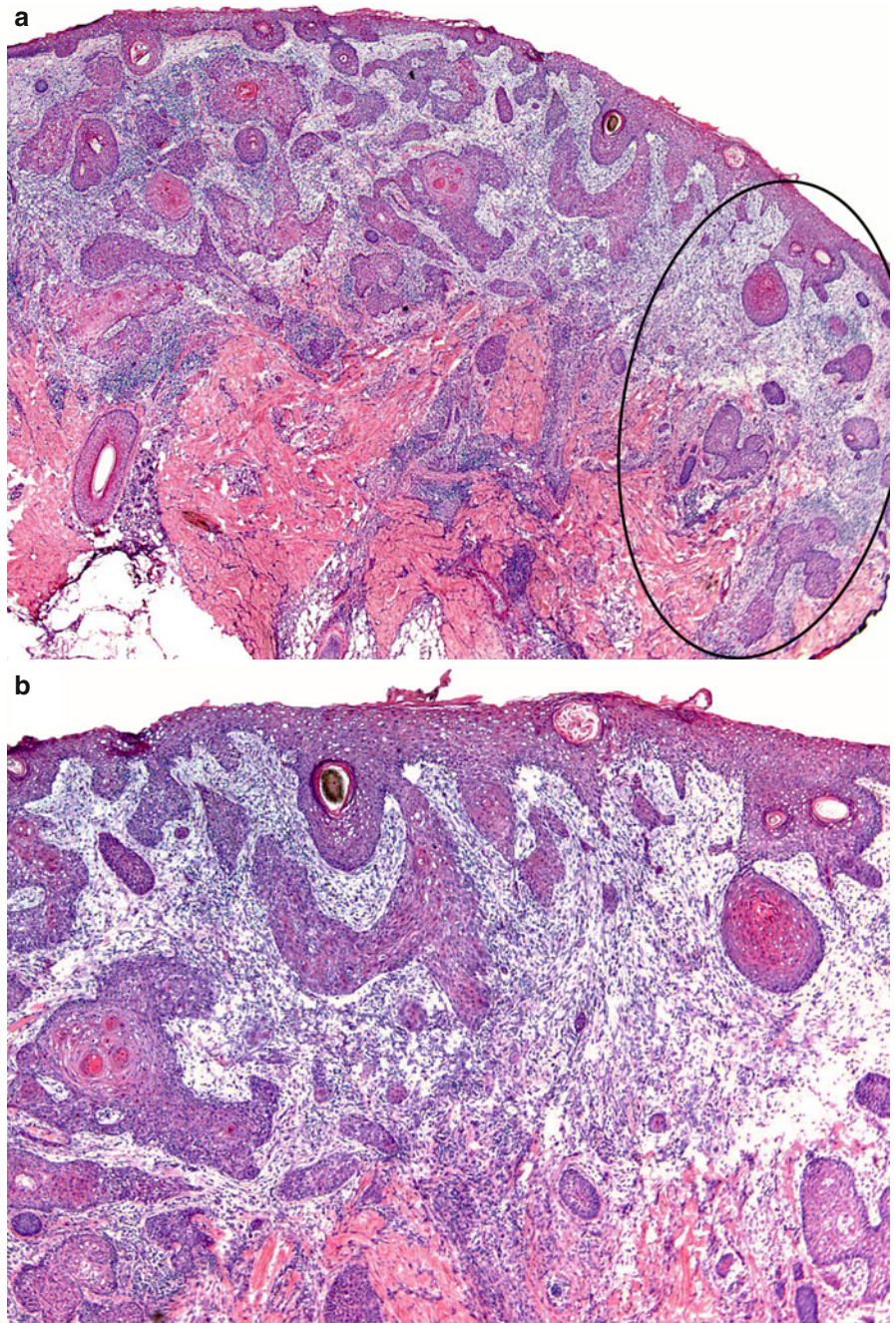


Fig. 11.8 Squamous cell carcinoma with adjacent pseudoepitheliomatous hyperplasia: **(a)** Well-differentiated tumor aggregates are seen in the dermis on the left. A focus of PEH is seen on the right side (*ellipse*). **(b)** Compare the large irregular neoplastic aggregates of SCC on the left, showing multiple foci of keratinization, to the well-differentiated epithelial projections of PEH on the right, representing extensions of follicular and adnexal epithelium



Histologic Features

1. Fibrohistiocytic dermal neoplasm of intermediate malignant potential that has a tendency to recur, but rarely metastasizes.
2. Poorly delineated tumor with infiltrative growth pattern.
3. Extension and infiltration into the subcutaneous fat showing honeycombing and lace-like pattern involving fat lobules with thickening of fibrous septae.
4. A Grenz zone between the tumor and the overlying epidermis.
5. Effacement of adnexal structures within the area occupied by tumor.
6. Tumor is composed of fascicles arranged in a storiform pattern within reticular dermis and subcutaneous fat.
7. Neoplastic cells are slender, bland, monomorphous, spindle-shaped with elongated nuclei and small amount of pale cytoplasm.
8. Rare mitotic figures.
9. Necrosis rarely seen.
10. Neoplastic cells are CD34 positive and Factor 13A negative.

Differentiating Dermatofibrosarcoma Protuberans and Scar Tissue

Dermatofibrosarcoma protuberans	Scar
1. Grenz zone present	1. Lack of Grenz zone
2. Neoplastic cells arranged in fascicular and storiform pattern	2. Fibroblasts and collagen bundles oriented parallel to the skin surface
3. Blood vessels are not prominent	3. Newly formed blood vessels oriented perpendicular to the skin surface
4. Greater cellular density	4. Less cellular
5. Extension within subcutaneous fat lobules with honeycombing and lace-like pattern and thickening of fibrous septae	5. Rare involvement of subcutaneous fat
6. Neoplastic cells are slender and monomorphous, closely opposed to each other	6. Plump fibroblasts parallel to each other
7. Lack of intervening collagen between neoplastic cells	7. Thickened collagen bundles in between fibroblasts
8. Overall color of the neoplasm at low magnification is bluish/gray	8. Overall color is pink due to the eosinophilic collagen laid out between fibroblasts
9. Fibrous septae thickened by the proliferation of slender monomorphous spindled neoplastic cells	9. Fibrous septae thickened by closely opposed thick collagen bundles and a small number of fibroblastic nuclei

Fig. 12.1 Dermatofibrosarcoma protuberans: (a) Scanning magnification showing a neoplasm within the lower reticular dermis and involving the subcutaneous fat, creating a honeycomb pattern. (b) Irregular storiform pattern of spindled cells within fibrous septae and fat lobules

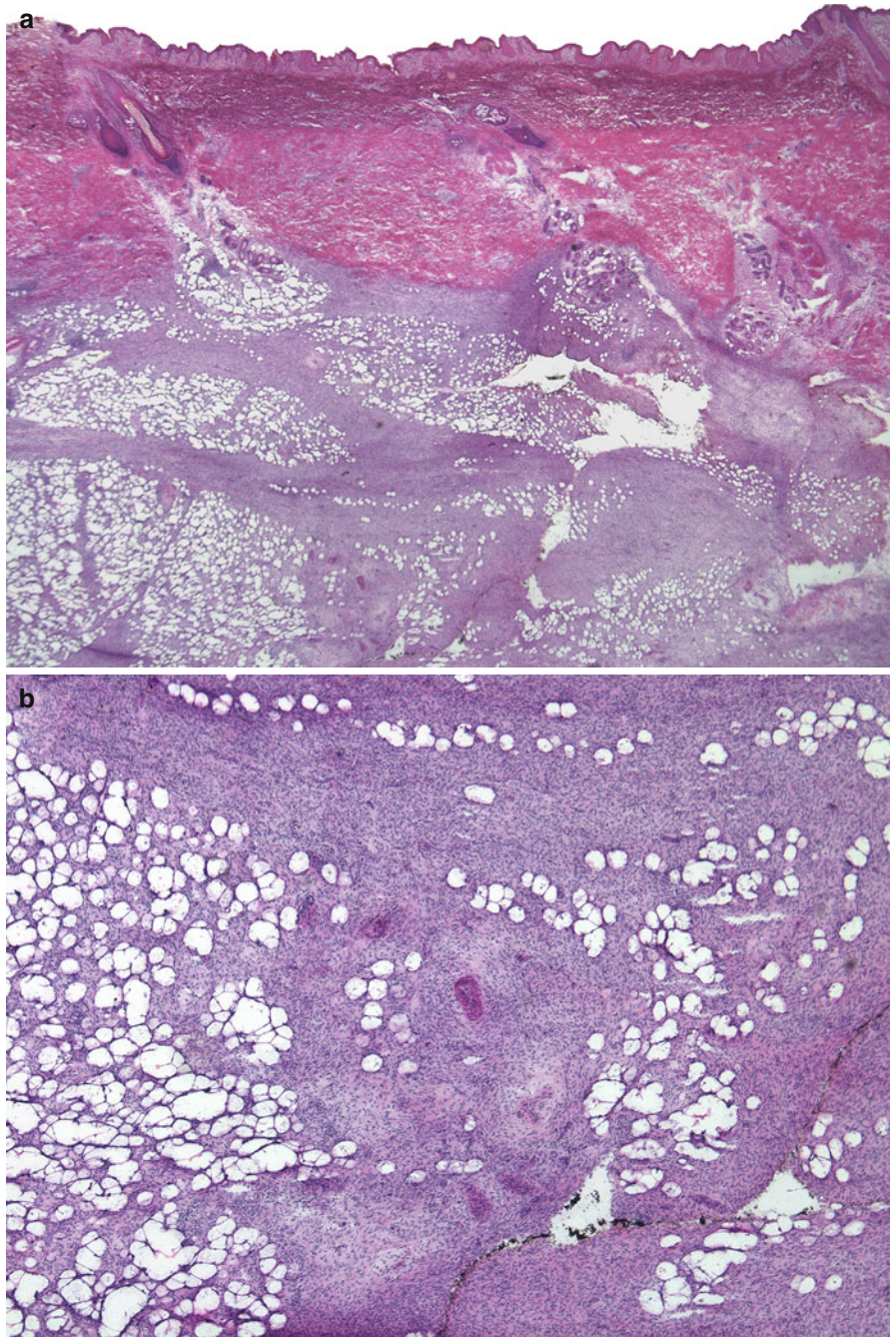


Fig. 12.1 (continued) (c) Infiltration of the fibrous septae and fat lobules by a spindle cell proliferation. The infiltrative pattern of the tumor creates a characteristic honeycomb appearance. (d) Dense proliferation of oval and spindle shaped monomorphic neoplastic cells. The nuclei are not hyperchromatic and the cells have a small amount of pale cytoplasm. Mitotic figures are not present and cellular pleomorphism is not appreciated. The neoplastic process has completely replaced a fat lobule

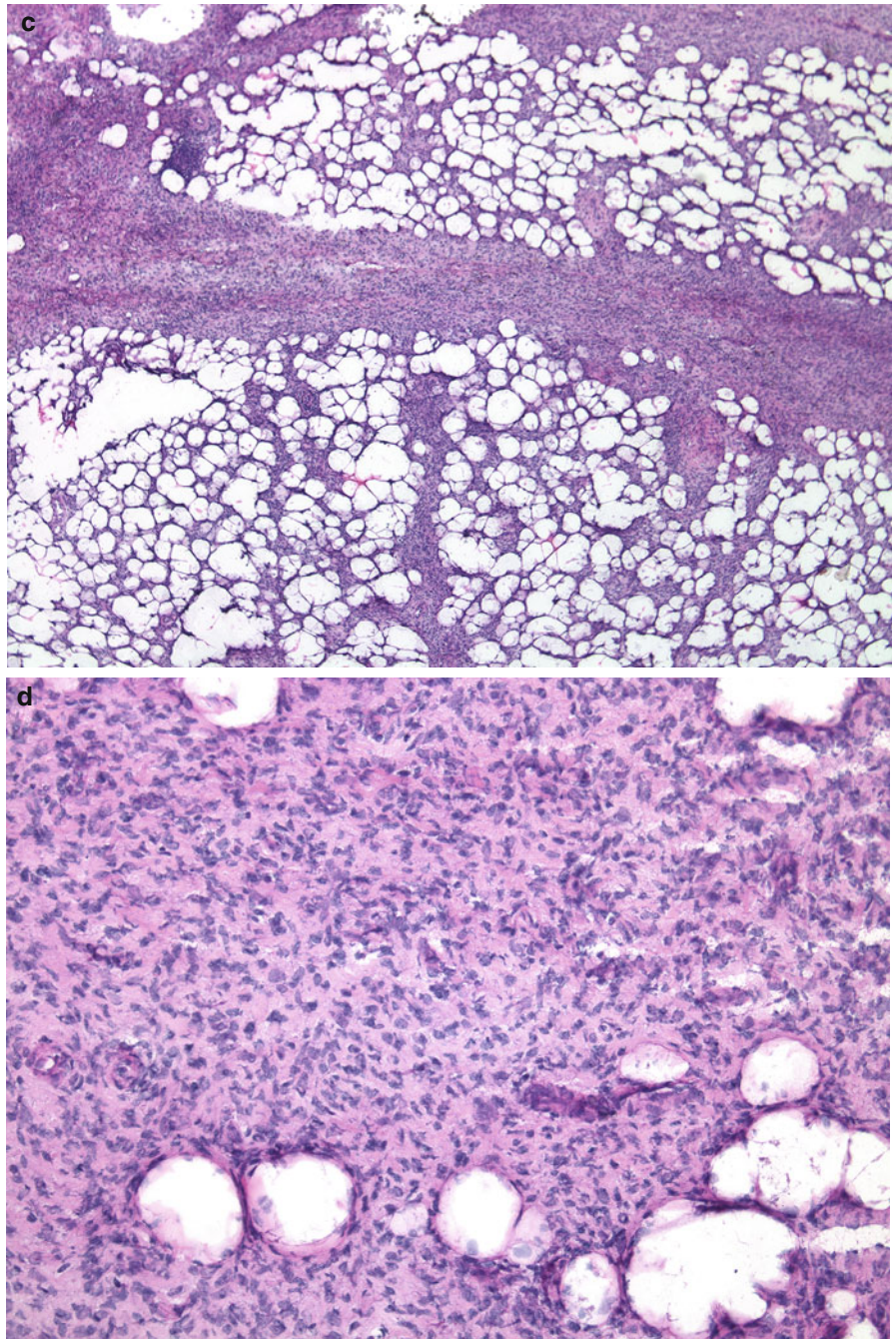


Fig. 12.2 Dermatofibrosarcoma protuberans: **(a)** Cellular area within the right lower portion of the photomicrograph. As opposed to the neoplastic process, scar tissue on the left is eosinophilic, sclerotic, and less cellular. **(b)** Densely packed spindled neoplastic cells in the subcutaneous fat. Fewer nuclei, prominent vessels, and sclerotic thickened collagen bundles are seen in the scar in the left upper corner

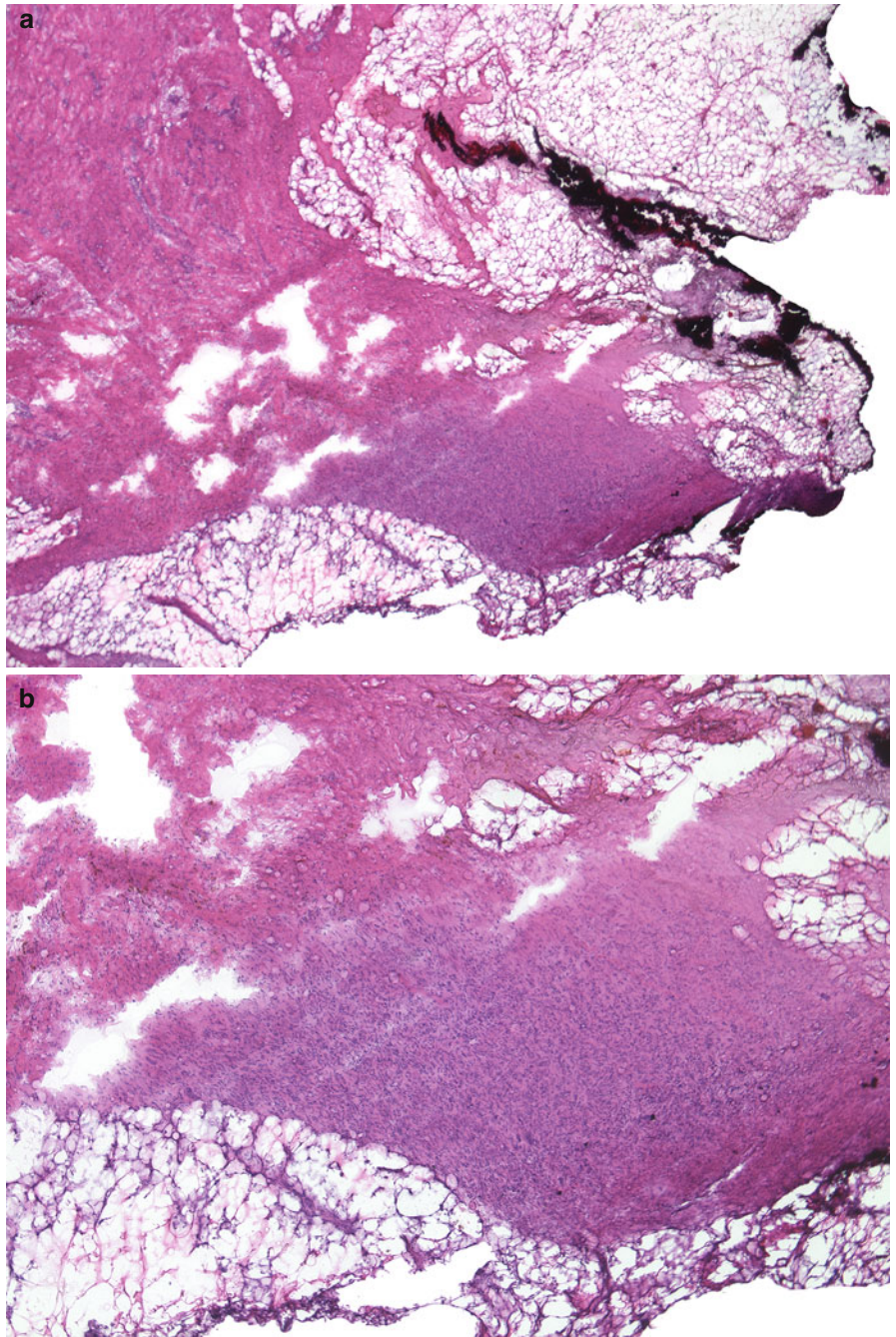


Fig. 12.3 Dermatofibrosarcoma protuberans: Tumor extends from upper dermis to subcutis. Note effacement of adnexal structures

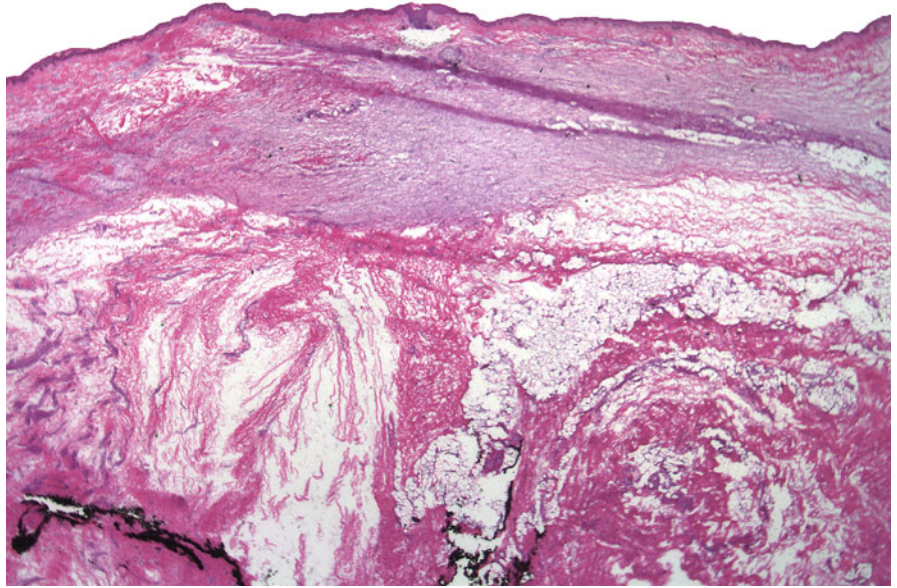


Fig. 12.4 Dermatofibrosarcoma protuberans: **(a)** Infiltration of the entire reticular dermis by tumor cells. A Grenz zone (area clear of tumor) can be appreciated between the epidermis and the tumor in the dermis. **(b)** Higher magnification demonstrates oval and spindled monomorphic cells infiltrating between bright eosinophilic collagen bundles

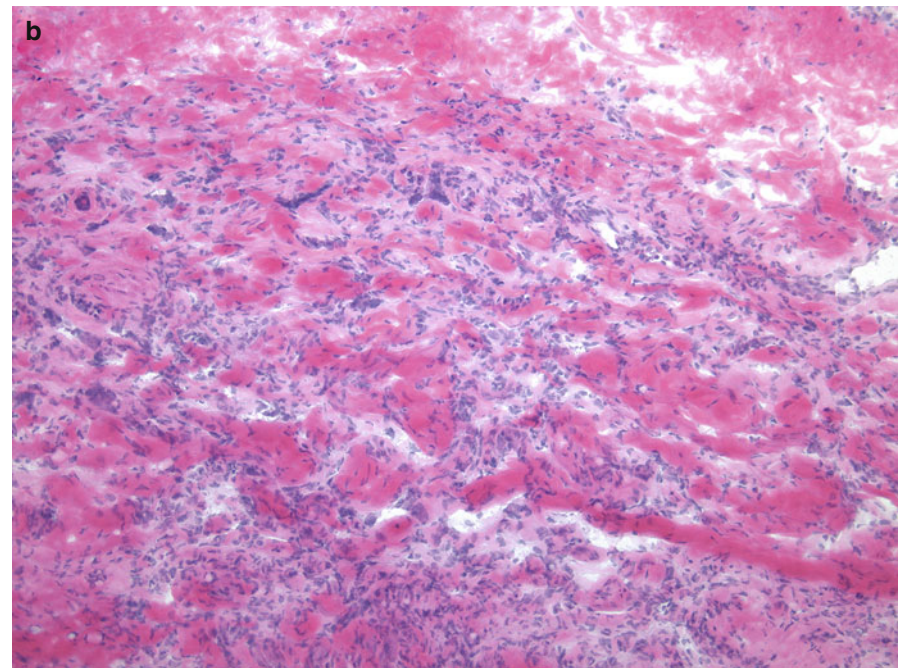
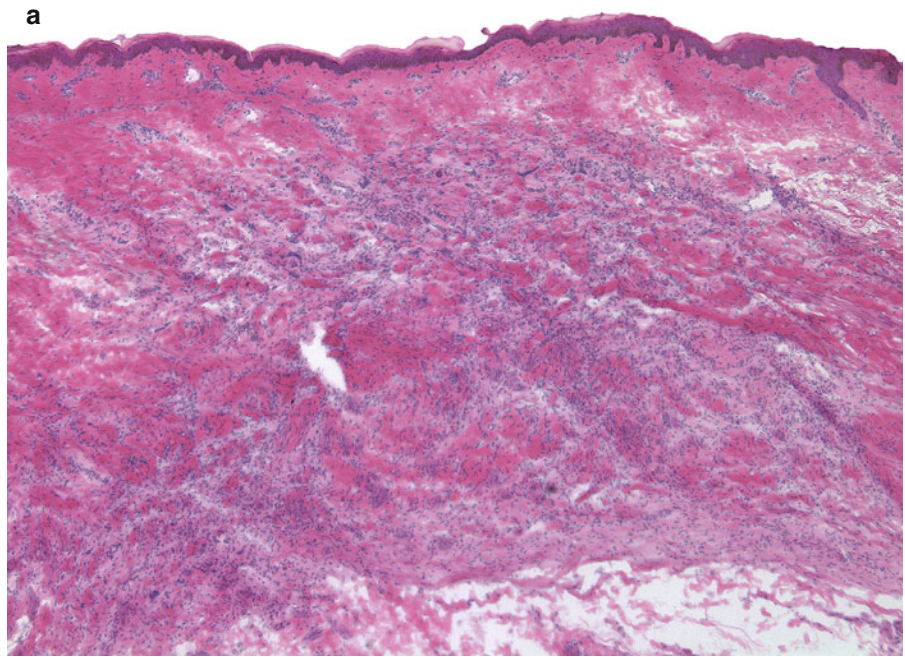


Fig. 12.4 (continued) (c) DFSP and scar: In the subcutaneous fat on the right (*ellipse*) there is a cellular area of DFSP involving a thickened fibrous septum and spilling out into the adjacent fat lobule. Thick sclerotic collagen of a scar is present on the left. (d) Scar: medium power view showing dense sclerotic area containing increased number of fibroblasts and numerous small blood vessels

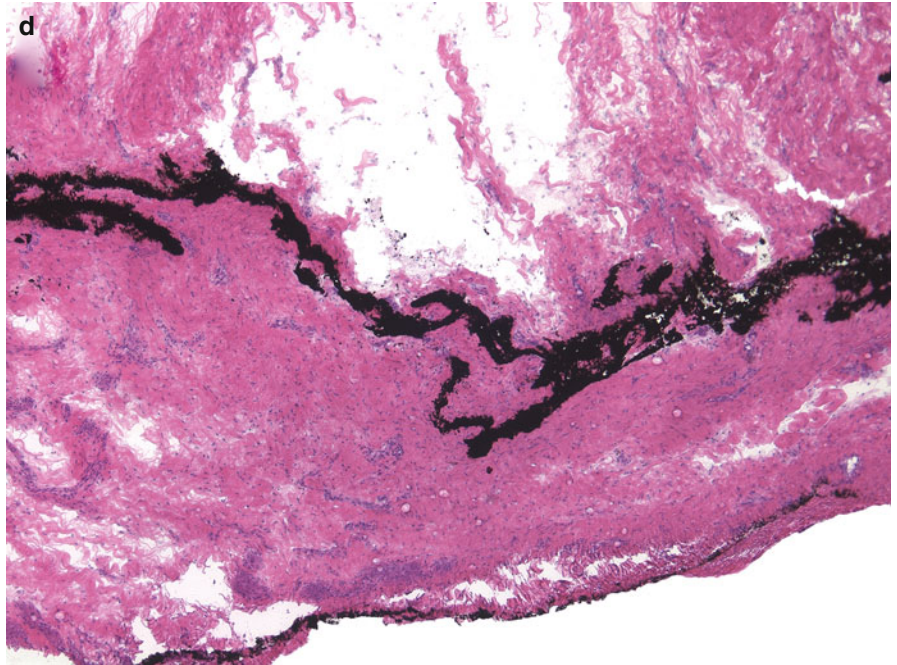
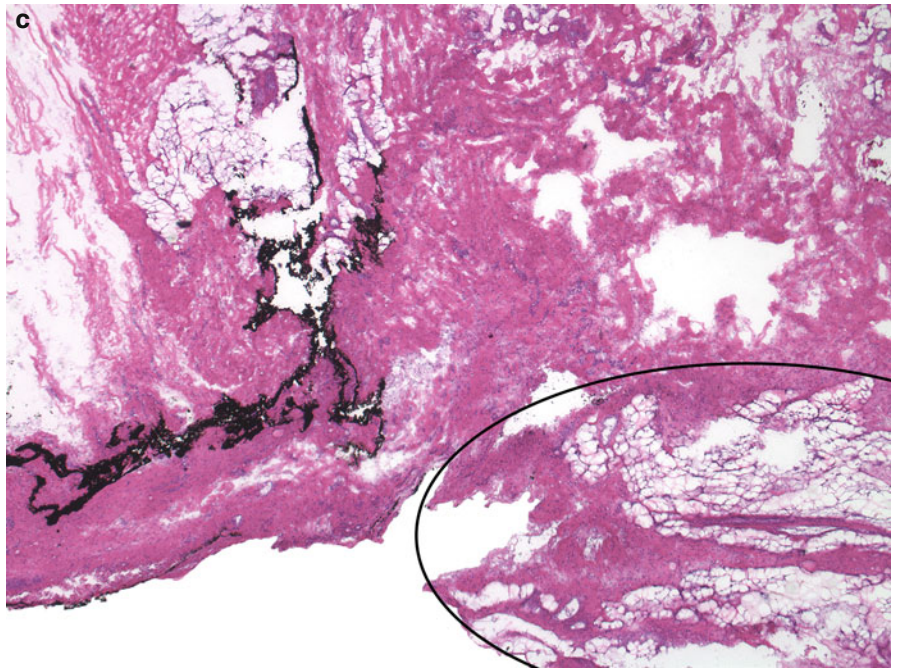


Fig. 12.4 (*continued*) (e) Delicate, slender, evenly spaced nuclei of fibroblasts in between thickened collagen bundles. (f) A small focus of tumor in the lower central portion of the photomicrograph. To the right and above that area is sclerotic scar tissue. The high cellularity and the lack of intervening thick collagen bundles distinguish the neoplastic focus from the adjacent scar

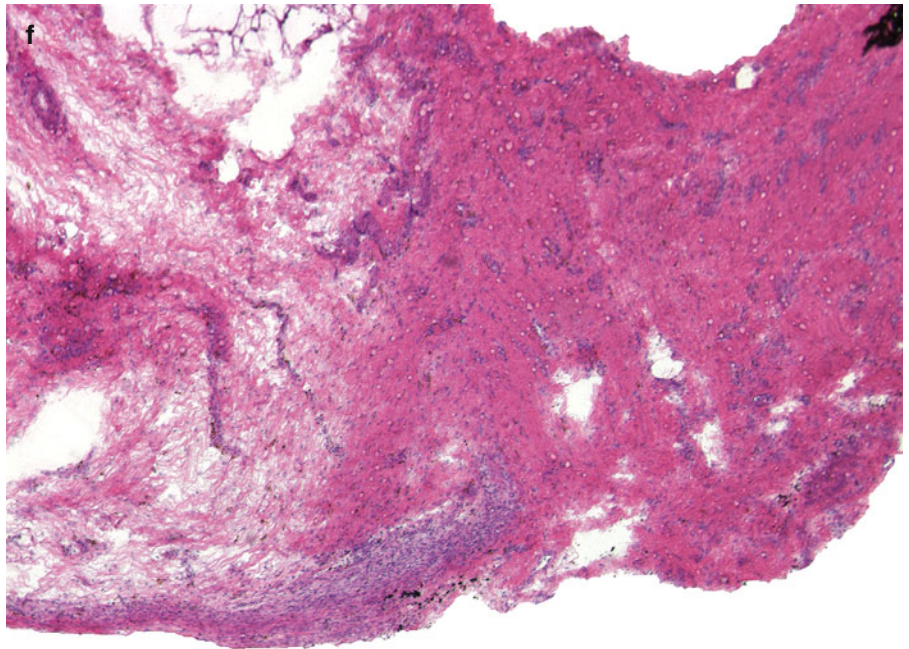
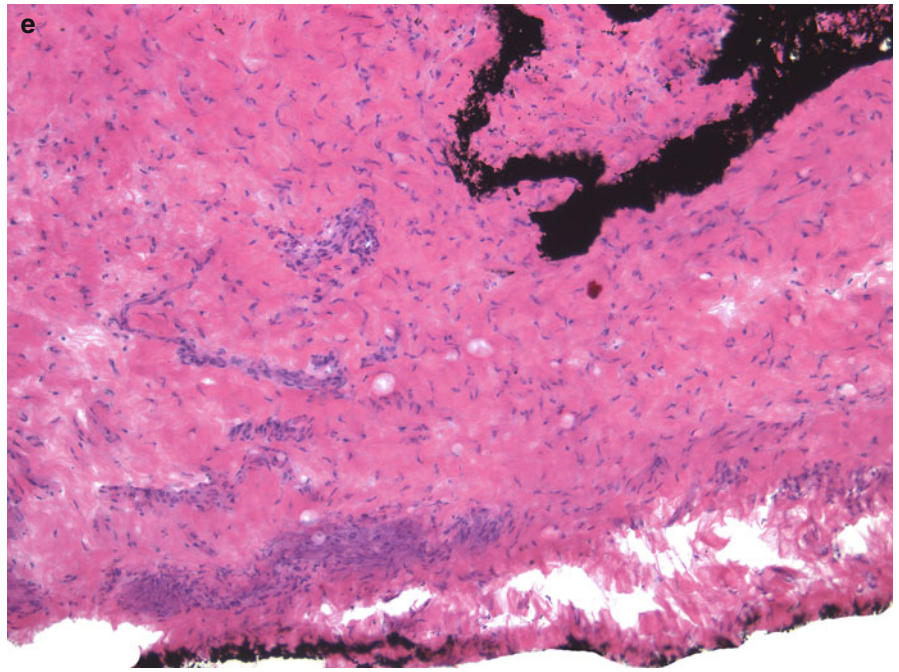


Fig. 12.4 (continued) (g) Higher magnification demonstrating a cellular focus of tumor surrounded by scar tissue. Scar tissue, in contrast to DFSP, contains fewer nuclei of fibroblasts in between bright eosinophilic collagen bundles, prominent small newly formed blood vessels and hemosiderin deposition

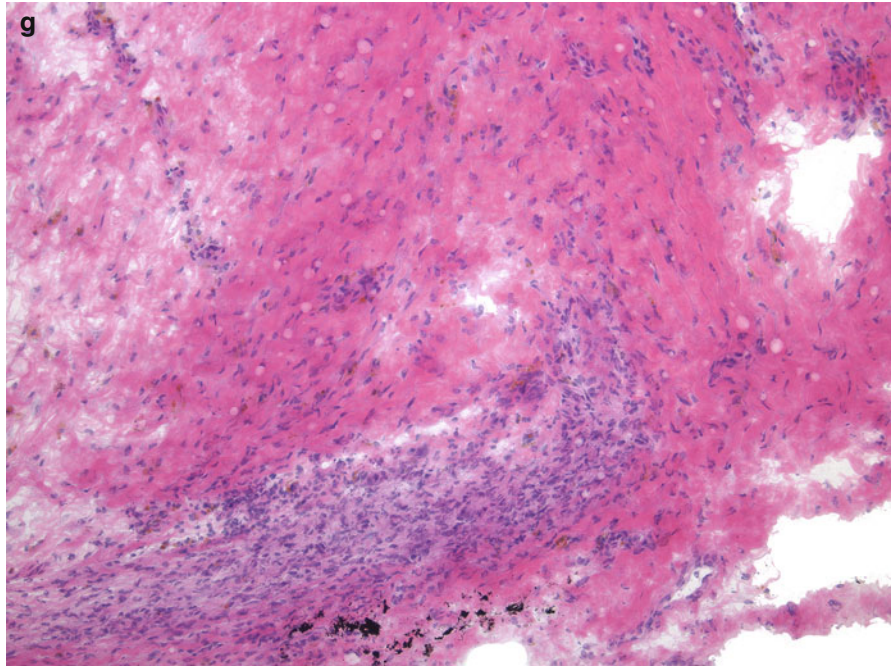


Fig. 12.5 Dermatofibrosarcoma protuberans: (a) Basophilic tumor in the mid dermis. (b) The dense cellular proliferation consists of small spindle-shaped cells in a haphazard storiform arrangement

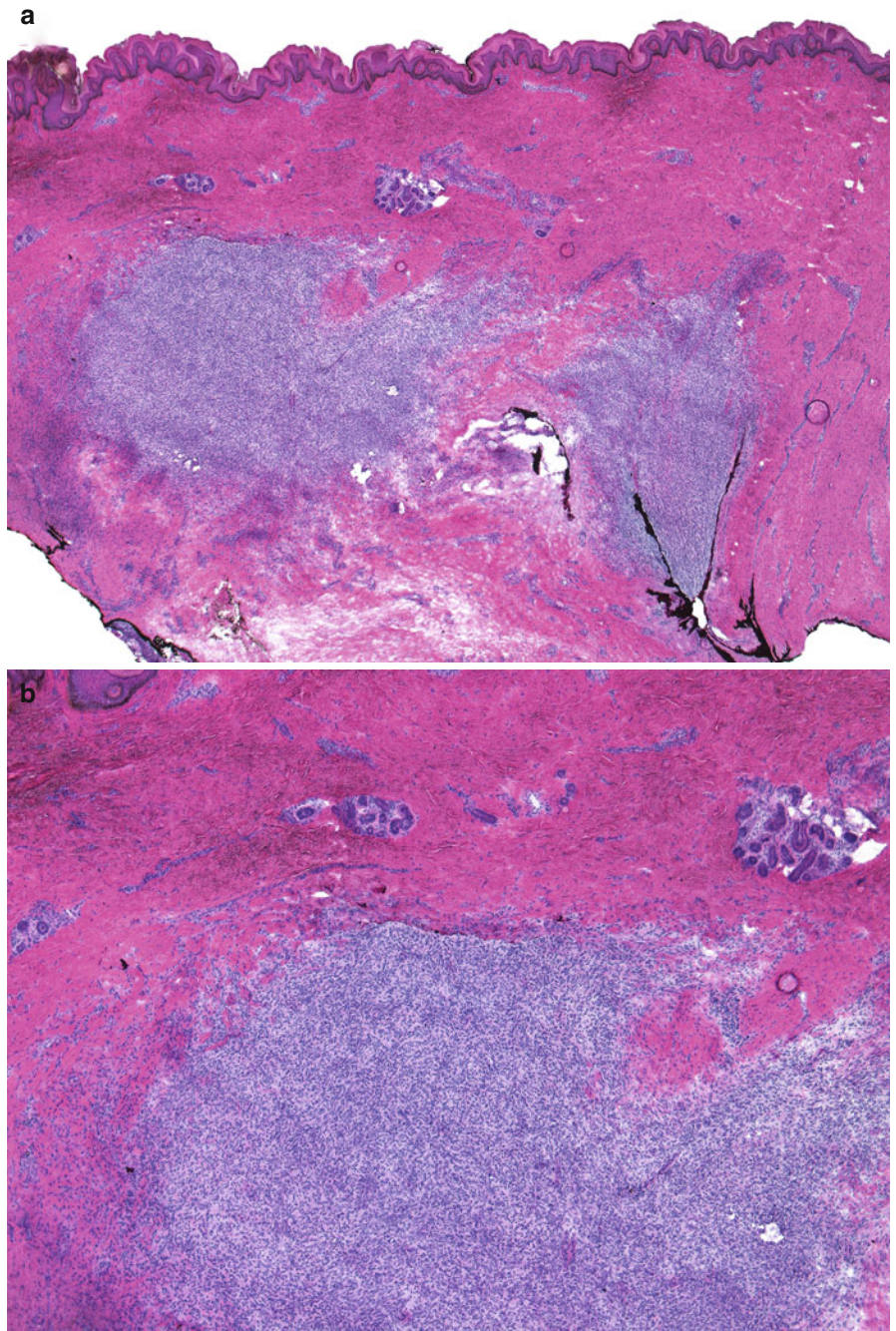


Fig. 12.5 (continued) (c) Scar in the superficial dermis and tumor in the right lower corner. Although subtle, this degree of cellularity in contrast to the surrounding scar should raise the suspicion of tumor. (d) With additional sections the tumor becomes less dense

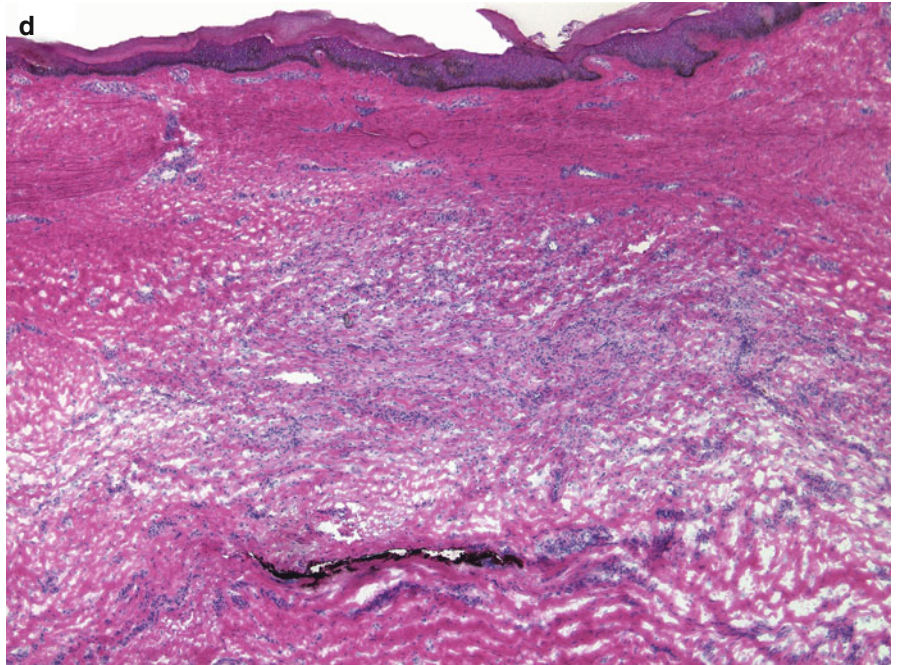
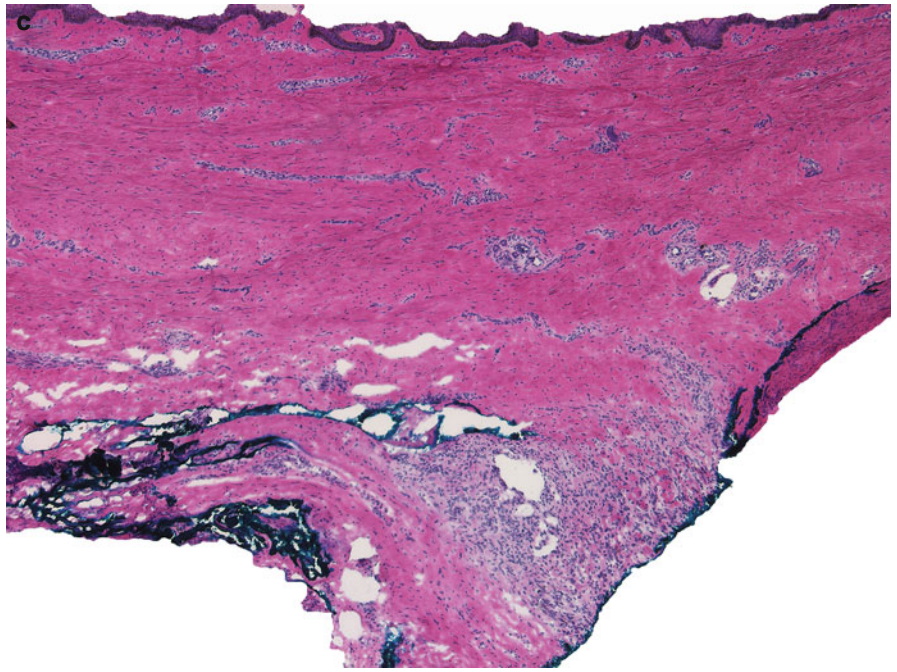


Fig. 12.5 (continued) (e) A focal area of increased cellularity is seen in the right lower portion of the tissue section (*arrows*). (f) Higher magnification confirms the presence of tumor (*ellipse*)

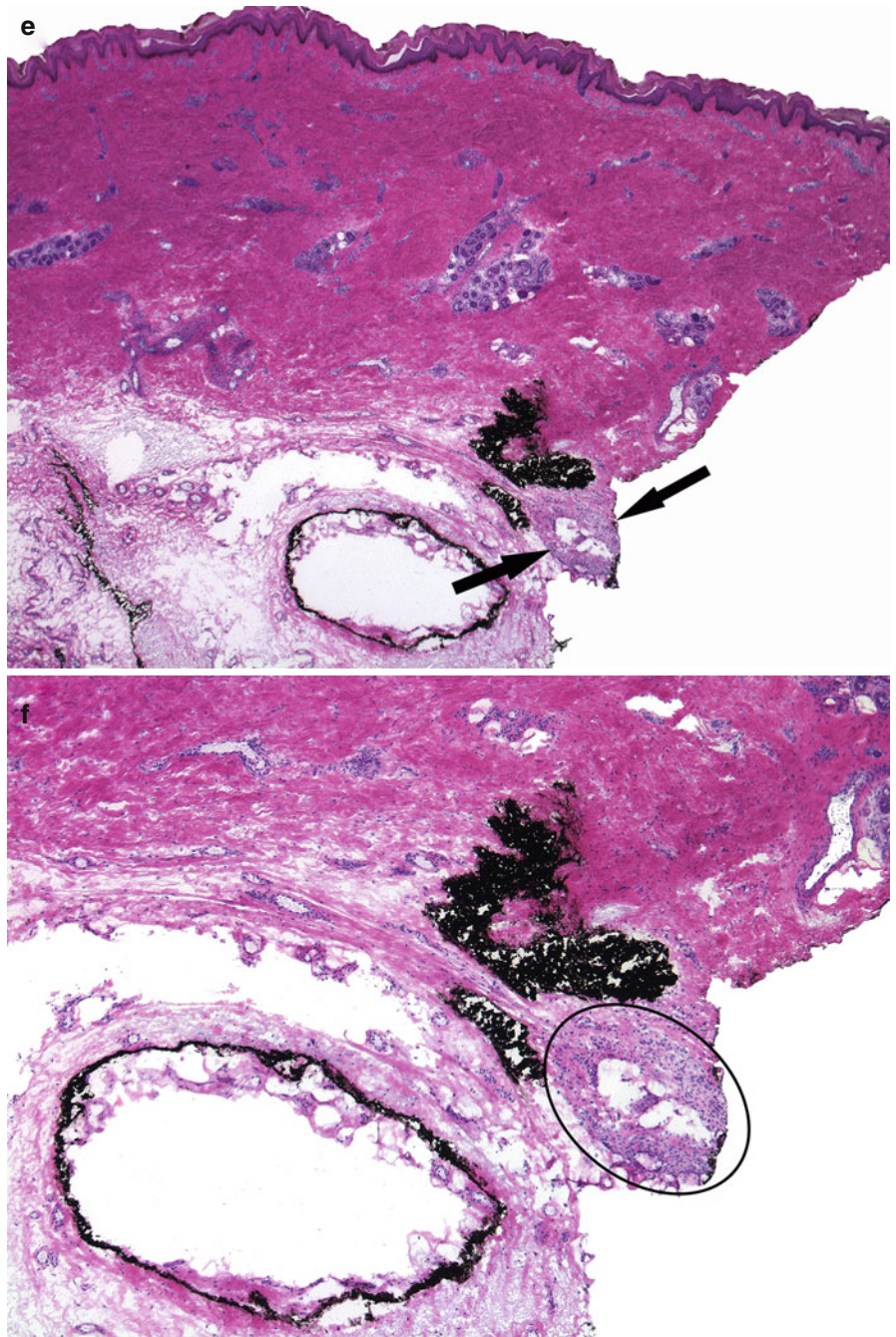


Fig. 12.5 (*continued*) (**g**) At this low magnification, tumor can be easily overlooked, highlighting the importance of examining all sections thoroughly. (**h**) An increased cellularity in the central portion of the photomicrograph. The neoplastic cells are bland and do not demonstrate pleomorphism

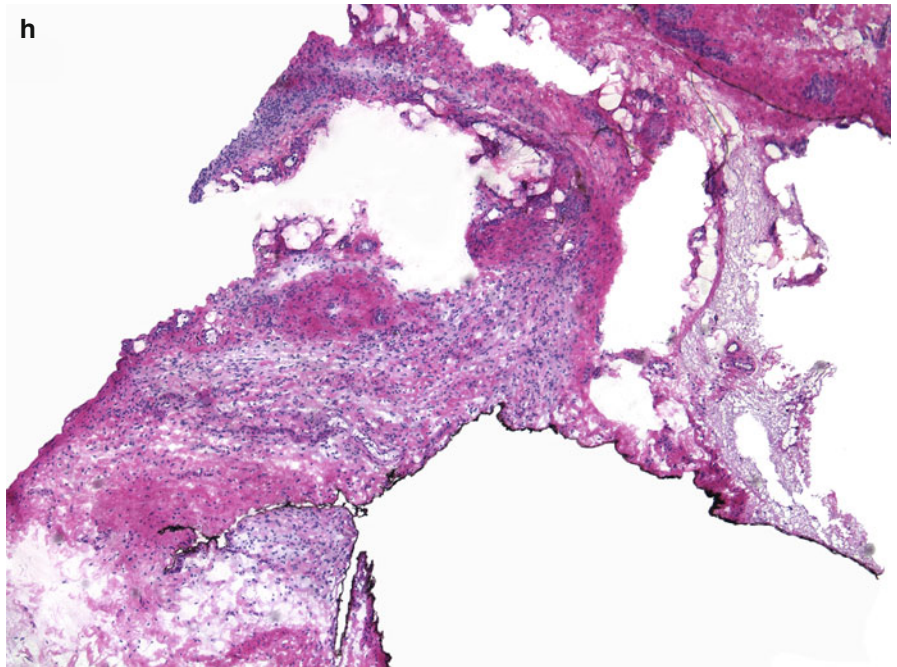
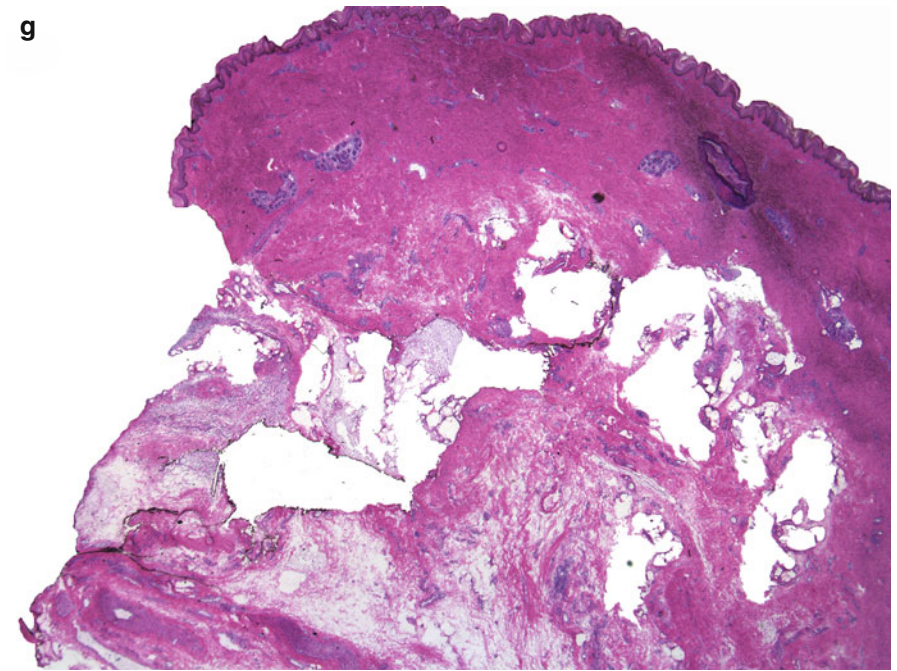


Fig. 12.5 (*continued*) (i) In the left portion of this photomicrograph is a scar with prominent vessels and mild perivascular inflammation. Adjacent to it on the right is a focus of densely packed neoplastic spindled cells. (j) Bland spindled neoplastic cells within the fat lobule and infiltrating a thickened fibrous septum

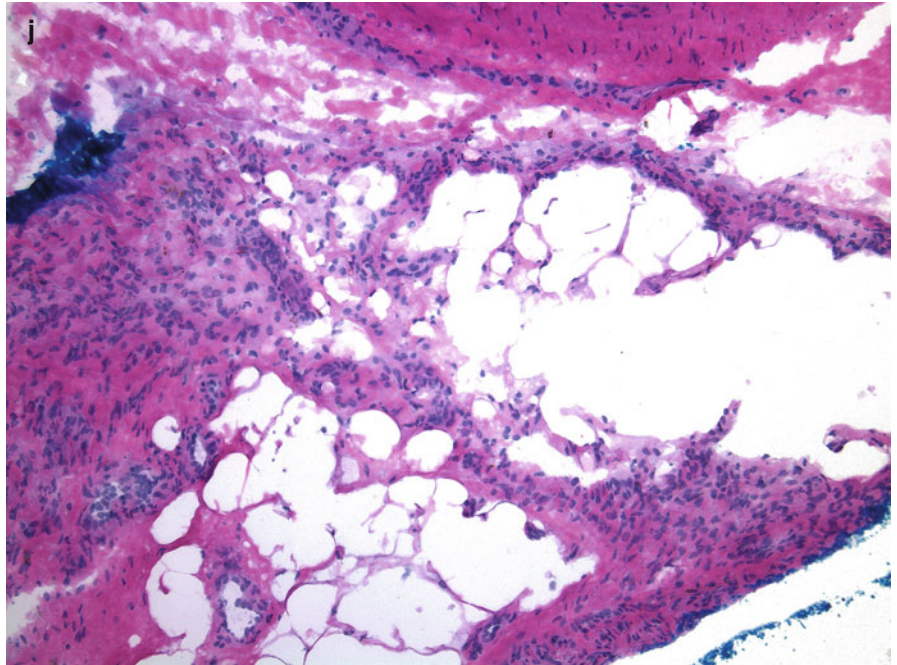
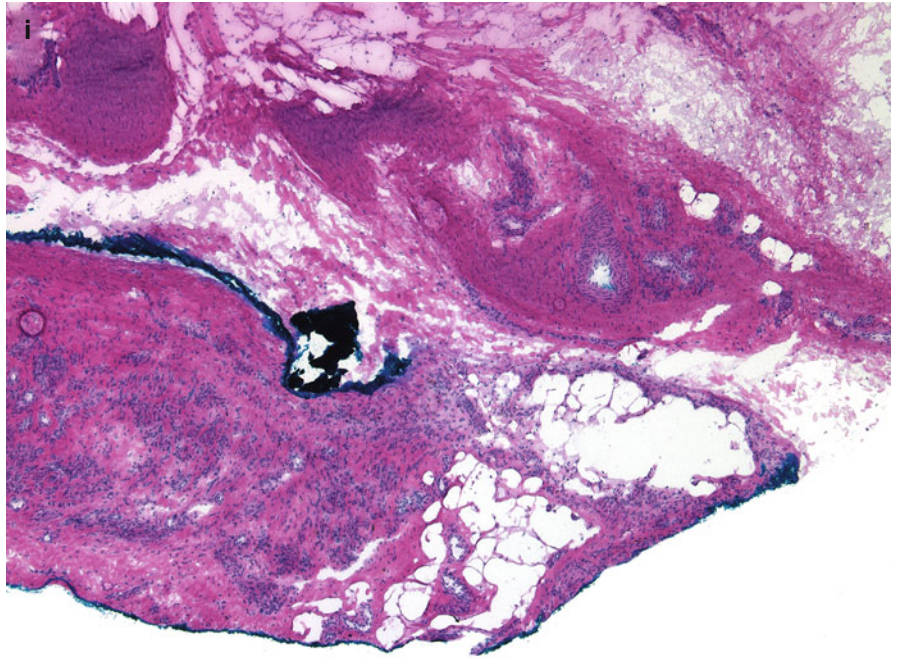


Fig.12.5 (*continued*) Dermatofibrosarcoma protuberans: **(k)** A focus of tumor in the center and on the right. Tumor is perceptible simply because of its cellularity in contrast to the surrounding tissue. **(l)** A densely cellular area with bland spindle nuclei within a markedly thickened fibrous septum in the subcutis. Note the trapping of the lipocytes surrounded by neoplastic cells

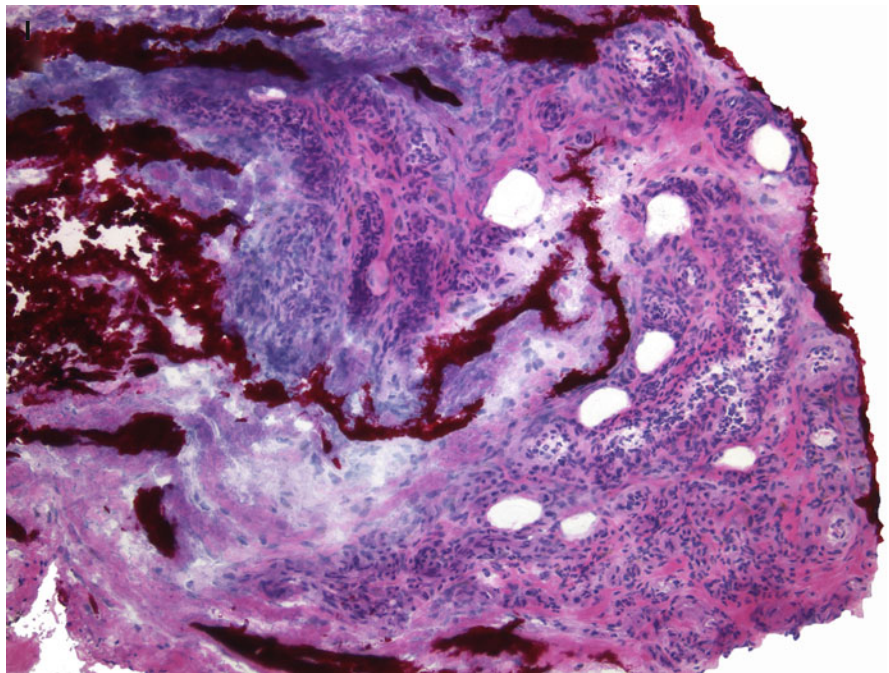
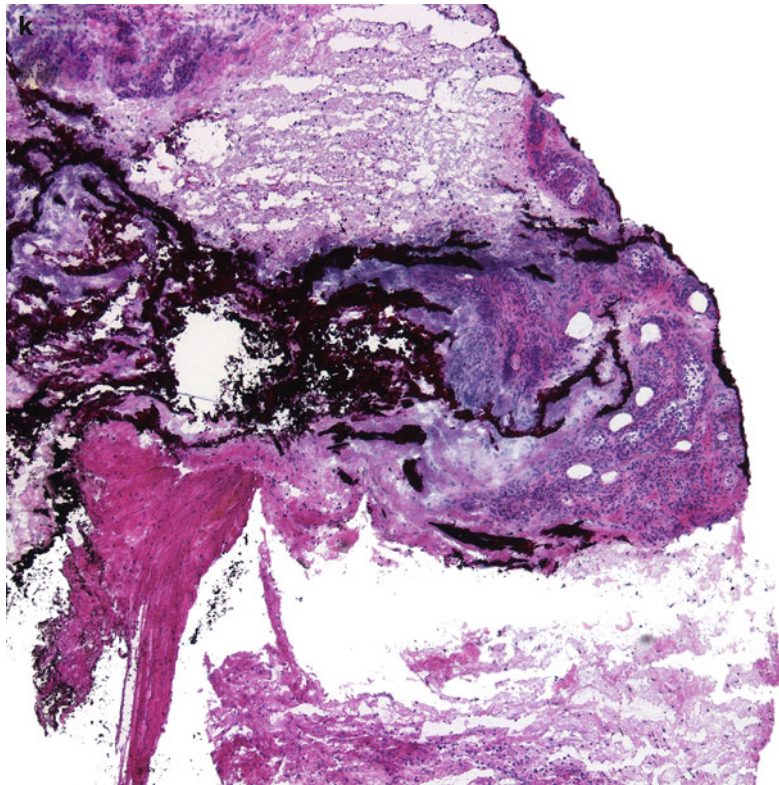
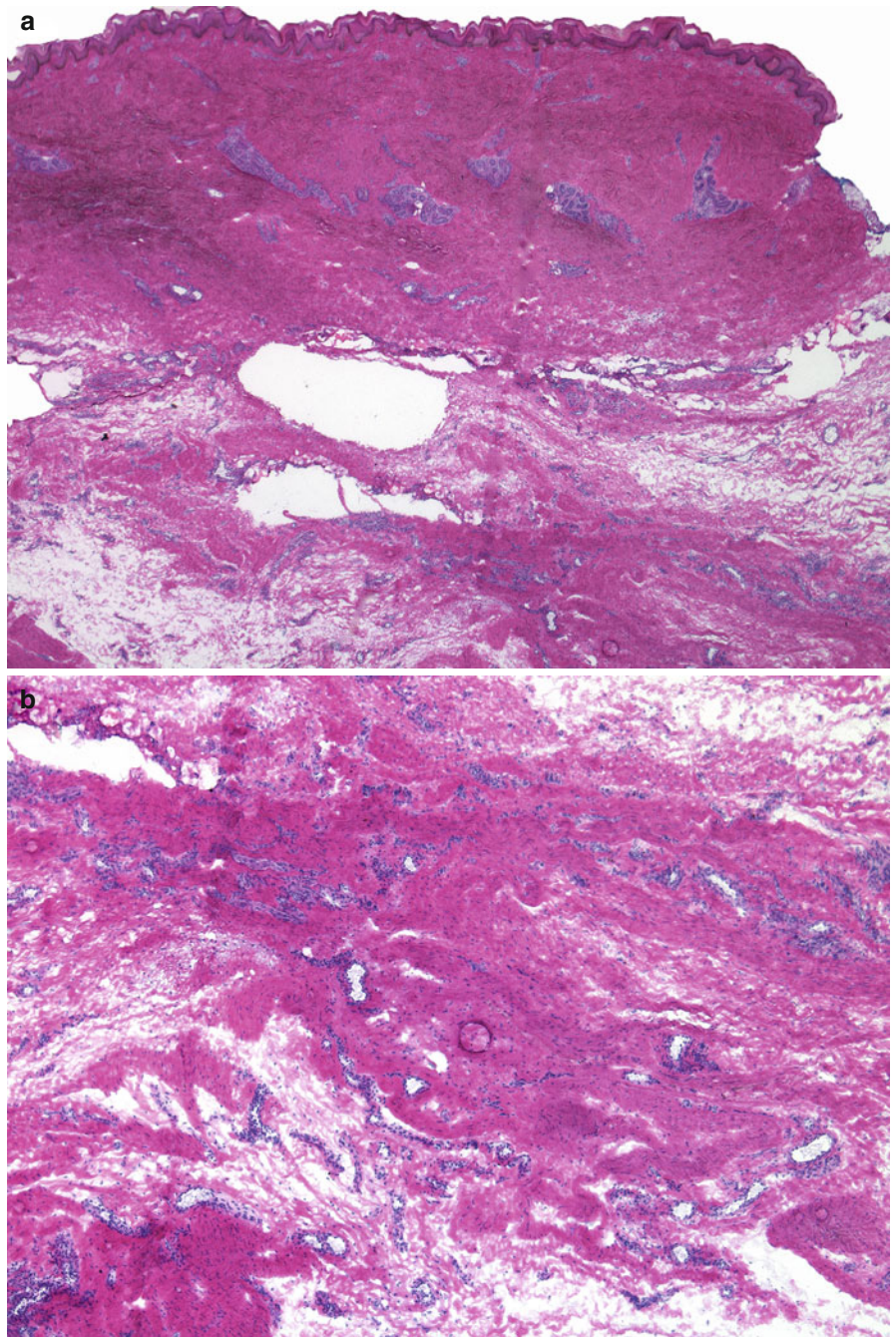


Fig. 12.6 Normal skin and scar: (a) The epidermis and dermis appear unremarkable. In the deep dermis and subcutaneous fat is a broad area of fibrosis consistent with scar tissue. (b) There is prominent scar tissue with dense eosinophilic collagen in between slender fibroblasts. Blood vessels, some with patent lumina, are easily identified within the area of fibrosis. There is also mild perivascular inflammation. There is no evidence of DFSP



Atypical Fibroxanthoma

Histologic Features

1. Malignant tumor of mesenchymal (fibrohistiocytic) origin.
2. Densely cellular.
3. Tumor starts beneath the epidermis, extends to the reticular dermis, and sometimes to the subcutis.
4. Tumor is non-encapsulated with indistinct borders and often infiltrates surrounding tissue.
5. Overlying epidermis is often ulcerated.
6. Grenz zone (a narrow layer of normal tissue beneath the epidermis that is uninvolved by the neoplastic process) can be seen.
7. Tumor is comprised of large, pleomorphic, atypical, tumor cells.
8. Neoplastic cells have hyperchromatic irregular nuclei and varying amounts of eosinophilic cytoplasm.
9. Bizarre multinucleated giant cells are often present.
10. Mitotic figures including atypical ones can be seen.
11. Adnexal structures are diminished or effaced by the tumor.
12. Solar elastosis in the adjacent dermis is invariably present.

Atypical Fibroxanthoma and Squamous Cell Carcinoma

Atypical fibroxanthoma	Squamous cell carcinoma
1. Sheet-like growth pattern of the tumor in the dermis	1. Neoplastic aggregates varying in size and shape
2. No connection between the neoplasm in the dermis and the overlying epidermis	2. Tumor originates from the overlying epidermis and extends into the dermis. Often adjacent actinic keratosis
3. Large pleomorphic cells with hyperchromatic atypical, sometimes bizarre nuclei with prominent nucleoli and moderately abundant pink cytoplasm	3. Large polygonal keratinocytes with hyperchromatic irregular nuclei and abundant eosinophilic cytoplasm
4. Tumor lacks areas demonstrating keratinization	4. Focal areas of keratinization with horn pearls and squamous eddies
5. Lack of intercellular bridges between the neoplastic cells	5. Intercellular bridges seen in between the neoplastic cells
6. Bizarre atypical multinucleated giant neoplastic cells	6. Multinucleated neoplastic cells are rare
7. Numerous mitotic figures, many of which atypical	7. Mitotic figures are present and can be atypical
8. Neoplastic cells may be spindle and may be arranged in fascicles with a storiform orientation	8. Aggregates of spindle shaped cells are present in the spindle cell variant of SCC. Individual neoplastic cells show evidence of keratinization

Extramammary Paget's Disease

Histologic Features

1. Large epithelioid cells in small groups or as individual cells scattered at all levels of the epidermis.
2. Paget cells have vesicular nuclei, large nucleoli and abundant pale, often vacuolated cytoplasm.
3. Low nuclear to cytoplasmic ratio, (abundant cytoplasm) and no intercellular bridges.
4. Atypical mitotic figures may be present.
5. Rarely the neoplastic cells contain pigment in their cytoplasm (pigmented Paget's disease variant).

A Note on Immunohistochemistry Stains

The role of the Mohs surgeon in treating spindle cell tumors is usually to differentiate tumor from non-cancerous tissue and to delineate the margin between the two which can usually be performed with hemotoxylin and eosin stains. However, the precise diagnosis of these tumors is quite challenging due to their similar cellular morphology and often a definitive diagnosis cannot be made without immunohistochemical stains. A table below serves as a quick reference for the special stains often used to discern between these tumors.

Immunohistochemical Staining Characteristics of Spindle Cell Neoplasms

	AFX	MM	LMSA*	SCC	DFSP
Cytokeratin	–	–	±	+	–
Vimentin	+	+	+	–	+
S-100	–	+	–	–	–
Desmin	–	–	+	–	–
CD34	±	–	–	–	+
CD10	+	±	±	±	±
Procollagen	+	±	±	±	+

*Leiomyosarcoma

Fig. 13.1 Atypical fibroxanthoma: (a) Low-power view of the initial biopsy of atypical fibroxanthoma showing an expansive and densely cellular nodular proliferation originating below the epidermis and extending to the deep reticular dermis. (b) Dense, spindle-cell proliferation within the dermis extending to but not involving the epidermis

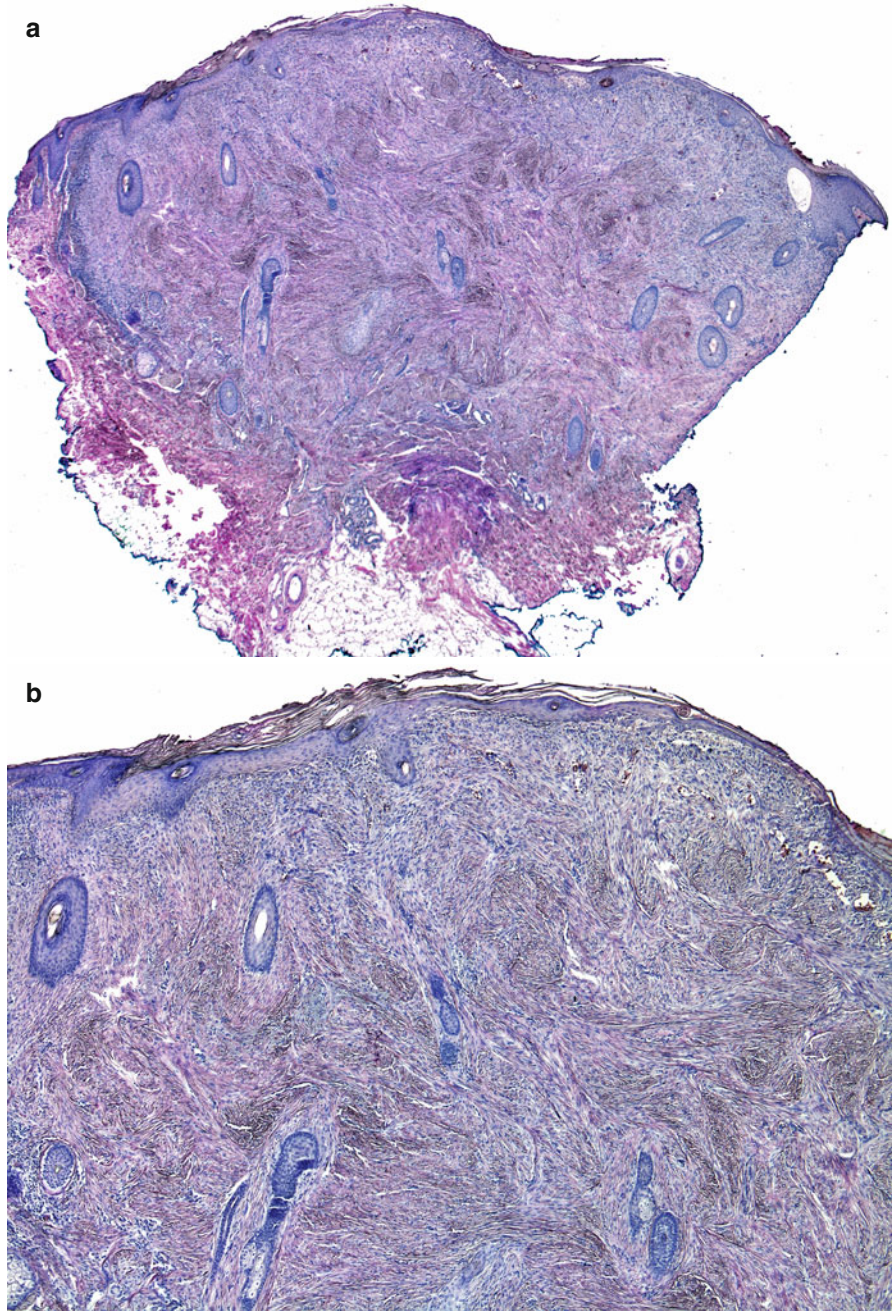


Fig. 13.1 (continued) (c) Tumor consists of fascicles of slightly pleomorphic spindle cells in a storiform arrangement. The epidermis is focally attenuated and covered by a scale crust. (d) Haphazardly arranged, pleomorphic spindled neoplastic cells admixed with inflammatory infiltrate. Numerous mitotic figures are present (thick arrows). A thin arrow designates an atypical mitosis

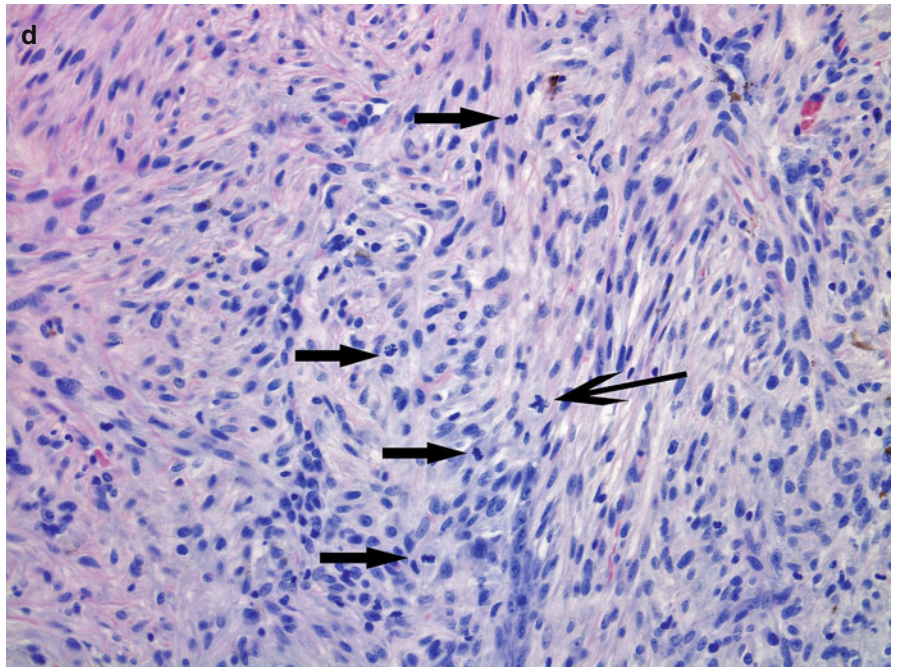
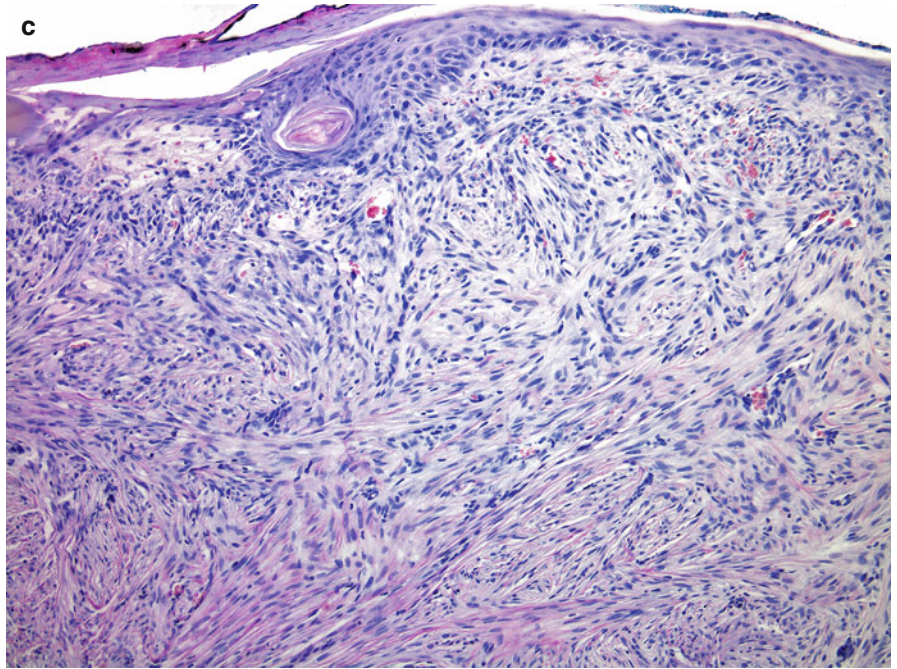


Fig. 13.2 Atypical fibroxanthoma: (a) Poorly circumscribed cellular proliferation originating immediately beneath the epidermis and extending to the mid reticular dermis. There is a narrow Grenz zone between the epidermis and tumor in the dermis. (b) Sheet-like dense proliferation of neoplastic cells throughout the subcutaneous fat, focally surrounding and invading skeletal muscle

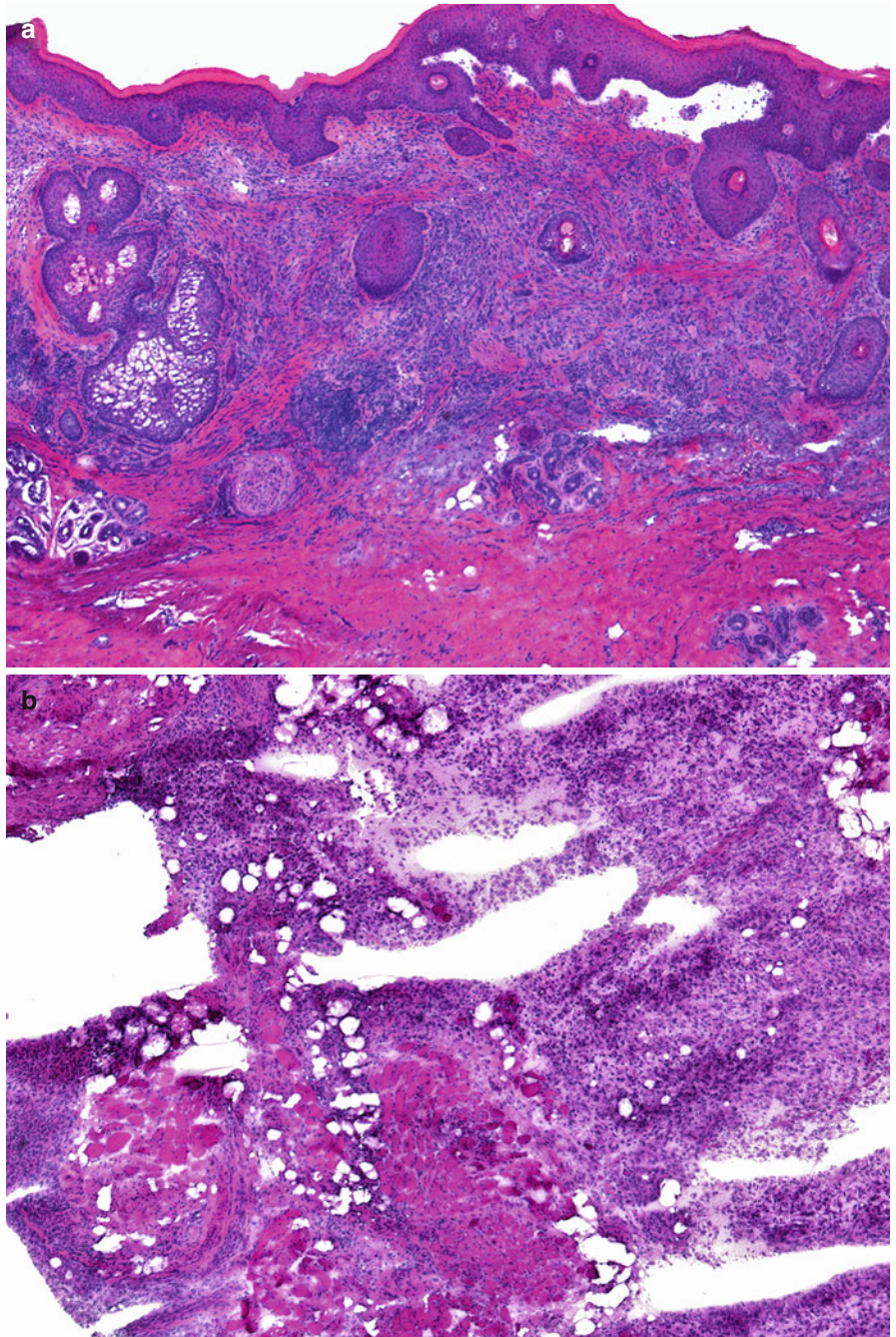


Fig. 13.2 (continued) (c) High magnification demonstrates polygonal and oval neoplastic cells with large pleomorphic and hyperchromatic nuclei. (d) This photomicrograph illustrates the spectrum of cellular and nuclear pleomorphism in this tumor. Note the several bizarre multinucleated neoplastic giant cells, characteristic of AFX and apparent at this magnification

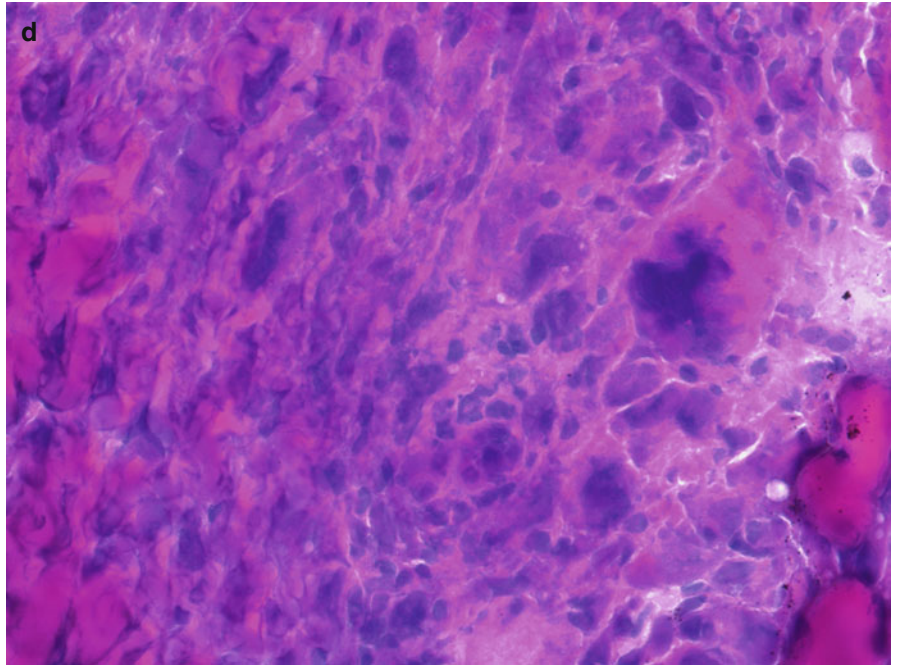
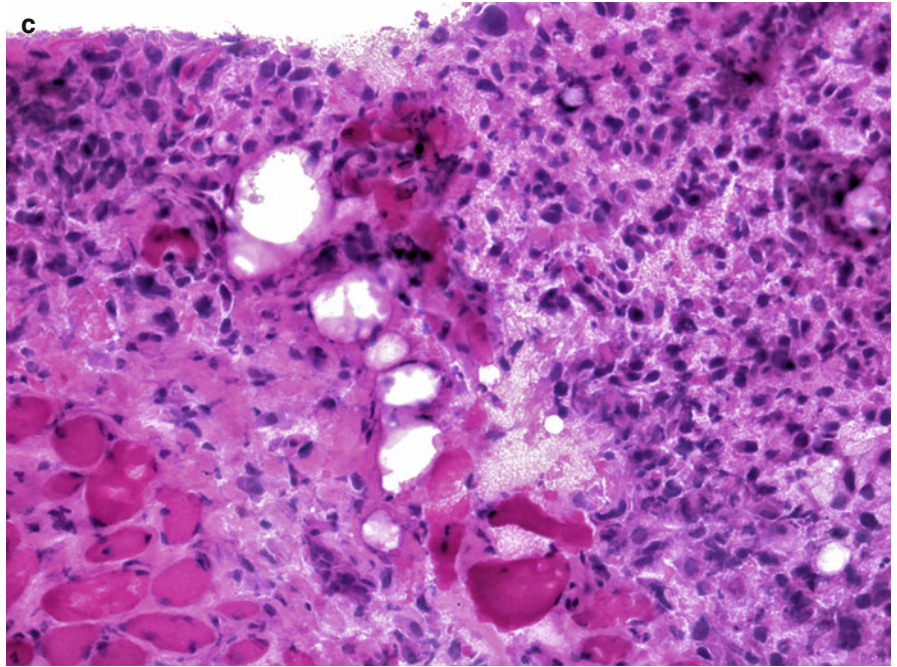


Fig. 13.3 Atypical fibroxanthoma:
(a) Expansive nodule deep in the subcutaneous fat and infiltrating skeletal muscle. (b) Neoplastic cells are arranged in a sheet-like and storiform fascicular pattern, infiltrating skeletal muscle

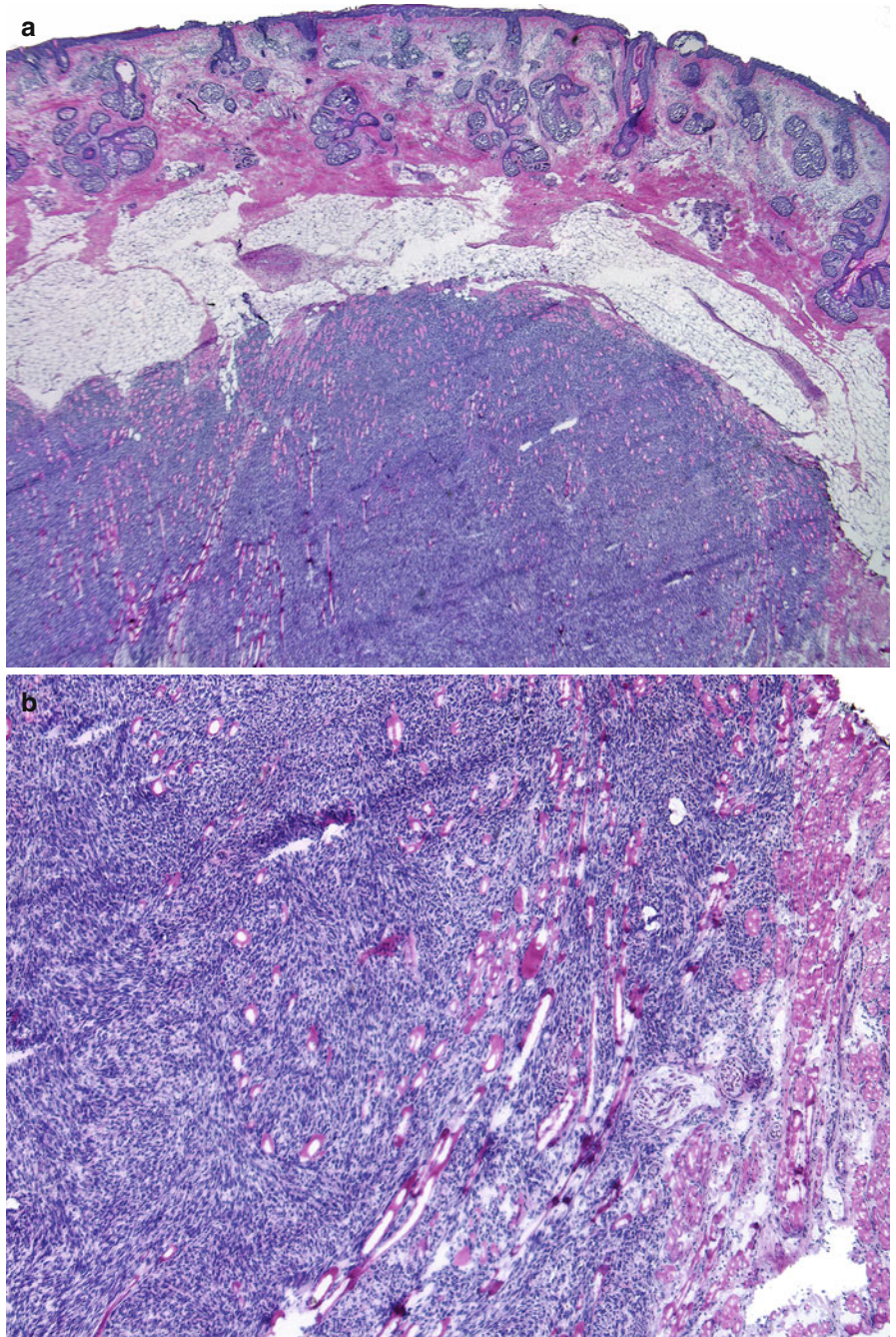


Fig. 13.3 (continued) (c) Dense proliferation of large, atypical, spindle-shaped neoplastic cells with irregular hyperchromatic nuclei, focally surrounding skeletal muscle in the right upper corner of the photograph

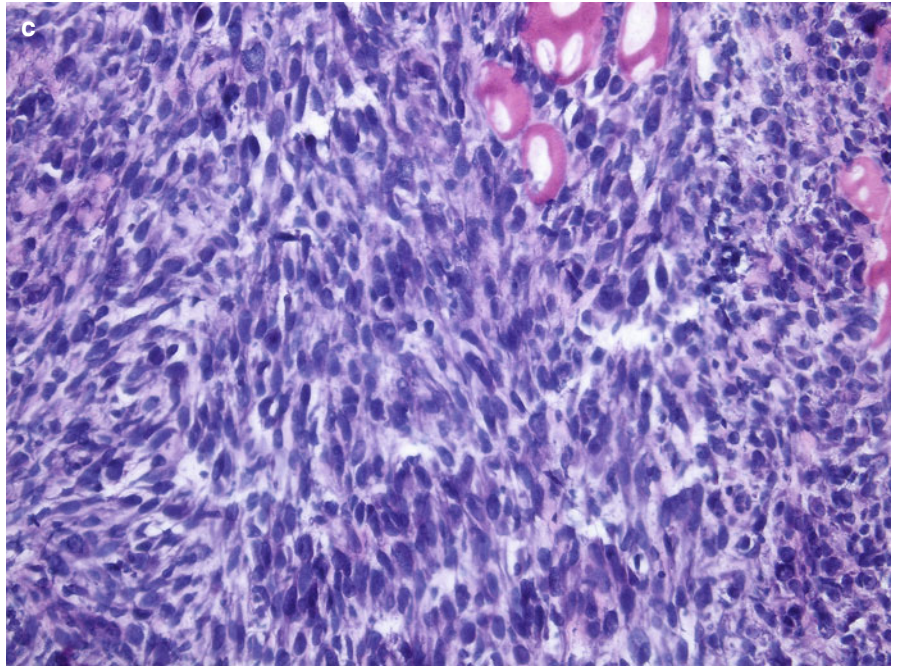


Fig. 13.4 Atypical fibroxanthoma:
(a) Tumor with ill-defined borders.
(b) Pleomorphic round and irregularly shaped neoplastic cells in a storiform arrangement in between collagen bundles and around adnexal structures

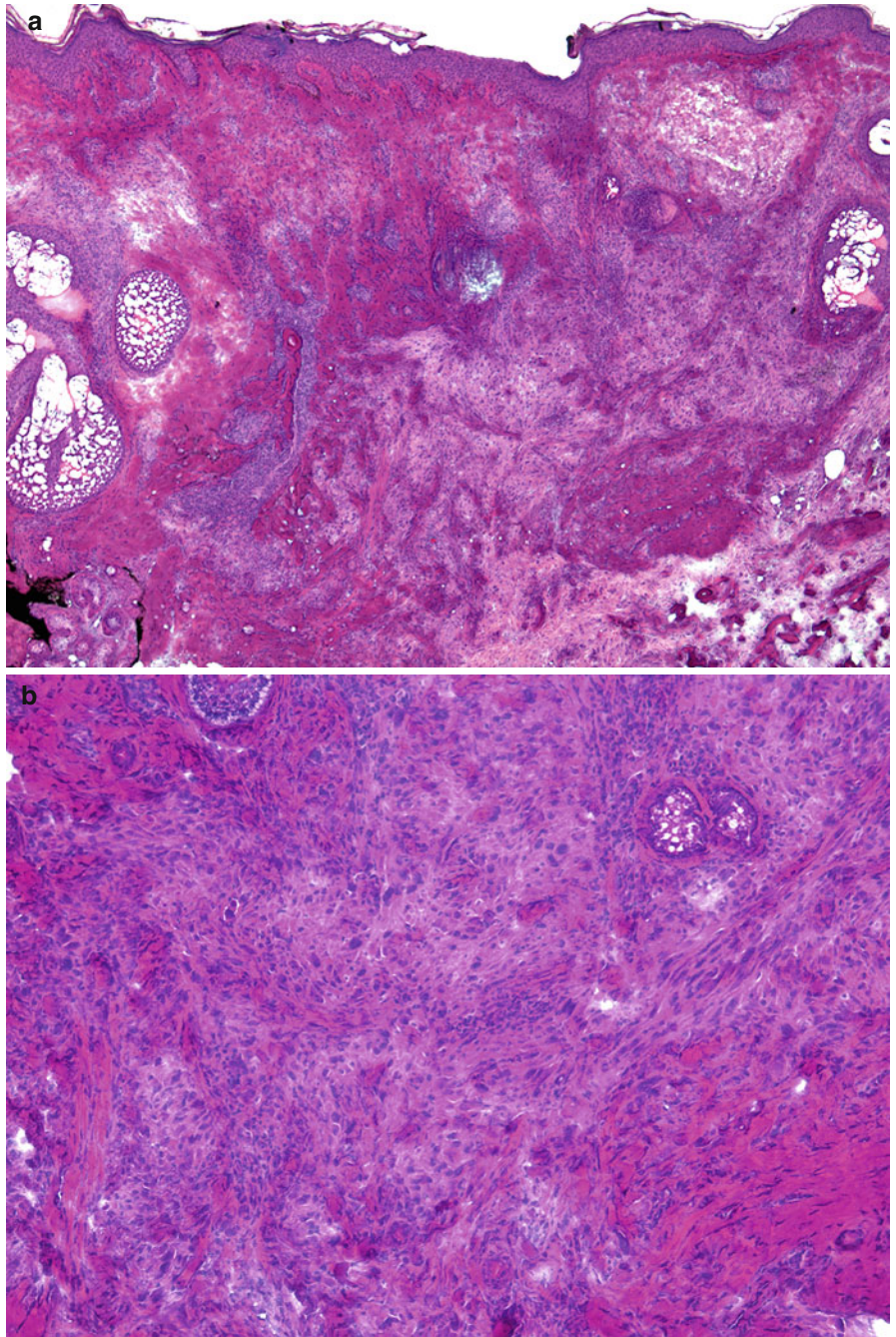


Fig. 13.5 Atypical fibroxanthoma:
(a) Scanning magnification shows a densely cellular proliferation in the reticular dermis with effacement of adnexal structures.
(b, c) Large, atypical hyperchromatic cells and numerous bizarre giant cells

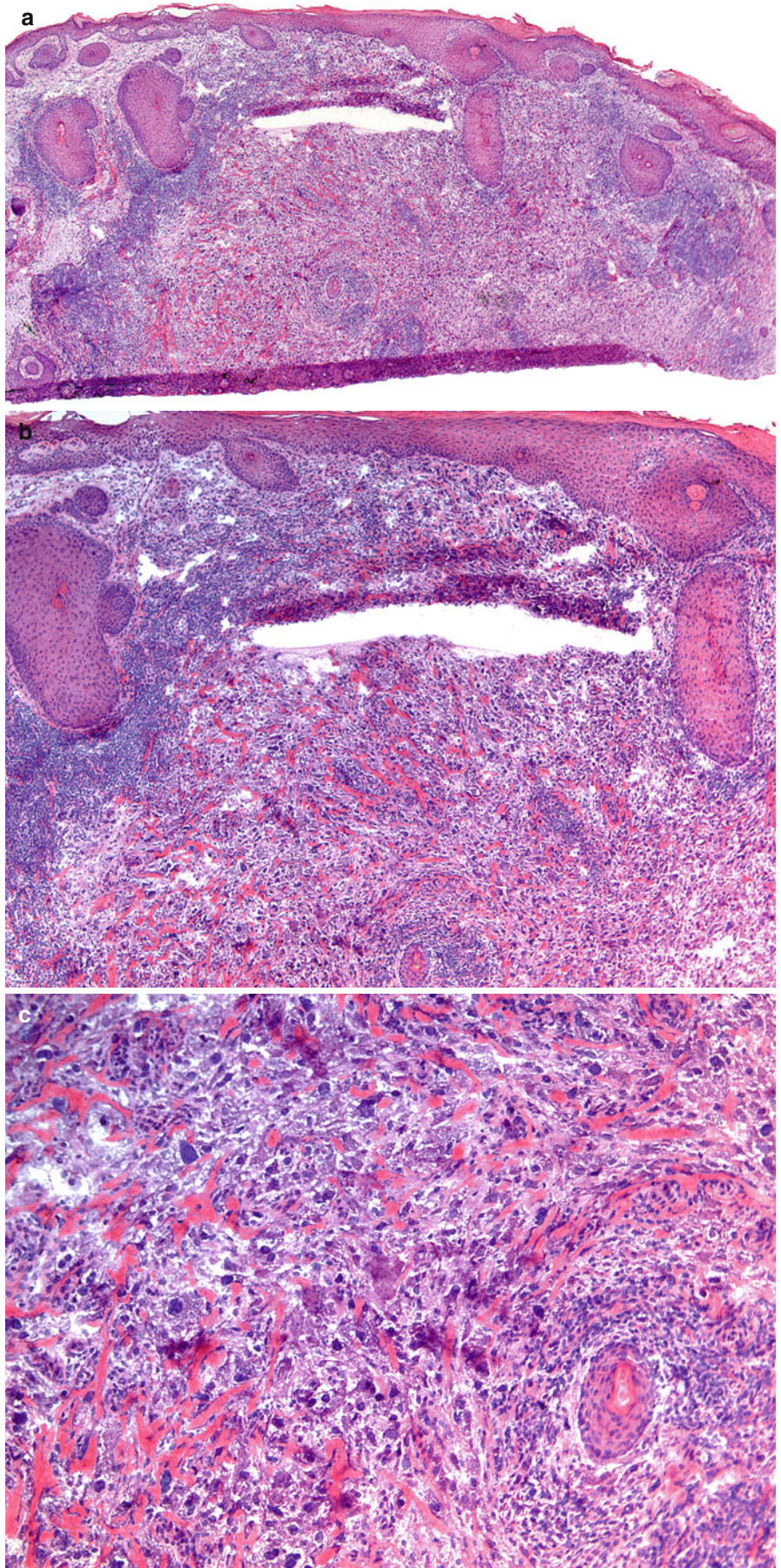
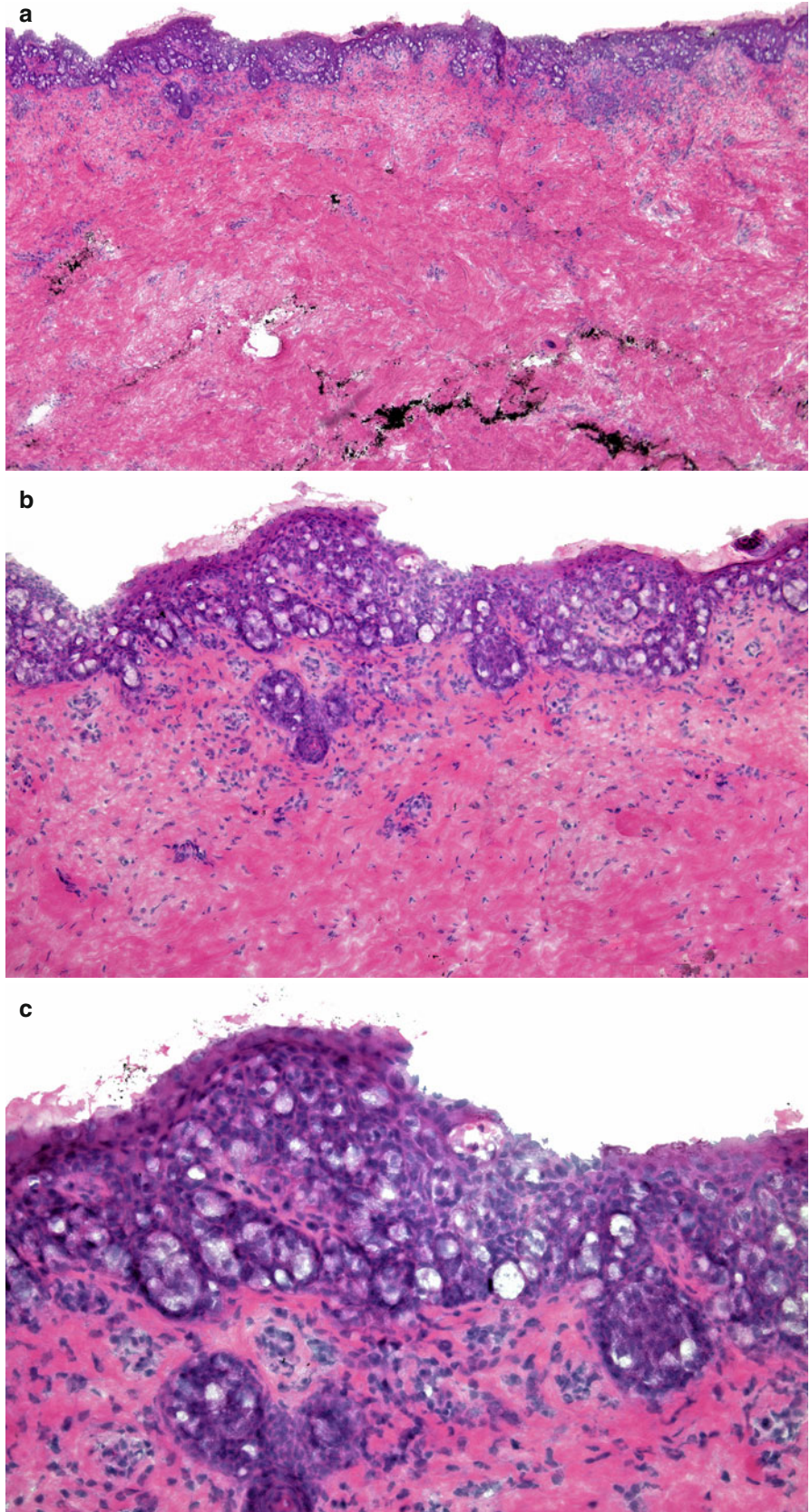


Fig. 13.6 Extramammary Paget's disease: (a) A low-power view showing numerous large pale cells throughout the epidermis. (b) Large pale cells of Paget's disease within the epidermis. Many of the Paget cells are clustered together, whereas others are dispersed as single cells at all levels within the epidermis. (c) Large vacuolated Paget cells with abundant pale cytoplasm, arranged individually or in groups. The neoplastic cells are seen above a flattened basal layer



Incidental Findings

Nevus

Benign intradermal or compound nevi are symmetrical and well circumscribed. Nevus cells are arranged in nests and cords. The nests are uniform in size and shape and mature with their descent into the dermis. The nevus cells have round or oval shape, vesicular nuclei, and scant pale cytoplasm. The melanocytes are monomorphous and mitotic figures are absent.

Neurofibroma

A neurofibroma is a circumscribed, non-encapsulated dermal neoplasm composed of slender spindled cells embedded in mucinous stroma. Numerous small blood vessels are seen throughout the neoplasm. The nuclei are wavy and slender. There are an increased numbers of mast cells.

Epidermal Inclusion Cyst

There is a cystic space in the dermis lined by epithelium that resembles the surface epidermis and the infundibular portion

of hair follicles. Within the cyst cavity is laminated keratin. With a ruptured cyst there is an associated granulomatous inflammation containing histiocytes and foreign-body type multinucleated giant cells.

Milium is a small cyst located in the superficial dermis, which arises from the infundibulum of vellus hairs. The wall is composed of thin, stratified, squamous lining.

Seborrheic Keratosis

Benign neoplasm with a flat base composed of monomorphous keratinocytes. There is acanthosis, pseudohorn cysts, and basket-woven hyperkeratosis. In addition, melanin pigment is often present. In cases of inflamed seborrheic keratoses, the keratinocytes may display significant reactive atypia.

Solar Lentigo

Elongated rete ridges with prominent melanin pigment at their bases. Invariably there is prominent solar elastosis in the dermis.

Fig. 14.1 Intradermal melanocytic nevus: (a) Dome-shaped intradermal melanocytic nevus composed of nests of darkly stained melanocytes. The nevus is symmetric and well delineated. (b) Basaloid nests of nevus cells with high nuclear to cytoplasmic ratio. There is maturation of the melanocytes with their descent into the dermis

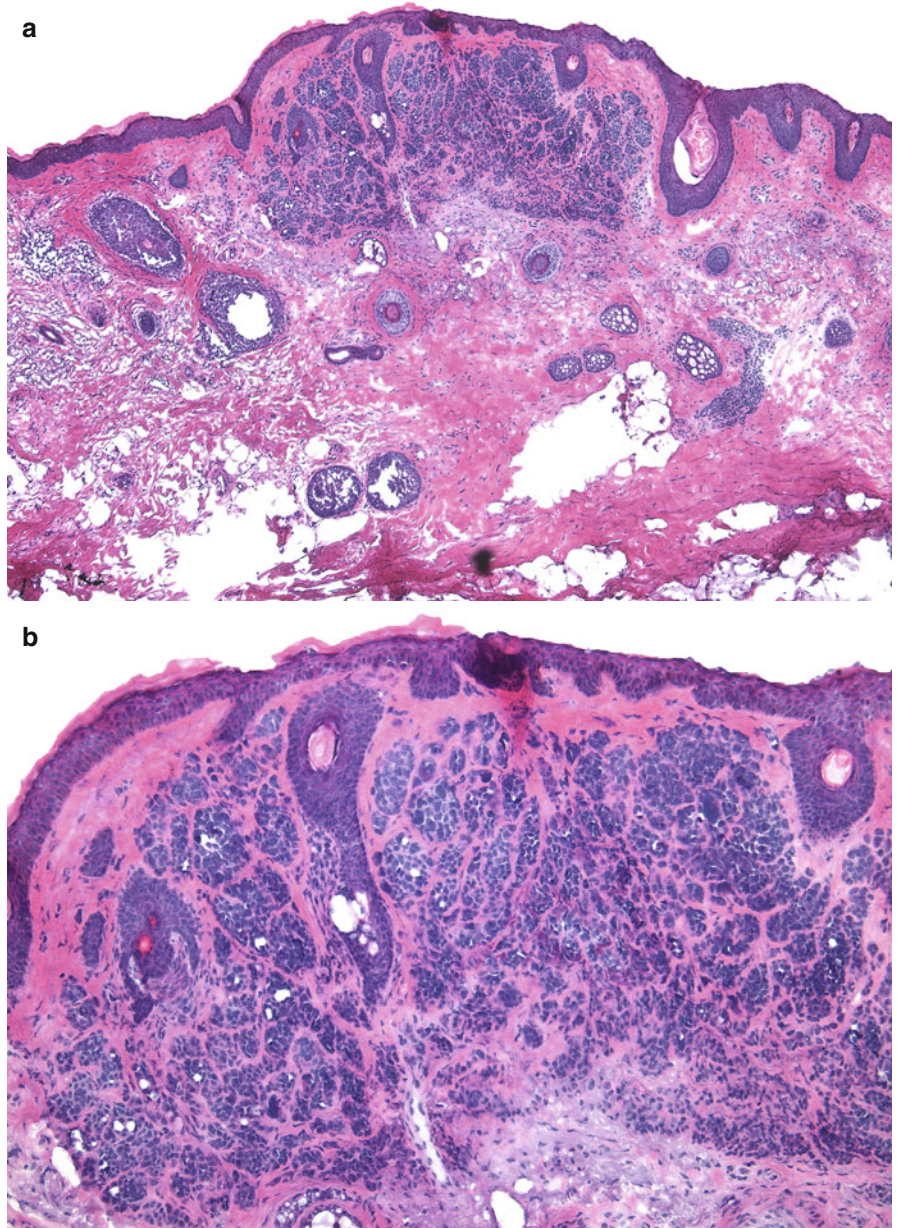


Fig. 14.2 Intradermal melanocytic nevus: (a) Nevus cells are grouped in clusters and nests that resemble the basaloid aggregates of basal cell carcinoma. (b) Round and oval melanocytic nests are seen in the superficial dermis. There is maturation with a decrease in size of the melanocytic nests in the dermis. Unlike the neoplastic aggregates of BCC, which have irregular angulated shapes, the melanocytic nests are round to oval. There is no peripheral palisading or clefting

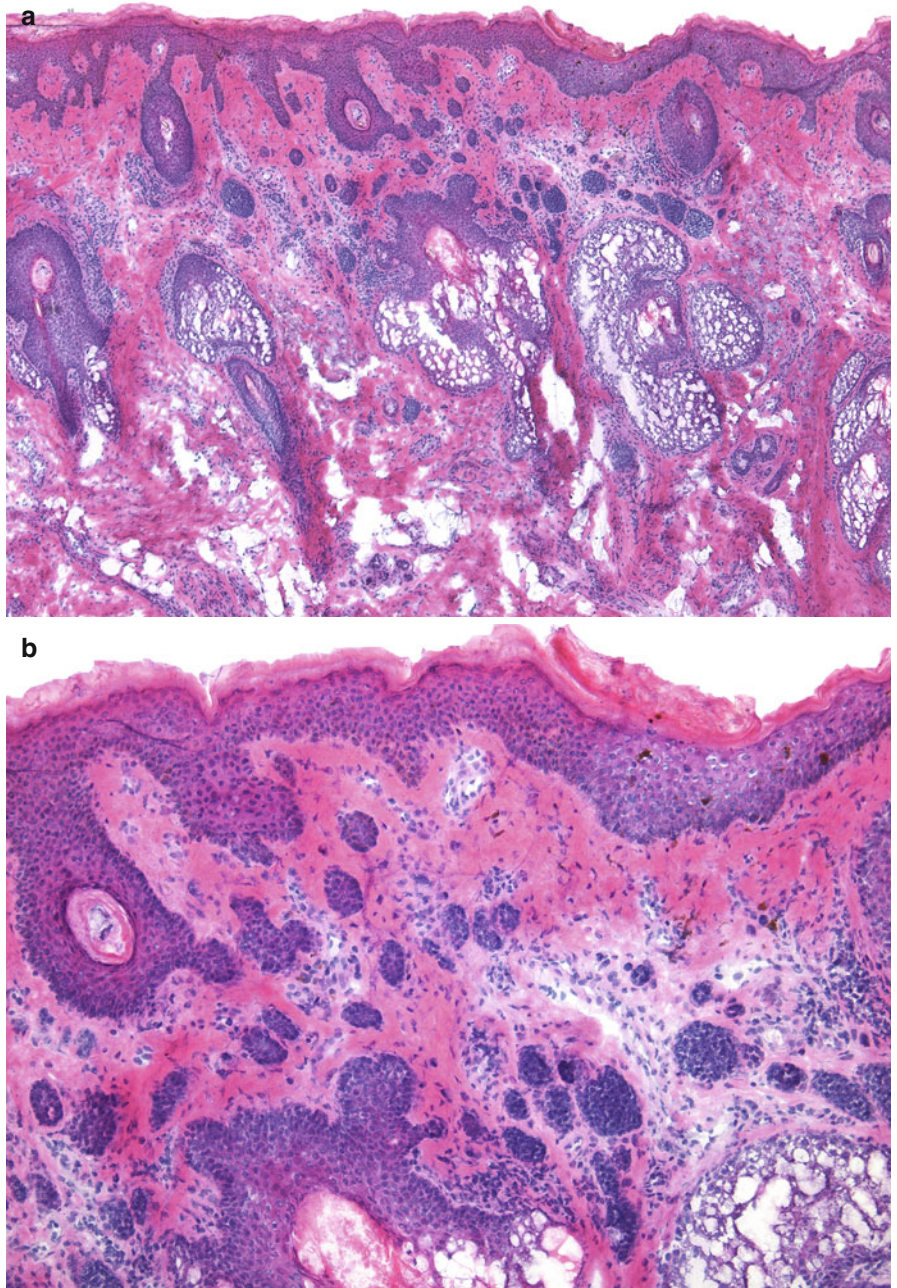


Fig. 14.3 Incidental intradermal melanocytic nevus and a small osteoma cutis: melanocytic nests are present in the papillary and upper reticular dermis. A round dark purple nodule in the right lower corner represents a small osteoma cutis

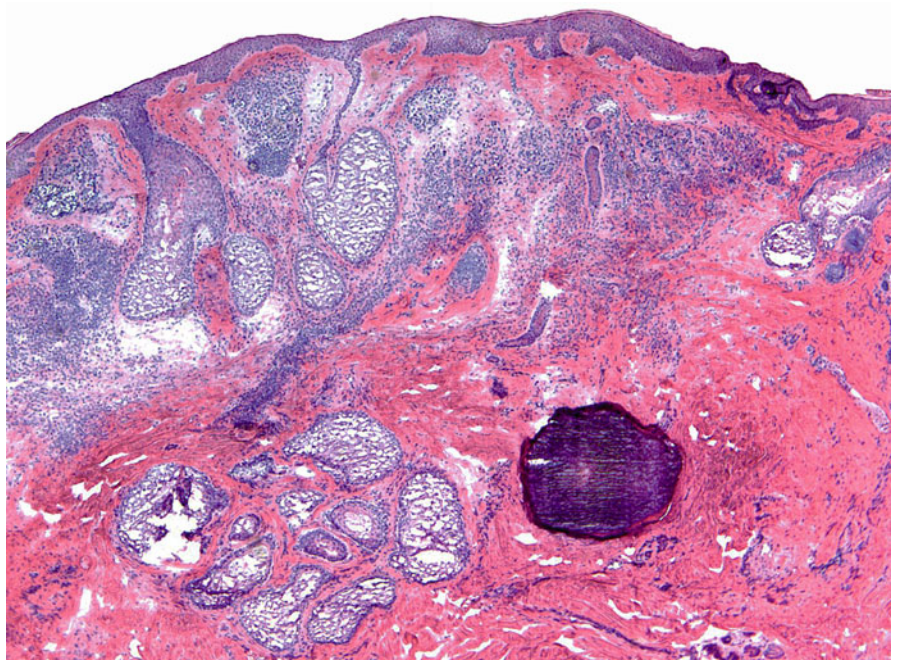


Fig. 14.4 Neurofibroma: (a) A well-delineated, non-encapsulated, basophilic nodule in the deep dermis. (b) The nodule is composed of slender spindle cells embedded in mucinous stroma

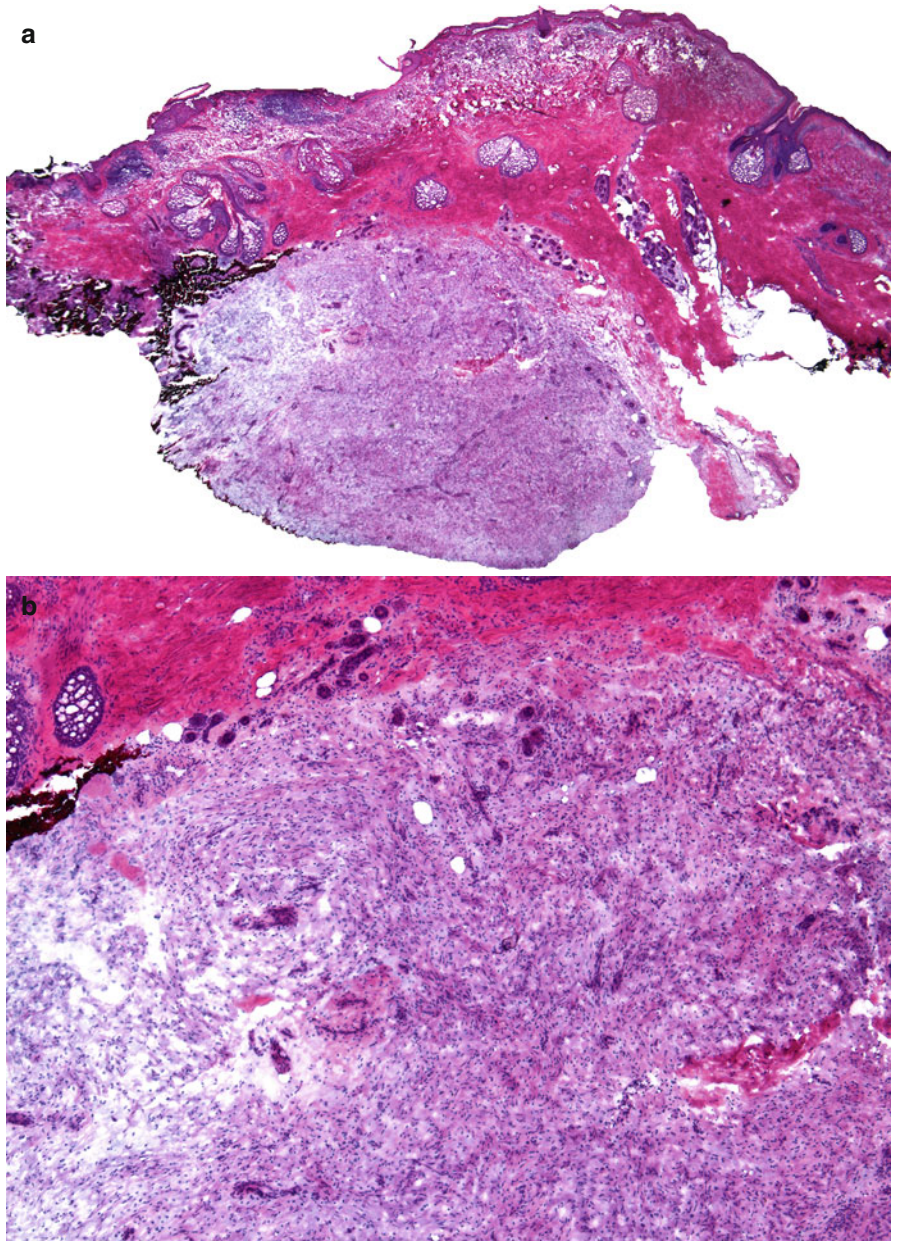


Fig. 14.4 (continued) (c) Bland, oval to spindled cells, surrounded by mucin. A few mast cells are present (arrows)

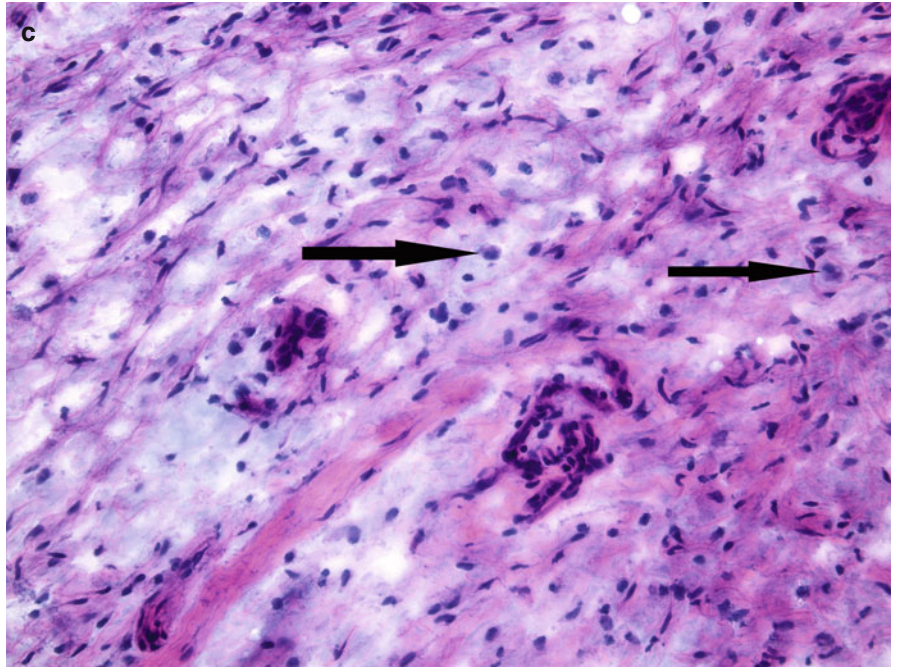


Fig. 14.5 Granulomatous inflammation: (a) In the center of this photomicrograph is a hair shaft surrounded by granulomatous inflammation. This process may be mistaken for a neoplasm if the inflammatory nature of the infiltrate containing multinucleated giant cells is not appreciated. (b) Centrally located, distorted hair shaft with surrounding granulomatous inflammation containing histiocytes and multinucleated giant cells

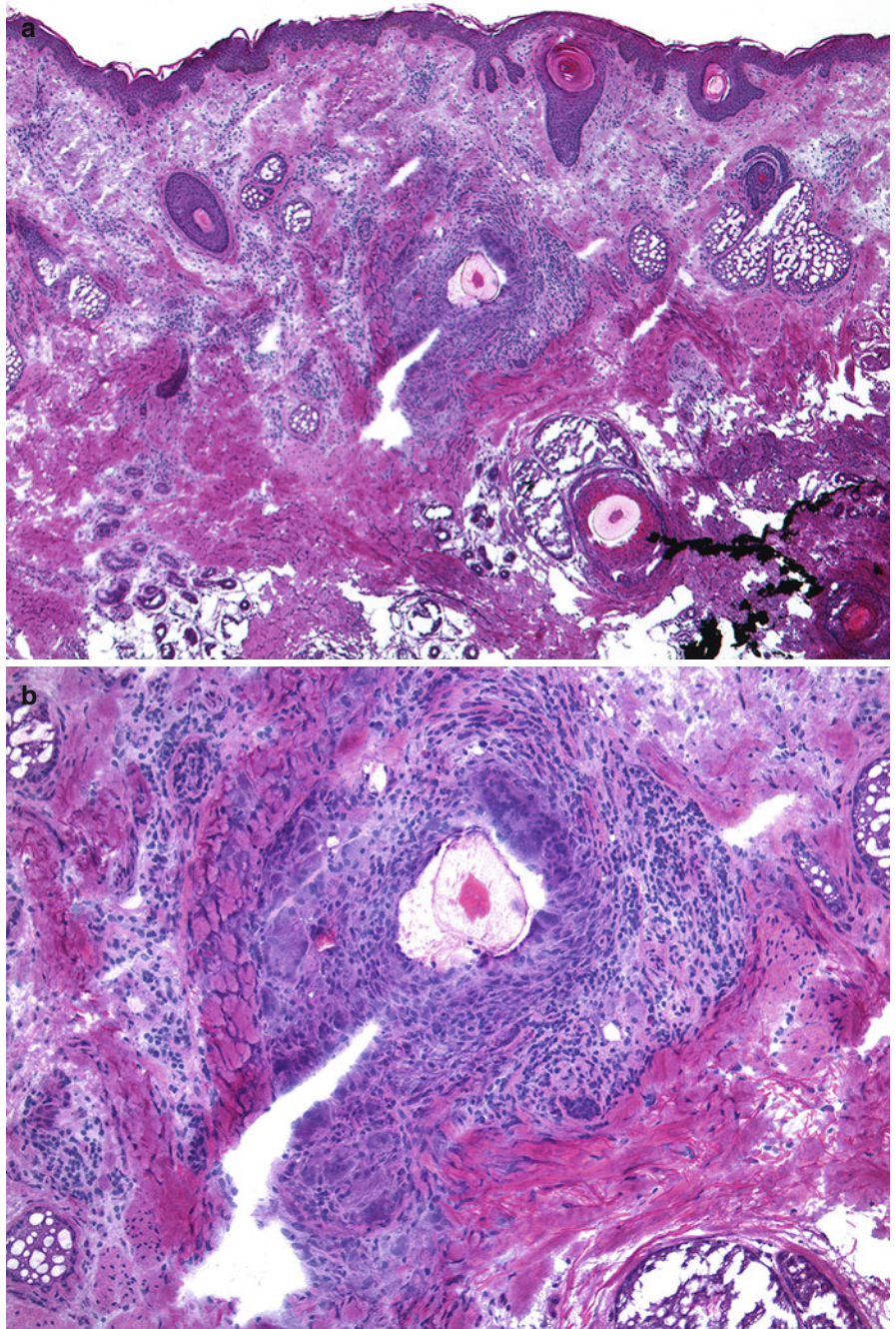


Fig. 14.5 (continued) (c) High-power view demonstrating numerous foreign body type multinucleated giant cells surrounding the hair shaft

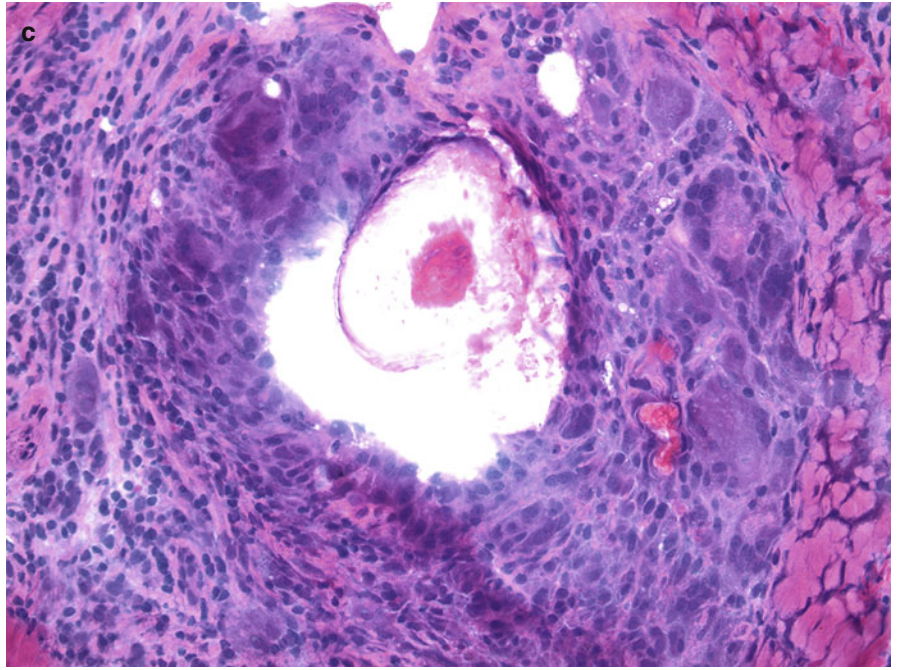


Fig. 14.6 Granulomatous inflammation:
(a) This section shows a recent scar with eosinophilic collagen and increased number of fibroblasts on the left. There is a focal area of granulomatous inflammation to the right of the scar. (b) The scar in the dermis on the left shows increased number of fibroblasts and newly formed eosinophilic collagen bundles. Many vessels are vertically oriented

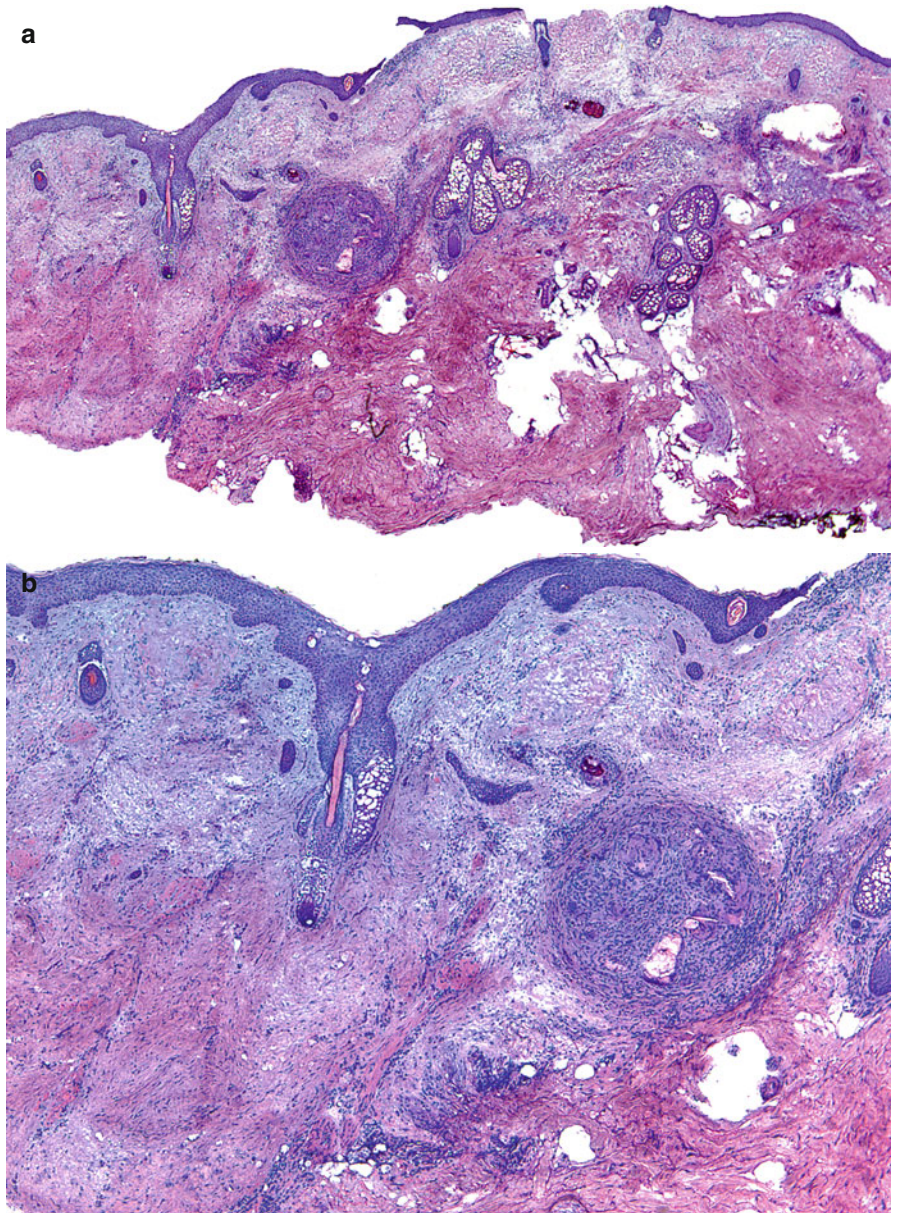


Fig. 14.6 (continued) (c) There is a granuloma composed of epithelioid histiocytes and foreign body type multinucleated giant cells, focally surrounding free keratin

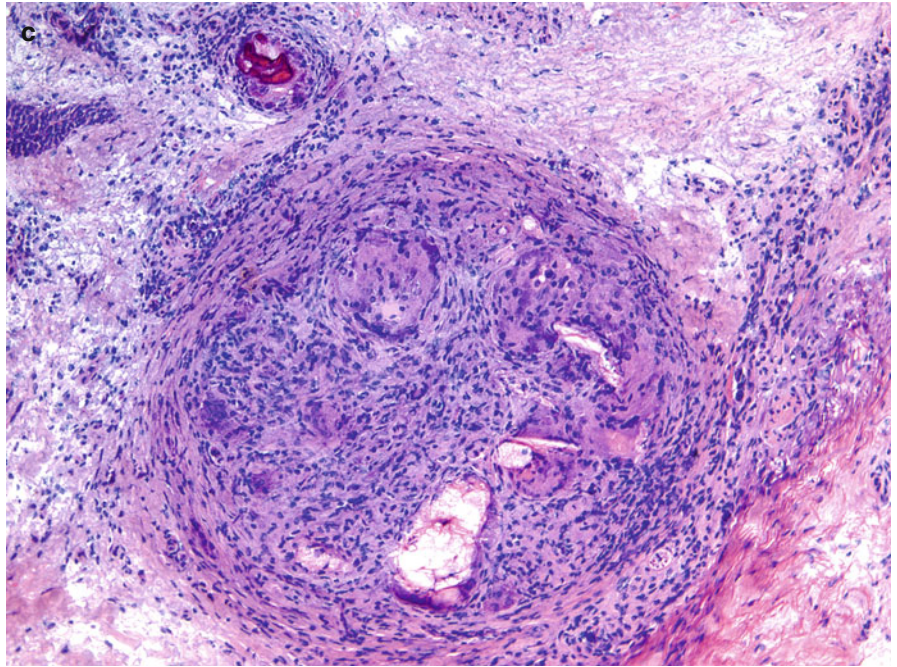


Fig. 14.7 Suture granuloma: (a) Focal dense inflammation surrounding suture fragments in the dermis. (b) Higher magnification demonstrates multinucleated giant cells as well other inflammatory cells surrounding linearly oriented suture material (*arrows*)

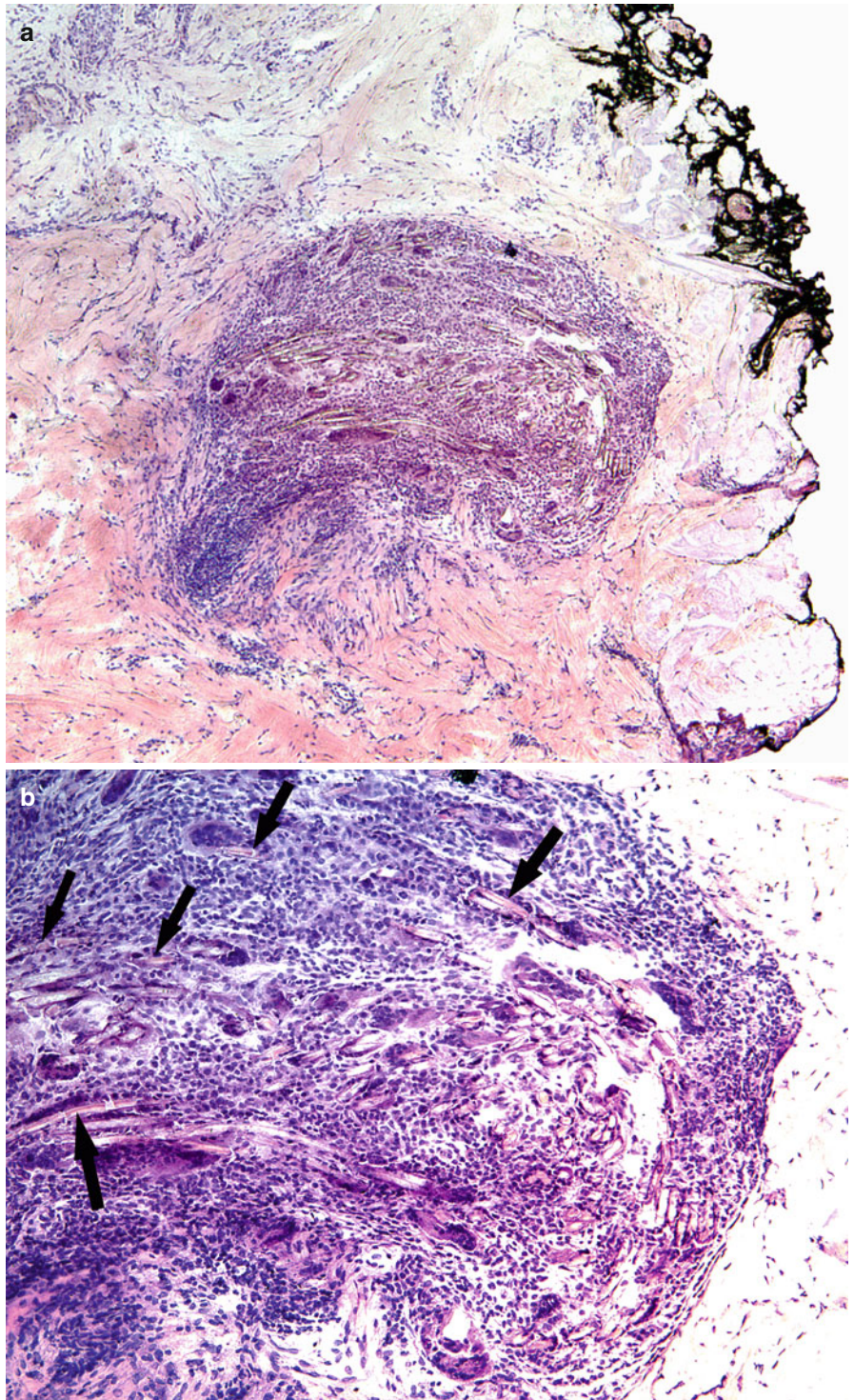


Fig. 14.8 Seborrheic keratosis, inflamed: (a) Acanthosis of the epidermis, flat base, keratin filled pseudohorn cysts, and a lichenoid lymphocytic inflammation. (b) The epidermis is tangentially cut and there is an a lymphocytic infiltrate at the base of the epidermis. The keratinocytes are small and monomorphous

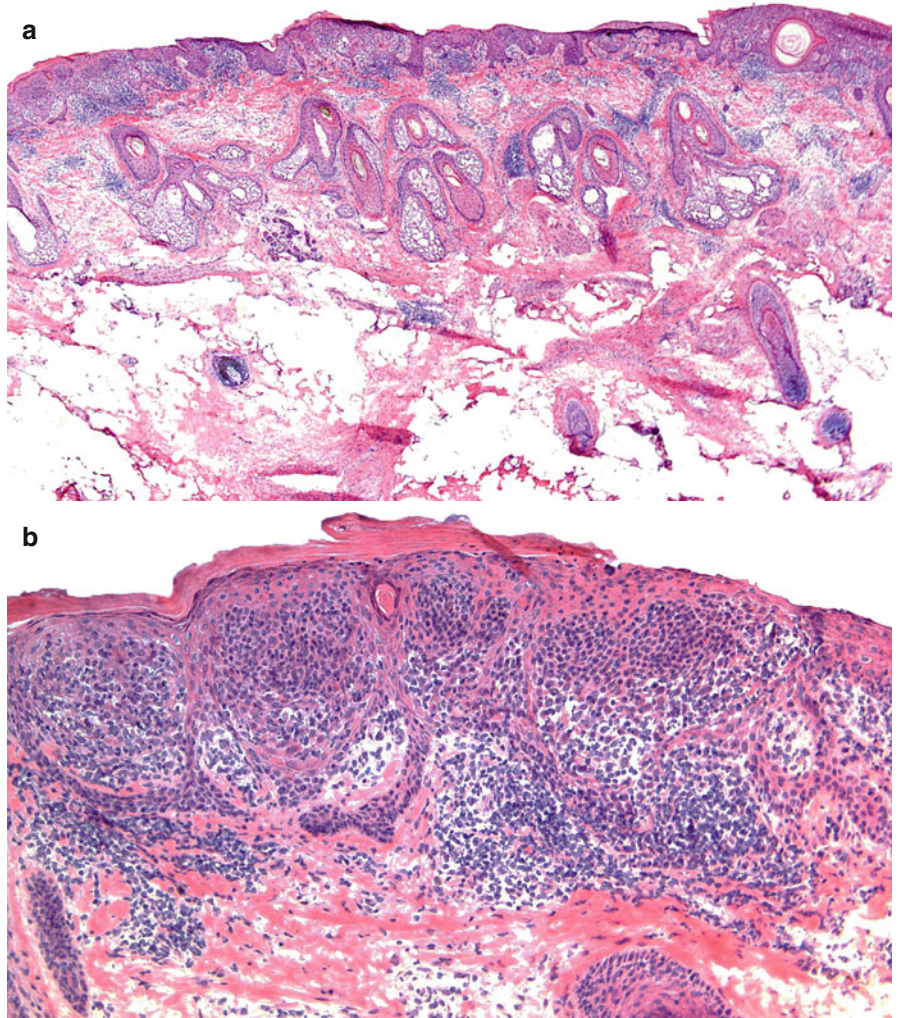


Fig. 14.9 Seborrheic keratosis, inflamed: (a) Acanthotic and slightly hyperkeratotic epidermis with a flat base and pseudohorn cysts. (b) There is mild cytologic atypia of the keratinocytes near the base of the epidermis secondary to inflammation

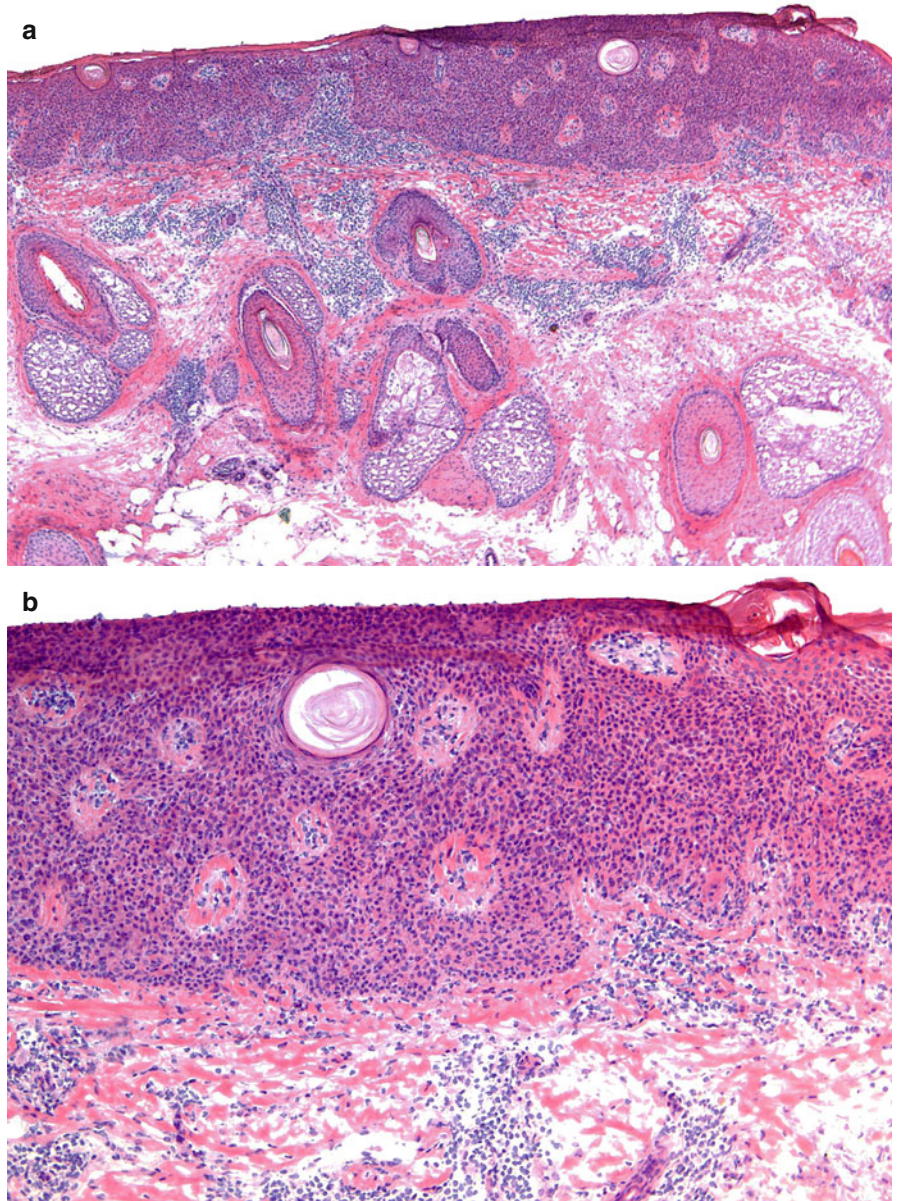


Fig. 14.10 Solar lentigo: (a) Hyperplastic epidermis with overlying hyperkeratosis. (b) Elongation of the rete ridges and basilar pigmentation are seen

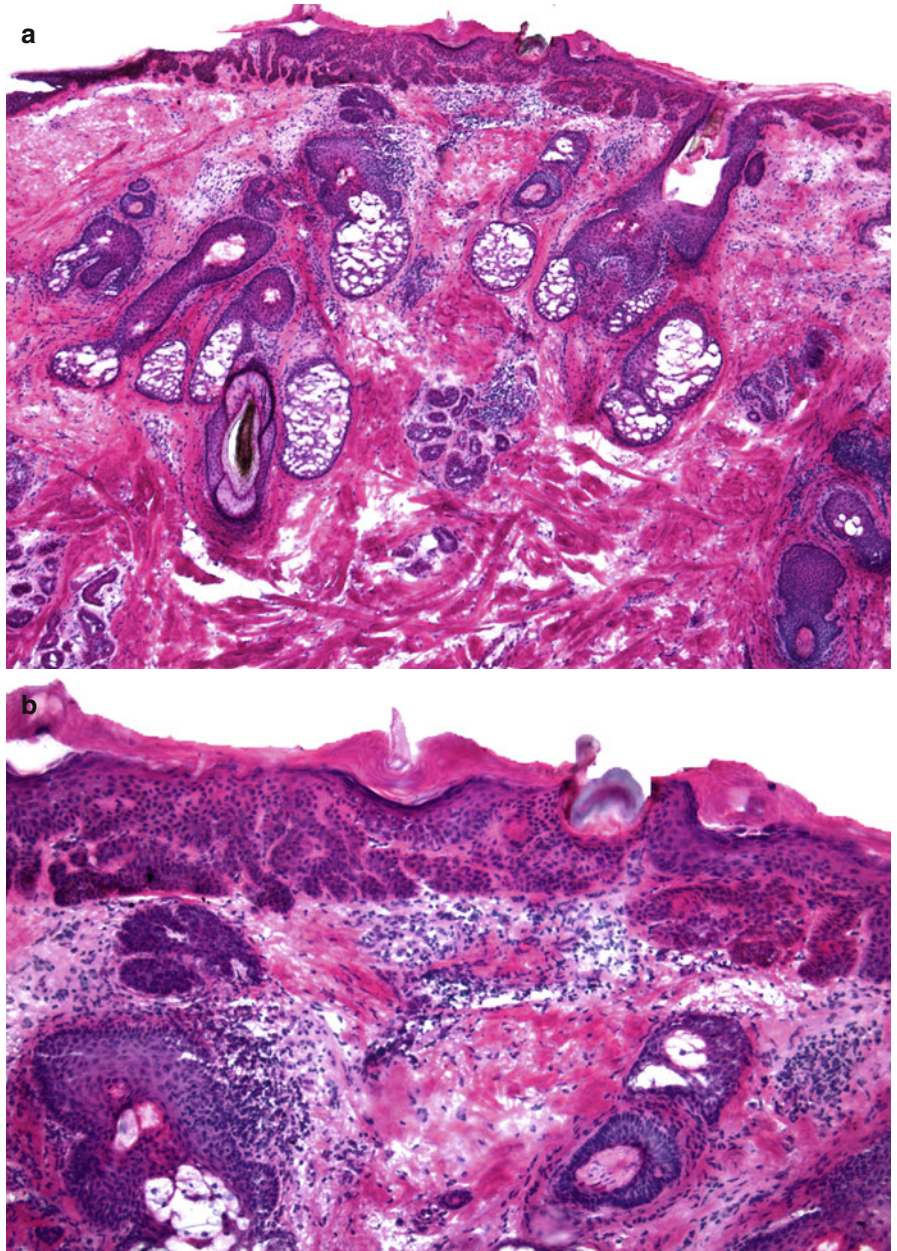


Fig. 14.11 Cyst and lentigo: (a) A small infundibular cyst is present in the superficial dermis. A solar lentigo with elongated pigmented rete ridges is noted in the overlying epidermis. (b) Laminated keratin fills a cystic space lined by a few layers of squamous epithelium. Heavily pigmented bases of elongated rete ridges are noted in conjunction with solar elastosis in the dermis

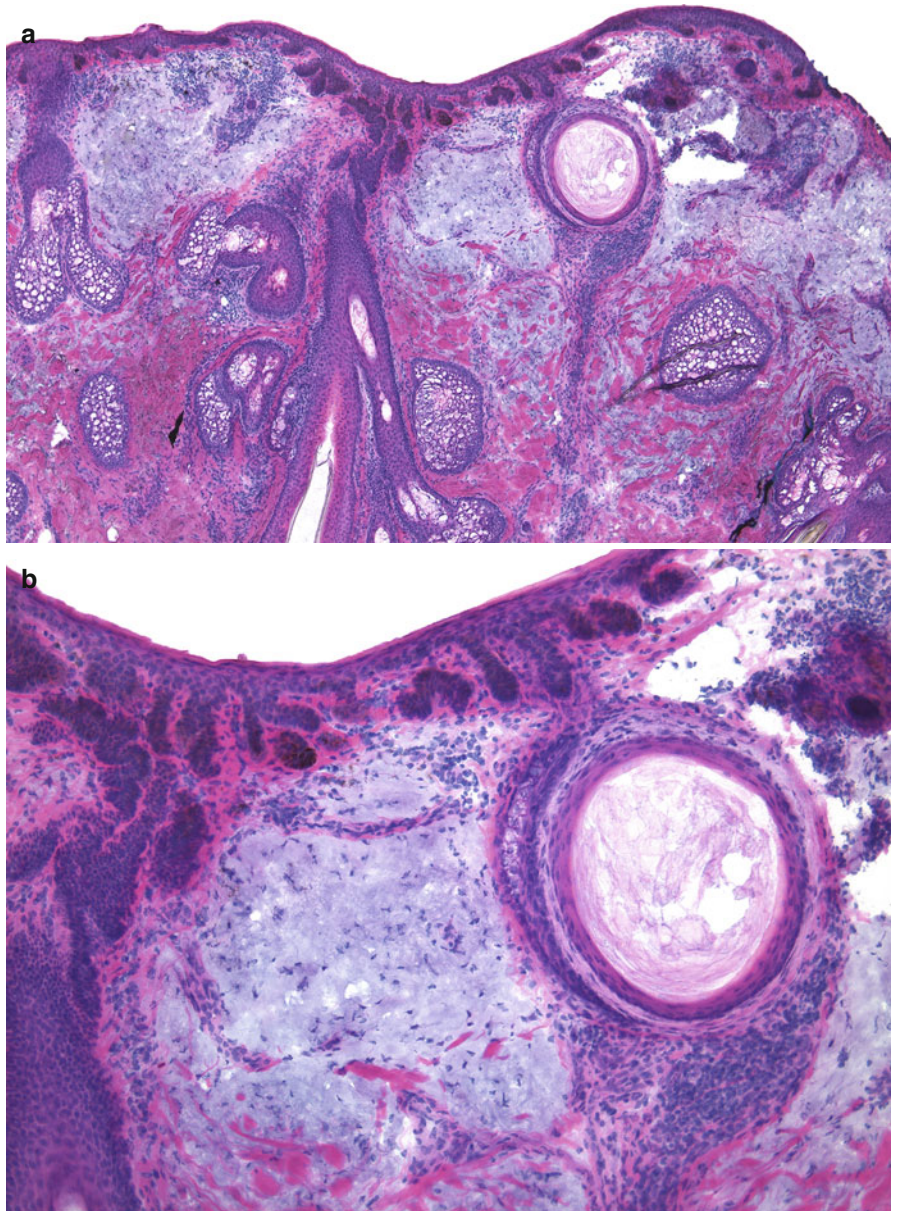


Fig. 14.12 Scar: (a) Newly formed scar tissue comprising the entire portion of dermis. (b) Thick, newly formed collagen in a somewhat branching fashion is seen in the right upper corner (*ellipse*). Thin, newly formed blood vessels, oriented perpendicular to the skin surface, are also noted (*arrows*). Newly excised scars can be challenging for the Mohs surgeon because of the dense cellularity and inflammation, which may be misconstrued as infiltrative carcinoma

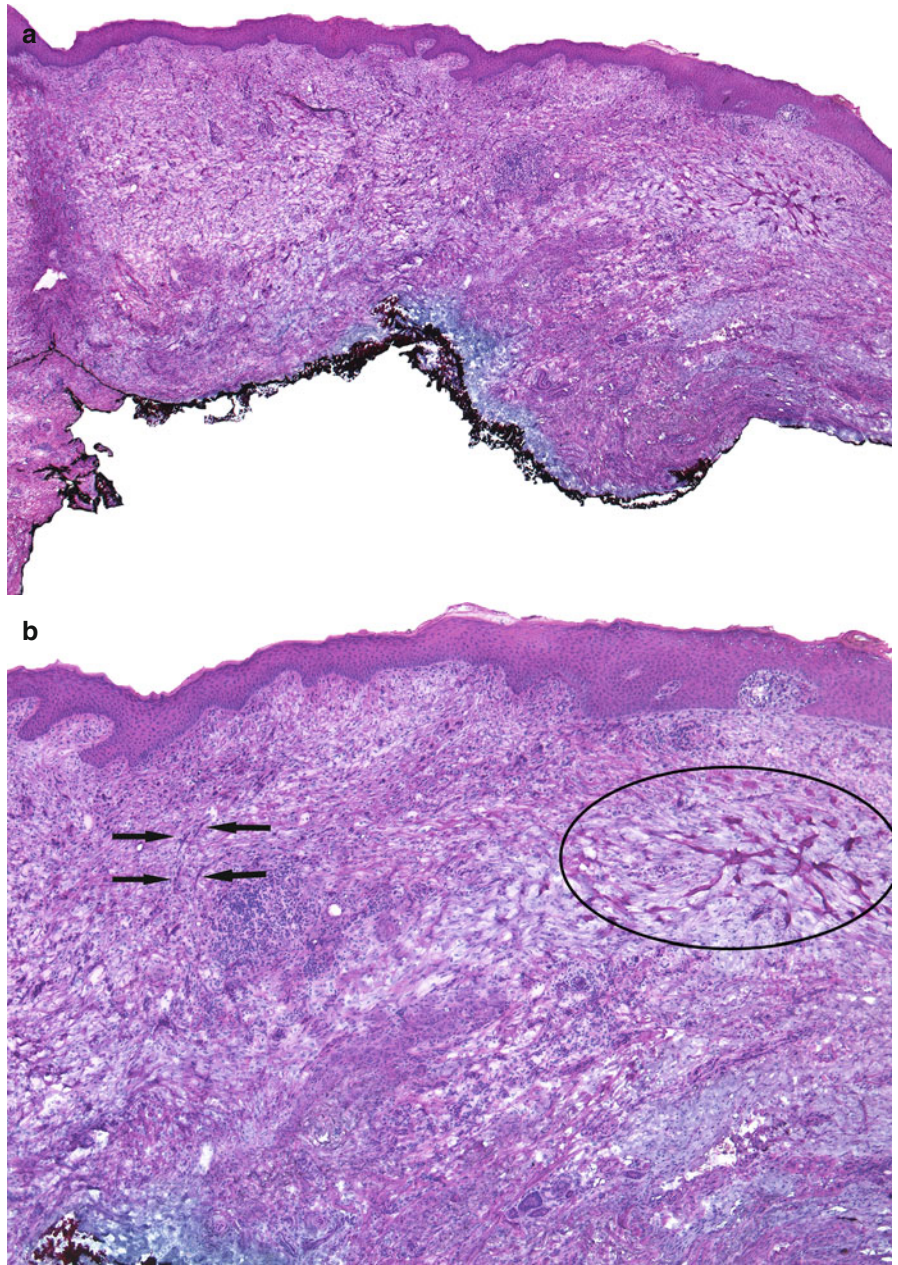


Fig. 14.12 (continued) (c) There is dense cellularity within the scar and a focus of granulomatous inflammation (arrows)

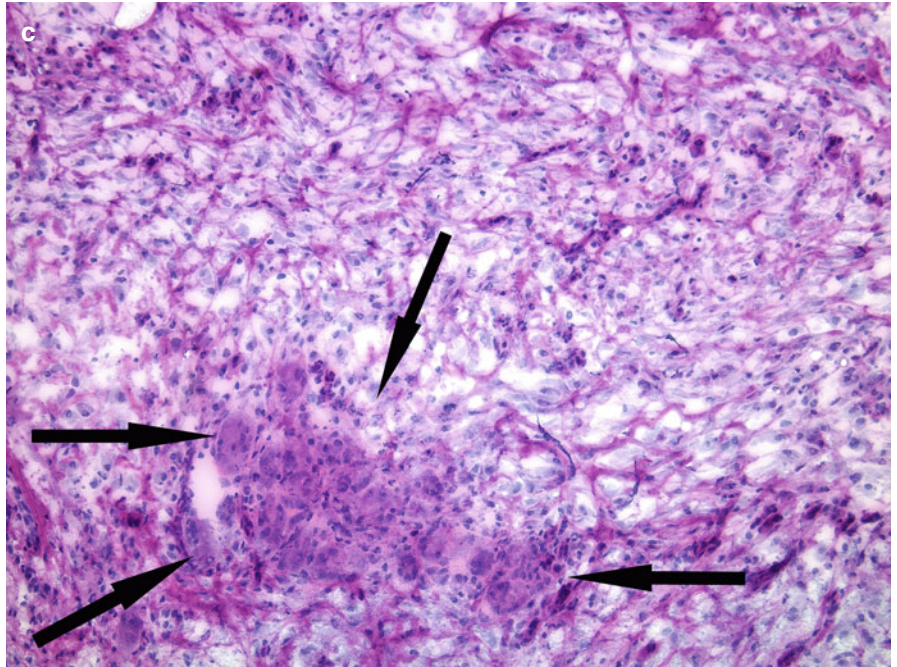


Fig. 14.13 New scar: **(a)** There are vertically oriented collagen bundles and blood vessels. Note also the obliteration of adnexal structures. **(b)** Plump fibroblasts and thickened collagen bundles are present. The overlying epidermis is hyperplastic

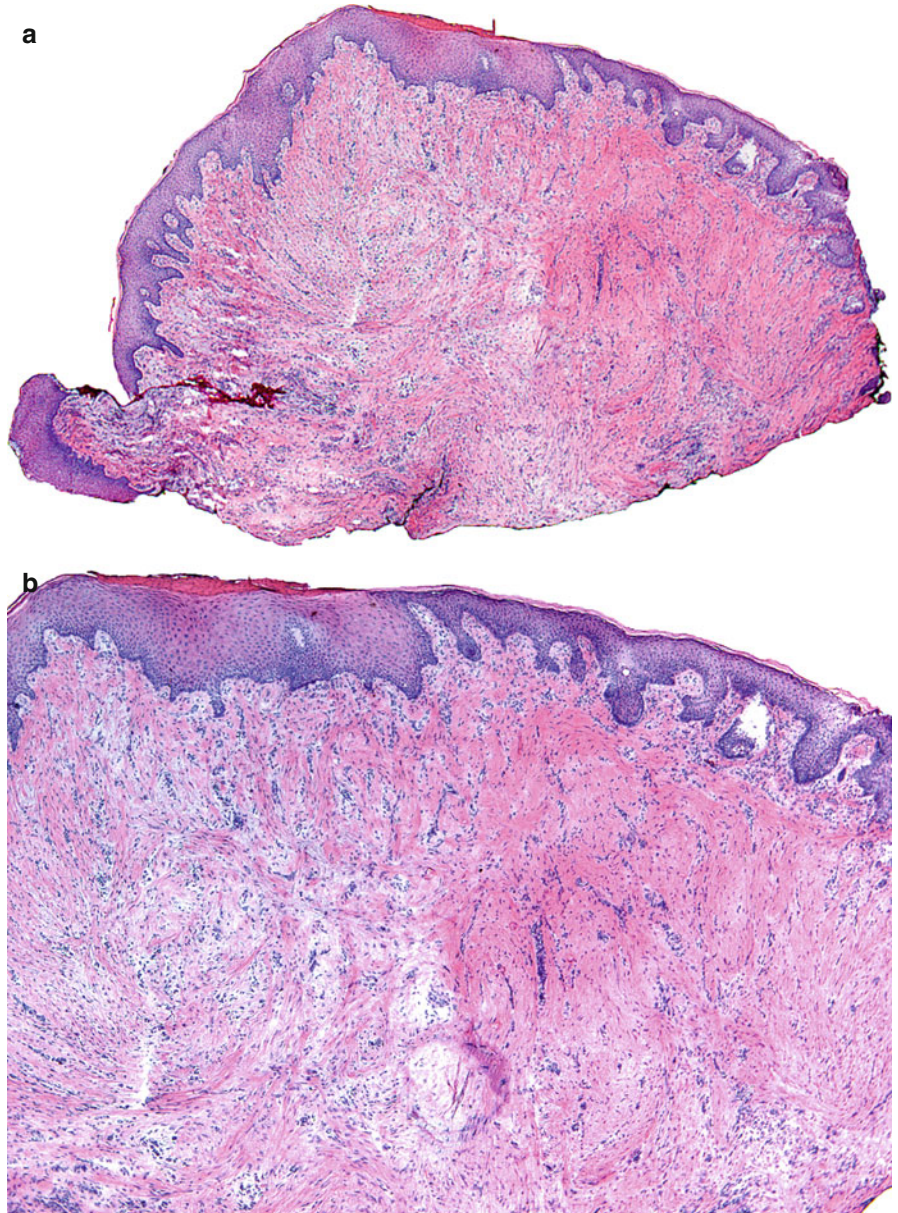


Fig. 14.13 (continued) (c) Newly formed blood vessels, which are slender, vertically oriented, compressed and surrounded by a few inflammatory cells

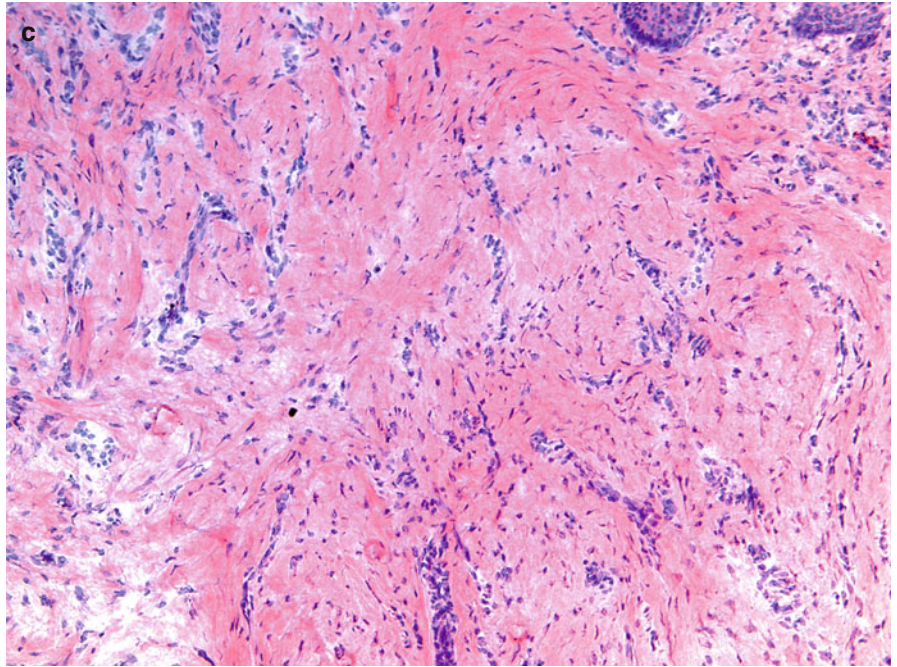


Fig. 14.14 Salivary gland: (a) Deeply situated within the subcutis is a portion of the submandibular gland. Unlike an infiltrative tumor the gland is well demarcated and shows a lobular architecture

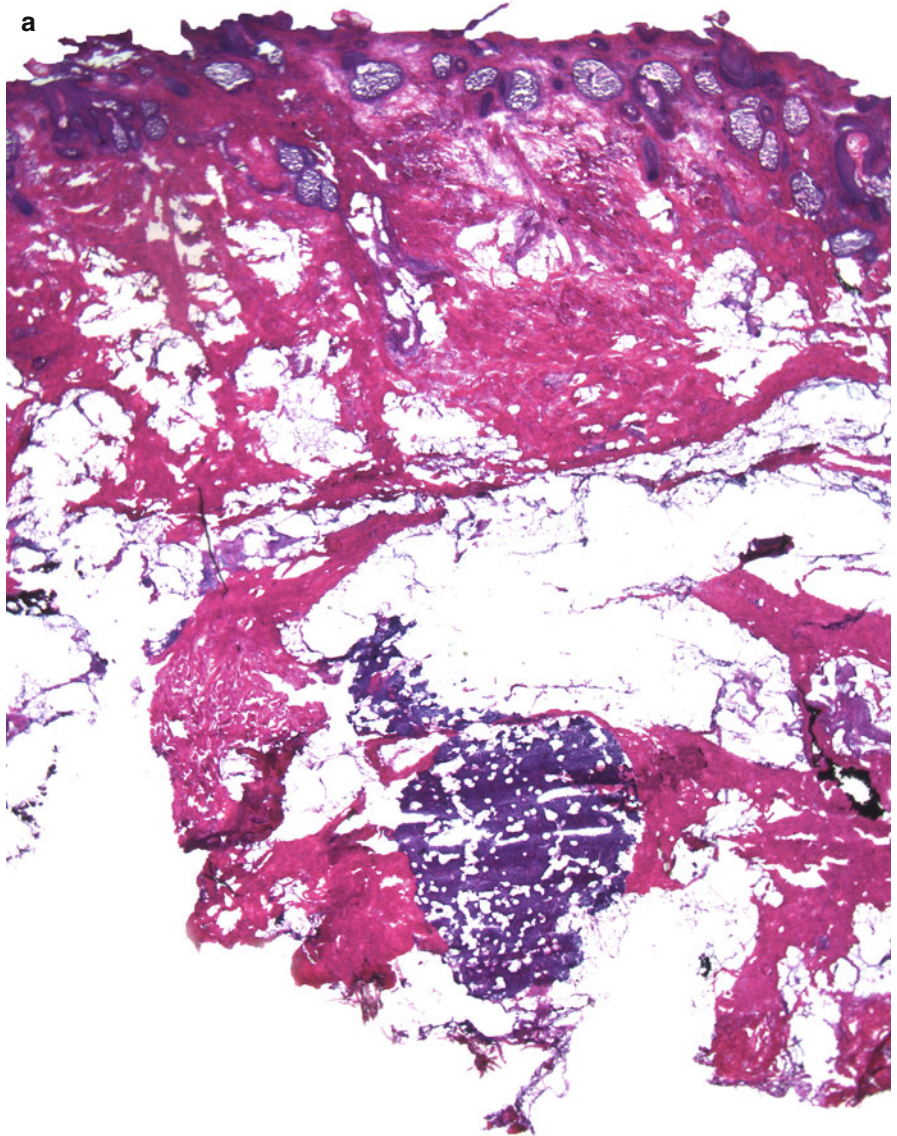


Fig. 14.14 (continued) (b) Organized glandular and ductal structures admixed with fatty tissue. (c) Ducts (*arrows*) containing pink secretions in their lumina are surrounded by glands

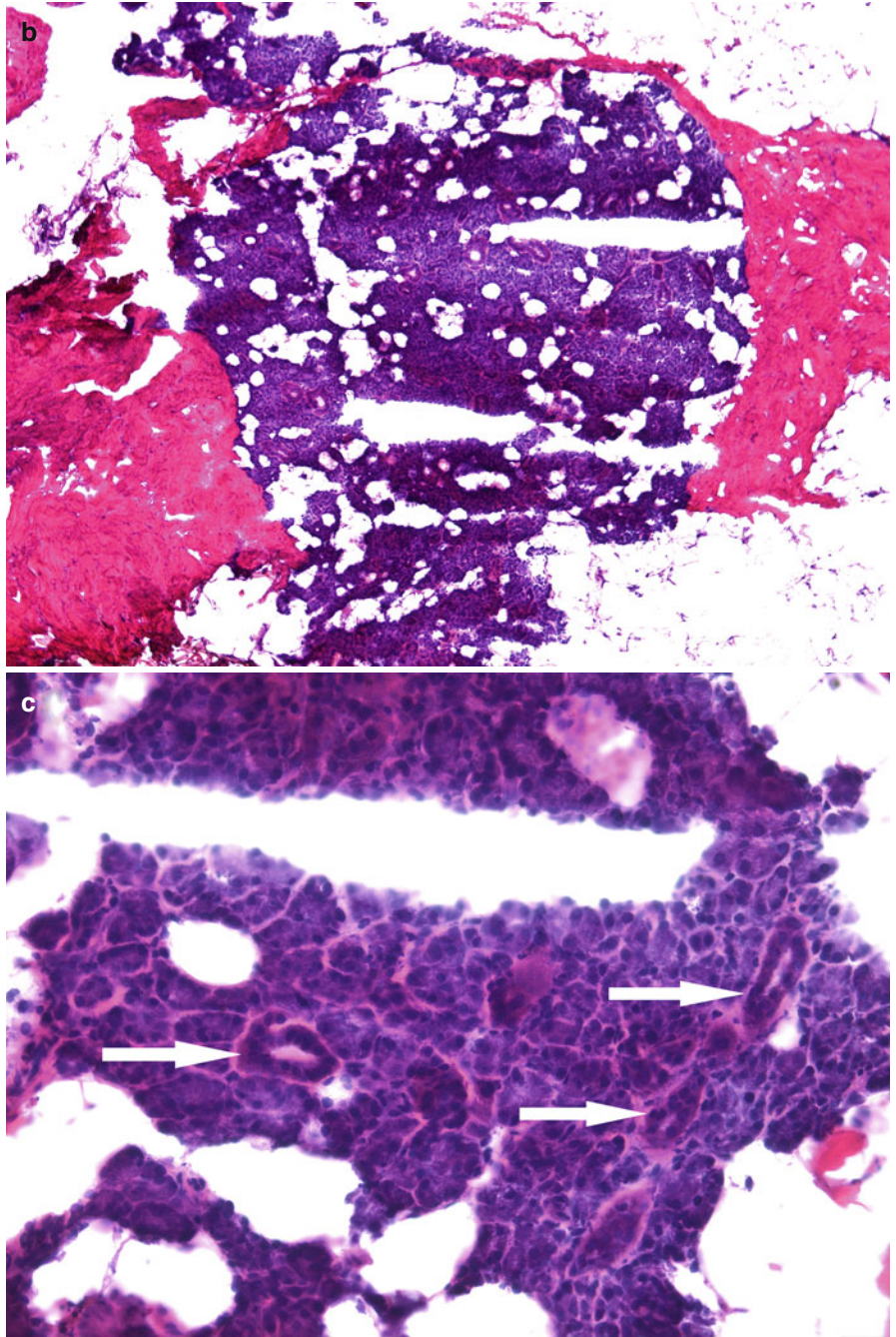


Fig. 14.15 Lymph node: (a) A basophilic well-delineated nodule is seen in the deep tissue in a section from the preauricular area. (b) Higher magnification demonstrates the architecture of the lymph node with lymphoid follicles (*arrows*)

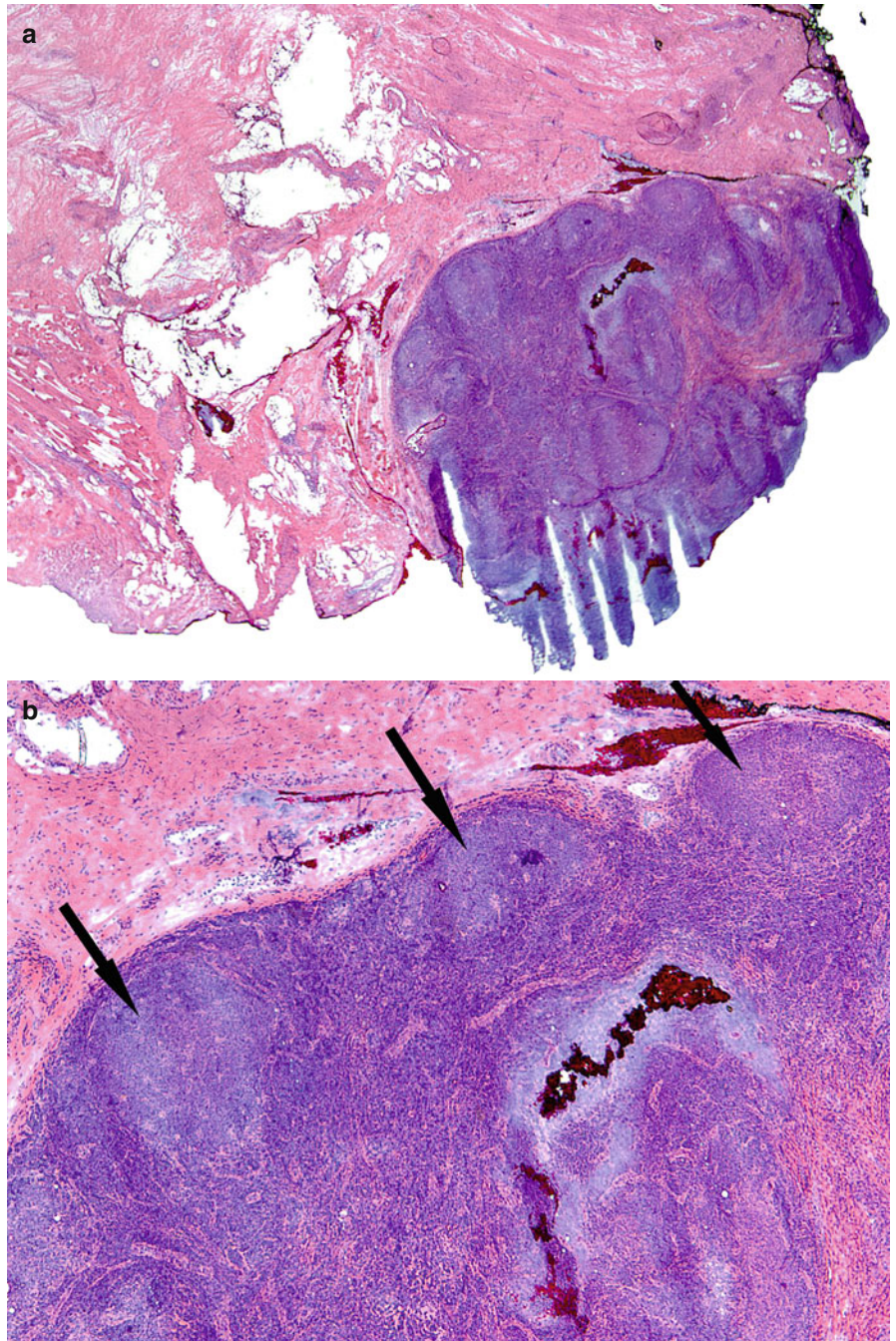


Fig. 14.16 Calcification in a vessel: (a) A medium size vessel in the lower portion of the photograph with calcifications within the vessel wall. (b) Purple calcium deposits within the wall of this blood vessel consistent with atherosclerosis

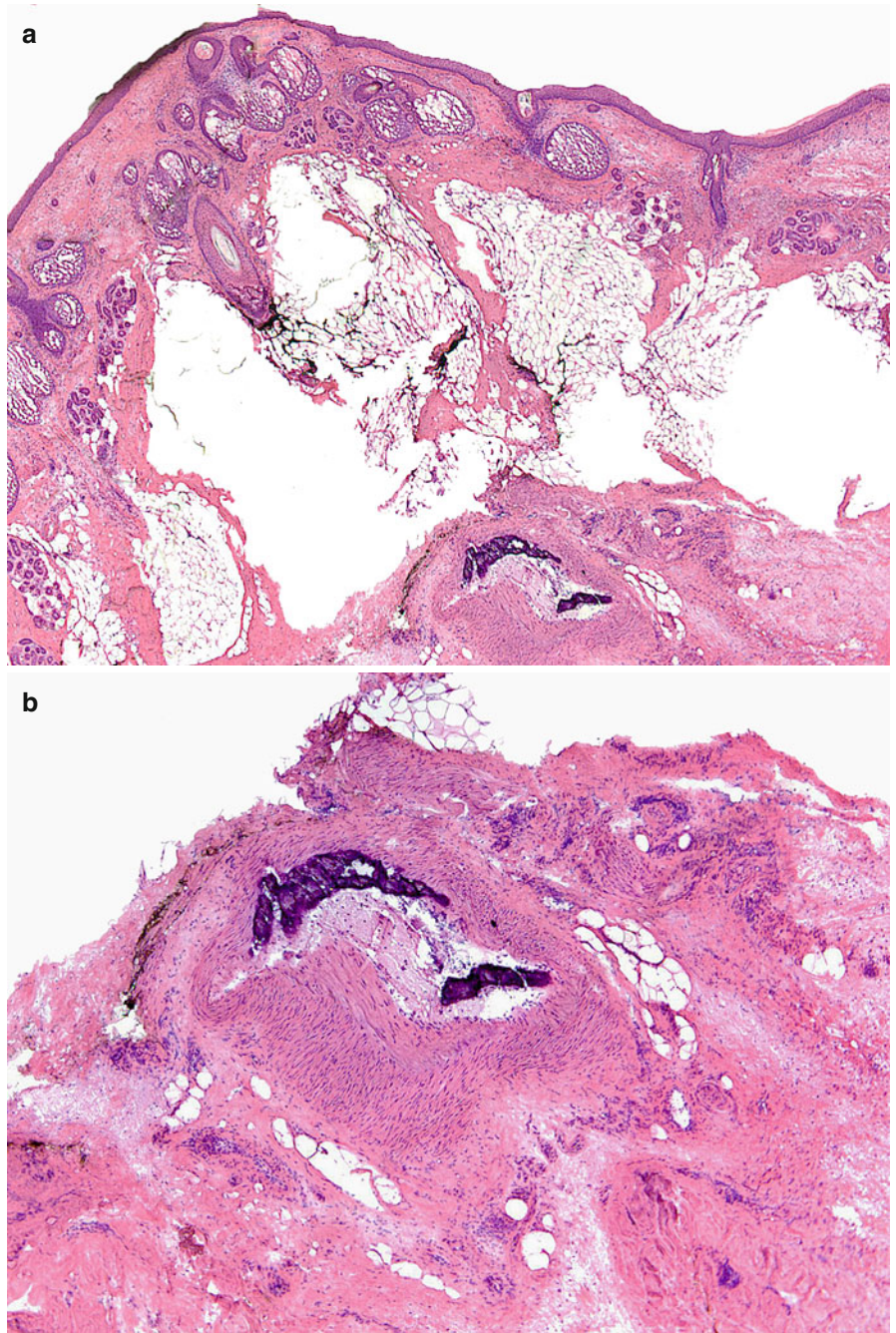


Fig. 14.17 Stasis changes: (a) Hyperplastic epidermis overlying edematous, papillary dermis with prominent, grouped, thick-walled blood vessels. There is a vertical linearity to the blood vessels in the dermis as well as prominent fibrosis. (b) The prominent edema and thickened walls of the papillary vessels are obvious

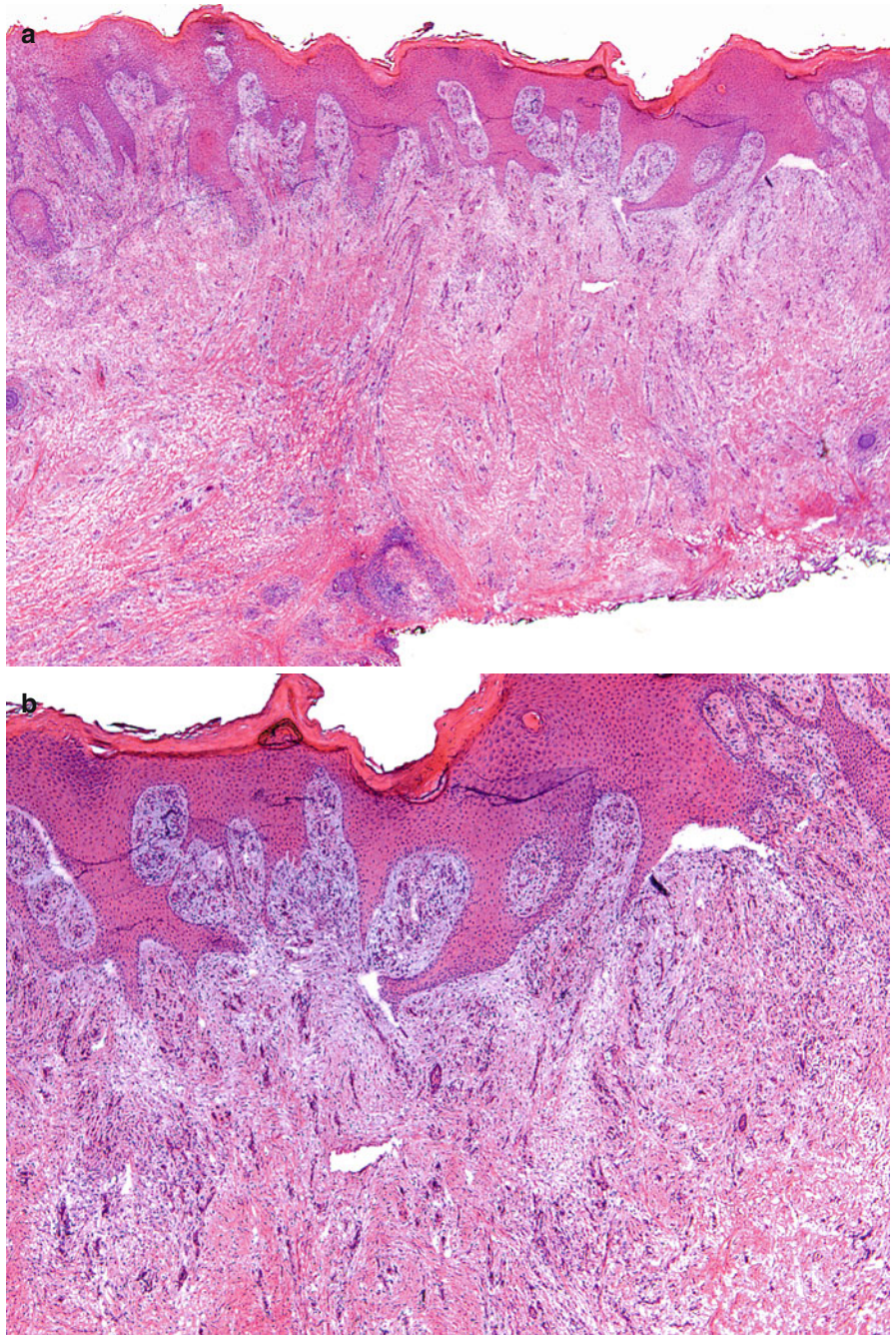


Fig. 15.1 The ideal specimen: An optimally prepared Mohs section shows epidermis, dermis, as well as subcutaneous tissue. The ink at the deep portion of the specimen should be visible so that the surgeon is assured that the deep margin of the tissue is seen in its entirety. There should be no epidermis missing and there should be no holes or missing areas in the dermis or in the deeper tissue. In addition, there should be a distinct contrast between the hematoxylin and eosin stains distinguishing adnexal structures and neoplastic aggregates from the surrounding dermis

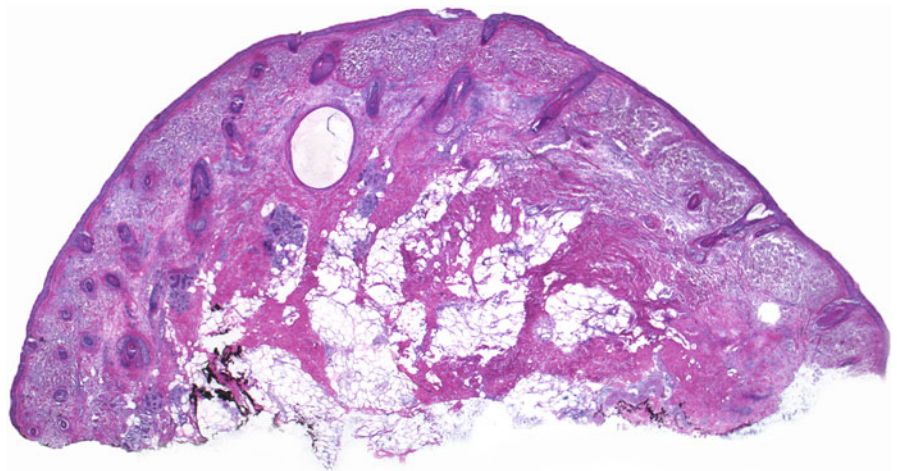


Fig. 15.2 Freeze artifact: this specimen shows pale cells in the epidermis along with vacuolization and ballooning

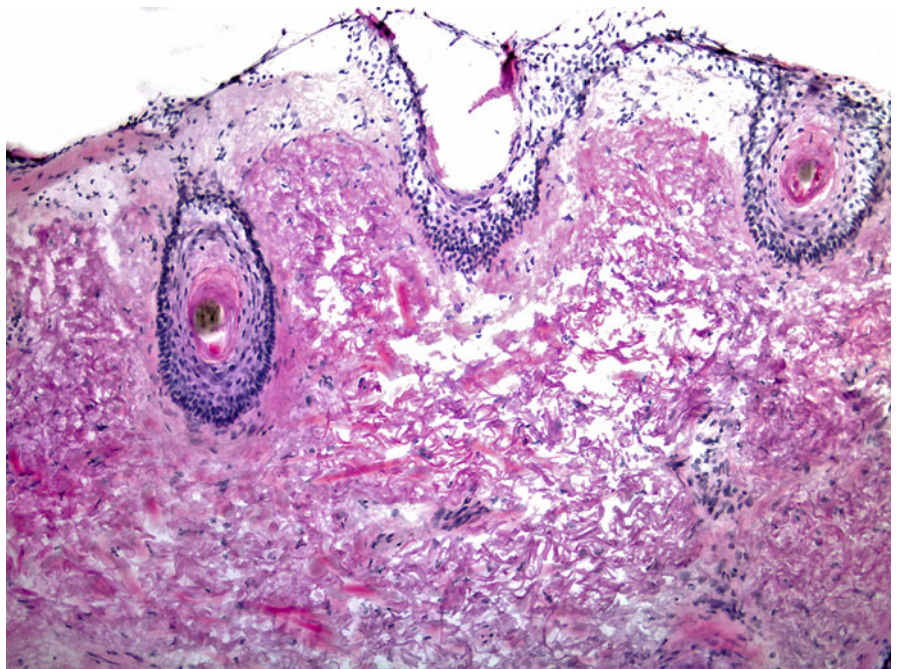


Fig. 15.3 Cautery artifact: (a) Normal epidermis adjacent to an area on the right, which shows cautery artifact. Keratinocytes are elongated and polarized and the cells appear stretched and smeared. Their nuclei are vertically oriented and polarized. (b) Another example of this effect along the entire length of the epidermis. There is loss of cellular detail and disruption of the tissue. (c) The hyperchromatic and large elongated nuclei as well as the cellular disarray demonstrate SCCIS in this case with superimposed cautery artifact. Such changes make evaluation of the specimen difficult. The dermis in the lower portion of the photomicrograph is amorphous due to coagulation of proteins

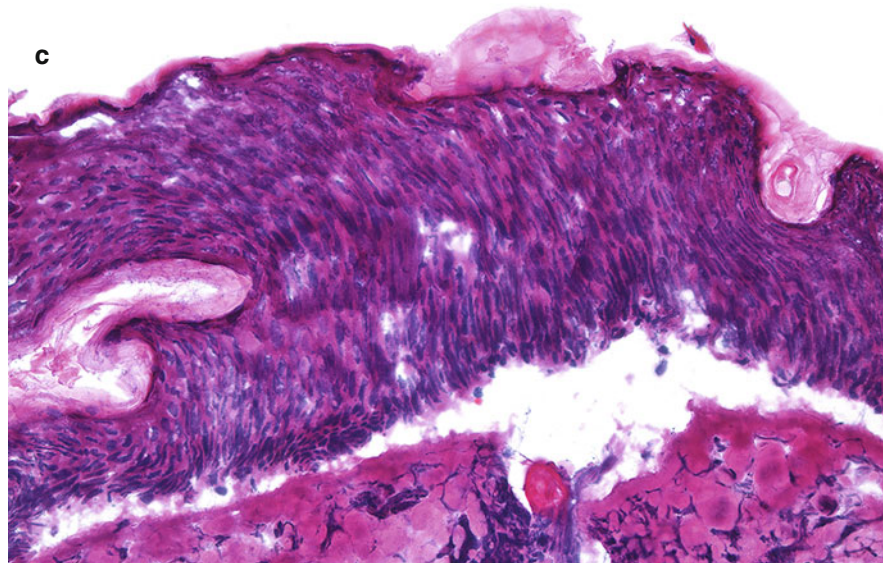
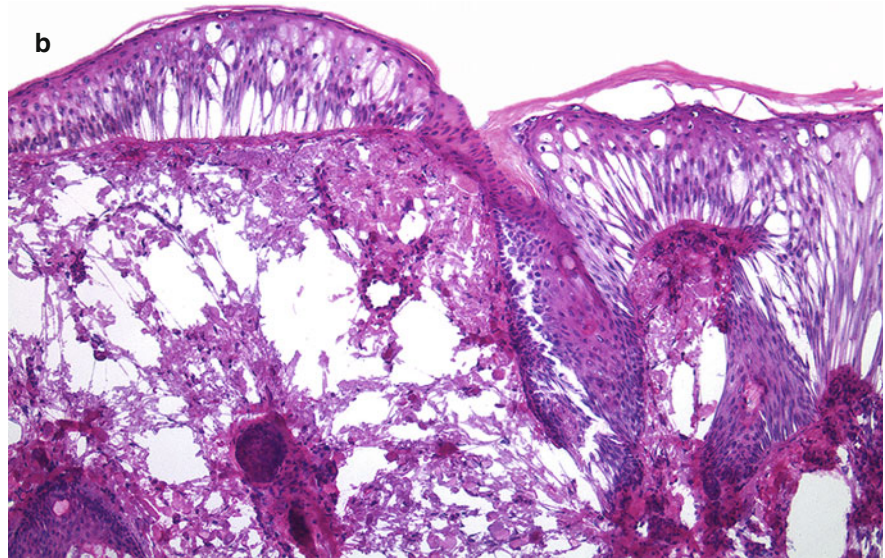
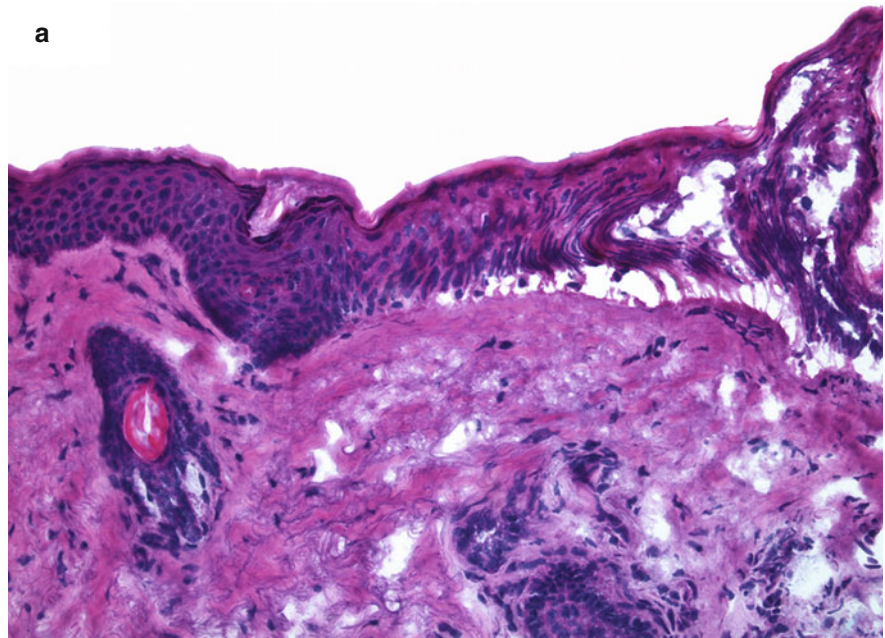


Fig. 15.4 Fold: a moderately sized fold will not allow the surgeon to examine the specimen completely and may also obscure the presence of tumor

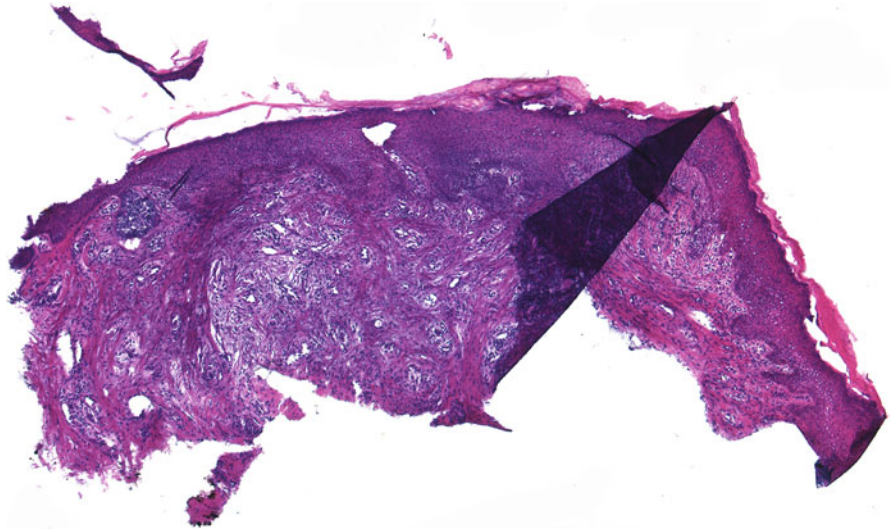


Fig. 15.5 Fold: essentially none of the epidermis and superior portion of the dermis can be appropriately examined. To prevent the specimen from folding, it must remain flat on the cryostat blade until it is transferred to a warm slide. The warmed slide allows the cold section to readily adhere

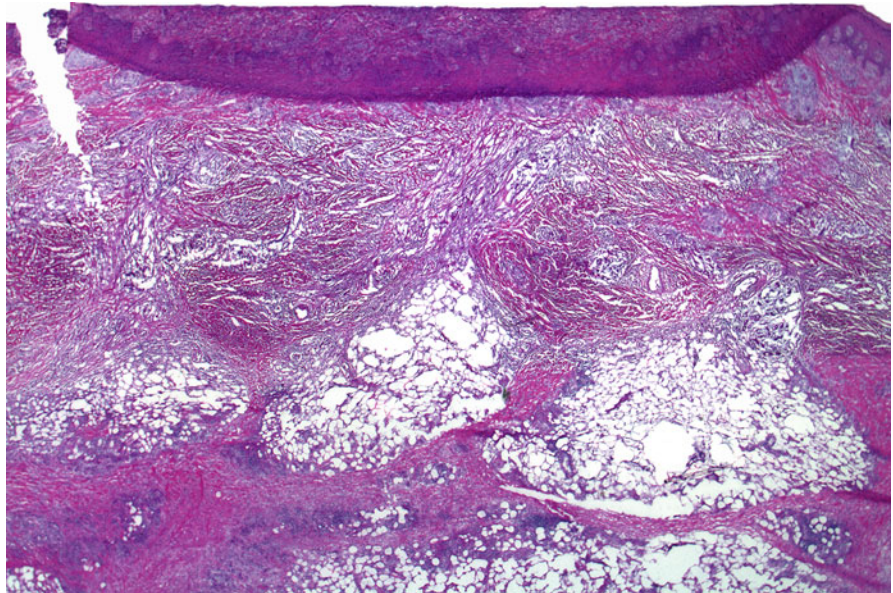


Fig. 15.6 Air bubble: this photomicrograph shows an early air bubble in the specimen. This occurs if the slide is too wet when the mounting medium is applied. The solvent evaporates allowing for separation of the coverslip from the slide and dries out the specimen. This can also occur if insufficient mounting media is applied to the slide before the coverslip is attached

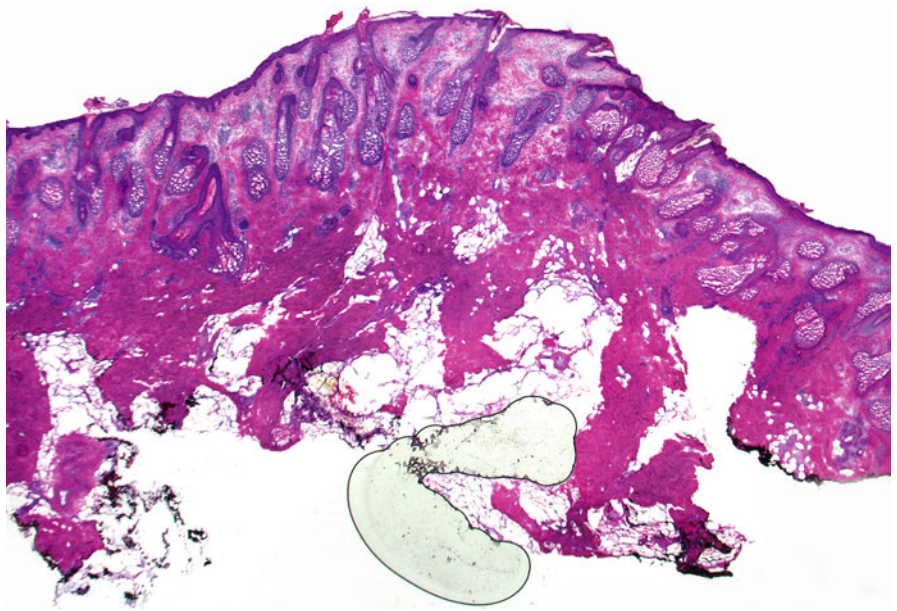


Fig. 15.7 Air bubble: a small early air bubble as shown above may not interfere with the interpretation of the slide. However, over time, as there is additional separation between the cover slip and the slide, the air bubble can expand drying out the specimen and leading to an illegible slide

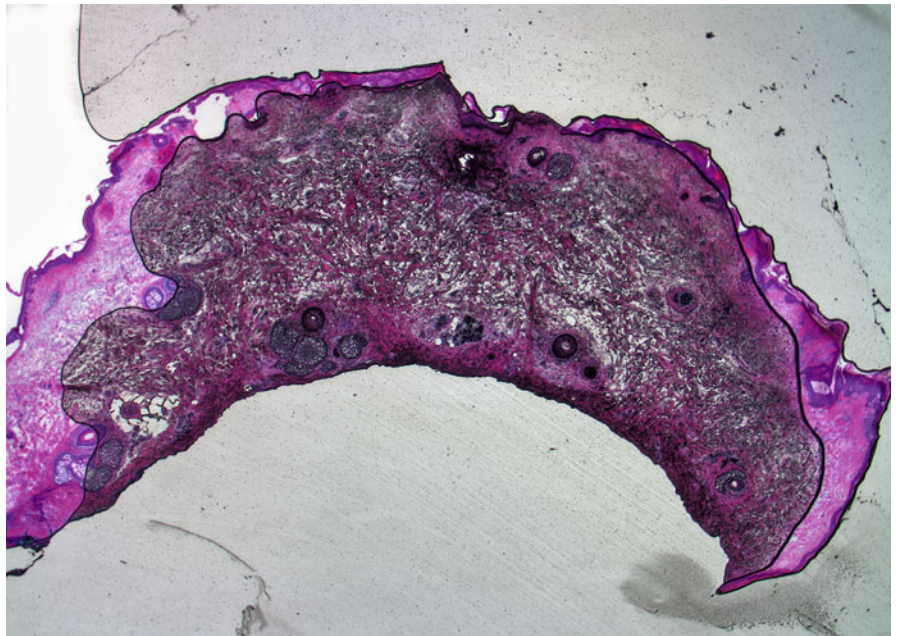


Fig. 15.8 Nicks: this photomicrograph shows a clear vertical mark in the specimen due to a nick in the blade

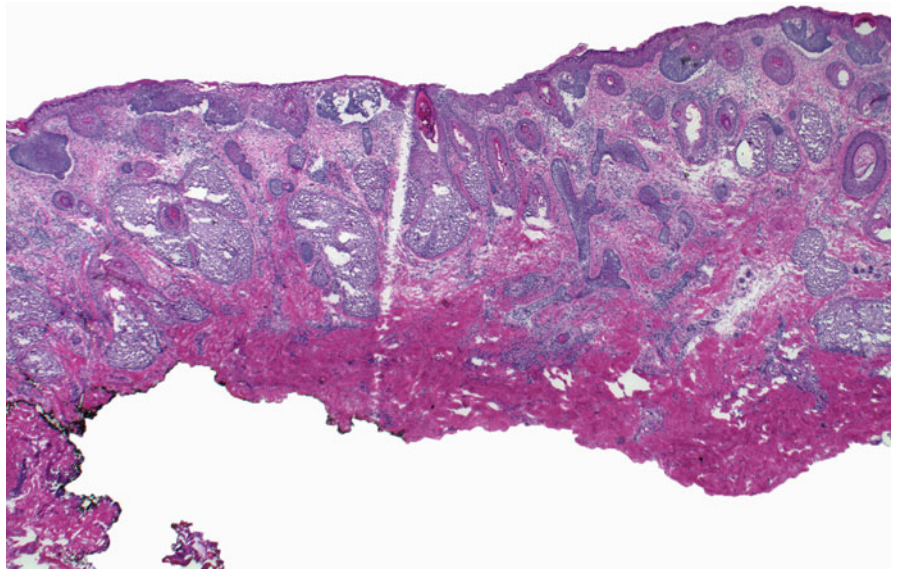


Fig. 15.9 Multiple wrinkles, folds, and separation within the specimen in a venetian blind pattern are indicative of a dull blade, a nick in the blade, or possibly a loose blade within the microtome

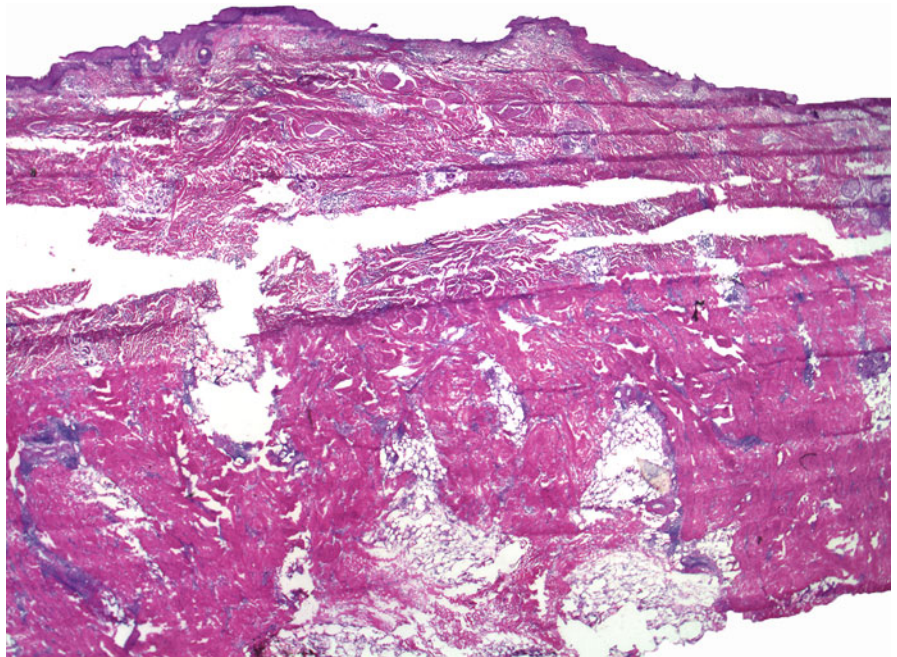


Fig. 15.10 (a, b) These are sections from the same specimen. However, in (b) the dermis is fragmented. There are spaces and irregularities within the slide and an uneven uptake of the tissue stains. This artifact occurs when a specimen is cut and laid on top of the excess OTC media from a previously cut specimen

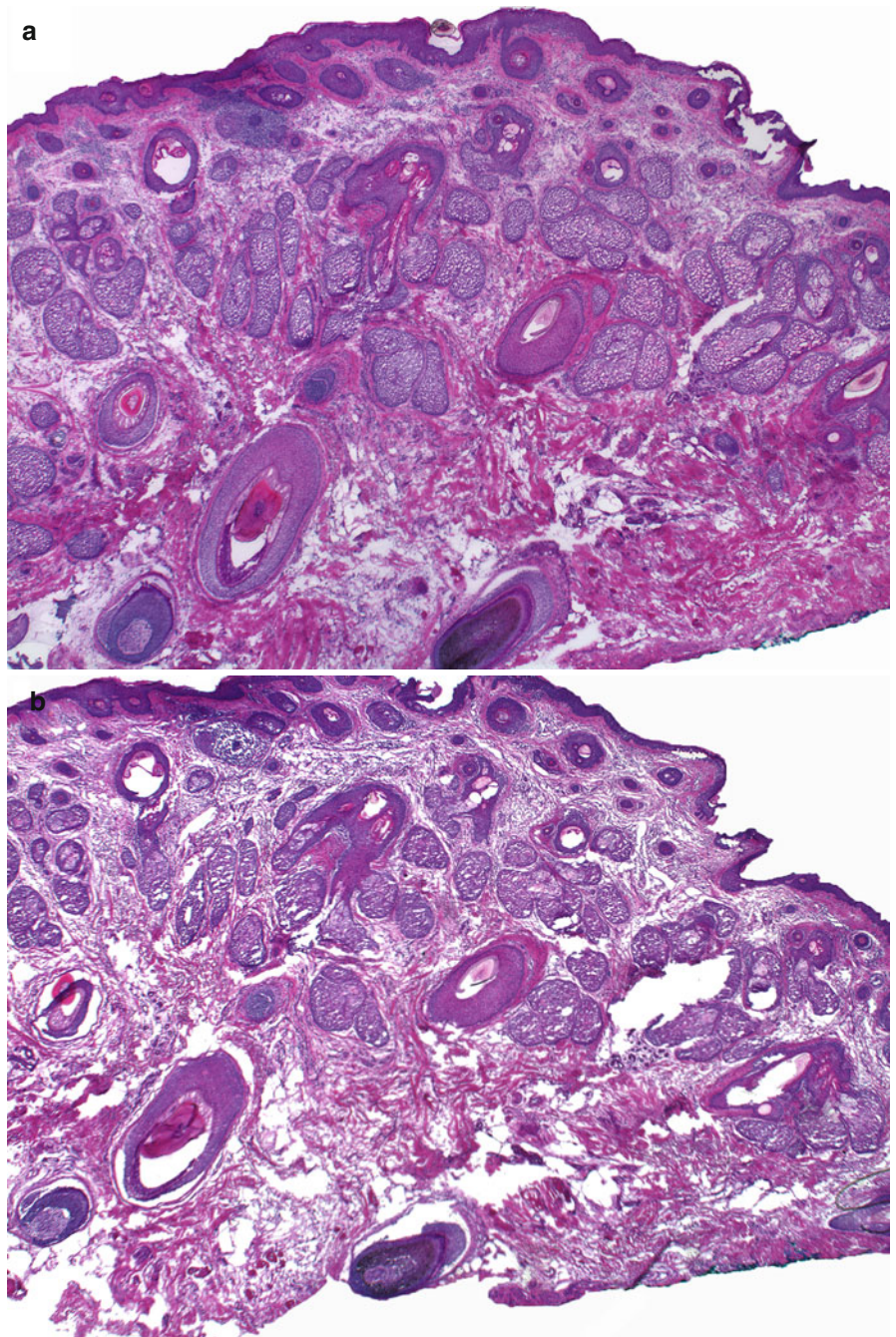


Fig. 15.11 (a, b) These are sections from the same specimen. In (b) the specimen was placed on top of underlying OTC media. The fat is fragmented. There are open spaces and the stain has an uneven uptake

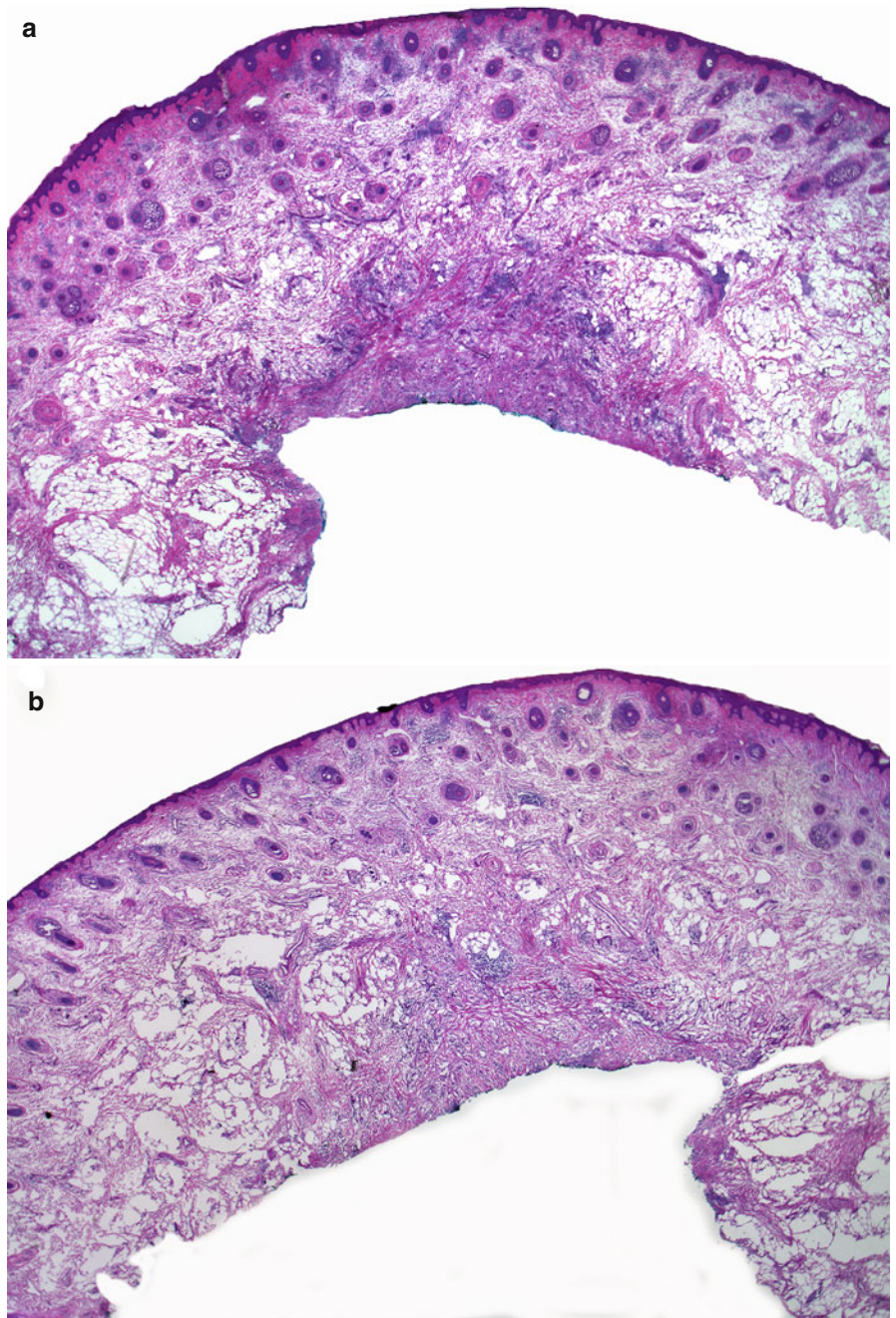


Fig. 15.12 This photomicrograph shows a section, of which the lower portion was placed on top of excess OTC media

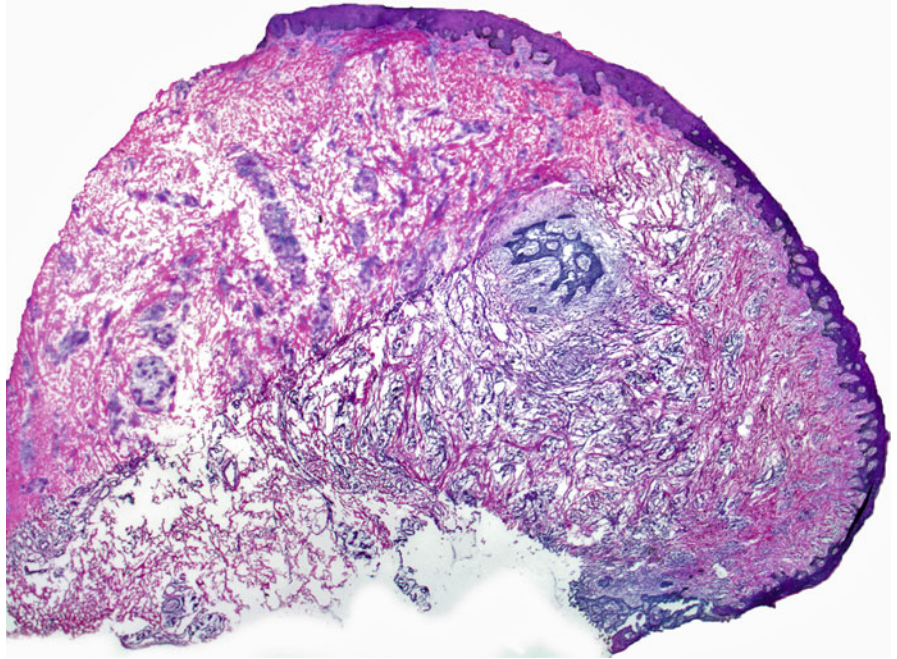
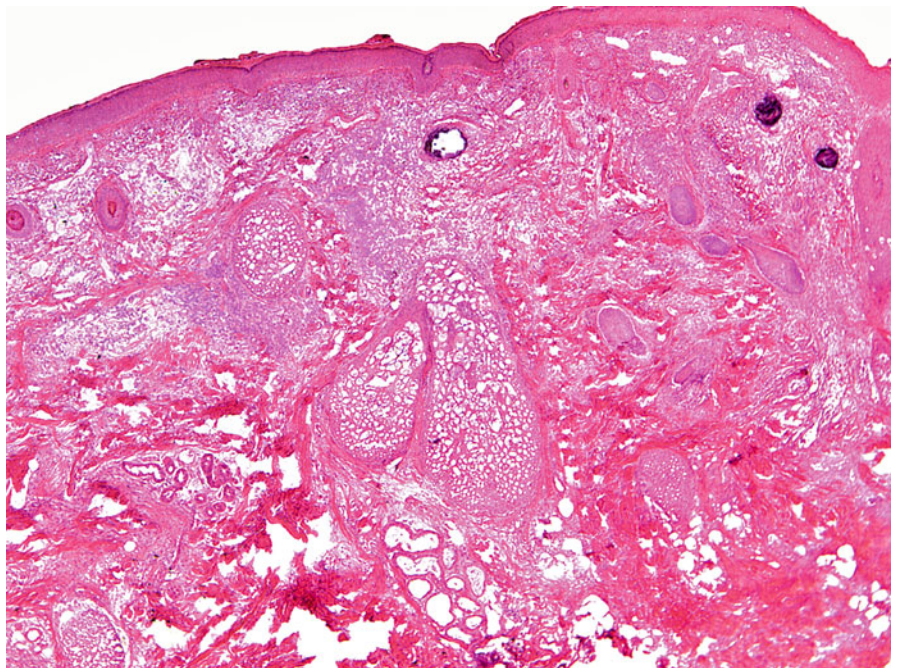


Fig. 15.13 Tissue stained abnormally pink. This processing error could be secondary to excess eosin, insufficient hematoxylin, or inadequate ammonia



Bibliography

- Abenzo P, Ackerman AB, editors. Neoplasms with eccrine differentiation. Philadelphia, London: Lea & Febiger; 1990.
- Ackerman AB, Mendonca AMN, Guo Y, editors. Differential diagnosis in dermatopathology I. 2nd ed. Philadelphia, London: Lea & Febiger; 1992. p. 58–61; 122–37; 170–3.
- Ackerman AB, Briggs PL, Bravo F, editors. Differential diagnosis in dermatopathology III. Philadelphia, London: Lea & Febiger; 1993a. p. 86–93; 98–101; 122–33; 138–41.
- Ackerman AB, de Viragh PA, Chongchitnant N, editors. Neoplasms with follicular differentiation. Philadelphia, London: Lea & Febiger; 1993b.
- Ackerman AB, Guo Y, Lazova R, Kaddu S, editors. Differential diagnosis in dermatopathology II. 2nd ed. New York: Ardor Scribendi; 2001. p. 90–101; 134–7; 142–9; 154–61; 170–3.
- Ackerman AB, Nussen-Lee S, Tan MA, editors. Histopathologic diagnosis of neoplasms with sebaceous differentiation. Atlas and text. 2nd ed. New York: Ardor Scribendi; 2009.
- Eisen DB, Michael DJ. Sebaceous lesions and their syndromes: part I. *J Am Acad Dermatol.* 2009a;61(4):549–60.
- Eisen DB, Michael DJ. Sebaceous lesions and their associated syndromes: part II. *J Am Acad Dermatol.* 2009b;61(4):563–78.
- Elder DE, Elenitsas R, Johnson Jr BL, Murphy GF, editors. *Lever's histopathology of the skin.* 9th ed. Philadelphia: Lippincott Williams & Wilkins; 2005.
- Grant-Kels JM, editor. *Color atlas of dermatopathology.* New York, London: Informa Healthcare; 2007.
- Leshin B, White WL. Folliculocentric basaloid proliferation. The bulge (der Wulst) revisited. *Arch Dermatol.* 1990;126(7):900–6.
- McKee PH, Calonje E, Granter SR, editors. *Pathology of the skin with clinical correlations.* 3rd ed. London: Mosby Elsevier; 2005.
- Mills O, Thomas LB. Basaloid follicular hamartoma. *Arch Pathol Lab Med.* 2010;134(8):1215–9.
- Rapini RP, editor. *Practical dermatopathology.* London: Mosby Elsevier; 2005.
- Steffen C, Ackerman AB, editors. *Neoplasms with sebaceous differentiation.* Philadelphia, Baltimore, Hong Kong, London, Munich, Sydney, Tokyo: Lea & Febiger; 1994.
- Weedon D, editor. *Skin pathology.* 2nd ed. Edinburgh, London, New York, Oxford, Philadelphia, St. Louis, Sidney, Toronto: Churchill Livingstone; 2002.
- Wheater PR, Burkitt HG, editors. *Functional histology. A text and colour atlas.* 2nd ed. Edinburgh, London, Melbourne, New York: Churchill Livingstone; 1987.
- Zayour M, Lazova R. Pseudoepitheliomatous hyperplasia: a review. *Am J Dermatopathol.* 2011;33(2):112–26.
- Zedeck DC, Smith Jr ET, Hitchcock MG, Feldman SR, Shelton BJ, White WL. Cutaneous lupus erythematosus simulating squamous neoplasia: the clinicopathologic conubdram and histopathologic pitfalls. *J Am Acad Dermatol.* 2007;56(6):1013–20.

Index

A

Acantholytic squamous cell carcinoma, 180

Actinic keratosis (AK)

acantholytic actinic keratosis, 174

seborrheic keratosis, 177

Adnexal tumors

description, 111

DTE (*see* Desmoplastic trichoepithelioma (DTE))

sebaceous carcinoma (*see* Sebaceous carcinoma)

syringoma (*see* Syringoma)

AFX. *See* Atypical fibroxanthoma (AFX)

AK. *See* Actinic keratosis (AK)

Apocrine sweat glands, 23

Artifacts

air bubble, 312

cautery, 310

freeze artifact, 309

Atypical fibroxanthoma (AFX)

bizarre giant cells, 282

immunohistochemistry stains, 274

B

Basal cell carcinoma (BCC)

desmoplastic trichoepithelioma, 147

infundibulocystic, 27, 29

keratinizing, 27, 31, 32

micronodular, 27, 30, 41

infiltrative, 27–29, 37

pigmented, 27

Basaloid follicular hamartoma (BFH), 65, 87

BCC. *See* Basal cell carcinoma (BCC)

BFH. *See* Basaloid follicular hamartoma (BFH)

D

Dermatofibrosarcoma protuberans (DFSP)

eccrine glands, 66, 108

Desmoplastic trichoepithelioma (DTE), 48, 112, 117, 130, 145, 148

DFSP. *See* Dermatofibrosarcoma protuberans (DFSP)

E

Eccrine carcinoma

microcystic adnexal (*see* Microcystic adnexal carcinoma)

Eccrine ducts, 137

actinic keratosis, 157, 174

SCCIS (*see* Squamous cell carcinoma in situ (SCCIS))

Extramammary Paget's disease, 274, 283

Eyeliner sign

SCCIS, 158, 160

F

FBP. *See* Folliculocentric basaloid proliferation (FBP)

Folliculocentric basaloid proliferation (FBP), 65

G

Granulomatous inflammation, 130, 146, 149, 291

H

Hair follicles

bulge, 3

follicular bulb and papilla, 5

SCCIS, 164, 166

Hypertrophic lupus erythematosus, 245, 248

I

Infiltrative basal cell carcinoma, 77, 111

DTE (*see* Desmoplastic trichoepithelioma (DTE))

microcystic adnexal carcinoma, 146

perineural invasion, 49, 58

syringoma (*see* Syringoma)

Infiltrative squamous cell carcinoma, 181, 210, 211, 215–230

K

Keratinizing BCC, 27, 31, 32

L

Lupus erythematosus, 247, 248

M

Melanocytic nevus, 286, 287

Microcystic adnexal carcinoma, 112

N

Neurofibroma, 285, 289

Nodular BCC, 27

Normal skin

apocrine sweat glands, 23

eccrine glands, 19

Normal skin (*cont.*)
 folliculo-sebaceous unit
 (*see* Hair follicles)
 nerves (*see* Nerves)
 periosteum, 24
 salivary glands, 20–22
 scar tissue, 25–26
 skeletal muscle, 13–14
 smooth muscle, 15–16

P

Paget's disease
 extramammary, 274, 283,
 intraepidermal, 153
 PEH. *See* Pseudoepitheliomatous hyperplasia (PEH)
 Periosteum, 24, 139–140
 calcification, vessel, 307
 epidermal inclusion cyst, 285
 lymph node, 306
 neurofibroma, 285, 289, 290
 nevus (*see* Melanocytic nevus)
 salivary gland, 304–305
 scar (*see* Scar tissue)
 seborrheic keratosis, 285, 296–297
 solar lentigo, 285, 298, 299

 stasis changes, 308
 suture granuloma, 295
 Pseudoepitheliomatous hyperplasia (PEH), 181, 246, 251, 252,
 254–256

S

Salivary glands, 20–22, 304
 Scar, 25–26, 97, 187–189, 242, 243, 257, 263–265, 272, 300
 SCC. *See* Squamous cell carcinoma (SCC)
 Sebaceous carcinoma
 Muir-Torre syndrome and cutaneous manifestations, 113
 Seborrheic keratosis (SK), 173, 180, 285, 297
 SK. *See* Seborrheic keratosis (SK)
 Solar lentigo, 285, 298
 Spindle cell squamous cell carcinoma, 180
 Squamous cell carcinoma (SCC)
 PEH (*see* Pseudoepitheliomatous hyperplasia (PEH))
 perineural invasion, 179
 SCCIS (*see* Squamous cell carcinoma in situ (SCCIS))
 well-differentiated, 233–236
 Squamous cell carcinoma in situ (SCCIS)
 SCC, 172, 197–198
 Superficial BCC, 28, 30, 39, 55, 69
 Suture granuloma, 295
 Syringoma, 48, 111, 112, 114, 146, 151